



# Book of Abstract

<b>PUBLIC TALK.....</b>	<b>2</b>
Public Talk   Examining Old Paintings With New X-Ray Methods: A Fresh Look At And Below The Surface.....	2
Public Talk   More than a century of Crystallography: What has it taught us and where will it lead?.....	3
<b>PLENARY .....</b>	<b>4</b>
PL1   The Cytomotive Switch In Actins And Tubulins.....	4
PL2   Quantum Crystallographic Studies Of Advanced Materials .....	5
<b>KEYNOTE .....</b>	<b>6</b>
KN01   Ground State Selection In Quantum Pyrochlore Magnets.....	6
KN02   New Experimental Techniques For Exploring Crystallization Pathways And Structural Properties Of Solids .....	7
KN03   Solar System Secrets Hidden In Quasicrystals .....	8
KN04   Metal-Organic Frameworks As Chemical Reactors: X-Ray Crystallographic Snapshots Of The Confined State .....	9
KN05   40 Years Of Ccp4: Where We Are, How We Got Here And Where We Are Going .....	10
KN06   Crystal Phase Control In Nanostructures As A Platform For Atomic Scale Tailoring Of Electronic, Optical And Chemical Properties. ....	11
KN07   Chemistry And Crystallography At Ultra-High Pressures .....	12
KN08   Diffuse Scattering - Past, Present And Future.....	13
KN09   Fertilization At The Atomic Level - Marrying Basic Science And Reproductive Medicine.....	14
KN10   One Million Structures And Counting: The Journey, The Insights, And The Future Of The Cambridge Structural Database .....	15
KN11   Enhancing The Success Of Macromolecular Crystallization .....	16
KN12   Application To E-Precession In Transmission Electron Microscope: Phase And Orientation Map.....	17
KN13   Mesophase Mirabilis. The Lipid Cubic Phase As A System For Investigating Membrane Proteins.....	18
KN14   Capturing Functional Nanostructures And Their Interfaces With Neutron Total Scattering.....	19
KN15   Changing Times In Structural Virology.....	20
KN16   Unusual Magnetic Orderings From The Interplay Of Triangular Topology And Magnetic Anisotropy .....	21
<b>MS01: SERIAL APPROACHES IN CRYSTALLOGRAPHY .....</b>	<b>2</b>
MS01-01   Elucidation Of No Reduction Mechanism In Soluble No Reductase By Time-Resolved Crystallography With Photosensitive Caged Compound .....	2
MS01-02   A Tale Of Two Sources: Serial Crystallography At Synchrotrons And Xfels.....	3
MS01-03   Swissmx: A New, Versatile Instrument For Fixed Target Femtosecond Macromolecular Crystallography At Swissfel.....	4
MS01-04   Ultra-Fast Raster-Scanning Synchrotron Serial Micro-Crystallography .....	5
MS01-05   Measuring The Dose: Photoelectron Escape In Micro-Crystals.....	6
MS01-P01   Data Analysis Infrastructure for Serial Crystallography Experiments at the EuXFEL.....	7
MS01-P02   TREXX: a new endstation for serial time-resolved crystallography at PETRA-III .....	8
MS01-P03   MicroMAX - New Possibilities for Serial Crystallography .....	9
MS01-P04   MetalJet source enabling advanced protein crystallography.....	10
MS01-P05   Serial crystallography at the ESRF Extremely Brilliant Source: The ID29 upgrade project .....	11
MS01-P06   Better SAUC -- Improving the Identification of Nearby Cells .....	12
MS01-P07   Optimized design for new scientific opportunities in macromolecular crystallography at the future microfocus XAIRA beamline .....	13
MS01-P08   Development of serial millisecond crystallography at BioMAX beamline .....	14
MS01-P09   P11 at PETRA III: A Versatile Beamline for Serial and High-Throughput Crystallography.....	15
MS01-P10   Liquid Application Method for time-resolved Analyses (LAMA) by serial synchrotron crystallography .....	16
MS01-P101 -LATE   P14 TREXX: First Results from the Jurassic Beamline.....	17
<b>MS02: FRAGMENT/LIGAND BINDING: TOOLS DEVELOPMENT .....</b>	<b>18</b>
MS02-01   How not to Shoot Yourself into the Foot.....	18
MS02-02   Polder Maps: Improving OMIT Maps for Ligand Building and Validation.....	19
MS02-03   FragMAX - The New Fragment Screening Facility of MAX IV Laboratory .....	20
MS02-04   Automated, Remote-Controlled Ligand Screening Pipelines for Drug Discovery .....	21
MS02-05   Structure-Based Fragment Screening on Dynamain GTPase Domain.....	22

MS02-P01   Structure-based drug design to tackle disorders of haem biosynthesis .....	23
MS02-P02   Getting the most from your crystals through the full automation of complex experiments.....	24
MS02-P03   PanDDA: extracting ligand-bound protein states from conventionally uninterpretable crystallographic electron density.....	25
MS02-P04   A Case Study of Fragment Screening: Protein Kinase A and PIM1-Kinase .....	26
MS02-P05   New fully Automatic measurement MX beamline BL45XU at SPring-8.....	27
MS02-P06   Fragment screening project management web application - FragMAX.....	28
MS02-P103 <b>LATE</b>   Long-Wavelength Native SAD Phasing at BL13-XALOC enabled by the presence of an Helium Cone .....	29

### **MS03: CRYSTALLISATION AND BIOPHYSICAL CHARACTERISATION ..... 30**

MS03-01   Protein Thermodynamic Parameters to Understand and Guide Crystallisation .....	30
MS03-02   High-Throughput Thermal Stability Approaches for Sample Optimization.....	31
MS03-03   In Numbers: Initial Screening at the MRC-LMB Protein Crystallization Facility .....	32
MS03-04   Biophysical Methods to Aid Protein Crystallization in a Pharmaceutical Setting.....	33
MS03-05   High-Throughput Stability Screening of Integral Membrane Proteins .....	34
MS03-P01   Structural Basis of Inactivation of Human Counterpart of Mouse Motor Neuron Degeneration 2 Mutant in Serine Protease HtrA2 .....	35
MS03-P02   The MORPHEUS protein crystallisation screens .....	36
MS03-P03   Molecular investigation of muscle Z-disc assembly centered on the complex human $\alpha$ -actinin isoform-2 and ZASP.....	37
MS03-P04   Crystal structure of an anti-tumour antibody in complex with a tumour-specific antigen .....	38
MS03-P05   Invitation to perform experiments on high end instruments: Centre of Molecular Structure in BIOCEV .....	39
MS03-P06   Crystal Production And Structure Solution Thanks ToThe Nucleating And Phasing Agent, Crystallophore.....	40
MS03-P07   Structural And Biophysical Analysis Of The Pyridoxal Phosphate Synthase From Plasmodium Vivax .....	41
MS03-P08   The Role Of Odd In The Biosynthesis Of Medically Important Alkaloids.....	42
MS03-P09   Crystal Structure Of Human Amacr Provides Insight Into Substrate Recognition And Catalytic Mechanism.....	43
MS03-P10   Sec-Saxs Analysis Of Oligomeric States Of Human Nkr-P1 With Its Ligand Lit1 In Solution.....	44
MS03-P11   A Reliable And Versatile Tool For High-End In-House Structural Studies.....	45
MS03-P12   All-In-One Sample Holder For Macromolecular Crystallography.....	46
MS03-P13   Profilins and the quest for structure-based IgE-epitope mapping.....	47
MS03-P14   One Step Co-Purification And Crystallization Of Three Soluble Proteins From Cyanobacteria, The Unique Crystallization Properties Of C-Phycocyanin .....	48
MS03-P15   Novel Biochemical Bases For Nuclear Factor I X (NFI)X.....	49
MS03-P16   Dynamic Formation And Internal Order Of Liquid Dense Protein Clusters Beyond Crystallography.....	50
MS03-P17   Crystal And Solution Structures Of SH2 Domain Of Signaling Molecule In Complex With The Co-Stimulatory Receptor CD28 .....	51
MS03-P19   Structural Determinants Of The Interaction Specificity At The G And Nc Interfaces Of Human Septins.....	52
MS03-P20   The Sod1-Hccs Mechanism Involved In Copper Homeostasis.....	53
MS03-P21   The N-terminal Domain of Lactobacillus acidophilus SlpA promotes Self-Assembly of the S-Layer Array .....	54
MS03-P22   Crystal Structure Of Histone Chaperone Anti Silencing Function 1 (Asf1) From Plasmodium Falciparum And Its Biochemical Characterization.....	55
MS03-P23   The Crystal Structure Of The Major Olive Pollen Allergen Ole E 1 .....	56
MS03-P24   Preliminary Diffraction Experiments On The E.Coli Toxin Sat.....	57
MS03-P105 <b>LATE</b>   ContaMiner and ContaBase: Automated Identification of Unwantedly Crystallized Protein Contaminants.....	58
MS03-P107 - <b>LATE</b>   Keeping Muscle Proteins In Shape – UCS-Proteins Acting As Myosin-Specific Quality Control Factors .....	59
MS03-P109 - <b>LATE</b>   How The Parg Protein Mark Keeps The Stress Response Kinase Mcsb Under Control.....	60
MS03-P111 - <b>LATE</b>   Dna Relaxase Traa Of The G+ Plasmid Pip501 As Key Player In Bacterial Conjugation ...	61

### **MS04: PROGRESS (METHODS) IN HIGH RESOLUTION CRYO-EM ..... 62**

MS04-01   Mechanisms Of C-Ring Protonation And Flexible F1-Fo Coupling In A Mitochondrial Atp Synthase ..	62
MS04-02   Recent Advances in Cryo-Electron Tomography for In Situ Structural Biology .....	63
MS04-03   A New and Simple Method for Cryo-EM Specimen Preparation.....	64

MS04-04   Automated Interpretation of Cryo-EM Density Maps with Convolutional Neural Networks .....	65
MS04-05   Micro Electron Diffraction is a Quick and Versatile Tool for Structure Determination of Macromolecules and Small Molecules .....	66
MS04-P01   CCP-EM: the Collaborative Computational Project for Electron cryo-Microscopy .....	67
MS04-P02 - <b>CANCELLED</b>   Tools for validation of maps and atomic model fits in Single Particle Cryo-EM .....	68
MS04-P03   Efficient Real-Space Refinement For Cryo-Em And Crystallography .....	69
MS04-P113 - <b>LATE</b>   Beam-Induced Movement Attenuation With Single Wall Carbon Nanotubes .....	70
<b>MS05: PROTEINS IN SIGNALLING (INCLUDING MEMBRANE PROTEINS) .....</b>	<b>71</b>
MS05-01   Protein Conformational and Oligomeric Rearrangements Control Intercellular Signaling .....	71
MS05-02   Structural Insights into Signal Processing to Chromatin .....	72
MS05-03   Transport Of Enantiomeric Neurotransmitters By Slc1a Family Of Proteins .....	73
MS05-04   Structural Basis for CD96 Immune Receptor Recognition of Nectin-like Protein-5, CD155 .....	74
MS05-05   Analysis of Cytomegalovirus Immune Evasion Protein UL144 Glycosylation Profile Revealed its Role in Immune Recognition .....	75
MS05-P01   The Critical Role Of The Fourth Position Of The Vxgfl Motif Of Pp2cs From Oryza Sativa In Regulation Of Aba Responsiveness .....	76
MS05-P02   Structural Studies of Type II TNF- $\alpha$ from Orange-spotted Grouper, Epinephelus coioides .....	77
MS05-P115 <b>LATE</b>   Structural studies of the atypical SLAMF3 receptor .....	78
MS05-P117 <b>LATE</b>   The BEP1 Fic-domain: Unravelling the mechanism of narrow selectivity towards Rac GTPases .....	79
MS05-139 <b>LATE</b>   Structural Characterization of the Linear Ubiquitin Chain Assembly Complex .....	80
<b>MS06: PROTEINS-NUCLEIC-ACID INTERACTIONS .....</b>	<b>81</b>
MS06-01   Structural Studies of the Leading Strand DNA Polymerase in Eukaryotes .....	81
MS06-02   Structural Basis of Ribosomal RNA Synthesis in Bacteria .....	82
MS06-03   RNA Translocation Mechanism of Spliceosomal DEAH-box ATPases .....	83
MS06-04   Molecular Mechanisms of TREX1 in DNA Repair and Immune Silencing .....	84
MS06-05   Structural Alphabets for Conformational Analysis of Nucleic Acids .....	85
MS06-P01   Structural Insights In A Mitochondrial Nucleoid Maintenance Factor .....	86
MS06-P02   Structural basis for RNA translocation and NTP hydrolysis by the Zika virus NS3 helicase .....	87
MS06-P03   Structural Studies of Temperate Phage Genetic Switches .....	88
MS06-P04   Chromosome partitioning system, ParABS .....	89
MS06-P05   Molecular Basis Of Self-Induced Genomic Degradation Inhibition By The Sub-Nanomolar Interaction Of Nin With Nuca And Nucb Endonucleases .....	90
MS06-P06   Structure and function of S. aureus YabJ as a novel chlorination-induced ribonuclease .....	91
MS06-P07   Structural Study Two Different Forms Of Smap From Halobacterium Salinarum Which Have A Different Rna-Binding Ability .....	92
MS06-P08   Use Of The Cocomaps Web Server To Analyze And Visualize The Interface Of Biomolecular Complexes In Crystal Structures .....	93
<b>MS07: STRUCTURAL ENZYMOLOGY .....</b>	<b>94</b>
MS07-01   Taking Crystallographic Snapshots of Vitamin B6 Biosynthesis and Treating Specific Radiation Damage .....	94
MS07-02   Crystallographic Enzymology: Using Synchrotron Radiation for High Resolution in Space and Time .....	95
MS07-03   Watching an Enzyme at Work: Breaking the Strongest Single Bond in Organic Chemistry .....	96
MS07-04   The Neutron Structure of Leishmania Mexicana Triose Phosphate Isomerase with Transition State Mimics Reveals General Base Catalyst .....	97
MS07-05   Arabidopsis and Chlamydomonas Phosphoribulokinase Crystal Structures Complete the Redox Structural Proteome of the Calvin-Benson Cycle .....	98
MS07-P01   Crystal structure of the cell wall binding domain of a novel bacteriophage PBC5 endolysin and its peptidoglycan interaction .....	99
MS07-P02   Oncogenic KRAS G12C mutation derived inhibitor development .....	100
MS07-P03   Structural and functional characterization of Phosphoglucomutase 5 .....	101
MS07-P04   Regioselective Carboxylation by Prenylated Flavin and Mn-Dependent Decarboxylases .....	102
MS07-P05   Studying the structural basis for selectivity in complexes of peptide inhibitors and serine-proteases of the complement system .....	103
MS07-P06   Covalent bond between side chains of tryptophan and histidine in bilirubin oxidase is essential for substrate binding .....	104
MS07-P07   Beetle Luciferases and their Color Emission .....	105
MS07-P08   New structural insight into the well known peptide flip observed in flavodoxins .....	106

MS07-P09   Active site evolution in biomass degrading enzymes .....	107
MS07-P10   Interdomain Conformational Flexibility Of The Peptidoglycan N-Acetylglucosaminidases Of Staphylococcus Aureus .....	108
MS07-P11   Differences In Crystallization Of Several Selected Haloalkane Dehalogenases And Their Mutation Variants.....	109
MS07-P12   Enzymatic control of O <sub>2</sub> reactivity and functionalization of the flavin cofactor.....	110
MS07-P13   Enzyme Activation by a Flavoprotein Redox Network .....	111
MS07-P14   Competitive binding of potential drug molecules at the active site of an acylpeptide-hydrolase .....	112
MS07-P15   Structural insight in peptidyl substrate binding to cysteine cathepsins .....	113
MS07-P16   Structural and mutational investigation of psychrophilic adenylate kinase reveals the importance of hydrophobic packing in protein thermal stability.....	114
MS07-P17   Porphyromonas gingivalis Tpr protease zymogen resembles calpain-calpastatin complex. ....	115
MS07-P18   High-resolution dimeric crystal structures of wild-type and mutant Aspergillus niger glucose oxidase .....	116
MS07-P19   Neutron protein crystallography at the Heinz Maier-Leibnitz Zentrum (MLZ): New developments and recent application examples.....	117
MS07-P20   Selective Inhibition Of Astacin Metallopeptidases By Mammalian Fetuin-B .....	118
MS07-P21   Structure-Function Characterisation Of Novel Galactosidases From Lactobacillus Plantarum: Exploring The Link Between Gut Bacteria And Lipid Levels .....	119
MS07-P22   Structural Comparison Of Two Mammalian Multicopper Oxidases, Hephaestin And Ceruloplasmin .....	120
MS07-P119 <b>LATE</b>   Crystal Structure Of The Crenarchaeal Membrane Family-2 Glycosyltransferase Reveals A Minimal Cellulose-Synthase Framework.....	121

## **MS08: HOT STRUCTURES..... 122**

MS08-01   Capturing Reaction Intermediates Of The Water Oxidation Reaction In Photosystem II At X-Ray Free Electron Lasers .....	122
MS08-02   Structural Basis of Adamantane Resistance in the Influenza A M2 Proton Channel .....	123
MS08-03   Structural Analysis of Chloroplast Tail-Anchored Membrane Protein Recognition by ArsA1 .....	124
MS08-04   Structural Basis of A-Actinin-2/Titin Interaction in the Z-Disk.....	125
MS08-05   Structure Of A-Actinin-2/Fatz-1 Fuzzy Complex And Implications In Z-Disk Formation Via Phase Separation.....	126
MS08-P01   Regulation Of P97 Atpase Activity By Cofactor-Mediated Remodeling And Post-Translational Modification.....	127
MS08-P02   Structure Of The A-Actinin Actin-Binding Domain/F-Actin Complex.....	128
MS08-P03   Traf Is An Essential Factor Of The Pip501 Type Iv Secretion System (T4ss) And Exhibits Structural Homology With The T7ss Protein Essb Of Staphylococcus Aureus. ....	129
MS08-P04   Structural Basis Of Ascorbate-Dependent Iron Reduction By Human Dcytb Involved In Intestinal Iron Absorption.....	130
MS08-P05   Atomic Structure Of Potato Virus X, The Prototype Of The Alphaflexviridae Virus Family .....	131
MS08-P06   Crystal Structure Of UHRF1:LIG1 Complex Revealed Structural Change Of UHRF1 And The Key Residues For High Affinity Binding.....	132
MS08-P07   Crystal Structures Of Streptococcus Pyogenes Cas1 And Cas2 In The Type II-A CRISPR-Cas System.....	133
MS08-P09   Structural Study For Recognition Of Ubiquitylated Histone H3 By DNA Methyltransferase .....	135
MS08-P121 <b>LATE</b>   The ESCRT-III Protein Vps24 Forms Double Stranded Filaments Composed Of Domain-Swapped Dimers.....	136

## **MS09: LOW RESOLUTION SOFTWARE DEVELOPMENT..... 137**

MS09-01   Tools To Aid Macromolecular Refinement At Low Resolution .....	137
MS09-02   Mask-Based Approach to Restoring and Phasing Single-Particle Diffraction Data.....	138
MS09-03   Vagabond: Redefining the Model for Macromolecular Refinement.....	139
MS09-04   ARCIMBOLDO Towards Low Resolution: Recent Updates.....	140
MS09-05   Molecular Replacement Model Preparation and its Automation in MoRDa and MrBUMP .....	141
MS09-P01   Improving density histogram by phase optimisation using a genetic algorithm .....	142

## **MS10: VALIDATION, ERRORS AND NOISE IN MACROMOLECULAR CRYSTALLOGRAPHY..... 143**

MS10-01   Combatting MX Measurement Errors at Source .....	143
MS10-02   Errors in Electron Scattering and Validation of Experimental Maps through Combination of MicroED and CryoEM.....	144
MS10-03   Staraniso: Use Of A WebGL-Based 3-D Interactive Graphical Display To Represent And Visualise Data Quality Metrics For Anisotropic Macromolecular Diffraction Data .....	145

MS10-04   Assessment of Model Bias in Crystallographic Maps and its Implications for Validation of Crystal Structures.....	146
MS10-05   Stereochemical Restraints for Nucleic Acids Revisited .....	147
MS10-P01   A New 3D Reflection data viewer based on NGL.....	148
MS10-P02   Analysis and validation of B values of macromolecular structures.....	149
MS10-P03   Improving identification and validation of water molecules in protein crystal structures with molecular dynamics simulations.....	150
MS10-P04   Validation in the PDB .....	151
MS10-P05   B-factors reflect the local dynamics of proteins and nucleic acids.....	152
<b>MS11: BIG DATA (AT FACILITIES) AND CLOUD COMPUTING IN CRYSTALLOGRAPHY.....</b>	<b>153</b>
MS11-01   Recalculating all X-ray Structures in the PDB by PDB_REDO: Going Cloud .....	153
MS11-02   CCP4 Cloud for Distributed Crystallographic Computations.....	154
MS11-03   EXI, the EXTended ISPyB Interface .....	155
MS11-04   Keeping Things 'N Synch: Analysing the Content and Completeness of CIF Metadata in the CSD..	156
MS11-05   Machine Learning for Experimental Phasing in MX.....	157
MS11-P01   New ARP/wARP web service integrated into virtual computation frameworks.....	158
MS11-P02   Harnessing the data: Integrating data flows across home laboratories, facilities and data repositories in protein crystallography.....	159
MS11-P03   SIMBAD: Structure based search model identification for molecular replacement using the PDB database.....	160
MS11-P04   Combining the use of libraries from several distant homologs in ARCIMBOLDO_SHREDDER spheres.....	161
MS11-P05   PReSTO Integrative Structure Biology software for all platforms.....	162
<b>MS12: STRUCTURAL BIOINFORMATICS .....</b>	<b>163</b>
MS12-01   Exploring Cancer Heterogeneity: From DNA Mutability to Protein Dysfunction.....	163
MS12-02   Darkness in the Human Gene and Protein Function Space Despite Big Omics Data and Decline in Molecular Mechanism Discovery after 2000 .....	164
MS12-03   Phaser.Voyager: Data-Guided Model Generation and Visualization .....	165
MS12-04   Molecular Replacement Using Structure Predictions from new Generation Databases .....	166
MS12-05   ALEPH: A New Software for Structural Analysis and Generation of Fragment Libraries for Molecular Replacement.....	167
MS12-P01   Crystallization and structure determination of aldo-keto reductase 1C3 in complex with steroidal inhibitors using in situ proteolysis.....	168
MS12-P02   Enhancing small molecule information in the Protein Data Bank in Europe.....	169
MS12-P03   Symmetry in structures of protein assemblies.....	170
MS12-P04   How Disease-Associated Mutations May Alter the Dynamic Motion of the N-terminal Domain of the Human Cardiac Ryanodine Receptor .....	171
MS12-P05   PDBe Knowledge Base (PDBe-KB) – infrastructure for FAIR structural and functional annotations .....	172
MS12-P06   Building the protein structure-specific side-chain rotamer libraries .....	173
MS12-P07   New covariance-based methods for unconventional MR of transmembrane proteins.....	174
MS12-P09   Structural comparison and evolutionary relationships between ceruloplasmin, hephaestin and blood coagulation factor VIII .....	175
<b>MS13: BIOMINERALOGY AND BIOINSPIRED MATERIALS.....</b>	<b>176</b>
MS13-01   Bioinspired Calcium Phosphates: Structural Modifications Induced by Functionalization.....	176
MS13-02   Alteration of Human Bone Mineralization in a Sclerosing Osteosarcoma.....	177
MS13-03   New Complexes of Silver(I) with Azoles .....	178
MS13-04   Surface layer proteins of lactobacilli – Determining the cell wall binding and their antibacterial effect .....	179
MS13-05   Dealing with Modulated Macromolecular Structures With Translational Non-Crystallographic Symmetry.....	180
MS13-P01   Brachiopod shell calcite mineralization occurs by ion-by-ion transport controlled by the epithelial cell membranes.....	181
MS13-P02   The bone mineral is carbonato-hydro-apatite and it transforms into hydroxyapatite by heating (cremation) beyond 700°C .....	182
MS13-P03   Structure and microstructure study of charonia lampas lampas shell .....	183
MS13-P04   Small-Angle X-ray Scattering Studies on the Interaction of Bicelles With Bovine Serum Albumin ..	184
MS13-P05   The interaction between calcium carbonate and calcium phosphate as the driving mechanism for carbonate-hydroxyapatite formation.....	185

MS13-P123 - LATE | Halogenesis and biomineralization in the residual basins of the Aral Sea ..... 186

**MS14: MINERALOGICAL AND INORGANIC CRYSTALLOGRAPHY ..... 187**

MS14-01   Search for New Tellurium and Selenium Oxides with Potential Ferroelectric and Multiferroic Properties .....	187
MS14-02   New Data about Topology and Modularity of Heteropolyhedral Frameworks in Minerals and Inorganic Compounds.....	188
MS14-03   Kahlenbergite, a New Potassium $\beta$ -Alumina Mineral.....	189
MS14-04   Modularity in Minerals: the Example of Biopyriboles-Palysepioles .....	190
MS14-05   The Structure of the Lanthanum Oxonitridophosphate La <sub>2</sub> P <sub>4</sub> O <sub>16</sub> N <sub>2</sub> .....	191
MS14-P01   Reassessing Pauling's Rules .....	192
MS14-P02   First-principles investigation of structural, electronic and optical properties of CsPb (I <sub>1-x</sub> Br <sub>x</sub> ) <sub>3</sub> (x = 0.0 - 1.0) compounds .....	193
MS14-P03   Electron crystallography of planetary materials: impactites and micrometeorites .....	194
MS14-P04   The dependence of Yb concentration on lattice parameters of YAG single crystals .....	196
MS14-P05   Synthesis and crystal structures of Zr <sub>2</sub> (OH) <sub>2</sub> (XO <sub>4</sub> ) <sub>3</sub> ·4H <sub>2</sub> O (X=S,Se) and Zr(SeO <sub>3</sub> ) <sub>2</sub> .....	198
MS14-P06   Order-disorder in the arsenopalladinite, Pd <sub>8</sub> As <sub>2.5</sub> Sb <sub>0.5</sub> , crystal structure .....	199
MS14-P07   Steric effect in tetracoordinated Ni(II) complexes with enaminketone ligands and their reaction products with heterocyclic amines .....	200
MS14-P08   Comparative crystal chemistry of the solid solution systems between kieserite (MgSO <sub>4</sub> ·H <sub>2</sub> O) and transition metal kieserite-type compounds (M <sup>2+</sup> SO <sub>4</sub> ·H <sub>2</sub> O; M <sup>2+</sup> = (Mn,Fe,Co,Ni,Zn) .....	201
MS14-P09   Crystal Structure and Hirshfeld Surface Analyses of a new Organogold (III) with Thiosemicarbazone .....	202
MS14-P10 - CANCELLED   New approaches for Rietveld refinement in size-strain, grain size distribution and dislocation-recrystallization analysis .....	203
MS14-P11   Synthesis of Calcium and Strontium Rare-Earth Aluminates and its use as host lattice for LEDs ..	204
MS14-P12   Nickel(II) complexes with dithiocarbamate ligand: crystal structures and spectroscopic analysis ..	205
MS14-P13   Periodic trend of stereochemical activity of lone electron pairs .....	206
MS14-P14   Powder Diffraction experiments on a Single Crystal Diffraction instrument - How far can we push this? .....	207
MS14-P15   Crystal structure and thermodynamic behavior of Bi <sub>6</sub> Te <sub>2</sub> O <sub>15</sub> : the likely structure of the rare mineral pingguite .....	208
MS14-P16   Isotope effects in recovered high-pressure phases of ice. ....	209
MS14-P17   Preparation, Spectral, Structural, Hirshfeld surface and molecular docking of tetrakis(pyridine- $\kappa$ N)bis(thiocyanato- $\kappa$ N) cobalt(II) complex .....	210
MS14-P18   Crystal structures of the first polymeric Cu(II) complexes with thiosemicarbazone methyl pyruvate .....	211
MS14-P19   Synthesis, spectroscopic properties, crystal structure, antimicrobial properties and molecular docking studies of the complex (1) 3(C <sub>36</sub> H <sub>24</sub> MnN <sub>6</sub> ) 6(PF <sub>6</sub> ) 0.5H <sub>2</sub> O .....	212
MS14-P20   Modular structures of layered uranyl minerals and synthetic compounds .....	213
MS14-P21   Inverse crystal structure behaviour of Ca <sub>3</sub> Al <sub>4</sub> ZnO <sub>10</sub> at high pressure and high temperature.....	214
MS14-P22   Synthesis and crystal structure of new alkali chalcogenido manganates/indates.....	215
MS14-P23   Structural ordering in the pyrite-related phases: PtSnS, PtSnSe and PtSnTe .....	216
MS14-P24   Pseudo-symmetry and order-disorder transitions in metal hydrides.....	217
MS14-P25   A new polymorph of trisodium hexachlororhodate .....	218
MS14-P26   Rare-earth pnictide chalcogenides REBiTe and RESbS (RE = La-Nd): structure determination by combination of transmission electron microscopy and microfocussed synchrotron radiation .....	219
MS14-P27   Doped single crystal TiO <sub>2</sub> series products by molten salt method used as photocatalytic materials .....	220
MS14-P28   New cubic borate Yb <sub>3</sub> [BO <sub>3</sub> ](OH) <sub>6</sub> ·2.1H <sub>2</sub> O with “antizeolite” framework and isolated BO <sub>3</sub> -triangles in cavities .....	221
MS14-P29   Evidence of anatase intergrowths formed during slow cooling of reduced ilmenite.....	222
MS14-P30   Insight into the crystallization and structural features of caesium-bearing chain-type borophosphates .....	223
MS14-P31   Crystal chemistry of struvite and its derivatives.....	224
MS14-P32   Layer Charge Influence on the Hydration Properties of Synthetic Na-Saturated Smectites .....	225
MS14-P33   Crystal structure and biological activities of a new proton transfer material .....	226
MS14-P34   Hexagonal Bariumtitanate stabilized as ultra-thin film on Pt(111): An X-ray diffraction and electron-energy-loss spectroscopy study.....	227
MS14-P35   The crystal structures of natural baryum beryllophosphates .....	228
MS14-P36   The crystal structure of koninckite.....	229

MS14-P37   Crystal structure of CaBaFe <sub>4</sub> O <sub>7</sub> .....	230
MS14-P38   Preparation, Spectral, Structural, Thermal and anticancer molecular docking studies of bis-(theophyllinato)-tetraaquocobalt(II) complex.....	231
MS14-P39   Stereochemistry of Tl(I) in inorganic oxysalts.....	232
MS14-P40   Calcium oxalate crystallization for a non-conventional CO <sub>2</sub> storage method.....	233
MS14-P41   Crystal structures of transition-metal halide complexes with cyanopyridine ligands: single chains, double chains, and networks.....	234
MS14-P125 - LATE   An occurrence of the acentric distortion due to Ag <sup>+</sup> /Bi <sup>3+</sup> ordering in the AgBi <sub>2</sub> B <sub>5</sub> O <sub>11</sub> borate.....	235
MS14-P127 - LATE   Does the iota-alumina phase exist?.....	236
MS14-P129 - LATE   Multi-scale characterisation of the cationic disorder in the novel borate Sr <sub>6</sub> Tb <sub>0.94</sub> Fe <sub>1.06</sub> (BO <sub>3</sub> ) <sub>6</sub> .....	237

## MS15: MINERALS AND MATERIALS UNDER EXTREME CONDITIONS ..... 238

MS15-01   Reactivity of Heavy Noble Gases Under High Pressures.....	238
MS15-02   High-Pressure Synthesis and Properties of Iron Oxides.....	239
MS15-03   The True Structural Relationship between Zircon and Scheelite Structure Types, and a New Polymorph of Zircon.....	240
MS15-04   Structural Behavior of the sII Clathrasil Chibaite at Low Temperatures and High Pressures.....	241
MS15-05   Crystallisation Studies of Biodiesel and Methyl Stearate at Extreme Conditions.....	242
MS15-P01   Reducing the background of ultra-low temperature X-ray diffraction data.....	243
MS15-P02   Xpress: latest results from the new dedicated high pressure diffraction beamline at Elettra.....	244
MS15-P03   Pressure-induced spin transitions in garnets.....	245
MS15-P04   Experimental Charge Density Distribution in Grossular Under High Pressure - a Feasibility Study.....	246
MS15-P05   Ab initio simulation and X-ray diffraction measurements of deviatoric stress in mineral inclusions.....	247
MS15-P06   Structure, crystal chemistry, and compressibility of iron-rich silicate perovskite at pressures up to 95 GPa.....	248
MS15-P07   Toward one-pot green synthesis of nanoporous carbon nitrides.....	249
MS15-P08   The microscopic origin of axial negative thermal expansion and negative linear compressibility in alpha- and beta-PbAlBO <sub>4</sub> .....	250
MS15-P09   New insights on the high pressure behaviour of the GeSe <sub>x</sub> Te <sub>1-x</sub> solid solution.....	251
MS15-P10   Squeezing the Most Data out of Your High-Pressure Experiment.....	252
MS15-P11   Synthesis, crystal structures and thermal expansion of novel lutetium-barium borates.....	253
MS15-P12   Antiferroelectric Pnma phase: The Missing Element to understand Morphotropic Phase Boundary lead-free Na <sub>1/2</sub> Bi <sub>1/2</sub> TiO <sub>3</sub> based piezoceramics.....	254
MS15-P13   High pressure x-ray imaging and diffraction on the Psiché beamline: Recent results and developments using large volume presses.....	255
MS15-P14   The influence of [2+2] photodimerization and high pressure on the structural transformations in crystals.....	256
MS15-P15   In-situ single crystal X-ray diffraction studies of proton transfer behaviour under an applied electric field on I19, Diamond Light Source.....	257
MS15-P16   Oxides under extreme conditions: pushing the limits of neutron diffraction.....	258
MS15-P131 - LATE   Thermal expansion of alluaudite group minerals (nickenichite and calciojohillerite).....	259
MS15-P133 - LATE   Thermal Expansion of Alkaline-Earth Borates.....	260

## MS16: STRUCTURAL CHARACTERIZATION OF FUNCTIONAL MATERIALS ..... 261

MS16-01   Polymorphism in Sesquioxides of Late Group-15: Work under Pressure.....	261
MS16-02   In Situ Methods for the Analysis of Functional Materials.....	262
MS16-03   Impact of Intense Electric Fields on the Structure of Centrosymmetric Relaxor Ferroelectric Sr <sub>0.85</sub> Pr <sub>0.15</sub> TiO <sub>3</sub> .....	263
MS16-04   Structural Control of thermomechanical Properties of Monoclinic Rare-Earth Calcium Oxoborates.....	264
MS16-05   MEAD, Salt, and Sunshine: Cation Distribution in CZTSe, CFTS, and CZSiSe.....	265
MS16-P01   Short-range structure of Zr and Pd bulk metallic glasses prepared during the melting and cooling process.....	266
MS16-P02   Pure gyrotropic ferroelastic phase transitions in the materials PbMXO <sub>4</sub> (M = Ba, Sr; X=Si,Ge): a new piezoelectric family.....	267
MS16-P03   Structure design of novel Ba <sub>3-x</sub> Sr <sub>x</sub> TeO <sup>6</sup> double perovskites and the effect of temperature and composition on structure stability.....	268
MS16-P04   Perovskite BaTiO <sub>3</sub> doped with pyrochlore Bismuth Zinc Niobate - a new perovskite relaxor ferroelectric BZN-BT.....	269
MS16-P05   Environmental effect on titanium alloy Ti6242S in air between 500 and 700 °C.....	270

MS16-P06   Forbidden/Non-Forbidden Bragg Reflections Study Under Phase Transitions And External Influences.....	271
MS16-P07   Crystal structure and dehydration behavior of Ag <sup>+</sup> -exchanged levyne .....	272
MS16-P08   Lattice Constants Prediction And Thermochemistry Of Hexahalometallate A <sub>2</sub> mx <sub>6</sub> .....	273
MS16-P09   Investegation of physical proprieties of equiatomic silver-rare earth compounds Ag-Re (Re=Nd, Ce ,Gd) from first Principles Calculations. ....	274
MS16-P10   LiTaO <sub>3</sub> defect structures by means of forbidden reflections .....	275
MS16-P11   Moringa oleifera waste as dopants for S, N, C-TiO <sub>2</sub> photocatalysts development .....	276
MS16-P12   Morphological analysis of the migration-induced field-stabilized polar phase in SrTiO <sub>3</sub> with Scanning X-ray Diffraction Microscopy .....	277
MS16-P13   How different do diffraction patterns of the same substance have to be to indicate polymorphism? .....	278
MS16-P135 - LATE   Synthesis and structural characterization of new salts containing 2-amino-3-methylpyridinium cations.....	279
MS16-P137 - LATE   Nanostructured flexible MOFs and related composite materials .....	280

## MS17: PRESSURE AND MECHANICAL STRESS INDUCED PHASE TRANSITION AND... ..... 281

MS17-01   Dynamic Compression of Materials at Pressures of Earth's Interior Using the dDAC .....	281
MS17-02   High-Pressure Polymorphs of Organic Compounds with Interactions Involving Nitrogen Atoms .....	282
MS17-03   Crystal Structure Compression and Pressure-Induced Polymerization of Arene-Perfluoroarene Co-Crystals Leading to Columnar Hydrofluorocarbons.....	283
MS17-04   Pressure Induced Phase Transition in CoSO <sub>4</sub> ·H <sub>2</sub> O .....	284
MS17-05   Pressure-Induced Polymerization and Electrical Conductivity of a Polyiodide.....	285
MS17-P01   Symmetry lowering in natrochalcite NaCu <sub>2</sub> (H <sub>3</sub> O <sub>2</sub> )(SO <sub>4</sub> ) <sub>2</sub> under pressure.....	286
MS17-P02   Structure–magnetic property correlations in metal–formate frameworks at high pressure.....	287
MS17-P03   Pressure-induced modification of molecular aggregation in crystals of benzocaine.....	288
MS17-P04   Effect of pressure on slit channels in hydrate of sodium salt of guanine: a link to nucleobase intermolecular interactions .....	289
MS17-P05   Ex-situ study of the pressure induced decomposition of iron nitride Fe <sub>4</sub> N .....	290
MS17-P06   Phase transformations of (RS)-2-Chloromandelic acid in the solid state: From racemic compound to conglomerate under mechanical force .....	291
MS17-P07   Phase transitions of Copper(I) Iodide compounds under High Pressure.....	292

## MS18: MATERIALS FOR ENERGY STORAGE AND CONVERSION ..... 293

MS18-01   Electrochemical Energy Storage beyond Lithium .....	293
MS18-02   Order-Disorder Transitions in Battery Electrodes Studied by Operando X-ray Scattering.....	294
MS18-03   Defects, Disorder and Electrochemistry in Phosphate-Based Metal-Ion Battery Cathodes.....	295
MS18-04   Crystal Growth and Structural and Electrochemical Properties of Garnet-type Lithium Ion Conducting Oxides.....	296
MS18-05   Structural Insights into Methanation Catalysts from MOF-Precursors via PDF.....	297
MS18-06   Increase your Energy with XRD.....	298
MS18-P01   Prussian Blue analogues as cathode material in low cost aqueous batteries .....	299
MS18-P02   Tailored exsolution of metal nanoparticles: Structural and chemical characterisation of doped Perovskites by XPS and XRD .....	300
MS18-P03   Phase Evolution During Perovskite Formation - Insight from PDF Analysis.....	301
MS18-P04   Ab-initio study of oxygen adsorption on PdZn(111) surface.....	302
MS18-P05   Combination of EXAFS and XRD for studies of the orthorhombic-tetragonal phase transformation in MAPb <sub>1-3x</sub> Cl <sub>x</sub> perovskites .....	303
MS18-P06   Synthesis and Crystal characterization of a new layered acidic diphosphate metallate .....	304
MS18-P07   First-principles study of oxygen adsorption structure on Ni <sub>3</sub> Al(210) surface .....	305
MS18-P08   Structure and Thermoelectric Characterization of Lithium-substituted Bismuth Palladium Oxide ...	306
MS18-P09   Determination of host and dopant ion distribution in Mg <sub>2</sub> Si <sub>1-x</sub> Sn <sub>x</sub> thermoelectric materials by electron channeling.....	307
MS18-P10   Structural modification of Perovskites by tailored Exsolution for enhanced Catalytic Activity .....	308
MS18-P11   Band Gap Depth Profile of Cu(In <sub>1-x</sub> Ga <sub>x</sub> )Se <sub>2</sub> Absorbing Layer in Thin-Film Solar Cell by Glancing Incidence X-Ray Diffraction.....	309
MS18-P12   In-situ carbonation of SrO at 298 K and controlled humidity for Thermochemical Energy Storage .	310
MS18-P13   Local structure of glass-ceramic sodium sulfidic solid state electrolytes .....	311
MS18-P14   New method for electromechanical losses evaluation of the electrostrictive energy efficiency: experiments and modeling.....	312
MS18-P15   Thermochromic Lead-Free Halide Double Perovskites .....	313

MS18-P16   Influence of Fe doping on the crystal structure, electronic structure and supercapacitance performance of birnessite with high areal mass loading .....	314
MS18-P17   The influences of Mg intercalation on the structure and supercapacitive behaviours of MoS <sub>2</sub> .....	315
MS18-P18   The surface phase diagram of La <sub>0.8</sub> Sr <sub>0.2</sub> MnO <sub>3</sub> in STM .....	316
MS18-P19   Combination Of Data Mining And Dft Modeling Of Ag <sup>+</sup> -Conductivity In S(Se)-Containing Inorganic Compounds.....	318
<b>MS19: QUANTUM MATERIALS .....</b>	<b>320</b>
MS19-01   Orbital Molecules in Oxides .....	320
MS19-02   Torque Magnetometry, a Tool for Magnetic Crystallography in Thin Films of Frustrated Magnets....	321
MS19-03   Crystal Growth Investigations of Lithium Iridate, Li <sub>2</sub> IrO <sub>3</sub> , and Lithium Ruthenates, Li <sub>2</sub> RuO <sub>3</sub> and Li <sub>3</sub> RuO <sub>4</sub> .....	322
MS19-04   Crystal Structure and Isotope Effect in Quantum Liquid H <sub>3</sub> LiIr <sub>2</sub> O <sub>6</sub> .....	323
MS19-05   Structure and Magnetic Phases in the Cs <sub>2</sub> CuCl <sub>4-x</sub> Br <sub>x</sub> Mixed System.....	324
MS19-P01   High-pressure synthesis, crystal structure, and magnetic properties of Ba <sub>3</sub> CuOs <sub>2</sub> O <sub>9</sub> .....	325
MS19-P02   Self-assembly of octanuclear complexes containing tetra- and pentacoordinate Co(II) centers .....	326
MS19-P03   Magnetism in Double Perovskites Ba <sub>2</sub> CrMoO <sub>6</sub> .....	327
<b>MS20: COMBINED APPROACHES FOR STRUCTURE CHARACTERIZATION OF COMPLEX.....</b>	<b>328</b>
MS20-01   Combined Analysis of Structure and Strain in Engineering Materials by Neutron and Synchrotron X-Ray Diffraction, and Electron Microscopy .....	328
MS20-02   X-Ray Characterization of Morphology and Structure of Materials at Multiple Length Scales .....	329
MS20-03   Characterization of Aperiodic Bi-based Layered Oxides Thin Films by TEM Multiscale Approaches	330
MS20-04   Orientational Disorder in Monomethyl-Quinacridone Investigated by Rietveld Refinement, Pair-Distribution Function Analysis and Lattice-Energy Minimisations .....	331
MS20-05   Small-angle Scattering Study for Developing Alkaline Durable Imidazolium-Based Grafted Anion Exchange Membranes for Pt-Free Fuel Cells .....	332
MS20-P01   Discovery of complex metal oxide materials by rapid phase identification and structure determination .....	333
MS20-P02   Synthesis and structure determination of SCM-15: a 3D large pore zeolite with interconnected straight 12×12×10-ring channels.....	334
MS20-P03   Raman and Surface Analysis Studies of (CuGaSe <sub>2</sub> ) <sub>0.8</sub> (CuAlSe <sub>2</sub> ) <sub>0.2</sub> Single Crystals .....	335
MS20-P04   Universal algorithm for prediction of new cleavage planes in single crystals .....	336
MS20-P05   Powder XRD structure determination of nanostructured, disordered MoS <sub>2</sub> -ethylenediamonium layered compound and molecular modeling of its deprotonation reactions.....	337
MS20-P100 - <b>LATE</b>   Effect of the side-chain on the topology of coordination polymers of copper(II) with amino acids .....	338
<b>MS21: MODERN QUANTUM CRYSTALLOGRAPHY.....</b>	<b>339</b>
MS21-01   Possible Quantum Crystallography Solutions for N-Representable One-Electron Reduced Density Matrices Reconstruction .....	339
MS21-02   Electron Configuration and Electronegativity of the Atoms Under Compression .....	340
MS21-03   Interactions between Stereo Chemically Active Lone Pairs in MnSb <sub>2</sub> O <sub>4</sub> .....	341
MS21-04   Quantum Crystallography for Macromolecules: the HAR-ELMO Method .....	342
MS21-05   Spin-Resolved Atomic Orbital Model Refinement for Combined Charge and Spin Density Analysis: Application to the Perovskite.....	343
MS21-P01   Structural investigations on bridging stibinidene complexes with Cu-Kβ-radiation: A comparison ..	344
MS21-P02   Electron densities of molecular crystals from powder X-ray diffraction .....	345
MS21-P03   Accurate Experimental Charge Density Data: Tips & Tricks for Data Collection & Processing .....	346
MS21-P102 - <b>LATE</b>   Non-Spherical Form Factors and Crystallographic Refinement .....	347
<b>MS22: STRUCTURE-PROPERTY RELATIONSHIPS VIA CHARGE DENSITY METHODS .....</b>	<b>348</b>
MS22-01   'Pancake' Bonding - A Charge Density Perspective .....	348
MS22-02   Elucidating the Mechanisms of Single Molecule Magnets using Diffraction Methods.....	349
MS22-03   Electron Densities of two Nonapeptides from Invariom Application.....	350
MS22-04   The Role of Electrostatic Interactions in IFIT Proteins Complexed with RNA with Different 5' End Predicted by the UBDB+EPMM Method .....	351
MS22-05   Using Crystal Structure, an Improved Electrochemical Method and Computational DFT Studies to Understand the Medicinal Properties of Celastraceae Species of Plants .....	352
MS22-P01   3D -Visualization and -Printing of Molecular Surfaces .....	353
MS22-P02   Evaluation of covalent bond density in molecular crystals using simplified virtual scattering centers .....	354

MS22-P03   Phase transitional behavior and charge density study of drug methimazole.....	355
MS22-P04   Assembly, crystal structures and (non)linear optical properties of multicomponent materials containing sulfonamides .....	356
MS22-P05   Charge density analysis of a series of 4-methylthiostilbene derivatives.....	357
MS22-P06   Insights into the Origin of Magnetic Anisotropy in Linear Iron Complexes from the Experimental Electron Density.....	358
MS22-P07   Quinoid dianion forming a lone-pair pi-hole contact .....	359
MS22-P08   Understanding of chromic phenomena: the examples of violuric acid - amino acid based salts and co-crystals.....	360
MS22-P09   Polymorphism and the Role of F...F Interactions in Crystal Packing of Fluorinated Tosylates .....	361

## MS23: APERIODIC AND MODULATED STRUCTURES ..... 362

MS23-01   Chemical vs Conformational Entropies at the Incommensurate and Lock-In Phase Transitions of Morpholinium Tetrafluoroborate.....	362
MS23-02   Evidencing of Charge Density Wave instabilities in even members of the Monophosphate Tungsten Bronzes Family .....	363
MS23-03   Multidimensional Aperiodic Structures from BGU.....	364
MS23-04   The 1D Modulated Structure of the Mixed-Valent Chain Sulfido Ferrate $K_{7.09}[FeS_2]_4$ .....	365
MS23-05   New Tools in Jana2006/Jana2020 to Study and Characterization of Pi-Pi Stacking of Incommensurate Modulated Structures: $\alpha$ & $\beta$ -Mn(dmp)Cl <sub>2</sub> .....	366
MS23-P01   Correction for phonons, phasons and multiple scattering in quasicrystals .....	367
MS23-P02   The real space refinement of the icosahedral quasicrystal .....	368
MS23-P03   From a single slit to periodic, modulated and quasiperiodic crystals – a new approach to the diffraction analysis of aperiodic systems.....	369
MS23-P04   Will PdPb confirm the prediction that its structure is modulated?.....	370
MS23-P05   Crystal Structure of Incommensurately Modulated $\beta$ -NaBrF <sub>4</sub> .....	371
MS23-P06   On the Puzzling Case of Sodium Saccharinate 1.875-Hydrate: Structure Description in (3+1)-Dimensional Superspace .....	372
MS23-P07   Modulated structure in Ni <sub>2</sub> MnGa <sub>0.95</sub> In <sub>0.05</sub> shape-memory alloy.....	373
MS23-P08   Novel approach to structure determination of complex protein system Hyp-1/ANS .....	374
MS23-P09   Incommensurately modulated structures in the series RETe <sub>2-δ</sub> .....	375

## MS24: MAGNETIC ORDER: METHODS AND PROPERTIES..... 376

MS24-01   A Symmetry Motivated Approach for Enumerating Magnetoelectric Couplings in Perovskites .....	376
MS24-02   Spiral Spin-Liquid, Multi-Step Order and the Emergence of a Vortex-Like State in MnSc <sub>2</sub> S <sub>4</sub> .....	377
MS24-03   High Symmetry Dictates a Vortex Magnetic Structure for the Mysterious Hidden Order in URu <sub>2</sub> Si <sub>2</sub> .....	378
MS24-04   Magnetic Inversion Symmetry Breaking and Spin Reorientation in Tb <sub>2</sub> MnNiO <sub>6</sub> : A Polar Strong Ferromagnet .....	379
MS24-05   Superspace Magnetic Structure and Topological Charges in Weyl Semimetal CeAlGe.....	380
MS24-P01   Structural disorder and magnetic correlations driven by oxygen doping in Nd <sub>2</sub> NiO <sub>4.11</sub> .....	381
MS24-P02   Oxygen order correlation to the incommensurately modulated magnetic stripes and their interaction in 214-type Pr <sub>2-x</sub> Sr <sub>x</sub> NiO <sub>4+δ</sub> .....	382
MS24-P03   Revisiting the magnetic structure of R <sub>1/3</sub> Sr <sub>2/3</sub> FeO <sub>3</sub> (R = La, Pr, Nd) by neutron powder and single crystal diffraction combined with spherical polarimetry .....	383
MS24-P04   MagStReX: Magnetic Structures through Resonant X-Ray Scattering.....	384
MS24-P05   Understanding and tuning magnetism of mesoscopic hollow oxide sphere by surface engineering .....	385
MS24-P06   Probing The Magnetic Ground-States Of Rare-Earth Compounds By Single Crystal Neutron Diffraction.....	386
MS24-P104 - LATE   Magnetic textures in non-magnetic systems .....	387

## MS25: ELECTRON CRYSTALLOGRAPHY AS A TOOL FOR STRUCTURE SOLUTION AND REFINEMENT ..... 388

MS25-01   Structure Determination of Nano-Precipitates in Metallic Alloys using Electron Crystallography Methods.....	388
MS25-02   Electron Crystallography is a Powerful and Feasible Extension to every X-Ray Facility .....	389
MS25-03   How Can We Directly See the Molecule Array in 3D Protein Crystal under TEM? .....	390
MS25-04   Serial Protein Crystallography in a S/TEM .....	391
MS25-05   Using ARCIMBOLDO's Fragment-Based MR for Solving microED Data from Macromolecular Structures.....	392
MS25-P01   Electron Crystallography for Studying MOF-Intercalated Guests .....	393

MS25-P02   Data processing of 3D precession electron diffraction data .....	394
MS25-P03   Automated electron diffraction: 3D structure determination with sub-ångström resolution .....	395
MS25-P04   Dedicated electron source for serial electron crystallography .....	396
MS25-P05   Continuous rotational electron diffraction method for structure determination of small organic molecules.....	397
MS25-P06   Low Dose Electron Diffraction Tomography (LD-EDT) solves the structure of a new (Na <sub>2/3</sub> Mn <sub>1/3</sub> ) <sub>2</sub> Mn <sub>3</sub> Ge <sub>3</sub> O <sub>12</sub> phase synthesized at high pressure and high temperature .....	398
MS25-P07   Dynamical structure refinement from data obtained with a dose of less than 1 E-/Å <sup>2</sup> .....	399
MS25-P08   Refinement of organic crystal structure with multipolar electron scattering factors .....	400
MS25-P09   Structure of a novel R2-like ligand-binding oxidase revealed by electron diffraction.....	401
MS25-P10   MicroED, Fast and Furious.....	402
MS25-P106 <b>LATE</b>   Exploration of Bragg in-line electron holography as a possible tool for crystal structure determination .....	403
MS25-P108 <b>LATE</b>   On the Design of a Dedicated Electron Diffractometer.....	404
<b>MS26: COMPLEX METALLIC ALLOYS: PERIODIC AND NON PERIODIC.....</b>	<b>405</b>
MS26-01   Some Recent Advances in the Surface Science of Complex Metallic Alloys.....	405
MS26-02   The Power of Analogy in Physics: From Faraday Waves through Soft Matter to Complex Metallic Alloys .....	406
MS26-03   Nucleation and Growth of Tenfold Twins of NiZr during Non-Equilibrium Solidification.....	407
MS26-04   Theoretical Study of Single-Element Quasi-Periodic Thin Films Formed on Ag-In-Yb Quasicrystal.....	408
MS26-05   Three Dimensional Local Atomic Configurations of Decagonal AlNiCo Quasicrystal Studied by X-Ray Fluorescence Holography .....	409
MS26-P01   Peculiarities Of Solid Solutions With NatI-Type Structure In Li-Zn-X (X=Al,Ga,In) Systems .....	410
MS26-P02   Chemical bonding and structural complexity in known intermetallic compounds o-Al <sub>13</sub> Co <sub>4</sub> and Al <sub>2.75</sub> Ir <sub>2</sub> .....	411
MS26-P03   New Ca/Mg/Zn intermetallics of one intergrowth family. ....	412
<b>MS27: STRUCTURAL DYNAMICS, DISORDER AND PHYSICAL PROPERTIES .....</b>	<b>413</b>
MS27-01   Combining Diffuse and Inelastic Scattering in the Exploration of Phase Transitions .....	413
MS27-02   Recent Developments in the Use of Single Crystal Diffuse Scattering to Study Materials Properties .....	414
MS27-03   Understanding Two-Dimensional Polymerisation Using Bragg and Diffuse X-Ray Scattering .....	415
MS27-04   Sub-Mesoscale Oxygen Ordering in Non-Stoichiometric Oxygen Ion Conductor Pr <sub>2</sub> NiO <sub>4+δ</sub> .....	416
MS27-05   Phase Transitions in Zr-Rich Lead Zirconate-Titanate Studied by Single Crystal Diffuse and Inelastic X-Ray Scattering.....	417
MS27-P01   Structural and physical properties of a 2,2',6',2"-terpyridine derivative in the solid state phase transition behavior.....	418
MS27-P02   New radiation-induced phase of MAPbI <sub>3</sub> - an unexpected surprise of synchrotron experiments. ....	419
MS27-P03   Local order in Co and Mn Prussian Blue analogues, the 3D-ΔPDF analysis. ....	420
MS27-P04   Endohedral Metallofullerene Crystals: Playing with Disorders .....	421
MS27-P05   Correlation of high-resolution X-ray diffraction with mechanical experiments and finite element analysis.....	422
MS27-P06   The Benefits of Cu-K <sub>β</sub> Radiation in Elucidating the Molecular Structure of Polypnictogen Cations.....	423
MS27-P07   Unique properties of geoinspired nanotubes as water nanocontainer.....	424
MS27-P110 - <b>LATE</b>   Towards phase transition in cocrystals of allylamine with aliphatic alcohols .....	425
<b>MS28: DYNAMICS AND DISORDER PROBED BY DIFFUSE SCATTERING .....</b>	<b>426</b>
MS28-01   Challenges in Measurement and Interpretation of Scattering from Protein Crystals.....	426
MS28-02   Beyond the Average Bragg Structure - Dynamics, Disorder and Diffuse Scattering.....	427
MS28-03   A Disordered Superspace Approach to Understand Highly Structured Diffuse Scattering .....	428
MS28-04   The Secret Life of MOFs' Functional Groups: Should we Trust Random Disorder? .....	429
MS28-05   Unraveling Local Correlations in Heavily Disordered Ferroelectric Sr <sub>x</sub> Ba <sub>1-x</sub> Nb <sub>2</sub> O <sub>6</sub> .....	430
MS28-P01   Solving the disordered structure of beta-Cu <sub>2</sub> Se using the three-dimensional difference pair distribution function .....	431
MS28-P02   Local Dipole Formation in IV-VI Semiconductors .....	432
MS28-P03 - <b>CANCELLED</b>   Understanding structural disorder in nickel cyanide using 1D statistical mechanical models .....	433
<b>MS29: ACCURATE TREATMENT OF HYDROGEN ATOMS .....</b>	<b>434</b>
MS29-01   Modelling of Hydrogen Atoms in Crystallography – An Overview.....	434
MS29-02   Influence of a Hydrogen Bond on Optical Properties of Materials .....	435

MS29-03   Structure Specific Restraints for Least-Squares Refinement from Tight Binding Quantum Chemistry .....	436
MS29-04   Hydrogen Positions in Small Organic Molecules Determined by 3D Electron Diffraction .....	437
MS29-05   Anisotropic Hydrogen Atoms in Charge Density Analysis .....	438
MS29-P01   KOALA - routine H-atom determinations by Laue neutron diffraction.....	439
MS29-P02   On precision and accuracy of X-ray and neutron diffraction results for single crystals of glycine....	440
MS29-P03   Comparison of Different Strategies for Modelling Hydrogen Atoms in Charge-Density Analyses ...	441
MS29-P04   TAAM: A reliable and user friendly tool for hydrogen atom location using X-Ray diffraction data ...	442
MS29-P05   Comparison of X-ray Wavefunction Refinement and Multipole Refinement Based on the Energetic Analysis of the Crystal Structures of 2-Hydroxo-8-X-Quinoline Derivatives (X = Cl, Br, I, S-Ph) .....	443
<b>MS30: CHIRALITY AND POLARITY IN CRYSTALS.....</b>	<b>444</b>
MS30-01   Solid-State Chiral Resolution via Metal Complexation.....	444
MS30-02   Electron Crystallography for Determining the Handedness of Chiral Crystals.....	445
MS30-03   Absolute Configuration of Pharmaceutical Molecules Determined from a Nanocrystal by Electron Diffraction.....	446
MS30-04   Optical Resolution of 2- and 4-Chloromandelic Acids with Cyclohexylethylamine Resolving Agent-Crystal Structures of the Diastereomers and the Double Salt.....	447
MS30-05   Highly Versatile Metal-Organic Frameworks.....	448
MS30-P01   Features of crystal formation of chiral derivatives of 1,5-dihydro-2h-pyrrole-2-one.....	449
MS30-P02   Absolute structure assignment through interplay of X-ray diffraction and EBSD.....	450
MS30-P03   Crystallization-Induced Stereoisomeric Recognition and Stereochemical Transformations of Chiral Organic Molecules: Role of Supramolecular Synthons .....	451
MS30-P04   Unexpected Polymorphic Behavior Of Four Racemic 3-Pyrrolin-2-One Derivatives .....	452
MS30-P05   Separation and resolution of methylcyclohexanones by enclathration with deoxycholic acid .....	453
MS30-P06   Peculiarities of supramolecular organization in centric, acentric and chiral ketones with vinylacetylene fragments.....	454
MS30-P112 - <b>LATE</b>   Structural similarities of 2D and 3D water frameworks in 3,3dimethyl-2-butylamine, tert-amylamine and azepane hydrates .....	455
<b>MS31: RESPONSIVE MATERIALS &amp; STRUCTURAL DYNAMICS IN CRYSTAL.....</b>	<b>456</b>
MS31-01   Mechanical Properties of Molecular Crystals: The Bigger Picture .....	456
MS31-02   Dynamic MOFs with Breathing-Dependent Redox Behavior .....	457
MS31-03   Energy Studies of Single Crystal to Single Crystal Transformations in Cyclic Peptoids .....	458
MS31-04   Insights from High-Pressure Crystallography and X-Ray Charge Density Analysis into Mechanical Flexibility of Metal-Organic Complex Crystals.....	459
MS31-05   Single-Crystal to Single-Crystal Transformations in Spin-Crossover Compounds. An Incredible Zoology!.....	460
MS31-P01   Structural analysis and IR-spectroscopy of a new anilinium hydrogenselenite hybrid compound: A subtle structural phase transition .....	461
MS31-P02   Triethylphosphine as a molecular gear — phase transitions in ferrocenyl-acetylide-gold(I) .....	462
MS31-P03   Photocrystallographic investigations of new nickel(II) nitro complexes .....	463
MS31-P04   Probing Spin Crossover In Novel Metal Organic Complexes .....	464
MS31-P05   Structural and computational studies of a series of new photoswitchable nickel nitro complexes..	465
MS31-P06   Pressure-induced polymerization and electrical conductivity of a polyiodide .....	466
MS31-P07   Breathing Metal-Organic Frameworks Based On Flexible Inorganic Building Units .....	467
MS31-P08   Conformational switching in single crystals of a calix[4]resorcinarene .....	468
MS31-P09   Wavelength-selective photoisomerisation of NO and NO <sub>2</sub> ligands.....	469
MS31-P10   Photoinitiated [2+2] cycloaddition reactions observed in d-metal(II) malonates with N,N'-containing linkers .....	470
MS31-P11   Molecular switches in nanocontainers.....	471
MS31-P12   Dynamic, Breathing, Water-stable, Mixed-Ligand Zn(II) Metal-organic Frameworks with differing water and vapour sorption properties.....	472
MS31-P13   Exceptionally flexible coordination polymers of Cd(II).....	473
MS31-P14   Thermo- / Mechano- Mechanically Responsive Cocrystals during Single-Crystal-to-Single-Crystal phase transitions.....	474
MS31-P15   Separation of Isomers by Host-Guest Chemistry: polymorphism, resolutions and templating. ....	475
MS31-P16   Structure / Reactivity Relationships from Detailed Reaction Mechanisms .....	476
<b>MS32: NEW INSIGHTS INTO NON-COVALENT BONDINGS &amp; TETREL, PNICTOGEN, CHALCOGEN.....</b>	<b>477</b>

MS32-01   Chalcogen Bonding in Crystal Engineering .....	477
MS32-02   Interactions Involving 13-17 Groups' Elements Acting as the Lewis Acid Centres – Comparison with the Hydrogen Bond .....	478
MS32-03   Can MEP Values Be Used to Predict the Supramolecular Connectivity in the Crystal Structure?.....	479
MS32-04   Phosphorus Can Do More: p-p Stacking of Planar Aromatic P5-rings.....	480
MS32-05   Supramolecular Synthons Orientation Rule in the Crystals of Benzodiazepines, Quinoxalines and Benzimidazoles as a Predictive Tool in the Material Design .....	481
MS32-P01   In situ PXRD monitoring the mechanosynthesis of metal-organic halogen-bonded cocrystals .....	482
MS32-P02   Efficient recognition of steroids by planar aromatic molecules: A novel biomolecular recognition motif and its potential applications .....	483
MS32-P03   Influence of the basicity of halogen bond acceptors on stoichiometry of cocrystals with 1,3,5-triiodo-2,4,6-trifluorobenzene .....	484
MS32-P04   Towards the Linear [S2X]+ Systems: Metal Complexes and Halogen Bonding.....	485
MS32-P05   Insights into Weak C-H...F-C Interactions in C <sub>6</sub> F <sub>6</sub> :C <sub>6</sub> H <sub>6-n</sub> Men Co-crystals using Variable Temperature Crystallography to follow Molecular Dynamics .....	486
MS32-P06   Identification of non-covalent interactions by Hirshfeld surface and energy frameworks in chalcone-flavanone isomers.....	487
MS32-P07   Intermolecular Head-to-Head Interactions of Carbonyl and Thiocarbonyl Groups .....	488
MS32-P08   Intermolecular chalcogen...halogen interaction in organic molecular crystals .....	489
MS32-P09   Non-covalent bonding in organic crystals: a combined X-ray and DFT study .....	490
MS32-P10   Structural Landscape of Cu(II) Coordination Compounds with Isomers and Derivatives of Cyclic Triimidazole.....	491
MS32-P11   Solid state structure of pharmaceutically important coumarin derivatives from in house collected XRPD data.....	492
MS32-P12   Examination of the intermolecular aurophilic interactions in the crystals of the (ArCOC=C)(PEt <sub>3</sub> )Au and [(ArCOC=C) <sub>2</sub> Au]-[Au(PEt <sub>3</sub> ) <sub>2</sub> ] <sup>+</sup> complexes. ....	493
MS32-P13   Effect of localized non-bonding/repulsive interactions on distribution of electron density in pi-conjugated systems .....	494
MS32-P14   Hypervalent chalcogen-chalcogen heteropentalenes and their charge transfer adducts .....	495
MS32-P15   Selenoureas as building blocks in binary and ternary cocrystals .....	496
MS32-P16   Interplay between occurrence frequencies of charged and neutral base pairs in small molecule crystals.....	497
MS32-P114 - LATE   2D Materials in Electron Microscope.....	498
MS32-P116 - LATE   Molecular interaction in hydrates of 4-methylpiperidine and 4-chloropiperidine .....	499

## MS33: TUNING CRYSTALLINE FRAMEWORKS AND THEIR APPLICATIONS THROUGH STRUCTURAL DESIGN..... 500

MS33-01   Understanding the Structure-Derived Function of Metal-Organic Frameworks and their Application in Separations.....	500
MS33-02   Modulated Self-Assembly of Hard and Soft Porous Crystals.....	501
MS33-03   Rules for Designing Rod Metal-Organic Frameworks: A Topological Approach.....	502
MS33-04   The Crystalline Sponge Method: Pitfalls, Challenges and Solutions .....	503
MS33-05   Exploring the Dynamic Gas Adsorption Behaviour of a Family of Coordination Polymers through in situ Diffraction Techniques.....	504
MS33-P01   Tunable Polar Linker Dynamics in Metal-Organic Frameworks.....	505
MS33-P02   Polarized fluorescence harvested from fullerenes loaded in non-centrosymmetric Ni-MOF .....	506
MS33-P03   Heterocyclic Ligands for Water Sorption in Metal–Organic Frameworks: A Structural Study Using the Rietveld Method .....	507
MS33-P04   Synthesis and characterization of new lanthanide MOFs using a semi-flexible bis-imide ligand.....	508
MS33-P05   Noble gas adsorption in MFU-4l frameworks with different metal atoms.....	509
MS33-P06   Controlled release of natural essential oils from microporous metal-organic framework.....	510
MS33-P07   Large pore MOFs as catalytic nanoreactors.....	511
MS33-P08   About the polymorphism of two anti-inflammatory drugs within thin films .....	512
MS33-P09   Prior evaluation of guest exchange in crystalline framework using preliminary diffraction data .....	513
MS33-P10   Mechanochemistry and electron crystallography: a winning combination for the discovery of new metal-organic materials.....	514
MS33-P11   Enhanced selectivity for CO <sub>2</sub> in mixed-ligand bis(pyrazolate) Zn(II) MOFs through dilution of functionalization: a structural and textural study .....	515
MS33-P12   Serial-MOF: Developing Serial Crystallography Methods for MOF Nano-crystals .....	516
MS33-P13   Crystal Engineering meets Stereochemistry: Investigations of the crystal structures and resulting properties of copper compounds featuring tartaric acid .....	517

MS33-P14   Constructing extended Bismuth(III) structures using tridentate organic linkers .....	518
MS33-P15   Coordination polymers and solvatomorphs – copper complexes with amino acids and 2,2'-bipyridine .....	519
MS33-P16   Giant Supramolecules as Molecular Containers .....	520
MS33-P17   Direct Structure Determination of Volatile Odor Compounds via Crystalline Sponge Method.....	521
MS33-P19   Complexation Studies of Chiral Cyclohexylhemicucurbit[n]uril to Metalloporphyrins in Solid-State	522
MS33-P20   Synthesis and crystal structure of a new bimetallic platinum complex [Pt <sub>2</sub> (μ-H)(μ-PPh <sub>2</sub> ) <sub>2</sub> Br <sub>2</sub> (PPh <sub>3</sub> ) <sub>2</sub> ]	523
MS33-P118 - LATE   Stability of non-toxic gamma-cyclodextrin-based metal–organic framework in various solvents.....	524
MS33-P120 - LATE   The Crystalline Sponge Method for the Structural Determination of Non-Crystalline Compounds using Metal Organic Framework.....	525
MS33-P122 - LATE   Using Metal Organic Frameworks to Determine the Crystal Structures of Non-Crystalline Compounds.....	526

## MS34: COMPUTER SIMULATION OF MOLECULAR INTERACTIONS AND CRYSTAL STRUCTURES

### ..... 527

MS34-01   Towards the Design of Molecular Materials.....	527
MS34-02   Towards Crystal Structure Solution of Organic Compounds by fit to the Pair Distribution Function without Prior Knowledge of Space Group and Lattice Parameters .....	528
MS34-03   CLPdyn: A Cheap and Reliable Tool for Molecular Dynamics Studies of Organic Molecules in Condensed Phase .....	529
MS34-04   Computational Protocol for Simulating the Anisotropic Lattice Expansion in Organic Crystals .....	530
MS34-05   Analysing Aromatic Interactions: Clarity out of Complexity.....	531
MS34-P01   Crystal structure and Hirshfeld surface analysis of 1,3,4-thiadiazol derivative .....	532
MS34-P02   Use of crystal structure prediction to design template crystallization experiments of nitrobenzoic acid derivatives.....	533
MS34-P03   Polymorphism of R-encenicline hydrochloride: Access to the highest number of structurally characterized polymorphs using desolvation of various solvates.....	534
MS34-P04   DFT Studies of Structural, Electronic and Magnetic Properties of InP and In <sub>0.75</sub> X <sub>0.25</sub> P (where X=Cr, Mn & Fe).....	535
MS34-P05   How to correctly sample unit cells in computer simulations of crystal structures.....	536
MS34-P06   A Combined Theoretical and Experimental Investigation into the High Throughput Screening of Cocrystal Cofomers .....	537
MS34-P07   Development of Accurate and Efficient ab initio Potentials for Effective Crystal Structure Prediction .....	538
MS34-P08   Understanding of cholesterol transport in NPC family protein: A computational study.....	539
MS34-P09   Affinity predictions for cocrystals' design: computational vs. experimental results.....	540

## MS35: FROM SYNTHON ENGINEERING TO PROPERTY ENGINEERING ..... 541

MS35-01   Synthons: Through the Looking-Glass, and What We Have Yet to Find There.....	541
MS35-02   Flexible Crystalline Coordination Polymers with Tunable Responses to Mechanical Stimuli .....	542
MS35-03   Crystallization of Chiral 2,4-Dinitrophenyl Pyridoxine Derivatives in «no Zonk» Groups: Regularity or Randomness?.....	543
MS35-04   Direct Proportionality between Structural Features and Property in Multicomponent Crystals of Salicylic Acid.....	544
MS35-05   Surface Properties of Organic Crystals Based on a Quantum Chemical Treatment of Crystal Facets .....	545
MS35-P01   Mononuclear cobalt, nickel and copper complexes with glycinamide: structural properties and biological activity .....	546
MS35-P02   Phase transitions associated with conformational changes of ligand and anion reorientation trigger normal and reverse spin crossover .....	547
MS35-P03   Luminescent [Os(Cl)(Co)(P <sup>^</sup> P)(Pbi)] Complexes .....	548
MS35-P04   Structural studies of the host-guest complexes of carboxylated pillar[n]arenes .....	549
MS35-P05   Graph-set analysis and non-linear optical properties of salts of L-arginine homologue .....	550
MS35-P06   Novel coordination compounds for biological applications .....	551
MS35-P07   Novel Schiff base-metal complexes; Synthesis, crystal structure and biological activity.....	552
MS35-P08   Two Composite Mn(II)-squarate-dpe Supramolecular Networks Showing Interesting Water Hysteresis Phenomenon in Water Vapor Ad-/de-sorption Isotherms.....	553
MS35-P09   New heterobimetallic complexes of Cu(II) and Mn(II) with cyclam derivatives .....	554
MS35-P10 cancelled  Hydrothermal Synthesis, Crystal Structure And Luminescent Properties Of A New Praseodymium Coordination Polymer.....	555

MS35-P11   Structural and Computational Study of Quinoline-Based Chalcogenesemicarbazones .....	556
MS35-P12   New Titanium Calix[n]arene-based Scaffolds as Anti-tumour Agents .....	557
MS35-P13   Exploring the Limits of Iodonium (I <sup>+</sup> ) Formation.....	558
MS35-P14   Crystal structure and self-assembly of pillar[n]pyridiniums.....	559
MS35-P15   Crystal structures and topological analysis of Ag(I) complexes with 1,4-heterodisubstituted cyclohexanes .....	560
MS35-P16   A Lamellar Structure Exhibiting Nano-Morphological Reversibility, Disassembly-and-Self-Assembly Crystallization into Novel Coordination Polymers.....	561
MS35-P17   Crystallographic Evidence for Aggregation Patterns of Two Cyclic Triimidazole Phosphors in Zn(II) and Cd(II) Complexes .....	562
MS35-P18   Crystal structures of cholesterol based photo-switchable mesogenic dimers. Strongly bent molecules versus an intercalated structure.....	563
MS35-P19   Cube Vs Dimer: Peculiarities Of Crystal Structure Of Cu <sub>2</sub> I <sub>2</sub> - And Cu <sub>4</sub> I <sub>4</sub> -Complexes Of 10-(Aryl)Phenoxarsines And 10-(Aryl)Phenarsazines .....	564
MS35-P20   Correlation between structural studies and third order NLO properties of three new semi-organic compounds .....	565
MS35-P21   Filling the gaps: what new polymorphs of acetylpyrene tell us about the fluorescence of pyrene derivatives.....	566
MS35-P22   Medium chain length (mcl)-PHA-based nanocomposites for biomedical applications: system evaluation through XRD.....	567
MS35-P23   Structural and vibrational study of new 2-ethylanilinium phosphite (C <sub>8</sub> H <sub>12</sub> N)H <sub>2</sub> PO <sub>3</sub> .....	568
MS35-P24   Supramolecular assemblies of copper(II) complexes: Supramolecular synthon transferability and magnetic properties .....	569
MS35-P25   Revealing Mechanical Plastic Bending in Coordination Polymer Crystals .....	570
MS35-P26   Organic cocrystals with mechanically interlocked architectures: Unprecedentedly stiff and hard with elastic flexibility .....	571
MS35-P27   Engineering of Supramolecular Coordination Spheres for Selective Fullerene Binding and Functionalisation .....	572
MS35-P28   Evaluation of trends in a series of halogenated isophthalamides.....	573
MS35-P29   Insights into the molecular arrangements of substituted hydroxypyridine carboxylic acids .....	574
MS35-P30   Halogenation dictates architectures and properties of amyloid peptides.....	575
MS35-P31   Design of cocrystals based on essential oils with a palette of different properties .....	576
MS35-P32   Hierarchical design of lipid-polymer composite nanofibers: the interplay of multiscale structures and biofunctions.....	577
MS35-P33   New synthons in supramolecular chemistry of short biologically active peptides.....	578
MS35-P34   Controlling the Salt-Cocrystal Continuum and pKa rule: The Multi-Drug Ionic-Cocrystals of Lamotrigine and Valproic Acid .....	579
MS35-P35   Effect of crystallization conditions on diuretic Clopamide and its copper(II) complexes .....	580
MS35-P36   Multicomponent crystal formation of baclofen with acids and bases .....	581
MS35-P37   Structurally diverse manganese(III) - salpn complexes with bridging formate ligand .....	582
MS35-P38   The photodimerization of Schiff bases: Benzophenone azine crystals and their weak C-H... $\pi$ interactions.....	583
MS35-P124 - LATE   Structural chemistry of binary cocrystals of diamines and diols .....	584
MS35-P126 - LATE   Hybrid polyoxomolybdate systems based on rationally designed asymmetric carbohydrazones .....	585
MS35-P128 - LATE   interactions in copper(II), nickel(II) and cobalt(II) complexes with N-methyl-, N-ethyl- and N-propylglycine: monomers, dimers and polymers.....	586

## MS36: AMORPHOUS SOLIDS, SOLID SOLUTIONS, COCRYSTAL ALLOYS AND COCRYSTALS .... 587

MS36-01   Ionic Co-Crystals .....	587
MS36-02   Manipulation of the Crystalline and Amorphous Physical States of Pharmaceutical Materials: Possibilities, Limits and Challenges.....	588
MS36-03   Characterisation of "Polyamorphism" and the Molecular Origins of Disorder using Complementary Methods .....	589
MS36-04   Pharmaceutical Solid Solutions from Non-Soluble Components .....	590
MS36-05   Charade Transfer Donor-Acceptor Complexes of Several Polycyclic Aromatic Molecules.....	591
MS36-P01   Four-component isomorphism in the crystal structure of [HL][Cd(HL)(NCS) <sub>2</sub> XY]·H <sub>2</sub> O, where L = 2-acetylpyridine-aminoguanidine, X = Cl-/Br-, and Y = Br-/SCN- .....	592
MS36-P02   Dynamical disorder in the solid state: insights from dielectric relaxation spectroscopies .....	593
MS36-P03   Molecular Basis of Water Sorption Behavior of Rivaroxaban-Malonic Acid Cocrystal.....	594
MS36-P130 - LATE   Cocrystals of cyclopentylamine with alcohols. Synthesis and structural studies.....	595

MS36-P132 - LATE   Polymorphism in ionic co-crystals - structural characterization .....	596
MS36-P141   Multicomponent Crystals of 2,2'-Bipyridine with Aliphatic Dicarboxylic Acids: Structure-Property Correlations.....	597
<b>MS37: NMR CRYSTALLOGRAPHY.....</b>	<b>598</b>
MS37-01   New Sensitivity-Enhanced NMR Crystallography Approaches to Investigate Crystallization and Polymorphism in Organic Materials .....	598
MS37-02   Understanding Self-Assembly of Molecular Organic Solids using NMR Crystallography: From Multicomponent Solids to Supramolecular Hydrogels.....	599
MS37-03   <sup>1</sup> H, <sup>19</sup> F and <sup>29</sup> Si MAS NMR Investigations of Synthetic Lepidolite Samples with Variable OH/F Ratios.....	600
MS37-04   Determination of Elusive Crystal Structure of Solvate-Hydrate of Catechin by Crystal Structure Prediction and NMR Crystallography .....	601
MS37-05   Understanding the Role of Molecular Mobility in Phase Transitions of Bulk and Confined Pharmaceuticals .....	602
MS37-P01   Expanding solid-state landscape of fluconazole: combined application of solid-state NMR, X-ray diffraction and computational methods to uncover polymorphism in fluconazole solvates.....	603
MS37-P02   Towards understanding phase transitions of confined pharmaceuticals .....	604
MS37-P03   { <sup>1</sup> H/ <sup>19</sup> F} -> <sup>29</sup> Si/ <sup>27</sup> Al CPMAS and HETCOR spectroscopy of synthetic lepidolites: Connectivities between F/OH and Si/Al in the octahedral and tetrahedral sheets.....	605
MS37-P04   The Drug Target Monoacylglycerol Lipase: Structure and dynamics, conservation and divergence .....	606
MS37-P05   Photoinitiated solid-state reactions of ketones with vinyl-acetylene fragments .....	607
MS37-P134 LATE   Configuration controlled crystal and/or gel formation of fully protected D-glucosamines.....	608
<b>MS38: NEW DETECTORS FOR HIGH ENERGY X-RAY APPLICATIONS .....</b>	<b>609</b>
MS38-01   Recent Advances in High-Z Pixel Detectors.....	609
MS38-02   Subpixel Spatial Resolution at 122 keV of an Spectroscopic Imager Composed of a pnCCD Coupled to a Columnar CsI(Tl) Scintillator .....	610
MS38-03   Photon Counting with Mixed Mode Detection.....	611
MS38-04   Eiger2 CdTe Detectors: Tools for Hard X-Ray Studies.....	612
MS38-05   Combining a Nine-Crystal Multianalyser Stage with a Hybrid CdTe Photon Counting Detector for High-Resolution X-Ray Powder Diffraction at ESRF-ID22 .....	613
MS38-P01   CdTe based 2D detectors for hard radiation .....	614
MS38-P02   Pushing data quality for laboratory Pair Distribution Function experiments .....	615
MS38-P03   The potential benefits of using higher X-ray energies for macromolecular crystallography.....	616
MS38-P04   Measuring accurate single crystal diffraction data using a Pilatus3 CdTe detector.....	617
MS38-P05   Resolution function for 2D pixel detectors .....	618
<b>MS39: TIME-RESOLVED DIFFRACTION AND SCATTERING TECHNIQUES .....</b>	<b>619</b>
MS39-01   Ultrafast Dynamics of Chemistry in Solution Studied by Time-Resolved X-Ray Diffuse Scattering at LCLS.....	619
MS39-02   Application of Ultrafast Strain Fields for X-Ray Pulse Shortening and Pulse Picking .....	620
MS39-03   Time-Resolved Structure Analysis of Piezoelectric Crystals Resonantly Vibrating Under Alternating Electric Field .....	621
MS39-04   Liquid-Metal-Jet X-Ray Source for Time-Resolved Saxes Studies in the Home Laboratory .....	622
MS39-05   At the Intersection of Crystallography and Spectroscopy - Studies of Selected Photoactive Coinage Metal Complexes .....	623
MS39-P01   Development of data processing methods in time-resolved Laue photocrystallography.....	624
MS39-P02   A Novel X-Ray Diffraction Technique for in-situ Observations of Cathode/Anode Reaction in Electrolytes .....	625
MS39-P03   Development of Channel-cut X-ray optics for laboratory small-angle X-ray scattering setups .....	626
MS39-P04   Silica nanoparticle agglomeration studies under physiological conditions using dynamical SAXS methods .....	627
MS39-P05   Structural mechanisms governing redox-linked proton pump in cytochrome c oxidase studied by time- resolved X-ray methods .....	628
MS39-P06   Recent developments towards high-flux time-resolved and THz -SAXS-experiments at the EMBL P12 BioSAXS beamline .....	629
<b>MS40: THE USE OF X-RAYS AND NEUTRONS FOR EXPERIMENTS IN NANOSCIENCE .....</b>	<b>630</b>
MS40-01   Nanoscale In-Situ 3D Imaging of Defect Dynamics in Oxide Ferroelectrics .....	630
MS40-02   Opportunities with Coherent X-Ray Nanobeams: A Short Perspective from a Beamline .....	631

MS40-03   Nano-Scale Strain Mapping in Complete Nanowire Based Electronic Devices by Bragg Coherent X-Ray Diffraction .....	632
MS40-04   In Situ X-Ray Scattering Study of Hydrothermal Synthesis of Anatase TiO <sub>2</sub> Nanoparticles from Commercial Precursor TiOSO <sub>4</sub> .....	633
MS40-05   Atomic Insight into Hydration Shells around Faceted Iron Oxide Nanoparticles .....	634
MS40-P01   Structural characterization of exchange biased Au-Fe <sub>3</sub> O <sub>4</sub> dumbbell nanoparticles .....	635
MS40-P02   Structural and optical properties of CuS nanoparticles .....	636
MS40-P03   Multiscale Structural decoding of electrospun nanofibers: from processing to possibilities for steering functionality .....	637
MS40-P04   A Laboratory Rheo-SAXS Setup - Relating Nanostructure to Macroscopic Properties in one go ...	638
MS40-P05   Possibilities of the X-ray diffraction method for the study of ultradispersed systems and nanopowders .....	639
MS40-P06   Study Of Structural Polymorphism In Molecular Composites:Application To Energy Storage .....	640
MS40-P07   Diffraction Experiments under Extreme Conditions on Single Crystals with Hot Neutrons on HEiDi .....	641
MS40-P08   Morphology characterization of anatase TiO <sub>2</sub> nanocrystals by advanced Rietveld refinement of powder X-ray diffraction data including anisotropic size broadening models .....	642
MS40-P09   Quantification of the strain relaxation processes in silicon nanowires arrays using combined X-ray diffraction analyses .....	643
MS40-P10   The Dynamic Structure of Au <sub>38</sub> (SR) <sub>24</sub> Nanoclusters Supported on CeO <sub>2</sub> under CO Oxidation .....	644
MS40-P11   Beam damage of single semiconductor nanowires during X-ray nano beam diffraction experiments .....	645
MS40-P12   Nanocrystalline CdS and (Cd,Mn)S particles: structure and morphology .....	646
MS40-P13   Interplay between Crystal Structure, Shape and Functionality of Colloidal Nanocrystals and Supercrystals .....	647

## MS41: CRYSTALLISATION FOR SMALL AND LARGE MOLECULES..... 648

MS41-01   Crystallisation for Serial Crystallography in Lipidic Cubic Phase (LCP) Made Simple.....	648
MS41-02   Four for the Price of One: Cross-Seeding to Obtain Crystals of Ancestral Elongation Factor Tus ...	649
MS41-03   Nano-crystallization: Applying the Methods of Macromolecular Crystallography for Small Molecules .....	650
MS41-04   Substrate Induced Polymorphism of Organic Electronic Molecules.....	651
MS41-05   Shaping Drug Process Development with Crystal Structure Databases.....	652
MS41-P01   Watching Nanodefects Grow in Si Crystals.....	653
MS41-P02   Multiferroic Bi <sub>2</sub> Fe <sub>4</sub> O <sub>9</sub> : Tuning of crystallization pathways and kinetics .....	654
MS41-P03   Amine-imine proton tautomerism in isomeric 2-phenylamino-1,3-thiazol-4(5H)- and 4-phenylamino-1,3-thiazol-2(5H)-one derivatives .....	655
MS41-P04   Two new polymorphs of CuCl <sub>2</sub> ·2DMF obtained via high-temperature crystallization .....	656
MS41-P05   Phytochemical and biological studies of Anacyclus pyrethrum L. from Ifrane-Morocco .....	657
MS41-P06   Dynamic theory of protein crystallization .....	658

## MS42: IN SITU AND IN OPERANDO ANALYSIS OF FUNCTIONAL MATERIALS..... 659

MS42-01   High Energy Surface X-Ray Diffraction from Surfaces and Nanoparticles in Operando Catalysis ...	659
MS42-02   Neutron Diffraction Studies of Energy Materials.....	660
MS42-03   Morphology and Structure of Metal-Organic Framework ZIF-8 during Crystallisation Measured by a New Technique: Dynamic Angle Resolved Second-Harmonic Scattering (AD-SHS).....	661
MS42-04   In Situ Mechanochemistry of Hybrid Materials.....	662
MS42-05   Inspecting Piezoelectricity in PbZr <sub>1-x</sub> Ti <sub>x</sub> O <sub>3</sub> Single Crystals with Ferroelastic Domains.....	663
MS42-P01   Phase diagram and redox behavior of (Nd/Pr) <sub>2</sub> NiO <sub>4+δ</sub> electrodes explored by in situ neutron powder diffraction during electrochemical oxygen intercalation.....	664
MS42-P02   Extracting coherent information about phase transformations in a functional material studied by X-ray powder diffraction.....	665
MS42-P03   Formation mechanism of epitaxial palladium-platinum core-shell nanocatalysts in a one-step supercritical synthesis.....	666
MS42-P04   SNBL's BM31 at ESRF beyond 2020 - Combined XRD-PDF-XAS .....	667
MS42-P05   Sequential SHELXL refinement of consecutive datasets: a tool to probe dynamically evolving single crystal structures.....	668
MS42-P06   Testing a home-made sample holder with flow-through capillary to study in-situ re-solvation process .....	669
MS42-P07   A new concept for sapphire single-crystal cells to study solid-gas reactions via real-time in situ neutron scattering .....	670
MS42-P08   Latest developments in non-ambient XRD attachments from Anton Paar .....	671

MS42-P09   Space- and time-resolved analysis of the decomposition of thermoelectric materials with mobile atoms under working conditions.....	672
MS42-P10   In-situ wide-angle X-ray scattering on liquid crystalline elastomers for orthopedic applications.....	673
MS42-P11   Crystallization of tin oxide quantum dots probed by coupled in situ high temperature SAXS and WAXS experiments on the BM02 beamline at the ESRF.....	674
MS42-P12   Operational non-uniformities of lithium distribution in Li-ion batteries probed by diffraction techniques.....	675
MS42-P13   Studying molecular crystals at high pressures: experimental strategy and hardware matters.....	676
MS42-P14   Diffusion Mechanisms of Gas Adsorption by Porous Frameworks from sub-Second Synchrotron Powder X-ray Diffraction.....	677
MS42-P15   In situ X-ray studies of electrodeposition of lead-halide compounds on the electrolyte-liquid mercury interface.....	678
MS42-P136 - LATE   In Situ Crystallization of the Viscous Organosilicon Liquids.....	679

## MS43: TOTAL SCATTERING STUDIES AND DISORDER..... 680

MS43-01   Hidden Vacancy-Network Polymorphism of Prussian Blue Analogues.....	680
MS43-02   Characterizing Structure, Microstructure and Morphology of Nanomaterials through Reciprocal Space Total Scattering Methods.....	681
MS43-03   Study of the Confinement Effect of Water in Bioactive Glasses Using Atomic Pair.....	682
MS43-04   Using Nuclear Magnetic Resonance Spectroscopy, Neutron and X-Ray Pair.....	683
MS43-05   Texture Correction for Total Scattering Functions.....	684
MS43-P01   Cooking Crystals: Radiation Damage in Molecular Modulated Materials.....	685
MS43-P02   Instrumental Effects in Laboratory Pair Distribution Function (PDF) Analysis.....	686
MS43-P03   Structures of the group 13 prenucleation clusters.....	687
MS43-P04   Mapping Non-Crystalline Nanostructure With Low-dose Scanning Electron Pair Distribution Function Analysis.....	688
MS43-P05   Investigation of the nanostructured materials by XRD method with use of simulation.....	689
MS43-P05   The inversion model and its limitations for spinel $ZnAl_2O_4$ : a multi technique study.....	690

## MS44: SOLVING STRUCTURES THROUGH COMBINATION OF RECIPROCAL AND DIRECT SPACE

### METHODS ..... 691

MS44-01   Crystal Structure of New and Highly Complex Organic Molecules Solved by 3D Electron Diffraction.....	691
MS44-02   Prospects of single molecule electron diffraction for structural biology.....	692
MS44-03   The Need for Correlation Coefficients in the Modeling of Stacking Faulted Crystal Structures.....	693
MS44-04   Structure Study of a Disordered Zeolite by cRED and HRTEM.....	694
MS44-05   Direct and Fourier Space Traveling: Multi-Dimensional Mapping of Lattice Strain and Tilt of a Suspended Silicon Nanowire in a Monolithic System.....	695
MS44-P01   Synthesis and study of highly sensitive SERS substrate by ferromagnetic hollow micro-spheres.....	696
MS44-P02   Hydraulic, structural and photocatalytic behavior of cementitious phases incorporating nanocomposite mixed Zn-Al-Ti oxydes.....	697
MS44-P03   Structural characterization of ZnO/graphene nanocomposite.....	698
MS44-P04   Effects of x-ray irradiation and thermal annealing on the Co dopant location in Co-doped $TiO_2$ nanocrystals.....	699
MS44-P05   Evaluation of crystal structures with partial occupancies using Boolean satisfiability techniques in STRUPLOX.....	700
MS44-P06   Automated Serial Rotation Electron Diffraction combined with Cluster Analysis as a Tool for Structure Determination.....	701
MS44-P07   Construction of Muqarnas from periodic and quasiperiodic 2-dim tiling.....	702
MS44-P08   Utilising MaXrd in the Study of Inclusion Compounds.....	703
MS44-P09   Evidence of Charge Density Wave transverse pinning by X-ray micro-diffraction.....	704
MS44-P10   Indexing Grazing Incidence X-ray Diffraction Patterns of Thin Films.....	705
MS44-P138 LATE   On phasing of oversampled diffraction data.....	706

## GI-MS45: HOW TO... SUCCESSFULLY COLLABORATE AS A CRYSTALLOGRAPHER ..... 707

GI-MS45-01   Fighting the wind mills: are crystallographers the successors of Don Quixote?.....	707
GI-MS45-02   Secrets to a Successful Collaboration.....	708
GI-MS45-03   Education for New Synchrotron Sources: An Interdisciplinary Master Program of the Novosibirsk State University.....	709
GI-MS45-04   How, and When, to Effect Collaborations.....	710
GI-MS45-05   Using Crystal Structures to Guide Pharmaceutical Drug Substance Development.....	711

GI-MS45-P01   Crystallochemical computational tools, web services, databases, and approaches for joining researchers over the world.....	712
GI-MS45-P02   StructureFinder .....	713
GI-MS45-P03   Extending NXmx metadata to facilitate data sharing.....	714
<b>GI-MS46: STATUS AND NEW ACTIVITIES @ LARGE SCALE FACILITIES .....</b>	<b>715</b>
GI-MS46-01   The ESRF-EBS and the Next Chapter in X-ray Science .....	715
GI-MS46-02   Megahertz Rate Serial Crystallography at the European XFEL.....	716
GI-MS46-03   EMBL Beamlines for Macromolecular Crystallography at PETRA III.....	717
GI-MS46-04   Macromolecular Crystallography at MAX IV .....	718
GI-MS46-05   Facility upgrades at the Australian Synchrotron: Extending the powder diffraction capabilities....	719
GI-MS46-P01   Establishment of a High Capacity X-ray Source in Austria for the Use in Materials Science .....	720
GI-MS46-P02   A Non-ambient Single Crystal X-ray Diffraction Beamline at Taiwan Photon Source.....	721
GI-MS46-P03   An effective neutron cross section for hydrogen in organic compounds .....	722
GI-MS46-P04   The high energy X-ray diffraction beamline at the PETRA III synchrotron light source at DESY. .....	723
GI-MS46-P05   Azimuthal integration and crystallographic algorithms on malleable hardware .....	724
GI-MS46-P06   Development of microspectrophotometer for the macromolecular crystallography beamline at the Photon Factory, Japan.....	725
GI-MS46-P07   Facilities for Macromolecular Crystallography at the HZB.....	726
GI-MS46-P08   New tricks for an old dog: The Powder Diffraction and Total Scattering Beamline P02.1 at PETRA III, DESY .....	727
GI-MS46-P09   NMX Macromolecular Diffractometer at ESS .....	728
GI-MS46-P10   Exploring new data collection protocols with the Eiger2 detector and SmarGon on the variable and microfocus beamline I04 at Diamond Light Source.....	729
GI-MS46-P11   Current Status of Sample Exchange Robots at the Photon Factory Macromolecular Crystallography Beamlines .....	730
GI-MS46-P12   Fxe Status: Femtosecond X-Ray Experiments For Chemical Dynamics Research At The European Xfel .....	731
GI-MS46-P13   CALIPSOplus - overview and targeted research possibilities.....	732
GI-MS46-P14   A new single crystal diffractometer at BM20/ESRF .....	733
GI-MS46-P15   Biological User Support at the European XFEL .....	734
GI-MS46-P16   Long-wavelength protein crystallography at Diamond Light Source.....	735
GI-MS46-P17   Advanced Protein Crystallisation for Neutron Macromolecular Crystallography.....	736
GI-MS46-P17   User Infrastructures at the Helmholtz-Zentrum Berlin für Materialien und Energie HZB .....	737
MS46-P140 <b>LATE</b>   XALOC, the MX beamline at ALBA synchrotron: Current status and perspectives .....	738
<b>GI-MS47: WOMEN IN CRYSTALLOGRAPHY .....</b>	<b>739</b>
GI-MS47-01   32 Years of Travels in Crystallography.....	739
GI-MS47-02   Women in Science – an African perspective .....	740
GI-MS47-03   Modest Recognition for High Achievements .....	741
GI-MS47-04   “It’s just like planning a dinner...” - Women in Crystallographic Computing .....	742
GI-MS47-05   Women in a Historical French Laboratory of Crystallography.....	743
<b>GI-MS48: TEACHING NEW DOGS OLD TRICKS .....</b>	<b>744</b>
GI-MS48-01   Some Reflections on Symmetry .....	744
GI-MS48-02   Seeing is Believing: Model Finalisation and Interpretation of Results.....	745
GI-MS48-03   The Difference Electron Density Map as a Crystal Structure Validation Tool .....	746
GI-MS48-04   Crystal Structure Exploration – I didn’t Know Mercury Could Do That!.....	747
GI-MS48-05   Resolution of Crystallographic Problems Using the Bilbao Crystallographic Server.....	748
GI-MS48-P01   How best to search and look for chaos in crystals by diffractometric methods.....	749
GI-MS48-P02   The HyPix-Arc 150° .....	750
GI-MS48-P03   MicaPenrose: a work of art as a tool to teach and popularize crystallography .....	751
GI-MS48-P04   CrysAlisPro 40: 64-bit, Synergy, HyPix-Arc 150°, AutoChem4.0, Ewald 3D .....	752
GI-MS48-P05   WANTED -- K-beta!.....	753
GI-MS48-P06   A life with crystallography.....	754
GI-MS48-P07   Benefits of transmission mode in XRD .....	755
GI-MS48-P08   Olex2: Teaching New Software Old AND New Tricks .....	756
GI-MS48-P09   Crenel or not crenel, what is the function? .....	757
GI-MS48-P10   Mathematical justifications for crystal systems, Bravais lattices and a new continuous classification.....	758

GI-MS48-P11   Pervasive approximate symmetry in P1 and high-Z' organic crystals .....	759
GI-MS48-P12   Overcoming ambiguous tautomer assignment in 1,2,4-triazole crystal structures.....	760
GI-MS48-P13   Optical simulation of crystal diffraction using modified video projectors - a teaching proposal...	761
GI-MS48-P14   Teaching old tricks: rotation conventions in crystallography and cryoEM .....	762
GI-MS48-P15   When are "Bad Data" "Good" Data?.....	763
GI-MS48-P16   Absolute structure of (E)-2,2'-[3-(4-Fluorophenyl)prop-2-ene-1,1-diyl]bis(3-hydroxy-5,5-dimethylcyclohex-2-en-1-one).....	764



# 32<sup>nd</sup> European Crystallographic Meeting (ECM32)

## Public Talk

---

### PUBLIC TALK | EXAMINING OLD PAINTINGS WITH NEW X-RAY METHODS: A FRESH LOOK AT AND BELOW THE SURFACE

Janssens, Koen (University of Antwerp, B)

Imaging of painted works of art such as oil and panel paintings is traditionally done by means of X-ray radiography and Infra-red reflectography, where the first method allows to obtain information on hidden/overpainted layers and the second is very suitable for visualization of underdrawings. In the last decade, a number of hyperspectral methods have been developed that allow to obtain more information in a non-invasive manner from such artworks. Two of these are macroscopic X-ray fluorescence (MA-XRF) and Macroscopic X-ray powder diffraction (MA-XRPD), allowing to record respectively large scale elemental and crystal phase maps. In the first half of this lecture, the examination by means of MA-XRF of well-known works of art such as Van Eyck's 'The Ghent Altarpiece', Bosch's 'Last Judgement' and Rubens' 'The Little Fur' will be discussed, revealing information that is highly relevant for art-historians and others interested in the creative process that gave rise to these artworks. In the second half of the lecture, the phenomenon of spontaneous (chemical) degradation of painted works of art will be the central theme. For the first time, MA-XRPD allows to visualize and detect the effect of subtle chemical transformations below or at the surface of painting. As examples, the examination of Vermeer's 'Girl with the Pearl Earring' and Van Gogh's 'Sunflowers' will be discussed. In many cases, to complement the macroscopic imaging, microscopic analysis of paint cross sections with synchrotron X-ray beams is also highly useful as this allows to better understand at which depth below the surface the degradation phenomena are taking place.

## PUBLIC TALK | **More Than A Century Of Crystallography: What Has It Taught Us And Where Will It Lead?**

Garman, Elspeth (University of Oxford, Oxford, GBR)

What has the art of the chocolatier got to do with drug discovery, proteins and DNA? The linking theme is crystals, which allow us to determine the three-dimensional shapes of all sizes of molecules, ranging from the tiny chocolate moiety to the much larger proteins that allow our bodies to function through to the DNA that carries our genetic information. Crystallography was born in 1913 with the determination of the 3-D structure of sodium chloride (salt) by the Bragg father and son team. It has flowered to elucidate many disciplines since then, with applications in engineering, physics, chemistry, earth sciences and biology. Using crystallography, we can unravel the shapes of biomolecules in our bodies that are targets for drugs against disease, and thus identify new treatments. I will focus on this last field, and give an overview of what is currently achievable and what may be possible in the future (my crystal ball permitting!).

### PL1 | THE CYTOMOTIVE SWITCH IN ACTINS AND TUBULINS

Löwe, Jan (Laboratory of Molecular Biology, Cambridge, GBR)

Protein filaments are used in cells of all sizes to position other molecules in time and space. These filaments can be called cytoskeletons, and they perform critical organising functions in a wide array of fundamental processes. The number of protein families used to form cytoskeletons is, perhaps, surprisingly small given the diversity of processes in which cytoskeletons play a role. In particular, in cytoskeletons across all domains of life, members of the actin and tubulin superfamily are found remarkably often, while the filaments they form are used in quite different processes. For example, prokaryotic actin and tubulin filaments such as ParM, FtsZ, MreB, TubZ, MamK, AlfA and BtubAB illustrate their functional diversity. One explanation for the structural but not functional conservation is that actin and tubulin proteins are special – that their structures encode hard-to-evolve mechanistic features that are useful in many contexts. Using a variety of structural bioinformatic analyses we integrated existing data about the tubulin superfamily to show that one conserved and (putatively) hard-to-evolve feature found across eukaryotic and bacterial tubulins is conformational switching upon polymerisation. We also showed that a similar feature is found across the actin superfamily. So far it is clear that conformational switching upon polymerisation mechanisms underlie the dynamics, and therefore functions, of microtubules and F-actin. Importantly, there are now several examples of the same conformational switching upon polymerisation feature being exploited in the functioning of prokaryotic actin and tubulin filaments as well: notably in the treadmilling FtsZ filament during bacterial cell division, and for the assembly of the magnetosome-positioning MamK filament (amongst other examples). Interestingly, actin MreB is an outlier in the sense that it does not seem to switch upon polymerisation, and this is in line with previous data that showed MreB filaments to be non-dynamic, being moved along by cell wall synthesis. Altogether, these findings suggest that conformational switching upon polymerisation is what makes both actin and tubulin special, and especially useful for building dynamic cytoskeletons using cytomotive filaments.

## PL2 | QUANTUM CRYSTALLOGRAPHIC STUDIES OF ADVANCED MATERIALS

Brummerstedt Iversen, Bo (Aarhus University, Aarhus, DNK)

Layered (2D) materials exhibit a variety of extraordinary properties, and recent focus has included topological insulators, electrode materials, monolayers, hetero structures – and thermoelectrics. The physical properties such as band gap or thermal and electrical conductivity are related to the detailed structural characteristics as well as the specific chemical bonding both within the covalent layers and across the van der Waal gap. It is generally assumed that layered materials exhibit anisotropic properties, but the properties are rarely discussed in direct relation to the specific chemical bonding characteristics of the solid.

Using advanced crystallographic analysis such as charge density modelling, NXMEM analysis, 3D-PDF as well as ab initio theoretical calculations, we have studied the crystal structures, chemical bonding and physical properties of a range of important thermoelectric materials including Cu<sub>2</sub>Se [1], Mg<sub>3</sub>Sb<sub>2</sub> [2], SnS<sub>2</sub> [3], TiS<sub>2</sub> [4], SnSe [5] and PbS [6].

[1] a) E. Eikeland et al., *IUCr-J* 2017, 4, 467-485, b) K. J. Dalgaard et al., *Adv. Theory Simul.* 2018, 1, 1800068, N. Roth & B. B. Iversen, *Acta Crystallogr. Sect. A* 2019, 75, 465–473

[2] J. Zhang et al., *Nature Commun.* 2016, 7, 10892; *Nature Commun.* 2017, 8, 13901; *Nature Commun.* 2018, 9, 4716; *npj comp. mater.* 2019, in press

[3] M. Filsø et al., *Dalton Trans.* 2016, 45, 3798 – 3805

[4] H. Kasai et al., *Nature Materials* 2018, 17, 249-252

[5] M. Sist et al., *Acta Crystallogr. Sect. B.* 2016, 72, 310–316

[6] C. Zeuthen et al., *J. Am. Chem. Soc.* 2019, 141,20, 8146-8157

## Keynote

---

### KN01 | GROUND STATE SELECTION IN QUANTUM PYROCHLORE MAGNETS

Gaulin, Bruce (McMaster University, Hamilton, CAN)

The pyrochlore lattice, a network of corner-sharing tetrahedra, is one of the most pervasive crystalline architectures in nature that supports geometrical frustration. We and others have been interested in a family of rare earth pyrochlore magnets, that can display quantum  $S=1/2$  magnetism on such a lattice. The ground states for some of these materials may be disordered, as occurs for "spin ice", a version of this phenomena with the same frustration and degeneracy as solid ice, as well as by a quantum version of this model known as "quantum spin ice" that possesses an emergent quantum electrodynamics. Non-collinear antiferromagnetic ground states are also expressed in rare earth pyrochlore magnets, and I will describe how this comes about and these ground states can be understood, with an emphasis on modern neutron scattering. I'll also discuss a generalized phase diagram for the ground states of these materials, with emphasis on the  $\text{Yb}_2\text{Ti}_2\text{O}_7$ ,  $\text{Er}_2\text{Ti}_2\text{O}_7$ , and  $\text{Er}_2\text{Pt}_2\text{O}_7$ , and comment on how fragile some of these quantum ground states seem to be with respect to weak quenched disorder, which is hard to avoid in real materials.

## KN02 | NEW EXPERIMENTAL TECHNIQUES FOR EXPLORING CRYSTALLIZATION PATHWAYS AND STRUCTURAL PROPERTIES OF SOLIDS

Harris, Kenneth (Cardiff University, Cardiff, GBR)

The lecture will highlight two experimental strategies that we are developing, specifically: (i) *in-situ* solid-state NMR techniques for monitoring the time-evolution of crystallization processes, and (ii) X-ray Birefringence Imaging, a new technique that allows the distribution of molecular orientations in anisotropic materials to be mapped in a spatially resolved manner.

Our *in-situ* solid-state NMR techniques for studying crystallization pathways exploit the ability of NMR to *selectively* detect the solid phase in heterogeneous solid/liquid systems of the type that exist during crystallization from solution. This strategy allows the sequence of solid phases formed during crystallization to be established, including the discovery of new transient polymorphs. A recent development is an *in-situ* NMR strategy (called "CLASSIC NMR") that yields simultaneous information on the time-evolution of *both* the solid phase *and* the liquid phase during crystallization. This strategy extends the scope and capability of *in-situ* NMR for gaining insights into the evolution of crystallization processes.

Following our early studies of X-ray birefringence in solids, we reported in 2014 an experimental set-up that allows spatially resolved measurements of X-ray birefringence to be carried out in "imaging mode". In many respects, this technique (called X-ray Birefringence Imaging) is the X-ray analogue of the polarizing optical microscope. The lecture will describe several applications of this technique, demonstrating the utility of X-ray Birefringence Imaging for characterizing changes in molecular orientations associated with solid-state phase transitions, determining the size and spatial distribution of domain structures in materials, and establishing molecular orientational ordering in anisotropic materials, including liquid crystals.

## KN03 | SOLAR SYSTEM SECRETS HIDDEN IN QUASICRYSTALS

Bindi, Luca (University of Florence, Firenze, ITA)

Quasicrystals are solids whose diffraction patterns are composed of diffraction peaks, like periodic crystals, but with symmetries forbidden to crystals. Natural quasicrystals (icosahedral and decagonal) were discovered a decade ago. The search took more than a dozen years and has opened a new frontier in mineralogy that could lead to new discoveries in geoscience, astronomy, condensed matter physics, and materials engineering. For the first time, minerals have been discovered that violate the symmetry restrictions of conventional crystallography. That nature could accomplish this without human intervention was unexpected, requiring the existence of petrological processes never considered previously. The fact that the quasicrystals were found in a meteorite formed in the earliest moments of the solar system means these processes have been active for over 4.5 billion years and influenced the mineral composition of the first objects to condense around the Sun. Finding quasicrystals formed in these extreme environments informs the longstanding debate about the stability and robustness of quasicrystals among condensed matter physicists. Recent shock experiments, with starting materials similar to the intermetallic alloys in the meteorite hosting the quasicrystals, lend support to the hypothesis that the extra-terrestrial quasicrystals formed as a result of hypervelocity impacts among objects in the early Solar system. Finally, the discovery inspired further searches for quasicrystals and other new forms of matter not seen in the laboratory previously which may provide valuable new materials for physics and engineering. This culminated in the discovery of an icosahedral phase with a composition not predicted before in laboratory experiments.

## KN04 | METAL-ORGANIC FRAMEWORKS AS CHEMICAL REACTORS: X-RAY

### CRYSTALLOGRAPHIC SNAPSHOTS OF THE CONFINED STATE

Armentano, Donatella (Università della Calabria, Rende, ITA); Pardo, Emilio (Universitat de València, ESP); Leyva-Pérez, Antonio (Instituto de Tecnología Química (UPV-CSIC), ESP)

Ultrasmall metal nanoclusters (NCs), consisting of aggregations of less than 10 atoms with a high percentage of them exposed to the external environment, have emerged as formidable catalysts capable to surpass the state-of-the-art catalysts in organic reactions of industrial interest, being thus capable to make feasible certain reactions which are currently financially prohibitive.[1] Such small NCs, that may give rise to a technological leap in a similar way as the irruption of metal nanoparticles (NPs) did, still show important weaknesses regarding the synthetic control of their shape and nuclearity as well as their lack of stability.[2] Metal-Organic Frameworks (MOFs) [3] show unique features to act as chemical nanoreactors for the in-situ synthesis and stabilization of otherwise not accessible functional species and to use single crystal X-ray crystallography as a definitive characterization tool, which offers the unique possibility –among porous materials– to contrast the success of synthetic methodologies, and even more important, to follow/understand what is actually happening within MOFs channels. Supporting these clusters within MOFs is a very promising strategy. MOFs own regular and well-defined channels and exhibit fascinating host-guest chemistry. [3] In principle, they are suitable platforms to synthesize, in a controlled manner, metal clusters below the nanometre allowing to gain information about their nature by means of X-ray crystallography, to shed light on every single step during their synthetic route.[4] Even Supramolecular Coordination Compounds (SCCs) with targeted properties can be self-assembled and stabilized within a MOF.

Here we report on the MOF-mediated chemical synthesis of structurally and electronically well-defined ultrasmall Pt<sub>2</sub>, Pt<sub>1+1</sub>, Fe<sup>III</sup>, Ru<sup>III</sup> and [Pd<sub>4</sub>]<sup>2+</sup> catalysts, together with PdII SCCs built within the confined space of preformed MOFs ([SCCs@MOF](#)) and their post-assembly metalation to give a Pd<sup>II</sup>-Au<sup>III</sup> supramolecular assembly, all crystallographically underpinned. [5] These results open new avenues in both the synthesis of novel NCs and SCCs and their use on heterogeneous metal-based Supramolecular Catalysis. Reactions in which the resulting hybrid materials outperform state-of-the-art metal catalysts will be illustrated.

#### References:

- [1] (a) Corma A. et al., *Nat. Chem.* 2013, 5, 775–781; (b) Liu, L.; Corma, A. *Chem. Rev.* 2018, 118, 4981–5079.
- [2] Lei Y. et al., *Science* 2010, 328, 224–228.
- [3] O’Keeffe, M.; Yaghi O. M. et al., *Science* 2013, 341, 974. (b) Férey, G. et al., *Chem. Soc. Rev.* 2017, 46, 3104–3107; (c) Zhou, H.-C. et al., *Adv. Mater.* 2018, 1704303.
- [4] (a) Corma, A.; Leyva-Perez, A.; Armentano, D.; Pardo E. et al., *Nat. Mater.* 2017, 16, 760; (b) A. Leyva-Perez, D. Armentano, E. Pardo et al., *J. Am. Chem. Soc.* 2016, 138, 7864–7867.; (c) D. Armentano, E. Pardo et al., *Angew. Chem., Int. Ed.* 2016, 55, 11167–11172; (d) Farha, O. K. et al., *Science* 2017, 356, 624–627; (e) Sumbly, C. J.; Doonan, C. J. et al., *Angew. Chem. Int. Ed.*, 2017, 129, 8532–8536;
- [5] (a) Leyva-Pérez, A.; Corma, A.; Armentano, D.; Pardo, E. J. et al., *Angew. Chem. Int. Ed.*, 2018, 57, 6186-6191; (b) Leyva-Pérez, A.; Armentano, D.; Pardo, E. J. et al., *Angew. Chem. Int. Ed.* 2018, 57, 17094 –17099; (c) Leyva-Pérez, A.; Armentano, D.; Pardo, E. J. et al., *J. Am. Chem. Soc.* 2018, 140, 8827–8832; (d) Leyva-Pérez, A.; Fernandez, A.; Armentano, D.; Pardo, E.; Ferrando-Soria, J. et al., *J. Am. Chem. Soc.* 2019, doi:10.1021/jacs.9b03914.

## KN05 | 40 YEARS OF CCP4: WHERE WE ARE, HOW WE GOT HERE AND WHERE WE ARE GOING

Noble, Martin (Newcastle University, Newcastle Upon Tyne, GBR); Wilson, Keith (York University, York, GBR); Dodson, Eleanor (York University, York, GBR); Krissinel, Eugene (Science & Technology Facilities Council, Didcot, Oxfordshire, GBR)

Collaborative Computational Project 4 (CCP4) was founded in 1979 with the aim of supporting computational macromolecular crystallography (MX) by promoting communication among developers, sharing algorithms as they were implemented, and promoting interoperability of software and data. From modest beginnings, CCP4 has contributed hugely to the growth and maturation of MX, enabling this discipline to obtain a central role in the investigation of mechanistic cell biology and in the exploitation of scientific insights in biotechnological and pharmaceutical applications. This talk will review some of the history of CCP4, and describe the current status and ambitions of the project as it continues to address important challenges during its fifth decade of activity.

## KN06 | CRYSTAL PHASE CONTROL IN NANOSTRUCTURES AS A PLATFORM FOR ATOMIC SCALE TAILORING OF ELECTRONIC, OPTICAL AND CHEMICAL PROPERTIES.

Mikkelsen, Anders (Lund University, Lund, SWE)

The III-V nanowire (NW) technology platform has reached a level of advancement that allows atomic scale control of crystal structure and surface morphology as well as flexible device integration. In particular, controlled axial stacking of Wurtzite (Wz) and Zincblende (Zb) crystal phases is uniquely possible in the NWs. We explore how this can be used to locally control electronic, optical, and chemical properties with atomic scale precision opening up for 1D, 2D and 3D structures with designed functionality for novel electronic, photonic and quantum technologies. To do this, we use atomically resolved Scanning Tunnelling Microscopy/Spectroscopy (STM/S), femtosecond Photo Emission Electron Microscopy (PEEM) and X-ray diffraction imaging techniques to study both individual nanowires as well as specially designed functioning nanoscale devices.

We measure local density of states of Zb crystal segments in Wz down to single atomic scale crystal lattice change and find that the "bulk" electronic structure is preserved locally in even the smallest possible segments. We demonstrate a novel device platform allowing true observation of single atom changes across a III-V NW device simultaneously with full electrical operation. We explore the surface alloying of Sb and Bi into GaAs NWs with controlled axial stacking of Wz and Zb crystal phases demonstrating a simple processing-free route to compositional control of 1D and 2D materials at the monolayer level on the NWs. We investigate local hot electron dynamic response and control down to a few femtoseconds temporally and a few tens of nanometre spatially using the Wz and Zb crystal phases.

## KN07 | CHEMISTRY AND CRYSTALLOGRAPHY AT ULTRA-HIGH PRESSURES

Bykova, Elena (Bayerisches Geoinstitut, Bayreuth, GER)

Many scientific disciplines including geophysics, geochemistry, mineralogy, material sciences and engineering are interested in study of materials exposed to extreme conditions as high pressures and high temperatures (HPHT). External stimuli can trigger structural, electronic and magnetic changes in a matter; chemical reactions conducted at HPHT can demonstrate unexpected behavior totally different from that at ambient conditions. However, the analysis and interpretation of the data collected at multimegabar pressures, especially after/during laser heating, is extremely difficult due to unknown (and often very exotic, not known at ambient conditions) chemistry of the materials. Single-crystal X-ray diffraction in diamond anvil cells provides a unique opportunity to study *in-situ* such important characteristic of a material as its crystal structure (unit cell parameters, a space group, atomic coordinates and atomic occupancies), and, if required, a phase composition. Here we demonstrate a great potential and novel opportunities provided by high-pressure crystallography in materials- and geo-sciences on the example of studies of iron oxides, silica and carbonates.

## KN08 | DIFFUSE SCATTERING - PAST, PRESENT AND FUTURE.

Welberry, Richard (Australian National University, Canberra, AUS)

Whereas analysis of Bragg peaks provides information about the average crystal structure (atomic coordinates, site-occupancies, or mean-square atomic displacements — *single* site properties), diffuse scattering contains information about how *pairs* of atoms behave and is thus potentially rich source of information on how atoms and molecules interact. Crystallographers have been aware of diffuse scattering since the earliest times, but development of techniques for recording and analysing it have lagged well behind the advances made in conventional crystallography.

A major impediment to the utilisation of this rich source of information is the diversity and often complex combination of disorder effects that arise in nature and the fact that until recently no one simple method of analysis has been available which can usefully deal with all of them. In this talk we show how computer simulation of a model crystal *does* provide such a general method by which diffuse scattering of all kinds and from all types of materials can be interpreted and analysed. Such methods have only been feasible since the advent of powerful and relatively inexpensive computers.

To trace these developments examples of different real materials are discussed. For organic systems the goal has been to move toward a truly quantitative solution where a pixel-by-pixel comparison between observed and calculated intensities gives agreement factors comparable to those achieved for Bragg intensities. For inorganic systems such as the ferroelectrics PZN and PMN there has been a move towards constructing atomistic potentials that allow diffuse scattering to be calculated *a priori*.

## KN09 | FERTILIZATION AT THE ATOMIC LEVEL - MARRYING BASIC SCIENCE AND REPRODUCTIVE MEDICINE

Jovine, Luca (Karolinska Institute, SWE)

Mammalian fertilization begins with the attachment of sperm to the zona pellucida (ZP), a specialized extracellular matrix that completely surrounds the egg and is essential for reproductive success *in vivo*. Despite the crucial role of the recognition between gametes and the fact that infertility affects more than 50 million couples worldwide, no mutations were until recently identified in the human genes that encode known egg-sperm interaction molecules. This paradoxical situation, which reflected the difficulty of genetically mapping mutations that are clinically silent in heterozygosis but cause sterility when homozygous, has now started to change as a result of the increasing availability of individual exome sequencing. Surprisingly however, the majority of infertility-associated mutations found in egg coat protein genes do not affect major ZP subunits ZP2 or ZP3, which are thought to interact with sperm, but rather ZP1, a minor glycoprotein component that covalently cross-links egg coat filaments into a three-dimensional matrix [1].

In my talk, I will describe a study [2] that started from the characterization of a ZP1 protein carrying a truncating mutation from infertile patients [3]. The analysis of this mutant unexpectedly suggested that, unlike in the mouse [4], filament cross-linking by ZP1 is crucial to form a stable ZP in human. Based on this finding, we mapped the function of ZP1 to its N-terminal ZP-N domain (ZP-N1) – an element also found in ZP2 (where it binds sperm) [5,6] as well as ZP4, a structurally-related egg coat component that is absent in the mouse [7]. We then determined crystal structures of ZP-N1 homodimers from a chicken homolog of the protein in different glycosylation states. These revealed that ZP filament cross-linking is highly plastic and can be modulated by ZP1 fucosylation and, potentially, zinc sparks. Moreover, we found that ZP4 ZP-N1 forms non-covalent homodimers in chicken but not human – explaining why ZP4 cannot functionally substitute for ZP1 in infertile patients. Together, these data identify human ZP1 cross-links as a promising target for non-hormonal contraception; at the same time, our work highlights the potential of structural biology as a tool to address key questions in reproductive medicine.

[1] Greve, J.M. and Wassarman, P.M. Mouse egg extracellular coat is a matrix of interconnected filaments possessing a structural repeat. *J. Mol. Biol.* 181, 253–264 (1985).

[2] Nishimura K., Dioguardi E., Nishio S., Villa A., Han L., Matsuda T. and Jovine L. Molecular basis of egg coat cross-linking sheds light on ZP1-associated female infertility. *Nat. Commun.* in press (2019).

[3] Huang, H.-L., Lv C., Zhao Y.C., Li W., He X.M., Li P., Sha A.G., Tian X., Papasian C.J., Deng H.W., Lu G.X. and Xiao H.M. Mutant ZP1 in familial infertility. *N. Engl. J. Med.* 370, 1220–1226 (2014).

[4] Rankin T., Talbot P., Lee E. and Dean J. Abnormal zonae pellucidae in mice lacking ZP1 result in early embryonic loss. *Development* 126, 3847–3855 (1999).

[5] Raj I., Sadat Al Hosseini H., Dioguardi E., Nishimura K., Han L., Villa A., de Sanctis D. and Jovine L. Structural basis of egg coat-sperm recognition at fertilization. *Cell* 169, 1315–1326.e17 (2017).

[6] Avella M.A., Baibakov B. and Dean, J. A single domain of the ZP2 zona pellucida protein mediates gamete recognition in mice and humans. *J. Cell Biol.* 205, 801–809 (2014).

[7] Conner S.J., Lefièvre L., Hughes D.C. and Barratt C.L.R. Cracking the egg: increased complexity in the zona pellucida. *Hum. Reprod.* 20, 1148–1152 (2005).

## KN10 | ONE MILLION STRUCTURES AND COUNTING: THE JOURNEY, THE INSIGHTS, AND THE FUTURE OF THE CAMBRIDGE STRUCTURAL DATABASE

Ward, Suzanna (The Cambridge Crystallographic Data Centre, Cambridge, GBR)

This year marks a huge milestone in structural chemistry – the sharing of one million organic and metal-organic crystal structures. The creation of the Cambridge Structural Database (CSD) to collate and distribute these structures is truly a worldwide effort, with the CCDC curating and enhancing data from hundreds of thousands of crystallographers.

The beginnings of the CSD can be traced back to 1965 with J.D. Bernal and Olga Kennard, who had the vision and foresight to understand that the collective use of data would lead to the discovery of new knowledge. Their vision has certainly come to fruition today. Both the structures and the database itself have evolved significantly since then, as has its value to scientists worldwide.

Major advances in technology, new structure solution methods, extraordinary developments in computing, and significant advancements in chemistry have all had a dramatic effect on how the CSD has evolved. The growing size, complexity and diversity of the database coupled with the development of new ways to search and analyse the CSD has meant that new insights have been possible, and the data can be used in ways that would once have been unimaginable. This presentation will take a journey through the CSD, highlighting significant milestones in the development of the database and the science that it has enabled. It will conclude by exploring some future possibilities, how the CSD and the field of crystallography might evolve and asking what role structural data may play in the future with the sharing and analysis of the next million structures.

## KN11 | ENHANCING THE SUCCESS OF MACROMOLECULAR CRYSTALLIZATION

Chayen, Naomi (Imperial College London, London, GBR)

Obtaining high quality crystals is a pivotal step to facilitate the structure determination of proteins and other biological macromolecules by X-ray crystallography.

In spite of momentous progress in the miniaturisation, automation and analysis of crystallisation experiments, the production of useful crystals still presents a major barrier to structure determination [1,2].

There is no 'magic bullet' that will guarantee well-diffracting crystals, hence rational approaches leading to the development of new and improved technologies for obtaining high quality crystals is of crucial importance to progress.

This talk will present strategies for increasing the chances of success and highlight a variety of practical methods that resulted in successful crystallization when standard procedures had failed [3-7]. The methods involve active influence and control of the crystallization environment in order to lead crystal growth to the desired result. Many of the techniques are automated for adaptation to high throughput mode and several have been patented and commercialised.

[1] Chayen and Saridakis (2008) *Nature Methods* 5, 147-153.

[2] Chayen, Helliwell and Snell *Macromolecular Crystallization and Crystal Perfection*, Oxford Univ. Press, Oxford, UK (2010).

[3] Saridakis et al. (2011) *Proc. Natl. Acad. Sci. U.S.A.* 108, 11081-11086.

[4] Khurshid et al. (2014) *Nature Protocols* 9, Pages: 1621–1633.

[5] Govada et al. (2016) *Scientific Reports Nature Publishing Group* 6:20053.

[6] Nanev et al. (2017) *Scientific Reports Nature Publishing Group* 7:35821.

[7] Govada and Chayen (2019) *Crystals* 9(2), 106.

## **KN12 | APPLICATION TO E-PRECESSION IN TRANSMISSION ELECTRON MICROSCOPE: PHASE AND ORIENTATION MAP**

Véron, Muriel (Grenoble Institute of Technology, FRA)

## **KN13 | MESOPHASE MIRABILIS. THE LIPID CUBIC PHASE AS A SYSTEM FOR INVESTIGATING MEMBRANE PROTEINS**

Caffrey, Martin (Trinity College Dublin, Dublin 4)

Membrane Structural and Functional Biology Group, School of Medicine and School of Biochemistry and Immunology, Trinity Biomedical Sciences Institute, Trinity College Dublin, Dublin 2, Ireland.

The lipid cubic phase (in meso) method for crystallizing membrane proteins has to its credit close to 700 structure records in the Protein Data Bank. Progress in applying the method reflects innovations that relate to protein enrichment, direct biophysical and biochemical characterization and refolding in the mesophase and in situ data collection at X-ray synchrotrons and free electron lasers using microcrystals. These varied methods will be reviewed and examples will be provided where they have contributed to the determination of high-resolution crystal structures of membrane integral enzymes, receptors, transporters and carriers with insights into mechanism of action and the prospect of drug discovery.

Funded in part by Science Foundation Ireland.

## KN14 | CAPTURING FUNCTIONAL NANOSTRUCTURES AND THEIR INTERFACES WITH NEUTRON TOTAL SCATTERING

Page, Katharine (Oak Ridge National Laboratory / University of Tennessee, Knoxville, Oak Ridge, USA)

It is widely recognized in catalysis, fuel cell and battery chemistry, bio- and geochemical processes, and a host of additional functional materials areas that unique properties and characteristics are governed by intricate structural-chemical relationships. Uncovering the identity and role of locally ordered motifs, including those of surface species and interfaces, remains a challenge because experimental tools to observe materials at atomic length-scales, in relevant operating conditions, or within sufficiently fine time scales are limited. We present our efforts to apply and extend neutron total scattering and related probes towards capturing the interplay of crystal chemistry and functionality in nano- and nanostructured materials. Examples include: (1) exploration of internal dipole-dipole ordering in ferroelectric nanocrystals, demonstrating the enhancing effects of cubic particle shape and polar surface termination; (2) investigation of layered manganese oxide structures, where interlayer water molecules, hydrogen bonding, and the nature of vacancies/intercalants strongly impact catalytically and electrochemically active variants; and (3) demonstrated abilities to probe the structure and dynamics of gas-solid interfaces in catalytic materials, where the signatures of interfacial species are enhanced through neutron isotope contrast techniques. These examples improve understanding of technologically and geologically significant materials and highlight a broader theme of our research aimed at extracting crystal structure models from experimental data with the detail needed to guide and validate modern nanoscale theories, and design new and improved functional materials. Current challenges and future opportunities in this arena will be discussed.

## KN15 | CHANGING TIMES IN STRUCTURAL VIROLOGY

Stuart, Dave (University of Oxford, Old Road Campus, GBR)

## KN16 | UNUSUAL MAGNETIC ORDERINGS FROM THE INTERPLAY OF TRIANGULAR TOPOLOGY AND MAGNETIC ANISOTROPY

Damay, Françoise (Laboratoire Léon brillouin, Gif sur Yvette Cedex, FRA)

Stackings of perfect triangular planes of transition metal ions offer a vast playground when looking for complex magnetic orderings, as geometrically induced frustration of antiferromagnetic exchanges leads to non-collinear magnetic structures; moreover, in the case of strong easy-axis magnetic anisotropy, magneto-elastic effects are often at play to lift the degeneracy of the magnetic ground state and allow the system to order. Several examples will be given, in which magnetic exchanges and/or magnetic anisotropy are tuned, to achieve multiferroic properties in particular, or to investigate more theoretical aspects of condensed matter, such as the well-known Transverse Field Ising Model. Those examples also illustrate the invaluable technique that is neutron scattering, both elastic and inelastic, especially when combined with the modelling tools that are available today.

## MS01: Serial Approaches in Crystallography

---

### MS01-01 | ELUCIDATION OF NO REDUCTION MECHANISM IN SOLUBLE NO REDUCTASE BY TIME-RESOLVED CRYSTALLOGRAPHY WITH PHOTOSENSITIVE CAGED COMPOUND

Tosha, Takehiko ; Nomura, Takashi (University of Hyogo, Akoh, JPN); Sugimoto, Hiroshi ; Shiro, Yoshitsugu (University of Hyogo, Akoh, JPN); Kubo, Minoru (University of Hyogo, Akoh, JPN)

Structural determinations of reaction intermediates in metalloenzyme-catalyzed reactions are great challenge in structural biology and very useful for understanding chemistry in metalloenzymes. Recently developed technique called serial femtosecond X-ray crystallography (SFX), in which micro-crystals are continuously supplied to the X-ray irradiation spot, using an X-ray free electron laser facility, SACLA, enabled time-resolved X-ray crystallography (TR-SFX). Since the X-ray laser from SACLA is a  $\sim 10$  fs pulse, it is possible to carry out a pump-probe type experiment. Here, we applied this method for the observation of enzymatic reaction using photosensitive caged-compound. We utilized a heme-containing enzyme, P450nor, which catalyzes a following reaction;  $2\text{NO} + \text{NADH} + \text{H}^+ \rightarrow \text{N}_2\text{O} + \text{H}_2\text{O} + \text{NAD}^+$ . Photosensitive caged-NO which release two equivalent of NO upon UV irradiation was utilized as a trigger and NO source for the P450nor reaction. We performed TR-SFX at SACLA, and obtained an intermediate structure, substrate NO-bound form, at 20 ms after the UV illumination<sup>1</sup>. Current results suggest that TR-SFX with photosensitive caged compound is promising approach for the characterization of the reactions catalyzed by metalloenzymes. In the presentation, characterization of next process of the P450nor-catalyzed reaction will be shown.

[1] Capturing an initial intermediate during the P450nor enzymatic reaction using time-resolved XFEL crystallography and caged substrate. T. Tosha et al., Nat. Commun. 2017, 8, 1585.

## MS01-02 | A TALE OF TWO SOURCES: SERIAL CRYSTALLOGRAPHY AT SYNCHROTRONS AND XFELS

Owen, Robin (Diamond Light Source, Didcot, GBR)

It was the best of times, it was the worst of times, it was the age of wisdom, it was the age of foolishness, it was the epoch of belief, it was the epoch of incredulity, it was the season of Light, it was the season of Darkness, it was the spring of hope, it was the winter of despair, we had everything before us, we had nothing before us, we were all going direct to Heaven, we were all going direct the other way—in short, the period was so far like the present period, that some of its noisiest authorities insisted on its being received, for good or for evil, in the superlative degree of comparison only. [1]

There are synchrotrons with a continuous wave available to many; XFELs with a pulsed wave available to few. At both sources it is clear that things in general are settled for ever. Developments at each source can, however, complement and advance experiments at the other. The need for serial delivery at XFELs has driven the emergence of serial synchrotron crystallography for example, while synchrotrons can provide lessons in reducing sample consumption and increasing throughput.

I will describe fixed target serial delivery methods developed and implemented at SACLA and DIAMOND, illustrating the gains that can be realised using a multi-source approach, through its application to identification and tracking of low-dose radiation driven effects in metalloproteins and high-throughput ligand binding studies.

[1] Dickens, C. (1859)

## **MS01-03 | SWISSMX: A NEW, VERSATILE INSTRUMENT FOR FIXED TARGET FEMTOSECOND MACROMOLECULAR CRYSTALLOGRAPHY AT SWISSFEL**

Martiel, Isabelle; Pradervand, Claude; Panepucci, Ezequiel; Zamofing, Thierry; Nass, Karol; Marsh, May; Vera, Laura; Huang, Chia-Yin; Olieric, Vincent; Buntschu, Domini); Gobbo, Alexandre; Kaelin, Rober); Thominet, Vincen); Leonarski, Fil); Hora, Jan; Glettig, Wayn); Lemke, Henri; Mozzanic); Redford, Sophi); Schmitt, Bern); Bunk, Oliv); Abela, Rafael; Wang, Meitian; Pedrini, Bill (Paul Scherrer Institute, Villigen, CH)

The SwissMX instrument for fixed target macromolecular crystallography (MX) provides robust and efficient data collection of challenging samples, in particular thanks to arbitrarily defined motions for prelocated sample supports. SwissMX consists of a fast and precise scanning stage enclosed in a chamber, and a high-throughput sample changer. Both cryogenic and room temperature data collection are possible. We summarize here the current and up-coming capabilities of the SwissMX instrument, based on examples from the commissioning phase at SwissFEL.

## MS01-04 | ULTRA-FAST RASTER-SCANNING SYNCHROTRON SERIAL MICRO-CRYSTALLOGRAPHY

Fuchs, Martin R. (National Synchrotron Light Source II, Upton, USA); Shi, Wuxian (National Synchrotron Light Source II, Upton, USA); Gao, Yuan (National Synchrotron Light Source II, Upton, USA); Andi, Babak (National Synchrotron Light Source II, Upton, USA); Jakoncic, Jean (National Synchrotron Light Source II, Upton, USA); Lazo, Edwin O. (National Synchrotron Light Source II, Upton, USA); Soares, Alexei (National Synchrotron Light Source II, Upton, USA); Myers, Stuart F. (National Synchrotron Light Source II, Upton, USA); Skinner, John (National Synchrotron Light Source II, Upton, USA); Liu, Qun (National Synchrotron Light Source II, Upton, USA); Bernstein, Herbert (School of Natural Science, Amherst, MA, USA); Nazaretski, Evgeny (National Synchrotron Light Source II, Upton, USA); McSweeney, Sean (National Synchrotron Light Source II, Upton, USA)

In recent years, serial micro-crystallography at synchrotrons has seen increases in beamline brightness and new sample delivery methods, greatly widening its appeal to structure determination of challenging proteins. The crystallography beamlines at National Synchrotron Light Source-II [1] provide beams of unprecedented brightness, stability and versatility. The Frontier MX-beamline, FMX, delivers  $3.5 \times 10^{12}$  ph/s at  $1 \text{ \AA}$  into a  $1 \times 1.5 \mu\text{m}$  focus. Its flux density surpasses current MX-beamlines by up to two orders of magnitude, with dose rates  $>500 \text{ MGy/s}$ .

The high dose rates cut measurement times for raster-scanning serial crystallography from hours to under a minute. To harness this new dose rate regime, we built the FastForward Goniometer, a high-speed goniometer with a unique XYZ piezo-positioner [2]. We obtained datasets up to the Eiger16M's maximum frame rate of 750Hz, with a shutter-open time under 20s [3]. Collecting rotation images, using a cluster analysis processing pipeline, required fewer crystals than still image measurements. Micro-patterned sample holders minimize background-scattering, enabling S-SAD phasing from  $5 \mu\text{m}$  crystals [3]. The high speed allows scanning any crystal distribution, to avoid loading crystals into a fixed-raster grid.

Complementing this for LCP-grown crystals, we established serial crystallography with a high-viscosity extrusion injector in a collaboration with Arizona State University [4].

This flexible sample delivery allows tailoring the experiment to a wide array of crystals – adding serial crystallography to the standard repertoire of the synchrotron MX community.

[1] Fuchs et al., AIP Conf Proc 2016

[2] Gao et al., JSR 2018

[3] Guo et al., IUCrJ 2019

[4] Weierstall et al., Nat Commun 2014

## MS01-05 | MEASURING THE DOSE: PHOTOELECTRON ESCAPE IN MICRO-CRYSTALS

Storm, Selina (Diamond Light Source, Didcot, GBR); Crawshaw, Adam (Diamond Light Source, Didcot, GBR); Devenish, Nicholas (Diamond Light Source, Didcot, GBR); Bolton, Rachel (University of Southampton, Southampton, GBR); Tews, Ivo (University of Southampton, Southampton, GBR); Evans, Gwyndaf (Diamond Light Source, Didcot, GBR)

With the trend of using microcrystals and intense microbeams, radiation damage becomes a more pressing problem. Theoretical calculations by Nave and Hill [1] show that the photoelectrons that primarily cause damage can escape very small crystals, reducing the effective dose, an effect which was demonstrated to be pronounced at higher energies [2].

To investigate photoelectronic escape, we measured radiation damage at cryo-temperatures on lysozyme crystals of 5um and 20um mounted on a cryo-EM grid. The data were collected at 13.5 keV and 20.1 keV using a 2M CdTe Pilatus and were analysed with DIALS [3] and RADDOSE3D [4]. Our data indicate a longer crystal lifetime for smaller crystals and support the theory of photoelectron escape.

[1] Nave & Hill, (2005), J. Synchrotron Rad. 12, 299–303

[2] Sanishvili et al. (2011), PNAS 108(15), 6127–6132

[3] Winter et al. (2018), Acta Cryst. D74, 85-97

[4] Zeldin et al. (2013), J. Appl. Cryst. 46, 1225-1230

## MS01-P01 | DATA ANALYSIS INFRASTRUCTURE FOR SERIAL CRYSTALLOGRAPHY

### EXPERIMENTS AT THE EUXFEL

Dall'Antonia, Fabio; Beg, Marijan; Bergemann, Martin; Bielecki, Johan; Bondar, Valerii; Carinan, Cammille; Costa Junior, Raul; Danilevski, Cyril; Ehsan, Wajid; Esenov, Sergey; Fabbri, Riccardo; Flucke, Gero; Fullà-Marsà, Daniel; Giovanetti, Gabriele; Göries, Dennis; Hickin, David; Jarosiewicz, Tobiasz; Kamil, Ebad; Kirienko, Yury; Kirkwood, Henry; Klimovskaia, Anna; Kluyver, Thomas; Mamchyk, Denys; Michelat, Thomas; Mohacsi, Istvan; Parenti, Andrea; Rosca, Robert; Rück, Denivy; Santos, Hugo; Schaffer, Robert; Silenzi, Alessandro; Spirzewski, Michal; Trojanowski, Sebastian; Youngman, Christopher; Zhu, Jun; Mancuso, Adrian P.; Fangohr, Hans; Brockhauser, Sandor: European XFEL GmbH, Schenefeld, GER

Data analysis applications for serial crystallography and single-particle imaging experiments at the European X-ray Free Electron Laser (EuXFEL) instrument SPB/SFX [1] range from near real-time data processing for experimental optimisation to computationally intensive offline analysis on stored data long after the experiment. Online analysis tasks for providing fast feedback during experiments are integrated into the EuXFEL-distributed control software Karabo [2]. Alternatively, user groups can connect their own processing tools to the Karabo-Bridge, a client software that provides a network interface to the data streams. Currently a C<sup>++</sup> and a Python API are available.

For offline analysis, we provide the Karabo-Data Python package [3] to help users working with the experimental data stored at EuXFEL. It provides routine analysis capabilities and data file conversion to be compatible with the most common analysis tools applied within the serial crystallography community.

Another field of active development is the implementation and integration of semi-automated high-performance computing crystallography pipelines to support user groups with computationally intensive offline data analysis tasks. We also aim at providing a full set of standard data analysis “sandbox” tools with example datasets and Jupyter notebooks to combine documentation and tutorials for less experienced users.

We present an overview of the available tools and interfaces with a selection of use-cases for online and offline data processing.

[1] A. P. Mancuso *et al.* (2019), *J. Synchrotron Rad.* 26:3, 1-17.

[2] B. Heisen *et al.* (2013), *Proc. ICALEPCS2013*, 1465-8.

[3] H. Fangohr *et al.* (2018), *Proc. ICALEPCS2017*, 245-52.

## MS01-P02 | TREXX: A NEW ENDSTATION FOR SERIAL TIME-RESOLVED CRYSTALLOGRAPHY AT PETRA-III

von Stetten, David (EMBL, Hamburg, GER); Agthe, Michael (Universität Hamburg, 22607, GER); Bourenkov, Gleb (EMBL, Hamburg, GER); Polikarpov, Maxim (EMBL, Hamburg, GER); Horrell, Sam (Universität Hamburg, Hamburg, GER); Yorke, Briony (University of Leeds, Leeds, GBR); Beddard, Godfrey S. (University of Edinburgh, Edinburgh, GBR); Nikolova, Marina (EMBL, Hamburg, GER); Karpics, Ivars (EMBL, Hamburg, GER); Gehrman, Thomas (EMBL, Hamburg, GER); Meyer, Jochen (EMBL, Hamburg, GER); Ristau, Uwe (EMBL, Hamburg, GER); Fiedler, Stefan (EMBL, Hamburg, GER); Monteiro, Diana C.F. (Hauptman-Woodward Medical Research Institute, Buffalo, USA); Trebbin, Martin (University at Buffalo, Buffalo, USA); Mehrabi, Pedram (Max Planck Institute for Structure and Dynamics of Matter, Hamburg, GER); Schulz, Eike (Max Planck Institute for Structure and Dynamics of Matter (MPSD), Hamburg, GER); Tellkamp, Friedjof (Max Planck Institute for Structure and Dynamics of Matter, Hamburg, GER); Miller, R. J. Dwayne (Max Planck Institute for the Structure and Dynamics of Matter, Hamburg, GER); Huse, Nils (Universität Hamburg, Hamburg, GER); Pearson, Arwen R. (Universität Hamburg, Hamburg, GER); Schneider, Thomas R. (EMBL, Hamburg, GER)

The EMBL operates two beamlines (P13 and P14) for macromolecular crystallography at the PETRA-III synchrotron in Hamburg. In addition, a new endstation (P14-2, TREX) for serial time-resolved crystallography has been in operation in a second hutch at the far end of P14 since October 2018. For this endstation, the P14 X-ray beam is refocussed with a compound refractive lens (CRL) transfocator to provide a 15x10  $\mu\text{m}$  beam with a flux of about  $2 \times 10^{12}$  photons/s at 12.7 keV. In order to be able to accommodate different microcrystal sample delivery systems suitable for serial crystallography, P14-2 is not equipped with a goniometer, but instead with a basic beam conditioning unit (BCU) that provides an on-axis viewer, beam shaping apertures, a fully motorized beamstop, and a scintillator for visualisation of the X-ray beam. For time-resolved pump/probe experiments, a laser system (355 and 532 nm) for initiating reactions is built into the setup, such that the laser and X-ray beams are almost parallel at the sample position, which facilitates alignment of the beams using the on-axis viewer. First experiments have yielded promising results using patterned chips as well as microfluidic flow cells. To be able to reach sub-millisecond timescales in time-resolved experiments, the Hadamard technique [1] will be employed in the future, either by gating the detector or alternatively by modulating the X-ray beam.

[1] Song BH et al., J Mater Chem A, 2015

## MS01-P03 | MICROMAX - NEW POSSIBILITIES FOR SERIAL CRYSTALLOGRAPHY

Ursby, Thomas (MAX IV Laboratory, Lund University, Lund, SWE); Milas, Mirko (MAX IV Laboratory, Lund University, Lund, SWE); Mueller, Uwe (MAX IV Laboratory, Lund University, Lund, SWE)

The beamline MicroMAX that will be in user operation in 2022 will provide unique possibilities to use serial crystallography methods to study macromolecular structures. The foreseen main applications are studies of microcrystals, structures at room temperature and with time-resolved techniques. This will in most cases imply using multicrystal data collections with different serial approaches. The X-ray beam will be variable in size from 1 micrometer and up and will have  $10^{13}$  photons/second in monochromatic mode and up to  $10^{15}$  photons/second using a wider energy bandpass mode. The beamline will cover the energy range 5 - 20 keV with a more limited energy range for the wider energy bandpass. The experiment setup will be flexible offering different sample delivery methods. The beamline will have two experiment hutches of which one can be used independently for preparing experiments while the other is used for data collections. Initially one hutch will be commissioned. The beamline will also include instrumentation for oscillation data collection of single crystals with automatic sample exchange. There will be an additional laboratory for working with different sample environments and a laboratory for sample preparation. Additional infrastructures including a bio-laboratory and resources for data handling and analysis are shared with other beamlines. The MAX IV Laboratory 3 GeV storage ring is the first multi-bend achromat ring in operation with already one macromolecular crystallography beamline, BioMAX, in operation. Different serial crystallography methods are already used at BioMAX.

## MS01-P04 | METALJET SOURCE ENABLING ADVANCED PROTEIN CRYSTALLOGRAPHY

Espes, Emil (Excillum AB, KISTA, SWE); Hållstedt, Julius (Excillum AB, Kista, SWE)

X-ray diffraction data from protein and bio crystals are typically of a much lower resolution and quality compared to measurements in chemical crystallography. This is mainly due to large molecules, poor crystalline quality in combination with very light atoms embedded in large amount of water. At the same time, unit cell size is extremely large and thus the Bragg reflections are very closely packed together. Protein crystallographers must rely on the strongest X-ray sources to combat the issues of air sensitivity, small crystals, weakly diffracting and densely packed reflections. Traditionally, a high brilliance synchrotron has been used to measure full protein data leading for structure determination, whilst home laboratory instruments have been used only for protein screening to identify the preferred crystals for measurement at the synchrotron. High brightness X-ray compact sources, such as the MetalJet have not only improved crystal screening but also made it possible to obtain publishable data from extremely difficult experiments such as GPCR membrane proteins. In this communication we will show a number of different examples how the MetalJet X-ray source can be a game changer for home laboratory macro molecular diffraction.

## MS01-P05 | SERIAL CRYSTALLOGRAPHY AT THE ESRF EXTREMELY BRILLIANT SOURCE: THE ID29 UPGRADE PROJECT

de Sanctis, Daniele (ESRF - The European Synchrotron, Grenoble, FRA)

The next generation of storage rings, such as the ESRF Extremely Brilliant Source will be able to produce an electron beam with a greatly reduced horizontal emittance. This will result in a small source size and a low divergent X-ray beam that will increase the brilliance by an order of magnitude and will permit to focalise the full beam on a submicron spot on the sample.

The delivered photon flux density will open new opportunities for serial crystallography experiments at room temperature and will permit to define new paradigms for data collection methods. Room temperature data collections and very short exposure time will be used to exploit time-dependant conformational changes that are relevant for biological mechanisms.

The EBSL8 project consists in the upgrade of the MAD beamline ID29, to become a new facility entirely dedicated to Serial Synchrotron Crystallography. The end-station will be equipped with a dedicated sample preparation laboratory and a data processing area.

The beamline is designed to deliver an X-ray beam of unequalled characteristics on different sample delivery systems and to collect still diffraction images from microcrystals. We will present the design of the new beamline and the current status of the EBSL8 project and discuss future plans and new scientific opportunities.

## MS01-P06 | BETTER SAUC -- IMPROVING THE IDENTIFICATION OF NEARBY CELLS

Bernstein, Herbert J. (Ronin Institute for Independent Scholarship, Upton, NY, USA)

As we move to faster data collection from very large numbers of small crystals, rapid identification of previously solved structures that have similar cells can be helpful both in identifying molecular replacement candidates and in sorting out images that may be suitable for clustering [1][2]. The PDB/COD cell search program SAUC has been speeded up by use of the new S6 cell metric [3] [4].

[1] V. Ramraj, G. Evans, J. M. Diprose, R. M. Esnouf. "Nearest-cell: a fast and easy tool for locating crystal matches in the PDB." *Acta Cryst.* D68:12 (2012): 1697 -- 1700.

[2] K. J. McGill, M. Asadi, M. T. Karakasheva, L. C. Andrews, H. J. Bernstein. "The geometry of Niggli reduction: SAUC—search of alternative unit cells." *J. Appl. Cryst.* 47:1 (2014): 360 -- 364.

[3] L. C. Andrews, H. J. Bernstein, N. K. Sauter. "Selling reduction versus Niggli reduction for crystallographic lattices." *Acta Cryst.* A75:1 (2019): 115 -- 120.

[4] L. C. Andrews, H. J. Bernstein, N. K. Sauter. "A space for lattice representation and clustering." *Acta Cryst.* to appear.

## MS01-P07 | OPTIMIZED DESIGN FOR NEW SCIENTIFIC OPPORTUNITIES IN MACROMOLECULAR CRYSTALLOGRAPHY AT THE FUTURE MICROFOCUS XAIRA BEAMLINE

Garriga, Damià (ALBA Synchrotron Light Facility, Cerdanyola del Vallès, ESP); González, Nahikari (ALBA Synchrotron Light Facility, Cerdanyola del Vallès, ESP); Colldelram, Carles (ALBA Synchrotron Light Facility, Cerdanyola del Vallès, ESP); Sics, Igors (ALBA Synchrotron Light Facility, Cerdanyola del Vallès, ESP); Marcos, Jordi (ALBA Synchrotron Light Facility, Cerdanyola del Vallès, ESP); Campmany, Josep (ALBA Synchrotron Light Facility, Cerdanyola del Vallès, ESP); Nicolas, Josep (ALBA Synchrotron Light Facility, Cerdanyola del Vallès, ESP); Juanhuix, Judith (ALBA Synchrotron Light Facility, Cerdanyola del Valles, ESP)

The BL06-XAIRA microfocus macromolecular crystallography (MX) beamline at the ALBA synchrotron light facility is foreseen to enter into user operation in 2021 and complies with a long-standing request from the scientific community. Three main MX scientific cases will be covered by XAIRA. Primarily XAIRA will tackle projects in which the macromolecular crystals only grow in micrometric sizes, possess a reduced diffracting power or require complex data collection strategies. To push these experiments the new beamline aims at providing a stable X-ray beam at 1 Å wavelength with a micrometric size ( $3 \times 1 \mu\text{m}^2$  FWHM), focused with plane-elliptical mirrors bent through Alba in-house Nanobenders and equipped with dynamical figure error correctors. The beam might be further reduced down to  $1 \times 1 \mu\text{m}^2$  by limiting the horizontal primary source produced by a prefocusing horizontal mirror.

The BL06-XAIRA beamline is also intended to cope with native phasing methods, which exploit the anomalous scattering of light metals naturally occurring in proteins. To this aim, the beamline will deliver 3 Å wavelength (4 keV) photons and the end station will include a helium atmosphere surrounding the sample up to the detector to reduce the background at the detector.

The new beamline will finally cater fixed-target serial crystallography experiments by providing a flexible sample environment, which will be operational also in air. To cover the need of high flux to perform these experiments, the photon wavelength will be selected using a double multilayer pseudo-channel cut monochromator, installed in addition to the channel-cut Si(111) monochromator.

## MS01-P08 | DEVELOPMENT OF SERIAL MILLISECOND CRYSTALLOGRAPHY AT BIOMAX

### BEAMLINE

Shilova, Anastasiia (MAXIV, Lund, SWE); Nan, Jie (MAXIV, Lund, SWE); Mueller, Uwe (MAXIV, Lund, SWE)

With the advent of X-ray free electron laser sources (XFELs), serial crystallography - a new method of data collection where thousands of crystals are delivered to the beam and exposed in random orientation at room temperature - was developed. During last years, serial crystallography was successfully implemented at synchrotron radiation sources (*serial synchrotron crystallography-SSX*) using a variety of sample presentation procedures. Due to the increased pulse length (around 100 ps) and reduced brilliance of synchrotron sources as compared to XFELs, SSX does not allow performing time-resolved experiments on ultra-fast time scales (fs-ps), nor to collect data from macromolecular nano-crystals. Nevertheless, SSX is well adapted to perform room temperature experiments on micro-crystals and to study events occurring on the ms-s timescale. Reduced costs, flexibility of the set-up and increased beamtime availability makes synchrotrons very attractive instruments to perform SSX experiments.

This work describes an implementation of different sample delivery approaches to perform room temperature serial crystallography at BioMAX beamline of recently inaugurated MAXIV facility. One of them is high viscosity injector-based serial millisecond crystallography, similar to the experiments with injectors originally developed at XFELs, where a continuous stream containing micro-crystals is injected into the microbeam. An alternative solid support approach is based on raster scanning micro-crystals deposited on silicon nitride membranes or capton based Xtal tools with very low background. Also, future perspectives for the dedicated serial crystallography beamline MicroMAX providing a very small but parallel and intense X-ray beam, will be discussed.

## MS01-P09 | P11 AT PETRA III: A VERSATILE BEAMLINE FOR SERIAL AND HIGH-THROUGHPUT CRYSTALLOGRAPHY

Burkhardt, Anja (DESY, Hamburg, GER); Crosas, Eva (DESY, Hamburg, GER); Saouane, Sofiane (DESY, Hamburg, GER); Hakanpää, Johanna (DESY, Hamburg, GER); Günther, Sebastian (DESY, Hamburg, GER); Pakendorf, Tim (DESY, Hamburg, GER); Reime, Bernd (DESY, Hamburg, GER); Meyer, Jan (DESY, Hamburg, GER); Urbschat, Jakob (DESY, Hamburg, GER); Fischer, Pontus (DESY, Hamburg, GER); Stübe, Nicolas (DESY, Hamburg, GER); Meents, Alke (DESY, Hamburg, GER)

Beamline P11 is dedicated to structural investigations of biological samples from atomic to micrometer length scales. The beamline provides two state-of-the-art endstations: a crystallography experiment which is operated between 5.5 and 28 keV and in user operation since 2013 [1] and an X-ray microscope which is currently under construction.

Basis of beamline design was to make full use of the excellent source properties of PETRA III and to deliver most of the photons into micrometer-sized focal spots at both experimental endstations. The beamline is equipped with two X-ray mirror systems which allow for tailoring the beam properties to the experimental requirements: A large parallel beam can be generated for bioimaging experiments, *e.g.* ptychography combined with X-ray fluorescence element mapping, and single crystal structure determination from large unit cell systems. A highly intense microbeam with more than  $10^{13}$  ph/s in a  $4 \times 9 \mu\text{m}^2$  focal spot ( $v \times h$ , FWHM) is available for the investigation of microcrystals and serial crystallography experiments using jets, tape-drives [2] or solid sample supports [3].

The rapid automatic sample changer and the Pilatus 6M detector in place provide a very stable setup for high-throughput crystallography. The implementation of a Roadrunner II goniometer, an Eiger2 16M detector and a 'pink' beam option will further reduce data collection times and will allow for screening whole ligand libraries in short time.

[1] Burkhardt et al., EPJ Plus 131:56 (2016);

[2] Beyerlein, IUCrJ 4, 439 (2017);

[3] Roedig et al., Sci. Rep. 5, 10451 (2015).

## MS01-P10 | LIQUID APPLICATION METHOD FOR TIME-RESOLVED ANALYSES (LAMA) BY SERIAL SYNCHROTRON CRYSTALLOGRAPHY

Mehrabi, Pedram (Max-Planck-Institute for Structure and Dynamics of Matter, Hamburg, GER); Schulz, Eike (Max Planck Institute for Structure and Dynamics of Matter (MPSD), Hamburg, GER); Agthe, Michael (Universität Hamburg, Hamburg, GER); Horrell, Sam (University of Hamburg, Hamburg, GER); Bourenkov, Gleb (EMBL Hamburg, Hamburg, GER); von Stetten, David (EMBL Hamburg, Hamburg, GER); Leimkohl, Jan-Philipp (Max Planck Institute for Structure and Dynamics of Matter (MPSD), Hamburg, GER); Schikora, Hendrick (Max Planck Institute for Structure and Dynamics of Matter (MPSD), Hamburg, GER); Schneider, Thomas (EMBL Hamburg, Hamburg, GER); Pearson, Arwen R. (University of Hamburg, Hamburg, GER); Tellkamp, Friedjof (Max Planck Institute for Structure and Dynamics of Matter (MPSD), Hamburg, GER); Miller, R. J. Dwayne (Max Planck Institute for the Structure and Dynamics of Matter, Hamburg, GER)

With the advent of serial crystallography and new light sources time-resolved crystallography has recently seen a resurgence. Since the majority of enzymatic reactions occur in the range hundreds of milliseconds, synchrotron light sources are a clear alternative to XFELs for these systems due to their wide distribution and their simpler experimental setup.

Previously we combined an established fixed target mount (chip), with a novel “*Hit And REturn*” (HARE) approach for data acquisition. Due to the HARE algorithm time delays from a few milliseconds to several minutes can be acquired with no increase in data collection time [1].

Extending the HARE approach with the use of a piezo droplet injector circumvents the use of physical or chemical triggers for reaction initiation, such as temperature-, pH jumps, or light pulses for systems that are not naturally amenable to light activation. Our “*Liquid Application Method for time-resolved Analysis*” (LAMA) in combination with the HARE approach uses minimal amounts of protein (1-3 mg) and ligand (1.5-3  $\mu$ l) per time point, making this scheme tremendously material efficient. Using Glucose Isomerase as a model system we were able to observe an open ring conformation of a glucose molecule in a reaction that spans several minutes in the enzyme. These newly developed methods are highly flexible, can be easily adapted to synchrotron and XFEL beamlines and are amenable to the majority of enzymatic systems, which now become accessible to time-resolved studies.

[1] Schulz, E. C., Mehrabi, P., Müller-Werkmeister, H.M. *et al Nat. Meth.* - 2018 doi:10.1038/s41592-018-0180-

## MS01-P101 -LATE | P14 TREXX: FIRST RESULTS FROM THE JURASSIC BEAMLIN

Horrell, Sam (Universität Hamburg, Hamburg, GER); Agthe, Michael (Universität Hamburg, Hamburg, GER); von Stetten, David (EMBL-Hamburg, Hamburg, GER); Mehrabi, Pedram (Max Planck Institute for Structure and Dynamics of Matter, Hamburg, AUT); Schulz, Eike-Christian (Max Planck Institute for Structure and Dynamics of Matter, Hamburg, GER); Bourenkov, Gleb (EMBL-Hamburg, Hamburg, AUT); Nikolova, Marina (EMBL-Hamburg, Hamburg, AUT); Karpics, Ivars (EMBL-Hamburg, Hamburg, GER); Fiedler, Stefan (EMBL-Hamburg, Hamburg, GER); Tellkamp, Friejof (Max Planck Institute for Structure and Dynamics of Matter, Hamburg, GER); Miller, R. Dwayne (Max Planck Institute for Structure and Dynamics of Matter, Hamburg, GER); Huse, Nils (Universität Hamburg, Hamburg, AUT); Pearson, Arwen R. (Universität Hamburg, Hamburg, AUT); Schneider, Thomas R. (EMBL-Hamburg, Hamburg, AUT)

T-REXX, a new end station co-developed by EMBL-Hamburg, and the Universität Hamburg on beamline P14 at PETRA III has recently entered user operation (March 2019), and aims to provide easy access to time-resolved measurements. Key to the T-REXX vision is that the end station is situated in a second experimental hutch, downstream from P14's main experimental hutch. This enables the time-resolved experiment team to optimise their set-up offline (photo-activation or rapid mixing) and make maximum use of their beamtime, as well as minimising the impact on P14 user operation. We present first results from T-REXX experiments over the last year, demonstrating the capabilities of the beamline. Beamtime is available through the usual EMBL SMIS application portal both via the T-REXX BAG and through rapid access.

## MS02: Fragment/Ligand Binding: Tools Development

---

### MS02-01 | HOW NOT TO SHOOT YOURSELF INTO THE FOOT

Rupp, Bernhard (Medical University Innsbruck, Innsbruck, AUT)

Protein-ligand complexes are some of the most interesting structures studied by crystallography and often support hypotheses directly relevant to therapeutic drug discovery and human health. The atomic models are the result of the interpretation of reconstructed electron density, which for the ligands is often weak or spurious, and the interpretation thus subject to discussion: telling what is from what is not becomes non-trivial. Some of the often concurrent fundamental difficulties regarding binding sites are that (i) out of principle, binding sites are only asymptotically fully occupied; (ii) by design, binding sites will seek to capture anything that is even remotely similar to the desired ligand; (iii) ligands are often present in multiple or varying conformations; and (iv) ligands displace solvent that is often close in density to that of the purportedly bound molecules. Particularly the latter points, in combination with certain features of the implementation of bulk solvent corrections can lead to self-deception and non-parsimonious modelling of ligands.

## MS02-02 | POLDER MAPS: IMPROVING OMIT MAPS FOR LIGAND BUILDING AND VALIDATION

Liebschner, Dorothee (Lawrence Berkeley National Laboratory, Berkeley, USA)

In macromolecular crystallography, electron density maps are used to build and validate models. In particular, OMIT maps [1] are a common tool to verify the presence of ligands. The simplest way to compute an OMIT map is to exclude the ligand from the model, update the structure factors and compute a residual map. If the ligand is present in the crystal structure, it is expected that the electron density of the ligand will appear as positive features in the OMIT map. However, this is complicated by the flat bulk-solvent model [2], which postulates constant electron density in the areas of the unit cell that are not occupied by the atomic model. Therefore, if atoms are removed from the model, the region where they were modeled will be filled with bulk-solvent, and if the density arising from the omitted atoms is weak, then the bulk-solvent model may obscure it further.

A possible solution to this problem is to prevent bulk-solvent from entering the OMIT regions, which may improve the interpretative power of residual maps. This approach is called polder (OMIT) map [3] and the tool is implemented in the software package Phenix. Polder OMIT maps can be particularly useful for displaying weak densities of ligands. Several examples are presented where polder OMIT maps show clearer features than conventional OMIT maps.

[1] Bhat & Cohen, *J. Appl. Cryst.* **17**, 244–248 (1984)

[2] Jiang & Brünger, *J. Mol. Biol.* **243**, 100–115 (1994)

[3] Liebschner *et al.*, *Acta Cryst. D*, **73**, 148–157 (2017)

## MS02-03 | FRAGMAX - THE NEW FRAGMENT SCREENING FACILITY OF MAX IV

### LABORATORY

Mueller, Uwe (MAX IV Laboratory, Lund, SWE); Lima, Gustavo (MAX IV Laboratory, Lund, SWE); Knecht, Wolfgang (Lund University, Lund, SWE); Logan, Derek (Saromics Biostructures AB, Lund, SWE); Sjögren, Tove (AstraZeneca, Mölndal, SWE)

Crystallographic fragment screening is a powerful tool to probe the functional surface of proteins and to assist pharmaceutical industry within their drug discovery process to identify small molecular binders. FragMAX is currently developed to a high throughput x-ray diffraction fragment screening facility using BioMAX, the first MX beamline at MAX IV Laboratory. FragMAX entails the infrastructure to produce apo-target protein crystals, to incubate those crystals with fragments via soaking or co-crystallisation, harvest the crystals and submit them to an screening experiment at BioMAX. The derived experimental data are automatically processed and further analysed in order to provide a initial ranking for potential hits to the user automatically. All experimental and analysis data are stored within a dedicated data base and are presented within an in house developed user interface. FragMAX is developed and operated in close coloboration with the Lund protein production platform LP3, AstraZeneca and Saromics Biostructures as a user facility for academic and industrial users.

## MS02-04 | AUTOMATED, REMOTE-CONTROLLED LIGAND SCREENING PIPELINES FOR DRUG DISCOVERY

Cornaciu, Irina (EMBL Grenoble, Grenoble, FRA); Marquez, Jose A. (EMBL Grenoble, Grenoble, FRA)

The evolution of automation in structural biology over the last decade has facilitated the study of challenging targets and extended the use of protein crystallography in drug discovery. However, manual crystal mounting and processing are time-consuming and resource-intensive, thus limiting the efficiency and productivity of small molecule screening in the context of drug design. We have developed a new approach called CrystalDirect™, enabling automated crystal soaking, harvesting, and cryo-cooling. This technology offers a remarkable level of control during sample processing, making crystal mounting a more reliable and systematic operation that can easily deal with problematic crystal morphologies and sizes. It also provides higher tolerance to organic solvents during soaking experiments. Thanks to the CrystalDirect™ technology, we are providing access to an integrated pipeline including high-throughput crystallization, crystal soaking and mounting, and synchrotron data collection into a fully automated and continuous workflow. This pipeline can support very-fast analysis of small molecule-target complexes as well as easy and efficient large-scale fragment screening and is available to scientists from both in industry and academia. All the experimental information and results are tracked in real-time through CRIMS (the Crystallization Information Management System). Automated data processing through the Global Phasing Pipedream software suite - including data reduction, phasing, ligand fitting, and automated refinement - enables real-time data processing. The capabilities of this new technology and the experience gained from the use of these automated pipelines for ligand screening will be discussed.

## MS02-05 | STRUCTURE-BASED FRAGMENT SCREENING ON DYNAMIN GTPASE DOMAIN

Taberman, Helena (Macromolecular Crystallography (HZB-MX), Helmholtz-Zentrum Berlin für Materialien und Energie, Berlin, GER); Wollenhaupt, Jan (Macromolecular Crystallography (HZB-MX), Helmholtz-Zentrum Berlin für Materialien und Energie, Berlin, GER); Metz, Alexander (Institut für Pharmazeutische Chemie, Philipps-Universität Marburg, Marburg, GER); Klebe, Gerhard (Institut für Pharmazeutische Chemie, Philipps-Universität Marburg, Marburg, GER); Daumke, Oliver (Max-Delbrück-Centrum for Molecular Medicine, Berlin, GER); Weiss, Manfred S. (Macromolecular Crystallography (HZB-MX), Helmholtz-Zentrum Berlin für Materialien und Energie, Berlin, GER)

Structure-based fragment screening concerns finding small organic molecules to occupy the active site or allosteric binding sites of a target protein. Fragments are low molecular weight compounds increasing the probability of finding hits, which can be optimised to higher affinity compounds to probe the biology of the target and to find drug candidates [1]. X-ray crystallography has been shown to be the most reliable and sensitive tool for detecting binders even with very low affinity [2].

The HZB fragment screening workflow provides libraries, for example, a novel 96 fragment F2X Entry Screen based on maximum structural and chemical diversity, tools for sample handling, as well as fully automated data processing and refinement for efficient evaluation of results. Furthermore, downstream optimization of hits with a web-server is used to identify purchasable, versatile follow-up compounds. Here, this workflow is used for finding fragments occupying the GTP binding site or allosteric sites of dynamin.

Dynamin is a multi-domain GTPase, which has a critical role in membrane fission in the endocytic pathway, for example, in cell signalling and nutrient intake [3]. Dynamin forms a helical oligomer around the neck of the invaginating clathrin-coated vesicle, and GTP hydrolysis introduces conformational changes inducing the fission of the tubular membrane. The fission-activity is entirely dependent on the nucleotide binding and hydrolysis, making the GTPase domain potential target for drug development studies.

[1] Murray, C.W. *et al.* (2012) *Trends Pharmacol. Sci.* 33, 224.

[2] Schiebel, J. *et al.* (2016) *Structure* 24, 1398.

[3] Faelber, K. *et al.* (2012) *Structure* 20, 1621.

## MS02-P01 | STRUCTURE-BASED DRUG DESIGN TO TACKLE DISORDERS OF HAEM

### BIOSYNTHESIS

Arruda Bezerra, Gustavo (University of Oxford - Structural Genomics Consortium, Oxford, GBR); Bailey, Henry (University of Oxford, Oxford, GBR); Foster, William (University of Oxford, Oxford, GBR); Rembeza, Elzbieta (University of Oxford, Oxford, GBR); Yue, Wyatt (University of Oxford, Oxford, GBR)

X-linked protoporphyria (XLP) is caused by gain-of-function mutations in erythroid-specific aminolevulinate synthase (ALAS2), the first and rate-limiting enzyme in haem biosynthesis. Additionally, inherited defects downstream of ALAS2 in the haem biosynthesis pathway of erythroids lead to several porphyrias. In this work, we aim to exploit inhibition of ALAS2 as substrate reduction therapy, whereby decreasing the influx of toxic haem intermediates in the pathway would ameliorate the aforementioned disorders. We have established a structural biology pipeline to generate milligram quantities of recombinant human ALAS2, suitable for large-scale crystallisation experiments. Hundreds of ALAS2 crystals were each soaked with a chemical fragment from a custom library, and their respective co-crystal structures were solved, in a week's timeframe, to identify fragments bound to ALAS2 as starting points for inhibitor design. From solving 295 crystal structures of ALAS2, we identified 19 bound fragments clustered in three different regions of the ALAS2 dimer interface, close to the C-terminal extension that is unique among higher eukaryotes. We have developed biophysical assays to evaluate the binding of fragments to ALAS2 and their impacts on enzyme activity, guiding us in future cycles of medicinal chemistry and drug design. As an obligate dimer, the ALAS2 active site is formed by residues from two subunits. This feature provides opportunities to develop inhibitors from fragments located at the dimer interface, aimed at disrupting protein dimerization. Additionally, fragments interacting with the mobile C-terminal extension, a key region for catalysis, could be developed into inhibitors aimed at restricting substrate access to the active site.

## MS02-P02 | GETTING THE MOST FROM YOUR CRYSTALS THROUGH THE FULL AUTOMATION OF COMPLEX EXPERIMENTS

Bowler, Matthew (European Molecular Biology Laboratory, Grenoble, FRA)

has been a key development in macromolecular crystallography allowing the remote operation of beamlines and the ability to screen thousands of samples and process the subsequent deluge of data. The full automation of data collection, where the process of mounting, locating, characterising and collecting data is left entirely to algorithms, is possible on the ESRF beamline MASSIF-1 [1,2]. In contrast to existing automatic beamlines, where automation is confined to mounting and loop centring of samples, MASSIF-1 uses mesh scans and characterisation combining data gathered during the process, such as crystal volume, with user input to calculate optimised strategies. The ability to make complex decisions at multiple stages of the location and characterisation phases mean that any sample can be processed in a wide variety of mounts allowing even the most challenging samples to be treated automatically.

The full automation of data collection from crystals of biological macromolecules opens the door to large scale screening for all laboratories without significant person hour investments. Projects from screening large numbers of highly variable crystals to small molecule fragment campaigns are now possible with thousands of data sets collected in a consistent manner day and night, often with better quality than human operators [3]. In combination with developments in the robotic mounting and soaking of crystals [4] we envision that the future of macromolecular crystallography is the provision of a fully automated high throughput service able to rapidly produce high quality structural models and screen for potential therapeutic and probe molecules.

## MS02-P03 | PANDDA: EXTRACTING LIGAND-BOUND PROTEIN STATES FROM CONVENTIONALLY UNINTERPRETABLE CRYSTALLOGRAPHIC ELECTRON DENSITY

Pearce, Nick (University of Utrecht, Utrecht)

X-ray crystallography is routinely used to determine the structures of small molecules (ligands) bound to proteins. Extended studies such as fragment screening probe the protein surface and elucidate information regarding the protein's flexibility, potentially stabilising rare alternative conformations, identifying allosteric sites or revealing cryptic pockets. However, ligand identification and modelling in X-ray crystallography remains subjective and error-prone: disordered solvent molecules give rise to uninterpretable or misleading density, and ordered solvent may obscure the binding of a low-occupancy ligand. The PanDDA method [1] enables weak signal to be objectively identified in crystallographic datasets through the simultaneous analysis of an ensemble of electron density maps from different crystals. In the case of ligand screening, the PanDDA method enables the identification of weakly-bound ligands by contrasting individual datasets against the background of "ground-state" datasets. After applying a correction to remove this background "noise", the density for partial-occupancy ligands is revealed, enabling weakly-bound ligands to be confidently modelled. The PanDDA method has been extensively tested in the context of crystallographic fragment screening at the XCHM facility at Diamond Light Source, and greatly increases the amount of structural information that can be derived from these experiments, compared to traditional data-analysis methods.

[1] Pearce, N. M. *et al.* A multi-crystal method for extracting obscured crystallographic states from conventionally uninterpretable electron density. *Nat. Commun.* 8, 15123 doi: 10.1038/ncomms15123 (2017).

## MS02-P04 | A CASE STUDY OF FRAGMENT SCREENING: PROTEIN KINASE A AND PIM1-KINASE

Heine, Andreas (Philipps-Universität Marburg, Marburg, GER); Siefker, Christof (Philipps-Universität Marburg, Marburg, GER); Klebe, Gerhard (Philipps-Universität Marburg, Marburg, GER)

Fragment screening may be used as an alternative to high-throughput screening of large compound libraries in the drug discovery process. Here, small molecules (<300 Da) contained in small libraries of a few hundred compounds are used in the screening process. An in-house developed fragment library was used to screen protein kinase A (PKA) and PIM1-kinase. As an initial screen we applied a thermal shift assay (TSA) to identify suitable fragments for follow-up crystallographic screening. High hit rates were obtained for both kinases in the TSA assay. These fragments were then selected for further crystallographic analysis to obtain detailed binding modes for the achieved protein-fragment complexes. Also here, high hit rates were obtained. Low fragment overlap was observed for both kinases, indicating that fragments might be selective binders. TSA screening results and observed fragment binding motifs will be discussed.

## MS02-P05 | NEW FULLY AUTOMATIC MEASUREMENT MX BEAMLINE BL45XU AT SPRING-8

Mizuno, Nobuhiro (JASRI, Hyogo, JPN); Baba, Seiki (JASRI, HYOGO, JPN); Hirata, Kunio (RIKEN SPring-8 Center, HYOGO, JPN); Yamashita, Keitaro (The University of Tokyo, Tokyo, JPN); Masunaga, Takuya (JASRI, HYOGO, JPN); Hasegawa, Kazuya (JASRI, HYOGO, JPN); Nakamura, Yuki (JASRI, HYOGO, JPN); Murakami, Hironori (JASRI, HYOGO, JPN); Kawano, Yoshiaki (RIKEN SPring-8 Center, HYOGO, JPN); Ueno, Go (RIKEN SPring-8 Center, HYOGO, JPN); Furukawa, Yukito (JASRI, HYOGO, JPN); Takeuchi, Tomoyuki (JASRI, HYOGO, JPN); Yamasaki, Hiroshi (JASRI, HYOGO, JPN); Yumoto, Hirokatsu (JASRI, HYOGO, JPN); Senba, Yasunori (JASRI, HYOGO, JPN); Ohashi, Haruhiko (JASRI, HYOGO, JPN); Yamamoto, Masaki (RIKEN SPring-8 Center, HYOGO, JPN); Kumasaka, Takashi (JASRI, HYOGO, JPN)

BL45XU operated as the SAXS beamline at SPring-8 was re-designed and reconstructed as fully automatic macromolecular crystallography (MX) beamline in response to the need for high flux, high-throughput data collection in recent years. We have been developing the unattended data collection system to make data collection rapid by eliminating complicated operation and the risk of human error.

From the commissioning results of the optics, the beamline can provide the beam size ranging from  $5.0 \mu\text{m} \times 5.0 \mu\text{m}$  -  $100 \mu\text{m} \times 100 \mu\text{m}$  with a photon flux of  $5.2 \times 10^{12}$  -  $1.8 \times 10^{13}$  photons/s at 12.4 keV. The beam size can be changed to fit crystal volume for the suitable data collection scheme.

The ZOO system [1] achieves fully automated data collection in various experimental schemes, such as the normal rotation, the multiple small wedge, the helical and SSROX schemes. The system exploits the double-arm SPACE and the beamline control software BSS. ZOO system conducts data collection with user defined experimental parameters including desired absorbed dose. Initial tests of the system at BL45XU was successfully done and the system is ready for user operation from the end of May 2019. The beamline BL45XU benefits MX users in worldwide to collect datasets just by shipping crystals here. This can save travel fee and time for coming to Japan for the sake of high resolution data collection at SPring-8.

[1] K. Hirata, *et al.*, *Acta Cryst. D*, 2019, 75, 138-150

## MS02-P06 | FRAGMENT SCREENING PROJECT MANAGEMENT WEB APPLICATION - FRAGMAX

Lima, Gustavo (MAX IV Laboratory, Lund, SWE)

Fragment screening as a tool for drug discovery has been extensively explored by industry and academia. In this method, small molecules are used to probe protein surface and pockets, identifying weak binders that can be developed into hits. While fast data collection is now widely available in modern photon sources, it generates a few terabytes of data within a single data collection, hindering data manipulation. At MAX IV, we are developing an OS-independent Web Application focused on Fragment Screening project management that gathers information from target and fragment library from ISPyB and present users with full data collection reports. The web-app provides data processing (XDSAPP, autoPROC, XIA2/Dials and XIA2/XDS), refinement (BUSTER, FSPipeline, Dimple) and ligand fitting (RhoFit, Phenix LigFit) from a simple and intuitive interface relying on MAX IV HPC, requiring minimal resource on user's computer for displaying a WebGL application. This tool allows 1-click automatic data analysis as well as advanced parameters input, with several pipelines to choose including Pipedream (Global Phasing) and PanDDA, and electron density visualisation through UglyMOL. In our current stage of development, we ran three commissioning projects whereas one using a custom fragment library. More information about FragMAX and our web-app is available at BioMAX webpage.

## MS02-P103 LATE | LONG-WAVELENGTH NATIVE SAD PHASING AT BL13-XALOC ENABLED BY THE PRESENCE OF AN HELIUM CONE

Calisto, Barbara (ALBA synchrotron, Barcelona, ESP); Gil-Ortiz, Fernando (ALBA Synchrotron, Cerdanyola del Vallès, ESP); Carpena, Xavier (ALBA Synchrotron, Cerdanyola del Vallès, ESP); González, Nahikari (ALBA Synchrotron, Cerdanyola del Vallès, ESP); Álvarez, José María (Alba Synchrotron, Cerdanyola del Vallès, ESP); Valcárcel, Ricardo; Ávila, José (Alba Synchrotron, Cerdanyola del Vallès, ESP); Villanueva, Jorge (Alba Synchrotron, Cerdanyola del Vallès, ESP); Juanhuix, Judith (Alba Synchrotron, Cerdanyola del Vallès, ESP); Boer, Roeland (Alba Synchrotron, Cerdanyola del Vallès, ESP)

The MX beamline BL13-XALOC (ALBA synchrotron, Barcelona, Spain) possesses a high-intense collimated beam and allows tailoring the beam size to the size of the sample, most commonly micrometer-sized crystals, by defocusing the beam thus minimizing the scattering background.

Native phasing for determining crystal structures of novel macromolecules is a very promising technique as it exploits the small anomalous signal from naturally occurring elements (atomic number  $< 20$ ). In particular, measuring the anomalous signal from sulfur at long wavelengths is very appealing because the macromolecules or the crystals need no further derivatization. However, at long wavelengths, X-ray absorption by air and sample dramatically hinders data collection. To partially overcome the air absorption drawback at BL13-XALOC we designed and commissioned a removable Helium Cone (HeC) consisting on a fixed-size chamber filled with helium gas. Comparison of data collected on tetragonal crystals of Hen egg white lysozyme at 2.7 Å (respective energy 4.6 keV) in absence or presence of the HeC highlights the benefit of measuring data for S-SAD phasing in a helium-enriched atmosphere and its most striking effect is observed in the S-substructure determination. The fully-automatic crystal structure determination of lysozyme collected at 2.1 Å (respective energy 6.0 keV) is also discussed.

For more challenging cases we urge MX beamline users to fully and rationally use the advanced data collection strategies available at BL13-XALOC. These include workflows designed by Global Phasing Ltd, and locally implemented strategies such as inverse-beam, low dose, multiple orientations and multiple crystal averaging.

## MS03: Crystallisation and Biophysical Characterisation

---

### MS03-01 | PROTEIN THERMODYNAMIC PARAMETERS TO UNDERSTAND AND GUIDE CRYSTALLISATION

Saridakis, Emmanuel (National Centre for Scientific Research "Demokritos", Athens)

Stability of protein molecules is recognised as a crucial parameter for their crystallisation. Melting (denaturation) temperature  $T_m$ , or thermostability, is an easily obtainable and widely used measure of stability, and choice of source organisms, ligands and co-factors of the protein to be crystallised is often guided by an increase in  $T_m$ . Thermodynamic stability ( $\Delta G$  of unfolding), consisting of enthalpic and entropic components due to intramolecular interactions, internal degrees of freedom and hydration effects, is a more complex and less well-studied parameter. We have shown using Differential Scanning Calorimetry, that common crystallisation salts can drastically influence the thermodynamic stability of proteins and these changes are not always reflected in the corresponding  $T_m$  shifts.

The Hofmeister series has for decades been associated with protein crystallisation. However, apart from the well-known effects of the various ions with respect to protein solubility (which have low predictive power for crystallisation), no specific "Hofmeister effects" have been discovered that could rationalise the preference of different proteins for specific salts with respect to crystallisation. Relating various components of thermodynamic stability to the presence of ions found at different points on the Hofmeister series, one such potential correlation is proposed.

Obtaining reliable thermodynamic data from a sufficiently large and varied set of proteins, needed for establishing meaningful, general conclusions and strategies, is a difficult task, especially when we do not know in advance what to look for. This talk will therefore mostly aim to give some general directions and ideas for future research.

## MS03-02 | HIGH-THROUGHPUT THERMAL STABILITY APPROACHES FOR SAMPLE OPTIMIZATION

Garcia, Maria (EMBL, Hamburg, GER)

Protein stability in detergent or membrane-like environments is the bottleneck for structural studies on integral membrane proteins (IMP). Irrespective of the method to study the structure of an IMP, detergent solubilization from the membrane is usually the first step in the workflow. Here, we describe a simple, high-throughput screening method to identify optimal detergent conditions for membrane protein structural biology. We apply differential scanning fluorimetry in combination with scattering upon thermal denaturation to study the unfolding of integral membrane proteins. Nine different prokaryotic and eukaryotic membrane proteins were used as test cases to benchmark our detergent screening method. Our results show that it is possible to measure the stability and solubility of IMPs by simple diluting them from their initial solubilization conditions into different detergents. We were able to identify groups of detergents with characteristic stabilization and destabilization effects for transporters. We further show that fos-choline detergents may lead to membrane protein unfolding/destabilization. Finally, we determined which thermodynamic parameters are most reliable as indicators for IMP stability.

## MS03-03 | IN NUMBERS: INITIAL SCREENING AT THE MRC-LMB PROTEIN CRYSTALLIZATION FACILITY

Gorrec, Fabrice (MRC Laboratory of Molecular Biology, Cambridge, GBR)

A strategy to bypass some difficulties related to protein crystallisation is to use a large initial screen containing many different initial crystallization conditions. We have adopted such a strategy at the MRC Laboratory of Molecular Biology (MRC-LMB, Cambridge, UK), combined with an automated vapour-diffusion sitting drop technique for setting up crystallization droplets. To further simplify the process when dealing with large screens, crystallization plates pre-filled with reservoir solutions are made ready to be used. Here, I present some statistics collected over a decade of running the facility at MRC-LMB: the numbers of plates pre-filled with initial screening kits, the resulting costs and the final yields of quality diffraction crystals. The numbers also highlight a recent decline in pre-filled plates consumption caused by the advent of a competing method that eliminates the need for crystallization – cryo-electron microscopy (cryo-EM) –, which now regularly produces atomic models comparable in quality to those obtained by X-ray crystallography.

## MS03-04 | BIOPHYSICAL METHODS TO AID PROTEIN CRYSTALLIZATION IN A PHARMACEUTICAL SETTING

Öster, Linda (AstraZeneca, Mölndal, SWE)

In the Protein Structure group at AstraZeneca, the overall goal is to support projects with structures. A key success factor is the quality control of the proteins of interest using a range of techniques including mass spectrometry, size exclusion chromatography and gel electrophoresis. The goal is to ensure high purity and homogeneity before entering crystallization trials. To learn more about the protein and further verify the quality we often use Dynamic Light Scattering and Thermal shift assay and these methods are also used to identify the best formulation.

As the great majority of our structures are protein-compound structures we are highly dependent on biophysical characterization of the protein-compound interaction. The purpose is to verify that we work on compounds that show specific binding, to rank the different compounds and identify differences in binding mode to further guide our crystallization trials. This is particularly important in a project during the hit identification campaign when many compounds from different sources are considered interesting but could be false positives. The methods used vary, and include Nuclear Magnetic Resonance, Surface Plasmon Resonance, Isothermal Titration Calorimetry and Thermal Shift Assay, and often several methods are in use for one project. Furthermore, we have seen that it can be very powerful to use biophysical methods to ensure compound binding to our specific crystallization construct and/or in the actual soaking/co-crystallization condition.

We will present our way of working including different project examples on how biophysical techniques have aided our efforts to support projects with structures.

## MS03-05 | HIGH-THROUGHPUT STABILITY SCREENING OF INTEGRAL MEMBRANE PROTEINS

Mlynek, Georg (University of Vienna MPL, Wien, AUT); Nagy, Michael (University of Vienna MPL, Wien, AUT); Koston, Julius (Department für Strukturbiologie und Computational Biology, AUT); Kotov, Vadim (University Medical Center Hamburg-Eppendorf (UKE), Hamburg, AUT); Marlovits, Thomas C. (University Medical Center Hamburg-Eppendorf (UKE), Hamburg, GER); Djinic-Carugo, Kristina (University of Vienna MPL, Vienna, AUT)

Structural analysis has changed the way we look at our world. The foremost technique used in structural analysis is X-ray crystallography. When applied on biological macromolecules the major bottleneck of this method is the production of well diffracting crystals [1]. As structural biology projects are becoming increasingly challenging, the failure in the crystallization step is even more significant [2]. Therefore, there is a strong requirement for improvement of methods to enable the growth of diffraction quality crystals.

Recently a number of studies tried to capture key factors that affect protein crystallization by either tapping the large amount of data available on macromolecular structures, or by experimental findings [3,4].

Besides the osmotic second virial coefficient ( $B_{22}$ ) [5] and monodispersity of protein solutions [6], protein thermal stability was shown to be a valuable criterion for assessment of crystallization propensity [7,8]. The rationale behind is that higher stability of the protein leads to higher amounts of chemically and conformationally pure samples throughout the purification process [8] and therefore to higher crystallization propensity as shown by systematic analysis of proteins by the high-throughput crystallization facility at EMBL-Grenoble [7].

The focus of this contribution is on the use of (nano)DSF for sample optimization and design of customized crystallization approaches. Additionally, emerging new concepts which employ analysis of thermodynamic data will be discussed.

[1] Derewenda and Vekilov, 2006

[2] Vincentelli and Romier, 2013

[3] Fusco et al., 2014

[4] Price et al., 2009

[5] Wilson and Delucas, 2014

[6] Proteau et al., 2010

[7] Dupeux et al., 2011

[8] Senisterra and Finerty, 2009

## MS03-P01 | STRUCTURAL BASIS OF INACTIVATION OF HUMAN COUNTERPART OF MOUSE MOTOR NEURON DEGENERATION 2 MUTANT IN SERINE PROTEASE HTRA2

Wagh, Ajay (TMC-ACTREC, MUMBAI, IND)

Serine protease HtrA2 (High temperature requirement protease A2), is involved in apoptosis and protein quality control. However, one of its murine inactive mutants, (S276C *aka* mnd2) is associated with motor neuron degeneration 2. Similarly, this conserved mutation in human HtrA2 (hHtrA2) also renders the protease inactive, implicating pathogenicity. However, the structural determinants for its inactivation have not yet been elucidated. Here, using multidisciplinary approach, we studied the structural basis of inactivity associated with this mutation in hHtrA2. Characterization of secondary and tertiary structural properties, protein stability, oligomeric properties and enzyme activity for both wild type and mutant has been performed using biophysical and functional enzymology studies. The structural comparison at atomic resolution has been carried out using X-ray crystallography. While enzyme kinetics showed inactivity, spectroscopic probes did not identify any significant secondary structural changes in the mutant. X-ray crystallographic analysis of the mutant protein at 2Å resolution highlighted the significance of a water molecule that plays important role in mediating intermolecular interactions for maintaining the functional ensemble of the protease. Overall, the crystallographic data, along with biophysical and enzymology studies helped decipher the structural basis of inactivity of hHtrA2S276C, which might pave way toward further investigating its correlation with aberration of normal cellular functions, hence pathogenicity.

## MS03-P02 | THE MORPHEUS PROTEIN CRYSTALLISATION SCREENS

Gorrec, Fabrice (MRC Laboratory of Molecular Biology, Cambridge, GBR)

Three MORPHEUS 96-condition protein crystallisation screens have been formulated de novo to solve novel structures of proteins and macromolecular complexes. Each MORPHEUS screen is a 3D grid where 8 mixes of additives are combined with 4 cryoprotected precipitant mixes and 3 buffer systems (Fig. 1). Systematic approaches were followed to select the reagents and formulate the screens, like the integration of ligands that are found in crystal structures of the Protein Data Bank (PDB). Additives that can act as protein stabilisers, crystal cross-linkers, etc. were integrated to increase the yield of quality diffraction crystals. To formulate the latest screen (MORPHEUS III), small drug-like compounds as additives were integrated (Fig. 1). In addition, pragmatic aspects that enable the steps towards structure solution were taken into consideration. For example, cryoprotectants are integrated for straightforward flash-freezing of crystals. In order to avoid biases towards a specific subset/class of targets, the formulation prototypes were tested on a broad range of samples purified at the LMB.

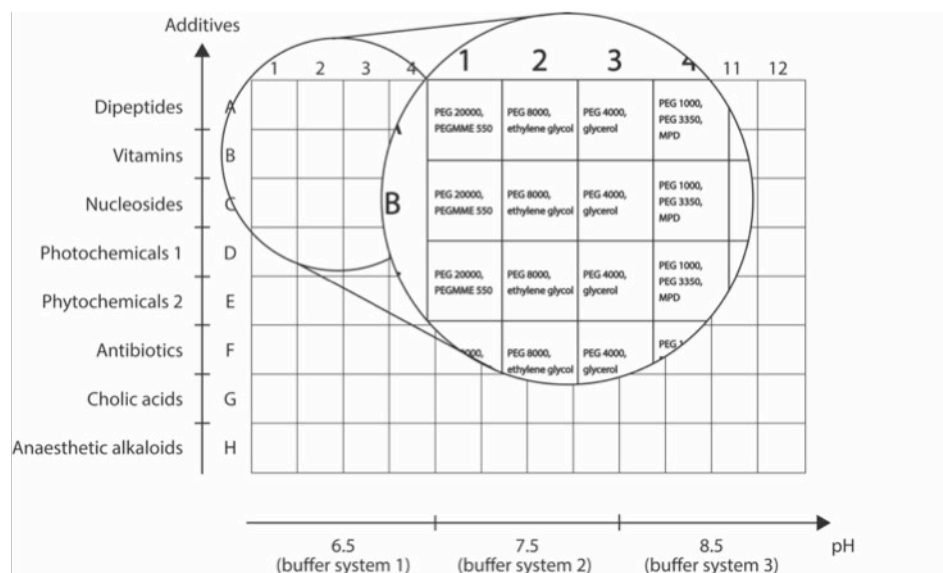


**Figure 1.** MORPHEUS III is a 3D grid screen composed of cryoprotecting precipitant mixes (e.g. PEG 4000 with glycerol), 3 buffer systems (pH 6.5, 7.5 and 8.5) and 8 additive mixes (Dipeptides, Vitamins, Nucleosides, etc.)

[1] Gorrec, F. (2009) The Morpheus protein crystallisation screen. *J Appl Cryst* 7, 1035–1042.

[2] Gorrec, F. (2015) The Morpheus II protein crystallisation screen. *Acta Cryst F* 71, 831–837.

[3] Gorrec, F. and Zinzalla, G. (2018) The MORPHEUS III protein crystallization screen: at the frontier of drug discovery. *IUCr Newsletter* 26.

## MS03-P03 | MOLECULAR INVESTIGATION OF MUSCLE Z-DISC ASSEMBLY CENTERED ON THE COMPLEX HUMAN A-ACTININ ISOFORM-2 AND ZASP

Konstan, Julius (University of Vienna, Vienna, AUT); Ribeiro, Euripides (Baxalta Innovations GmbH-Takeda, Vienna, AUT); Stefania, Valeria (University of Vienna, Vienna, AUT); Djinovic, Kristina (University of Vienna, Vienna, AUT)

In skeletal and cardiac muscle, proteins are organized into sarcomeric units, which lateral borders are delineated by the Z-discs. ZASP is a Z-disc protein involved in the early stage of myofibrillogenesis. It belongs to the Enigma family, which is one of the prevailing protein families involved in dilated cardiomyopathies [1]. ZASP acts as a mediator between cytoskeletal elements and signaling cascades and its presence in the Z-disc is essential for integrity of the sarcomere during contraction [1]. In the Z-disc protein network, ZASP interacts with various binding partners [2;3], in particular with  $\alpha$ -actinin 2 (ACTN2), which is one of the most abundant proteins in the Z-disc, designed to cross-link actin filaments from adjacent sarcomeres [4]. By integrative structural approaches, we aim to explore the function and dynamics of ACTN2-ZASP complex in presence of its binding partners FATZ, titin and F-actin. We show that ZASP binds ACTN2 with nanomolar affinity, which makes the complex amenable for crystallization and subsequent X-ray diffraction experiments. Moreover, preliminary XL-MS analysis delineated the binding sites of ZASP on ACTN2, providing constraints for modeling of solution structure ZASP-ACTN2 complex using the data obtained by small-angle X-ray scattering. We also show that ZASP and ACTN2 can form a ternary complex with the Z-disc protein FATZ-1. Further studies will provide insights into formation and function of the ZASP-ACTN2-FATZ-1 complex as well its organization at molecular level, which might help to reveal essential implications of ZASP in the formation of the Z-disc.

[1] Lin, 2014

[2] Au, 2004

[3] Ming Zheng, 2009

[4] Ribeiro, 2014

## MS03-P04 | CRYSTAL STRUCTURE OF AN ANTI-TUMOUR ANTIBODY IN COMPLEX WITH A TUMOUR-SPECIFIC ANTIGEN

Johannesen, Hedda (University of Oslo, Department of Chemistry, Oslo, NOR); Bjerregaard-Andersen, Kaare (Department of Chemistry - University of Oslo, Oslo, NOR); Heggelund, Julie (Department of Pharmacy - University of Oslo, Oslo, NOR); Løset, Geir Åge (Department of Biosciences - University of Oslo, Oslo, NOR); Krengel, Ute (Department of Chemistry - University of Oslo, Oslo, NOR)

When a healthy cell mutates into a cancerous cell, it exhibits altered gene expression and uncontrolled proliferation. These changes can be exploited by cancer immunotherapy for diagnostic and therapeutic purposes. One such tumour-specific antigen is the *N*-glycolyl GM3 ganglioside that is highly similar to the most common ganglioside *N*-acetyl GM3, differing only by a terminal hydroxyl group instead of a hydrogen. It is located on the cell surface of several different tumours, but not in healthy adult human cells [3] The ganglioside is recognised by a monoclonal IgG antibody named 14F7 that was developed at the Centre for Molecular Immunology in Havana, Cuba [2]. To be able to exploit the favourable properties of 14F7 it would be helpful to know precisely how the *N*-glycolyl GM3 ganglioside and the 14F7 antibody interact at a molecular level. To this end, we have generated recombinant 14F7 in scFv format, expressed the protein using a periplasmic expression system and crystallised the scFv [1]. Here, we show how the ganglioside binds to a groove created by the heavy chain CDR H3-loop.

[1] Bjerregaard-Andersen, K., Johannesen, *et al.*, (2018). Crystal structure of an L chain optimised 14F7 anti-ganglioside Fv suggests a unique tumour-specificity through an unusual H-chain CDR3 architecture. *Scientific Reports*, 8(1), 10836.

[2] Carr, A., *et al.*, (2000). A mouse IgG1 monoclonal antibody specific for *N*-glycolyl GM3 ganglioside recognized breast and melanoma tumors. *Hybridoma*, 19(3), 241-247.

[3] Malykh, Y. N. *et al.*, (2001). *N*-Glycolylneuraminic acid in human tumours. *Biochimie*, 83(7), 623-634.

## MS03-P05 | INVITATION TO PERFORM EXPERIMENTS ON HIGH END INSTRUMENTS: CENTRE OF MOLECULAR STRUCTURE IN BIOCEV

Stránský, Jan (Institute of Biotechnology, Academy of Sciences of the Czech Republic, Vestec u Prahy, CZE); Pavlíček, Jiri (Institute of Biotechnology, Academy of Sciences of the Czech Republic, Vestec, CZE); Charnavets, Tatsiana (Institute of Biotechnology, Academy of Sciences of the Czech Republic, Vestec, CZE); Pompach, Petr (Institute of Biotechnology, Academy of Sciences of the Czech Republic, Vestec, CZE); Vanková, Pavla (Institute of Biotechnology, Academy of Sciences of the Czech Republic, Vestec, CZE); Škultétyová, Lubica (Institute of Biotechnology, Academy of Sciences of the Czech Republic, Vestec, CZE); Schneiderová, Magdalena (Institute of Biotechnology, Academy of Sciences of the Czech Republic, Vestec, CZE); Dohnálek, Jan (Institute of Biotechnology of the Czech Academy of Sciences, Vestec, CZE)

The Centre of Molecular Structure offers wide range of methods of structural biology. It operates in BIOCEV as a part of Institute of Biotechnology, AS CR. CMS consists of facilities devoted to crystallization of macromolecules, X-ray diffraction and scattering, biophysical characterization, advanced mass spectrometry, and infrared and fluorescence spectroscopy. The open access services are provided via the Czech Infrastructure for Integrative Structural Biology (CIISB) and Instruct-ERIC. The essential core equipment consists of 15T-Solarix XR FT-ICR (Bruker Daltonics) for mass spectrometry, D8 Venture (Bruker) diffractometer with MetalJet X-ray source (Excillum), crystallization hotel RI-1000 (Formulatrix), Prometheus and two Monoliths (Nanotemper) for protein characterization and affinity measurements, and Chirascan for circular dichroism measurements. Recently, this instrument portfolio was extended by SAXSPoint 2.0 (Anton Paar) with MetalJet X-ray source (Excillum) for small angle X-ray scattering studies of biomolecules in solution, MALDI TOF mass spectrometer, excimer laser for induced protein modification, and newly equipped room for spectroscopy with Fourier-transformed Infrared (FTIR) spectrometer and a FLS1000 spectrofluorometer. The Centre of Molecular Structure also participate in active development of the instruments and methods.

[1] The Centre of Molecular Structure is supported by: MEYS CR (LM2015043 CIISB); project Czech Infrastructure for Integrative Structural Biology for Human Health (CZ.02.1.01/0.0/0.0/16\_013/0001776) from the ERDF; project Structural dynamics of biomolecular systems (CZ.02.1.01/0.0/0.0/15\_003/0000447) from the ERDF.

## MS03-P06 | CRYSTAL PRODUCTION AND STRUCTURE SOLUTION THANKS TO THE NUCLEATING AND PHASING AGENT, CRYSTALLOPHORE.

Girard, Eric (Institute of Structural Biology IBS, Grenoble, FRA); Engilberge, Sylvain (Institute for Structural Biology (IBS), Grenoble, FRA); Riobé, François (École Normale Supérieure, Lyon, FRA); Santoni, Gianluca (European Synchrotron Radiation Facility, Grenoble, FRA); Wagner, Tristan (Max-Planck-Institute for Marine Microbiology, Bremen, GER); Maury, Olivier (École Normale Supérieure, Lyon, FRA)

Obtaining crystals and solving the phase problem remain major hurdles encountered by bio-crystallographers in their race to get new high-quality structures.

The crystallophore, Tb-Xo4, is a lanthanide complex formed from a molecular cage chelating a terbium atom [2]. We will present the results obtained on about fifteen proteins which show that Xo4 induces unique crystallization conditions and promotes new crystal packing showing that Tb-Xo4 acts an efficient nucleating agent. The crystalline forms promoted by the crystallophore bypass crystal defects often encountered by crystallographers such as low-resolution diffracting samples or crystals with twinning.

We will also present few examples of Tb-Xo4 phasing properties [1,2,4], showing, in particular that the crystallophore is compatible with serial crystallography approaches.

Finally, the versatility of the interactions between Xo4 and the surface of proteins explains its exceptional properties [3] making this molecule a unique tool for simultaneously solving the two major locks of biocrystallography.

[1] Bernhardsgrütter, I., et al. (2018). *Nature Chemical Biology*. 14, 1127–1132.

[2] Engilberge, S., et al. (2017). *Chem. Sci.* 8, 5909–5917.

[3] Engilberge, S., et al. (2018). *Chemistry*. 24, 9739–9746.

[4] Vögeli, B., et al. (2018). *Proceedings of the National Academy of Sciences*. 115, 3380–3385.

## MS03-P07 | STRUCTURAL AND BIOPHYSICAL ANALYSIS OF THE PYRIDOXAL PHOSPHATE SYNTHASE FROM *PLASMODIUM VIVAX*

Ullah, Najeeb (University of Hamburg, Hamburg, GER); Mudogo, Celestin Nzanzu (University Hamburg, Institute for Biochemistry and Molecular Biology, Hamburg, GER); Falke, Sven (University of Hamburg, Hamburg, GER); Perbandt, Markus (University of Hamburg, Hamburg, GER); Wrenger, Carsten (University of São Paulo, São Paulo, BRA); Betzel, Christian (University of Hamburg, Hamburg, GER)

Malaria is still one of the leading causes of morbidity and mortality in developing countries, especially in Africa, but also in Asia and Latin America caused by *Plasmodium* species [1]. A potential drug target and till now mostly not analysed are the structurally unique enzymes of *Plasmodium spec.* involved in vitamin B<sub>6</sub> (pyridoxal 5-phosphate) biosynthesis. Vitamin-B<sub>6</sub> is synthesized by PLP synthase complex consisting of pyridoxal biosynthesis lyase (Pdx1) and glutamine amido-transferase (Pdx2) [2]. Pdx1 exist as hexamer–dodecamer equilibrium in solution formed by two interdigitating rings, each consisting of six Pdx1 molecules and Pdx2 subunits attach to the Pdx1 oligomer [3].

To study structure-function relationship and dynamicity of the Pdx1-Pdx2 complex bacterial expression, purification and biophysical characterization of both proteins were established. Initial characterization of the recombinant proteins was performed by size exclusion chromatography and dynamic light scattering revealing that the Pdx1 protein is monodisperse and dodecameric in solution, whereas, Pdx2 appears as both monomeric and multimeric. The complex formation was analysed by Nanoparticle tracking and small-angle X-ray scattering to obtain insights about the three-dimensional structure in solution.

Further, we obtained crystals of Pdx1 and the complex applying the vapor diffusion method. Diffraction data up to 2.5 Å applying synchrotron radiation were collected and processed.

Details about structure solution, final refinement and interpretation will be presented.

[1] Guédez *et al.* 2012 *Structure*, 20, 172–184.

[2] Sangwoo Kim and Kyung-Jin Kim. *Structural Biology and Crystallization Communications*, F69 (2013), 578–580.

[3] Neuwirth *et al.* 2009, *FEBS Letters*, 583, 2179–2186.

## MS03-P08 | THE ROLE OF ODD IN THE BIOSYNTHESIS OF MEDICALLY IMPORTANT ALKALOIDS

Kot, Ewa (Jerzy Haber Institute of Catalysis and Surface Chemistry Polish Academy of Sciences, Krakow, POL); Kurpiewska, Katarzyna (Jerzy Haber Institute of Catalysis and Surface Chemistry Polish Academy of Science, Krakow, POL); Borowski, Tomasz (Jerzy Haber Institute of Catalysis and Surface Chemistry Polish Academy of Science, Krakow, POL)

Most of drugs belong to substances produced by plants and called with a common name as alkaloids. It is a group of organic compounds with one or more nitrogen atoms which are mostly alkaline. To one of the most popular alkaloids morphine or codeine can be counted; both have similar chemical properties. Morphine is mainly used as a painkiller in heroin addiction or as a counter the effects of opioid overdose. Codeine also can be analgesic but causes the disappearance of feeling hungry [1]. Both, morphine and codeine, belong to alkaloids which are produced in opium poppy (*Papaver somniferum*) at the morphine biosynthesis pathway [2]. The biosynthesis pathways for morphine and berberine engage 2-oxoglutarate dependent dioxygenases (ODD) [3].

Presented project concerns production, crystallization, catalytic characterization and engineering of plant enzymes belonging to the superfamily of 2-oxoglutarate dependent dioxygenases. Three enzymes: codeine O-demethylase (CODM), thebaine 6-O-demethylase (T6ODM) and protopine O-dealkylase (PODA) are under investigation. Two of them, CODM and T6ODM, catalyze penultimate and final steps in morphine biosynthesis, while PODA can catalyze the O,O-demethylenation of methylenedioxy bridges on protopine and on protoberberine alkaloids. All three enzymes can catalyze reactions for a relatively wide range of alkaloids as a substrate [2].

Number of expression and purification experiments were performed so far, including optimization of different bacterial hosts systems, culture conditions and purification protocols. As a result, active and stable enzymes were obtained. Results of biochemical experiments will be presented.

[1] Rang et al., 1995

[2] Runguphan et al., 2012

[3] Farrow and Facchini, 2013

## MS03-P09 | CRYSTAL STRUCTURE OF HUMAN AMACR PROVIDES INSIGHT INTO SUBSTRATE RECOGNITION AND CATALYTIC MECHANISM

Lin, Meng Hsuan (National Taiwan University, Taipei, TWN); Lee, Ming Ying (National Taiwan University, Taipei, TWN); Hsu, Chun-Hua (National Taiwan University, Taipei, TWN)

Human  $\alpha$ -methylacyl CoA racemase (AMACR; P504S) plays a pivotal role in catalysing a key chiral inversion step in the metabolism of branched-chain fatty acid, ibuprofen, and related drugs. Recently, AMACR was found to be overproduced in prostate cancer and has been used as a cancer biomarker and an attractive drug target. Moreover, human AMACR is associated with human diseases because of function deficiency caused by single base mutation such as the SNP mutants S52P and L107P. Here, we report the crystal structures of human AMACR in apo form and in complex with a substrate analog, isobutyrylCoA (IBCoA). The structure of human AMACR presents an interlocked dimeric architecture. In addition, the structural information delineates the residues involved in catalysis and identifies a hydrophobic plateau for acyl or aromatic groups binding. For the binding effect of large side-chain substrates, the evidence implies that the hydrophilic side-chain would not contribute to binding. Finally, based on the results of MD simulation and in vivo thermal shift assay, we find that L107P and S52P mutants located very close to the binding pocket, and S52P are less stable than wildtype AMACR. These studies will shed new light on the drug development and understanding of AMACR function, and thus will be of great research and therapeutic value.

## MS03-P10 | SEC-SAXS ANALYSIS OF OLIGOMERIC STATES OF HUMAN NKR-P1 WITH ITS LIGAND LLT1 IN SOLUTION

Skalova, Tereza (Institute of Biotechnology CAS, v.v.i., Vestec, CZE); Blaha, Jan (Department of Biochemistry, Faculty of Science, Charles University, Prague, CZE); Stransky, Jan (Institute of Biotechnology, The Czech Academy of Sciences, v.v.i., Vestec, CZE); Koval, Tomáš (Institute of Biotechnology of the Czech Academy of Sciences, Vestec, CZE); Duskova, Jarmila (Institute of Biotechnology, The Czech Academy of Sciences, v.v.i., Vestec, CZE); Skorepa, Ondrej (Department of Biochemistry, Faculty of Science, Charles University, Prague, CZE); Kalousková, Barbora (Department of Biochemistry, Faculty of Science, Charles University, Prague, CZE); Pazicky, Samuel (Department of Biochemistry, Faculty of Science, Charles University, Prague, CZE); Vanek, Ondrej (Department of Biochemistry, Faculty of Science, Charles University, Prague, CZE); Dohnálek, Jan (Institute of Biotechnology of the Czech Academy of Sciences, Vestec, CZE)

Natural killer (NK) cells are a type of lymphocytes able to kill tumour and virally infected cells. Human NKR-P1 is one of the plenty of receptors anchored in the membrane of the cell and LLT1 is its ligand on a partner cell. Both NKR-P1 and LLT1 have extracellular part with C-type lectin like fold.

The extracellular domains of NKR-P1 and LLT1 have been expressed and characterised.<sup>1,2</sup> The crystal structures of LLT1 oligomers have been published<sup>3</sup> and structures of NKR-P1 and NKR-P1:LLT1 have been deposited. We discovered that NKR-P1 and LLT1 form a chain in the crystal structure of the NKR-P1:LLT1 complex. In order to study the form of the interaction of NKR-P1 with LLT1 in solution, we have performed small angle X-ray scattering coupled with size exclusion chromatography (SEC-SAXS). The SEC-SAXS intensity curve shows two distinct peaks, the smaller one corresponding to higher oligomers and the larger one corresponding basically to the NKR-P1:LLT1 complex. However, deeper analysis showed that in fact, each point of the SEC-SAXS curve corresponded to a combination of several oligomeric states.

[1] Bláha, J. et al (2015). *Protein Expr. Purif.* 109, 7-13.

[2] Bláha, J. et al (2017). *Protein Expr. Purif.* 140, 36-43.

[3] Skálová, T. et al (2015). *Acta Cryst.* D71, 578-591.

This study was supported by BIOCEV (ERDF CZ.1.05/1.1.00/02.0109), CIISB4HEALTH (ERDF CZ.02.1.01/0.0/0.0/16\_013/0001776), Czech Science Foundation (15-15181S and 18-10687S), MEYS of the Czech Republic (LTC17065 within the COST Action CA15126), Charles University (SVV260427/2018, GAUK 161216), and Instruct (R&D pilot scheme APPID 56 and 286).

## MS03-P11 | A RELIABLE AND VERSATILE TOOL FOR HIGH-END IN-HOUSE STRUCTURAL STUDIES

Mrosek, Michael (Bruker AXS GmbH, Karlsruhe, GER); Smith, Vernon (Bruker AXS GmbH, Karlsruhe, GER); Adam, Martin (Bruker AXS GmbH, Karlsruhe, GER)

In house X-ray structure determination has seen steady improvements, now being capable of handling ever smaller and weaker diffracting samples. Modern diffraction systems address the need for increased throughput that is essential e.g. for ligand binding studies in the pharmaceutical industry. Performance of these systems has increased so much that protein crystals that previously required synchrotron data collection, now often can be collected in house significantly improving the speed of the projects moving forward.

Here we demonstrate that the D8 VENTURE platform is capable of collecting data of protein crystals with a broad array of challenging properties. High-performance X-ray sources, such as the  $\mu$ S DIAMOND, and the PHOTON III—a large active-area photon-counting mixed-mode detector—provide data to high resolution of samples with extremely large unit cells or very small crystal sizes. During development special attention has been given to keeping the system virtually maintenance free and minimizing running costs.

We will also present a number of examples that all benefit from new and advanced system features that were added to achieve an unprecedented ease of use:

- Automated visual and X-ray based crystal centering,
- Improved crystal visualisation features for both, cryo and *in situ* applications
- Extended import and export functionalities to modern crystallographic pipelines.
-

## MS03-P12 | ALL-IN-ONE SAMPLE HOLDER FOR MACROMOLECULAR CRYSTALLOGRAPHY

Feiler, Christian (Helmholtz Zentrum Berlin, Berlin, GER); Wallacher, Dirk (Helmholtz Zentrum Berlin, Berlin, GER); Weiss, Manfred (Helmholtz Zentrum Berlin, Berlin, GER)

Various types of sample holders have been developed and are widely used in protein X-ray crystallography [1, 2].

Collection of diffraction data from a single protein crystal involves a number of manual handling step, including crystal fishing, cryo protection and mounting onto an individual sample holder. Numerous enhancements have been done in order to improve many handling steps, including *in-situ screening* to characterize well-diffracting crystals [3, 4].

We have developed a novel type of sample holder, which acts as an all-in-one platform. As a replacement of commonly used cover slips, it supports all steps in the workflow from crystal setup to data collection without any direct crystal handling. Further, crystal manipulation is realized in-place and does not require any handling steps of individual crystals.

Diffraction data collection can be carried out at both, ambient and cryogenic temperature. Additionally, the sample holder is compatible with the SPINE standard format and can therefore be used with automatic sample mounting robots. Finally, with using the new type of sample holder, the number of crystals / dewar can be drastically increased.

The patent pending sample holder can be used on both, 22- and 18-millimeter standard 24-well plates. Auxiliary tools support a straightforward workflow, using the novel sample holder with a minimized chance of damaging sensitive crystalline material.

[1] Papp, G. *et al.* doi:10.1107/S2059798317013742

[2] Pflugrath, J.W. doi:10.1107/S2053230X15008304

[3] le Maire, A. *et al.* doi:10.1107/S0907444911023249

[4] Soliman, A.S.M. *et al.* doi:10.1107/S090744491101883X

## MS03-P13 | PROFILINS AND THE QUEST FOR STRUCTURE-BASED IGE-EPIOTOPE MAPPING

Wortmann, Judith (Institute for Molecular Biosciences, University of Graz, Graz, AUT); Gottstein, Nina Alice (Institute for Molecular Biosciences, University of Graz, Graz, AUT); Hofer, Gerhard (University of Graz, Graz, AUT); Keller, Walter (Institute for Molecular Biosciences, University of Graz, Graz, AUT)

**Background:** Panallergens frequently cause respiratory allergy and oral allergy syndrome. Profilins are important panallergens because of their highly conserved structure and ubiquitous presence in allergy sources. Therefore, determination of the structure and biophysical characterization are important tasks to complement IgE-binding studies and enable structure-based epitope prediction. Here we give an overview of important profilin allergens and present our most current research results.

**Methods:** Six profilins were expressed in *E.coli*. The food allergen Cuc m 2 (melon - Cucumis melo) and Cit s 2 (orange – Citrus sinensis), the pollen allergen Ole e 2 (olive tree – Olea europaea), Fra e 2 from the European ash (*Fraxinus excelsior*) and Phl p 12 (timothy grass - Phleum pratense) as well as the storage mite allergen Tyr p 36 (*Tyrophagus putrescentiae*). Biophysical characterization including Circular Dichroism spectroscopy, Differential Scanning Fluorimetry and Size Exclusion Chromatography are used to verify the proteins' native fold. Crystallization and homology modeling coupled to bioinformatics provide structural information and IgE-binding assays immunological data on cross-reactivity.

**Results:** All six profilin allergens included in this study were recombinantly expressed and purified to homogeneity. Biophysical characterization revealed the structural integrity of the allergens and their monomeric state, which makes them well suited for immunological testing. Homology modeling elucidated the surface-accessible regions of the allergens.

**Conclusion:** Immunological data regarding cross-reactivity of a wide range of homologous proteins in combination with structural information will enable more accurate IgE-epitope predictions using a structure based IgE-epitope mapping approach for the profilin family of allergens.

## MS03-P14 | ONE STEP CO-PURIFICATION AND CRYSTALLIZATION OF THREE SOLUBLE PROTEINS FROM CYANOBACTERIA, THE UNIQUE CRYSTALLIZATION PROPERTIES OF C-PHYCOCYANIN

Sarrou, Iosifina (CFEL, DESY, Hamburg, GER); Falke, Sven (Institute for Biochemistry, Hamburg, GER); Komadina, Dana (CFEL, DESY, Hamburg, GER); Tritschler, Felix (CFEL, DESY, Hamburg, GER); Yefanov, Oleksandr (CFEL, DESY, Hamburg, GER); Chapman, Henry (CFEL, DESY, Hamburg, GER)

Cyanobacteria have gained a lot of attention in recent years because of their potential applications in various fields of biotechnology. The establishment of cost and time-efficient purification protocols for cyanobacterial proteins and complexes, especially from their natural source, is highly desirable in structural biology and other areas of research.

We are presenting a highly time-efficient optimized co-purification protocol for three native key proteins of the photosynthetic cyanobacteria *T. elongatus* and *A. platensis*:

The cytochrome c6, a redox protein acting as an electron mediator between the cytochrome b6/f complex and photosystem I. The 2Fe-2S cluster Ferredoxin (Fed1) which is reduced by Photosystem I and carries one electron to a Fd-NADP<sup>+</sup> reductase. The antenna protein C- Phycocyanin (C-PC), a pigment with massive commercial value as natural colorants in nutraceutical, cosmetics, and pharmaceutical industries, besides its health benefits.

As obtained, we were able to characterize and optimize crystallization conditions for cytc6 and Fed1 from *T. elongatus* and collected X-ray diffraction data from crystals with resolutions higher than 2 Å.

Further, C-Phycocyanin from *T. elongatus* and *A. platensis* show unique crystallization properties. They crystallize in hundreds of significantly different conditions with various crystal morphologies. We collected high resolution data from 160 different crystallization conditions in the pH range 4 to 9 and will present the changes in the symmetry and the unit cell parameters under different conditions. This extraordinary behaviour of the C-PC will contribute to the comprehension of the fundamental principles of protein crystallography.

## MS03-P15 | NOVEL BIOCHEMICAL BASES FOR NUCLEAR FACTOR I X (NFI X)

Lapi, Michela (Università degli studi di Milano, Milano (MI), ITA)

My PhD project focuses on Nuclear Factor I X (NFI X), which is a transcription factor belonging to the NFI DNA-binding proteins family. NFI X plays an essential role in the development of several organs, most importantly skeletal muscle. It has been shown that upon NFI X inhibition in a dystrophic mice model there is an amelioration in the pathological features of the muscular dystrophy. Thus, these data demonstrated that the absence of NFI X protects from the progression of the disease *in vivo*. This study shed a light on the possible use of NFI X as a genetic tool to slow down the progress of muscular dystrophy, which is still incurable.

On these bases, my project aims of purifying and solving the novel structure of NFI X alone and in complex with its palindromic DNA consensus sequence. The goal of the study is to find small molecules able to inhibit NFI X transcriptional function.

During my PhD, I managed to find an acceptable protocol for expression and purification of truncated constructs of NFI X *via* a prokaryotic expression system. I was also able to find crystallization conditions suitable for NFI X-DNA complex, but I still have to work on crystals optimization. Moreover, I performed several biophysical analysis to better characterize the binding of NFI X to the target DNA and the protein stability.

## MS03-P16 | DYNAMIC FORMATION AND INTERNAL ORDER OF LIQUID DENSE PROTEIN CLUSTERS BEYOND CRYSTALLOGRAPHY

Falke, Sven (University Hamburg, Hamburg, GER); Brognaro, Hevila ; Mudogo, Celestin Nzanzu ; Wang, Mengying ; Cheng, Qing-di ; Betzel, Christian (University Hamburg, Institute for Biochemistry and Molecular Biology, Hamburg, GER)

Ellipsoidal liquid-dense clusters (LDCs) can be formed by liquid-liquid phase separation, which is a process known *in vitro* as initial step in crystal nucleation [1]. A rapidly increasing number of studies also describe dense protein or nucleic acid clusters *in vivo*, mainly formed in the context of RNA signaling, stress, neurodegenerative diseases like Alzheimer and potentially even *in vivo* crystallization [1]. However, insights into structure and dynamics of macromolecules inside LDCs and how to induce or manipulate molecular order are till now missing. Insights will not only provide new options to optimize protein crystal growth but will also potentially provide new routes to utilize LDCs of nanomaterials for structural investigation in a non-crystalline environment in the future, for example applying particle imaging methods at highly brilliant radiation sources, including coherent X-ray diffractive imaging (CXD).

In order to investigate formation and internal structure of LDCs we apply particularly DLS, EM, CD spectroscopy, particle tracking and X-ray imaging techniques. We selected proteins of medical and biological relevance, including a  $\beta$ -lactamase, concanavalin A,  $\beta$ -lactoglobulin, *Tb*IMPDPH and tau, as well as RNAs to prepare and analyse LDCs. The physico-chemical conditions for formation, stabilization and labelling of selected macromolecule LDCs were systematically established in multi-dimensional phase diagrams. Further, external electromagnetic fields have been applied to analyse the response towards two-dimensional ordering. Further details will be presented.

[1] Falke, S. et al. (2018). Encyclopedia of Analytical Chemistry, Vol. edited by R.A. Meyers, pp. 1–25. Chichester, UK: John Wiley & Sons, Ltd.

## MS03-P17 | CRYSTAL AND SOLUTION STRUCTURES OF SH2 DOMAIN OF SIGNALING MOLECULE IN COMPLEX WITH THE CO-STIMULATORY RECEPTOR CD28

Inaba-Inoue, Satomi (JASRI/SPring-8, Hyogo, JPN); Inoue, Katsuaki (Diamond Light Source, Oxfordshire, GBR); Hikima, Takaaki (RIKEN SPring-8 Center, Hyogo, JPN); Sekiguchi, Hiroshi (JASRI/SPring-8, Hyogo, JPN); Rambo, Robert (Diamond Light Source, Oxfordshire, GBR)

In addition to the signalling produced by the binding of antigen-major histocompatibility complex to T-cell receptors, co-stimulatory signals from other receptor-ligand interactions are required for full activation of T-cells. One of co-stimulatory receptor, CD28, has no enzymatic activity and its cytoplasmic region consists of 41 amino acids that contain the sequence YMNM, in which the tyrosine residue is phosphorylated by kinase. The phosphorylated sequence, pYMNM, is recognized by SH2 adaptor proteins, such as Grb2, Gads, and PI3-kinase regulatory subunit, p85. We had reported the high resolution X-ray crystal structures of Grb2 SH2, Gads SH2, p85 nSH2, and p85 cSH2 in complex with the CD28 phosphopeptide, showing that the four SH2 domains had highly conserved secondary structure and overall structures in the complex states were similar to each other [1]. In this study, we evaluate the solution structures of those SH2 domain and its complex with CD28 phosphopeptide using small angle X-ray scattering connected to size exclusion chromatography (SEC-SAXS) and compared them with the crystal structures. The radius of gyration of SH2 domains in the free states are smaller than those in the CD28 phosphopeptide complex states, as well as the maximum values of distance distribution. The experimental scattering curves were well fitted to theoretical scattering curves calculated from the PDB information, indicating that the solution states are almost similar to crystal structures. We will discuss the protein dynamics in the solution with results obtained from another biophysical methods.

[1] Inaba et al., J. Biol. Chem., 292, 1052, 2017

## MS03-P19 | STRUCTURAL DETERMINANTS OF THE INTERACTION SPECIFICITY AT THE G AND NC INTERFACES OF HUMAN SEPTINS

Leonardo, Diego (Instituto de Física de Sao Carlos, Sao Carlos, BRA); Nascimento, André (Laboratório Nacional Luz Síncrotron - CNPEM, Campinas, BRA); Valadares, Napoleao (Universidade de Brasília, Brasília, BRA); André, Ingemar (Lund University, Lund, SWE); Uson, Isabel (ICREA, Catalan Institution for Research and Advanced Studies, Barcelona, ESP); Garratt, Richard (Instituto de Física de Sao Carlos, Sao Carlos, BRA)

Septins are proteins involved in several cellular processes and to perform their functions, at least three of the four different groups must associate to form heterofilaments by forming two types of interface: The G and NC interface. Although the type of contact interface and the specific order of the septins in the assembly of the filament are known, the molecular mechanisms that control the correct polymerization of the filament are still unknown. Here, we describe studies performed at the G and NC interfaces of septins in order to uncover the structural determinants of the interaction specificity. "G" combinations of septins were purified to be characterized using biophysical techniques, showing dimers in solution with the presence of GTP/GDP. The dimers exhibit a different thermal stability, which could indicate preferences during complex formation. This condition was studied with MST, demonstrating that there is no significant difference in the dissociation constants, which strengthens the idea of substitution between septins in the same group. In the "NC" interface studies, the structures of the coiled-coil in the septins 1, 4 and 5 were solved. An antiparallel orientation was observed for SEPT1 and SEPT4, with a hydrophilic and a hydrophobic side (a novel motif not yet reported) whereas the coiled-coil of SEPT5 has a parallel orientation (with classic contact interface). This suggests that these sequences can adopt the two orientations, which could explain the formation of structures of high complexity such as networks of filaments which have been observed in vivo and in TEM images.

## MS03-P20 | THE SOD1-HCCS MECHANISM INVOLVED IN COPPER HOMEOSTASIS

Sala, Fernanda Angelica (University of Sao Paulo, Sao Carlos, BRA); Wriqth, Gareth (University of Liverpool, Liverpool, GBR); Antonyuk, Svetlana (University of Liverpool, Liverpool, GBR); Garratt, Richard Charles (University of Sao Paulo, Sao Carlos, BRA); Hasnain, S. Samar (University of Liverpool, Liverpool, GBR)

The copper concentration in cell is maintained at low levels and regulatory processes control its homeostasis. Once soluble  $\text{Cu}^{+1}$  has been transferred to the cytosol through CTR1, glutathione or recipient proteins immediately bind to the metal and deliver it to its target. Cu,Zn-Superoxide dismutase (SOD1) is one of the proteins which requires copper as a cofactor for enzymatic activity. However, SOD1 is not expected to acquire copper via direct interaction with CTR1. It is well known that hCCS (human copper chaperone for SOD1) forms stable heterodimers with SOD1. This interaction suggests subsequent amendments which involve reorientation of hCCS-D1, copper transfer and oxidation of a disulphide bond. The objective of this work is to investigate the recognition processes and sequence of post translational modifications during the maturation of SOD1 catalyzed by hCCS and particularly if the  $\text{Cu}^{+1}$  transfer occurs within the context of a membrane scaffold involving CTR1-hCCS or CTR1-hCCS-SOD1 interactions. Crystals of heterodimeric complexes which were either SOD1 copper free or loaded in complex with its metallochaperone were obtained, processed and analyzed. Protein-Membrane association experiments on different combinations of hCCS and SOD1 mutants suggested that copper acquisition occurs via hCCS, in its homodimeric state, engaging with the lipid bilayer and subsequently forming heterodimers off the membrane. Moreover, the analysis of the structures of heterodimeric complexes showed a novel conformation for the SOD1 disulphide sub-loop which communicates the presence of hCCS to the SOD1 active site and coordinates the timing of copper transfers prior to the disulphide bond formation.

## MS03-P21 | THE N-TERMINAL DOMAIN OF LACTOBACILLUS ACIDOPHILUS SLP<sub>A</sub> PROMOTES SELF-ASSEMBLY OF THE S-LAYER ARRAY

Sagmeister, Theo; Eder, Markus (University of Graz, Graz, AUT); Damisch, Elisabeth (University of Graz, Graz, AUT); Vejzovic, Djenana (University of Graz, Graz, AUT); Dordic, Andela (University of Graz, Graz, AUT); Millán Nebot, Claudia Lucía (Institut de Biologia Molecular de Barcelona, Barcelona, ESP); Usón, Isabel (Molecular Biology Institute of Barcelona (IBMB) CSIC, Barcelona, ESP); Vonck, Janet (Max-Planck-Institut für Biophysik, Frankfurt am Main, GER); Pavkov-Keller, Tea (University of Graz, Graz, AUT)

Surface layer proteins (S-layers) represent the outermost cell envelope in many bacteria and archaea. They assemble into highly regular 2D crystalline arrays composed of mostly single protein or glycoprotein species. These arrays are in close contact with their surrounding and fulfil various functions like bacterial adherence to other cells or substrates, protection against life-threatening conditions and maintenance of the cell shape.

The S-layer of *L. acidophilus* consists of two proteins. Slp<sub>A</sub> is mainly expressed under normal physiological conditions, whereas Slp<sub>X</sub> expression is increased under osmotic stress. They have two functional regions: the C-terminal region that is important for the attachment to the cell wall and the N-terminal region for the self-assembly of the S-layer array.

Our goal is to structurally characterize the S-layer protein Slp<sub>A</sub> of *L. acidophilus* and further understand the mechanism of the self-assembly. Since full length S-layers form insoluble 2D crystal we designed three functional protein fragments. We obtained crystals of fragments important for self-assembly formation. The structure of the first fragment was solved with a serine to cysteine mutant co-crystallized with mercury by Hg-SAD and later by molecular replacement with data from native crystals at 2.2 Å resolution. The structure of the second fragment was solved *ab initio* with ARCIMBOLDO with a resolution of 1.4 Å. Both structures together suggest the mode of action how the self-assembly of the Slp<sub>A</sub> protein occurs. Furthermore, the putative exposed areas of the S-layer, which are important for potential interactions with the environment are analysed.

## MS03-P22 | CRYSTAL STRUCTURE OF HISTONE CHAPERONE ANTI SILENCING FUNCTION 1 (Asf1) FROM PLASMODIUM FALCIPARUM AND ITS BIOCHEMICAL CHARACTERIZATION

Kr. Srivastava, Dushyant (CSIR-Indian Institute of Chemical Biology, Kolkata, IND); Gunjan, Sarika (National Centre for Cell Science, Pune, IND); Seshadri, Vasudevan (National Centre for Cell Science, Pune, IND); Das, Chandrima (Saha Institute of Nuclear Physics, Kolkata, IND); Roy, Siddhartha (CSIR-Indian Institute of Chemical Biology, Kolkata, IND)

Chromatin structure and its dynamics are central to regulation of DNA template mediated cellular processes such as replication, transcription and repair. The chromatin structure continuously undergoes assembly and disassembly for facilitating access to nascent DNA sequence. This assembly and disassembly of chromatin is tightly governed and orchestrated by histone chaperone proteins. Anti silencing function 1 (Asf1) is a central histone chaperone which mediates deposition of histone H3-H4 into nucleosome structure in both replication dependent and independent manner. In this study we have done the structural characterization and molecular identification of Asf1 from *Plasmodium falciparum* (PfAsf1), which is the causative agent of severe form of malaria in humans. We have solved the high resolution crystal structure of histone chaperone domain of PfAsf1 protein. Two monomeric units of PfAsf1 molecule was observed in the asymmetric unit of the crystal structure of PfAsf1 indicating the protein might exists in a dimeric state which is different in comparison to its yeast and human homologues. This observation was further substantiated by in solution cross-linking experiments. Further, PfAsf1 interacted with histone H3 and H4 in our *in-vitro* protein interaction assay. Identification of critical residues mediating interaction of PfAsf1 and histone H3-H4 has been done and validated by site directed mutagenesis approach. Biophysical characterization of the PfAsf1-histone interaction was done by surface plasmon resonance (SPR) wherein high affinity interaction of PfAsf1 with H3-H4 was observed. The dimeric structure of PfAsf1 may be indicative of its divergent role in regulating the chromatin landscape in this pathogenic parasite.

## MS03-P23 | THE CRYSTAL STRUCTURE OF THE MAJOR OLIVE POLLEN ALLERGEN OLE E 1

Wortmann, Judith (University of Graz, Graz, AUT); Hofer, Gerhard (University of Graz, Graz, AUT); Dorofeeva, Yulia (University of Graz, Graz, AUT); Focke-Tejkl, Margarete (University of Graz, Graz, AUT); Aschauer, Philipp (University of Graz, Graz, AUT); Pavkov-Keller, Tea (University of Graz, Graz, AUT); Valenta, Rudolf (University of Graz, Graz, AUT); Keller, Walter (University of Graz, Graz, AUT)

In the field of molecular allergology, structural investigations of important allergens are crucial for the development of hypoallergenic derivatives and the design of efficient vaccines. An important allergen source in the Mediterranean area is the olive tree pollen. Its main allergen is Ole e 1 which is recognized by 90% of atopic individuals with olive tree pollinosis. This work elucidates a new structural understanding of this protein family.

Recombinant Ole e 1 was produced natively folded in *E. coli*, characterized with biophysical methods and compared to natural Ole e 1. The three-dimensional structure was solved using X-ray crystallography. Peptide-based IgE-binding and inhibition assays were performed to map the dominant IgE-epitope regions of Ole e 1.

We here present the 3D crystal structure of the major olive tree pollen allergen Ole e 1, the prototypic member of the Ole e 1-like family. The structure exhibits a 6-stranded  $\beta$ -barrel in the core, resembling the fold of Pla I 1, which is the only other known structure of this allergen family (PDB-Code: 4Z8W). Additionally, the extended C-terminus, which is missing in the homologous structure, forms an  $\alpha$ -helix that serves as the interface for a homodimer formation. Stable dimer formation was also proven in solution. Immunological characterization revealed the high allergenicity of the allergen and enabled the determination of IgE-epitope regions.

## MS03-P24 | PRELIMINARY DIFFRACTION EXPERIMENTS ON THE E.COLI TOXIN SAT

Meza, Domingo (European XFEL, Schenefeld, GER); Fromme, Raimund (Arizona State University, Tempe, USA); Thifault, Darretn (Arizona State University, Tempe, USA)

**Background:** Sat belongs to the serine protease autotransporter of *Enterobacteriaceae* (SPATEs). This family of proteins is normally associated with virulence of Gram-negative pathogens. Sat function has been studied specifically in Uropathogenic *Escherichia coli* strains (UPEC) responsible for urinary tract infections. **Results:** The Sat construct with the proteolytic activity abolished (S256I-S258A) from *E. coli* strain HB101 was used for overexpression in LB broth medium. The supernatant of the cell culture was incubated with ammonium sulfate (1.7 M) for protein precipitation (Overnight at 4 °C) and the pellet thus obtained was re-suspended in 20 mM Tris-HCL, 5 mM EDTA, pH 7.5, desalted and equilibrated using 6-8 KDa molecular-weight-cutoff (MWCO) dialysis membrane. Subsequently, 50 ml of this solution was loaded onto a preequilibrated Q-sepharose anionic exchange column equilibrated with 20 mM Tris-HCL, 5 mM EDTA, pH 7.5. A second chromatography purification was performed using size exclusion Superdex200 10/300. The process of the purification was monitored by SDS-PAGE (4-20 %). The crystals were obtained by sitting drop method and measured at beamline 19-ID at APS, Detector distance was 1000 mm, wavelength 0.9729 Å. A data set was taken with 1 sec exposure for each image and 0.333 degree oscillation, in total 540 images. The unit cell has been determined to belong to the space group F432 with  $a=b=c=485$  Å and  $\alpha=\beta=\gamma=90$  degree. Currently the resolution is limited to 9.5 Å.

## MS03-P105 LATE | CONTAMINER AND CONTABASE: AUTOMATED IDENTIFICATION OF UNWANTEDLY CRYSTALLIZED PROTEIN CONTAMINANTS

Hungler, Arnaud (King Abdullah University of Science and Technology, Thuwal, SAU); Momin, Afaque (King Abdullah University of Science and Technology, Thuwal, SAU); Diederichs, Kay (Universität Konstanz, Konstanz, GER); Arold, Stefan (Computational Bioscience Research Center (CBRC), King Abdullah University of Science and Technology, Thuwal, SAU)

Solving the phase problem in protein X-ray crystallography relies heavily on the identity of the crystallized protein, especially when molecular replacement (MR) methods are used. Yet, it is not uncommon that a contaminant crystallizes instead of the protein of interest. Such contaminants may be proteins from the expression host organism, protein fusion tags or proteins added during the purification steps. Many contaminants co-purify easily, crystallize and give good diffraction data. Identification of contaminant crystals may take time, since the presence of the contaminant is unexpected, and its identity unknown. We have established a webserver (*ContaMiner*) and a contaminant database (*ContaBase*), both available at [strube.cbrc.kaust.edu.sa/contaminer/](http://strube.cbrc.kaust.edu.sa/contaminer/), to allow fast automated MR-based screening of crystallographic data against currently ~80 known contaminants from several different expression systems and contaminating microbes. Here we present the latest developments of *ContaMiner*, and highlight a curious case of a structurally altered domain-swapped maltose-binding protein (MBP).

## MS03-P107 - LATE | KEEPING MUSCLE PROTEINS IN SHAPE – UCS-PROTEINS ACTING AS MYOSIN-SPECIFIC QUALITY CONTROL FACTORS

Vogel, Antonia (IMP - Research Institute of Molecular Pathology, Vienna, AUT); Gudino, Ricardo (Max Perutz Labs, Vienna, AUT); Arnese, Renato (IMP - Research Institute of Molecular Pathology, Vienna, AUT); Clausen, Tim (IMP - Research Institute of Molecular Pathology, Vienna, AUT)

The broad variety of movement-based organismal functions - ranging from muscle contraction to cytokinesis and endocytosis - rely on the motor protein myosin. Given the intricate fold, myosin family members require help of several chaperones to attain their native conformation. Interestingly, the chaperone UCS (UNC45/CRO1/SHE4) has been additionally shown to facilitate degradation of misfolded myosin by acting as an adaptor for UFD2-mediated ubiquitination [1, 2].

The aim of this study is to unravel how myosin interacts with UCS-proteins and how this is connected to protein quality control. Initially, we investigated interaction motifs of the fungal UCS-protein SHE4 with myosin and determined a co-crystal structure with the respective peptide. Subsequently, focusing on myosin interactions with the more complex, metazoan UCS-protein UNC45, we demonstrated that within the interaction motif a strictly conserved tyrosine residue is critical for chaperone engagement. Guided by crosslinking mass spectrometry, we obtained a model of full-length UNC45-myosin interactions, suggesting that the identified chaperone recognition motif can flip to recruit UNC45.

Our work provides molecular insight into how UCS-proteins bind to myosin and is fundamental for subsequent studies addressing the regulated formation of the myosin-chaperone complexes and their role in muscle myosin proteostasis.

[1] D. Hellerschmied, M. Roessler, A. Lehner, L. Gazda, K. Stejskal, R. Imre, K. Mechtler, A. Dammermann, T. Clausen, *Nature Communications*, 9, (2018), 484

[2] D. Hellerschmied, T. Clausen, *Current Opinion in Structural Biology*, 25, (2014), 9

## MS03-P109 - LATE | HOW THE PARG PROTEIN MARK KEEPS THE STRESS RESPONSE KINASE MCSB UNDER CONTROL

Hajdusits, Bence (Research Institute of Molecular Pathology (IMP), Vienna, AUT); Suskiewicz, Martin J. (Research Institute of Molecular Pathology (IMP), Vienna, AUT); Hundt, Nikolas (Department of Chemistry, University of Oxford, Oxford, GBR); Meinhart, Anton (Research Institute of Molecular Pathology (IMP), Vienna, AUT); Kukura, Philipp (Department of Chemistry, University of Oxford, Oxford, GBR); Clausen, Tim (Research Institute of Molecular Pathology (IMP), Vienna, AUT)

Protein arginine phosphorylation is an emerging post-translational modification found in gram-positive bacteria. Here, the phospho-arginine (pArg) mark serves as degradation signal directing aberrant proteins to the ClpC:ClpP protease. The chemically demanding phosphorylation of arginine residues is carried out by the protein arginine kinase McsB. Recent structural studies revealed the organizing of the McsB kinase, having an allosterically coupled dimer as basic functional unit. In vivo data suggest that the McsB's activity needs to be tightly controlled in the cell, most likely to keep the pArg death-marking function under control. However, molecular details of McsB regulation are still elusive.

Here, we present a comprehensive structural, biochemical and biophysical investigation of the *Bacillus subtilis* McsB kinase. Most importantly, single-molecule data reveal the presence of various functionally relevant oligomeric forms, which differ in their substrate-targeting activities. Moreover, we show that the change in oligomeric state depends on a phospho-arginine switch, allowing pArg effector proteins to modulate McsB activity. Delineating the molecular mechanism of the pArg-dependent oligomer conversion of McsB will help to better understand the bacterial stress-response system, which is a one of the most critical assets underlying bacterial pathogenicity.

## MS03-P111 - LATE | DNA RELAXASE TRAA OF THE G+ PLASMID PIP501 AS KEY PLAYER IN BACTERIAL CONJUGATION

Reisenbichler, Anna Maria (University of Graz, Graz, AUT)

The accelerated emergence of antibiotic resistant bacteria is one of the biggest threats to human health in the world. Dissemination of antibiotic resistance and virulence determinants in clinical settings is caused by horizontal gene transfer even among only distantly related bacteria, and is mediated by a multi-protein complex termed type IV secretion system (T4SS), encoded by conjugative plasmids. The T4SS of the broad host-range, self-transmissible plasmid pIP501 consists of 15 proteins, which assemble into the Gram-positive cell wall-spanning mating core complex, the cytosolic relaxosome and the coupling factor connecting the components.

This project aims to bring about a crystal structure of the relaxase TraA, the central element of the relaxosome, and further elucidate function and intermolecular interactions thereof within its T4SS. With the pipeline for new antibiotics to treat drug-resistant infections running dry, there is an immediate need for novel therapeutics, and in the light of the DNA-mobilizing enzyme TraA acting as initiator, regulator and terminator of bacterial conjugation, we view comprehending its structure and detailed function as potential key to impede the rapid dissemination of antibiotic resistance genes.

## MS04: Progress (Methods) in High Resolution Cryo-EM

---

### MS04-01 | MECHANISMS OF C-RING PROTONATION AND FLEXIBLE F<sub>1</sub>-F<sub>0</sub> COUPLING IN A MITOCHONDRIAL ATP SYNTHASE

Murphy, Bonnie (Max Planck Institute of Biophysics, Frankfurt am Main, GER); Klusch, Niklas (Max Planck Institute of Biophysics, Frankfurt am Main, GER); Langer, Julian (Max Planck Institute of Biophysics, Frankfurt am Main, GER); Mills, Deryck (Max Planck Institute of Biophysics, Frankfurt am Main, GER); Yildiz, Özkan (Max Planck Institute of Biophysics, Frankfurt am Main, GER); Kühlbrandt, Werner (Max Planck Institute of Biophysics, Frankfurt am Main, GER)

F<sub>1</sub>F<sub>0</sub>-ATP synthases play a central role in cellular metabolism across all domains of life. Although much is known about the structure and mechanism of these complexes, open questions remain. The stoichiometric mismatch between processes at F<sub>1</sub> (3-fold symmetry) and F<sub>0</sub> (8- to 17-fold symmetry) is a challenge to efficient energy conversion within the complex. Flexible coupling between the two nanomotors is proposed to mitigate this challenge, but the structural basis is not established. We have determined the single-particle cryo-EM structure of active dimeric ATP synthase from mitochondria of *Polytomella* sp. at 2.7- 2.8 Å resolution, and have used 3D classification to separate 13 well-defined rotary sub states, providing a detailed picture of the molecular motions that accompany c-ring rotation. We show that the F<sub>1</sub> head rotates along with the central stalk and c-ring rotor for the first ~30° of each 120° primary rotary step, which would result in flexible coupling of F<sub>1</sub> and F<sub>0</sub>. Rotation of F<sub>1</sub> is mediated primarily by the interdomain hinge of the conserved OSCP subunit, a well-established target of physiologically important inhibitors. The membrane-bound F<sub>0</sub> subunit, where proton translocation drives c-ring rotation, is resolved at 2.7Å, allowing us to model ordered water molecules in the aqueous half-channels and at the conserved gating Arg-239. A histidine residue essential to proton translocation binds a metal ion in the proton access channel, and the coordination of the metal changes with c-ring position, suggesting that this may play a role in synchronising c-ring protonation with rotation.

## MS04-02 | RECENT ADVANCES IN CRYO-ELECTRON TOMOGRAPHY FOR IN SITU STRUCTURAL BIOLOGY

Plitzko, Juergen (MPI of Biochemistry, Martinsried, GER)

As a consequence of the 'resolution revolution' cryo-EM has become the most versatile method for structural biology. Clearly, advances made in instrumentation, in automation and in image processing over the recent past have expanded its capabilities in a profound manner. Cryo-EM is used to determine the structure of isolated and purified macromolecular structures, i.e. *ex situ* but, biological functions are only rarely carried out by individual molecules. They arise from the interactions of the many molecular species found within the cells. In order to investigate these *in situ*, i.e. in an undisturbed cellular context, cryo-electron tomography is the method of choice. However, in tomography, several different high-end instruments are involved and many different tasks are chained into a complex, but not yet fully streamlined workflow. The fragile and delicate sample has to be prepared, information derived during these workflow steps have to be passed on and most importantly the sample has to be transferred (safely and reliably) from one system to the other. To realize the full potential of such a workflow and to apply it to many different sample materials (i.e. from cells to tissue) in a routine fashion there is an urgent need for further technology and methodology development spanning its entire range.

This lecture will present our recent work in the field of cryo-electron tomography and *in situ* structural biology and highlights technological developments, limitations and their opportunities and also provide a perspective for obtaining 'anatomical' detail at the molecular level from larger cells or tissues.

## MS04-03 | A NEW AND SIMPLE METHOD FOR CRYO-EM SPECIMEN PREPARATION

Zhou, Jingjing (Stockholm University, Stockholm, SWE); Xu, Hongyi (Stockholm University, Stockholm, SWE); Carroni, Marta (Stockholm University, Stockholm, SWE); Lebrette, Hugo (Stockholm University, Stockholm, SWE); Wallden, Karin (Stockholm University, Stockholm, SWE); Högbom, Martin (Stockholm University, Stockholm, SWE); Zou, Xiaodong (Stockholm University, Stockholm, SWE)

Cryo-electron microscopy (cryo-EM), including single-particle cryo-EM and micro-crystal electron diffraction (MicroED), has made great impacts on structural biology. Specimen preparation remains as one of the major bottlenecks. The pipetting-blotting-plunging routine has been the most widely used method for preparing cryo-EM specimen. The main drawback of the method is that 99.9% of the particles ends up on the blotting paper<sup>1,2</sup>. On the other hand, the method is not optimized for preparing specimen of micro-crystals used in MicroED, an emerging method for structure determination of small- and macro-molecules. Here, we present a novel method for preparing cryo-EM specimen (in manuscript). The new method can be implemented in two simple setups, one for single particles and the other for micro-crystals. Using the method, protein consumption can be reduced by at least one order of magnitude compared to the blotting method, offering biologists new opportunities to work with samples of low concentration. Furthermore, the method is able to handle protein crystals grown in viscous mother liquid, allowing MicroED to be applied to a large variety of micro-crystals<sup>3</sup>.

[1] Razinkov, I. *et al.* A new method for vitrifying samples for cryoEM. *J. Struct. Biol.* **195**, 190–198 (2016)

[2] Glaeser, R. M. How good can cryo-EM become? *Nat. Methods* **13**, 28–32 (2016)

[3] Xu, H. *et al.* Solving the first novel protein structure by 3D micro-crystal electron diffraction. *bioRxiv* (2019)  
doi:10.1101/600387

## MS04-04 | AUTOMATED INTERPRETATION OF CRYO-EM DENSITY MAPS WITH CONVOLUTIONAL NEURAL NETWORKS

Mostosi, Philipp (University of Würzburg, Würzburg, GER); Philip, Kollmannsberger (University of Würzburg, Würzburg, GER); Schindelin, Hermann (University of Würzburg, Würzburg, GER); Thorn, Andrea (University of Würzburg, Würzburg, GER)

In recent years, three-dimensional density maps reconstructed from single particle images obtained by electron cryo-microscopy (Cryo-EM maps) have reached unprecedented resolution. However, assigning a fold to map regions can be a challenge, in particular if the constituting macromolecules are unknown or mobile. Convolutional neural networks (CNNs) combine traditional image analysis with machine learning by cascading layers of trainable convolution filters and are exceptionally well suited for map annotation [1]. CNNs have been successfully applied to biological problems such as breast cancer mitosis recognition [2] and volumetric data segmentation [3].

Here, we will give a general perspective on the potential of CNNs for the interpretation of Cryo-EM maps and present a network which was trained on a carefully curated set of 293 experimentally derived reconstruction maps from the EMDB [4] to automatically annotate protein secondary structure as well as nucleotides. The network, named Haruspex, can be straightforwardly applied to predict structures in newly reconstructed maps to facilitate model building. It can also support domain placement, and due to its high median recall and precision rates of 94.2% and 79.2%, respectively (on an independent test set of 167 EMDB entries), it can be used for structure validation. The network and a plugin for COOT [5] will be available from our website.

[1] Cireşan et al. (2011). IJCNN, 1918

[2] Cireşan et al. (2013). MICCAI, 411

[3] Çiçek et al. (2016). MICCAI, 424

[4] Tagari et al. (2002). Trends Biochem. Sci. 27, 589

[5] Emsley et al. (2010). Acta Cryst. D66, 486

## **MS04-05 | MICRO ELECTRON DIFFRACTION IS A QUICK AND VERSATILE TOOL FOR STRUCTURE DETERMINATION OF MACROMOLECULES AND SMALL MOLECULES**

Yakushevskaya, Alevtyna (Thermo Fisher Scientific, Ecublens, CH); Reyntjens, Steve (Materials and Structural Analysis Division, Ecublens, CH)

X-ray crystallography experiments require large, well-ordered protein crystals for diffraction data collection. Growing protein crystals is difficult, requires a lot of time and effort and it is sometimes even impossible. However, crystallization experiments quite often produce plenty of microcrystals which are too small for conventional X-ray diffraction experiments. Moreover, large protein crystals are frequently imperfect and often suffer from different defects like high mosaicity. Small crystals are usually not affected by such defects and may yield better quality data. These kind of small crystals could be used for high-resolution structure determination by electron microscopy methods.

Cryo-transmission electron microscope (cryo-TEM) and diffraction are increasingly powerful methods for the analysis of biological structures at near atomic resolution. However, the very strong interaction of electrons with matter limits the thickness of specimens that can be analyzed at high resolution, by the current implementations of these methods, to a few hundreds of nanometers. To efficiently collect MicroED data, software automation, dedicated hardware components and customized optical setting can be installed on a cryo-TEM. Combined with the intrinsic microscope performance, we show that data collection is now fully automated and can be realized in a matter of minutes

## MS04-P01 | CCP-EM: THE COLLABORATIVE COMPUTATIONAL PROJECT FOR ELECTRON CRYO-MICROSCOPY

Winn, Martyn (STFC, Didcot, GBR); Burnley, Tom (STFC, Didcot, GBR); Palmer, Colin (STFC, Didcot, GBR); Joseph, Agnel (STFC, Didcot, GBR); Mirecka, Jola (STFC, Didcot, GBR)

The Collaborative Computational Project for Electron cryo-Microscopy is a community project to support computation in cryoEM. It is modelled closely on the long-running CCP4 project for MX, but is separately managed and with a remit to include all cryoEM modalities from high resolution single particle analysis through to tomography. I will present an overview of CCP-EM activities, together with two specific projects in the key areas of validation and machine learning.

The CCP-EM software suite is currently focussed on single particle analysis. It combines pre-processing and reconstruction in Relion with building of atomic models. Several workflows are possible, depending on the resolution of the cryoEM map and the availability of atomic models. Some crystallographic programs are included, which have been adapted to take into account different map distributions and lower resolution.

CCP-EM is a partner in a validation consortium which is developing tools for validating cryoEM reconstructions and fitted atomic models. Together with the EMDB, CCP-EM is responsible for disseminating these tools to the cryoEM community. We have developed a set of tools for the CCP-EM software suite with the aim of catching problems early, and anticipating future deposition requirements.

As an experimental technique generating large and numerous datasets, cryoEM is ripe for the application of machine learning. We are developing machine learning models for recognising features in cryoEM maps, at a range of lengthscales from components of complexes down to individual side chains. We are investigating the dependence of these models on data quality and resolution.

## MS04-P02 - CANCELLED | TOOLS FOR VALIDATION OF MAPS AND ATOMIC MODEL FITS IN SINGLE PARTICLE CRYO-EM

Warshamanage, Rangana (MRC Laboratory of Molecular Biology, Cambridge, GBR); Murshudov, Garib N. (MRC Laboratory of Molecular Biology, Cambridge, GBR)

Most of the current validation tools used in Single Particle Cryo-EM analyses are global metrics. They provide summaries of the global quality of maps or map-model fits. In order to reveal local variation of the signal in maps and map-model fits, a new set of tools have been developed. In these tools the correlation is calculated in each voxel of the image space resulting in a three-dimensional (3D) correlation map. This map when calculated using half maps can be used to assess the signal quality of the consensus map. Similarly, if the map and the model are used, then it can be used to evaluate the correctness of the map-model fit. Also, the 3D correlation map between the true map and model [1] should serve as the upper limit of map-model fit. The 3D correlation map calculated in Fourier space yields directional dependence of the signal and is useful to quantify preferential orientation of samples as well as for calculation of the variance in each Fourier coefficient.

Conformational changes of protein molecules or a protein with and without ligand bound to it can result in multiple maps during single particle cryo-EM analyses. A new tool utilizing the common information of multiple maps to generate average maps with enhanced signals has been developed. In this presentation, some examples of the usage of correlation tools and preliminary results on averaging of multiple maps will be discussed.

[1] Nicholls, R.A., Tykac, T., Kovalevskiy, O & Murshudov, G.N. (2018). *Acta. Cryst.*, **D74**, 492-505

## MS04-P03 | EFFICIENT REAL-SPACE REFINEMENT FOR CRYO-EM AND CRYSTALLOGRAPHY

Urzhumtsev, Alexandre (IGBMC, Illkirch, FRA); Afonine, Pavel V. (LBNL, Berkeley, USA); Poon, Billy K. (LBNL, Berkeley, USA); Read, Randy (Department of Haematology, Cambridge Institute for Medical Research, University of Cambridge, Cambridge, GBR); Sobolev, Oleg V. (LBNL, Berkeley, AUT); Terwilliger, Thomas C. (LANL, Los Alamos, USA); Adams, Paul D. (LBNL, Berkeley, USA)

Recent progress in cryoEM made it possible to refine atomic models against cryoEM maps,  $\rho_{\text{exp}}$ , at resolutions  $\sim 2.5\text{--}3\text{\AA}$ . Usually such real-space refinement calculates a map  $\rho_{\text{model}}$  from an atomic model and matches it with  $\rho_{\text{exp}}$ , e.g. by calculating their correlation value *CCmaps*. An accurate but computationally expensive way to calculate  $\rho_{\text{model}}$  is by obtaining the model Fourier coefficients, truncating them up to the resolution of  $\rho_{\text{exp}}$  and calculating the respective Fourier series. Alternatively,  $\rho_{\text{model}}$  can be calculated as a sum of contributions of individual atoms where each contribution reflects the resolution of  $\rho_{\text{exp}}$ . In both cases, the calculation time of the refinement target grows at least as a product of the number of atoms by a cube of the value inverse to the grid step of the map.

We have developed a new refinement procedure *phenix.real\_space\_refine* [1] that does not require calculating  $\rho_{\text{model}}$  at all thus saving both the computational time and memory. We showed that *CCmaps* can be approximated by a sum of the  $\rho_{\text{exp}}$  values in the positions of atomic centers for any resolution and not only at a very low resolution as suggested earlier [2]. This leads to the refinement algorithm with a very low computational cost independent of the grid size. In turn, this allowed to automate a number of refinement stages, e.g. the weight optimization between the data and restraints terms.

[1] Afonine\_et\_al.,2018,*ActaCryst.*,D74,531

[2] Rossmann,2000,*ActaCryst.*,D56,1341

## MS04-P113 - LATE | BEAM-INDUCED MOVEMENT ATTENUATION WITH SINGLE WALL CARBON NANOTUBES

Borsa, Christopher (Paul Scherrer Institute, Villigen, CH)

Protein crystallization has long been seen as the principal bottle-neck in traditional X-ray crystallography, recent advances in cryo-electron microscopy now allow for structural elucidation without the need for crystallization with structural resolutions rivalling that of crystallographic methods. Despite these advances, sample movement and drift hamper image alignment making the acquisition of high-resolution structures difficult. Methods used to counter the effects of beam-induced motion include image alignment processing algorithms along with physical interventions such as the use of ultra-stable gold grids and graphene sample supports. Herein we utilize carbon nanotubes as a support scaffold to prevent beam-induced motion without modification of sample buffers.

## MS05: Proteins in Signalling (Including Membrane Proteins)

---

### MS05-01 | PROTEIN CONFORMATIONAL AND OLIGOMERIC REARRANGEMENTS CONTROL INTERCELLULAR SIGNALING

Janssen, Bert (Utrecht University, Utrecht)

Intercellular communication, orchestrated by cell-surface expressed proteins, is a fundamental process in the formation, function and pathology of all tissues and organs. Protein structure, interaction and conformational change determine signaling and adhesion events. Using three target systems with central roles in the formation and maintenance of our nervous system; transmembrane receptors Myelin associated glycoprotein (MAG), Sortilin and Teneurin, we show how interactions and conformational changes on the cell surface and between cells underlie the molecular mechanisms of signal transduction and adhesion. Protein conformational flexibility, important for function, imposes challenges on the structural studies. Strategies will be shown on how to handle such samples and how to overcome problems. Ultimately, we used a hybrid approach of structural biology techniques to resolve protein structures and conformational rearrangements, biophysical methods to determine protein interactions and cellular assays to unify the mechanistic insights with function in the nervous system.

## MS05-02 | STRUCTURAL INSIGHTS INTO SIGNAL PROCESSING TO CHROMATIN

Panne, Daniel (University of Leicester, Leicester, GBR)

Signals that emerge from cellular receptors ultimately impinge on chromatin to regulated gene expression. As part of such signalling reactions chromatin becomes extensively modified. The precise mechanisms that allow cellular signalling to control chromatin modification and how such modifications contribute to gene regulation remain unclear. One such modification is Lysine acetylation which has long been correlated with active gene transcription. p300 is a multivalent adaptor for Transcription factors (TFs) and an acetyltransferase that is typically recruited to enhancers and contributes to gene regulation by acetylating chromatin and other transcriptional regulators. We have recently discovered that the activation of p300 depends on the activation and oligomerization status of TFs. We found that TF dimerization enables *trans*-autoacetylation of p300 in a highly conserved and intrinsically disordered autoinhibitory lysine-rich loop. Structural and biochemical studies, in combination with molecular modelling, indicate that TF dimerization enables trans-autoacetylation of the lysine-rich loop thus relieving autoinhibition and enabling activation of the enzyme. A large fraction of TFs operate as functional dimers and dimerization is frequently inducible by exogenous stimuli. We therefore propose that cellular signalling directly controls activation and genome targeting of p300 thus explaining why chromatin acetylation is associated with transcriptionally active chromatin. Our working model is that acetylation contributes to nucleation and concentration of dynamic TF–p300 assemblies on enhancers and thereby to active gene regulation. Dysregulation of p300-mediated chromatin acetylation by oncogenic TFs can lead to formation of aberrant chromatin condensates and profound changes in gene expression programs that drive the malignant cell state.

## MS05-03 | TRANSPORT OF ENANTIOMERIC NEUROTRANSMITTERS BY SLC1A FAMILY OF PROTEINS

Guskov, Albert (University of Groningen, Groningen)

Mammalian glutamate transporters (belonging to Solute Carrier Family 1 of transporters) are crucial players in neuronal communication as they perform neurotransmitter reuptake from the synaptic cleft. Besides L-glutamate and L-aspartate, they also recognize D-aspartate, which might participate in mammalian neurotransmission and/or neuromodulation. We investigated binding and transport of enantiomeric substrates in archaeal homologue of glutamate transporters - Glt<sub>TK</sub> from *Thermococcus kodakarensis*. We observed that Glt<sub>TK</sub> transports D-aspartate with identical Na<sup>+</sup> : substrate coupling stoichiometry as L-aspartate, and that the affinities ( $K_d$  and  $K_m$ ) for the two substrates are very similar. Additionally, we solved a crystal structure of Glt<sub>TK</sub> with bound D-aspartate at 2.8 Å resolution and compared it with the L-aspartate bound Glt<sub>TK</sub> structure. The new structure explains how the geometrically different molecules L- and D-aspartate are recognized and transported by the protein in the same way and provides a clue to explain the puzzling observation why mammalian SLC1A transporters readily transport L- but not D-glutamate.

## MS05-04 | STRUCTURAL BASIS FOR CD96 IMMUNE RECEPTOR RECOGNITION OF NECTIN-LIKE PROTEIN-5, CD155

Deuss, Felix (Monash University, Clayton, AUS); Watson, Gabrielle (Monash University, Clayton, AUS); Fu, Zihui (Monash University, Clayton, AUS); Rossjohn, Jamie (Monash University, Clayton, AUS); Berry, Richard (Monash University, Clayton, AUS)

CD96, DNAM-1, and TIGIT constitute a group of immunoglobulin superfamily receptors that are key regulators of tumor immune surveillance. Within this axis, CD96 recognizes the adhesion molecule nectin-like protein-5 (necl-5), although the molecular basis underpinning this interaction remains unclear. We show that the first immunoglobulin domain (D1) of CD96 is sufficient to mediate a robust interaction with necl-5, but not the DNAM-1 and TIGIT ligand, nectin-2. The crystal structure of CD96-D1 bound to the necl-5 ectodomain revealed that CD96 recognized necl-5 D1 via a conserved “lock-and-key” interaction observed across TIGIT/necl complexes. Specific necl-5 recognition was underpinned by a novel structural motif within CD96, namely an “ancillary key”. Mutational analysis showed that this specific residue was critical for necl-5 binding, while simultaneously providing insights into the unique ligand specificity of CD96.

## MS05-05 | ANALYSIS OF CYTOMEGALOVIRUS IMMUNE EVASION PROTEIN UL144

### GLYCOSYLATION PROFILE REVEALED ITS ROLE IN IMMUNE RECOGNITION

Nemcovicová, Ivana (Biomedical Research Center SAV, Bratislava, SVK); Nemcovic, Marek (Institute of Chemistry, Bratislava, SVK); Benko, Mário (Biomedical Research Center SAV, Bratislava, SVK); Lenhartová, Simona (Biomedical Research Center SAV, Bratislava, SVK); Holíková, Viera (Biomedical Research Center SAV, Bratislava, SVK); Zajonc, Dirk (La Jolla Institute for Immunology, La Jolla, USA)

The immune system is designed to provide protection against various pathogens, however several pathogens, including large double stranded DNA viruses have evolved multiple strategies to avoid immune recognition. This is in part achieved by removing immune activating ligands from cell surface and at the same time to express viral mimic on the cell surface to prevent killing of the infected cell by missing self-recognition. Human cytomegalovirus (HCMV) belongs to the beta herpes virus family that has co-evolved with the host immune system. UL144 is found exclusively in clinical HCMV strains and encodes a structural homologue of the herpesvirus entry mediator. UL144 plays a role in virus-mediated immune evasion by transmitting inhibitory signals to downregulate T-cell responses. Its sequence shows 10 N-linked glycosylation sites located in extracellular part. Many of them are not present in other viral species that suggest glycosylation is important only in humans and may play a role in ligand-binding recognition. Here, we present characterization of recombinant HCMV UL144 glycoprotein by liquid chromatography-tandem mass spectrometry (LC-MS/MS). Intact protein analysis determined the accurate masses of these proteins. We have also analyzed the glycan profiles and identified the most glycosylated species. The binding studies showed specific function of UL144 glycosylation in immune recognition.

IN is Marie Curie Fellow financed by Programme SASPRO, co-funded by EU and the Slovak Academy of Sciences. The authors gratefully acknowledge the contribution of the Slovak Research and Development Agency (APVV-14-0839) and the contribution of the Scientific Grant Agency of the Slovak Republic (2/0020/18 and 2/0130/18).

## MS05-P01 | THE CRITICAL ROLE OF THE FOURTH POSITION OF THE VxGFL MOTIF OF PP2CS FROM ORYZA SATIVA IN REGULATION OF ABA RESPONSIVENESS

Han, Seungsu (Sungkyunkwan University, Suwon, KOR); Lee, Ji-Young (Duksung Women's University, Seoul, KOR); Lee, Yongmok (Sungkyunkwan University, Suwon, KOR); Kim, Tae-Houn (Duksung Women's University, Seoul, KOR); Lee, Sangho (Sungkyunkwan University, Suwon, KOR)

Regulation of abscisic acid (ABA) signaling is crucial in balancing responses to abiotic stresses and retaining growth in planta. An ABA receptor (PYL/RCAR) and a protein phosphatase (PP2C), a co-receptor, forms a complex upon binding to ABA. Previously we reported that the second and fourth positions in the VxGFL motif of PP2Cs from *Oryza sativa* are critical in the interaction of PP2Cs with PYL/RCARs. Considering substantial effects of the VxGFL motif on ABA signaling outputs, further comprehensive characterization of residues in the second and fourth positions are required. Here we surveyed the second and fourth positions of the VxGFL motif by combination of biochemical, structural and physiological analyses. We found that the fourth position of the VxGFL motif, highly conserved to small hydrophobic residues, was a key determinant of the OsPP2C50:OsPYL/RCAR interactions across subfamilies. Large hydrophobic or any hydrophilic residues in the fourth position abrogated ABA responsiveness. Comparison of crystal structures of OsPP2C50 mutants, S265L/I267V ("LV"), I267L ("SL") and I267W ("SW"), in complex with ABA and OsPYL/RCAR3, along with energy calculation of the complexes, revealed that a bulky hydrophobic residue in the fourth position of the VxGFL motif pushed away side chains of nearby residues, conferring side-chain rotameric energy stress. Hydrophilic residues in this position imposed solvation energy stress to the PP2C:PYL/RCAR complex. Germination and gene expression analyses corroborated that OsPP2C50 AS and AK mutants modulated ABA responsiveness in *Arabidopsis*. Our results suggest that ABA responsiveness could be finely-controlled by the fourth position of the VxGFL motif on PP2Cs.

## MS05-P02 | STRUCTURAL STUDIES OF TYPE II TNF- $\alpha$ FROM ORANGE-SPOTTED GROUPEL, EPINEPHELUS COIODES

Lin, Shih-Ming (Department of Biotechnology and Bioindustry Sciences, National Cheng Kung University, Tainan City, TWN); Lin, John Han-You (Institute of Veterinary Medicine, National Taiwan University, Taipei, TWN); Kuo, Wan-Ching (Department of Biotechnology and Bioindustry Sciences, National Cheng Kung University, Tainan city, TWN); Yu, Ming (Department of Biotechnology and Bioindustry Sciences, National Cheng Kung University, Tainan city, TWN)

TNF- $\alpha$  is one of the most important cytokines regulating the immune system in vertebrates. It is mainly secreted by macrophage to induce multiple immune responses of innate immunity. So far, a single type of TNF- $\alpha$  is found in the mammalian system. However, it is known that two types of TNF- $\alpha$  exist in teleost fish. Revealing the structural and functional variety between teleost and mammalian TNF- $\alpha$  would be important to understand the immunoregulation in the vertebrates. Here, we present the crystal structure of type II TNF- $\alpha$  from Orange-spotted Grouper, *Epinephelus coioides* at 3.6 Å resolution. The *Ec*TNF- $\alpha$ 2 structure showed a typical jelly-roll fold with eight beta strands and formed a homotrimer complex like the mammalian TNF- $\alpha$  proteins. Superposition of each protomer showed the r.m.s.d. is small than 2Å, indicating that the trimeric conformation does not have the orientational specificity. The interacting surfaces between protomers mainly consisted of hydrophobic residues and several highly conserved residues contribute to maintaining the robust trimeric conformation. The receptor-interacting regions of *Ec*TNF- $\alpha$ 2 are composed of several acidic residues, which means the electrostatic interaction is the major force to recognize the TNF- $\alpha$  receptor. Compare to the human TNF- $\alpha$ , *Ec*TNF- $\alpha$ 2 showed a highly structural homology but the receptor binding sites are relatively different. This study provides evidence revealing the functional and structural homology in the immune system of vertebrates. Further studies on the type I teleost TNF- $\alpha$  will be conducted to reveal the differences between the two types of TNF- $\alpha$  proteins.

## MS05-P115 LATE | STRUCTURAL STUDIES OF THE ATYPICAL SLAMF3 RECEPTOR

Shaikh, Ra'eessah (University of Leicester, Leicester, GBR); Burschowsky, Daniel (University of Leicester, Leicester, GBR)

The signalling lymphocyte activation module family (SLAMF) of type I transmembrane receptors has nine members, expressed broadly on hematopoietic cells. SLAMF3 is also expressed on hepatocytes. Generally, SLAMF receptors have two extracellular Ig-like domains, except for SLAMF3, which has four (D1 to D4). All SLAMF receptors, apart from SLAMF2, homodimerise via their extracellular N-terminal IgV-like domain (D1). On their cytoplasmic region, most SLAMF receptors have multiple immunoreceptor tyrosine-based switch motifs (ITSMs), which act as ligands for the adaptor proteins SAP and EAT-2. SLAMF3 is implicated in systemic lupus erythematosus (SLE), multiple myeloma (MM), hepatocellular carcinoma (HCC) and enhancing hepatitis C virus infection.

Here we present the high-resolution crystal structure of SLAMF3 D1. Similar to other known SLAMF N-terminal IgV-like domains, it comprises a two-layered  $\beta$ -sheet, however it appears to associate more strongly than any previously characterised SLAMF dimers. The interface contains 20 hydrogen bonds and 8 salt bridges, surrounding a hydrophobic patch, compared to the 9 hydrogen bonds and single salt bridge in the SLAMF6 interface and the 17 hydrogen bonds and zero salt bridges in the SLAMF5 interface. The c' loop of SLAMF3 D1 is truncated. SLAMF3 D2-3 has an atypical distribution of cysteines, which raises the possibility of an interdomain disulphide bond. We have expressed, refolded, crystallised and collected diffraction data of SLAMF3 D2-3, however we have so far been unable to solve the structure by molecular replacement or by sulphur SAD. We suggest that these domains have diverged since the gene duplication event that created them.

## MS05-P117 LATE | THE BEP1 FIC-DOMAIN: UNRAVELLING THE MECHANISM OF NARROW SELECTIVITY TOWARDS RAC GTPASES

Dietz, Nikolaus (University of Basel, Basel, CH); Huber, Markus (Biozentrum - University of Basel, Basel, CH); Sorg, Isabel (University of Basel, Basel, CH); Schirmer, Tilman (University of Basel, Basel, CH); Dehio, Christoph (University of Basel, Basel, CH)

Small GTPases of the Rho-family are molecular switches that regulate fundamental biological processes in mammalian cells. They thus represent favored targets of pathogens that strive to influence host cell behavior to their advantage. While most virulence factors target a wide range of GTPases, we recently discovered an effector of the gram-negative bacterium *Bartonella* spp. with unprecedented GTPase selectivity.

Here we show that the FIC-domain of *Bartonella* effector protein 1 (Bep1) exclusively AMPylates the Rac subfamily of Rho GTPases. Based on a co-crystallized FIC-target complex (IbpAFIC2-Cdc42), we generated an atomic model of the Bep1-Rac interaction and support the model with mutational studies and quantitative enzyme kinetics of wild-type and designed GTPases. This allowed us to pinpoint critical molecular details needed for Bep1-target selectivity.

## MS05-139 LATE | STRUCTURAL CHARACTERIZATION OF THE LINEAR UBIQUITIN CHAIN ASSEMBLY COMPLEX

Rodriguez, Alan (Institute of Molecular Biotechnology, Vienna, AUT); Vogel, Antonia (IMP - Research Institute of Molecular Pathology, Vienna, AUT); Orban-Nemeth, Zsuzsanna (Universitäts-Sportinstitut, AUT); Mechtler, Karl (AUT); Clausen, Tim (Department für Mikrobiologie, Immunbiologie und Genetik, AUT); Haselbach, David (AUT); Ikeda, Fumiyo (AUT)

The Linear Ubiquitin Chain Assembly Complex (LUBAC) is the only known mammalian ubiquitin ligase complex capable of assembling linear ubiquitin chains, which are essential in immune response, autophagy, and development. LUBAC is comprised of two ubiquitin ligases, HOIP and HOIL-1L, as well as the accessory protein Sharpin. HOIP is the ligase necessary in generation of linear ubiquitin chains, which are assembled by formation of a peptide bond between the C-terminal Gly of one ubiquitin and the N-terminal Met of another. HOIL-1L and Sharpin are needed for activation and stabilization of LUBAC although their precise roles remain unclear. The biological functions of LUBAC have been extensively studied, however structural work on the holoenzyme or its constituent components has been difficult given that recombinant expressions yield little protein of poor quality and stability. Furthermore gel filtration analysis indicates that the complex cannot be readily reconstituted *in vitro*. We have recently established a method to isolate recombinant LUBAC with high yield, stability, and purity. Using this protein we have begun to determine the structure of LUBAC by single particle negative stain- and cryo-electron microscopy. Sorting negatively stained particles into 2D class averages reveals a distinct elongated structure with a long axis of 12-15nm. We are aiming to obtain the first 3D map of the LUBAC holoenzyme from these 2D class averages and to collect micrographs from cryo-preparations for high-resolution structural determination. Additionally we are carrying out cross-linking mass spectrometry analysis to determine the relative domain positioning of the proteins in the complex.

## MS06: Proteins-Nucleic-Acid Interactions

---

### MS06-01 | STRUCTURAL STUDIES OF THE LEADING STRAND DNA POLYMERASE IN EUKARYOTES

Johansson, Erik (Umeå University, Umeå, SWE)

In eukaryotes, the duplication of the genome requires three different DNA polymerases with separate functions. Both genetic experiments and biochemical experiments have shown that DNA Polymerase epsilon is responsible for the bulk synthesis of the leading strand during DNA replication. In addition, it was recently shown that a mutation in the exonuclease domain of Pol epsilon, leads to an impaired proofreading capacity and is responsible for a very high mutation load in sporadic tumors. We have in addition to biochemical and genetic experiments solved a series of ternary structures of the catalytic core of Pol2 (142 kDa), the catalytic subunit of yeast Pol epsilon. I will here discuss some of our most recent findings, for example the structural basis for the very high processivity of DNA polymerase epsilon, the presence of an Fe-S cluster in the catalytic domain, and how a single amino acid substitution (P301R in yeast, orthologous to P286R in human Pol epsilon) can alter the high-fidelity polymerase to become a very strong mutator polymerase. The structure, in combination with molecular dynamics simulations, revealed major differences between Pol epsilon - P301R and the catalytically inactive Pol epsilon - D290A,E292A in the mechanism of exonuclease inactivation, and help explain the vastly stronger mutagenic and tumorigenic effects of the cancer variant.

## MS06-02 | STRUCTURAL BASIS OF RIBOSOMAL RNA SYNTHESIS IN BACTERIA

Wahl, Markus (Freie Universität Berlin, Berlin, GER)

Ribosomal RNA synthesis in *Escherichia coli* involves a transcription elongation complex (EC), in which RNA polymerase is modified by a signal element on the transcript, Nus factors A, B, E and G, ribosomal protein S4 and inositol mono-phosphatase SuhB. This EC is resistant to  $\rho$ -dependent termination and facilitates ribosomal RNA folding, maturation and subunit assembly. I will report on recent results from our lab on the functional architecture of the ribosomal RNA EC.

## MS06-03 | RNA TRANSLOCATION MECHANISM OF SPLICEOSOMAL DEAH-BOX ATPASES

Hamann, Florian (Georg-August-University Goettingen, Goettingen, GER); Schmitt, Andreas (Georg-August-University Goettingen, Goettingen, GER); Favretto, Filippo (Max Planck Institute for Biophysical Chemistry, Goettingen, GER); Zweckstetter, Markus (Max Planck Institute for Biophysical Chemistry, Goettingen, GER); Ficner, Ralf (Georg-August-University Goettingen, Goettingen, GER)

Spliceosomal DEAH-box ATPases were long thought to fulfill their tasks by direct unwinding of RNA duplexes. Recent studies, however, suggest that they rather function as ssRNA translocases and remodel the spliceosome from a distance by a mechanism called winching. Crystallographic studies on DEAH-box ATPases over the last decade have tried to shed light onto their motor function and the analyses of different ligand-bound states have been key to unravel the molecular dynamics. While early ADP-bound structures of Prp43 revealed the global architecture, later ATP- and RNA-bound structures unmasked insights into the RNA-loading and -binding mechanism and first domain movements could be described. More recently, adenosine nucleotide-free structures of Prp22 showed that DEAH-box ATPases are able to adopt more open conformations of the helicase core in the absence of ADP/ATP. By toggling between these closed and open conformations of the helicase core they are able to translocate along an ssRNA in 3'-5' direction with a step-size of one RNA nucleotide per hydrolyzed ATP. These dynamics additionally pose a particular challenge for other interaction partners, such as G-patch proteins that modulate the function of Prp43 and Prp2. The G-patch motif of the intrinsically disordered protein Spp2 is mostly unfolded in solution but its N-terminal part stably binds Prp2 *via* an amphipathic  $\alpha$ -helix, while the C-terminal part of this motif adopts two alternative conformations in different crystal structures. The increased conformational freedom of this region likely allows the G-patch to adapt to the different adenosine nucleotide-dependent conformations of the helicase core.

## MS06-04 | MOLECULAR MECHANISMS OF TREX1 IN DNA REPAIR AND IMMUNE SILENCING

Huang, Kuan-Wei (Department of Biological Science and Technology, National Chiao-Tung university, Hsinchu, TWN); Liu, Tung-Chang (Institute of molecular medicine and bioengineering, National Chiao-Tung university, Hsinchu, TWN); Hsiao, Yu-Yuan (Department of Biological Science and Technology, National Chiao-Tung university, Taiwan, Hsinchu, TWN); Hsiao, Yu-Yuan (Institute of molecular medicine and bioengineering, National Chiao-Tung university, Hsinchu, TWN)

Mammalian TREX1 provides the major 3'-to-5' exonuclease activity in immune silencing and DNA repair, and its defects are related to multiple inflammation and autoimmune disorders. A long-standing mystery is how TREX1 conducts 3'-overhang excision in DNA repair and dsDNA degradation in immune silencing. Here, the molecular basis of such unique catalytic activities are established by crystal structure analyses of TREX1 bound with a variety of structural DNA bearing a short 3'-overhang or damaged nucleotides. We found that the Leu24-Pro25-Ser26 cluster serves to cap the non-scissile 5'-end of the DNA for precise removal of the 3'-overhang or it wedges into the duplex region for dsDNA degradation. We also revealed the behaviours of TREX1 in acting on DNA lesions in the various DNA repair pathways and cooperating with HMGB-2 in immune silencing. This study thus uncovered unprecedented knowledge on the molecular mechanism of TREX1 in DNA processing.

## MS06-05 | STRUCTURAL ALPHABETS FOR CONFORMATIONAL ANALYSIS OF NUCLEIC ACIDS

Cerny, Jiri (Institute of Biotechnology, Czech Academy of Sciences, Vestec, CZE); Bozikova, Paulina (Institute of Biotechnology, Czech Academy of Sciences, Vestec, CZE); Schneider, Bohdan (Institute of Biotechnology, Czech Academy of Sciences, Vestec, CZE)

We present a universal nucleic acids structural alphabet suitable for conformational analysis of DNA as well as RNA structures. The underlying local conformational classes of dinucleotide step are characterized by seven torsion angles of the sugar-phosphate backbone, two torsions around glycosidic bonds, and three parameters describing the mutual orientation of bases within the step. Our previous definition of 44 DNA classes [1,2] was extended to incorporate also RNA conformers. We have obtained 84 conformational classes covering the combined structural variability of DNA and RNA.

The newly determined set of conformers substantially extends the previously determined set of RNA conformers [3]. All the classes are defined by means of hierarchical clustering of data from a sequentially non-redundant set of high resolution crystal structures containing about 60 and 60 thousands steps for DNA and RNA, respectively.

We have found that many of the previously defined conformational classes determined as specifically DNA [1] or RNA [3] are shared among nucleic acids. The most significant feature of new conformational classes is a high number of conformers with non-stacked steps. Despite the larger diversity of the molecular architecture of RNA molecules, many unstacked ("open") conformations are also found in DNA. The assignment of nucleic acids conformation is available at <https://dnatco.org> as a freely accessible web service [4].

[1] Schneider et al., *Acta Cryst. D* 2018, 74, 52-64.

[2] Schneider et al., *Genes (Basel)* 2017, 8, 278.

[3] Richardson et al., *RNA* 2008, 14, 465–481.

[4] Černý et al., *Nucleic Acids Research* 2016, 44, W284.

## MS06-P01 | STRUCTURAL INSIGHTS IN A MITOCHONDRIAL NUCLEOID MAINTENANCE FACTOR

Tarrés-Solé, Aleix (IBMB-CSIC, Barcelona, ESP)

*Candida albicans* is a human pathogen causative of a number of infectious diseases that can lead to life-threatening disorders in immunocompromised patients. Our aim is the structural characterization of a *C.albicans* mitochondrial DNA maintenance factor. This factor is indispensable for mitochondrial DNA maintenance and for *C.albicans* survival, thus representing a potential therapeutic target. We successfully expressed and purified the protein, and identified the DNA substrates suitable for crystallization. After performing serial screening from a custom DNA library we obtained crystals that diffract from low to medium resolution. We are currently working on structure solution by applying experimental phasing methods. Our current efforts are focused in dealing with highly anisotropic data which shows very weak anomalous signal. Strategies include addition of extra methionines by mutagenesis and heavy atom screenings. Complementary studies consist in SAXS analysis of the unbound protein and molecular microscopy imaging that shows DNA compaction by the protein.

## MS06-P02 | STRUCTURAL BASIS FOR RNA TRANSLOCATION AND NTP HYDROLYSIS BY THE ZIKA VIRUS NS3 HELICASE

Ge, Mengyu (York Structural Biology Laboratory, Department of Chemistry, University of York, York, GBR); Jenkins, Huw (York Structural Biology Laboratory, Department of Chemistry, University of York, York, GBR); Chechik, Maria (York Structural Biology Laboratory, Department of Chemistry, University of York, York, GBR); Jin, Yi (Cardiff Catalysis Institute, School of Chemistry, Cardiff University, Cardiff, GBR); Greive, Sandra (York Structural Biology Laboratory, Department of Chemistry, University of York, York, GBR); Antson, Fred (York Structural Biology Laboratory, Department of Chemistry, University of York, York, GBR)

Flaviviruses are single-stranded positive sense RNA viruses. Several members of this family, such as Dengue, Yellow Fever, and Zika viruses, are associated with important human diseases. Flaviviral non-structural protein 3 (NS3) helicase participates in RNA unwinding and capping, and is crucial for viral replication [1,2]. X-ray structures for protein complexes with a polynucleotide and/or NTP analogs have been reported for several Flaviviral NS3 helicases. However, the mechanism of coupling NTP hydrolysis with RNA translocation remains unclear.

In this study, we determined the first crystal structure for the Zika virus NS3 helicase complex with an ssRNA segment containing 5'-phosphate. Notably, the presence of the 5'-phosphate induces significant remodeling of the interactions with the 5'-nucleotide of RNA, unveiling the breadth of structural changes that can occur during RNA unwinding. Additionally, we determined the X-ray structures of the NS3 helicase in several different functional states of NTP hydrolysis, including the pre-hydrolysis, transition state and post-hydrolysis. Structural observations indicate how a catalytically important loop, that is involved in ATP hydrolysis, can mediate coupling with RNA translocation. Structural data are substantiated by NMR analysis of the NS3 helicase transition state complex, which demonstrate that the presence of RNA enhances the transition state formation. Taken together, our data clarify the mechanism for RNA unwinding that is applicable to all Flaviviridae family NS3 helicases.

[1] C. J. Neufeldt, *et al.*, *Nat. Rev. Microbiol.* **2018**, *16*, 125–142.

[2] V. J. Klema, *et al.*, *Viruses* **2015**, *7*, 4640–4656.

## MS06-P03 | STRUCTURAL STUDIES OF TEMPERATE PHAGE GENETIC SWITCHES

Varming, Anders (Department of Chemistry, University of Copenhagen, Copenhagen Ø, DNK); Rasmussen, Kim Krighaar (University of Copenhagen, Copenhagen Ø, DNK); Kilstrup, Mogens (Technical University of Denmark, Kgs Lyngby, DNK); Hammer, Karin (Technical University of Denmark, Kgs Lyngby, DNK); Ringkjøbing Jensen, Malene (CNRS, IBS, Grenoble, FRA); Ingmer, Hanne (University of Copenhagen, Frederiksberg, DNK); Lo Leggio, Leila (University of Copenhagen, Copenhagen Ø, DNK)

Temperate bacteriophages (TPs) may alternatively enter a lytic or a lysogenic cycle and have been shown to play a major role in the horizontal gene transfer of virulence and resistance genes between bacterial populations. The choice of lytic or lysogenic cycle in TPs is controlled by regulatory proteins and operator sites on the DNA creating a bi-stable genetic switch.

Here we present our work on the lysogeny switches of lactococcal TP901-1 phage and the staphylococcal phi13 phage, controlled by the CI repressor and the MOR anti-repressor.

We have taken an integrative structural biology approach to characterize the proteins and their interactions with DNA and each other, using a wide range of techniques, including crystallography, SAS, CD and NMR spectroscopy, ITC, DSF, MS, gel filtration and EMSA. We have previously structurally characterized CI repressor interaction with DNA through the N-terminal domain (NTD), the CI C-terminal dimerization domain and the hexameric full-length CI (Pedersen et al, 2008; Frandsen et al, 2013, Rasmussen et al, 2016, Rasmussen et al, 2018). Recently we have characterized the role of the flexible linker between the CI NTD and the C-terminal domain (CTD) and a heterodimeric complex between the CI NTD and the MOR anti-repressor.

Furthermore, we have initiated studies of the phi13 phage genetic switch and biochemical and biophysical characterization of its CI, which has a similar NTD structure, but a diverse CTD. These studies help us understand the diverse molecular mechanisms of phage genetic switches, and potentially their role in transfer of antibiotic resistance.

## MS06-P04 | CHROMOSOME PARTITIONING SYSTEM, PARABS

Sun, Yuh-Ju (National Tsing Hua University, Hsinchu, TWN)

ParABS is an important DNA partitioning process in chromosome segregation. ParABS consists of three major components: ParA (an ATPase), ParB (a *parS* binding protein) and *parS* (a centromere-like DNA). The homologous proteins of ParA and ParB in *Helicobacter pylori* are *HpSoj* and *HpSpo0J*, respectively. From the complex crystal structures of *HpSoj* and *HpSpo0J*, the *HpSoj*-DNA complex, *HpSoj* nonspecifically binds DNA through a continuous basic binding patch formed and the *HpSpo0J*-DNA complex, *HpSpo0J* folds into an elongated structure with a flexible N-terminal domain for protein-protein interaction and a conserved DNA-binding domain for *parS* DNA binding. Also, we detected the *HpSpo0J*-*HpSoj*-DNA complex, the nucleoid adaptor complex (NAC), by electron microscopy. NAC formation is promoted by *HpSoj* participation and specific *parS* DNA facilitation.

## MS06-P05 | MOLECULAR BASIS OF SELF-INDUCED GENOMIC DEGRADATION INHIBITION BY THE SUB-NANOMOLAR INTERACTION OF NIN WITH NUCA AND NUCB ENDONUCLEASES

Booth, Simon (Newcastle University, Newcastle upon Tyne, GBR); Norton, Lois (Newcastle University, Newcastle upon Tyne, GBR); Gaimster, Hannah (Centre for Bacterial Cell Biology, Newcastle upon Tyne, GBR); Basle, Arnaud (Newcastle University, Newcastle upon Tyne, GBR); Rao, Vincenzo (Newcastle University, Newcastle upon Tyne, GBR); Hewitt, Lorraine (Newcastle University, Newcastle upon Tyne, GBR); Murray, Heath (Centre for Bacterial Cell Biology, Newcastle upon Tyne, GBR); Lewis, Richard J. (Newcastle University, Newcastle upon Tyne, GBR)

Biofilms are communities of sessile bacteria that form on a wide variety of natural and man-made surfaces, sometimes at a detriment to human health. Bacteria in biofilms are held together by an extracellular matrix of polysaccharides, lipids, proteins, and extracellular DNA (eDNA). Species of *Bacillus* secrete two closely related endonucleases, Nuclease A and B (NucA & NucB), into their environment to degrade eDNA to ease its uptake by the cell either to enhance their genetic diversity, or for metabolic purposes, respectively. As a mechanism of protection from self-induced genome degradation, the genes for NucA and a putative cytosolic inhibitor, Nin, are present in a bi-cistronic operon presumably to drive co-expression.

Through a combination of biophysical/biochemical techniques, we probed the interaction between NucA/B and Nin from *Bacillus subtilis*. The structures of NucA/NucB in complex with Nin were solved by X-ray crystallography, revealing the mechanism of inhibition by Nin, and allowing for the calculated dismantling of the complexes by site-directed mutagenesis. We found that single alanine substitutions in Nin at the interface between the two proteins were insufficient to disrupt the interaction, however, reversing charges on Nin at electrostatic interfaces in conjunction with alanine mutations were sufficient to abrogate binding, whilst maintaining the overall fold of Nin. Genetic studies confirmed the importance of the interfacial residues, and this model system now permits future studies of how the Nin/Nuc complexes are disassembled at the membrane to permit secretion of the endonuclease whilst leaving the host genome intact.

## MS06-P06 | STRUCTURE AND FUNCTION OF *S. AUREUS* YABJ AS A NOVEL CHLORINATION-INDUCED RIBONUCLEASE

Kwon, Ae-Ran (Daegu Haany University, GyungSan-City, KOR)

The characteristic fold of a protein is the decisive factor for its biological function. However, small structural changes to amino acids can also affect their function, for example in the case of post-translational modification (PTM). Many different types of PTMs are known, but for some, including chlorination, studies elucidating their importance are limited. A recent study revealed that the YjgF/YER057c/UK114 family (YjgF family) member RidA from *Escherichia coli* shows chaperone activity after chlorination. Thus, to identify the functional and structural differences of RidA upon chlorination, we studied an RidA homolog from *Staphylococcus aureus*: YabJ. The overall structure of *S. aureus* YabJ was similar to other members of the YjgF family, showing deep pockets on its surface, and the residues composing the pockets were well conserved. *S. aureus* YabJ was highly stable after chlorination, and the chlorinated state is reversible by treatment with DTT. However, it shows no chaperone activity after chlorination. Instead, YabJ from *S. aureus* shows chlorination-induced ribonuclease activity, and the activity is diminished after subsequent reduction. Even though the yabJ genes from *Staphylococcus* and *Bacillus* are clustered with regulators that are expected to code nucleic acid-interacting proteins, the nucleic acid-related activity of bacterial RidA has not been identified before. From our study, we revealed the structure and function of *S. aureus* YabJ as a novel chlorination-activated ribonuclease. The present study will contribute to an in-depth understanding of chlorination as a PTM.

## MS06-P07 | STRUCTURAL STUDY TWO DIFFERENT FORMS OF SMAP FROM HALOBACTERIUM SALINARUM WHICH HAVE A DIFFERENT RNA-BINDING ABILITY

Fando, Maria (Institute of Protein Research, Pushchino, RUS); Lekontseva, Natalia (Institute of Protein Research, Pushchino, RUS); Buyuklyan, Julia (South Ural State Humanitarian Pedagogical University, Chelyabinsk, RUS); Nikulin, Alexey (Institute of Protein Research, Pushchino, RUS)

Archaeal Sm-like proteins belong to the large LSM family, which is characterized by the ability to adopt Sm fold. It is comprised of a 5-stranded  $\beta$ -sheet capped by an N-terminal  $\alpha$ -helix. Despite Lsm proteins are structurally conserved, the functions of the proteins in Archaea, Bacteria and Eukarya are different. Eukaryotic Sm/Lsm are part of several RNP particles and involved in the RNA processing. Bacterial Lsm protein Hfq exhibits RNA-chaperone activity, facilitate the interaction of regulatory sRNA with mRNA, thus regulating gene expression. Nowadays, there is little information about the functions of the archaeal Lsm proteins SmAP; some data shows that they appear to be involved in the processing of RNA.

Our work is concerned by structural and functional studies of SmAP from *Halobacterium salinarum* (HsaSmAP). We've found this protein is represented in databases in two forms: a length of 60 and 69 amino acids. Both variants of HsaSmAP have been isolated and their affinity to oligo(A) RNA, oligo(U) RNA, AMP and GMP have been measured. A difference in the affinity of the alternatives to the RNA has been found. The proteins were crystallized and X-ray diffractions data have been collected at ERSF in Grenoble. In contrast with majority of Lsm proteins, HsaSmAP has no unstructured N- and C-terminus or extended loops between secondary structure elements thus representing a minimal Lsm core. However, SmAP from *H. salinarum* has the characteristic for the Lsm proteins doughnut-shape form with seven monomers organized into a torus.

The work is supported by RFBR grant #18-04-00222

## MS06-P08 | USE OF THE COCOMAPS WEB SERVER TO ANALYZE AND VISUALIZE THE INTERFACE OF BIOMOLECULAR COMPLEXES IN CRYSTAL STRUCTURES

Oliva, Romina (University of Naples "Parthenope", Naples, ITA); Cavallo, Luigi (Kaust Catalysis Center, King Abdullah University of Science and Technology, Thuwal, SAU)

Interactions between biomolecules are at the basis of many of the most important molecular processes in the cell. Therefore, characterizing the interface of biological complexes is a fundamental step for possible biomedical and biotechnological applications and the number of crystal structures solved for them is steadily increasing.

COCOMAPS (bioCOMplexes CONTACT MAPS) is a user-friendly web application for the analysis, visualization and comparison of the interaction surface in biological complexes, such as protein-protein, protein-DNA and protein-RNA assemblies. It provides information, organized in tables, on the: i) interacting residues, defined on the basis of a cut-off distance, ii) residues at the interface, defined on the basis of the accessible surface area, and iii) intermolecular H-bonds. However, the hallmark of COCOMAPS is the contact map it provides, that is a two-dimensional representation of the interface where a dot is present at the cross-over of two residues which are in contact, i.e. within a cut-off distance. An online 3D visualization of the complex in Jmol and a ready-to-run PyMol script are also provided.

Input files can be downloaded directly from the wwPDB or uploaded locally. More chains can be selected for each interacting partner. Therefore, COCOMAPS can be used to analyze the interface between two molecules, between one molecule and an assembly or between two assemblies, depending on how many chains are specified.

Examples of the use of COCOMAPS for the analysis of crystal structures of biomolecular complexes in the corresponding original papers will be presented and discussed.

COCOMAPS is available at: <https://www.molnac.unisa.it/BioTools/cocomaps>.

## MS07: Structural Enzymology

---

### MS07-01 | TAKING CRYSTALLOGRAPHIC SNAPSHOTS OF VITAMIN B6 BIOSYNTHESIS AND TREATING SPECIFIC RADIATION DAMAGE

Tews, Ivo (University of Southampton, Southampton, GBR)

The enzyme complex PLP synthase catalyses a complex sequence of chemical reactions in the biosynthesis of vitamin B6. Structures of covalent enzyme-intermediate complexes illuminate the reaction cascade, starting from simple triose and pentose carbohydrates and the amino acid glutamine, and ending in formation of the aromatic heterocycle PLP, an active form of vitamin B6.

The main catalyst for this reaction is the Pdx1 enzyme which possesses a TIM-like ( $\beta\alpha$ )<sub>8</sub>-barrel fold. Together with the Pdx2 glutaminase, Pdx1 forms the PLP synthase complex with a molecular weight of ~750 kDa. The Pdx1 dual-specificity active site binds pentose and triose carbohydrates in sequence. The final product PLP, however, is observed in a second binding site.

An intermediate with a characteristic absorbance is key to understand the sophisticated enzyme structure. This intermediate is formed from the pentose ribose 5-phosphate and ammonia and bridges across binding sites by double Schiff base formation. A lysine relay mechanism to migrate carbonyl intermediates provides an elegant solution to the challenge of coordinating a complex sequence of reactions that follow a path of over 20 Å between substrate- and product-binding sites.

Electron rich compounds such as these intermediates are prone to specific radiation damage that can lead to misinterpretation. Dose-conservative diffraction analysis can limit the effects of radiation induced damage. Radiation induced decay was monitored using the spectroscopic signature of the intermediates, detected *in crystallo* using on-line micro-spectrophotometry at the time of crystallographic data collection. Low-dose multi-crystal data support the bridging structure of the intermediate.

## MS07-02 | CRYSTALLOGRAPHIC ENZYMOLOGY: USING SYNCHROTRON RADIATION FOR HIGH RESOLUTION IN SPACE AND TIME

Schneider, Thomas R. (EMBL c/o DESY, Hamburg, GER)

With the advent of highly brilliant synchrotron sources such as PETRA III, MAX IV (and a number ongoing or planned upgrades of other synchrotrons), it has become possible to produce X-ray beams optimally tailored to applications in structural enzymology. While highly homogenous and stable X-rays can be used to extract the best possible data from large ( $> 20 \mu\text{m}$ ) crystals, micro-focus beams can be used to obtain data from small ( $< 20 \mu\text{m}$ ) crystals. Being able to exploit small crystals is of particular value in the context of time-resolved crystallography as – in a pump-probe scenario - a homogeneous and synchronized triggering of a chemical reaction is often only possible for limited sample volumes. The routine availability of micro-focus X-ray beams on synchrotrons in combination with novel ‘serial’ sample presentation technologies (in many cases originating from experiments designed for XFELs) is now paving the way to a renaissance of pump-probe time-resolved macromolecular crystallography.

The EMBL beamline P14 on PETRA III (DESY, Hamburg) offers a wide range of beam properties and sample presentation modalities. We will discuss how high-resolution structural data can be obtained on large molecular machineries such as the 20S proteasome, how serial approaches can be used to extract structural data from micro-crystals, and how pump-probe time-resolved diffraction data can be collected on the new T-REXX endstation.

## MS07-03 | WATCHING AN ENZYME AT WORK: BREAKING THE STRONGEST SINGLE BOND IN ORGANIC CHEMISTRY

Schulz, Eike (Max Planck Institute for Structure and Dynamics of Matter (MPSD), Hamburg, GER); Mehrabi, Pedram (Max Planck Institute for Structure and Dynamics of Matter (MPSD), Hamburg, GER); Dsouza, Raison (Max Planck Institute for Structure and Dynamics of Matter (MPSD), Hamburg, GER); Müller-Werkmeister, Henrike M. (University of Potsdam, Potsdam, GER); Tellkamp, Friedjof (Max Planck Institute for Structure and Dynamics of Matter (MPSD), Hamburg, GER); Miller, R. J. Dwayne (Max Planck Institute for the Structure and Dynamics of Matter, Hamburg, GER); Pai, Emil F. (University of Toronto, Toronto, CAN)

The functional characterization of biomolecular catalysis requires a correlation of the three-dimensional structural ensemble with time-dependent changes. The advent of serial femtosecond time-resolved crystallography (TR-SFX) has provided insight into ultrafast time-scales of biomolecular function. This renaissance triggered the emergence of time-resolved serial synchrotron crystallography (TR-SSX), which simplifies accessing prevalent biological time-scales (> ns). To this end we have applied the recently developed the *hit-and return* (HARE)<sup>1</sup> approach which allows to collect several time points along the reaction coordinate of an enzyme during a single synchrotron beamtime. This contrasts conventional methods, which require several hours up to several beamtimes per time-point. We used the HARE approach to capture 18 time points from 30 milliseconds to 30 seconds during the non-reversible turnover cycle of fluoroacetate dehalogenase (FACD). These time points include all key states involved in enzymatic C-F bond cleavage: substrate binding and reorientation, covalent-intermediate formation, location of the water nucleophile and product release. In total four substrate turnovers can be observed between the two subunits, which are highly coupled but display different conformations. Reactivity is coupled to molecular breathing, expressed by dynamic changes in lateral FACD dimensions and modulation in water content pointing at an allosteric communication pathway between the two subunits. These results demonstrate the excellent suitability of TR-SSX to unravel biomolecular catalysis and provide key insights into protein dynamics.

[1]Schulz, E. C., Mehrabi P., Müller-Werkmeister H. *et al.* The hit-and-return system enables efficient time-resolved serial synchrotron crystallography. *Nature Methods*, 2018, doi:10.1038/s41592-018-0180-2

## MS07-04 | THE NEUTRON STRUCTURE OF LEISHMANIA MEXICANA TRIOSE PHOSPHATE ISOMERASE WITH TRANSITION STATE MIMICS REVEALS GENERAL BASE CATALYST

Kelpsas, Vinardas (Lund University, Lund, SWE); Caldararu, Octav (Lund University, Lund, SWE); Kulkarni, Yashraj (Uppsala University, Uppsala, SWE); Wierenga, Rikkert (University of Oulu, Oulu); Ryde, Ulf (Lund University, Lund, SWE); Kamerlin, Lynn (Uppsala University, Uppsala, SWE); von Wachenfeldt, Claes (Lund University, Lund, SWE); Oksanen, Esko (European Spallation Source ESS ERIC, Lund, SWE)

Triose phosphate isomerase (TIM) is a key enzyme in glycolysis that catalyses the interconversion of glyceraldehyde-3-phosphate and dihydroxyacetone phosphate. This simple reaction involves the shuttling of protons mediated by protolysable sidechains. The catalytic power of TIM is believed to stem from the ability to deprotonate a carbon next to a carbonyl group, generating an enediolate intermediate. The enediolate intermediate is believed to be mimicked by the inhibitor 2-phosphoglycolate (PGA) and the following enediol intermediate by phosphoglycolohydroxamate (PGH). We have determined the neutron structure of *Leishmania mexicana* TIM with both inhibitors and performed joint neutron-X-ray refinement followed by quantum refinement. The structures clearly show that in the complex PGA the postulated general base E167 is protonated, while in the PGH complex it remains deprotonated. The deuteron is also clearly localised on E167, which suggests that the hydrogen bond is a double-well hydrogen bond instead of a low-barrier hydrogen bond. The full picture of active site protonation states allows us to simulate the deprotonation step of the reaction at the empirical valence bond level as well as snapshots with *ab initio* quantum chemistry, confirming our mechanistic explanation.

## MS07-05 | ARABIDOPSIS AND CHLAMYDOMONAS PHOSPHORIBULOKINASE CRYSTAL STRUCTURES COMPLETE THE REDOX STRUCTURAL PROTEOME OF THE CALVIN-BENSON CYCLE

Fermani, Simona (University of Bologna, Department of Chemistry "G. Ciamician", Bologna, ITA)

Photosynthetic CO<sub>2</sub> fixation is a fundamental source of food, fuels and chemicals for human society. In land plants and algae, carbon fixation is operated by the Calvin-Benson cycle (CBC), a pathway of 13 distinct reactions catalyzed by 11 enzymes that takes place in the chloroplast, a specialized organelle operating the photosynthetic process. Thioredoxins (TRXs) are small ubiquitous proteins that coordinate the two stages of photosynthesis through a thiol-based mechanism. Among the CBC enzymes, the TRX target phosphoribulokinase (PRK) has yet to be characterized at the atomic scale. To fill this gap, the crystal structures of PRK were determined from two model species: the green alga *Chlamydomonas reinhardtii* (CrPRK) and the land plant *Arabidopsis thaliana* (AtPRK). PRK is an elongated homodimer characterized by a large central  $\beta$ -sheet of 18 strands, extending between two catalytic sites positioned at its edges. The electrostatic surface potential of the catalytic cavity shows a positive region suitable for binding the substrate phosphate groups and an exposed negative region to attract positively charged TRX-f. In the catalytic cavity, the regulatory cysteines are 13 Å apart and connected by a flexible region (clamp-loop) exclusive to photosynthetic eukaryotes which is believed to be essential for structural rearrangements required by the oxidation. Structural comparisons with prokaryotic and evolutionarily older PRKs revealed that both AtPRK and CrPRK have a strongly reduced dimer interface and increased number of random coiled regions, suggesting that a general loss in structural rigidity correlates with TRX sensitivity acquisition during the molecular evolution of PRKs in eukaryotes.

## MS07-P01 | CRYSTAL STRUCTURE OF THE CELL WALL BINDING DOMAIN OF A NOVEL BACTERIOPHAGE PBC5 ENDOLYSIN AND ITS PEPTIDOGLYCAN INTERACTION

Suh, Jeong-Yong (Seoul National University, Seoul, KOR)

Phage endolysins are hydrolytic enzymes that cleave the bacterial cell wall during the lytic cycle. In this study, we isolated the bacteriophage PBC5 against *Bacillus cereus*, a major foodborne pathogen, and describe the molecular interaction between its endolysin LysPBC5 and the host peptidoglycan structure. LysPBC5 has an N-terminal glycoside hydrolase 25 domain, and a C-terminal cell-wall binding domain (CBD) that is crucial for specific cell-wall recognition and lysis. The crystal and solution structure of CBD reveals tandem SH3b domains that are tightly engaged with each other. CBD binds to peptidoglycan in a bidentate manner via distal beta-sheet motifs with pseudo two-fold symmetry, which can explain its high affinity and host specificity. CBD primarily interacts with the glycan strand of the peptidoglycan layer instead of the peptide crosslink, implicating the tertiary structure of peptidoglycan as the recognition motif of endolysins

## MS07-P02 | ONCOGENIC KRAS G12C MUTATION DERIVED INHIBITOR DEVELOPMENT

Leveles, Ibolya (Budapest University of Technology and Economics, Budapest, HUN); Koppány, Gergely (Budapest University of Technology and Economics, Budapest, HUN); Nyíri, Kinga (Budapest University of Technology and Economics, Budapest, HUN); G. Vertessy, Beata (Budapest University of Technology and Economics, Budapest, HUN)

KRAS (Kirsten Rat Sarcoma Viral Proto-Oncogene) is a guanine binding signalling protein, which works as a molecular switch in controlling cell growth, differentiation and proliferation. GTP-bound KRAS is in active conformation that can interact with the downstream effectors, like SOS protein, while in the GDP-bound state the signalling decays. It has a high rate of mutagenesis, the most frequent G12C mutation is proven to play a significant role in almost 25 percent of all human cancers. Tumorous malignancies caused by KRAS mutations, such as pancreatic and lung cancer are generally difficult to treat, therefore in the recent years, there was a successful attempt to create promising KRAS inhibitors, that bind covalently to the cysteine of the G12C mutant protein.

In the present work we aim to develop new effective covalent inhibitors to KRAS G12C mutants, since at the time being there is no clinically suitable drugs for cancer therapy.

As a strategy, we applied the fragment-based drug development approach in the research of covalent KRAS inhibitors. Based on this approach we first tested small molecules (fragments) containing the reactive group which is responsible for forming the covalent bond. After validating the most efficient fragment hits, we develop an inhibitor that fits to the binding pocket of KRAS by gradually increasing the size of the fragment.

After successful protein cloning and purification, we managed to crystallize the apo- and inhibited KRAS G12C proteins, collecting X-ray data at BESSY Berlin synchrotron, data processing being in progress.

## MS07-P03 | STRUCTURAL AND FUNCTIONAL CHARACTERIZATION OF PHOSPHOGLUCOMUTASE 5

Pühringer, Dominic (University of Vienna, Vienna, AUT)

Phosphoglucomutase-like protein 5 (PGM5), also known as “Aciculin” or phosphoglucomutase-related protein (PGM-RP) is a member of the phosphohexose mutase protein family.

It is closely related to phosphoglucomutase 1 (PGM1), which catalyzes isomerization of glucose-1-phosphate to glucose-6-phosphate via its phosphotransferase activity.

PGM5 is expressed in smooth and cardiac muscle at high levels, it is localized at intercalated disks of cardiac muscle and myotendinous junctions of skeletal muscle, is part of the mature Z-disk and has been found to be a highly dynamic and mobile protein which is essential for myofibril formation, maintenance and remodelling. Knockdown of PGM5 has been shown to lead to failure of myofibril assembly, alignment and membrane attachment. The protein is also involved in areas of myofibrillar damage [1].

It has first been described as a novel dystrophin and utrophin binding protein [2], which has a purely structural role and lacks phosphoglucomutase activity [3]. Recently, the list of binding partners has been extended to also include striated muscle Z-disk proteins filamin C, Xin [1] and FATZ-1.

Revisiting the studies done in the early 90s, we can show in biochemical assays that PGM5 does possess phosphoglucomutase activity, albeit less than PGM1 and present the first crystal structure of the protein obtained in complex with an inhibitor of PGM1, fructose-1,6-bisphosphate, at 1.57 Å resolution.

[1] Molt S., et al., J Cell Sci. (2014) 127, 3578-92

[2] Molseeva, E. P., et al., Eur. J. Biochem. (1996) 235, 103-113

[3] Belkin, A.M., et al., Journal of Cell Science (1994) 107, 159-173

## MS07-P04 | REGIOSELECTIVE CARBOXYLATION BY PRENYLATED FLAVIN AND MN-DEPENDENT DECARBOXYLASES

Hofer, Gerhard (University of Graz, Graz, AUT); Payer, Stefan E. (University of Graz, Department of Chemistry, Organic & Bioorganic Chemistry, Graz, AUT); Plasch, Katharina (University of Graz, Department of Chemistry, Organic & Bioorganic Chemistry, Graz, AUT); Bärland, Natalie (Max-Planck Institute of Biophysics, Frankfurt am Main, GER); Marschall, Stephen A. (University of Manchester, Manchester Institute of Biotechnology, Manchester, GBR); Sheng, Xiang (Stockholm University, Department of Organic Chemistry, Stockholm, SWE); Vonck, Janet (Max-Planck Institute of Biophysics, Frankfurt am Main, GER); Gruber, Karl (University of Graz, ZMB, Graz, AUT); Himo, Fahmi (Stockholm University, Department of Organic Chemistry, Stockholm, SWE); Leys, David (University of Manchester, Manchester Institute of Biotechnology, Manchester, GBR); Faber, Kurt (University of Graz, Department of Chemistry, Organic & Bioorganic Chemistry, Graz, AUT); Keller, Walter (University of Graz, ZMB, Graz, AUT); Glueck, Silvia M. (University of Graz, Department of Chemistry, Organic & Bioorganic Chemistry, Graz, AUT); Pavkov-Keller, Tea (University of Graz, ZMB, Graz, AUT)

Carboxylation reactions received considerable attention in view of the use of CO<sub>2</sub> as abundant C<sub>1</sub>-building block for sustainable chemical production. However, to date only a few examples of CO<sub>2</sub> fixation reactions have been realized on industrial scale, mainly due to the high-energy input required for substrate activation. In order to expand the biocatalytic carboxylation toolbox, we searched and characterized enzymes enabling the regiocomplementary *para*- and *ortho*-carboxylation of electron-rich aromatic compounds.

The enzyme-catalyzed *para*-carboxylation of catechols employs 3, 4-dihydroxybenzoic acid decarboxylase (AroY). Crystal structures and accompanying solution data confirm AroY utilizes the recently discovered prenylated FMN cofactor (prFMN), and requires oxidative maturation to form the catalytically competent prFMN<sup>iminium</sup> species. The enzymes form hexameric assemblies, arranged as a trimer of dimers. The same quaternary structure is observed for all crystallographically independent AroY monomers, and in the 4.6 Å cryo-EM solution structure of *apo*-AroY. The putative flexibility of individual domains and its influence on enzyme mechanism is discussed.

The *ortho*-carboxylation of resorcinol is achieved by utilization of 2, 3-dihydroxybenzoic acid decarboxylase from *Aspergillus oryzae*. The tetrameric arrangement of its amidohydrolase fold subunits, as well as metal ion promiscuity allowing for the incorporation of Mg<sup>2+</sup> in its active site instead of Mn<sup>2+</sup> are explored.

*Acknowledgment:* Supported by the Austrian Science Fund (FWF - P26863 and P29432).

## MS07-P05 | STUDYING THE STRUCTURAL BASIS FOR SELECTIVITY IN COMPLEXES OF PEPTIDE INHIBITORS AND SERINE-PROTEASES OF THE COMPLEMENT SYSTEM

Dürvanger, Zsolt (Laboratory of Structural Chemistry and Biology, Eötvös Loránd University, Budapest, HUN); Boros, Eszter (Department of Biochemistry, Eötvös Loránd University, Budapest, HUN); Hegedus, Rózsa (MTA-ELTE Research Group of Peptide Chemistry, Budapest, HUN); Dobó, József (Institute of Enzymology, Research Centre for Natural Sciences, Hungarian Academy of Sciences, Budapest, HUN); Kocsis, Andrea (Institute of Enzymology, Research Centre for Natural Sciences, Hungarian Academy of Sciences, Budapest, HUN); Fodor, Krisztián (Department of Biochemistry, Eötvös Loránd University, Budapest, HUN); Gál, Péter (Institute of Enzymology, Research Centre for Natural Sciences, Hungarian Academy of Sciences, Budapest, HUN); Mezo, Gábor (MTA-ELTE Research Group of Peptide Chemistry, Budapest, HUN); Pál, Gábor (Department of Biochemistry, Eötvös Loránd University, Budapest, HUN); Harmat, Veronika (Eötvös Loránd University, Institute of Chemistry, Budapest, HUN); Karancsiné Menyhárd, Dóra (MTA-ELTE Protein Modelling Research Group, Budapest, HUN)

Mannan-binding lectin-associated serine proteases (MASPs) are trypsin-type serineproteases that play a key role in the activation of the complement system via the lectin pathway. Selective peptide inhibitors of MASP-1 and MASP-2 were developed using the phage display technique based on the sunflower trypsin inhibitor (SFTI). SFTI is a member of the Bowman-Birk inhibitor family and forms a stable  $\beta$ -hairpin structure in solution, which is stabilized by a disulfide bond. This structure remains essentially unchanged upon complex formation with trypsin. The metabolic stability of the evolved inhibitors were increased by replacing the disulfide bond with a thioether containing linker. The efficiency of the peptides proved to be highly dependent on the linker length.

To find the structural basis of the selectivity and the significantly different efficiency of the peptides, we studied the inhibitors and their complexes with MASPs using X-ray crystallography, ECD spectroscopy and MD simulations. We solved the crystal structure of the MASP-1 specific inhibitor, SFMI-1 in complex with MASP-1 and refined the structure to 2.7Å resolution. It was found that directed evolution of SFTI, a peptide with a stable  $\beta$ -hairpin structure, resulted in highly flexible peptides. Despite the high flexibility of the selected inhibitors, the binding mode of the most efficient peptides is highly similar to that of found in the SFTI / trypsin complex.

This study was supported by the MedInProt program of the Hungarian Academy of Sciences, OTKA grants K116305, K100769 and K119386, the VEKOP-2.3-2-16-2017-00014 and VEKOP-2.3.3-15-2017-00018 grants. We acknowledge ESRF for providing synchrotron radiation beamtime.

## MS07-P06 | COVALENT BOND BETWEEN SIDE CHAINS OF TRYPTOPHAN AND HISTIDINE IN BILIRUBIN OXIDASE IS ESSENTIAL FOR SUBSTRATE BINDING

Dohnálek, Jan (Institute of Biotechnology of the Czech Academy of Sciences, Vestec, CZE); Koval, Tomáš (Institute of Biotechnology of the Czech Academy of Sciences, Vestec, CZE); Švecová, Leona (Institute of Biotechnology of the Czech Academy of Sciences, Vestec, CZE); Švecová, Leona (Faculty of Nuclear Sciences and Physical Engineering, Czech Technical University in Prague, Prague, CZE); Østergaard, Lars (Novozymes A/S, Bagsvaerd, DNK); Skálová, Tereza (Institute of Biotechnology of the Czech Academy of Sciences, Vestec, CZE); Dušková, Jarmila (Institute of Biotechnology of the Czech Academy of Sciences, Vestec, CZE); Kolenko, Petr (Institute of Biotechnology of the Czech Academy of Sciences, Vestec, CZE); Kolenko, Petr (Faculty of Nuclear Sciences and Physical Engineering, Czech Technical University in Prague, Prague, CZE); Fejfarová, Karla (Institute of Biotechnology of the Czech Academy of Sciences, Vestec, CZE); Stránský, Jan (Institute of Biotechnology of the Czech Academy of Sciences, Vestec, CZE); Trundová, Mária (Institute of Biotechnology of the Czech Academy of Sciences, Vestec, CZE); Hašek, Jindrich (Institute of Biotechnology of the Czech Academy of Sciences, Vestec, CZE)

Bilirubin oxidase (EC 1.3.3.5) from *Myrothecium verrucaria* is a blue multicopper oxidase capable of oxidation of organic and inorganic substrates, including bilirubin. It utilizes two active sites with one and three copper ions to transfer electrons from substrates from site T1 to the trinuclear cluster and to reduce molecular oxygen to water [1,2]. The enzyme is used in a number of fields, including medicine and biotechnologies. The substrate oxidation site has an exceptional feature - a covalent link between His398, coordinating T1 Cu, and Trp396, forming the substrate binding site [3]. Here we show that the covalent modification, verified by mass spectrometry and crystallography, alters the T1 copper coordination and is crucial for formation of the properly organized substrate binding site. Mutagenesis of Trp396 leads to conclusions that the adduct is crucial for oxidation of substituted phenols and substantially influences the rate of bilirubin oxidation. Even if the link likely participates in the actual electron transfer, its importance lies rather in formation of the substrate binding site. Our crystallographic data for substrate binding uncover important amino acid residues of the substrate binding site and explain why in the absence of the Trp396 side chain the activity of the enzyme remains unchanged for some substrates. This work was supported by ERDF (CZ.02.1.01/0.0/0.0/15\_003/0000447, CZ.02.1.01/0.0/0.0/16\_013/0001776) and MEYS CR (LM2015043).

[1] Murao, S., Tanaka, N. (1981) *Agric. Biol. Chem.* **45**, 2383–2384.

[2] Mizutami, K., et al. (2010) *Acta Cryst.*, **F66**, 765–770.

[3] Akter, M., et al. (2018) *Chemistry* **24**, 18052–18058.

## MS07-P07 | BEETLE LUCIFERASES AND THEIR COLOR EMISSION

Rabeh, Wael (New York University Abu Dhabi, Abu Dhabi, ARE)

The different colors of light emitted by bioluminescent beetles ranging from yellow–green to red are related to slightly different enzymes (luciferases) that catalyze the same two–stage chemical reaction, conversion of luciferin to oxyluciferin in presence of ATP and oxygen. However, luciferases with known crystal structures emit only green light with several mutations resulted in red emission ( $\lambda_{\text{max}}$  610 nm) that is still far from the emission of the only red-emitting beetle luciferases (623 nm) from *Phrixothrix hirtus* (RE<sub>ph</sub>). To shed light on the mechanism of color “tuning” in beetle luciferases, we determined the crystal structure of RE<sub>ph</sub> in addition to a blue-shifted green-emitting luciferase from the firefly *Amydetes vivianii* (GB<sub>Av</sub>). The structure of RE<sub>ph</sub> was found to be an oligomer with monomers with a/b structural fold, similar to other known luciferase structures. The active site is located between the large N-terminal and small C-terminal domains, where it opens or closes by motion of the latter. Multiple mutations were introduced in two loops to evaluate their roles in the emission color. First, loop<sup>346–361</sup> at the bottom of the active site was found to have an effect on the energy of the emitted light. However, loop<sup>346–361</sup> contains amino acids that affected emission of the RE<sub>ph</sub> and GB<sub>Av</sub> luciferases.

## MS07-P08 | NEW STRUCTURAL INSIGHT INTO THE WELL KNOWN PEPTIDE FLIP OBSERVED IN FLAVODOXINS.

Gudim, Ingvild (University of Oslo, Oslo, NOR); Lofstad, Marie (University of Oslo, Oslo, NOR); Hammerstad, Marta (University of Oslo, Oslo, NOR); van Beek, Wouter (European Synchrotron Radiation Facility, Grenoble, FRA); Hersleth, Hans-Petter (University of Oslo, Oslo, NOR)

Flavodoxins (Flds) are small proteins that shuttle electrons in a range of reactions in microorganisms. Flds contain a redox-active cofactor, a flavin mononucleotide (FMN), and it is well established that when Flds are reduced by one electron, a peptide bond close to the FMN isoalloxazine ring flips to form a new hydrogen bond with the FMN N5H, stabilising the one-electron reduced state. Here, we present high-resolution crystal structures of Flavodoxin 1 from *Bacillus cereus* in both the oxidised and one-electron reduced (semiquinone) state. We observe a mixture of conformers in the oxidised state; a 50:50 distribution between the established oxidised conformation where the peptide bond is pointing away from the flavin, and a conformation where the peptide bond is pointing toward the flavin, approximating the conformation in the semiquinone state. We use single-crystal spectroscopy to demonstrate that the mixture of conformers is not caused by radiation damage to the crystal. This is the first time that such a mixture of conformers is reported in a wild-type Fld. We therefore carried out a survey of published Fld structures, which show that several proteins have a pronounced conformational flexibility of this peptide bond. The degree of flexibility seems to be modulated by the presence, or absence, of stabilising interactions between the peptide bond carbonyl and its surrounding amino acids [1,2].

[1] I. Gudim, M. Lofstad, W. van Beek, H.-P. Hersleth, *Protein Sci.* 27 (2018) 1439-1449.

[2] I. Gudim, M. Hammerstad, M. Lofstad, H.-P. Hersleth, *Biochemistry* 57 (2018) 5427–5436.

## MS07-P09 | ACTIVE SITE EVOLUTION IN BIOMASS DEGRADING ENZYMES

Frandsen, Kristian E.H. (University of Copenhagen, Copenhagen, DNK); Tandrup, Tobias (University of Copenhagen, Copenhagen, DNK); Poulsen, Jens-Christian N. (University of Copenhagen, Copenhagen, DNK); Mazurkewich, Scott (Chalmers University of Technology, Gothenburg, SWE); Huang, Qian (University of Copenhagen, Copenhagen, DNK); Labourel, Aurore (INRA, Aix Marseille University, Marseille, FRA); Garcia-Santamarina, Sarela (Duke University, Durham, USA); Arnling Bååth, Jenny (Chalmers University of Technology, Gothenburg, SWE); Tovborg, Morten (Novozymes A/S, Bagsværd, DNK); Berrin, Jean-Guy (INRA, Aix Marseille University, Marseille, FRA); Thiele, Dennis J. (Duke University, Durham, USA); Larsbrink, Johan (Chalmers University of Technology, Gothenburg, SWE); Johansen, Katja S. (University of Copenhagen, Frederiksberg, DNK); Lo Leggio, Leila (University of Copenhagen, Copenhagen, DNK)

Plant polysaccharides are important resources for energy and biomaterials production, but many applications rely on breaking down the biomass to monosaccharides, thus the recalcitrance of *eg* lignocellulose is an obstacle to its full utilization.

Lytic polysaccharide monooxygenases (LPMOs) and glucuronoyl esterases (GEs) are enzymes characterized within the last ten years and can boost the action of longer-known polysaccharide- degrading enzymes, which are primarily glycoside hydrolases.

LPMOs have a characteristic histidine brace motif binding the active site copper, which activates oxygen leading to oxidative breakage of the glycosidic bond [1]. LPMOs have relatively flat binding surfaces, allowing them to attack regions on the surface of crystalline polysaccharides inaccessible to most glycoside hydrolases.

GEs act through a classic Ser, His, Asp/Glu catalytic triad [2]. GEs are believed to attack ester bonds between hemicellulose and lignin, thus making the polysaccharides in lignocellulose more accessible to other enzymes.

Focus of this presentation will be our recent results showing how the active sites of LPMOs and GEs have diversified to tune/change their function, providing fascinating examples of enzyme evolution. In particular:

- The active site carboxylate in GEs can be positioned differently on the structure, and sometimes two carboxylate residues are present
- A newly discovered family of LPMOs has a carboxylate as additional copper ligand and has taken roles in copper homeostasis
- Some LPMO homologues have lost their copper site, yet still play roles in biomass degradation

[1] Tandrup et al, BST, 2018

[2] Baath et al, JBC, 2019

## MS07-P10 | INTERDOMAIN CONFORMATIONAL FLEXIBILITY OF THE PEPTIDOGLYCAN N-ACETYLGLUCOSAMINIDASES OF STAPHYLOCOCCUS AUREUS

Pintar, Sara (Jožef Stefan Institute, Ljubljana, SVN); Borišek, Jure (National Institute of Chemistry, Ljubljana, SVN); Usenik, Aleksandra (Jožef Stefan Institute, Ljubljana, SVN); Perdih, Andrej (National Institute of Chemistry, Ljubljana, SVN); Turk, Dušan (Jožef Stefan Institute, Ljubljana, SVN)

Bacterial cell wall enables the cell to withstand the osmotic pressure and thus enables its survival in a large set of different habitats. Yet for cells to grow and divide it has to be remodeled in a controlled manner. Cell wall is composed of glycan strands comprising alternating N-acetylglucosamine (NAG) and N-acetylmuramic acid (NAM) and cross-linked by peptides. Peptidoglycan hydrolases have been shown to be important for peptidoglycan maturation, turnover and recycling as well as antibiotic resistance.

Bacterial peptidoglycan N-acetylglucosaminidases have a typical lysozyme-like fold with active site glutamate in centre of the highly conserved core that consists of five or six helices. Crystal structures of two N-acetylglucosaminidases, SagB and AtlA-gl, revealed very similar fold to another *S. aureus* N-acetylglucosaminidase, AtlE, however with unexpectedly different L- and R-domain packing. Consequentially, the substrate binding clefts of SagB and AtlA-gl are significantly wider than in that of AtlE.

Structural analysis and mutational studies confirmed that substrate interacts with active site residues on the left and right side of the active site cleft. This suggests that a substantial conformational change has to take place to enable productive binding of the substrate and subsequential reaction to transpire.

## MS07-P11 | DIFFERENCES IN CRYSTALLIZATION OF SEVERAL SELECTED HALOALKANE DEHALOGENASES AND THEIR MUTATION VARIANTS

Kuta Smatanova, Ivana (University of South Bohemia, Ceske Budejovice, CZE); Prudnikova, Tatyana (University of South Bohemia, Ceske Budejovice, CZE); Kutý, Michal (University of South Bohemia, Ceske Budejovice, CZE); Damborsky, Jiri (Masaryk university Brno, Brno, CZE); Chaloupkova, Radka (Masaryk university Brno, Brno, CZE)

Knowledge of the structure of proteins is a key in identifying and describing the detailed mechanism of biological processes, the development of therapeutics, the degradation of pollutants from the environment, etc. One of the methods used to determine the structure of proteins on atomic resolution is X-ray crystallography. For many years, our laboratory has been researching structures of different types and mutant variants of haloalkane dehalogenases (HLDs) that are responsible for one of the key reactions in the bacterial degradation of various halogenated pollutants - environmentally unfriendly compounds. HLDs can be potentially applying in bioremediation, biosensing of pollution, biosynthesis, cellular imaging and protein immobilization. These enzymes catalyze the cleavage of a carbon-halogen bond in haloalkanes with water as the sole co-substrate, resulting in formation of a halide ion, a corresponding alcohol, and a proton. To date, several tertiary structures of different HLDs enzymes have been solved by X-ray diffraction analysis, providing a good theoretical framework for their modification by protein engineering. Crystallization conditions for haloalkane dehalogenases such as DhaA from *Rhodococcus rhodochrous* NCIMB 13064, LinB from *Sphingobium japonicum* UT26, and DbeA from *Bradyrhizobium elkanii* USDA94 and their mutant variants were compared and analyzed. Based on carefully designed experiments and by combination of the information obtained from complementary techniques it was possible to get inside into conformational changes of selected enzymes upon their interactions with substrates as well as location of hydrogen atoms inside the enzyme active site and the access tunnels.

This research is supported by the GACR (17-24321S).

## MS07-P12 | ENZYMATIC CONTROL OF O<sub>2</sub> REACTIVITY AND FUNCTIONALIZATION OF THE FLAVIN COFACTOR

Saleem Batcha, Raspudin (University of Freiburg, Freiburg, GER); Teufel, Robin (University of Freiburg, Freiburg, GER)

The chemical reactions of enzymes and cofactors with gaseous molecules such as dioxygen (O<sub>2</sub>) are demanding to study and remain a contentious field in biochemistry. Until now, it remains partially cryptic how enzymes steer their reactions with O<sub>2</sub>, as exemplified by the ubiquitous flavoenzymes that mostly facilitate redox reactions such as the oxygenation of organic substrates. We employed O<sub>2</sub>-pressurized X-ray crystallography and quantum mechanical calculations to reveal how particular positioning of O<sub>2</sub> within flavoenzyme active sites enables the regiospecific formation of covalent flavin-N5-oxygen adducts that may serve as oxygen transferring agent (e.g. the flavin-N5-oxide) by mimicking a critical transition state. This study establishes how flavoenzymes may control the O<sub>2</sub> functionalization of an organic cofactor as prerequisite for oxidative catalysis. Our work thus illustrates how O<sub>2</sub> reactivity can be harnessed in an enzymatic environment and provides important knowledge for future rational design of O<sub>2</sub>-reactive enzymes.

## MS07-P13 | ENZYME ACTIVATION BY A FLAVOPROTEIN REDOX NETWORK

Hammerstad, Marta (University of Oslo, Oslo, NOR); Gudim, Ingvild (University of Oslo, Oslo, NOR); Lofstad, Marie (University of Oslo, Oslo, NOR); Kjendseth Røhr, Åsmund (Norwegian University of Life Sciences, Ås, NOR); Hersleth, Hans-Petter (University of Oslo, Oslo, NOR)

Ribonucleotide reductases (RNRs) reduce ribonucleotides to deoxyribonucleotides by employing radical chemistry. In class Ib RNRs, reduced NrdI, a flavodoxin-like protein, is essential for the activation of a dimanganese center in the radical generating RNR  $\beta$  subunit. It has been proposed that NrdI is recycled *in vivo* by an NrdI reductase, but no such reductase had been identified. Ferredoxin/flavodoxin-NADP<sup>+</sup> oxidoreductases (FNRs) are probable reductants of NrdI. We identified three FNRs in the genome of *Bacillus cereus* and carried out structural and functional studies in order to characterize their ability to reduce NrdI. By comparing reduction kinetics, binding affinities, redox potentials and 3D structure, we have shown that one FNR reduces NrdI at a much higher rate than the two remaining FNRs. Using this FNR as an NrdI reductase, we were also able to activate the RNR  $\beta$  subunit under aerobic conditions, mimicking cellular conditions. Altogether, our observations suggest that this FNR might be the superior NrdI reductase *in vivo*, and hence, an essential activator of the class Ib RNR system.

In addition to NrdI, *B. cereus* encodes two flavodoxins (Flds). We have performed biochemical and structural investigations of the full FNR-Fld/NrdI redox network, and identified that one FNR-Fld pair is more efficient than the others. By studying the interactions between proteins in flavoprotein networks, which are poorly characterised in bacteria, we aim to map defining features that govern recognition and selectivity for electron transfer between flavoproteins.

## MS07-P14 | COMPETITIVE BINDING OF POTENTIAL DRUG MOLECULES AT THE ACTIVE SITE OF AN ACYLPEPTIDE-HYDROLASE

Kiss-Szemán, Anna (Eotvos Loránd University, Budapest, HUN)

Acylaminoacyl-peptidases (AAP) are oligopeptidases that cleave short peptides or protein segments, while they function as exopeptidases (processing N-terminal acylated peptides) and endopeptidases too.

For members of its enzyme family two basic ways of substrate selection have been discovered: flexible domain movement between opened and closed form, or multimerization of rigid monomers. The formation of multimers is linked to the shielding of the "sticky edge" of a  $\beta$ -sheet - to avoid aggregation. In archeal *PhAAP* formation of hexamers with a complex channel system is responsible for  $\beta$ -edge shielding and for the size selection too, in contrast, *Aeropyrum pernix* AAP (*ApAAP*) forms dimers capable for a gating mechanism by domain movements providing size selection of the substrates [1]. The mammalian enzyme – present also in the human liver – is a key protein in the upstream regulation of the proteasome [2]. It was also proven to be part of a competitive binding process with a carbapenem type of antibiotics, such as meropenem [3]. The goal of our study is to determine the process of this competition with the help of protein crystallography on the archaeal analogues, since the structure of the mammalian AAP has not yet been determined.

The *ApAAP* S445A and D524A mutants were crystallized and the obtained crystals were soaked into the meropenem solution for 1, 8 and 20 days to study the effect of time on degradation.

[1] Menyhárd 2013, 2015

[2] Palmieri 2011

[3] Yokogawa 2001

## MS07-P15 | STRUCTURAL INSIGHT IN PEPTIDYL SUBSTRATE BINDING TO CYSTEINE

### CATHEPSINS

Loboda, Jure (Institute Jozef Stefan, Ljubljana, SVN); Tusar, Livija (Jozef Stefan Institute, Ljubljana, SVN)

Jure Loboda<sup>1</sup>, Piotr Sosnowski<sup>2</sup>, Livija Tusar<sup>1,2</sup>, Robert Vidmar<sup>1</sup>, Matej Vizovisek<sup>1</sup>, Jaka Horvat<sup>5</sup>, Gregor Kosec<sup>5</sup>, Francis Impens<sup>3,4</sup>, Hans Demol<sup>3</sup>, Boris Turk<sup>1</sup>, Kris Gevaert<sup>3,4</sup>, Dusan Turk<sup>1,2</sup>

1 Department of Molecular and Structural Biology, Jozef Stefan Institute, Jamova 39, Ljubljana, Slovenia

2 Centre of excellence CIPKEBIP, Jamova 39, Ljubljana, Slovenia

3 VIB Center for Medical Biotechnology, A. Baertsoenkaai 3, Ghent, Belgium

4 Department of Biomolecular Medicine, Ghent University, A. Baertsoenkaai 3, Ghent, Belgium

5 Acies Bio d.o.o., Tehnološki park 21, 1000 Ljubljana, Slovenia

We are trying to understand how cysteine cathepsins select their endogenous substrates. Analysis of proteomic study of the cell lysate, which was enriched with selected cathepsins, suggested representative peptides as a model of protein substrates based on cathepsin's specific cleavages. Using a structural approach we attempted to validate the peptide model with the crystal structures of active-site mutant human cathepsin V in complex with those peptides. The first generation peptides were designed to explore possible cooperative effects of amino acids binding into S1 and S2' subsites of the enzyme. The second generation peptides were hexapeptides selected from the proteomic data. We observed electron density of mainly cleaved or shifted peptides at the active site, possibly due to interactions of their charged termini. The analysis of the third generation peptides of various lengths, which have N- and C- termini protection, is ongoing.

## MS07-P16 | STRUCTURAL AND MUTATIONAL INVESTIGATION OF PSYCHROPHILIC ADENYLATE KINASE REVEALS THE IMPORTANCE OF HYDROPHOBIC PACKING IN PROTEIN THERMAL STABILITY

Koo, Jasung (Seoul National University, Seoul, KOR)

Sojin Moon<sup>1</sup>, Junhyung Kim<sup>1</sup>, Jasung Koo<sup>1</sup>, Euiyoung Bae<sup>1,2</sup>

<sup>1</sup>Department of Agricultural Biotechnology, Seoul National University, Seoul 08826, Korea

<sup>2</sup>Research Institute of Agriculture and Life Sciences, Seoul National University, Seoul 08826, Korea

Protein thermal stability has been of particular interest since thermally stable proteins are desirable in both academic and industrial settings. Information on protein thermal stabilization can be obtained by contrasting homologous proteins from organisms living at distinct temperatures. Here, we report structural and mutational analyses of adenylate kinases (AKs) from psychrophilic *Bacillus globisporus* and mesophilic *Bacillus subtilis*. Comparison of their crystal structures showed suboptimal hydrophobic packing in the central CORE domain of the psychrophilic AK, where a polar side chain makes contacts with hydrophobic neighboring residues. Thermal stability measurement of AK mutants confirmed that optimization of hydrophobic interactions in the CORE domain is important for overall thermal stability. We also determined the crystal structures of AK mutants, which showed the largest thermal stability transition compared to the wild-type AKs. Taken together, our results provide a structural basis of the stability difference between the psychrophilic and mesophilic AK homologues, highlighting the role of hydrophobic interactions in protein thermal stabilization.

## MS07-P17 | PORPHYROMONAS GINGIVALIS TPR PROTEASE ZYMOGEN RESEMBLES CALPAIN-CALPASTATIN COMPLEX.

Staniec, Dominika (Jagiellonian University, Krakow, POL)

Calcium dependent proteases of calpain family are widespread in eukaryotes, but no homologues in the kingdom of prokaryotes have been described to date. Here we present the crystal structure of the first prokaryotic calpain-like protease. The structure of Tpr protease zymogen from *Porphyromonas gingivalis* resembles a calpain-calpastatin complex. The core structure of the proteolytic domain is largely identical to calpain, while the propeptide only distantly resembles calpastatin and its function is distinct from enzyme inhibition. The structural similarity between calpain and Tpr suggests that the latter could have been acquired by horizontal gene transfer from animal host. Thus, *P. gingivalis*, one of the major periodontal pathogens responsible for formation of teeth disease (periodontitis) have likely acquired an additional virulence factor from its mammalian host. To help understand the role of Tpr in pathogenesis we characterized in detail substrate preference of Tpr and provided sensitive synthetic substrates for the detection of Tpr activity.

## MS07-P18 | HIGH-RESOLUTION DIMERIC CRYSTAL STRUCTURES OF WILD-TYPE AND MUTANT ASPERGILLUS NIGER GLUCOSE OXIDASE

Pavlovic, Jelena (Institute of molecular biology, SAS, Bratislava, SVK); Szalayová, Andrea (Institute of Molecular Biology, SAS, Bratislava, SVK); Kostan, Julius (Department für Strukturbiologie und Computational Biology, AUT); Djinovic-Carugo, Kristina (Department for Structural and Computational Biology, Max F. Perutz Laboratories, University of Vienna, Vienna, AUT); Bauerova, Vladena (Institute of Molecular Biology, SAS, Bratislava, SVK); Bauer, Jacob (Institute of Molecular Biology, SAS, Bratislava, SVK)

Glucose oxidase (GOx) is an enzyme that catalyzes the oxidation of  $\beta$ -D-glucose to hydrogen peroxide ( $H_2O_2$ ) and  $\delta$ -glucono lactone using molecular  $O_2$ . It is a homodimeric glycoprotein non-covalently bound to a flavin adenine dinucleotide (FAD) cofactor. GOx is used for commercial applications and it is among the most important enzymes used in pharmaceutical, clinical chemistry, biotechnology, and other industries. Its most important application is in biosensors for the detection and estimation of glucose in blood and urine. Our goal in this project is better understand the reaction mechanism and dynamics of glucose oxidase.

Here, we describe a 1.63 and 2.0 Å crystal structures of *Aspergillus niger* wt-GOx and its mutant G513S bound to FAD. The enzyme crystallized in the  $P2_1$  monoclinic space group with unit-cell dimensions 84.549, 81.920, and 103.190 Å and  $\beta=106.30^\circ$ . The asymmetric unit contained one GOx homodimer, making it the first structure to have a complete dimer in the asymmetric unit. The current  $R$  factor and  $R_{free}$  are 18.29 and 21.43 %. The refined model includes 580 amino acid residues for each subunit, two FAD cofactors, fifteen N-acetylglucosamine residues, ten mannose residues, and five bromide anions.

This work was supported by a Grant from the Slovak Academy of Sciences: VEGA 2/16/0140.

## MS07-P19 | NEUTRON PROTEIN CRYSTALLOGRAPHY AT THE HEINZ MAIER-LEIBNITZ ZENTRUM (MLZ): NEW DEVELOPMENTS AND RECENT APPLICATION EXAMPLES

Schrader, Tobias E. (Forschungszentrum Jülich GmbH, Garching bei München, GER); Ostermann, Andreas (Heinz Maier-Leibnitz Zentrum (MLZ), Garching bei München, GER); Monkenbusch, Michael (Forschungszentrum Jülich GmbH, Jülich, GER); Laatsch, Bernhard (Forschungszentrum Jülich GmbH, Jülich, GER); Jüttner, Philipp (Heinz Maier-Leibnitz Zentrum (MLZ), Garching bei München, GER); Petry, Winfried (Heinz Maier-Leibnitz Zentrum (MLZ), Garching bei München, GER); Richter, Dieter (Forschungszentrum Jülich GmbH, Jülich, GER)

The neutron single crystal diffractometer BIODIFF at the research reactor Heinz Maier-Leibnitz (FRM II) is especially designed to collect data from crystals with large unit cells. The main field of application is the structural analysis of proteins, especially the determination of hydrogen atom positions. BIODIFF is a joint project of the Jülich Centre for Neutron Science (JCNS) and the FRM II. BIODIFF is designed as a monochromatic instrument with a narrow wavelength spread of less than 3 %. To cover a large solid angle the main detector of BIODIFF consists of a neutron imaging plate in a cylindrical geometry with online read-out capability.

BIODIFF is equipped with a standard Oxford Cryosystem “Cryostream 700+” which allows measurements at 100 K. A new kappa goniometer head was added recently. This allows an automated tilting of the crystal in order to increase the completeness of the data set when recording another set of frames in the tilted geometry. Typical scientific questions addressed are the determination of protonation states of amino acid side chains in proteins and the characterization of the hydrogen bonding networks between the protein active centre and an inhibitor or substrate.

Picking out some recent highlights from measurements at BIODIFF it will be shown how the method of neutron protein crystallography could be used to answer mechanistic questions in enzymatic processes or help to improve inhibitor fragment screening.

## MS07-P20 | SELECTIVE INHIBITION OF ASTACIN METALLOPEPTIDASES BY MAMMALIAN FETUIN-B

Cuppari, Anna (IBMB-CSIC, Barcelona, ESP); Körschgen, Hagen (University of Mainz, Mainz, GER); Fahrenkamp, Dirk (Karolinska Institutet, Huddinge, SWE); Schmitz, Carlo (RWTH Aachen University Medical Faculty, Aachen, GER); Jahn-Dechent, Willi (RWTH Aachen University Medical Faculty, Aachen, GER); Stöcker, Walter (University of Mainz, Mainz, GER); Jovine, Luca (Karolinska Institutet, Huddinge, SWE); Gomis-Rüth, F. Xavier (IBMB-CSIC, Barcelona, ESP)

Mammalian fetuin-A and -B are abundant serum proteins with pleiotropic functions. Fetuin-B is a highly selective and potent inhibitor of metallopeptidases (MPs) of the astacin family, which includes ovastacin in mammals. By inhibiting ovastacin, fetuin-B is essential for female fertility. We determined the crystal structure of fetuin-B, unbound and in complex with archetypal astacin, and found that the inhibitor has tandem cystatin-type modules (CY1 and CY2). They are connected by an exposed linker with a rigid, disulfide-linked “CPDCP-trunk” and followed by an C-terminal region with little regular secondary structure (CTR). The CPDCP-trunk and a hairpin of CY2 form a bipartite wedge, which slots into the active-site cleft of the MP. These elements occupy the non-primed and primed sides of the cleft, respectively, but spare the specificity pocket so that the inhibitor is not cleaved. The trunk aspartate blocks the catalytic zinc of astacin while the CY2 hairpin binds through a QWVXGP motif. Module CY1 assists in structural integrity and the CTR is not involved in inhibition, as verified by *in vitro* studies with a cohort of mutants and variants. Overall, inhibition conforms to a novel “raised-elephant-trunk” mechanism for MPs, which is reminiscent of single-domain cystatins that target cysteine peptidases. Over 200 sequences from vertebrates are annotated as fetuin-B, which underpins its ubiquity and physiological relevance; accordingly, we found sequences with conserved CPDCP and QWVXGP-derived motifs from mammals to cartilaginous fishes. Thus, the raised-elephant-trunk mechanism is likely to be generally valid for the inhibition of astacins by fetuin-B orthologs.

## MS07-P21 | STRUCTURE-FUNCTION CHARACTERISATION OF NOVEL GALACTOSIDASES FROM LACTOBACILLUS PLANTARUM: EXPLORING THE LINK BETWEEN GUT BACTERIA AND LIPID LEVELS

Feliciotti, Irene (University of Reading, Reading, GBR); Kolida, Sofia (Optibiotix HPLC, London, GBR); Rastall, Bob (University of Reading, Reading, GBR); Watson, Kim (University of Reading, Reading, GBR)

The human gut microbiome is a complex ecosystem, which plays a crucial role not only in intestinal health but also significantly impacts on factors such as appetite regulation, cardiovascular health, immunomodulation, mood and neuronal developmental disorders. Current research is suggesting that there may be a link between blood lipid profile regulation and the metabolic activity of certain gut microbiome members, suggesting possible applications in the management of cardiovascular disease.

This project focuses on *Lactobacillus plantarum*, a GRAS (generally regarded as safe) probiotic strain used to regulate the metabolism of bile acids and impact on coronary disease risk biomarkers such as serum lipid profiles and blood pressure. Recent sequencing of *Lactobacillus plantarum* has revealed potential novel beta-galactosidase sequences responsible for galacto-oligosaccharide (GOS) synthesis. These enzymes will be targeted for detailed structure-function studies to elucidate their functional role in GOS production. The enzymes will be isolated; X-ray crystallography will be used for their structural characterisation and functional testing will be performed to characterise their GOS production. The resulting GOS products will be isolated, characterized structurally and their cholesterol lowering potential and impact on gut microbiome composition and activity will be tested in batch cultures. Their non-prebiotic effects will be tested in different pathways, using relevant mammalian cell lines.

We anticipate that this work will be valuable for understanding detailed mechanisms of action of specific galactosidase enzymes in the synthesis of oligosaccharides with the ability to enhance the numbers and activity of the parent strain and improve human health by targeting specific health biomarkers.

## MS07-P22 | STRUCTURAL COMPARISON OF TWO MAMMALIAN MULTICOPPER OXIDASES, HEPHAESTIN AND CERULOPLASMIN

Zaitsev, Viatcheslav (Independent researcher, Dundee, GBR); Lindley, Peter (ITQB NOVA, Oeiras)

The evolutionary family of multicopper oxidases (MCO) includes laccase, ascorbate oxidase, CueO, Fet3p and ceruloplasmin [1-2]. A new mammalian MCO and ceruloplasmin (Cp) evolutionary paralogue, hephaestin (Heph) has been recently discovered [3-5]. While Heph shares ~50% sequence identity with serum Cp, it includes an additional transmembrane domain at the C-terminus and a short cytoplasmic tail.

A structural model for the ecto-domain of human Heph has been created using Phyre2 [6] and Swiss-Model [7] protein modelling software. The Heph model shows high similarity to the human Cp (hCp) structure [8] with the overall RMSD value of 0.45 Å. Detailed structural comparison of six integral copper centres and putative divalent cation binding sites has revealed that Heph, in contrast to hCp, contains the 3rd 'blue' mononuclear copper site in domain 2. In addition, three putative iron binding sites in domains 2, 4 and 6 were identified in the Heph structure, whereas hCp holds only two iron binding sites in domains 4 and 6 [1,8]. Based on these observations, distinct physiological roles of the two ferroxidases, intracellular Heph and plasma blood hCp, will be discussed.

[1] <https://slavazaitsev914078364.wordpress.com>

[2] P.Lindley et. al. (1999). In: *Perspect. Bioinorg. Chem.*, 4: 51-82

[3] C.Vulpe et. al. (1999). *Nat. Genet.* 21: 195–199

[4] B.Syed et. al. (2002). *Protein Eng.* 15: 205-214

[5] H.Chen et al. (2010) *J. Nutr.* 140: 1728–1735.

[6] L.Kelley et. al. (2015). *Nature Protocols* 10: 845-858

[7] A.Waterhouse et. al. (2018). *Nucleic Acids Res.* 46(W1): W296-W303

[8] I.Bento et. al. (2007). *Acta Cryst.* D63(2): 240-248

## MS07-P119 LATE | CRYSTAL STRUCTURE OF THE CRENARCHAEAL MEMBRANE FAMILY-2 GLYCOSYLTRANSFERASE REVEALS A MINIMAL CELLULOSE-SYNTHASE FRAMEWORK

Reichenbach, Tom (KTH Royal Institute of Technology, Stockholm, SWE)

Proteins in all three domains of life are subjected to post-translational modification *via* glycosylation to enable an immense number of biological functions. The majority of these constitute *N*-glycosylation of archaeal and eukaryotic proteins, where the archaeal *N*-glycans is considerably more diverse compared to eukaryotes. Archaea belonging to the TACK superphylum are considered to be most similar to eukaryotes. From the few functionally characterized archaeal glycosyltransferases, it has been shown that a donor substrate, usually an NDP sugar, as well as an acceptor substrate, typically a polyisoprenyl-based lipid carrier, are needed. Here, we report the first crystal structures of a glycosyltransferase of TACK origin, namely the membrane glycosyltransferase *PcManGT* from *P. calidifontis*, in complex with both nucleotide and donor substrate. The structural investigation shows stabilization of the nucleotide within the active site, and further indication of interaction with the donor's mannosyl group. In the absence of a suitable acceptor substrate, our functional studies reveal enzymatic hydrolysis of the donor substrate. Furthermore, the comparison with similar 3D structures suggests that *PcManGT* is an enzyme that catalyzes a single glycosyl-transfer reaction to a Dol-PP-linked acceptor molecule as part of the *N*-glycan biosynthesis in this crenarchaeon, rather than acting as a sugar polymerase.

## MS08: Hot Structures

---

### MS08-01 | CAPTURING REACTION INTERMEDIATES OF THE WATER OXIDATION REACTION IN PHOTOSYSTEM II AT X-RAY FREE ELECTRON LASERS

Yano, Junko (LBNL, Berkeley, USA)

The water oxidation reaction in nature occurs in Photosystem II (PS II), multi-subunit protein complex, in which the  $\text{Mn}_4\text{CaO}_5$  cluster catalyzes the reaction. The reaction comprises four (meta)stable intermediates ( $S_0$ ,  $S_1$ ,  $S_2$  and  $S_3$ ) and one transient  $S_4$  state, which precedes dioxygen formation occurring in a concerted reaction from two water-derived oxygens bound at the OEC. This reaction is coupled to the two-step reduction and protonation of the mobile plastoquinone  $Q_B$  at the acceptor side of PS II.

Using serial femtosecond X-ray crystallography (SFX) and simultaneous X-ray emission spectroscopy (XES) with multi-flash visible laser excitation at room temperature, we studied all (meta)stable states with resolutions of 2.04-2.08 Å. We also collected some timepoint data between the S-states in order to understand the sequence of events. The current status of this research and the mechanistic understanding of the water oxidation reaction based on the X-ray techniques is presented.

[1] J. Kern, et al. Structures of the intermediates of Kok's photosynthetic water oxidation clock, *Nature*, **563**, 421 (2018).

## MS08-02 | STRUCTURAL BASIS OF ADAMANTANE RESISTANCE IN THE INFLUENZA A M2

### PROTON CHANNEL

Thomaston, Jessica (University of California, San Francisco, San Francisco, USA); Wu, Yibing (University of California, San Francisco, San Francisco, USA); Liu, Lijun (Peking University Shenzhen Graduate School, Shenzhen, CHN); Wang, Jun (University of Arizona, Tucson, USA); DeGrado, William (University of California, San Francisco, San Francisco, USA)

The M2 protein is a homotetrameric proton channel found in the influenza A virus. It is the target of the anti-influenza drugs amantadine and rimantadine. However, in the past decade, viral resistance has emerged in the majority of currently circulating strains of influenza. The most prevalent drug-resistant M2 mutants are S31N and V27A. Here we report X-ray crystal structures of both of these mutants. A newly solved 2.1 Å structure of the S31N mutant contains two conformations of the channel (Inward<sub>open</sub> and Inward<sub>closed</sub>) in the asymmetric unit of a novel crystal form, allowing us to observe the Inward<sub>closed</sub> conformation of the S31N mutant for the first time. In the Inward<sub>open</sub> conformation, Asn31 faces the center of the channel pore and sterically occludes the binding site of the adamantane drugs. In the Inward<sub>closed</sub> conformation, Asn31 faces away from the channel pore and instead forms hydrogen bond interactions with backbone carbonyls. We have also characterized the V27A mutant bound to a spiroadamantane inhibitor in a 2.5 Å structure. The mutation of Val to Ala removes hydrophobic contacts that previously stabilized binding of the adamantane drugs; the spiroadamantane inhibitor is observed to bind to this larger pocket. This work provides a structural explanation for adamantane resistance in the M2 channel that will be useful for the design of new compounds targeting these drug-resistant mutants.

## MS08-03 | STRUCTURAL ANALYSIS OF CHLOROPLAST TAIL-ANCHORED MEMBRANE PROTEIN RECOGNITION BY ARSA1

Hsiao, Chwan-Deng (Academia Sinica, Taipei, TWN)

Tail-anchored (TA) membrane proteins destined for the posttranslational pathway are safely delivered to the endoplasmic reticulum (ER) membrane by a well-known targeting factor, TRC40/Get3, in mammals and yeast. In contrast, the underlying mechanism for translocation of TA proteins in plants remains obscure. How this unique eukaryotic membrane-trafficking system correctly distinguishes different subsets of TA proteins destined for various organelles, including mitochondria, chloroplasts and the ER, is a key long-standing question. Here, we present crystal structures of algae ArsA1 (the Get3 homolog) in a new distinct open state of nucleotide-free and AMPPNP-bound. This ~80-kDa protein possesses a monomeric architecture, with two ATPase domains in a single polypeptide chain. It is capable of binding chloroplast (TOC34 and TOC159) and mitochondrial (TOM7) TA proteins based on features of its transmembrane domain as well as the regions right before and after the transmembrane domain. Several helices located above the TA-binding groove comprise the interlocking hook-like motif implicated in TA substrate recognition by mutational analyses. Our data provide new insights into the molecular basis of the highly specific selectivity of algae ArsA1 interactions with the correct sets of TA substrates before membrane targeting in plant cells.

## MS08-04 | STRUCTURAL BASIS OF $\alpha$ -ACTININ-2/TITIN INTERACTION IN THE Z-DISK

Lopez Arolas, Joan (Max F. Perutz Laboratories, University Vienna, Vienna, AUT); Sponga, Antonio (Max F. Perutz Laboratories, University Vienna, Vienna, AUT); Smith, Luke (King's College London, London, GBR); Gautel, Mathias (King's College London, London, GBR); Djjinovic-Carugo, Kristina (Max F. Perutz Laboratories, University Vienna, Vienna, AUT)

$\alpha$ -Actinin-2 plays a central role in Z-disk assembly and stability as it crosslinks actin filament thanks to its unique antiparallel dimeric architecture. The organization and spacing between each  $\alpha$ -actinin-2 dimer is regulated via two specific interactions with titin, the giant blueprint protein of the sarcomere: (i)  $\alpha$ -actinin-2 EF3-4 interact with specific titin Z-repeats in a PIP2-regulated manner and (ii)  $\alpha$ -actinin-2 rod domain interacts with Zq titin. The first interaction has been studied in detail at all levels, but the molecular basis behind the second interaction as well as on how the two binding events translate into Z-disk assembly remain unknown.

Here, CD and SAXS analyses of Zq and Zr7-Zq titin constructs revealed that they are intrinsically disordered. Subsequent ITC experiments showed the binding affinity of rod/Zq and EF3-4/Zr7 plus rod/Zq binding events. We next managed to crystallize rod/Zq and solve its structure to 2.8 Å resolution using MR, data from XL/MS and PMF MS of the crystals, as well as Se-Met labeled variants of Zq mutants. We further validated rod/Zq interacting regions by generating different mutants whose effect is currently being analyzed in muscle cells. In addition, we modelled the flexible regions of Zr7-Zq in complex with  $\alpha$ -actinin-2 using SAXS to have a complete molecular model of the complex. Finally, we designed a collection of MBP-fused titin constructs and are currently analyzing their complexes with  $\alpha$ -actinin-2 using SEC-MALS and NS EM. Altogether, our results point to an important role for Zq in  $\alpha$ -actinin-2/titin interaction which might regulate proper Z-disk assembly.

## MS08-05 | STRUCTURE OF $\alpha$ -ACTININ-2/FATZ-1 FUZZY COMPLEX AND IMPLICATIONS IN Z-DISK FORMATION VIA PHASE SEPARATION

Sponga, Antonio (Max F. Perutz Laboratories, University of Vienna, Vienna, AUT); Lopez Arolas, Joan (Max F. Perutz Laboratories, University of Vienna, Vienna, AUT); Rodriguez-Chamorro, Ariadna (Max F. Perutz Laboratories, University of Vienna, Vienna, AUT); De Almeida Ribeiro, Euripedes (Max F. Perutz Laboratories, University of Vienna, Vienna, AUT); Geist, Leonhard (Max F. Perutz Laboratories, University of Vienna, Vienna, AUT); Drepper, Friedel (University of Freiburg, Freiburg, GER); Peterbauer, Thomas (Max F. Perutz Laboratories, University of Vienna, Vienna, AUT); Mlynek, Georg (Max F. Perutz Laboratories, University of Vienna, Vienna, AUT); Warscheid, Bettina (University of Freiburg, Freiburg, GER); Konrat, Robert (Max F. Perutz Laboratories, University of Vienna, Vienna, AUT); Djinic-Carugo, Kristina (Max F. Perutz Laboratories, University of Vienna, Vienna, AUT)

$\alpha$ -Actinin-2 plays a pivotal role in Z-disk assembly and stability as it crosslinks actin filaments from adjacent sarcomeres and acts as a binding platform for a number of Z-disk proteins. Among them is FATZ-1, a 30-kDa protein that appears when Z-bodies, the precursors of Z-disks, are formed. Accordingly, FATZ-1 is believed to have a central role at initial stages of myofibrillogenesis by serving as focal point for interactions with Z-disk proteins, but its structure and function remain unknown.

Here, we used bioinformatics, CD and SAXS to show that FATZ-1 is intrinsically disordered after generating a soluble construct (D91 FATZ-1). We next studied the affinity and binding stoichiometry of  $\alpha$ -actinin-2/FATZ-1 complex by ITC and SEC-MALS, and mapped down a shortest construct (mini FATZ-1) using XL/MS, NMR and LP/MS, as the disordered nature of this protein was a challenge for our crystallographic studies. We then managed to solve the structure of  $\alpha$ -actinin-2 rod/mini FATZ-1 complex at 2.7Å and  $\alpha$ -actinin-2 half dimer/D91 FATZ-1 complex at 3.2Å using MR and Se-Met variants of FATZ-1. In addition, we modelled the flexible regions of D91 FATZ-1 in complex with  $\alpha$ -actinin-2 by SAXS to have a complete molecular model of the complex. Finally, we studied FATZ-1 capacity to phase separate and form liquid droplets in the presence of  $\alpha$ -actinin-2. Together, our results provide a complete and detailed structural model of the  $\alpha$ -actinin-2/ FATZ-1 fuzzy complex as well as a plausible model on how FATZ might attract Z-disk proteins and form membrane-less compartmentalization at initial stages of myofibrillogenesis.

## MS08-P01 | REGULATION OF P97 ATPASE ACTIVITY BY COFACTOR-MEDIATED REMODELING AND POST-TRANSLATIONAL MODIFICATION

Heinemann, Udo (Max Delbrück Center for Molecular Medicine, Berlin, GER); Arumughan, Anup (Max Delbrück Center for Molecular Medicine, Berlin, GER); Banchenko, Sofia (Max Delbrück Center for Molecular Medicine, Berlin, GER); Petrovic, Sasa (Max Delbrück Center for Molecular Medicine, Berlin, GER); Roske, Yvette (Max Delbrück Center for Molecular Medicine, Berlin, GER); Wanker, Erich E. (Max Delbrück Center for Molecular Medicine, Berlin, GER)

AAA proteins are ATPases associated with diverse cellular activities. The abundant human ATPase p97 is functionally regulated by a family of ubiquitin regulatory-X (UBX) domain-containing cofactors. We demonstrated that the UBX protein ASPL (alveolar soft-part sarcoma locus) modifies p97 function by remodeling p97 hexamers into p97:ASPL heterotetramers with reduced ATPase activity [1]. This activity depended on the presence in ASPL of an extended UBX (eUBX) domain with N-terminal lariat that wraps around the p97-N domain, disrupting the functional p97 hexamer and reducing its ATPase activity.

A database search for eUBX sequence signatures identified the *Arabidopsis thaliana* protein PUX1 protein. By biochemical studies and crystal structure analysis of the *A. thaliana* p97 ortholog CDC48 and a p97:PUX1 complex we provided evidence for an ATPase remodeling process in plants analogous to p97 remodeling by ASPL.

Further, we observed that the conversion of p97 into p97:ASPL heterotetramers led to the surface exposure of peptide segments deeply buried inside functional p97 hexamers, some of which harbored post-translationally modified residues. We hypothesized that structural remodeling by ASPL or homologous proteins might facilitate the modification of these residues and tested this hypothesis by studying the trimethylation of p97 Lys315 by the protein lysine methyltransferase METTL21D. Biochemical evidence and the crystal structure of heterotetrameric p97:ASPL:METTL21D complex confirmed our hypothesis and suggested a novel mode of functional regulation of p97 and, possibly, related ATPases by coupling of structural remodeling and post-translational modification.

[1] Arumughan, A. et al. (2016) Nat. Commun. 7, 13047 (2016).

## MS08-P02 | STRUCTURE OF THE $\alpha$ -ACTININ ACTIN-BINDING DOMAIN/F-ACTIN COMPLEX

Vujin, Slobodan (Max F. Perutz Laboratories, University of Vienna, Vienna, AUT); Zheng, Weili (University of Virginia, Charlottesville, USA); Arolas, Joan (Max F. Perutz Laboratories, University of Vienna, Vienna, AUT); Höllerl, Eneda (Max F. Perutz Laboratories, University of Vienna, Vienna, AUT); Drepper, Friedel (University of Freiburg, Germany, Freiburg, GER); Schwarz, Thomas (Max F. Perutz Laboratories, University of Vienna, Vienna, AUT); Konrat, Robert (Max F. Perutz Laboratories, University of Vienna, Vienna, AUT); Warscheid, Bettina (University of Freiburg, Germany, Freiburg, GER); Egelman, Edward (University of Virginia, Charlottesville, USA); Djinovic-Carugo, Kristina (Max F. Perutz Laboratories, University of Vienna, Vienna, AUT)

$\alpha$ -Actinin plays a crucial role in cytoskeleton organization by crosslinking actin filaments. All four human  $\alpha$ -actinin isoforms consist of an N-terminal actin binding domain (ABD; 252-271 residues) comprising two calponin homology domains (CH1 and CH2) connected each other via a flexible linker. Accordingly, mutations on ABD that increase or decrease binding to F-actin lead to disease. Here, we took advantage of a high-affinity, disease-associated  $\alpha$ -actinin-4 mutant (K255E) to obtain a 4.2 Å cryo-EM structure of the ABD/F-actin complex. We confirmed previously reported actin binding sites present in CH1, but could not observe CH2 most likely due to orientational flexibility. We could not observe the N-terminal part of the ABD either which is predicted to be disordered in all  $\alpha$ -actinin isoforms based on bioinformatics studies. To examine the role of this N-terminal part, which ranges from 10 residues in  $\alpha$ -actinin-1 to 28 residues in  $\alpha$ -actinin-4, we performed actin cosedimentation assays with different N-terminally truncated constructs of all  $\alpha$ -actinin isoforms. We further investigated ABD/F-actin interaction by XL/MS and NMR which proved that not only CH1 but also CH2 is involved in binding to F-actin. Taken together, our results provide a complete molecular model of the  $\alpha$ -actinin ABD/F-actin complex and highlight the importance of the N-terminal part in direct interaction with F-actin.

## MS08-P03 | TRAF IS AN ESSENTIAL FACTOR OF THE PIP501 TYPE IV SECRETION SYSTEM (T4SS) AND EXHIBITS STRUCTURAL HOMOLOGY WITH THE T7SS PROTEIN ESSB OF STAPHYLOCOCCUS AUREUS.

Stallinger, Amrutha (University of Graz, Graz, AUT); Kohler, Verena (University of Graz, Graz, AUT); Lammer, Anna (University of Graz, Graz, AUT); Berger, Tamara (University of Graz, Graz, AUT); Probst, Ines (University Medical Center Freiburg, Freiburg, GER); Grohmann, Elisabeth (Beuth University of Applied Sciences, Berlin, GER); Keller, Walter (University of Graz, Graz, AUT)

The rapid spread of antibiotic resistances and the occurrence of multi-resistant strains among pathogenic bacteria, in particular those causing nosocomial infections, is one of the most pressing problems of our health system. Bacterial conjugation is the most prevalent route of DNA transfer between bacteria and mediates the rapid spread of bacterial resistances within bacterial communities. Type IV secretion systems (T4SS) are responsible for the efficient transport of nicked, single-stranded plasmid DNA across the cell walls of the donor as well as the recipient cell<sup>1</sup>. The T4SS from the antibiotic resistance plasmid pIP501, occurring in *Enterococci* and related Gram-positive bacteria, is encoded within a single operon comprised of 15 putative transfer factors. The 6<sup>th</sup> open reading frame encodes TraF, a bitopic trans-membrane protein of 52.8 kDa. Here we present the crystal structure of the N-terminal, cytosolic domain determined at 1.4 Å and show that TraF<sub>N</sub> exhibits a surprising structural homology with the EssB proteins of *Staphylococcus aureus* and *Geobacillus thermodenitrificans*. The solution structure of both the N- and the C-terminal domains were determined by SAXS methods. Western blot analysis revealed that TraF is part of the isolated T4SS complex. Interaction studies using the bacterial-two-hybrid system (BACTH) showed that TraF and its domains interact with the VirB8-like protein TraM, which was proposed to be an integral part of the functional T4SS<sup>2,3</sup>. Generating knock-out mutants we proved that TraF is an essential component of the transfer machinery, as the transfer rates were basically abolished when the TraF gene was missing.

## MS08-P04 | STRUCTURAL BASIS OF ASCORBATE-DEPENDENT IRON REDUCTION BY HUMAN DCYTB INVOLVED IN INTESTINAL IRON ABSORPTION

Sugimoto, Hiroshi (RIKEN SPring-8 Center, Hyogo, JPN); Ganasen, Menega (University of Hyogo, Hyogo, JPN); Togashi, Hiromi (RIKEN SPring-8 Center, Hyogo, JPN); Takeda, Hanae (University of Hyogo, Hyogo, JPN); Shiro, Yoshitsugu (University of Hyogo, Hyogo, JPN); Mauk, Grant (University of British Columbia, Vancouver, CAN); Sawai, Hitomi (University of Hyogo, Hyogo, JPN)

Duodenal cytochrome *b* (Dcytb) is a  $\text{Fe}^{3+}$  reductase that was identified in the duodenal brush border. Since DMT-1 favors the absorption of divalent metal including  $\text{Fe}^{2+}$ , the reduction of  $\text{Fe}^{3+}$  to  $\text{Fe}^{2+}$  by Dcytb in the duodenum is essential for effective intestinal iron absorption. Dcytb is an integral membrane protein that catalyzes reduction of nonheme  $\text{Fe}^{3+}$  by electron transfer from ascorbate across the membrane. Here we report the crystallographic structures of human Dcytb and its complex with ascorbate and  $\text{Zn}^{2+}$  [1]. Each monomer of the homodimeric protein possesses six transmembrane helices and cytoplasmic and apical heme groups, as well as cytoplasmic and apical ascorbate-binding sites located adjacent to each heme.  $\text{Zn}^{2+}$  coordinates to two hydroxyl groups of the apical ascorbate and to a histidine residue. Biochemical analysis indicates that  $\text{Fe}^{3+}$  competes with  $\text{Zn}^{2+}$  for this binding site. These results provide a structural basis for the mechanism by which  $\text{Fe}^{3+}$  uptake is promoted by reducing agents and should facilitate structure-based development of improved agents for absorption of iron.

[1] Ganasen et al. *Commun. Biol.* 1,120 (2018)

## MS08-P05 | ATOMIC STRUCTURE OF POTATO VIRUS X, THE PROTOTYPE OF THE ALPHAFLEXVIRIDAE VIRUS FAMILY

Grinzato, Alessandro (University of Padua, Padova, ITA); Kandiah, Eaashisai (ESRF, Grenoble, FRA); Lico, Chiara (ENEA C.R Casaccia, Rome, ITA); Betti, Camilla (ENEA C.R Casaccia, Rome, ITA); Baschieri, Selene (ENEA C.R Casaccia, Rome, ITA); Zanotti, Giuseppe (University of Padova, Padova, ITA)

Potato virus X (PVX) is a ss(+)ssRNA filamentous plant virus belonging to the *Alphaflexviridae* family. In recent years, PVX has been considered as a tool for nanotechnology applications, in particular in the biomedical field. Here, we present the cryo-electron microscopy structure of the PVX particle at a resolution of 2.2 Å, the highest currently obtained for a flexible filamentous virus. The density of the coat proteins and of the genomic RNA is particularly well-defined and has allowed a detailed analysis of protein-RNA interactions, including those mediated by solvent molecules, within the virion. The PVX particle itself is formed by repeats of segments made of 8.8 coat protein protomers, arranged to form a left-handed helical structure. The viral RNA is inserted in an internal crevice running along the virus length of the particle, packaged in 5-nucleotide repeats in which the first four bases are stacked in the classical way, while the fifth is rotated such that it is nearly perpendicular. The atomic resolution structure of PVX suggests a mechanism for the virion assembly and potentially provides a platform both for the rational design of antiviral compounds working as agonists of the viral genomic RNA to block infection and the use of PVX as a carrier of foreign RNA sequences or polypeptides/chemicals.

## MS08-P06 | CRYSTAL STRUCTURE OF UHRF1:LIG1 COMPLEX REVEALED STRUCTURAL CHANGE OF UHRF1 AND THE KEY RESIDUES FOR HIGH AFFINITY BINDING

Kori, Satomi (Graduate School of Medical Life Science, Yokohama City University, Yokohama, JPN); Ferry, Laure (Univ. Paris Diderot, Sorbonne Paris Cité, Epigenetics and Cell Fate, Paris, FRA); Matano, Shohei (Graduate School of Medical Life Science, Yokohama City University, Yokohama, JPN); Kodera, Noriyuki (Bio-AFM Frontier Research Center, Kanazawa University, Kanazawa, JPN); Oda, Takashi (Graduate School of Medical Life Science, Yokohama City University, Yokohama, JPN); Defossez, Pierre-Antoine (Univ. Paris Diderot, Sorbonne Paris Cité, Epigenetics and Cell Fate, Paris, FRA); Arita, Kyohei (Graduate School of Medical Life Science, Yokohama City University, Yokohama, JPN)

DNA methylation is an important epigenetic modification, which involved in development, X-chromosome inactivation, genome imprinting, and carcinogenesis. DNA methylation patterns are re-established after DNA replication and UHRF1 plays an essential role in this process. Tandem Tudor Domain (TTD) of UHRF1 is critical for its function. It binds various partners by intra or inter-molecule interaction; histone H3K9me<sub>2/3</sub>, linker 2 or spacer. Recently, we reported that a methylated histone-like region of DNA Ligase1 (LIG1K126me<sub>2/3</sub>) binds to the UHRF1 TTD. We also revealed that the affinity of LIG1K126me<sub>3</sub> binding to TTD is higher than that of H3K9me<sub>3</sub>. However, the underlying mechanism by which the binding of LIG1K126me<sub>3</sub> to TTD with high affinity is unclear. Here, we show the crystal structure of the UHRF1 TTD in complex with LIG1K126me<sub>3</sub> peptide. Mutational studies revealed the key residues for high affinity binding of LIG1K126me<sub>3</sub> and that the interaction probably regulated by phosphorylation of LIG1. Furthermore, SAXS and high-speed AFM analysis indicated that the binding of LIG1K126me<sub>3</sub> changes the overall structure of UHRF1 to flexible. These results suggest that LIG1K126me<sub>3</sub> is an allosteric regulator that modulates the conformation of UHRF1 in a different manner from H3K9me<sub>3</sub>. We will also discuss development of UHRF1 targeting inhibitor that compete with the binding of LIG1.

## MS08-P07 | CRYSTAL STRUCTURES OF STREPTOCOCCUS PYOGENES CAS1 AND CAS2 IN THE TYPE II-A CRISPR-CAS SYSTEM

Ka, Donghyun (Seoul National University, Seoul, KOR); Jung, Seungyong (Seoul National University, Seoul, KOR); Bae, Euiyoung (Seoul National University, Seoul, KOR)

Clustered regularly interspaced short palindromic repeats (CRISPRs) and CRISPR-associated (Cas) proteins constitute a microbial adaptive immune system against invading mobile genetic elements such as bacteriophages and plasmids. CRISPR acts as a genetic memory that has an array of invariable 'repeat' sequences interspaced with variable 'spacer' sequences. CRISPR adaptation is achieved by integrating short fragments of the invading foreign nucleic acids into CRISPR array as new 'spacer' sequences. Cas1 and Cas2 are conserved in almost all CRISPR types and form the 'spacer' integrase complex in the CRISPR adaptation process. Here, we report the crystal structures of *Streptococcus pyogenes* Cas1 and Cas2 proteins in the type II-A CRISPR-Cas system. Cas1 reveals a unique structural features distinct from type I Cas1 homologues, including extensive dimerization interface, globular overall structure, and disrupted metal-binding sites for catalysis. Cas2 displays a significant structural difference from *Enterococcus faecalis* Cas2 of the same CRISPR type, suggesting conformational variability in the type II-A Cas2 homologues. We also characterized interactions of Cas1 and Cas2. A single Cas2 dimer interacts with two Cas1 dimers through its C-terminal tails to form a heterohexameric complex. The Cas1-Cas2 complex and Csn2 comprise a larger type II-A CRISPR adaptation module. Furthermore, we demonstrated that the Cas1-Cas2 integrase complex interacts with Cas9 via Csn2. Our results provide structural information for *S. pyogenes* Cas proteins and lay a foundation for a network of molecular interactions among type II-A Cas components involved in the adaptation and interference stages of CRISPR-mediated immunity.

Bærentsen, René (Aarhus University, Aarhus C, DNK)

Bacteria are exposed to ever-changing environments and have evolved responsive systems to address this. In times of low availability of nutrients, or the presence of antibiotics, they reduce their growth rate. One way that bacteria signals stress is via the hyperphosphorylated guanosine nucleotides ppGpp and pppGpp, collectively called (p)ppGpp, that have been shown to regulate replication, transcription, translation, and metabolic pathways. PpnN, a pyrimidine/purine nucleotide 5'-monophosphate nucleosidase from *Escherichia coli*, has previously been determined to be able to bind (p)ppGpp.

In our recent publication we were able to show the crystal structures of PpnN, both in an apo form and pppGpp-bound state. When bound to pppGpp it undergoes a dramatic conformational shift, exposing its active site, which we also show translates to an increased catalytic activity. By performing mutations in the pppGpp-binding site we were able to show that loss of pppGpp binding lead to antibiotic sensitivity, but also an improved fitness in competition against other bacteria in a state of abundance. By making a  $\Delta ppnN$ -strain we saw the opposite effect.

We have since then been able to crystallize new forms of PpnN shedding light on the interaction between (p)ppGpp and PpnN, and will expand upon the complexities of bacterial mechanisms leading to tolerance. This information becomes increasingly important when discussing the emerging threat of multiresistant bacteria, since antibiotic tolerance is a necessary step for the evolution of antibiotic resistance, and that *ppnN* is conserved amongst most Proteobacteria.

## MS08-P09 | STRUCTURAL STUDY FOR RECOGNITION OF UBIQUITYLATED HISTONE H3 BY DNA METHYLTRANSFERASE

Arita, Kyohei (Graduate School of Medical Life Science, Yokohama City University, Yokohama, JPN); Ishiyama, Satoshi (Graduate School of Medical Life Science, Yokohama City University, Yokohama, JPN); Nishiyama, Atsuya (Division of Cancer Cell Biology, The Institute of Medical Science, The University of Tokyo, Tokyo, JPN); Defossez, Pierre-Antoine (Univ. Paris Diderot, Sorbonne Paris Cité, Epigenetics and Cell Fate, Paris, FRA); Nakanishi, Makoto (Division of Cancer Cell Biology, The Institute of Medical Science, The University of Tokyo, Tokyo, JPN)

Cytosine methylation in CpG dinucleotide plays an important role in gene silencing, genome imprinting, X-chromosome inactivation and carcinogenesis. After DNA replication, DNA methylation patterns in somatic cells are faithfully maintained to uphold the cell identity. Two proteins are essential for the maintenance of DNA methylation; DNA methyltransferase DNMT1 and its recruiter UHRF1. After genome replication, UHRF1 SRA domain specifically recognize hemi-methylated DNA and subsequently catalyzes the multi-monoubiquitylation on histone H3 at K14, K18 and K23. DNMT1 RFTS domain recognizes the ubiquitylated histone H3, which recruits the DNMT1 on the DNA methylation sites.

Here, we present the structural basis for recognition of dual-monoubiquitylated histone H3 (ubiquitylated at K18 and K23) by DNMT1 RFTS domain. We show the sample preparation of ubiquitylated histone H3 analogs, detail of recognition of ubiquitylated histone H3, and activation of DNMT1 methyltransferase activity upon binding of the ubiquitylated histone H3. These data suggest that activation of DNMT1 at proper timing and location ensures the DNA methylation maintenance. Finally, we will discuss the recognition of triple monoubiquitylated histone H3 by DNMT1 RFTS.

## MS08-P121 LATE | THE ESCRT-III PROTEIN Vps24 FORMS DOUBLE STRANDED FILAMENTS COMPOSED OF DOMAIN-SWAPPED DIMERS

Huber, Stefan (TU Delft, Delft); Mortensen, Simon A. (Forschungszentrum Jülich GmbH, Juelich, GER); Sachse, Carsten (Forschungszentrum Jülich GmbH, Juelich, GER)

ESCRT-III proteins mediate a range of membrane remodeling events such as multivesicular body biogenesis, cytokinesis and viral budding. Little atomic resolution information is available on how ESCRT-III monomers come together to facilitate membrane remodeling. In this study we determined the cryo-EM structure of a filamentous assembly of yeast Vps24 at 3.2 Å resolution. We found that Vps24 monomers adopt an elongated open conformation and bind together with another monomer to form a domain-swapped dimer with a central symmetry axis. The dimers combine to form an apolar ribbon, and two of those form a double stranded filament. The observation of such an architecture is unexpected in the context of ESCRT-III assemblies and strikingly different from proposed linear Snf7 filaments. Our structure of homopolymeric Vps24 suggests a new architecture on how Vps24 may assemble in hetero-polymers as they form in the cell during membrane remodelling events.

## MS09: Low Resolution Software Development

---

### MS09-01 | TOOLS TO AID MACROMOLECULAR REFINEMENT AT LOW RESOLUTION

Nicholls, Robert (Medical Research Council, Cambridge, GBR); Emsley, Paul (Medical Research Council, Cambridge, GBR); Kovalevskiy, Oleg (Medical Research Council, Cambridge, GBR); Long, Fei (Medical Research Council, Cambridge, GBR); Murshudov, Garib (Medical Research Council, Cambridge, GBR)

Effects such as crystal mosaicity and disorder lead to poor diffraction quality and weak intensities, resulting in only low-resolution data being available. Low observation-to-parameter ratio and suboptimal parameterisation cause unstable refinement, overfitting, and ultimately result in an unreliable model.

Regularisers stabilise macromolecular refinement, ensuring consistency between derived models and prior knowledge. Restraints representing chemical information help local structure adopt chemically reasonable conformations. At lower resolutions, supplementary restraints are used: encouraging consistency with models of homologous structures, formation of hydrogen bonding networks, nucleotide base pairing and stacking. Jelly-body restraints stabilise model refinement without injecting externally derived information. An anharmonic penalty function is used in order to control robustness to outliers due to inconsistencies between data and prior. Additional restraints and robust estimation are also useful for model building, increasing real space refinement convergence radius and stability.

Where several datasets and models are available for a macromolecule, restraints can facilitate information transfer between structures, potentially improving refinement and thus resultant model quality. Pragmatically, determining suitability of reference structures and refinement parameters can be challenging; the automated pipeline *LORESTR* facilitates this process by trialling multiple protocols.

This contribution will discuss techniques to facilitate high-quality models being routinely achieved in cases where only low-resolution data are available, focussing on implementation in *REFMAC5*, *Coot*, *ProSMART*, *LibG* and *LORESTR*. Other developments in refinement, map calculation, analysis and validation tools will also be discussed.

[1] Nicholls R.A., Kovalevskiy O. and Murshudov G.N. (2017) Low resolution refinement of atomic models against crystallographic data. *Protein Crystallography: Methods and Protocols*, 565-93.

## MS09-02 | MASK-BASED APPROACH TO RESTORING AND PHASING SINGLE-PARTICLE DIFFRACTION DATA

Lunin, Vladimir (Keldysh Institute of Applied Mathematics, Pushchino, RUS)

The development of experimental techniques, in particular the emergence of the X-ray free-electron lasers, allows to approach the practical solution of the problem of registration of the scattering from an isolated particle and thereby to obtain information about the three-dimensional structure of non-crystalline biological objects by X-ray diffraction methods. The possibility to measure non-Bragg reflections makes experimental data mutually dependent and essentially simplifies the structure solution. Sampling of experimental scattering data to a fine enough grid makes the structure determination equivalent to phasing of structure factor magnitudes for an 'imaginary' crystal with extremely large solvent content. This makes density modification phasing methods especially powerful supposing the object envelope is known. At the same time, such methods may be sensitive to the accuracy of the envelope and completeness of experimental data and may suffer from nonuniqueness of the phase problem solution. The mask based approach is a preliminary phasing method that performs random search for connected object envelopes that produce the estimates of structure factor magnitudes close to the values observed in X-ray experiment. Alignment, clusterization, and averaging of the phase sets corresponding to selected putative envelopes produce an approximate solution of the phase problem [1,2]. Beside the estimating of unknown phase values this approach allows to estimate the values of structure factor magnitudes lost in the experiment, *e.g.* ones corresponding to beam-stop shade zone or to oversaturated reflections.

[1] Lunin et al.: Acta Cryst. D72, 147-157

[2] Acta Cryst. D75, 79-89

## MS09-03 | VAGABOND: REDEFINING THE MODEL FOR MACROMOLECULAR REFINEMENT

Ginn, Helen (Diamond Light Source Ltd, Didcot, GBR)

Model refinement for biomolecular crystallography, at present, relies on a model defined in atomic x, y, z parameters and associated B factors. Vagabond is a new refinement project which takes an unconventional approach, revisiting the concept of refining in torsion space by defining the model in terms of bond lengths, angles and torsion angles. B factors have been replaced by defining the flexibility of the protein through allowing variation in the torsion angles. The distribution of the torsion angles within this model can then be sampled multiple times, creating an ensemble of individual structures: the sum of this ensemble is equivalent to the estimation of electron density. This significantly reduces the number of parameters to describe the structure and is capable of describing atomic distributions which are not accessible from isotropic or anisotropic B factor models alone. The combination of describing a more complex distribution with fewer parameters leads to a reduction in overfitting and increased clarity of maps as developed against existing structures from X-ray crystallography data. This reveals verifiable electron density differences in the reported structures from the Protein Data Bank, particularly revealing features in low resolution structures which, formerly, could only be obtained by optimisation of crystal conditions and collecting a new high resolution data set. Although the improvement in electron density quality is conspicuous across all resolution ranges, the parameter reduction is particularly powerful at low resolution, where fewer observations are available to support the model parameterisation.

## MS09-04 | ARCIMBOLDO TOWARDS LOW RESOLUTION: RECENT UPDATES

Borges, Rafael; Millán Nebot, Claudia Lucía (Institut de Biologia Molecular de Barcelona, Barcelona, ESP); Medina, Ana; Soler, Nicolas; Uson, Isabel (ICREA, Catalan Institution for Research and Advanced Studies, Barcelona, ESP)

In high resolution macromolecular crystallography, the use of small fragments in phasing is currently well established. A small fraction of a structure, if highly accurate, may render phases good enough to allow density modification and autotracing algorithms to complete the structure. The method implemented in ARCIMBOLDO [1] relies on the placement with PHASER [2] of ubiquitous fragments, such as  $\alpha$ -helices or libraries of  $\beta$ -sheets, followed by density modification and autotracing with SHELXE. The same principle, whereby a very incomplete but highly accurate structure, when subject to density modification reveals new elements in the structure holds at resolutions down to 3-4Å. Nevertheless, phasing becomes very challenging. The pattern recognition-based interpretation of an electron density into a model with its refinement implemented in ARP/wARP has been efficiently dealing with model completion in this range of resolution [3]. In ARCIMBOLDO, further development in ARCIMBOLDO\_LITE with coil coiled mode, in ARCIMBOLDO\_SHREDDER and integrating anomalous signal allowed also to address this scenario [4]. With SEQUENCE\_SLIDER, impossibility to expand is overcome by improving the polyaniline chains by assembling and refining the most probable side chain conformations. Sequence hypotheses may be generated on a secondary structure basis or using the optimum alignment between a remote homologous structure and target sequences.

[1] Sammito, M.D. et al. (2016). *Acta Crystallogr. Sect. Found. Adv.* 72, s23.

[2] McCoy, A.J. et al., (2007). *J. Appl. Cryst.* 40, 658–674.

[3] Langer, G. et al. (2008). *Nat. Protoc.* 3, 1171–1179.

[4] Ferrero, D. et al. (2019). *PLOS Pathogens* (accepted).

## MS09-05 | MOLECULAR REPLACEMENT MODEL PREPARATION AND ITS AUTOMATION IN MoRDA AND MrBUMP

Lebedev, Andrey (STFC-UKRI, Didcot, GBR); Vagin, Alexy (CCP4, Didcot, GBR); McNicholas, Stuart (YSBL, York, GBR); Thomas, Jens (Institute of Integrative Biology, Liverpool, GBR); Uski, Ville (CCP4, Didcot, GBR); Rigden, Daniel (Institute of Integrative Biology, Liverpool, GBR); Keegan, Ronan (CCP4, Didcot, GBR)

Performing molecular replacement (MR) with low resolution data presents many challenges. A plethora of new techniques are available to isolate fragment search models and perform post-MR density modification suitable for high resolution data, but many of these are not applicable where the data resolution is no better than 3 Angstroms. Here, we rely on the availability of search models constituting a sizeable fraction of the scattering content of the target crystal. The selection and preparation of such search models is key to the success of the MR procedure. The correct placement of a model in the unit cell of the target relies heavily on not just the sourcing of the search model, but also on the selection from the model of that part of it most similar to the target. This selection process can be guided by exploiting any available information such as sequence alignment or the alignment of homologues against similar homologues to isolate a common structural core. In difficult cases, a lot of trial and error can be required to optimize both the choice of model and its preparation. Automated MR pipelines such as MoRDa and MrBUMP have been developed to derive many potential search models automatically. They make use of leading structural bioinformatics techniques to identify candidate search models and help guide the selection of atoms from that model to optimize their similarity to the target. Here we present how these programs work, as well as how they can help in cases of low resolution structure solution.

## MS09-P01 | IMPROVING DENSITY HISTOGRAM BY PHASE OPTIMISATION USING A GENETIC ALGORITHM

Kantamneni, Sravya Mounika (European Molecular Biology Laboratory, Hamburg, GER); Sobolev, Egor (European Molecular Biology Laboratory, Hamburg, GER); Lamzin, Victor S (European Molecular Biology Laboratory, Hamburg, GER)

In macromolecular crystallography the initial phases obtained by experimental phasing or molecular replacement may not always be sufficiently accurate to produce an interpretable density map. Additional phase improvement steps using density modification and/or model refinement approaches may be required. Given the complexity of the phase space to be sampled, heuristic global optimisation techniques based on genetic algorithms may have their own advantages.

A sampling of the phase space and phase optimisation using genetic algorithms has been attempted and has produced promising results for reflections at low resolution of the data and for the use of the third moment of density distribution, skewness, as a target function [1, 2].

Here we present a phase optimisation approach using a genetic algorithm with several characteristics of the density map as a target function. For two selected test cases with X-ray data to 2.5 Å resolution, we observe the development of the density histogram with a gradual shift towards the histogram of the map computed from the refined and deposited model.

**Keywords:** Electron density, Skewness, Genetic algorithm

[1] Lunin et al., (2016) Acta Cryst. D72, 147-157.

[2] Uervirojnangkoorn et al., (2013) Acta Cryst. D69, 2039-2049.

## MS10: Validation, Errors and Noise in Macromolecular Crystallography

---

### MS10-01 | COMBATTING MX MEASUREMENT ERRORS AT SOURCE

Evans, Gwyndaf (Diamond Light Source, Didcot, GBR)

Micro-crystal diffraction has, in the past two decades, played an essential role in the success of synchrotron macromolecular crystallography (SMX) allowing major progress to be made in structural biology and biomedicine [1]. It has however become clear that even with major advances in detectors, X-ray sources and optics, automation and software, micro-crystallography (crystal dimensions < 5 microns) is fundamentally limited by crystal lifetime and, linked to this, the signal to noise ratio in diffraction data. Principal sources of noise come from X-ray background generated by disordered material in the sample (solvent regions in the crystal and solvent or other material surrounding the crystal) and scatter from air in the sample environment.

The VMXm beamline at Diamond Light Source has been developed to address these major sources of X-ray background and bring micro-crystallography closer to the true physical limits of microcrystal SMX. The presentation will describe novel approaches to X-ray focusing, crystal imaging, sample mounting and sample environments that together produce more than an order of magnitude reduction in X-ray background. The improved signal to noise ratio has the immediate effect of either improving the diffraction resolution limit from microcrystals, or extending the lifetime of crystals due to the fact that a reduced dose can deliver an equivalent signal-noise ratio. The results of benchmark comparison experiments will be presented together with early scientific results from VMXm.

[1] G. Evans, D. Axford, D. Waterman, R.L. Owen, Macromolecular microcrystallography, *Crystallogr. Rev.* 17 (2011) 105–142.

## MS10-02 | ERRORS IN ELECTRON SCATTERING AND VALIDATION OF EXPERIMENTAL MAPS THROUGH COMBINATION OF MICROED AND CRYOEM

Usón, Isabel (ICREA at IBMB-CSIC, Barcelona, ESP); Millán Nebot, Claudia Lucía (Institut de Biologia Molecular de Barcelona, Barcelona, ESP); Borges, Rafael (Crystallographic Methods, Institute of Molecular Biology of Barcelona (IBMB-CSIC), Barcelona, ESP)

Electron scattering is described in crystallography and EM in terms of spherical atoms, whereas the potential map determined depends both on the interactions with electrons and nuclei, and thus on the environment of each atom, not just on the scattering element. Advances in MicroED have opened exciting possibilities in the determination of structures from micro-crystals. We have adapted our fragment-based phasing methods to microED structures, incorporating maps as search fragments.

On borderline cases, we are exploring differences between the use of tabulated electron scattering factors to calculate the scattering from a helix, as we do for X-rays vs. cutting an helix out of a cryoEM map and thus resorting to the experimental scattering. This entails exploring the differences derived from using one map or another.

Within the ARCIMBOLDO framework, which combines fragment location with PHASER and density modification and autotracing with SHELXE, we are investigating both aspects: solution of microED data and examination of cryoEM map genesis, treatment and resolution through its performance against microED data. The potential of this approach lies in introducing an external experimental method as a validation probe for cryoEM. Are CryoEM maps currently too biased towards crystallography without accounting for a fundamental difference in scattering behaviour?

## MS10-03 | STARANISO: USE OF A WebGL-BASED 3-D INTERACTIVE GRAPHICAL DISPLAY TO REPRESENT AND VISUALISE DATA QUALITY METRICS FOR ANISOTROPIC MACROMOLECULAR DIFFRACTION DATA

Tickle, Ian (Global Phasing Ltd., Cambridge, GBR)

The STARANISO webserver for processing macromolecular diffraction data, either in the unmerged (unscaled or already scaled) state or in the already-scaled and merged state, has been available for use by the community since January 2016, during which time around 6500 user datasets have been successfully processed and the results returned to users. The server is specifically targeted at datasets with significant anisotropic diffraction in the hope that mitigation of the effects of the anisotropy will lead to improved electron-density maps, and this has indeed turned out to be the case for a significant proportion of datasets submitted.

In our view a critical component of the server is a WebGL-based 3-D interactive graphical display to represent and visualise data quality metrics for anisotropically-corrected macromolecular diffraction data. We are of the view that it is impossible to adequately specify the quality of data in terms of a small number of metrics such as completeness,  $R_{meas}$ , mean  $I / \sigma(I)$  or  $CC(\frac{1}{2})$ , whether specified as spherical bin averages or as overall averages. Equally, even knowledge of the overall anisotropy tensor and associated metrics such as anisotropic diffraction limits do not provide a full picture of the data quality. The 3-D interactive display provided by the server provides full access not only to the anisotropy analysis but also to properties and quality criteria for the dataset, such as the error model, redundancy, completeness and statistical significance.

## MS10-04 | ASSESSMENT OF MODEL BIAS IN CRYSTALLOGRAPHIC MAPS AND ITS IMPLICATIONS FOR VALIDATION OF CRYSTAL STRUCTURES

Neumann, Piotr (Georg-August-Universität Göttingen, Göttingen, GER); Ficner, Ralf (Georg-August-Universität Göttingen, Göttingen, GER)

Since decades, model bias has been considered as the Achilles' heel of macromolecular crystallography due to the necessity of deriving the crystallographic phases from an atomic model and utilizing them for the calculation of an electron density map. As a consequence, the resulting map tends to possess features present in the atomic model regardless of their existence in the structure, in particular in cases when a partial model with errors has been used. The awareness of limitations caused by model bias, has led to the development of several methods aiming to reduce it: prime-and-switch phasing, composite omit map, ping-pong map, 'kicked' OMIT map, 'iterative-build' OMIT map, Feature-Enhanced Map (FEM), sigma-A weighting. Most of the mentioned methods address only one or a few map quality-related problems at a time and thus provide maps of different reliability and applicability for model re-building or validation. In order to assess both the quality and the level of model bias in commonly used crystallographic maps, a set of about 260 deposited crystal structures, for which a bias free SAD experimental electron density map of good quality could be obtained, has been analysed. Numerous map comparisons in both real and reciprocal space (the Fourier Shell Correlation, FSC) have been performed in an attempt to determine the least biased electron density map which should be the most suited for verification of structural model as well as for the subsequent validation. Application of the FSC for estimation of the quality of the crystal structure will be discussed.

## MS10-05 | STEREOCHEMICAL RESTRAINTS FOR NUCLEIC ACIDS REVISITED

Jaskolski, Mariusz (A. Mickiewicz University, Poznan, POL); Brzezinski, Dariusz (Poznan University of Technology, Poznan, POL); Kowiel, Marcin (Institute of Bioorganic Chemistry, Polish Academy of Sciences, Poznan, POL); Gilski, Mirosław (A. Mickiewicz University, Poznan, POL); Zhao, Jianbo (University of Rochester, Rochester, USA); Turner, Douglas (University of Rochester, Rochester, USA)

The reference dictionary of nucleic-acid stereochemistry was compiled (using CSD) in 1996, as presented by Parkinson et al. 23 years later and with 10x expanded CSD, it is time to re-assess the validity of those standards and to see if more sophisticated paradigms (e.g. conformation-dependent functions) might be used. We based our analysis on rigorous statistical treatment of CSD fragments, divided into three main classes of the principal nucleic-acid constituents. The covalent geometry of the phosphodiester group is indeed dependent on conformation, albeit in a discrete way, where the O-P-O bond angles and distances are grouped into six conformational categories. The same clustering results were obtained by manual analysis and by machine-learning algorithms, confirming that artificial intelligence can be successfully applied for the discovery of complicated structural patterns. The nucleobase geometry is not expected to be conformation-dependent but in this class we tested different hypotheses, e.g. if the CSD data correctly represent WC base pairs, or if advanced quantum mechanical (QM) calculations could provide sufficiently accurate restraints. While the QM models are remarkably good, they are still inferior to high-quality CSD data. For the glycosidic moiety, the situation is complex because some of the geometrical parameters (e.g. the glycosidic bond) depend on conformation, while other do not. Our results confirm that the Parkinson library is still valid. However, since there are some parameters that require adjustment, we suggest to use the current library. For convenience, a webserver (<http://achesym.ibch.poznan.pl/restraintlib/>) has been created to generate restraints for the most popular refinement programs.

## MS10-P01 | A NEW 3D REFLECTION DATA VIEWER BASED ON NGL

Oeffner, Robert (University of Cambridge, Cambridge, GBR); Echols, Nathaniel (Molecular Biophysics and Integrated Bioimaging, Berkeley, CA, USA); Sammito, Massimo (Department of Haematology, aCambridge Institute for Medical Research, Cambridge, AUT); McCoy, Airlie J (University of Cambridge, Cambridge, GBR); Hatti, Kaushik (Department of Haematology, Cambridge Institute for Medical Research, Cambridge, GBR); Stockwell, Duncan H (Department of Haematology, Cambridge Institute for Medical Research, Cambridge, GBR); Croll, Tristan I (Department of Haematology, Cambridge Institute for Medical Research, Cambridge, GBR); Read, Randy (Department of Haematology, Cambridge Institute for Medical Research, University of Cambridge, Cambridge, GBR)

The 3D-Reflection data viewer in Phenix [1] is based on the OpenGL library which is deprecated on MacOS. A replacement based on supported libraries, was urgently required. The NGL-HKL-viewer has been developed in a way that leverages the codebase of the original viewer while extending the functionality.

Protein crystallography involves processing raw X-ray images to indexed intensities. Subsequent steps may associate additional data with these indices. As part of the changes to the 3D-Reflection data viewer the types of reflection data that can be displayed were expanded.

Real valued data are displayed as spheres scaled according to their magnitudes. Colour coding through both hue and saturation can be applied as well. The viewer allows associating one data parameter with the sizes of the spheres but colour them according to another data parameter. For example, phased structure factors can be displayed as spheres scaled by amplitudes, coloured according to phases and colour saturation used to represent figures of merit. Data can be sorted into bins and be shown or hidden.

NGL-HKL-viewer is scriptable from Python and part of CCTBX [2]. It is based on NGL [3] and therefore portable to all computing platforms with a modern web browser. The viewer can be embedded in graphical user interfaces such as Qt5 or PySide. It is part of Phaser.Voyager [4].

[1] Echols et al. J. Appl. Cryst. (2012). 45, 581

[2] Grosse-Kunstleve et al. J. Appl. Cryst. (2002). 35, 126.

[3] Rose et al. Bioinformatics (2018). 34, 3755

[4] Read et al. per comms

## MS10-P02 | ANALYSIS AND VALIDATION OF B VALUES OF MACROMOLECULAR STRUCTURES.

Masmaliyeva, Rafiga (ANAS Institute of Molecular Biology and Biotechnology, Baku, AZE); Murshudov, Garib (MRC Laboratory of Molecular Biology, Cambridge, GBR)

This presentation will describe a global analysis of macromolecular B values. It is shown that the distribution of B values generally follows the Shifted Inverse Gamma Distribution (SIGD). SIGD parameters are estimated using the Fisher scoring technique with the expected information matrix. It is demonstrated that a contour plot based on the parameters of SIGD can be used to validate macromolecular structures. The analysis of the dependence of the peak heights (PH) on resolution and atomic B values is shown. It is demonstrated that PH distribution depends on resolution and B values. A comparative analysis neighbouring atoms must account for resolution and B values. A combination of SIGD, PH distribution and outlier detection are used to identify entries from the PDB that require attention. It is also shown that presence of a multimodal B value distribution indicates that some parts of the molecule have been mismodelled or have different mobility, depending on their environment. These distributions can also indicate the level of sharpening/blurring of Fourier coefficients. Often sharpening/blurring is an artefact of data scaling, absolute average B value depends on the scaling technique used; the shape of B value distribution is invariant to scaling.

Sometimes atomic models exhibit multimodal B value distribution. In such cases, expectation maximisation method is used to model B value distributions as a mixture of SIGD.

Local analysis of B values and PH, a tool to identify mismodelled/misidentified atoms, will also be demonstrated.

Developed algorithms have been implemented in an open source software – ToBeValid.

## MS10-P03 | IMPROVING IDENTIFICATION AND VALIDATION OF WATER MOLECULES IN PROTEIN CRYSTAL STRUCTURES WITH MOLECULAR DYNAMICS SIMULATIONS

Caldararu, Octav; Misini Ignjatovic, Majda (Lund University, Lund, SWE); Oksanen, Esko (European Spallation Source, Lund, SWE); Ryde, Ulf (Lund University, Lund, SWE)

Water molecules in close proximity to the protein surface are fundamental to multiple biological processes, such as protein folding, stability or enzymatic reactions. Furthermore, water molecules mediate protein-ligand interactions and play an important role in the energetics of ligand-binding. Thus, knowledge of the position of water molecules around the protein is crucial for the correct prediction of protein-ligand affinities.

Peak-finding algorithms in crystallographic software packages usually perform well for finding the position of well-ordered water molecules but sometimes fail for water molecules with a less clearly-defined electron density and cannot discern between water molecules and ions or other solvent molecules used in crystallization. These algorithms can be improved by using chemical information, for example from molecular dynamics (MD) simulations.

We performed MD simulations of a sugar-binding protein, galectin-3, in complex with various inhibitors, for which high-resolution crystal structures exist both at cryo-temperature and at room temperature. The simulations were done both in solution and in a crystallographic unit cell. Then, we compared water density maps obtained with grid inhomogeneous solvation theory (GIST) from these MD simulations to X-ray electron density maps and added water molecules if the peaks matched in the two maps. Solution MD simulations gave rather poor agreement to the experimental electron density maps. In contrast, MD simulations in crystallographic unit cells show a better performance in identifying weakly-defined crystal water molecules and are a promising tool in the future development of water molecule identification algorithms.

## MS10-P04 | VALIDATION IN THE PDB

Armstrong, David (PDBe, Hinxton, GBR); wwPDB consortium (wwPDB consortium, AUT)

The Protein Data Bank (PDB) is one of the oldest biological archives. Having started with 7 entries in 1971, it has grown to over 150,000 entries. The way the quality of archival entries was understood and evaluated has evolved over the years. In 2008-2009, the wwPDB, the worldwide organisation which manages the PDB, set up community expert task forces to obtain recommendations on validation metric for coordinate models in the PDB archive, supporting experimental data and the correspondence between them. These recommendations were implemented in the wwPDB validation pipeline and presented in the wwPDB validation reports.

The wwPDB validation reports summarise the overall quality of each PDB entry in a simple slider image. The sliders allow non expert users to quickly judge the quality of each PDB entry at a glance and select the best quality model for their work, without having to understand all the validation metrics that were used to create the sliders. The wwPDB validation service also produces a comprehensive report which contains details of every outlier in the PDB entry in PDF and XML format.

The wwPDB validation service is made freely available via the wwPDB website ([validate.wwpdb.org](http://validate.wwpdb.org)) and through an API and users are encouraged to use these services prior to deposition to the PDB. Following curation of a PDB entry an official wwPDB validation report is produced which depositors are encouraged to provide to the referees of their publication and is required by an increasing number of journals.

## MS10-P05 | B-FACTORS REFLECT THE LOCAL DYNAMICS OF PROTEINS AND NUCLEIC ACIDS

Schneider, Bohdan (Institute of Biotechnology of the Czech Academy of Sciences, Vestec, CZE); Cerný, Jirí (Institute of Biotechnology of the Czech Academy of Sciences, Vestec, CZE)

Our recent analysis of scaled B factors in over 700 crystal structures of protein–DNA complexes showed that the B factor distributions of biopolymer residues, amino acids and nucleotides, as well as ordered water molecules, are a primary function of their neighborhood [1]. Amino acids in the interior of proteins have the tightest B factor distributions, residues forming the biopolymer interfaces have the distribution shifted to higher B factor values, and residues exposed to the solvent have the widest distribution with the mode at the highest B factor values. The distributions are also different for the backbone and side chain atoms and for the DNA backbone and base atoms. The behavior is evident in the group of structures with resolution higher than 1.9 Å and represents well the local protein and DNA dynamics. However, the distributions are much less telling at lower resolution bins and the factual meaning of B factors is lost. It stands to reason that residues in low resolution structures have principally similar local dynamics as residues in the high resolution structures. We therefore propose that the high resolution B factor distributions can be used to formulate the initial constraints for B factor values in structures refined at lower resolution.

[1] Schneider B et al. *Acta Cryst. D70*, 2413–2419 (2014). doi: 10.1107/S1399004714014631.

## MS11: Big Data (at Facilities) and Cloud Computing in Crystallography

---

### MS11-01 | RECALCULATING ALL X-RAY STRUCTURES IN THE PDB BY PDB\_REDO: GOING CLOUD

Joosten, Robbie (NKI, Amsterdam); Perrakis, Anastassis (Netherlands Cancer Institute, Amsterdam)

PDB-REDO is a refinement procedure that used REFMAC together many decision making and model building and restraints generation algorithms, to improve macromolecular structures determined by X-ray crystallography. PDB-REDO is available as a web server, a software package for local installation, and - crucially - as the "back-end" for creating the PDB-REDO databank: a collection of all the PDB structures with X-ray diffraction data (well over one hundred thousand entries), re-refined and partially re-built.

To be able to offer our web services to the user community rapidly and efficiently, enable easier installation of our software, and use Grid and Cloud computing resources, PDB-REDO is available as a singularity container. This architecture has been used, among others, to re-calculate the entire PDB-REDO databank within a week in the San Diego Super-Computing center.

We will discuss the current achievement and future plans for utilising shared computing infrastructure for PDB-REDO, specifically also in the context of efficient fragment-based lead discovery campaigns based on X-ray crystallography.

## MS11-02 | CCP4 CLOUD FOR DISTRIBUTED CRYSTALLOGRAPHIC COMPUTATIONS

Krissinel, Eugene (Science & Technology Facilities Council, Didcot, GBR); Lebedev, Andrey (STFC-UKRI, Didcot, GBR); Uski, Ville (Science & Technology Facilities Council, Didcot, GBR); Ballard, Charles (Science & Technology Facilities Council, Didcot, GBR); Keegan, Ronan (Science & Technology Facilities Council, Didcot, GBR); Nicholls, Robert (MRC Laboratory of Molecular Biology, Cambridge, GBR); Kovalevskiy, Oleg (MRC Laboratory of Molecular Biology, Cambridge, GBR); Berrisford, John (European Bioinformatics Institute, Cambridge, GBR); Wojdyr, Marcin (Global Phasing Ltd, Cambridge, GBR); Simpkin, Adam (Institute of Integrative Biology, Liverpool, GBR); Thomas, Jens (Institute of Integrative Biology, Liverpool, GBR); Oliver, Christopher (Theoretical Physics Group, Birmingham, GBR); Pannu, Navraj (Biophysical Structural Chemistry, Leiden); Skubak, Pavol (Leiden University Medical Center, Leiden)

The Collaborative Computational Project Number 4 in Protein Crystallography (CCP4) exists to maintain, develop and provide world-class software that allows researchers to determine macromolecular structures by X-ray crystallography and other biophysical techniques. Over 40 years of existence, CCP4 Software was assembled and distributed as an integrated Suite of programs, traditionally operated via CCP4i (2) GUI in Linux, OSX and Windows platforms.

Modern trends in computing suggest a fast-growing interest to mobile platforms and cloud solutions for data management and operations in practically all areas. Answering to these trends, CCP4 releases beta version of CCP4 Cloud, developed for essentially remote and distributed deployment of CCP4 Software. CCP4 Cloud allows a user to keep all necessary data and projects in the cloud and perform all scope of crystallographic computations, from image processing to final refinement, ligand fitting and deposition, remotely via a common web-browser, optionally complemented with CCP4 Cloud Client for interactive model building with Coot.

The talk will present architectural solutions and key features of CCP4 Cloud such as ability to seamlessly import data from 3rd party sites (e.g., synchrotrons), high scalability of computational background, convenient (big) data management for multiple users, rich graphical interface with built-in molecular graphics, enhanced data and structure solution pathway provenance.

CCP4 Cloud may be used from CCP4 Web portal with any device running a modern web-browser (including tablets and smartphones). All the source code is open and freely available for installation elsewhere to serve local researchers in a lab, or institution, or pharma, or a synchrotron.

## MS11-03 | EXI, THE EXTENDED ISPYB INTERFACE

Santoni, Gianluca (ESRF, Grenoble, FRA)

The ISPyB database and web interface have been the mainstays of a Laboratory Information Management System for structural biology experiments which has been in use at the ESRF since 2001. EXI is an upgraded interface for ISPyB, currently used in the context of MX, bioSAXS and Cryo EM experiments and which allows the preparation of synchrotron experiments from the home laboratory, the tracking of samples to/from at the synchrotron, the visualisation of all experimental steps carried out on an individual sample and the presentation and download of the results of automatic data processing pipelines carried out at the synchrotron. This functionality is vital for remote and automated data collection but has also proven to be a powerful tool for managing experiments involving many samples and/or spanning over multiple experimental sessions. Recent improvements to EXI will be presented, including the visualization of molecular replacement structure solution for MX experiments, the reporting of statistics resulting from cryo-EM image analysis and the presentation of the results of auto processing pipelines for bioSAXS experiments.

## MS11-04 | KEEPING THINGS 'N SYNCH: ANALYSING THE CONTENT AND COMPLETENESS OF CIF METADATA IN THE CSD

Johnson, Natalie (Cambridge Crystallographic Data Centre, Cambridge, GBR); Wiggin, Seth (Cambridge Crystallographic Data Centre, Cambridge, GBR); Ward, Suzanna (Cambridge Crystallographic Data Centre, Cambridge, GBR)

Alongside structural information, Crystallographic Information Files (CIF)s can store metadata detailing how the crystal data was collected and processed [1]. Complete and accurate experimental metadata is important as it provides additional insights about the experiment [2] and can be useful in a variety of cases. Databases of crystal structure information could be mined for specific material or to assess trends within a field. One such database is the Cambridge Structural Database (CSD), containing 1 million small-molecule organic and metal organic crystal structures, which has an archive of over 750,000 underlying CIFs. Scripts can be written to utilise the CSD Python API [3] to examine the completeness and content of certain CIF attributes.

CIF metadata has been used to assess the possibility of attributing structures identified as being collected using synchrotron radiation to particular facilities, or even specific beamlines. Data from a number of CIF fields was probed for *'facility identifying information'*. For facilities with at least 100 attributed single crystal structures, over 90% of the structures can be attributed to a named beamline – although percentages varied by facility. This information could be used to provide increased traceability of data measured at synchrotron facilities and help establish community guidelines.

[1] Hall, S R et al., Acta Cryst., 1991, **A47**, 665-685.

[2] Kroon-Batenburg, L M J, et al., IUCrJ, 2017, **4**, 87-99.

[3] Groom, C R, et al., Acta Cryst., 2016, **B72**, 171-179.

## MS11-05 | MACHINE LEARNING FOR EXPERIMENTAL PHASING IN MX

Vollmar, Melanie (Diamond Light Source Ltd, Didcot, GBR); Parkhurst, James (Diamond Light Source Ltd, Didcot, GBR); Jaques, Dominic (Diamond Light Source Ltd, Didcot, GBR); Elliott, Jenna (Univeristy of Oxford, Oxford, GBR); Basle, Arnaud (Institute for Cell and Molecular Biosciences, Newcastle upon Tyne, GBR); Murshudov, Garib (MRC Laboratory of Molecular Biology, Cambridge, GBR); Waterman, David (CCP4, Didcot, GBR); Winn, Martyn (STFC, Didcot, GBR); Evans, Gwyndaf (Diamond Light Source Ltd, Didcot, GBR)

Large-scale facilities such as synchrotrons face an increasing demand for computational resources due to rapid increases in data rates, data volumes, and growing interest in real-time feedback to researchers during their experiments. The efficient use of these high performance computing resources is an important factor in the overall efficiency of the facility. Machine learning applications geared towards user assistance offer great opportunities to improve experiment outcomes. These can be trained using a large archive of previously-collected data, enabling more efficient experiments to be performed by rapidly providing information that can be used for decision making.

Here we describe a method to estimate the likelihood of success when determining a protein structure by experimental phasing using X-ray crystallography. Such a predictive tool has the potential to accelerate the structure determination process, as data can be rapidly assessed regarding its usefulness and either discarded or extended until an appropriate data set of sufficient quality is available. In this way, computational and synchrotron beamtime resources can be focused on the most promising data sets.

We have developed applications based on statistical and machine learning methods to predict the success of X-ray crystallographic experimental phasing outcomes ~95% accuracy and to assist in identifying electron density maps of sufficient quality for model building.

## MS11-P01 | NEW ARP/wARP WEB SERVICE INTEGRATED INTO VIRTUAL COMPUTATION

### FRAMEWORKS

Sobolev, Egor (EMBL, Hamburg Unit, Hamburg, GER); Heuser, Philipp (DESY, Hamburg, GER); Chojnowski, Grzegorz (EMBL, Hamburg Unit, Hamburg, GER); Oezugurel, Umut (EMBL, Hamburg Unit, Hamburg, GER); Kantamneni, Sravya (EMBL, Hamburg Unit, Hamburg, GER); Lamzin, Victor (European Molecular Biology Laboratory Hamburg, GER)

The remote web service for macromolecular model building using ARP/wARP [1] was established in 2004 and has had over 5,000 users. Since 2017 it has undergone a complete redesign and now offers the use of all modules of the latest ARP/wARP software version 8.0 for crystallographic model building, including interpretation of cryo-electron microscopy maps. The new web service includes advanced options for real-time monitoring, re-running computational tasks with modified parameters and a comparison of the results.

The redesigned web service is gaining popularity: 900 remote users ran 9,400 model-building tasks in 2018. 92% of the tasks follow a molecular replacement-like scenario where some initial model is already available. Recent developments implemented in ARP/wARP enable to build atomic structures not only in maps of a medium-to-high resolution but also within 3.0–4.0 Å resolution range.

Half of the users operate Mac and Linux computers and 30% use Windows. A considerable portion of users (20%) submit or monitor tasks from tablets and smartphones.

The ARP/wARP web service is gradually integrated into virtual frameworks [2]. Most of the tasks (58%) are submitted via the dedicated web interface. Other model-building tasks are submitted to the web service automatically from the CCP4i interface and the molecular replacement pipelines Balbes, MoRDa and MrBump. The users also have an option to direct the built ARP/wARP model to PDB-REDO.

[1] Langer et al., (2008) Nature Protocols. 3, 1171–1179.

[2] Morris et al., (2019) J Struct Biol. 1, 100006.

## MS11-P02 | HARNESSING THE DATA: INTEGRATING DATA FLOWS ACROSS HOME LABORATORIES, FACILITIES AND DATA REPOSITORIES IN PROTEIN CRYSTALLOGRAPHY

Marquez, Jose Antonio (EMBL, Grenoble, Grenoble, FRA)

The systematic introduction of automation in structural biology over the last decades has enabled the study of ever more challenging targets. However, it has brought new challenges, concerning data management and integration. Typically, crystallography experiments are carried out across multiple sites including home laboratories and synchrotron facilities and spans relatively long periods of time before data is deposited in one of the worldwide Protein Data Bank sites. While some of these facilities use data management systems they are not interconnected. Moreover, new applications, like fragment screening and serial, crystallography, producing large amounts of data in a short time are becoming mainstream. To address these problems, we have developed the Crystallography Information Management System, CRIMS. A web-based software suit enabling automated sample tracking along the experimental crystallography workflow, from pure protein to model refinement. This system provides interfaces for crystallization screening and optimization that can be connected to the most popular crystallization robots, can establish communication with multiple synchrotron facilities, exchanging unique sample identifiers to support both manual and automated data collection and provides for the first time, automated, uninterrupted sample tracking along the whole process. Recently, we have incorporated communication with automated data processing pipelines to support large scale fragment screening. The CRIMS system is installed in multiple laboratories in Europe and is being used by over 1500 scientists. The experience on the use of this system and its potential to support automated data tracking and deposition and foster the development of an European Open Science Cloud will be discussed.

## MS11-P03 | SIMBAD: STRUCTURE BASED SEARCH MODEL IDENTIFICATION FOR MOLECULAR REPLACEMENT USING THE PDB DATABASE.

Simpkin, Adam (University of Liverpool, Liverpool, GBR); Simkovic, Felix (University of Liverpool, Liverpool, GBR); Thomas, Jens (University of Liverpool, Liverpool, GBR); Savko, Martin (synchrotron SOLEIL, Gif-sur-Yvette, FRA); Lebedev, Andrey (STFC-UKRI, Didcot, GBR); Uski, Ville (CCP4, STFC, Oxford, GBR); Wojdyr, Marcin (CCP4, STFC, Global phasing, Oxford, GBR); Ballard, Charles (CCP4, STFC, Oxford, GBR); Shepard, William (synchrotron SOLEIL, Gif-sur-Yvette, FRA); Rigden, Daniel (University of Liverpool, Liverpool, GBR); Keegan, Ronan (CCP4, STFC, Oxford, GBR)

The conventional approach to identifying search models in molecular replacement (MR) is to use the sequence of the target to search against a database of known structures. This approach is based on the assumption that sequence similarity is a useful guide to structural similarity. While largely true, this strategy is not always effective: for example, conformational changes may mean that the most structurally similar Protein Data Bank (PDB) entries to the unknown structure are not those most closely related in sequence. A conceptually straightforward alternative approach to this problem would be to perform full MR on everything in the PDB. This strategy, however, would be extremely slow. SIMBAD is a CCP4 development that provides an alternate route to identify suitable search models. A rotation search is performed on every entry in the MoRDa database, a non-redundant derivative of the PDB containing ~100,000 structural domains. Through assessing the scores of these rotation searches, suitable search models can be obtained relatively quickly.

The SIMBAD pipeline also allows users to test if a contaminant has been crystallised in place of the desired protein. The use of SIMBAD post data collection on synchrotron beamlines has helped to avoid misspent research effort by quickly identifying these contaminants.

Recent developments include the use of Phaser and ensembles to enhance the sensitivity of SIMBAD as well as the deployment SIMBAD on CCP4 cloud resources.

## MS11-P04 | COMBINING THE USE OF LIBRARIES FROM SEVERAL DISTANT HOMOLOGS IN ARCIMBOLDO\_SHREDDER SPHERES

Jiménez-Mellado, Elisabet (IBMB - CSIC, Barcelona, ESP); Millán Nebot, Claudia Lucía (Institut de Biologia Molecular de Barcelona, Barcelona, ESP); Medina, Ana (IBMB - CSIC, Barcelona, ESP); Sammito, Massimo (Cambridge Institute for Medical Research, University of Cambridge, Cambridge, GBR); Usón, Isabel (IBMB - CSIC, Barcelona, ESP)

ARCIMBOLDO [1] is a software that exploits secondary and tertiary structure constraints for phasing by using fragments such as ideal polyalanine alpha helices or libraries of local folds derived from structures deposited in the PDB [2]. ARCIMBOLDO combines the location of such small, accurate models with PHASER [3] followed by density modification and auto tracing with SHELXE [4].

ARCIMBOLDO\_SHREDDER [5] produces fragment models from homologs whose deviation to the final structure is too large for successful location. Models are cut in equivalent volumes respecting structural units and annotated into separate rigid groups with ALEPH [6]. Gyre and gimble refinement enhance the convergence of the method, improving starting models with large deviations from the target.

This work explores the combination of model fragments from several distant homologs within the SHREDDER program, collaborating with SBGrid [7]-supported high-performance computing resources to overcome the massive scale computing requirements needed. Our goal is to be able to exploit the maximum amount of prior information about our unknown fold and to evaluate if we get larger discrimination by the use of multiple homologs.

[1] Millán *et al.*, (2015) IUCrJ. 1, 95.

[2] Burley *et al.* (2019) Nucleic Acids Research 47: D464

[3] McCoy *et al.* (2007) Appl Crystallogr. 40, 658

[4] Usón & Sheldrick (2018) Acta Crystallogr. D74, 106

[5] Millán *et al.* (2018) Acta Crystallogr D 74: 290

[6] Medina *et al.* (2019) In preparation

[7] Morin *et al.* (2013) eLife. 2: e01456

## MS11-P05 | PRESTO INTEGRATIVE STRUCTURE BIOLOGY SOFTWARE FOR ALL PLATFORMS

Unge, Johan (MAX IV, Lund University, Lund, SWE)

### Objective

With the larger amount of data generated in lesser time the need for better resources to share and analyse the data is increasing. Projects tend to span over several techniques to answer the scientific questions leading to Integrative Structure Biology. The need to be able to share the results, software and competence across the fields is accelerating. The software project PRESTO has been initiated with the aim of providing a common software package for all technique's analysis of structure biology data on local, remote, single and multimode platforms, with the emphasis of High-Performance Computing infrastructures.

### Result

Protein Science Facility (PSF) from Karolinska Institute in Stockholm and National Supercomputer Centre (NSC) in Linköping, the Swedish synchrotron light source MAX IV and Lunarc, the supercomputer centre in Lund, Sweden, runs PRESTO to support Swedish structural biologist with powerful analysing tools and an interface to the data generated to MAX IV. PRESTO can run on any machine and is especially designed to be make an efficient use of the High-Performance Computing facilities using several nodes in an user friendly way. It supports a virtual desktop with menu based support for parallel processing and batch or interactive processing of data.

### Future

The project has funding to invite all parties of Integrative Structural Biology including Neutron MX (NMX), Nuclear Magnetic Resonance (NMR) and cryo-electron microscopy (CryoEM). The techniques used can be ported to any user, institution of facility around Europe.

## MS12: Structural Bioinformatics

---

### MS12-01 | EXPLORING CANCER HETEROGENEITY: FROM DNA MUTABILITY TO PROTEIN DYSFUNCTION

Panchenko, Anna (Queen's University, Kingston, CAN)

Many different mutagenic processes cumulatively shape the observed somatic mutational trends in cancer and the growing body of evidence supports the dependence of mutation rates on local DNA sequence context and other factors. In our pursuit to decipher the mechanisms of cancer driver events, we develop methods to explore DNA context-dependent mutational patterns, identify underlying mutagenic processes related to infidelity of DNA replication and repair machinery, and various exogenic mutagenic factors. We derive mutagen and cancer-specific mutational background models and apply them to calculate expected DNA and protein site mutability to decouple relative contributions of mutagenesis and selection in carcinogenesis. Next we investigate molecular mechanisms of the impact of candidate driver missense mutations on protein structure and interactions and verify our predictions by different experimental approaches.

## MS12-02 | DARKNESS IN THE HUMAN GENE AND PROTEIN FUNCTION SPACE DESPITE BIG OMICS DATA AND DECLINE IN MOLECULAR MECHANISM DISCOVERY AFTER 2000

Eisenhaber, Birgit (Bioinformatics Institute Singapore, Singapore, SGP); Eisenhaber, Frank (Bioinformatics Institute (BII) A\*STAR, Singapore, SGP)

It is generally believed that full human genome sequencing was a watershed event in human history that boosted biomedical research, biomolecular mechanism discovery and life science applications. At the same time, researchers in the field of genome annotation see that there is a persisting, substantial body of functionally insufficiently or completely not characterized genes (for example, ~10,000 protein-coding in the human genome) despite the availability of full genome sequences. A survey of the biomedical literature shows that the number of reported new protein functions had been steadily growing until 2000 but the trend reversed to a dramatic decline thereafter [1,2] when, at the same time, the annual amount of new life science publications doubled between 2000 and 2017. Examples of gene function discovery for chronic myeloid leukaemia and from the GPI lipid biosynthesis pathway [3, 4] show the difficulties and the application potential when molecular functions are really understood.

[1] Darkness in the human gene and protein function space. Sinha et al. *Proteomics* 2018, 10.1002/pmic.201800093

[2] A decade after the first full human genome sequencing: when will we understand our own genome? Eisenhaber F. *JBCB* 2012 10.1142/S0219720012710011

[3] Transamidase subunit GAA1/GPAA1 is a M28 family metallo-peptide-synthetase that catalyzes the peptide bond formation between the substrate protein's omega-site and the GPI lipid anchor's phosphoethanolamine. Eisenhaber et al., *Cell Cycle*. 2014, 10.4161/cc.28761

[4] Function of a membrane-embedded domain evolutionarily multiplied in the GPI lipid anchor pathway proteins PIG-B, PIG-M, PIG-U, PIG-W, PIG-V, and PIG-Z. Eisenhaber et al. *Cell Cycle*. 2018, 10.1080/15384101.2018.1456294

## MS12-03 | PHASER.VOYAGER: DATA-GUIDED MODEL GENERATION AND VISUALIZATION

Sammito, Massimo D (University of Cambridge, Cambridge, GBR); McCoy, Airlie J (University of Cambridge, Cambridge, GBR); Hatti, Kaushik (University of Cambridge, Cambridge, GBR); Oeffner, Robert D (University of Cambridge, Cambridge, GBR); Stockwell, Duncan H (University of Cambridge, Cambridge, GBR); Croll, Tristan I (University of Cambridge, Cambridge, GBR); Read, Randy (Department of Haematology, Cambridge Institute for Medical Research, University of Cambridge, Cambridge, GBR)

Although molecular replacement is a mature technique, new and established users alike can still find it challenging to generate ensemble models and to cope with uncertainty about the contents of the asymmetric unit. Ensembles should include information not only from homologous domains, but also their assembly into macromolecular complexes. Moreover, when multiple homologs are available with varying predicted structural similarity to the target, their optimal clustering into ensembles should depend also on the data resolution. We have developed an automated procedure for building ensembles that accounts for data quality. Ensemble generation is calibrated to the difficulty of the problem, via the expected LLG [1]. Our procedure to rank possibilities for asymmetric unit content takes into account any translational non-crystallographic symmetry and previously observed oligomeric states. We expect to optimize the path to structure solution particularly in challenging cases involving large complexes, low-resolution data, high order non-crystallographic symmetry, low-homology models and combinations thereof.

The automated procedure, *phaser.voyager*, is supported by a graphical interface to

- Visualize data features and their corrections to identify sources of error
- Automate the retrieval, selection and preparation of atomic models, building ensembles optimized to account for limitations in experimental data.
- Guide user decisions including description of the crystal content
- Visualize in real-time the MR tree search, introducing a new user interaction that will allow dynamically branching alternative MR strategies from any intermediate step.
- Optimize the MR solution to output the best model and map.

[1] Airlie J. McCoy et al., (2017) PNAS 114(14):3637-3641

## MS12-04 | MOLECULAR REPLACEMENT USING STRUCTURE PREDICTIONS FROM NEW GENERATION DATABASES

Rigden, Daniel (University of Liverpool, Liverpool, GBR); Simpkin, Adam (University of Liverpool, Liverpool, GBR); Thomas, Jens (University of Liverpool, Liverpool, GBR); Simkovic, Felix (University of Liverpool, Liverpool, GBR); Keegan, Ronan (STFC, Didcot, GBR)

Molecular Replacement (MR) is the predominant route to solution of the phase problem in macromolecular crystallography. Where the lack of a suitable homologue precludes conventional MR, one option is predicting the target structure with bioinformatics. Such modelling, in the absence of homologous templates, is called *ab initio* or *de novo* modelling. Recently the accuracy of such models has improved significantly as a result of the availability, in many cases, of residue contact predictions derived from evolutionary covariance analysis. Covariance-assisted *ab initio* models representing structurally uncharacterised Pfam families are now available on a large scale in databases, potentially representing a valuable and easily accessible supplement to the PDB as a source of search models.

Here we deploy the unconventional MR pipeline AMPLE to explore the value of structure predictions in the Gremlin and PconsFam databases. We test whether these deposited predictions, processed in various ways, can solve the structures of PDB entries subsequently deposited. The results were encouraging: nine of 26 Gremlin cases solved, covering target lengths of 112-355 residues and a resolution range of 1.35-2.85Å, and with target-model shared sequence identity as low as 37%. AMPLE's cluster-and-truncate approach proved essential for most successes. For the overall lower quality structure predictions in the PconsFam database, remodelling with Rosetta within the AMPLE pipeline proved to be the best approach, generating ensemble search models from single structure deposits. Overall the results help point the way towards the optimal use of expanding *ab initio* structure prediction databases.

## MS12-05 | ALEPH: A NEW SOFTWARE FOR STRUCTURAL ANALYSIS AND GENERATION OF FRAGMENT LIBRARIES FOR MOLECULAR REPLACEMENT

Medina, Ana (Institute of Molecular Biology of Barcelona, Spanish National Research Council (IBMB-CSIC), Barcelona, ESP); Triviño, Josep (Institute of Molecular Biology of Barcelona, Spanish National Research Council (IBMB-CSIC), Barcelona, ESP); Millán Nebot, Claudia Lucía (Institut de Biologia Molecular de Barcelona, Barcelona, ESP); J. Borges, Rafael (Institute of Molecular Biology of Barcelona, Spanish National Research Council (IBMB-CSIC), Barcelona, ESP); Usón, Isabel (Catalan Institution for Research and Advanced Studies (ICREA), IBMB-CSIC, Barcelona, ESP); Sammito, Massimo (Cambridge Institute for Medical Research, Cambridge, GBR)

RCIMBOLDO [1] is a fragment based molecular replacement framework where Local Folds (LF: small discontinuous fragments) are located with PHASER [2] providing phases that are improved and interpreted in SHELXE [3].

ALEPH [4] is a program for retrieving structural properties of proteins from the PDB [5], based solely on geometrical descriptors, Characteristic Vectors (CVs) [6], computed as centroid C $\alpha$ -O vectors on consecutive tripeptides. Networks of CVs hold angles and distances representing protein structure.

ALEPH implements four different tasks:

- Annotation: a customizable secondary and tertiary structure analysis to map general or local properties controlling the strictness of the annotation.
- Decomposition: structure subdivision into smaller compact folds. ARCIMBOLDO\_SHREDDER [1] gives the model internal degrees of freedom based on this decomposition.
- Library generation: to extract and cluster fragment libraries collecting structural variations of the same fold. Each library expresses a common pattern as the hypothesis for phasing whereas ARCIMBOLDO\_BORGES [1] jointly evaluates results for all models, revealing correct solutions.
- Superposition: align a fragment onto a complete structure.
- A graphical user interface is provided to perform each task and to visualize and plot the results in real time.

[1] Millán, C. *et al.*, (2015) IUCrJ., 1, 95.

[2] McCoy, AJ, *et al.* (2007). J Appl Crystallogr 40, 658.

[3] Usón, I & Sheldrick, G. (2018) Acta Cryst. D74, 106.

[4] Medina, A., *et al.* (2019) In preparation.

[5] Berman, H., *et al.* (2015) Nucleic Acids Research. 35, D301

[6] Sammito, M., *et al.* (2013). Nat Methods. 10, 1099.

## MS12-P01 | CRYSTALLIZATION AND STRUCTURE DETERMINATION OF ALDO-KETO REDUCTASE 1C3 IN COMPLEX WITH STEROIDAL INHIBITORS USING IN SITU PROTEOLYSIS

Petri, Edward (Faculty of Sciences, Univeristy of Novi Sad, Novi Sad); Celic, Andjelka (Faculty of Sciences, Novi Sad)

Human aldo-keto reductase 1C (AKR1C) isoforms are NADPH-dependent oxidoreductases that metabolize carbonyl containing drugs and are overexpressed in many cancers, where they confer resistance to chemotherapies such as doxorubicin and abiraterone. Structural methods could facilitate design of drugs that are more resistant to AKR1C activity, or inhibitors with potential as adjuvant drugs, to improve the effectiveness of current chemotherapies. To design more effective steroidal inhibitors of AKR1C isoforms, X-ray structural data were used as templates for molecular docking simulations. Potential ligands for AKR1C isoforms were then investigated using *in vitro* biochemical assays, yeast-based assays for nuclear receptor affinity, and computational simulations. Results were correlated with anti-proliferation tests using human cancer cell lines. Based on these screening results, steroidal inhibitors of AKR1C isoforms were identified, and X-ray crystal structures of new steroidal inhibitors in complex with human aldo-keto reductase 1C3 were determined. Recombinant AKR1C3 was expressed from a pET28(a+) vector with a thrombin-cleavable N-terminal His<sub>6</sub>-tag for structural studies. *In situ* proteolysis with thrombin was used to remove the His-tag during crystallization, resulting in improved crystal morphology and diffraction quality. Our combined results were applied to help design more potent, selective inhibitors of human aldo-keto reductase 1C3 and 1C2 isoforms.

We thank the Ministry of Education and Science of the Republic of Serbia for financial support (Grants No. 173014 and 172021).

## MS12-P02 | ENHANCING SMALL MOLECULE INFORMATION IN THE PROTEIN DATA BANK IN EUROPE

Pravda, Lukáš (GBR); PDBe (PDBe, Hinxton, GBR)

The Protein Data Bank (PDB) provides a wealth of data on biomacromolecules and their complexes with small molecules/ligands. Information about each unique small molecule is provided through the PDB chemical component dictionary (CCD), including chemical composition, connectivity, model and idealized coordinates, and descriptors such as InChI or SMILES. Entries in the CCD and PDB, however, lack information on the role of bound molecules, e.g. as a cofactor, drug or inhibitor. Information on structural similarity, e.g. common scaffolds or fragments, and data on common interactions formed between small molecules and macromolecules are also difficult to access.

As part of the data enrichment process in the Protein Data Bank in Europe [1] we have extended small molecule information to include scaffolds, fragments, physicochemical properties, and 2D coordinates for collision-free depictions. We also provide cofactor annotation within a biological context and mapping of unique small molecules in the CCD to other common databases using UniChem. Interaction information between macromolecules and small molecules is already available through the new aggregated views for proteins [2] which are part of the Protein Data Bank in Europe Knowledge Base (PDBe-KB; [pdbe-kb.org](http://pdbe-kb.org)) a new, community-driven resource of functional annotations for structure data.

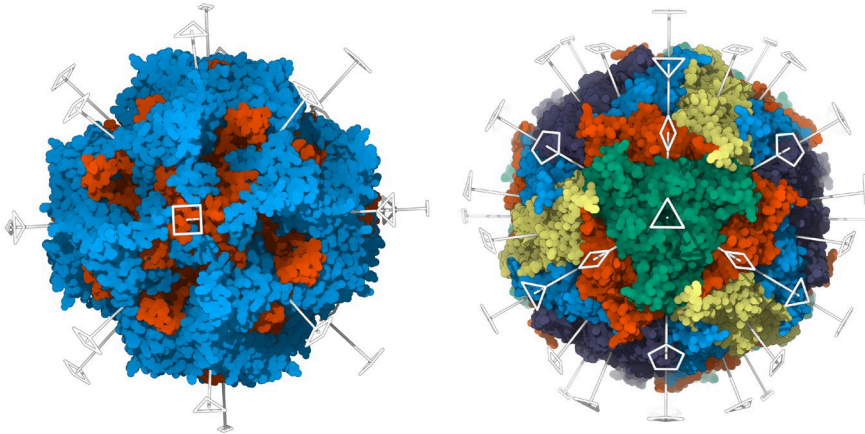
Enrichment of small molecule data provides the basis for a new service presenting aggregated views for small molecules/ligands in the PDB, putting them in their biological context. The service is planned to be introduced at the end of 2019.

[1] PDBe; <https://pdbe.org>

[2] <https://pdbe-kb.org/proteins>

## MS12-P03 | SYMMETRY IN STRUCTURES OF PROTEIN ASSEMBLIES

Grudin, Sergei (Inria / CNRS, Grenoble, FRA); Pages, Guillaume (Inria, Univ. Grenoble Alpes, LJK-CNRS, Grenoble, FRA)



Many protein complexes in the Protein Data Bank (PDB) are symmetric homo-oligomers. Indeed, it appears that large symmetrical protein structures have evolved in many organisms because they carry specific morphological and functional advantages compared to small individual protein molecules. There is therefore considerable interest in studying and modelling these assemblies.

Recently we have proposed a novel free-docking method for protein complexes with arbitrary point-group symmetry [1]. It assembles complexes with cyclic symmetry, dihedral symmetry, and also those of high order (tetrahedral, octahedral, and icosahedral). Later on we discovered that the inverse problem, i.e. identification of symmetry in a protein assembly, is even more interesting. Given a structure of the assembly, it consists in the identification of the symmetry measure, and also of the computations of the symmetry axes [2-4]. We tackled this problem using two orthogonal approaches, (i) analytical minimization of a geometrical mismatch score over transformation operators within a symmetry group [2-3]; and (ii) convolutional neural networks trained on 3D density maps [4]. Using these tools, we performed exhaustive analysis of all symmetric structures in the PDB and found some organization patterns that are worth discussing.

[1] Ritchie, D. W. & Grudin, S (2016). *J. Appl. Cryst.*, **49**, 1-10.

[2] Pages, G., Kinzina, E, & Grudin, S (2018). *J. Struct.Biology*, **203** (2), 142-148.

[3] Pages, G. & Grudin, S (2018). *J. Struct.Biology*, **203** (3), 185-194.

[4] Pages, G. & Grudin, S (2018). *arXiv preprint arXiv:1810.12026*.

## MS12-P04 | HOW DISEASE-ASSOCIATED MUTATIONS MAY ALTER THE DYNAMIC MOTION OF THE N-TERMINAL DOMAIN OF THE HUMAN CARDIAC RYANODINE RECEPTOR

Bauer, Jacob (Institute of Molecular Biology, SAS, Bratislava, SVK); Pavlovic, Jelena (Institute of Molecular Biology, SAS, Bratislava, SVK); Kutejová, Eva (Institute of Molecular Biology, SAS, Bratislava, SVK); Bauerova, Vladena (Institute of Molecular Biology, SAS, Bratislava, SVK)

The cardiac Ryanodine receptor (RyR2), one of the largest known ion channels, releases  $\text{Ca}^{2+}$  ions from the sarcoplasmic reticulum of cardiomyocytes into the cytoplasm, thereby triggering heart cell contraction [1]. Mutations to this channel are associated with inherited cardiac arrhythmias and appear to cluster in distinct parts of the N-terminal, central, and C-terminal areas of the channel [2]. Starting with our previous structure of the human RyR2 N-terminal domain (NTD) [3], we used molecular dynamics simulation to study how the R414L, I419F and R420W mutations affect its structure and dynamics. The R414L and I419F mutations diminish the overall amplitude of motion without greatly changing its direction; R420W both enhances the amplitude and changes the direction of motion. These results suggest that R414L and I419F hinder channel closing, while R420W may enhance channel opening. It appears that the wild-type protein possesses a moderate level of flexibility which allows the gate to close and not open easily without an opening signal. These mutations disrupt this balance by making the gate either too rigid or too loose, making closing difficult or less effective [4].

This work was supported by VEGA research grant 2/0140/16 from the Slovak Grant Agency.

[1] K. Otcu, et al. (1990) *J. Biol. Chem.* 265, 13472–13483

[2] J. T. Lanner et al. (2010) *Cold Spring Harb. Perspect. Biol.* 2, a003996

[3] Ľ. Borko et al. (2014) *Acta Cryst. D70*, 2897–2912

[4] J. A. Bauer et al. (2019) *J. Biomol. Struct. Dyn.* (in press) 10.1080/07391102.2019.1600027

## MS12-P05 | PDBe KNOWLEDGE BASE (PDBe-KB) – INFRASTRUCTURE FOR FAIR

### STRUCTURAL AND FUNCTIONAL ANNOTATIONS

Velankar, Sameer (Protein Data Bank in Europe (PDBe), Cambridge, GBR)

Growth in the number and complexity of macromolecular structures deposited to the Protein Data Bank (pdb.org) has continually increased, due to rapid advances in structure determination techniques. The PDB archive currently contains ~150,000 structures, referencing more than 45,000 unique UniProtKB entries, which facilitate greater understanding of protein function and mechanism. In addition to the PDB, over 400 further data resources are able to derive additional annotations related to structures. This both enhances the inherent value of macromolecular structures and provides their biological context. PDBe-KB (Protein Data Bank in Europe - Knowledge Base; pdbe-kb.org), established in 2018, is an international, community-driven resource with the primary goal of collating and making available structural and functional annotations contributed by partner resources. It is managed by the Protein Data Bank in Europe team at EMBL-EBI.

PDBe-KB partner data resources provide manually curated or computationally predicted annotations for ligand binding sites, catalytic sites, protein-protein interfaces and post-translational modification sites, as well as selected physico-chemical parameters (solvent accessibility, residue depth). These enriched data are combined with manual curations of functional sites and quaternary structure assemblies and other annotations available in PDBe. PDBe-KB facilitates data exchange and allows insights into the biological function by providing a comprehensive view of the functional context of the protein structure. Functional annotations are made available on PDBe-KB web pages, programmatically via an API, and as a distributed Neo4J graph database. As a first example, PDBe-KB has launched aggregated views of structure data for UniProtKB accessions, referenced by PDB structures.

## MS12-P06 | BUILDING THE PROTEIN STRUCTURE-SPECIFIC SIDE-CHAIN ROTAMER LIBRARIES

Grybauskas, Algirdas (Vilnius University Institute of Biotechnology, Vilnius, LTU); Gražulis, Saulius (Vilnius University Institute of Biotechnology, Vilnius, LTU)

Identifying the probable positions of the protein side-chains is one of the protein modeling steps that can greatly improve the prediction of protein-ligand, protein-protein interactions. Most of the strategies predicting the side-chain conformations use pre-determined angles, also called rotamer libraries, that are usually generated from the subset of high-quality protein structures from PDB. Grouping the amino acids by their type and calculating the frequencies of the most occurring dihedral angles in that group are then performed. Depending on the library, groups can be further divided by the structure of the main-chain atoms, solvent accessibility or other criteria.

Although these methods are fast, they tend to be too generalized and ignore basic assumptions about the geometry and surroundings of the target protein that can result in inaccuracies when predicting the possible side-chain atom positions; Hence we propose the approach that takes into account both of these terms by scanning through the conformationally restricted side-chain positions and generating dihedral angle libraries specific to the target proteins. The method avoids the drawbacks of lacking conformations due to unusual or rare protein structures. The core principle of the approach is a limited movement of side-chains imposed by the fixed number of degrees of freedom. Combinatorial explosion is avoided by using dead-end elimination and cell-list neighbor search while calculating potential energy.

Building such dynamic libraries could increase the likelihood of detecting rare rotamers and reveal the broader picture on the impact of side-chain positions.

## MS12-P07 | NEW COVARIANCE-BASED METHODS FOR UNCONVENTIONAL MR OF TRANSMEMBRANE PROTEINS.

Sanchez Rodriguez, Filomeno (University of Liverpool, Liverpool, GBR); Rigden, Daniel (University of Liverpool, Liverpool, GBR); Keegan, Ronan (CCP4, STFC, Didcot, GBR); Evans, Gwyndaf (CCP4, STFC, Didcot, GBR); Vollmar, Melanie (CCP4, STFC, Didcot, GBR)

The most prevalent technique for the solution of the phase problem in macromolecular crystallography is molecular replacement (MR). In most cases, selection of a suitable search model, typically a solved structure homologous to the target of interest, is the key limitation of conventional MR. In those cases where no such structure is available, other more challenging and time consuming unconventional MR approaches are used. Nevertheless, recent results suggest that even in those cases where no homologous structures are found for a given target, it may still be possible to find suitable search models among these unrelated structures, in the form of regions that share high, albeit local, structural similarity with the target. The challenge then becomes the accurate determination of such search models among all the solved structures.

Here we propose a novel pipeline for the solution of structures of transmembrane proteins, which exploits the latest advances in residue contact predictions for the detection of fragments later to be used as search models. Preliminary data already show that contact predictions play a pivotal role in the process of search model selection: those fragments that better match the contact information predicted for the target tend to constitute a better match. The ultimate aim is to develop a pipeline which would provide valid search models originating from already solved structures, even in those cases where no related structures have been already solved. This would enable solution of these structures without the use of experimental phasing techniques.

## MS12-P09 | STRUCTURAL COMPARISON AND EVOLUTIONARY RELATIONSHIPS BETWEEN CERULOPLASMIN, HEPHAESTIN AND BLOOD COAGULATION FACTOR VIII

Zaitsev, Viatcheslav (Independent researcher, Dundee, GBR); Prof. Lindley, Peter (ITQB NOVA, Qeiras)

Copper proteins form an extremely diverse group of proteins with a broad variation in function ranging from electron transfer, metal transport, oxidation of a variety of substrates, to the blood coagulation factors V and VIII (FVIII). A separate class of multicopper oxidases (MCOs) includes laccase, ascorbate oxidase, metallo-oxidases CueO and Fet3p, hephaestin and ceruloplasmin [1-3]. It is widely accepted that the MCOs have evolved from a two-domain ancestral protein (gene duplication of cupredoxin).

The A domains of FVIII show some 40% sequence identity to the six-domain ceruloplasmin. Unlike ceruloplasmin, FVIII contains a large insertion domain B and two extra domains C1 and C2 at the C-terminus. Structural comparisons of human ceruloplasmin (hCp) [2] and its evolutionary paralogue, hephaestin (Heph) [3], with the three X-ray structures of recombinant FVIII [4-6] have been undertaken. The A domains of FVIII heterotrimers show significant similarity to the hCp/Heph structure with the overall RMSDs varying from 1.4 to 1.7 Å. However, a detailed comparison of the copper binding sites indicates that FVIII may have evolved from the Heph precursor, but not from that of hCp, whilst losing the interdomain trinuclear copper cluster and the mononuclear copper of domain 4. The evolutionary relationships within the broader copper proteins superfamily will be discussed.

[1] P. Lindley et.al. (1999), In: *Perspect. Bioinorg. Chem.* 4: 51-82

[2] I.Bento et.al. (2007), *Acta Cryst. D*63(2): 240-248

[3] <https://slavazaitsev914078364.wordpress.com>

[4] A.Svensson et.al. (2013), *Biol.Chem.* 394(6):761-765

[5] B. Shen et.al. (2008), *Blood*, 111(3): 1240-1247

[6] J.Ngo et.al. (2008), *Structure*, 16: 597-606

## MS13: Biomineralogy and Bioinspired Materials

---

### MS13-01 | BIOINSPIRED CALCIUM PHOSPHATES: STRUCTURAL MODIFICATIONS INDUCED BY FUNCTIONALIZATION

Boanini, Elisa (University of Bologna, Bologna, ITA)

Thanks to their excellent biocompatibility and bioactivity, calcium orthophosphates are widely employed in the preparation of biomaterials for hard tissues substitution and repair. Improvement of tissue response can be achieved through the development of functionalized calcium phosphate based materials. Furthermore, tailor-made multi-functionalized calcium phosphates may be exploited to provide local release of the functionalizing agents and prevent the drawbacks of systemic treatments. This lecture will focus on the role played by the structural approach on the comprehension of the important influence of functionalization with bioactive ions and molecules on the structure, morphology, and stability of some calcium orthophosphates of biological interest.

## MS13-02 | ALTERATION OF HUMAN BONE MINERALIZATION IN A SCLEROSING OSTEOSARCOMA

Zanghellini, Benjamin (Universität für Bodenkultur Wien (BOKU), Wien, AUT); Grünewald, Tilman (Institut Fresnel, Marseille, FRA); Burghammer, Manfred (The European Synchrotron (ESRF), Grenoble, FRA); Rennhofer, Harald (Universität für Bodenkultur Wien (BOKU), Wien, AUT); Liegl-Atzwanger, Bernardette (Medizinische Universität Graz, Graz, AUT); Leithner, Andreas (Medizinische Universität Graz, Graz, AUT); Lichtenegger, Helga (Universität für Bodenkultur Wien (BOKU), Wien, AUT)

Osteosarcoma is the most common primary bone cancer type in humans. It is predominantly found in young individuals, with a second peak later in life. The tumour is formed by malignant osteoblasts and consists of collagenous, sometimes also mineralized, bone matrix. While the morphology of osteosarcoma has been well studied, there is virtually no information about the nanostructure of the tumour and changes in mineralization on the nanoscale level. We have studied human bone tissue inside, next to and remote from a sclerosing osteosarcoma with small angle x-ray scattering, x-ray diffraction and electron microscopy. Quantitative evaluation of nanostructure parameters was combined with high resolution, large area mapping to obtain microscopic images with nanostructure parameter contrast. It was found that the tumour regions were characterized by a notable reduction in mineral particle size, while the mineral content was even higher than that in normal bone. Furthermore, the normal preferential orientation of mineral particles along the longitudinal direction of corticalis or trabeculae was largely suppressed. Also, the bone mineral crystal structure was affected: severe crystal lattice distortions were detected in mineralized tumour tissue pointing to a different ion substitution of hydroxyl apatite in tumorous tissue than in healthy tissue.

[1] B. Zanghellini et al. J Struct Biol. 2019 Apr 17. pii: S1047-8477(19)30078-4. doi: 10.1016/j.jsb.2019.04.012

### MS13-03 | NEW COMPLEXES OF SILVER(I) WITH AZOLES

Checinska, Lilianna (University of Lodz, Faculty of Chemistry, Lodz, POL); Komerist, Yevgeniy (University of Lodz, Faculty of Chemistry, Lodz, POL); Ochocki, Justyn (Medical University of Lodz, Department of Bioinorganic Chemistry, Lodz, POL)

This research project is a part of our ongoing studies concerning the biological activity of new silver(I) compounds, which have drawn much attention as potential antimicrobial agents.

We determined crystal and molecular structures of silver(I) complexes with azole ligands (as clotrimazole, fluconazole etc). Azole agents are widely used in medicine due to their antifungal and antibacterial activity. Complexes of azoles with biometals (eg. with Ag) may extend the range of potential drugs and affect the diversity of their properties, selectivity and efficiency.

The next step is to determine whether the obtained complexes are effective antimicrobial agents and whether they represent a possible alternative to commonly used drugs.

## MS13-04 | SURFACE LAYER PROTEINS OF LACTOBACILLI – DETERMINING THE CELL WALL BINDING AND THEIR ANTIBACTERIAL EFFECT

Eder, Markus (University of Graz, Graz, AUT); Dordic, Andela (University of Graz, Graz, AUT); Sagmeister, Theo (University of Graz, Graz, AUT); Damisch, Elisabeth (University of Graz, Graz, AUT); Vejzovic, Djenana (University of Graz, Graz, AUT); Berni, Francesca (Leiden University, Leiden); Codee, Jeroen (Leiden University, Leiden); Palva, Airi (University of Helsinki, Helsinki); Vonck, Janet (Max-Planck-Institut für Biophysik, Frankfurt am Main, GER); Oberer, Monika (University of Graz, 8010, AUT); Pavkov-Keller, Tea (University of Graz, 8010, AUT)

Surface layers (S-layers) are 2D crystalline lattices of proteins which cover the whole surface of many archaeal and bacterial cells. Since these proteins are in close contact with the environment, they fulfil many important tasks like bacterial adherence to other cells, protection against life-threatening conditions, maintenance of the cell shape and, auto- coaggregation. They play an important role in the stimulation of gut dendritic cells by interacting with specific receptors. Interaction with the cell wall occurs by binding to Lipoteichoic acids (LTA).

These proteins are not just important for our immune system. They are equally important for the role of lactobacilli in the microbiome of the gut. Lactobacillus S-Layers harbor outstanding therapeutic potential, especially for vaccines. Furthermore, it was reported that the cell wall binding domain of Lactobacilli surface layer proteins possess a murein hydrolase activity, which shows antibacterial activity against *Escherichia coli*.

Our goal is to characterize the surface layer proteins SlpA and SlpX of *L. acidophilus* and SlpA of *L. amylovorus*. Both species are of high biological and medical relevance because of their probiotic properties. We elucidated the 3D structures of the three cell wall binding domains by x-ray crystallography. Isothermal titration calorimetry experiments were performed to characterize the binding partner of these domains. Ongoing experiments focus on the co-crystallization with LTA fragments and the antibacterial effect of this domain.

## MS13-05 | DEALING WITH MODULATED MACROMOLECULAR STRUCTURES WITH TRANSLATIONAL NON-CRYSTALLOGRAPHIC SYMMETRY

Caballero, Iracema (SBU - IBMB - CSIC, Barcelona, ESP); Sammito, Massimo (Department of Haematology, Cambridge Institute for Medical Research, University of Cambridge, Cambridge, GBR); Usón, Isabel (SBU - IBMB - CSIC, Barcelona, ESP); Read, Randy (Department of Haematology, Cambridge Institute for Medical Research, University of Cambridge, Cambridge, GBR); McCoy, Airlie J (University of Cambridge, Cambridge, GBR)

Translational non-crystallographic symmetry (tNCS) is a pathology of protein crystals in which multiple copies of a molecular assembly are found in similar orientations. This causes an overall modulation with systematically strong and weak intensities, affecting structure determination and refinement. Addressing this pathology is less developed in macromolecules than in chemical crystallography, as severe cases preclude solution altogether.

Modulation gives rise to strong peaks in the Patterson function. In commensurate modulation, peaks are located at simple fractions of the vectors of the reciprocal lattice whereas in incommensurate modulation peaks occupy positions that do not represent a simple fraction.

In order to take into account the statistical effects of these modulations, the Patterson map can be used to determine the translation relating the copies. Then any small rotational differences in their orientations, and the size of random coordinate differences caused by conformational differences can be refined against a likelihood function to account for the effects of tNCS [1,2].

In the present project we deal with the determination from the experimental data of the parameters describing the tNCS before a structure is solved and in order to aid structure solution. For this purpose a database containing a representative PDB [3] subset with nearly 80000 protein structures has been characterized and used to train a decision algorithm.

[1] Read RJ *et al.* (2013). *Acta Cryst.* D69, 176-183

[2] Sliwiak J *et al.* (2013). *Acta Cryst.* D69, 176-183

[3] Burley SK *et al.* (2019) *Nucleic Acids Research* 47: D464–D474.

## MS13-P01 | BRACHIOPOD SHELL CALCITE MINERALIZATION OCCURS BY ION-BY-ION TRANSPORT CONTROLLED BY THE EPITHELIAL CELL MEMBRANES

Griesshaber, Erika (LMU Munich, Munich, GER); Simonet Roda, Maria (LMU Munich, Munich, GER); Ziegler, Andreas (University of Ulm, Ulm, GER); Fernandez-Diaz, Lurdes (Universidad Complutense de Madrid, Madrid, ESP); Schmahl, Wolfgang (LMU Munich, Munich, GER)

Most biocarbonates show a nanoparticulate morpho-topology in the 50-100 nm size range in high resolution imaging studies. Accordingly, a paradigm evolved claiming that biominerals form by accretion of carbonate-filled vesicles exocytosed by the mineralizing cells. We investigated numerous marine calciumcarbonate shells with AFM, SEM/EBSD, TEM and XRD over the last decade, and we likewise examined calcite crystals grown abiotically in a protein or polysaccharide gel matrix. A number of observations speak against nanoparticle accretion as a general model for biomineralization and for an ion-by-ion growth mechanism:

(1) Gel-grown calcite incorporates a fibrous gel network with connected pores in the 50-100 nm range. These crystals thus show a superficial “nanoparticulate” mesocrystal-like appearance where the ~100 nm subcrystals result from the gel pores rather than from pre-existing nanoparticles. The crystals show {104} morphologies which are created by ion-by-ion growth.

(2) For most marine biocarbonates the “nanogranule-like” morphologies are also in the 50-100 nm range, and the biocarbonate crystals also contain incorporated organic networks with pores in the corresponding size-range. One exception are coccoliths, which do not contain organic matrix and show a classical crystallography; moreover, THEY form in intracellular vesicles.

(3) Packing of any round similarly-sized particles leaves ~25% pore space. However, most marine biocarbonates are rather dense.

(4) We showed for brachiopods that the shell mineral morphology is tightly controlled by the epithelial cell membranes and that “extrapallial space” is absent, which speaks for ion-by-ion growth. No vesicles supporting the paradigm of “nanoparticle-accretion” of the shell calcite were found.

## MS13-P02 | THE BONE MINERAL IS CARBONATO-HYDRO-APATITE AND IT TRANSFORMS INTO HYDROXYAPATITE BY HEATING (CREMATION) BEYOND 700°C

Greiner, Martina (LMU Munich, Munich, GER); Rodríguez-Navarro, Alejandro (Universidad de Granada, Granada, ESP); Schmahl, Wolfgang (LMU Munich, Munich, GER); Kocsis, Balazs (LMU Munich, Munich, GER); Grupe, Gisela (LMU Munich, Planegg-Martinsried, GER); Mayer, Katrin (LMU Munich, Planegg-Martinsried, GER)

We studied thermal changes in bovine bone mineral between 100°C and 1000°C. Complementary analytical methods were applied to the same unheated and heat treated material to ensure data consistency: quantitative powder X-ray diffraction, Fourier Transform Infrared Spectroscopy (FTIR), and Infrared-coupled Thermogravimetric Analysis (TGA-FTIR). At temperatures from 700 °C onwards after 30 minutes of heating, a considerable recrystallization reaction from the original bioapatite to hydroxyapatite occurred. No hydroxyl ions are discernible in FTIR spectra of original bone mineral while  $\text{CO}_3^{2-}$  and  $\text{H}_2\text{O}$  spectral features are prominently visible. Bovine bone bioapatite thus should be referred to “carbonate-hydro-apatite” rather than hydroxyapatite. The treatment at temperatures  $\geq 700$  °C induced a pronounced recrystallization reaction, increasing both the crystallite size and the amount of hydroxyl groups in the apatite lattice. Above 800 °C buchwaldite,  $\text{CaNaPO}_4$ , is formed from the Na component of the bone mineral. The changes in the state of the bone mineral are not only dependent on temperature but also on time. The recrystallization reaction strongly accelerates after organic matrix compounds and their residues have been combusted and the apatite grains get into direct contact.

### SHELL

BOUFALA, Khaled (Université de Bejaia, Bejaia, DZA); Salim, OUHENIA (University of Bejaia, Bejaia, DZA); LOUIS, Ghislain (Université de Lille, Lille, FRA); BETRANCOURT, Damien (Université de Lille, Lille, FRA); CHICOT, Didier (Université de Lille, Lille, France., FRA); BELABBAS, Imad (Université de Béjaia, Bejaia, DZA)

Molluscs' shells are biogenic composite materials built by the mollusc following biomineralisation process. These biocomposite materials are dense and present acellular arrangement tissues which contain at least 95% of minerals and 5% of proteins and traces of polysaccharides. It is recognised that the most part of the organic phase is located between the crystallites (inter-crystalline). However, some organic molecules (intra-crystalline) are also intercalated within the crystalline lattice. This particular combination of organic matter and inorganic material gives to the mollusc shells their remarkable mechanical properties, which render them  $10^2$  to  $10^3$  tougher than pure geological minerals. This biomaterial is obtained with a minimum consumption of energy and a precise control of the polymorphism and crystal morphology at the nanometric-scale by the use of various macromolecules secreted by the organism according to its genetic programming.

In the present work, scanning electron microscopy observations are performed on the shell (broken in nitrogen liquid) of Charonia Lampas Lampas mollusc in order to explore the different orientations of the crystal through its thickness. On the other hand, the phase identification of the shell has been determined by X-ray diffraction and FT-IR analysis.

## MS13-P04 | SMALL-ANGLE X-RAY SCATTERING STUDIES ON THE INTERACTION OF BICELLES WITH BOVINE SERUM ALBUMIN

Lin, Tsang-Lang (National Tsing Hua University, Hsinchu, TWN)

It is essential to understand how bicelles interact with proteins in order to develop bicelle drug delivery systems. In this study, the interaction of cationic lipid bicelles with the Bovine Serum Albumin (BSA) was investigated by small-angle X-ray scattering (SAXS). Disc-shaped bicelles can be formed spontaneously by mixing long-chain lipids with short-chain lipids at suitable ratios [1]. The long-chain lipids form the bilayer core of the bicelle while the short-chain lipids form the protecting rim of the bicelle. The surface charge of such bicelles can be varied by doping with cationic lipids, such as DC-Cholesterol, to form cationic bicelles [2]. For the cationic bicelles consist of 8.5 mM DPPC, 3.3 mM diC7PC and 1.5 mM DC-cholesterol, at low BSA concentrations of 0.029 mM to 0.058 mM, the presence of BSA induces the bicelles to form long stacking lamellar structure by encapsulating the BSA molecules between the lipid bilayers. When the BSA concentration is further increased above 0.072 mM, the lamellar structure is transformed to a rectangular column structure. It is likely that the mixed bilayers become modulated due to the strong charge interaction between the cationic lipid bilayers and the BSA molecules at high BSA concentrations.

[1] Yang, P.-W.; Lin, T.-L.; Hu, Y. & Jeng, U-S. (2012) *Chinese J. of Phys.*, **50**, 349.

[2] Yang, P.-W.; Lin, T.-L.; Hu, Y. & Jeng, U-S. (2013) *Soft Matter*, **9**, 11542.

## MS13-P05 | THE INTERACTION BETWEEN CALCIUM CARBONATE AND CALCIUM PHOSPHATE AS THE DRIVING MECHANISM FOR CARBONATE-HYDROXYAPATITE FORMATION

Pastero, Linda (Department of Earth Sciences-University of Turin, Turin, ITA); Bruno, Marco (Department of Earth Sciences-University of Turin, Turin, ITA); Aquilano, Dino (Department of Earth Sciences-University of Turin, Turin, ITA)

The mechanisms involved in carbonate-hydroxyapatites (CAp) growth in both biological and geological environments still represent a challenge for mineralogists and crystallographers, even if it is commonly accepted from crystallographic studies on CAp, that carbonate ions could be placed into both the OH<sup>-</sup> and PO<sub>4</sub><sup>3-</sup> sites of the apatite, originating the A-type or B-type of CAp [1-4].

We experimentally demonstrated that the presence of carbonate in solution affects both, the morphology and structure of apatites, the extent of the effects depending on the concentration. The continuity between morphological and structural effects of calcium carbonate on calcium hydroxyapatites was explained in the light of the cooperative effect [4-7] between Ca-carbonates in solution and Ca-hydroxyapatites, considering the modification of growth habit and the stabilization of carbonate-containing structures as a consequence of the epitaxy as the driving mechanism during crystal growth.

- [1] J. C. Elliott, Queen Mary University of London, 1964.
- [2] R. Z. Legeros, O. R. Trautz, E. Klein and J. P. Legeros, *Experientia*, 1969, **24**, 5–7.
- [3] J. C. Elliott, D. W. Holcomb and R. A. Young, *Calcif. Tissue Int.*, 1985, **37**, 372–375.
- [4] S. Shimoda, T. Aoba, E. C. Moreno and Y. Miake, *J. Dent. Res.*, 1990, **69**, 1731–1740.
- [5] L. Pastero and D. Aquilano, *Cryst. Growth Des.*, 2008, **3**, 0–9.
- [6] D. Aquilano and L. Pastero, *Cryst. Res. Technol.*, 2013, **48**, 819–839.
- [7] L. Pastero and D. Aquilano, *Cryst. Growth Des.*, 2016, **16**, 852–860.

## MS13-P123 - LATE | HALOGENESIS AND BIOMINERALIZATION IN THE RESIDUAL BASINS OF THE ARAL SEA

Reykhart, Liudmila (Shirshov Institute of Oceanology, Russian Academy of Sciences, Moscow, RUS); Sapozhnikov, Philipp (Shirshov Institute of Oceanology, Russian Academy of Sciences, Moscow, RUS); Izhitskiy, Alexander (Shirshov Institute of Oceanology, Russian Academy of Sciences, Moscow, RUS); Dara, Olga (Shirshov Institute of Oceanology, Russian Academy of Sciences, Moscow, RUS); Boev, Andrey (Shirshov Institute of Oceanology, Russian Academy of Sciences, Moscow, RUS); Andrulionis, Natalia (Shirshov Institute of Oceanology, Russian Academy of Sciences, Moscow, RUS); Kozina, Nina (Shirshov Institute of Oceanology, Russian Academy of Sciences, Moscow, RUS); Kalinina, Olga (Shirshov Institute of Oceanology, Russian Academy of Sciences, Moscow, RUS); Reikhard, Arsenii (Public school ?2086, Moscow, RUS)

Catastrophic desiccation transformed the Aral Sea into a system of residual basins with different hydrophysical and hydrochemical characteristics. Extremely high gradients of salinity values and concentrations of hydrogen sulfide and methane observed previously in the Western Large Aral Sea and Lake Tshchebas provoke unique conditions for processes of halogenesis and biomineralization.

Here we present the results of field survey to the Aral Sea taken place in October, 2018. Biogenic opal was actively formed in the well-mixed water column of Lake Tshchebas with salinity values of 47 g/kg by the blooming euryhaline diatom *Cyclotella meneghiniana*, and was located in the diatom frustules *Pleurosigma sp.*, *Proschkinia complanata*, *Navicula sp.*, *Tryblionella apiculata*. The coastal surface crusts consist of the microcrystalline aggregates of thenardite, halite, eugsterite, blödite with inclusions of the opal frustules of diatoms *Mastogloia pumila*. Crusts contain microzones of hydrotroilite and filaments of green alga *Cladophora*, often encrusted with crystals of chemogenic minerals.

In the Chernyshev Bay of the Western Large Aral Sea, the measured salinity was 72 g/kg in the surface layer and 235 g/kg in the bottom layer. The opal frustules of diatoms *Tabularia tabulata*, *Halamphora cymbifera*, *Cocconeis placentula var. euglipta*, *Cyclotella meneghiniana* were found in the water column. Coastal dense crusts from microcrystalline aggregates of eugsterite, blödite, konyaite, and thenardite were studied.

These results can be used as indicators of changes in the ecological situation in the Aral region.

The work has been realized in the framework of the state assignment (theme №0149-2019-0004).

## MS14: Mineralogical and Inorganic Crystallography

---

### MS14-01 | SEARCH FOR NEW TELLURIUM AND SELENIUM OXIDES WITH POTENTIAL FERROELECTRIC AND MULTIFERROIC PROPERTIES

BARRIER, Nicolas (CNRS-CRISMAT, CAEN, FRA)

The synthesis of new non-centrosymmetric compounds is a very interesting challenge for solid-state chemistry. Indeed, non-centrometry is the prerequisite for obtaining materials with functional properties such as piezoelectricity, pyroelectricity, ferroelectricity. Conjugated to a magnetic order, it can induce multiferroicity. In the family of oxides, the use of cations subject to Second Order Jahn-Teller (SOJT) distortions able to provide asymmetric coordination environments with local dipole moments, may favor the emergence of the non-centrosymmetry. Among these cations we can find those with active non-bonded electron pair such as  $\text{Se}^{\text{IV}}$  and  $\text{Te}^{\text{IV}}$ . With these cations numerous of noncentrosymmetric oxydes have already been synthesized by solid state reactions. Alternative reaction routes are now exploring to get new non-centrosymmetric phases. The solvothermal syntheses and more particularly hydrothermal syntheses are promising methods to explore chemical systems to get new compounds or new polymorphs with original crystal structures as well as for growing crystals. Compare to solid state synthesis, many parameters (pH, concentration, precursors, oxido-redox conditions, temperature, pressure, time, etc.) are adjustable in hydrothermal synthesis which offer a substantial number of configurations and thus increased the chances of getting new phases. In a second time, the X-ray and neutron diffraction experiments are necessary to solve the new structures and follow the phase-transitions. During the presentation, I will present chemical systems such as (Ca, Sr, Co) -  $\text{Te}^{\text{IV}}$  - O and Co -  $\text{Se}^{\text{IV}}$  - O explored by conjugating hydrothermal synthesis assisted by microwave, conventional hydrothermal synthesis and crystallographic studies.

## MS14-02 | NEW DATA ABOUT TOPOLOGY AND MODULARITY OF HETEROPOLYHEDRAL FRAMEWORKS IN MINERALS AND INORGANIC COMPOUNDS

Aksenov, Sergey (FSRC "Crystallography and Photonics" RAS, Moscow, RUS)

Zeolites compose an important class of inorganic crystalline materials that have been widely used in technology. A family of microporous materials demonstrates that frameworks can be built by  $TO_4$  tetrahedra and  $MO_6$  octahedra ( $M$  – predominantly transitional metals: Ti, Nb, Zr, Sn, Fe, Mn, etc.). Such heteropolyhedral zeolite-like materials are also characterized by many useful physical and chemical properties and attract interest (especially titanium silicates) as ion-exchangers because of their efficient absorption of heavy elements from aqueous solutions.

The modern topological analysis of zeolite structures using the ToposPro software is based on the types of linkage of natural tiles, the smallest tetrahedral clusters, to form a framework structure. In this case, it can be also useful to characterize a topology of the heteropolyhedral frameworks as they represent the same 3D cationic nets.

Another way for describing complex structures of minerals and inorganic compounds is the modular approach, when the structure is described as a combination of a number of fragments – modules. It is closely related to the concepts of order/disorder (OD) structures and polysomatic series.

Both approaches have been recently applied for the analysis of hybrid lanthanide-based silicates, uranyl germanates and vanadates, and series of minerals and related compounds with heteropolyhedral frameworks. The relationships between such heteropolyhedral frameworks and tetrahedral framework types were found and described in details and hypothetical zeolite-type materials were predicted.

## MS14-03 | KAHLENBERGITE, A NEW POTASSIUM $\beta$ -ALUMINA MINERAL

Krüger, Biljana (University of Innsbruck, Innsbruck, AUT); Galuskin, Evgeny V. (University of Silesia, Faculty of Earth Sciences, Sosnowiec, POL); Galuskina, Irina O. (University of Silesia, Faculty of Earth Sciences, Sosnowiec, POL); Krüger, Hannes (University of Innsbruck, Institute of Mineralogy and Petrography, Innsbruck, AUT); Vapnik, Yevgeny (Ben-Gurion University of the Negev, Beer-Sheva, ISR)

Kahlenbergite (IMA 2018-158) is a natural potassium  $\beta$ -alumina, with an empirical formula of  $(K_{0.87}Mg_{0.09}Ca_{0.03}Ba_{0.01})_{S1}(Al_{9.46}Fe^{3+}_{1.36}Mg_{0.14}Cr^{3+}_{0.02}Si_{0.02})_{S11}O_{17}$ . It occurs in small hematite segregations within wollastonite-gehlenite rocks. The mineral association suggests formation temperature between 1000 and 1200 °C (Sharygin, 2019). Kahlenbergite forms platy, light-brown crystals, epitaxially replaced and overgrown by hibonite. The unit cell dimensions ( $a=5.64860(6)$ ,  $b=22.8970(3)$  Å) and space group  $P6_3/mmc$  of kahlenbergite corresponds to that of synthetic K  $\beta$ -alumina. The crystal structure was refined using synchrotron diffraction data (beamline X06DA, SLS, PSI). Compared to synthetic K  $\beta$ -alumina, which often shows considerable amounts of positional and occupational cation disorder, the structure of kahlenbergite is fairly simple. It exhibits a fully occupied position of the K atom at ( $\frac{2}{3}$ ,  $\frac{1}{3}$ ,  $\frac{1}{4}$ ). The structure of kahlenbergite is made of spinel blocks, divided along  $c$  into mixed ( $M$ ) layers with  $AlO_6$  octahedra and  $(Al_{0.56}Fe_{0.44})O_4$  tetrahedra, Kagome ( $K$ ) layers with  $(Al_{0.92}Fe_{0.08})O_6$ , and pillar ( $P$ ) layers with two  $AlO_4$  tetrahedra and K-atoms. The presented structure model of kahlenbergite describes an idealised ordered structure. All investigated crystals exhibit one-dimensional diffuse scattering. In one crystal additional reflections can be identified, which obviously belong to the  $Fe^{3+}$ -analog of hibonite.

The structure of kahlenbergite and the  $Fe^{3+}$ -analog of hibonite contain identical blocks, which are connected by  $P$ -layers in kahlenbergite and so-called  $R$ -layers in the  $Fe^{3+}$ -analog of hibonite. The  $R$ -layers contain Ca atoms,  $AlO_5$ -bipyramids, and further  $AlO_6$  octahedra. Therefore, the connecting layers are most likely the source of the disorder.

[1] Sharygin, (2019) Mineralogical Magazine 83, 123–135

## MS14-04 | MODULARITY IN MINERALS: THE EXAMPLE OF BIOPYRIBOLES-PALYSEPIOLES

Nespolo, Massimo (Université de Lorraine, Vandoeuvre-lès-Nancy, FRA); Umayahara, Akihiro (Université de Lorraine and Radboud University Nijmegen, Vandoeuvre-lès-Nancy and Nijmegen, FRA)

Modularity expresses the way in which the same building blocks, larger than the coordination polyhedron, occur in various crystal structures, which can therefore be gathered in series of structurally related compounds. Two well-known examples are those of biopyriboles and palysepioles, which have been described as two polysomatic series. A new unifying scheme describes all the minerals in these two series as built by TOT rods of variable width extracted from the structure of phyllosilicates. The close structural similarity between any two members of these two series can be shown by expressing the fractional atomic coordinates in a common reference. Accordingly, the two polysomatic series can actually be interpreted as a single series whose prototype is a phyllosilicate

The operations mapping pairs of modules in each of the member of this series are partial operations; the symmetry operation of each module are local operations. Both partial and local operations act on the given module(s) but not necessarily on other modules. The set-theoretical union of all the partial and local operations gives a Brandt groupoid. The subset of these operations that act on the whole structure are global operations and they form the space group of the structure. We show that the groupoid analysis explains the structural relations between pairs of rods in each member of the series. We also show that the global operations obtained by analysing the groupoid of a given structure indeed result in the space group of that member.

## MS14-05 | THE STRUCTURE OF THE LANTHANUM OXONITRIDOPHOSPHATE La<sub>21</sub>P<sub>40</sub>O<sub>46</sub>N<sub>57</sub>

Günther, Daniel (Leipzig University, Leipzig, GER); Nentwig, Markus (Leipzig University, Leipzig, GER); Kloß, Simon D. (LMU München, 81377, GER); Neudert, Lukas (Leipzig University; LMU München, 04275, 81377, GER); Eisenburger, Lucien (Leipzig University, LMU München, Leipzig; München, GER); Schnick, Wolfgang (LMU München, München, GER); Oeckler, Oliver (Leipzig University, Leipzig, GER)

High-pressure metathesis is a successful method for syntheses of intriguing nitridophosphates, e.g. LiNdP<sub>4</sub>N<sub>8</sub> or LiPr<sub>2</sub>P<sub>4</sub>N<sub>7</sub>O<sub>3</sub> [1]. The reaction of LiPN<sub>2</sub> and LaCl<sub>3</sub> at either 7 GPa and 750 °C or 9 GPa and 950 °C yields the new oxonitrodophosphate La<sub>21</sub>P<sub>40</sub>O<sub>46</sub>N<sub>57</sub> if water is present, e.g. by hydrolysis of LaCl<sub>3</sub> or the used BN crucible. The microcrystalline product was characterized by single-crystal structure determination using microfocussed synchrotron radiation after preselecting suitable crystallites by transmission electron microscopy and electron diffraction. The compound crystallizes in the monoclinic space group *P*2<sub>1</sub>/*n* with a *c* lattice parameter of ca. 41.4 Å. Its complicated structure is built up from vertex-sharing P(O,N)<sub>4</sub> tetrahedra forming loop-branched chains with *dreier* ring branches. Lanthanum atoms are embedded between these loops. The chains are built up by *21er* units. These units are interconnected either by vertex- or by edge-sharing tetrahedra; alternatively, the chain can interrupt. These different variants are described by disordered tetrahedra. An additional split position involving La and N/O atoms leads to eight different local structure variants. Tentative structure refinements in lower-symmetric space groups such as *Pn*, taking into account twinning where appropriate, do not result in ordered models and thus confirm the disorder.

We thank Dr. J. Wright, Dr. V. Dyadkin (ESRF, Grenoble) for their help with synchrotron measurements and the ESRF for granting beamtime (projects CH-5142 and CH-4612).

[1] S. D. Kloß, W. Schnick, *Angew. Chem. Int. Ed.* **2019**, *58*, 2-14.

## MS14-P01 | REASSESSING PAULING'S RULES

George, Janine (Université Catholique de Louvain, Louvain-la-Neuve, BEL); Waroquiers, David (Université catholique de Louvain, Louvain-la-Neuve, BEL); Di Stefano, Davide (Université catholique de Louvain, Louvain-la-Neuve, BEL); Rignanese, Gian-Marco (Université catholique de Louvain, Louvain-la-Neuve, BEL); Hautier, Geoffroy (Université catholique de Louvain, Louvain-la-Neuve, BEL)

Pauling's rules play an essential role for solid state chemistry [1,2]. In the first publication of the rules, Pauling has already mentioned several of their drawbacks [2]. For instance, they are expected to only work for very ionic compounds such as oxides [2]. Surprisingly, there is no statistical sound answer on how well *all* Pauling's rules perform for oxides up to today. We will provide such an answer in this contribution. To do so, all five Pauling rules are checked on around 6000 oxides from the Materials Project [3] that originally stem from the experimental database ICSD. We will start from a very recent analysis of the statistics of the coordination environments of oxides [4]. Structural exceptions from the rules and trends within the exceptions will be discussed.

Computational resources have been provided by the Consortium des Équipements de Calcul Intensif (CÉCI).

[1] L. Pauling, *J. Am. Chem. Soc.* **1929**, *51*, 1010.

[2] L. Pauling, *The Nature of the Chemical Bond and the Structure of Molecules and Crystals*, Cornell University Press, Ithaca, New York, **1960**.

[3] A. Jain, S.P. Ong, G. Hautier, W. Chen, W.D. Richards, S. Dacek, S. Cholia, D. Gunter, D. Skinner, G. Ceder, K.A. Persson, *APL Materials* **2013**, *1*, 011002.

[4] D. Waroquiers, X. Gonze, G.-M. Rignanese, C. Welker-Nieuwoudt, F. Rosowski, M. Göbel, S. Schenk, P. Degelmann, R. André, R. Glaum, G. Hautier, *Chem. Mater.* **2017**, *29*, 8346

## MS14-P02 | FIRST-PRINCIPLES INVESTIGATION OF STRUCTURAL, ELECTRONIC AND OPTICAL PROPERTIES OF CsPb (I1-xBrx )3 (x = 0.0 - 1.0) COMPOUNDS

Ghaithan, Hamid (king saud university, Riyadh, SAU)

The structural, electronic and optical properties of the CsPb(I<sub>1-x</sub>Br<sub>x</sub>)<sub>3</sub> (x = 0, 0.25, 0.33, 0.5, 0.66, 0.75 and 1) were investigated using the full potential augmented plane wave (FP-LAPW) scheme in the frame of generalized gradient approximation (GGA). The two exchange potentials, PBE-GGA and mBJ-GGA are used to study the electronic and optical properties. In this study, we have observed an increase in band gap values by 0.56 eV with increasing the concentration of Br atoms in CsPb(I<sub>1-x</sub>Br<sub>x</sub>)<sub>3</sub> alloys whereas the refractive indices, reflection and real part of dielectric function have reverse effect. It is noted that all of the compounds are wide and direct band gap semiconductors with band gap located at A-symmetry point. The optical properties of these compounds like optical conductivities, absorption coefficients, real and imaginary parts of dielectric functions, refractive indices, extinction coefficients, and reflectivity, are also calculated. The direct band gap nature and high absorption power of these compounds in the visible ultraviolet energy range imply that these perovskites can be used in optical and optoelectronic devices working in this range of the spectrum by replacing I by Br.

## MS14-P03 | ELECTRON CRYSTALLOGRAPHY OF PLANETARY MATERIALS: IMPACTITES AND MICROMETEORITES

Mugnaioli, Enrico; Gemmi, Mauro (Istituto Italiano di Tecnologia, Pisa, ITA); Campanale, Fabrizio (Università di Pisa, Pisa, ITA); Suttle, Martin D. (Università di Pisa, Pisa, ITA); Folco, Luigi (Università di Pisa, Pisa, ITA)

Electron crystallography have evolved in the last years into a technique able to furnish fast and reliable structural information from nanocrystals. 3D electron diffraction (ED) methods provide diffraction data from nm-sized domains, which are suitable for ab-initio structure solution. Moreover, it is now possible to derive a phase and orientation map with nanometric resolution by recording a sequence of ED patterns while scanning an area. Therefore, we have access to the crystal structure and to the phase and topotactic relations between the crystalline grains at a scale of few nanometers at the same time.

Cutting-edge electron diffraction methods guarantee a new opportunity for understanding the kinetic and the thermodynamic history of a geological sample with a cryptocrystalline habit. We will show specific applications of this analysis to impact rocks shocked by a hypervelocity impacts of cometary and asteroidal bodies on Earth crust. The investigation at the nanoscale with ED methods shows evidence of coesite formation directly from quartz and not from a dense amorphous phase during shock unloading as previously thought.

A second field of application is the identification of nanocrystalline phases in micrometeorites. We show the determination of magnetite and pyroxene crystals in a hydrated chondritic micrometeorite (CP94-050-052). These phases have been determined with a 3D ED data collection with a 150 nm beam by diffracting only on the nanocrystalline grains of interest, avoiding any contribution by the surrounding matrix. This research was supported through Programma Nazionale delle Ricerche in Antartide (ID# PNRA16\_00029).



## MS14-P04 | THE DEPENDENCE OF Yb CONCENTRATION ON LATTICE PARAMETERS OF YAG SINGLE CRYSTALS

Kodess, Boris (FSUE "VNIIMS", Moscow, RUS)

The garnet single crystals containing rare-earth additives applicate in many fields, including electronic and lasers. The impurities change the structural characteristics of these crystals and their properties as well. The dependence lattice parameters from Yb concentration in yttrium – aluminium garnet (YAG:Yb) have been constructed. Using the Czochralski method, single crystals were grown. The high quality of the single crystals was proved by the measurement of the half-width of the Bragg reflections. The Yb content and the low-impurity composition (31 elements) was monitored at the calibrated M1 MISTRAL (Bruker). The high-precision experiments carried out both on a 4-circle single diffractometer XCalibur (Rigaku-Oxford Diffraction) using spheres with of 0.3-0.4 mm (MoK-alpha radiation in the full Ewald-sphere) and on equipment with Bartels-monochromator using the Bond method analogous (polishing plate of 10\*15 mm). The parameters were determined by a high-angle region measurement.

The maximum in the lattice parameter values at 2 at. % Yb was not found in our experiment, as was stated in some early publications. A smooth change from the initial value of 1.20095 nm was observed right from the start, for a sample with 2 at. % (1.20063 nm), then it continued for the sample with 5 at. % (1.20039 nm) and then, with the increase of the Yb concentration, the change began to slow down for a sample with 10 at. % Yb (1.20024 nm). The distribution of electron density and its characteristics for a sample with 10 at. % Yb is consistent with the data in other publications.



## MS14-P05 | SYNTHESIS AND CRYSTAL STRUCTURES OF $Zr_2(OH)_2(XO_4)_3 \cdot 4H_2O$ ( $X=S, Se$ ) AND $Zr(SeO_3)_2$

Giester, Gerald (Universität Wien, Wien, AUT); Lengauer, Christian (universität Wien, Wien, AUT); Wildner, Manfred (Universität Wien, Wien, AUT)

In the course of a study on the crystal chemistry of zirconium oxysalts synthesized at low-hydrothermal conditions [1-3] we also prepared the title compounds from  $Zr_2O_2(CO_3)(OH)_2$ , the respective acids and minor contents of water.

The  $Zr_2(OH)_2(XO_4)_3 \cdot 4H_2O$  ( $X=S, Se$ ) salts crystallize isotypic in space group  $C2/c$ , the structure of the sulfate has been described earlier [4]. The present single crystal X-ray data allowed high-quality refinements disclosing the hydrogen bonding system and its role in the framework structure of  $Zr^{[8]}_2O_{14}$  dimers and  $XO_4$  groups.

For  $Zr(SeO_3)_2$ , only a microcrystalline precipitate could be extracted so far, hence X-ray powder data were measured on a Bruker D8eco system. A previous description [5] in  $Pmmm$  ( $a=8.555$ ,  $b=6.479$ ,  $c=15.232$  Å) resulted in several unindexed main peaks. The new cell is re-indexed in  $P2_1/c$  with  $a=4.9724(3)$ ,  $b=8.5992(5)$ ,  $c=6.9447(3)$  Å,  $\beta=110.128(3)^\circ$ . The structure obtained from our Rietveld refinement proves isotypism with other  $M^{4+}(SeO_3)_2$  compounds, i.e.  $Ti(SeO_3)_2$ ,  $\beta-Sn(SeO_3)_2$  and  $Pb(SeO_3)_2$  [6,7]. The  $Zr^{[6]}-O$  (2.031–2.083 Å) and  $Se-O$  (1.710–1.718 Å) bond lengths are in good agreement with values from literature.

- [1] G. Giester, M. Wildner, Monatsh. Chem. **149**, 1321 (2018)
- [2] M. Wildner, G. Giester, Monatsh. Chem. **150**, 593 (2019)
- [3] G. Giester, D. Talla, M. Wildner, Monatsh. Chem., submitted (2019)
- [4] D.B. McWhan, G. Lundgren, Inorg. Chem. **5**, 284 (1966)
- [5] J. Henry et al., J. Chil. Chem. Soc. **58**, 1759 (2013)
- [6] J.P. Legros, J. Galy, Comptes Rend. Ser. C **286**, 705 (1978)
- [7] G. Steinhäuser et al., J. Alloys Compounds **419**, 45 (2006)

## MS14-P06 | ORDER-DISORDER IN THE ARSENOPALLADINITE, $\text{Pd}_8\text{As}_{2.5}\text{Sb}_{0.5}$ , CRYSTAL

### STRUCTURE

Karimova, Oxana (Institute of Geology of Ore Deposits RAS, Moscow, RUS); Zolotarev, Andrey (St.-Petersburg State University, Saint-Petersburg, RUS); Evstigneeva, Tatiyana (Institute of Geology of Ore Deposits, Russian Academy of Sciences, Moscow, RUS)

Keywords: arsenopalladinite,  $\text{Pd}_8\text{As}_{2.5}\text{Sb}_{0.5}$ , order-disorder, polymorphism, crystal structure determination, single-crystal X-ray diffraction

The crystal structure of the mineral arsenopalladinite,  $\text{Pd}_8\text{As}_{2.5}\text{Sb}_{0.5}$ , from the Kaarreoja River, Inari commune, Finnish Lapland, Finland, was solved on the basis of X-ray diffraction data collected from the single crystal. The two polymorph modifications established.

The both polymorphs are triclinic, space groups are  $P-1$ . The unit cell parameters are:  $a=7.3344(7)$  Å,  $b=7.3870(8)$  Å,  $c=7.5255(7)$ ,  $\alpha=98.869(8)^\circ$ ,  $\beta=102.566(8)^\circ$ ,  $\gamma=119.10(1)^\circ$ ,  $V=331.19(1)$  Å<sup>3</sup>,  $Z=4$ ,  $R1=0.0481$  for (I) and  $a=7.329(2)$  Å,  $b=7.384(2)$  Å,  $c=14.137(3)$  Å,  $\alpha=95.983(4)^\circ$ ,  $\beta=92.027(4)^\circ$ ,  $\gamma=119.053(4)^\circ$ ,  $V=661.80(2)$  Å<sup>3</sup>,  $Z=8$ ,  $R1=0.0533$  for (II).

A net of atoms parallel to the plane constitute the structure. As and Sb occupy separate sites in the structure and located in a triangular,  $3^6$  type, nets. Pd atoms separated in another nets: distorted triangular  $3^6$  and pentagon-triangular  $3.5^3$ . The atomic nets of different orientation stack along the  $c$  axis.

All Sb atoms are ordered in one of the inversions centre ( $1a$  Wyckoff position) in the structure of the  $7\text{Å}$ -arsenopalladinite. In the  $14\text{Å}$ - arsenopalladinite Sb atoms disordered on to two positions. A half of Sb atoms occupy  $1a$  position, and a half – the  $1h$  position. In the result, one of the (As, Sb)-net is shifted in the  $ab$  plane caused stacking fault and doubling of the unit cell. The unit cell of the arsenopalladinite  $7\text{Å}$ -polymorph contains 6 nets, the  $14\text{Å}$ -polymorph contains 12 nets.

Acknowledgements: Author thanks Dr. Kari Kojonen for providing the mineral samples. X-Ray diffraction data were collected at the Center of X-ray diffraction studies at St. Petersburg State University (XRD Center SPbSU).

## MS14-P07 | STERIC EFFECT IN TETRACOORDINATED Ni(II) COMPLEXES WITH ENAMINOKETONE LIGANDS AND THEIR REACTION PRODUCTS WITH HETEROCYCLIC AMINES

Zep, Anna (University of Warsaw, Warsaw, POL)

Tetradentate ONNO coordinating ligands, such a Schiff base type salen/salphen and enaminone type acacen/acacphen, are wide studied ligands in chemistry due to the interest in their applicability. They have been successfully employed as ligands in combination with various metals to give catalyst capable of realizing a variety of synthetic transformations.

In this work two types of Ni (II) complexes based on acacen type ligands with variation in the N,N' bridge: 1,2-bis(4-methylbenzoylvinylamino) ethane Ni (II) – compound C2 and 1,3-bis(4-methylbenzoylvinylamino) propane Ni (II) – compound C3 have been synthesized and characterized by elemental analysis, FT-IR, UV-VIS, <sup>1</sup>H NMR and <sup>13</sup>C NMR spectral techniques.

In our studies we have observed that due the steric preferences compound C3 exhibit the ability to attach small molecules with N-donors. The structures of compounds C2, C3 and octahedral complexes of C3 with heterocyclic aromatic amines were determined by single crystal X-ray diffraction. Structural changes and the stability of the resulting complexes depending on the substituents in the molecules of N-donors will be discussed.

## MS14-P08 | COMPARATIVE CRYSTAL CHEMISTRY OF THE SOLID SOLUTION SYSTEMS BETWEEN KIESERITE ( $\text{MgSO}_4 \cdot \text{H}_2\text{O}$ ) AND TRANSITION METAL KIESERITE-TYPE COMPOUNDS ( $\text{M}^{2+}\text{SO}_4 \cdot \text{H}_2\text{O}$ ; $\text{M}^{2+} = (\text{Mn, Fe, Co, Ni, Zn})$ )

Wildner, Manfred (Institut für Mineralogie und Kristallographie, Wien, AUT); Talla, Dominik (University of Vienna, Vienna, AUT)

The extensive presence of low-hydrated sulfates, e.g. kieserite ( $\text{MgSO}_4 \cdot \text{H}_2\text{O}$ ), on the surface of Mars and probably also on icy moons of Jupiter and Saturn has gained much attention during the past 40 years. Given the local abundance of cosmochemically relevant transition metals (TM), the actual composition of extraterrestrial kieserite likely differs from its ideal formula. Hence, the confirmation and characterisation of continuous solid solutions between kieserite and the isotopic  $3d$ TM-compounds is crucial for interpretation of data from orbiter and rover space missions.

We have synthesized and structurally characterized the solid solution series between kieserite and the  $3d$ TM-sulfate monohydrates of Mn, Fe, Ni, Zn and previously Co [1]. All these systems form continuous solid solutions with linear Vegard-type behaviour of lattice and structural parameters. Nonetheless, it appeared that kieserite itself shows crystal chemical peculiarities compared to the  $3d$ TM-compounds, which do not follow simple expectations deduced from the different  $\text{M}^{2+}$  ionic radii: Mg-dominant phases show clearly expanded bond angles at polyhedra-linking oxygens, leading to larger cell volumes than expected.

We attribute this to the absence of  $3d$  orbitals in Mg, in contrast to their presence in the TM-compounds, leading to anisotropy of the electron density around the TM cations and affecting the bond critical point  $r_c$  along the  $M\text{--O}$  bond path [2]. This influences the electron density at the oxygen atoms and hence the second coordination sphere.

[1] Bechtold A, Wildner M (2016) Eur J Mineralogy 28, 43–52

[2] Bader RFW (1998) Encyclopedia Comput Chem 1, 64–86

## MS14-P09 | CRYSTAL STRUCTURE AND HIRSHFELD SURFACE ANALYSES OF A NEW ORGANOGOLD (III) WITH THIOSEMICARBAZONE

Almeida, Carolane (University of Brasília, Brasília, BRA); Macron, Pedro (University of Brasília, Brasília, BRA); Gatto, Claudia (University of Brasília, Brasília, BRA)

The thiosemicarbazones have been extensively studied, mainly due to their biological activities, properties and facility of coordination with many transition metals, due the presence of electron donor NNS atoms.

We describe the synthesis and crystal structure of new organogold(III) [Au(L)Cl] with 2-acetyl thiophene N4-methylthiosemicarbazone (HL). The metal center is coordinated by the N(1) and S(1) atoms and also by the C(3) - ketothyl group present on the thiosemicarbazone double-desprotonated. The coordination sphere with planar square geometry to the metal center is completed with a chloride ion with Au-Cl distance of 2.288(4) Å. The compound were characterized also by and spectral analyzes (IR, UV-Vis, <sup>1</sup>H NMR and <sup>13</sup>C NMR) and the results are agree with similar works reported in the literature.

The Hirshefeld Surface Analysis is fundamental to study unusual interactions present in the packing architectures revealed by single crystal X-ray diffraction analysis. Interestingly, intermolecular hydrogen bonds form a one-dimensional molecular arrangement.

## MS14-P10 - CANCELLED | NEW APPROACHES FOR RIETVELD REFINEMENT IN SIZE-STRAIN, GRAIN SIZE DISTRIBUTION AND DISLOCATION-RECRYSTALLIZATION ANALYSIS

Kristály, Ferenc (University of Miskolc, Institute of Mineralogy and Geology, Miskolc-Egyetemváros, HUN); Mikó, Tamás (University of Miskolc, Institute of Physical Metallurgy, Metalforming and Nanotechnology, Miskolc-Egyetemváros, HUN); Gácsi, Zoltán (University of Miskolc, Institute of Physical Metallurgy, Metalforming and Nanotechnology, Miskolc-Egyetemváros, HUN)

We have used Ti powder in milling and sintering experiments to obtain novel nanocomposites. The main properties to control were particle and grain (crystallite) size, sintered density and hardness. For particle size development we applied X-ray powder diffraction (Bruker, Cu  $K_{\alpha 1+2}$ , Göbel mirror, Vantec-1 PSD) and Rietveld refinement. The results revealed that we can delimit multimodal grain size distributions with discrete size ranges, simultaneously applying size-strain modeling and calculating quantitative distribution of size fractions. Grain shapes are extracted with size distribution data. Recrystallization by pressing and sintering produces changes in size-strain, texture and grain shapes which are readily solved in Rietveld refinement as newly developed fractions described with size, strain and lattice parameters different from starting material. The development of highly textured fractions can be quantitatively differentiated by combining orientation distribution and Rietveld refinement. Interrelation between dislocation density and recrystallization is observed from peak profile data. Changes upon sintering in size-strain and texture were observed also by in-situ sintering (Anton Paar HTK1200, vacuum, Cu  $K_{\alpha 1+2}$ , Göbel mirror, LynxEye X-ET). The results have been validated on standard materials (diamond, corundum) and by microscopy methods.

Due to severe broadening and overlapping of peaks of nanocrystalline phases, Rietveld refinement with multiple size/strain/texture fractions gives more realistic results than conventional size-strain analysis. Size and strain related broadening can be differentiated by the refinement and grain shapes are calculated from peak profile fitting following Rietveld refinement. Density and hardness developed during sintering show correlation with type and amount of recrystallized fractions.

## MS14-P11 | SYNTHESIS OF CALCIUM AND STRONTIUM RARE-EARTH ALUMINATES AND ITS USE AS HOST LATTICE FOR LEDs

Otgonbayar, Chimednorov (University of Halle/Saale/, Halle an der Saale, GER); Poellmann, Herbert (University of Halle/Saale/, Halle an der Saale, GER)

Long luminescent material based on  $\text{MRAIO}_4$  and  $\text{MR}_2\text{O}_4$  ( $\text{M} = \text{Ca, Sr, Ba}$ ;  $\text{R} = \text{Rare Earth Elements}$ ) as host lattice are gaining more interest due to their smooth emission spectra and long lifetimes.

The abstract reports on the results of studies on solid solution of  $\text{MEu}_{2-x}\text{Al}_x\text{O}_4$  ( $\text{M} = \text{Sr, Ba}$ ) and monophasic synthesised  $\text{MRAIO}_4$  – phases ( $\text{M} = \text{Ca, Sr, Ba}$ ;  $\text{R} = \text{La, Nd, Sm, Eu, Gd, Dy, Y}$  and  $\text{Yb}$ ). The compounds prepared using sol gel based Pechini method are studied by powder X-ray diffraction analysis, IR, TG and REM. Furthermore,  $\text{CaEuAlO}_4$  and  $\text{SrEuAlO}_4$  are doped with  $\text{Dy}^{3+}$  and  $\text{Sm}^{3+}$  to study the potential use in white light emitting diodes (W-LED).

The study of the system of  $\text{SrEu}_{2-x}\text{Al}_x\text{O}_4$  showed, that when  $x = 1$  there exists an intermediate phase with composition  $\text{SrEuAlO}_4$ . Phases with composition  $\text{MRAIO}_4$  ( $\text{M} = \text{Ca, Sr}$ ;  $\text{R} = \text{Nd, Sm, Eu, Gd, Dy, Y}$  and  $\text{Yb}$ ), which are isotypic to  $\text{SrEuAlO}_4$ , are not all stable, depending on the ionic size of alkaline earth and rare earth elements (unstable are  $\text{SrDyAlO}_4$ ,  $\text{SrYAlO}_4$  and  $\text{SrYbAlO}_4$ )

The present study demonstrates the synthesis of monophasic  $\text{MRAIO}_4$  ( $\text{M} = \text{Ca, Sr, Ba}$ ;  $\text{R} = \text{La, Nd, Sm, Eu, Dy, Y}$  and  $\text{Yb}$ ) by sol gel based Pechini method at sintering temperature ( $1300^\circ\text{C}$ , 2-4h).

## MS14-P12 | NICKEL(II) COMPLEXES WITH DITHIOCARBAZATE LIGAND: CRYSTAL STRUCTURES AND SPECTROSCOPIC ANALYSIS

Lima, Francielle (University of Brasilia, Brasilia, BRA); Gatto, Claudia (University of Brasilia, Brasilia, BRA)

Dithiocarbazates and their metal complexes have been the subject of many studies because they have a wide range of pharmaceutical applications and great chemical and structural versatility. These Schiff bases present varied structures coordination sites and allow the formation of complexes with several transition metals [1,2]. The present study describe the synthesis and crystal structures of the two new nickel(II) complexes with 2-hydroxyacetophenone-S-benzylidithiocarbazate ( $H_2L^1$ ) ligand and additionally pyridine or triphenylphosphine to form respectively,  $[NiL^1Py]$  (1) and  $[NiL^1PPh_3]$  (2). The compounds were characterized also by elemental analysis and spectral measurements (IR, UV-Vis,  $^1H$  NMR and  $^{13}C$  NMR) and the results are agreeing with similar works reported in the literature [3,4].

In both complexes the metal center shows planar square geometry connected to the ONS donor-atoms of the dithiocarbazate and additionally the phosphorus of the  $PPh_3$  for the complex 1 and the nitrogen of the Py for the complex 2. The ligand adopts an E configuration and tautomeric and thiol form. Interestingly,  $\pi$ - $\pi$  stacking interaction between the rings of triphenylphosphine are observed to the complex 1.

Acknowledgements: FAPDF, Capes and UnB.

[1] Lima, F. C. *et al.* (2018). *Inor. Chim. Acta.* 483, 464-472.

[2] Takjoo, R., Centore, R., Hayatolgheibi, S. S. (2018). *Inor. Chim. Acta.* 471, 587-594.

[3] Maia, P. I. S. *et al.* (2010). *J. Inor. Biochemistry.* 104, 1276-1282.

[4] Ali, M. A. *et al.* (1996). *Transition Met. Chem.* 21, 351-357.

## MS14-P13 | PERIODIC TREND OF STEREOCHEMICAL ACTIVITY OF LONE ELECTRON PAIRS

Murshed, M. Mangir (Universität Bremen, Institut für Anorganische Chemie und Kristallographie, FB Biologie/Chemie, Bremen, GER); Gesing, Thorsten M. (Universität Bremen, Institut für Anorganische Chemie und Kristallographie, FB Biologie/Chemie, Bremen, GER)

In a series of papers, Wang and Liebau [1-3] pointed out that the bond valence sum calculated for a lone electron pair (LEP) cation increases as the cation's coordination environment becomes more distorted. They proposed to associate the geometric distortion of the LEP-coordination as the measures of the stereochemical activity of the LEP using the term eccentricity which we later coined as Wang-Liebau eccentricity (WLE) parameter [4]. Most of the polyhedral distortion indices [5-9] are purely geometric and cannot account for the interaction strength between the atoms. In contrast, the WLE parameter describes the weighted bond length with an exponential function, allowing the strength of a bond to exponentially decrease with increasing bond length. Sampling on crystal information data of As-, Se-, Sn-, Sb-, Te-, Tl-, Pb- and Bi-oxide coordination, a statistical approach demonstrates that the WLE parameter of the LEP-cations follows a periodic trend.

- [1] X. Wang, F. Liebau, *Z. Krist.* 211 (1996) 437.
- [2] X. Wang, F. Liebau, *Acta Crystallogr. B* 63 (2007) 216.
- [3] F. Liebau, X. Wang, W. Liebau, *Chem. - A Eur. J.* 15 (2009) 2728.
- [4] M. Curti, T.M. Gesing, M.M. Murshed et al., *Z. Krist.* 288 (2013) 629.
- [5] K. Robinson, G. V. Gibbs, P.H. Ribbe, *Science* (80-. ). 172 (1971) 567.
- [6] J.M. Gaithe, *Phys. Chem. Miner.* 6 (1980) 9.
- [7] W.A. Dollase, *Acta Crystallogr. A* 30 (1974) 513.
- [8] E. Makovicky, T. Balić-Žunić, *Acta Crystallogr. Sect. B Struct. Sci.* 54 (1998) 766.
- [9] P.S. Halasyamani, *Chem. Mater.* 16 (2004) 3586.

## MS14-P14 | POWDER DIFFRACTION EXPERIMENTS ON A SINGLE CRYSTAL DIFFRACTION INSTRUMENT - HOW FAR CAN WE PUSH THIS?

Stuerzer, Tobias (Bruker AXS GmbH, Karlsruhe, GER); Adam, Martin (Bruker AXS GmbH, Karlsruhe, GER); Smith, Vernon (Bruker AXS GmbH, Karlsruhe, GER); Ott, Holger (Bruker AXS GmbH, Karlsruhe, GER)

Modern single crystal X-ray diffraction (SC-XRD) allows – often within minutes – the reliable structure determination from one small single crystal. Complementing SC-XRD, powder X-ray diffraction (P-XRD) is typically used on bulk material for qualitative and quantitative phase analysis, texture investigations and structure refinement.

Advances in X-ray diffraction technology are pushing the limits of what information can be extracted from more complicated samples. This development seems to go hand-in-hand with researchers working on tiny, poorly crystalized, samples which often are multiply twinned or intergrown. Many of these compounds are hardly suitable for conventional SC-XRD and only accessible with investing unreasonable amounts of time. For some of these cases P-XRD may help but often not enough sample material is available, a dedicated instrument is not accessible or the researcher is no familiar with the respective hard- and software.

We will present results from a number of experiments where we compare data obtained with typical P-XRD and SC-XRD systems. With a focus on phase identification, quick quantitative analysis and texture investigations we will discuss the impact of wavelength, beam and detector properties, particularly for tiny samples. We will also discuss whether a standard SC-XRD system can outperform a dedicated P-XRD setup. We hope to answer the question: “how far we can we push P-XRD on a SC-XRD instrument?”

## MS14-P15 | CRYSTAL STRUCTURE AND THERMODYNAMIC BEHAVIOR OF $\text{Bi}_6\text{Te}_2\text{O}_{15}$ : THE LIKELY STRUCTURE OF THE RARE MINERAL PINGGUILITE

Nenert, Gwilherm (Malvern Panalytical B. V., Almelo); Prugovecki, Stjepan (Malvern Panalytical B. V., Almelo); Lian, Hong (Zernike Institute for Advanced Materials, University of Groningen, Groningen); Blake, Graeme (Zernike Institute for Advanced Materials, University of Groningen, Groningen)

Pingguitite is a rare mineral reported for the first time in 1994 [1]. However, its crystal structure was not reported, only cell parameters and the existence of a phase transition around 800°C [1, 2].

With this contribution, we aim to shed some new light onto this rare mineral by investigating in details the structural properties at room temperature and as function of temperature coupled to detailed TGA/DSC experiment.

We synthesized  $\text{Bi}_6\text{Te}_2\text{O}_{15}$  using a solid state reaction according to the literature [3]. We were able to solve its crystal structure using powder diffraction. The system crystallizes in the space group Pnma with  $a = 10.61156(7)$  Å,  $b = 22.7446(2)$  Å and  $c = 5.39906(4)$  Å in good agreement with the initial report on pingguitite [1]. In addition, we confirm the existence of a phase transition from  $\text{Bi}_6\text{Te}_2\text{O}_{15}$  to the cubic phase  $\text{Bi}_6\text{Te}_2\text{O}_{13}$  around 840°C.

We investigated the crystal structure of synthetic pingguitite as function of temperature and were able to solve its crystal structure and demonstrate the existence of the reduction of  $\text{Te}^{+VI}$  to  $\text{Te}^{+IV}$  around 840°C giving rise to the cubic phase  $\text{Bi}_6\text{Te}_2\text{O}_{13}$  at high temperature.

[1] Sun Zhifu, et al. (1994) Pingguitite; a new bismuth tellurite mineral. *Acta Mineralogica Sinica*, 14(4), 315–321

[2] John L. Jambor, et al., *American Mineralogist*, Volume 81, pages 766-770, 1996

[3] Hiroshi Sakai, et al., *Hyperfine Interactions* 90 (1994), pp 401-405

## MS14-P16 | ISOTOPE EFFECTS IN RECOVERED HIGH-PRESSURE PHASES OF ICE.

Fortes, Dominic (ISIS neutron spallation facility, Chilton, GBR); Howard, Christopher (University College London, London, GBR); Baron, Geoffrey (University College London, London, GBR); Wood, Ian (University College London, London, GBR)

Water ice is one of the most fundamental molecular solids and one of the most abundant minerals in the cosmos. In addition to being less dense than its own liquid, the ambient-pressure polymorph of ice (ice *Ih*) exhibits two other atypical properties: firstly, negative volume thermal expansion below 60 K; secondly, an anomalous volume difference due to isotopic substitution (i.e., the molar volume of D<sub>2</sub>O is larger than H<sub>2</sub>O).

Here we report some new results for the high-pressure forms of ice. We have prepared samples of both H<sub>2</sub>O and D<sub>2</sub>O in the ice II, ice III / IX and ice VI structures and recovered them to ambient pressure under liquid nitrogen. The specimens were mixed with a silicon standard and high-precision lattice parameters were measured between 10-150 K at ambient pressure using HRPD, one of the highest resolution neutron powder diffraction instruments in the world.

We determined that the volume isotope effect is normal in ices II, III / IX and VI, although this fact hides some interesting subtleties. Notably, the isotope effect in ice III / IX is normal along the *c*-axis and anomalous along the *a*-axis. This is noteworthy because the *a*-axis of ice III / IX exhibits negative linear expansion below ~ 40 K. Thus it seems, on the basis of only a few examples, that there may be a relationship between anomalous isotope effects and negative expansivity that remains to be explored further.

## MS14-P17 | PREPARATION, SPECTRAL, STRUCTURAL, HIRSHFELD SURFACE AND MOLECULAR DOCKING OF TETRAKIS(PYRIDINE- $\kappa$ N)BIS(THIOCYANATO- $\kappa$ N) COBALT(II) COMPLEX

El Hamdani, Hicham (student, Meknes, MAR); EL Amane, Mohamed (Moulay Ismail University, School of sciences, Meknes, MAR); Duhayon, Carine (bCNRS, LCC (Laboratoire de Chimie de Coordination), 205, route de Narbonne, F-31077 Toulouse, Meknes, FRA)

The structure of the title complex,  $[\text{Co}(\text{NCS})_2(\text{C}_5\text{H}_5\text{N})_4]$  was synthesized, studied by FTIR, UV-visible and single crystal X-ray diffraction analysis. The asymmetric unit of compound, consists of one cobalt(II) cation, one thiocyanate anions and two pyridine ligands. In the structure of cobalt complex, the cobalt(II) cations are octahedrally coordinated by two terminal N-bonding thiocyanate anions and by the N atoms of four pyridine ligands, resulting in discrete and slightly distorted octahedral complex. The complexes are linked into a three-dimensional network via intramolecular hydrogen bonds Interactions C-H $\cdots$ S, C-H $\cdots$ C, and  $\pi$ - $\pi$  stacking interactions [centroid-centroid distances = 3.753 Å] between pyridine ring systems. The different intermolecular interactions studied through Hirshfeld surface analysis enables contributions to the crystal packing of the cobalt complex to be quantified. The schemes 2D and 3D, associated with the Hirshfeld surface clearly display each significant interaction involved in the structure, by quantifying them in an effective visual manner. The molecular docking studies were also performed against various cancer target proteins 4FLH (colon cancer), 1SVC (pancreatic cancer), 1MOX (lung cancer) and 2DSQ (breast epithelial cancer). The complex showed good molecular interactions with all the receptors.

## MS14-P18 | CRYSTAL STRUCTURES OF THE FIRST POLYMERIC Cu(II) COMPLEXES WITH THIOSEMICARBAZONE METHYL PYRUVATE

Radanovic, Mirjana (University of Novi Sad, Faculty of Sciences, Novi Sad); Rodic, Marko (University of Novi Sad, Faculty of Sciences, Novi Sad); Miškov-Pajic, Vukoslava (University of Stuttgart, Stuttgart, GER); Vojinovic-Ješić, Ljiljana (University of Novi Sad, Faculty of Sciences, Novi Sad); Belošević, Svetlana (University of Priština, Faculty of Technical Sciences, Kosovska Mitrovica); Leovac, Vukadin (University of Novi Sad, Faculty of Sciences, Novi Sad)

Thiosemicarbazones and their metal complexes are in the focus of many researchers due to easy complexation with d- and p-metals, but also wide spectrum of biological activities. Among them, pyruvic acid thiosemicarbazone ( $H_2pt$ ) stands out. A large number of metal complexes with this ligand are characterized and tridentate and tetradentate modes of coordination are found.

The synthesis and crystal structure of two polymeric complexes of Cu(II) of the general formula  $[Cu(\mu-Hpt)H_2O]X$  ( $X = NO_3^-$  (1),  $ClO_4^-$  (2)) are described. Complex 1 is obtained in the reaction of ethanolic solution of  $Cu(NO_3)_2 \cdot 3H_2O$  and  $H_2pt$ , while the reaction of acetone solution of  $Cu(ClO_4)_2$  and methyl pyruvate thiosemicarbazone yielded in formation of complex 2.

Molecular structures of the complexes 1 and 2 consist of polymeric monocation  $[Cu(\mu-Hpt)H_2O]^+$  and  $NO_3^-$  or  $ClO_4^-$  anion. In both complexes copper(II) is situated in ideal square-pyramidal surroundings ( $\tau=0.00$ ). Basal plane is defined by sulphur atom S1, azomethine nitrogen N1 and carboxylate oxygen O1 from the same asymmetric unit, while the fourth coordination place is occupied by bridging carboxylate oxygen of the neighbouring asymmetric unit. The apical position is occupied by the oxygen atom of the coordinated water molecule. In both complexes, the ligand is coordinated in monoanionic form.

## MS14-P19 | SYNTHESIS, SPECTROSCOPIC PROPERTIES, CRYSTAL STRUCTURE, ANTIMICROBIAL PROPERTIES AND MOLECULAR DOCKING STUDIES OF THE COMPLEX (1)

### $3(\text{C}_{36}\text{H}_{24}\text{MnN}_6) \cdot 6(\text{PF}_6) \cdot 0.5\text{H}_2\text{O}$

El Hamdani, Hicham (Meknes, MAR); EL Hamdani, Mohamed (Université Moulay, Ismail, faculté des sciences, Meknes, MAR); Duhayon, Carine (bcNRS, LCC (Laboratoire de Chimie de Coordination), 205, route de Narbonne, F-31077 Toulouse, Toulouse, FRA)

The complex (1) of general formula  $3(\text{C}_{36}\text{H}_{24}\text{MnN}_6) \cdot 6(\text{F}_6\text{P}) \cdot 0.5\text{H}_2\text{O}$  was prepared and characterized by IR, UV-visible spectroscopy and single crystal X-ray structure analysis. The complex (1) is crystallized in the monoclinic system ( $z = 2$ ) with space group of  $P 2_1/c$ , the unit cell parameters are  $a = 15.1490(3) \text{ \AA}$ ,  $b = 15.2154(2) \text{ \AA}$ ,  $c = 23.1114(3) \text{ \AA}$ ,  $b = 90.5152[1]$ , and  $V = 5326.92 \text{ \AA}^3$ . The asymmetric unit contains one and a half Manganese (II) complex (2)  $[\text{Mn}(\text{II})(\text{C}_{12}\text{H}_8\text{N}_2)_3]^{2+}$ ; one of the cations having crystallographic twofold rotational symmetry. Each Mn (II) is pseudo-octahedrally coordinated by three 1,10-phenanthroline molecules with Mn-N distances included between 1.96 and 1.99  $\text{ \AA}$ . Besides, the intermolecular hydrogen bonds: C-H/F, C-H/O and  $\pi$ - $\pi$  interactions are together playing a vital role in the stabilization of the crystal packing. In addition, the antibacterial activity of the complex (1) was evaluated against some bacterial species: *Escherichia coli*, *Staphylococcus aureus*, *Klebsiella pneumoniae*, *Bacillus Spp*, *Serratia marcescens*, *Acinetobacter Bounannue*, *Staphylococcus saprophiticus*; and the antifungal activity against: *Aspergillus niger*, *Aspergillus spp*, *Aspergillus nidulans* and *Candida albicans*. Finally, the 1,10-phenanthroline was docked against various target proteins from diverse bacterial species 1E15 (*S. marcescens*), 3BU2 (*S. saprophiticus*), 3GFX (*Klipsila pnumani*), 1BY3 (*E. coli*) and 5IDV (*acinetobacter baumannii*) to confirm those obtained results from antibacterial activity. In short, the results of synthesized complex (1) can be exploited in medical field.

## MS14-P20 | MODULAR STRUCTURES OF LAYERED URANYL MINERALS AND SYNTHETIC COMPOUNDS

Nazarchuk, Evgeny (Saint-Petersburg State University, Saint-Petersburg, RUS)

There are many ways to describe topology of polyhedral complexes in the structures of uranyl compounds, one of them is a modular approach. The  $[(\text{UO}_2)(\text{T}^{6+}\text{O}_4)(\text{H}_2\text{O})_n]^0$  ( $\text{T} = \text{Cr}^{6+}, \text{S}^{6+}, \text{Se}^{6+}, \text{n} = 0-2$ ) chains are the building block for a numbers of layers. Uranium compounds obtained from aqueous solutions often inherit fundamental building blocks. The layers in the structures of uranyl selenates can be obtained by the self-assembly of the  $[(\text{UO}_2)_2(\text{SeO}_4)_4(\text{H}_2\text{O})_4]^{4-}$  complexes. This approach will be generalized for all layered uranyl compounds with  $\text{TO}_4$  ( $\text{S}^{6+}, \text{Se}^{6+}, \text{Cr}^{6+}, \text{Mo}^{6+}, \text{P}^{6+}, \text{As}^{6+}$ ) tetrahedra in this contribution.

Tetramers  $[(\text{UO}_2)_2(\text{TO}_4)_4(\phi)_4]^{4-}$  ( $\phi = \text{O}, \text{H}_2\text{O}, \text{F}, \text{Cl}, \text{OH}$ ) in uranyl compounds are binding by free vertexes of  $\text{TO}_4$  tetrahedra to form three types of fundamental chains. Chains connected by vertex of uranium and  $\text{TO}_4$  polyhedral form layers with different  $\text{UO}_2:\text{TO}_4 = 1:2, 2:3, 3:5, 4:7, 5:8$  ratios. Thus, the layers are modular units built from separate chains.

This work was financially supported by the Russian Science Foundation through the grant 16-17-10085 and internal travel grant of SPbSU.

## MS14-P21 | INVERSE CRYSTAL STRUCTURE BEHAVIOUR OF $\text{Ca}_3\text{Al}_4\text{ZnO}_{10}$ AT HIGH PRESSURE AND HIGH TEMPERATURE

Hejny, Clivia (Universität Innsbruck, Innsbruck, AUT); Kahlenberg, Volker (Universität Innsbruck, Innsbruck, AUT); Krüger, Hannes (Universität Innsbruck, Innsbruck, AUT)

$\text{Ca}_3\text{Al}_4\text{ZnO}_{10}$  was initially found in an investigation on the incorporation of ZnO into Portland cement clinker phases [1]. In contrast to a previous description of the structure in space group  $Pbc2_1$  [2]  $\text{Ca}_3\text{Al}_4\text{ZnO}_{10}$  was found to be isotopic with  $\text{Ca}_3\text{Al}_4\text{MgO}_{10}$  [3].  $\text{Ca}_3\text{Al}_4\text{ZnO}_{10}$ ,  $a = 5.1364(3)$ ,  $b = 16.7403(9)$ ,  $c = 10.7019(6)$  Å,  $V = 920.20(8)$  Å<sup>3</sup>,  $Z = 4$ , crystallizes in  $Pbcm$ . Crystals were obtained in a crystal growth experiment and studied in-situ between ambient pressure and 6.8(1) GPa as well as 25(2)-797(2) °C. Lattice parameters change continuously in the examined P-T-range, thus allowing computation of a second-order Birch-Murnaghan equation-of-state. The structure represents a three-dimensional network of corner-sharing  $[\text{AlO}_4]$ - and  $[\text{ZnO}_4]$ -tetrahedra with Ca ions in six- and eightfold coordination. Analysis of the pressure- and temperature-induced response of the structure shows an inverse relationship of all observed mechanism contributing to overall structural changes. To give an example: The only Ca-O bond distance increasing with increasing pressure, i.e. Ca2-O3, is found to decrease with increasing temperature.

[1] H. Bolio-Arceo, F.P. Glasser; *Adv. Cem. Res.* **1998**, *10*, 25–32.

[2] V.D. Barbanyagre, T.I. Timoshenko, A.M. Ilyinets, V.M. Shamshurov; *Powder Diffr.*, **1997**, *12*, 22–26.

[3] V. Kahlenberg, R. Albrecht, D. Schmidmair, H. Krüger, B. Krüger, M. Tribus, A. Pauluhn; *J. Am. Ceram Soc.* **2019**, *102*, 2084-2093.

## MS14-P22 | SYNTHESIS AND CRYSTAL STRUCTURE OF NEW ALKALI CHALCOGENIDO MANGANATES/INDATES

Langenmaier, Michael (Albert-Ludwigs-Universität Freiburg, Freiburg, GER)

In the system A-Fe-Q mixed-valent alkali chalcogenido ferrates are well known [1-3]. Recently we mimiced an equivalent mixed-valent state for Mn, by a partially replacement of Mn(II) by In(III) [4]. Now we present newly obtained metalates  $\text{Na}_{12}\text{MnIn}_2\text{Q}_{10}$  (Q=S, Se) (1,2) as well as so far unknown indates  $\text{K}_6\text{In}_2\text{S}_6$  (3) and  $\text{K}_6\text{InS}_{4.5}$  (4). In all these compounds there are  $[\text{MQ}_4]$  tetrahedra, either isolated or connected via edges.

The compounds were obtained by heating stoichiometric mixtures of the elements or binary phases at  $T_{\text{max}}=1200\text{K}$ . All structures were determined by means of X-ray single crystal diffraction.

The compounds 1 & 2 crystallize in the space group  $P2_1/m$  and contain isolated  $[\text{InQ}_4]^{5-}$  tetrahedra as well as  $[\text{M}_2\text{Q}_6]^{7-}$  dimers with  $M=\text{Mn}$  and In.

$\text{K}_6\text{In}_2\text{S}_6$  crystallizes in  $P2_1/c$ . Though not isotypic, it shows similarities to  $\text{K}_6\text{Fe}_2\text{S}_6$  [5] with its  $[\text{In}_2\text{S}_6]^{6-}$  dimers of edge-sharing tetrahedra.

$\text{K}_6\text{InS}_{4.5}$  crystallizes in  $P6_3mc$  and is almost isotypic to  $\text{K}_6\text{MnS}_4$  [6]. The only difference is an additional S position, which is only partially occupied.

[1] P. Stüble, S. Peschke, D. Johrendt, C. Röhr, *J. Solid State Chem.*, **258**, 416, (2018).

[2] P. Stüble, A. Berroth, C. Röhr, *Z. Naturforsch. B*, **71**, 485, (2016).

[3] K. O. Klepp, H. Boller, *Monatsh. Chem.*, **112**, 83, (1981).

[4] M. Langenmaier, J. Brantl, C. Röhr, *Z. Kristallogr. Suppl.*, **39**, 68 (2019).

[5] M. Schwarz, M. Haas, C Röhr, *Z. anorg. allg. Chem.*, **639**, 360 (2013).

[6] W. Bronger, H. Balk-Hardtdegen, *Z. Anorg. Allg. Chem.*, **574**, 89 (1989).

## MS14-P23 | STRUCTURAL ORDERING IN THE PYRITE-RELATED PHASES: PtSnS, PtSnSe AND PtSnTe

Laufek, Frantisek (Czech Geological Survey, Prague, CZE); Vymazalová, Anna (Czech Geological Survey, Prague, CZE)

The ternary PtSnX (X= S, Se or Te) phases were prepared and their crystal structures were characterized using powder X-ray diffraction. The ternary compounds were synthesized from elements by solid state reactions using silica glass tube technique at 600°C. From earlier investigations it is known that the crystal structures of the title phases can be derived from the pyrite structure type (FeS<sub>2</sub>) by replacing of S-S the dumbbells by Sn-X heteroatomic anion pairs. Weihrich et al. (2004) suggested three ordering variants of these phases according to the relative orientation of Sn-X dumbbells: the cubic ulmannite type (*P2<sub>1</sub>3*), the orthorhombic cobaltite type (*Pca2<sub>1</sub>*) and the trigonal type (*R3*). Based on the DFT studies of Weihrich et al. (2004), PtSnSe and PtSnTe crystalizes in the cobaltite structure type, whereas the PtSnS prefers the trigonal one. A careful Rietveld analysis of powder X-ray diffraction patterns was performed in order to reveal the preferred structure type. The superstructure reflections indicating the structural ordering and apparent peak splitting in the diffraction patterns clearly indicated the cobaltite structure type for all prepared PtSnX phases. The cubic and trigonal structure models cannot fit satisfactorily the measured diffraction data. The crystal structure of title phases is based on a three-dimensional framework of corner-sharing distorted [PtSn<sub>3</sub>X<sub>3</sub>] octahedra. The Sn-X bond distances range from 2.497(5) Å (in PtSnS) to 2.842(2) Å (in PtSnTe).

[1] Weihrich, R. et al. (2004). J. Solid. State Chem. 177, 2591.

## MS14-P24 | PSEUDO-SYMMETRY AND ORDER-DISORDER TRANSITIONS IN METAL HYDRIDES

Kohlmann, Holger (Leipzig University, Leipzig, GER)

Pseudo-symmetry is a well-known phenomenon in inorganic compounds and very common in metal hydrides for various reasons. Metallic hydrides typically exhibit non-stoichiometry by partial occupation of crystallographic sites by hydrogen. Ordered low-temperature modifications often show pronounced pseudo-symmetry, e. g. monoclinic or triclinic pseudo-cubic Laves phase hydrides. In complex hydrides, order-disorder transitions may arise due to rotational degrees of freedom in groups such as  $\text{BH}_4$  ( $\text{NaBH}_4$ ),  $\text{SiH}_3$  ( $\text{KSiH}_3$ ) or  $\text{NiH}_4$  ( $\text{Mg}_2\text{NiH}_4$ ). Sometimes, only an ordered arrangement is found showing pseudo-symmetry of a hypothetical disordered polymorph, e. g.  $\text{IrH}_4$  and  $\text{IrH}_5$  groups in monoclinic pseudo-hexagonal  $\text{Mg}_6\text{Ir}_2\text{H}_{11}$ . Directional (covalent) bonds are yet another reason for developing pseudo-symmetry. Zintl phases are a good example, since upon formation of Si-H and Si-Si bonds in  $\text{CaSiH}_{1.33}$  and  $\text{SrSiH}_{1.67}$ , a superstructure of the parent hydrogen free phase occurs. Even in mainly ionic compounds like  $\text{Eu}_6\text{Mg}_7\text{H}_{26}$  the more covalent nature of metal-hydrogen bonds introduces pseudo-symmetry as compared to more ionic fluorides and chlorides. Pseudo-symmetry in metal hydrides may thus occur for many different reasons. Resulting crystallographic pitfalls will be discussed on examples and advice given for dealing with such problems in structure solution and refinement.

## MS14-P25 | A NEW POLYMORPH OF TRISODIUM HEXACHLORORHODATE

Etter, Martin (Deutsches Elektronen-Synchrotron, Hamburg, GER)

Several trisodium hexachlorometalates ( $\text{Na}_3\text{MCl}_6$  with e.g.  $\text{M} = \text{Ir}, \text{Rh}$ ) are highly hygroscopic and often exhibit simultaneously multiple hydrated phases at ambient conditions. In order to determine the different crystal structures of these hydrated compounds, *in situ* powder X-ray diffraction experiments are performed, where the temperature is slowly increased and the evaporation of water leads to less hydrated compounds with lower water content until finally the anhydrous phase is formed. Usually, during this process the different hydrated phases become separated, which makes it easier to distinguish them and to start crystal structure solution attempts.

However, after performing a couple of *in situ* powder X-ray diffraction measurements on  $\text{Na}_3\text{RhCl}_6$  and  $\text{Na}_3\text{IrCl}_6$  it became clear, that also at elevated temperatures mixtures of hydrated phases are always present until the anhydrous compound is formed. Therefore, only the crystal structures of the anhydrous phases of  $\text{Na}_3\text{RhCl}_6$  and  $\text{Na}_3\text{IrCl}_6$  have been determined so far.

Intriguingly, in some of the heating experiments on  $\text{Na}_3\text{RhCl}_6$  a second phase coexisted at elevated temperatures together with the anhydrous phase until it was transformed fully into the known anhydrous  $\text{Na}_3\text{RhCl}_6$  compound. This phase was determined to be a polymorph of  $\text{Na}_3\text{RhCl}_6$  which surprisingly possesses the same space group as the stable anhydrous  $\text{Na}_3\text{RhCl}_6$  phase, although lattice parameters and motif are different.

In this presentation structural details of the dehydrated  $\text{Na}_3\text{RhCl}_6$  polymorph will be given as well as an overview to the so far performed *in situ* powder X-ray diffraction experiments on the hydrated phases.

## MS14-P26 | RARE-EARTH PNICTIDE CHALCOGENIDES REBiTe AND RESbS (RE = La-Nd): STRUCTURE DETERMINATION BY COMBINATION OF TRANSMISSION ELECTRON MICROSCOPY AND MICROFOCUSSED SYNCHROTRON RADIATION

Lindemann, Tobias (Universität Leipzig, Leipzig, GER); Wright, Dr. Jonathan P. (European Synchrotron Radiation Facility, Grenoble, FRA); Benndorf, Dr. Christopher (Universität Leipzig, Leipzig, GER)

Searching for compounds such as LaSbTe [1], which form charge density waves (CDW), investigations of rare-earth (RE) pnictide chalcogenides yielded a new series of compounds REBiTe with layered crystal structures. These can be described as an alternating stacking of 2D extended [Bi]<sup>-</sup> and [RETe]<sup>+</sup> sheets with predominantly ionic interaction between them. In the microcrystalline products, suitable crystallites for data collection using microfocussed synchrotron radiation (beamline ID11, ESRF) were selected using TEM imaging, EDX and electron diffraction [2]. The compounds crystallize with a monoclinic distortion variant of the PbFCl-type structure characterised by small distortions within the square-like arrangement of Bi atoms. Investigation of electrical transport properties showed differences, most remarkable for CeBiTe, which is a semiconductor between 5 and 300 K, in contrast to NdBiTe, which exhibits a metal to semiconductor transition at 150 K. Further investigations of pnictide chalcogenides lead to the discovery of isotopic compounds RESbS. Synthesis was carried out by cold-pressing mixtures of the elements with the ideal atomic ratio to pellets and heating them to 1223 K in evacuated silica tubes for 5-7 d. The phase-pure samples appeared as dark greyish polycrystalline substances with slight metallic lustre.

[1] E. DiMasi, B. J. Foran, M. C. Aronson, S. Lee, *Phys. Rev. B* **1996**, *54*, 13587-13596.

[2] F. Fahrnbauer, T. Rosenthal, T. Schmutzler, G. Wagner, G. B. M. Vaughan, J. P. Wright, O. Oeckler, *Angew. Chem.* **2015**, *127*, 10158-10161.

## MS14-P27 | DOPED SINGLE CRYSTAL TiO<sub>2</sub> SERIES PRODUCTS BY MOLTEN SALT METHOD USED AS PHOTOCATALYTIC MATERIALS

Zhao, Zengying (China University of Geosciences, Beijing, Beijing, CHN)

Doped single crystal TiO<sub>2</sub> (DSCT) is a promising material among the various photocatalytic catalysts. Series of DSCT, such as N doped, N, F doped, and N, B doped DSCT, have been prepared by molten salt method (MSM) using mixed nitrates, like NaNO<sub>3</sub> and KNO<sub>3</sub>. The mixed nitrates can not only be used as a morphology modifier to form a single-crystal-like structure of TiO<sub>2</sub> in the sample, but also can be used as a synergistic doping agent. As a result, the doping nitrogen content in the DSCT samples can be improved and adjusted easily because of the adding of the mixed nitrates in the calcination process of the MSM method, when compared with using urea as a single nitrogen doping source. The as prepared DSCT materials, such as N-TiO<sub>2</sub>, N, F-TiO<sub>2</sub>, N, B-TiO<sub>2</sub>, etc., all have an enhanced photocatalytic activity compared with the samples without the molten salt process.

[1] Hamukwaya L., Zengying Zhao\*, Enhanced Photocatalytic Activity of B, N-Codoped TiO<sub>2</sub> by a New Molten Nitrate Process, *J. Nanosci. Nanotech.*, 2019, 19(2): 839-849.

[2] Zengying Zhao\*, Molten-salt fabrication of (N,F)-codoped single-crystal-like titania with high exposure of (001) crystal facet for highly efficient degradation of methylene blue under visible light irradiation, *J. Mater. Res.*, 2018, 33(10): 1411-1421.

[3] Chenxi Li, Zengying Zhao\*, Enhanced visible photocatalytic activity of nitrogen doped singlecrystal-like TiO<sub>2</sub> by synergistic treatment with urea and mixed nitrates. *J. Mater. Res.*, 2017, (32): 737-747.

## MS14-P28 | NEW CUBIC BORATE $\text{Yb}_3[\text{BO}_3](\text{OH})_6 \cdot 2.1\text{H}_2\text{O}$ WITH “ANTIZEOLITE”

### FRAMEWORK AND ISOLATED $\text{BO}_3$ -TRIANGLES IN CAVITIES

Topnikova, Anastasiia; Eremina, Tatiana (Lomonosov Moscow State University, Moscow, RUS); Belokoneva, Elena (Lomonosov Moscow State University, Moscow, RUS); Dimitrova, Olga (Lomonosov Moscow State University, Moscow, RUS); Volkov, Anatoly (Lomonosov Moscow State University, Moscow, RUS)

Single crystals of new borate,  $\text{Yb}_3[\text{BO}_3](\text{OH})_6 \cdot 2.1\text{H}_2\text{O}$ , have been synthesized under hydrothermal conditions in multicomponent system at the temperature 280°C and pressure of 90-100 atm. Symmetry of new structure corresponds to quite rare cubic space group  $I432$ . Anionic radical is presented by isolated  $\text{BO}_3$ -triangles of 32 symmetry and the borate belongs to monoborates. Yb-atom have high coordination number equal to 8 and forms polyhedra with typical for rare earth elements pentagonal caps. They are condensing into cationic framework via common apexes and edges forming channels parallel to coordinate axes  $a$ ,  $b$ ,  $c$  and 3-fold axis. Water molecules and hydroxyl groups fill large channels along crystallographic axes. New borate have structural similarity with tetragonal  $\text{ABa}_{12}(\text{BO}_3)_7\text{F}_4$ ,  $A = (\text{Li}, \text{Na})$ ,  $I4/mcm$  [1] and iso-structural  $\text{Li}_x\text{Na}_{1-x}\text{Ba}_{12}(\text{BO}_3)_7\text{F}_4$ ,  $P4_2bc$  [2]. All structures have cationic “antizeolite” framework [2] filled by anionic cluster including  $\text{BO}_3$ -triangles and principally differ from traditional zeolite, in which anions form anionic framework filled by cations.

The reported study was funded by RFBR according to the research project № 18-35-00645.

[1] Zhao J., Li R.K. (2014) Inorg. Chem., 53, 2501-2505.

[2] Bekker T.B., Rashchenko S.V., Solntsev V.P. et al. (2017). Inorg. Chem., 56, 5411-5419.

## MS14-P29 | EVIDENCE OF ANATASE INTERGROWTHS FORMED DURING SLOW COOLING OF REDUCED ILMENITE

D'Angelo, Anita (Australian Synchrotron (ANSTO), Clayton, AUS); Webster, Nathan (CSIRO, Clayton, AUS)

Worldwide, ilmenite ( $\text{FeTiO}_3$ ) is industrially important as it is the main source of titanium dioxide,  $\text{TiO}_2$ , which has applications in sunscreens, as pigments and in photocatalysis. Controlling the parameters during synthetic rutile production is essential to minimise production costs and ensure final product quality. To improve the properties of the final product and economics upgrading, the synthetic rutile industry simulates reactions that occur in the rotary kiln within pots. In this work, unusual and distinct changes were observed between the powder X-ray diffraction (PXRD) patterns of RIs produced after rapid and slow cooling from small and large pots, respectively. The PXRD pattern of the slow-cooled RI showed the  $M_3O_5$  peak at  $20.6^\circ$  (002)  $2\theta$  was not apparent, and the peaks at  $37.9^\circ$  (203) and  $38.3^\circ$  (203), and  $47.9^\circ$  (204) and  $48.4^\circ$  (402)  $2\theta$  had significantly decreased in intensity. Using transmission electron microscopy (TEM), selected area electron diffraction (SAED) and pair distribution function (PDF) analysis, we attribute these features to  $M_3O_5$ -anatase intergrowth formation, which causes a loss in long-range order along the  $M_3O_5$   $c$ -axis. Overall, these results demonstrate the importance of cooling rate during the formation of these materials, and may be used to guide process developments within the industry.

## MS14-P30 | INSIGHT INTO THE CRYSTALLIZATION AND STRUCTURAL FEATURES OF CAESIUM-BEARING CHAIN-TYPE BOROPHOSPHATES

Shvanskaya, Larisa (M.V. Lomonosov Moscow State University, Moscow, RUS); Yakubovich, Olga (M.V. Lomonosov Moscow State University, Moscow, RUS); Krikunova, Polina (M.V. Lomonosov Moscow State University, Moscow, RUS)

Three borophosphates,  $\text{CsBP}_2\text{O}_6(\text{OH})_2$  (I),  $\text{CsMn}[\text{BP}_2\text{O}_8(\text{OH})]$  (II) and  $\text{Cs}_{0.54}\text{Mn}_{1.17}\text{BP}_2\text{O}_8(\text{H}_2\text{O})_{2.32}$  (III), were grown under hydrothermal conditions. Their crystal structures were solved using single crystal X-ray diffraction: (I)-monoclinic,  $I2/a$ ,  $a=14.5329(3)$  Å,  $b=7.4869(2)$  Å,  $c=13.4002(3)$  Å,  $\beta=90.059(2)^\circ$ ,  $V=1458.03(6)$  Å<sup>3</sup>,  $Z=8$ ; (II)-monoclinic,  $P2_1/c$ ,  $a=9.1446(2)$  Å,  $b=8.6946(1)$  Å,  $c=9.6361(2)$  Å,  $\beta=100.139(2)^\circ$ ,  $V=754.19(2)$  Å<sup>3</sup>,  $Z=4$ ; (III)-hexagonal,  $P6_122$ ,  $a=9.6292(3)$  Å,  $c=15.8051(3)$  Å,  $\beta=100.139(2)^\circ$ ,  $V=754.19(2)$  Å<sup>3</sup>,  $Z=6$ . The crystal architecture of (I) presents a unique structural type, whereas (II) and (III) are novel cesium-manganese representatives of known families. The structural features of (I)-(III) are infinite anionic chains with tB:tP ratio of 1:2 as main structural building blocks. The chains of (II) consist of alternating corner sharing tetrahedral  $\text{BO}_3(\text{OH})$  borate and  $\text{PO}_4$  phosphate groups with an additional branched phosphate tetrahedron. In the case of (I) and (III) the borate and phosphate tetrahedra share oxygen vertices to form four-ring chains with identical topology. These chains are extended along [010] direction in the crystal structure of (I) and are twisted along  $6_1$  axes in the structure of (III). The influence of different crystallization conditions on the structure formation of obtained cesium borophosphates will be discussed. The work was supported by the RFBR (№18-03-00908).

## MS14-P31 | CRYSTAL CHEMISTRY OF STRUVITE AND ITS DERIVATIVES

Kiriukhina, Galina (Lomonosov Moscow State University, Moscow, RUS); Yakubovich, Olga (Lomonosov Moscow State University, Moscow, RUS)

Single crystals of  $\text{CsMn}(\text{H}_2\text{O})_6(\text{PO}_4)$  were synthesized under medium-temperature hydrothermal conditions. The new compound was established to be the first Mn member and the second hexagonal modification in the struvite morphotropic series of phosphates and arsenates, with hydrogen bonding between the main structural units.

Crystal chemical analysis of the new phosphate in comparison with other members of the family revealed general features for the struvite morphotropic series,  $AM(\text{H}_2\text{O})_6(\text{XO}_4)$ , where  $A = \text{K}, \text{NH}_4, \text{Rb}, \text{H}_2\text{O}, \text{Cs},$  and  $\text{Tl}$ ,  $M = \text{Mn}, \text{Fe}, \text{Co}, \text{Ni},$  and  $\text{Mg}$ , and  $X = \text{P}, \text{As}$ . It has been shown that a regular increase of the unit-cell parameters of the arsenate members correlates to the larger size of  $\text{AsO}_4$  tetrahedra compared to the size of  $\text{PO}_4$  tetrahedra. The morphotropic transformation of orthorhombic structures for hexagonal and cubic ones is discussed to be caused by the size of the atoms in the  $A$  position. The tendency for growth of the  $c$  and reduction of the  $a$  unit-cell parameter of orthorhombic Mg members of the struvite family was shown to correlate with the ionic radius of the  $A$  atom ( $A = \text{K}, \text{NH}_4, \text{Tl}$  and  $\text{Rb}$ ).

The symmetry change from cubic in  $\text{CsMg}(\text{H}_2\text{O})_6(\text{PO}_4)$  to tetragonal in  $\text{Na}(\text{H}_2\text{O})\text{Mg}(\text{H}_2\text{O})_6(\text{PO}_4)$  was demonstrated to be caused by the ordering of Na atoms and water molecules in their surroundings. Crystal structure transformation from struvite-K,  $\text{KMg}(\text{H}_2\text{O})_6(\text{PO}_4)$ , to hazenite,  $\text{KNa}(\text{H}_2\text{O})_2\text{Mg}_2(\text{H}_2\text{O})_{12}(\text{PO}_4)_2$ , was discussed in order to explain the fourfold increase of the  $b$  axis in the case of hazenite.

## MS14-P32 | LAYER CHARGE INFLUENCE ON THE HYDRATION PROPERTIES OF SYNTHETIC NA-SATURATED SMECTITES

Vinci, Doriana (University of Bari, Bari, ITA)

Smectite hydration controls dynamical properties of interlayer cations and thus the fate and transport of water and pollutants. The influence of smectite crystal chemistry, and more especially of the amount and location of isomorphous substitutions, on smectite hydration has been largely documented over the last decade.[1] The influence of layer charge location, however, remains incompletely documented. The present study thus reports the influence of layer charge location on interlayer species organization by combining Powder X-Ray Diffraction (PXRD) profile modelling and Monte Carlo simulation in Grand Canonical ensemble. A set of octahedrally charged hectorites, with a common structural formula  $^{inter}[\text{Na}_x]^{oct}[\text{Mg}_{6.0-x}\text{Li}_x]^{tet}[\text{Si}_{8.0}]\text{O}_{20}(\text{OH})_4$  and a layer charge (x) varying from 0.8 to 1.6, was synthesized hydrothermally. Interlayer water contents were monitored as a function of relative humidity (RH) from H<sub>2</sub>O vapor (de)sorption isotherms. The evolution in proportions of both mono- and bi-hydrated layers was then determined from PXRD profile modeling as a function of RH. Then, Monte Carlo simulations were performed in the Grand Canonical ensemble to get additional details on the distribution of water molecules and charge-compensating cations within interlayers. Based on the comparison between octa- and tetrahedrally charged smectites [1] with contrasting layer charge, it is concluded that the evolution of layer-to-layer distance with the amount of layer charge differs for tetrahedrally and octahedrally charged smectites.

[1] Ferrage, E.; Lanson B.; Michot, L.J.; Robert J.L. (2010) Journal of Physical Chemistry C, 114: 4515-4526.

## MS14-P33 | CRYSTAL STRUCTURE AND BIOLOGICAL ACTIVITIES OF A NEW PROTON TRANSFER

### MATERIAL

HAMDI, NAJLAA (Faculty of Sciences University Sidi Mohamed Ben Abdelah, FES, MAR); CHAOUCH, Souad (USMBA, FEZ, MAR); IDBOUMLIK, Meryem (USMBA, FEZ, MAR); LACHKAR, Mohammed (USMBA, FEZ, MAR); EL BALI, Brahim (UMP, oujda, MAR)

A novel hybrid phosphite was synthesized using 1,4- diaminobutane (dabn) as structure-directing agent using slow evaporation method. Single crystal X-ray diffraction analysis shows that it crystallizes in the triclinic system (S.G: P-1). The crystal structure is built up from corner sharing  $[\text{CoO}_6]$  octahedrons running in a form of chain along [001], interconnected by  $\text{H}_2\text{PO}_3$  pseudo-pyramid units. The diprotonated organic molecule residing between the parallel chains, interacts with the inorganic moiety via hydrogen bonds leading thus to the formation of a three dimensional network. The biological tests exhibit significant activity against *C. albicans* and *E. coli* strains in all used concentrations while less activity was pronounced when tested against *S. epidermidis*, *S. cerevisiae* whilst there was no activity against the nematode model *S. feltiae*.

## MS14-P34 | HEXAGONAL BARIUMTITANATE STABILIZED AS ULTRA-THIN FILM ON Pt(111): AN X-RAY DIFFRACTION AND ELECTRON-ENERGY-LOSS SPECTROSCOPY STUDY

Meyerheim, Holger (MPI Halle, Halle an der Saale, GER); Mohseni, Katayoon (MPI Halle, Halle an der Saale, GER); Förster, Stefan (Martin-Luther-Universität Halle-Wittenberg, Halle an der Saale, GER); Zollner, Eva Maria (Martin-Luther-Universität Halle-Wittenberg, Halle an der Saale, GER); Schumann, Florian (Martin-Luther-Universität Halle-Wittenberg, Halle an der Saale, GER); Felici, Roberto (Consiglio Nazionale delle Ricerche - SPIN, Roma, ITA); Hergert, Wolfram (Martin-Luther-Universität Halle-Wittenberg, Halle an der Saale, GER); Widdra, Wolf (Martin-Luther-Universität Halle-Wittenberg, Halle an der Saale, GER)

Bariumtitanate ( $\text{BaTiO}_3$ ) is one of the most intensely studied oxides. Besides the perovskite- (PV) type phases, a high-temperature hexagonal (h) phase exists, which is stable above 1705 K. The h- type structure is distinctly different from the PV-type, as it contains  $\text{TiO}_6$  octahedra linked by common faces rather than by common corners. Many attempts have been made to stabilize h- $\text{BaTiO}_3$  at ambient conditions, but thus far only a mixture of PV- h- type (17%)  $\text{BaTiO}_3$  could be obtained in crystals of 140 nm in size [1].

We present an x-ray diffraction (XRD) and electron-energy loss spectroscopy (EELS) study in combination with theoretical simulations which shows that h- $\text{BaTiO}_3$  exists as a 7 nm thick film on Pt(111) deposited by radiofrequency magnetron sputtering. The film forms a (2x2) superstructure with respect to the Pt(111) surface unit cell. XRD experiments carried out at the ESRF in Grenoble indicate that the h- $\text{BaTiO}_3$  unit cell parameters are in-plane contracted by -3.04% and vertically expanded by +3.89% relative to the bulk parameters ( $a=b=5.724$  Å,  $c=13.965$  Å). Based on the fitting of the intensities of 14 symmetry independent reflections the formation of h- $\text{BaTiO}_3$  is unambiguously confirmed. Along the c-axis the film is disordered by the presence of two terminations of the h-  $\text{BaTiO}_3$  unit cell. In parallel, comparison of EELS spectra collected for PV-type  $\text{BaTiO}_3$  and for the film with simulations also confirm the h-  $\text{BaTiO}_3$  formation.

[1] M. Yashima, T. Hoshina, D. Ishimura et al., J. Appl. Phys. 98, 014313 (2005)

## MS14-P35 | THE CRYSTAL STRUCTURES OF NATURAL BARYUM BERYLLOPHOSPHATES

Hatert, Frederic (University of Liège, Liege, BEL); Dal Bo, Fabrice (University of Oslo, Oslo, NOR); Bruni, Yannick (University of Liège, Liege, BEL)

Three new Ba-bearing beryllorphosphates were recently described. Minjiangite,  $\text{BaBe}_2\text{P}_2\text{O}_8$ , occurs in the Nanping No. 31 pegmatite, China (space group  $P6/mmm$ ,  $a = 5.028(1)$ ,  $b = 7.466(1)$  Å). It shows a phyllophosphate structure consisting of double layers of tetrahedra, which contain both Be and P in a 1:1 ratio. Inside the layers,  $(\text{Be,P})\text{O}_4$  tetrahedra form six-membered rings by sharing corners. The Ba atoms are located in regular 12-coordinated polyhedra and connect two successive double layers. Wilancookite,  $(\text{Ba,K,Na})_8(\text{Ba,Li,[]})_6\text{Be}_{24}\text{P}_{24}\text{O}_{96}\cdot 32\text{H}_2\text{O}$ , occurs in the Lavra Ponte do Piauí pegmatite, Minas Gerais, Brazil. Its crystal structure ( $I23$ ,  $a = 13.5398(2)$  Å) is identical to those of pahasapaite and of synthetic zeolite RHO; the framework is based on corner-sharing  $\text{BeO}_4$  and  $\text{PO}_4$  tetrahedra forming a large cavity in which occur Ba atoms and water molecules. Three different types of rings are building the cavity: eight-, six-, and four-membered rings. A third new species was discovered in the Vilatte-Haute pegmatite, Limousin, France, with the ideal formula  $\text{BaCa}[\text{Be}_4\text{P}_4\text{O}_{16}]\cdot 6\text{H}_2\text{O}$ . This beryllorphosphate (space group  $P2_1/c$ ,  $a = 9.4958(4)$ ,  $b = 13.6758(4)$ ,  $c = 13.4696(4)$  Å,  $\beta = 90.398(3)^\circ$ ) shows a zeolite framework identical to that of phillipsite, based on corner-sharing  $\text{BeO}_4$  and  $\text{PO}_4$  tetrahedra forming inter-connected 4-membered and 8-membered rings. Large cages within this zeolite framework contain Ba, Ca and water molecules.

## MS14-P36 | THE CRYSTAL STRUCTURE OF KONINCKITE

Bruni, Yannick (University of Liège, Liege, BEL); Hatert, Frederic (University of Liège, Liege, BEL); Puccio, Stephane (University of Liege, Liege, BEL); Blondieau, Michel (University of Liège, Liege, BEL)

The name koninckite designates a phosphate mineral discovered in Richelle (Belgium) by G. Cesàro, who carefully examined the chemical composition and defined the formula  $\text{Fe}^{3+}(\text{PO}_4)\cdot 3\text{H}_2\text{O}$ . The mineral forms pale brownish spheroidal aggregates constituted by tiny needle-like crystals; due to this fibrous habit, the crystal structure was very difficult to solve from single-crystal X-ray diffraction data. Recently, the structure of koninckite from Kociha, Slovakia, was solved by using synchrotron powder X-ray diffraction data (space group  $P4_12_12$ ,  $a = 11.9800(5)$  and  $c = 14.618(1)$  Å); the H atoms were localized from DFT calculations. A re-investigation of samples from the type locality allowed us to find good quality isolated crystals of koninckite, which were used to obtain single-crystal X-ray diffraction data. The structure was solved in space group  $P4_12_12$  ( $a = 11.9852(2)$  and  $c = 14.6239(3)$  Å), to a  $R_1$  factor of 0.0375. The asymmetric unit contains 2 Fe, 2 P, 14 O and 12 H atoms; Fe atoms are coordinated by 4 O atoms and 2 water molecules, forming fairly regular octahedral sites. These octahedra are connected to tetrahedral  $\text{PO}_4$  sites by corner-sharing, and the resulting heteropolyhedral framework shows large channels running along the  $c$  axis. The channels contain two water molecules; according to their site multiplicities, the formula of the mineral is revised as  $\text{Fe}^{3+}(\text{PO}_4)\cdot 2.75\text{H}_2\text{O}$ . Hydrogen-bonding scheme of the structure is discussed in detail.

## MS14-P37 | CRYSTAL STRUCTURE OF $\text{CaBaFe}_4\text{O}_7$

Gutmann, Matthias (Rutherford Appleton Laboratory, Chilton Didcot, GBR)

Magnetic materials that transport information via magnetic excitations are promising candidates for spintronics applications. Such materials are often chemically complex and difficult to synthesise. Such materials should be ferro- or ferri-magnetic with a high Curie temperature and have a large charge gap to minimize particle-hole excitations along with long magnon lifetimes and mean-free paths. Swedenborgite,  $\text{CaBaFe}_4\text{O}_7$  has been identified as a possible new candidate being a ferrimagnet with a polar space group. It displays two magnetic transitions at 210K and 275K and a structural phase transition at around 350K to a hitherto unknown phase. The resulting crystal structure in the high-temperature phase has now been solved from X-ray and neutron single crystal diffraction at 400K and verified against high-resolution neutron powder diffraction data. Similar to the room-temperature phase in that it consists of alternating layers of triangular and Kagome Fe-O tetrahedra. The compound is found to retain its polar character in the high-temperature phase and shows a rather complex modulation of the Fe-O tetrahedra. A bond-valence analysis indicates mixed Fe<sup>+2</sup>/Fe<sup>+3</sup> [1].

[1] R. S. Perry, H. Kurebayashi, A. Gibbs, and M. J. Gutmann, *Phys. Rev. Materials* 2, 054403 (2018).

## MS14-P38 | PREPARATION, SPECTRAL, STRUCTURAL, THERMAL AND ANTICANCER

### MOLECULAR DOCKING STUDIES OF BIS-(THEOPHYLLINATO)-TETRAAQUOCOBLALT(II) COMPLEX

El Hamdani, Hicham (student, Meknes, MAR); EL Amane, Mohamed (Moulay Ismail University, School of sciences, Meknes, MAR); Duhayon, Carine (CNRS ; LCC (Laboratoire de Chimie de Coordination), toulouse, FRA)

The compound of the general formula:  $[\text{Co}(\text{C}_7\text{H}_8\text{N}_4\text{O}_2)_2(\text{H}_2\text{O})_4]$  has been prepared and characterized by X-ray diffraction analysis, UV-visible and infrared spectroscopy (FTIR),  $^1\text{H}$ ,  $^{13}\text{C}$  NMR and thermal analyses (TGA and DTA). The complex was crystallized in the monoclinic system (P 21/c). The unit cell parameters are  $a = 7.6304 (3) \text{ \AA}$ ,  $b = 13.1897 (6) \text{ \AA}$ ,  $c = 9.6670 (4) \text{ \AA}$ ,  $\beta = 104.9744 (17)^\circ$  and  $V = 939.87 (7) \text{ \AA}^3$ . The cobalt ions are pseudo-octahedrally coordinated by two theophyllinato ligands with Co-N distance is  $2.1847 \text{ \AA}$ , and four coordinated water with Co-O distances included between  $2.0756$  and  $2.1022 \text{ \AA}$ . The three-dimensional network stabilized by the intermolecular hydrogen bonds (O-H...O and O-H...N) which incorporated 2 4 (8) and 2 2 (18) graph-set motifs. The fingerprint plots associated with the Hirshfeld surface clearly display each significant interaction involved in the structure, by quantifying them in an effective visual manner. Additionally, the molecular docking studies between the tumor suppressor protein p53 with the cobalt complexes. The results of molecular docking show that the complex has a good affinity complex-P53 (docking score = 7.19).

## MS14-P39 | STEREOCHEMISTRY OF Tl(I) IN INORGANIC OXYSALTS

Markovski, Mishel (Saint Petersburg State University, Sankt-Petersburg, RUS); Siidra, Oleg (Saint Petersburg State University, Sankt-Peterburg, RUS)

183 monovalent thallium oxysalts for which good refinements exist were reviewed. 303  $Tl^+-O_n$  and 11  $Tl^+-O_nX_m$  ( $X = F, Cl, Br$ ) polyhedra consisting of 2449  $Tl^+-O$  ( $\leq 3.55 \text{ \AA}$ ) and 74  $Tl-X$  ( $\leq 3.7 \text{ \AA}$ ) bonds were taken into consideration. Bond-valence calculations and geometrical parameters ( $[\Delta]$  displacement parameter,  $[Pd]$  distortion,  $[V_p]$  polyhedral volume,  $[R_{sph}]$  sphere radius,  $[V_{sph}]$  sphere volume,  $[S]$  sphericity,  $[ECC_l]$  linear eccentricity and  $[ECC_v]$  volume eccentricity) were calculated in order to evaluate the influence of the 'lone pair' (LP) stereoactivity on the distortion of  $Tl-O_n$  polyhedra. In 2/3 of complexes the LP stereoactivity is pronounced. Complexes with active LP are generally built of strong  $Tl-O$  bonds ( $\leq 3 \text{ \AA}$ ).  $Tl-O_n$  polyhedra were classified into five types: I-hemidirected convex, II-hemidirected concave, III-equatorial, IV-bisdirected and V-holodirected. Different geometrical parameters and trends for each type were evaluated and will be discussed.

This work was financially supported by the Russian Science Foundation through the grant 16-17-10085 and internal travel grant of SPbSU.

## MS14-P40 | CALCIUM OXALATE CRYSTALLIZATION FOR A NON-CONVENTIONAL CO<sub>2</sub> STORAGE

### METHOD

Pastero, Linda (Department of Earth Sciences-University of Turin, Turin, ITA); Curetti, Nadia (Department of Earth Sciences-University of Turin, Turin, ITA); Ortenzi, Marco Aldo (Department of Chemistry - University of Milan, Milan, ITA); Schiavoni, Marco (Department of Chemistry - University of Milan, Milan, ITA); Destefanis, Enrico (Department of Earth Sciences - University of Turin, Turin, ITA); Pavese, Alessandro (Department of Earth Sciences - University of Turin, Turin, ITA)

The increase in the concentration of carbon dioxide in the atmosphere is a relevant and outstanding problem. A synergic approach to the problem is needed: many complementary methods of sequestration should be combined with the reduction of production to decrease the total amount of CO<sub>2</sub> in the atmosphere.

A direct and green method to convert C(IV) into C(III) and trap CO<sub>2</sub> into a stable crystalline structure other than a carbonate (*i.e.* calcium oxalate, weddellite) is proposed <sup>1</sup>. CO<sub>2</sub> is reduced and precipitated as weddellite through Ca-ascorbate (CaAsc) as a sacrificial reductant. The reaction has been validated. Reaction's kinetics and trapping yield are under evaluation. Weddellite crystals precipitated show very high quality, as demonstrated by single crystal X-ray measurements. Moreover, crystals obtained exhibit stable flat (F) forms, even if the morphology reflects the crystal growth conditions. The crystal quality of the precipitate reflects on its stability, essential for storage purposes.

The precipitation of weddellite from CO<sub>2</sub> was described as a two-step process, following two separate reactions: i) a red-ox reaction that involves the reductant (CaAsc); ii) the nucleation of calcium oxalate. The red-ox is the rate-determining step of the process and should be enhanced to increase the overall reaction rate. The reaction rate of the whole process is dependent on the extent of the interface between the solution and CO<sub>2</sub> as well. The reaction yield could be increased explosively working with very large reaction surface.

[1] Pastero et al. (2019), STOTEN, 666, 1232-1244; doi: 10.1016/j.scitotenv.2019.02.114

## MS14-P41 | CRYSTAL STRUCTURES OF TRANSITION-METAL HALIDE COMPLEXES WITH CYANOPYRIDINE LIGANDS: SINGLE CHAINS, DOUBLE CHAINS, AND NETWORKS.

Heine, Miriam (Goethe-University Frankfurt, Frankfurt am Main, GER); Fink, Lothar (Goethe-University Frankfurt, Frankfurt am Main, GER); Schmidt, Martin U. (Goethe-Universität, Frankfurt a.M., Frankfurt am Main, GER)

We describe the structural variety of  $[M^{\text{II}}X_2(\text{CNpy})_2]_n$  and  $[M^{\text{II}}X_2(\text{CNpy})_1]_n$  with  $M^{\text{II}} = \text{Mn, Fe, Co, Ni}$ ;  $X = \text{Cl, Br}$  and  $\text{CNpy} = 3\text{-cyanopyridine, 4-cyanopyridine}$ . All crystal structures were determined by X-ray powder diffraction.

Single chains are the distinctive structural motif in  $[M^{\text{II}}X_2(\text{CNpy})_2]_n$  compounds: the metal atoms are coordinated octahedrally to four halogen atoms and two cyanopyridine ligands. The halogen atoms bridge two metal atoms, resulting in  $[M^{\text{II}}X_2]_n$  single chains. The CNpy molecules coordinate at their pyridine nitrogen atoms ( $N_{\text{py}}$ ) and form lateral “wings” on the chains.

In  $[M^{\text{II}}X_2(\text{CNpy})_1]_n$  compounds two different structure types are observed:

In case of  $X = \text{Cl}$ , 3-CNpy coordinates monodentately, which results in double chains of  $[M^{\text{II}}_2\text{Cl}_4]_n$ . 4-CNpy acts as a bidentate ligand connecting single chains *via* the two nitrogen atoms, forming two-dimensional networks.

In instance of  $X = \text{Br}$ , 4-CNpy and 3-CNpy both act as bidentate ligands to assemble networks.

By selecting the suitable combination of metal, halogen and ligand, single chains, double chains or networks easily become accessible.

## MS14-P125 - LATE | AN OCCURRENCE OF THE ACENTRIC DISTORTION DUE TO $\text{Ag}^+/\text{Bi}^{3+}$

### ORDERING IN THE $\text{AgBi}_2\text{B}_5\text{O}_{11}$ BORATE

Volkov, Sergey (Grebenshchikov Institute of the Silicate Chemistry of the Russian Academy of Sciences, Saint-Petersburg, RUS); Bubnova, Rimma (Grebenshchikov Institute of the Silicate Chemistry of the Russian Academy of Sciences, Saint Peterburg, RUS); Krzhizhanovskaya, Maria (Department of Crystallography, Saint Petersburg State University, Saint-Petersburg, RUS); Charkin, Dmitri (Department of Chemistry, Lomonosov Moscow State University, Moscow, RUS); Stefanovich, Sergey (Department of Chemistry, Lomonosov Moscow State University,, Moscow, RUS); Povolotskiy, Alexey (Institute of Chemistry, Saint Petersburg State University, Saint-Petersburg, RUS)

The first silver bismuth borate,  $\text{AgBi}_2\text{B}_5\text{O}_{11}$  has been synthesized and its crystal structure was characterized by a single-crystal X-ray diffraction. Crystal structure is orthorhombic, sp.gr.  $Pna2_1$  and based on isolated  $\text{B}_5\text{O}_{10}$  pentaborate groups. Its structure is derived from that of centrosymmetric  $\text{Bi}_3\text{B}_5\text{O}_{12}$  by ordered substitution of one  $\text{Bi}^{3+}$  ion for  $\text{Ag}^+$ , which results in the disappearance of the mirror plane and inversion centre. Second harmonic generation (SHG) measurements confirm the acentric crystal structure. Thermal expansion of this borate was studied by high-temperature X-ray powder diffraction in the 20–550 °C temperature range. It is strongly anisotropic:  $\alpha_a = 20.4(2)$ ,  $\alpha_b = 7.8(2)$ ,  $\alpha_c = 3.1(1) \times 10^{-6} \text{ }^\circ\text{C}^{-1}$  at 200 °C. The new compound was also characterized by thermal analysis, DFT calculations, vibrational and UV–Vis–NIR spectroscopy.

The optical measurements were performed at the Centre for Optical and Laser Materials Research, Research Park, Saint Petersburg State University. Powder X-ray diffraction experiments were performed at the Centre for X-ray Diffraction Studies, Research Park, Saint Petersburg State University. This work was financially supported by the Russian Science Foundation through the grant 18-73-00176.

## MS14-P127 - LATE | DOES THE IOTA-ALUMINA PHASE EXIST?

Lenz, Stephan (University of Bremen, Bremen, GER); Schneider, Hartmut (University of Bremen, Bremen, GER); Fischer, Reinhard X. (University of Bremen, Bremen, GER)

Several authors (e.g., [1,2,3]) reported on the synthesis of a pure alumina, designated iota-alumina ( $\iota$ -Al<sub>2</sub>O<sub>3</sub>), with a mullite-like X-ray diffraction pattern. Formally, this would be the aluminium-endmember of the mullite compositional series Al<sub>2</sub>[Al<sub>2+x</sub>Si<sub>2-x</sub>]O<sub>10-x</sub> with  $x = 1$ . However, none of the authors presented a crystal-structure model of this phase. So the existence of the iota-alumina is still not confirmed. To elucidate this question, we reproduced the synthesis procedure proposed by Ebadzadeh & Sharifi [3] and examined the synthesis products by X-ray powder diffraction and electron-dispersive X-ray spectroscopy (EDX).

The powder pattern of the synthesised material corresponds to the X-ray powder data provided by [3], but Rietveld analysis showed that the resulting phase is Na-aluminate mullite (see [4]) with lattice parameters:  $a = 7.6776(4) \text{ \AA}$ ,  $b = 7.6762(3) \text{ \AA}$ , and  $c = 2.9163(1) \text{ \AA}$ . This aluminate exhibits a mullite-type crystal structure with a pseudotetragonal metric and Na being located at the oxygen vacancy sites. The presence of sodium could be unambiguously identified by EDX. Also in other synthesis routes of putative  $\iota$ -Al<sub>2</sub>O<sub>3</sub> described in the literature, sodium can be found in the starting materials. We therefore assume that in most of the cases compounds denominated as iota-alumina actually correspond to Na-aluminate mullite. Thus, the existence of this hypothetical endmember needs to be reevaluated.

[1] Foster, P.A. *J. Electrochem. Soc.*, 106, 1959

[2] Perrotta, A.J. & Young, J.E. *J. Am. Ceram. Soc.*, 57, 1974

[3] Ebadzadeh, T. & Sharifi, L. *J. Am. Ceram. Soc.*, 91, 2008

[4] Fischer, R.X., Schmücker, M., Angerer, P., & Schneider, H. *Am. Min.*, 86, 2001

## MS14-P129 - LATE | MULTI-SCALE CHARACTERISATION OF THE CATIONIC DISORDER IN THE NOVEL BORATE $\text{Sr}_6\text{Tb}_{0.94}\text{Fe}_{1.06}(\text{BO}_3)_6$

Péchev, Stanislav (ICMCB - CNRS, University of Bordeaux INP, Pessac, FRA); Velázquez, Matias (ICMCB - CNRS, University of Bordeaux INP, Pessac, FRA); Duttine, Mathieu (ICMCB - CNRS, University of Bordeaux INP, Pessac, FRA); Wattiaux, Alain (ICMCB - CNRS, University of Bordeaux INP, Pessac, FRA); Labrugère, Christine (PLACAMAT - CNRS, University of Bordeaux, Pessac, FRA); Veber, Philippe (ILM - CNRS, University Lyon 1, Villeurbanne, FRA); Buffière, Sonia (ICMCB - CNRS, University of Bordeaux INP, Pessac, FRA); Denux, Dominique (ICMCB - CNRS, University of Bordeaux INP, Pessac, FRA)

The remarkable magnetic-optical properties of Tb-based compounds focused a number of works on the tailoring of novel crystals [1-2].

Millimetre sized single crystals of  $\text{Sr}_6\text{Tb}_{0.94}\text{Fe}_{1.06}(\text{BO}_3)_6$  were prepared by crystal growing from high-temperature solution. The crystal structure of this new borate was resolved by single-crystal X-ray diffraction with the trigonal  $R\bar{3}$  space group:  $a = 12.2164(2)$  Å,  $c = 9.1943(2)$  Å. The refinement of the crystal structure led to a final model with a long range disorder relative to the Tb and Fe statistical distribution over the  $3a$  and  $3b$  sites. Previously, the  $^{57}\text{Fe}$  Mössbauer spectroscopy revealed the only presence of  $\text{Fe}^{3+}$  with two different environments. Diffuse reflectance experiments showed no luminescence under excitation, consistent with a point disorder in the Tb/ $\text{FeO}_6$  octahedra and a local loss of the centre of symmetry. Finally, XPS and magnetic susceptibility measurements excluded the presence of  $\text{Tb}^{4+}$  and helped to settle down the cationic distribution in the final structure model. The cationic disorder in  $\text{Sr}_6\text{Tb}_{0.94}\text{Fe}_{1.06}(\text{BO}_3)_6$  is discussed in comparison with the structure of a close phase, synthesised in different conditions [3].

[1] P. Veber, M. Velázquez, G. Gadret, D. Rytz, M. Peltz, R. Decourt, *CrystEngComm*, **2015**, 17, 492.

[2] K. Shimamura et al., *Cryst. Growth Des.*, **2010**, 10, 3466.

[3] H. Inoue, Y. Doi, Y. Hinatsu, *J. Alloys Comp.*, **2016**, 681, 115-119.

## MS15: Minerals and Materials Under Extreme Conditions

---

### MS15-01 | REACTIVITY OF HEAVY NOBLE GASES UNDER HIGH PRESSURES

Sanloup, Chrystele (Sorbonne University, Paris, FRA); Crepisson, Celine (Sorbonne University, Paris, FRA); Leroy, Clemence (Sorbonne University, Paris, FRA); Blanchard, Marc (Université de Toulouse, Toulouse, FRA); Bureau, Helene (Sorbonne University, Paris, FRA); Cormier, Laurent (Sorbonne University, Paris, FRA)

Xenon (Xe) is the most reactive amongst noble gases, with over hundred compounds synthesised at ambient pressure. Increasing pressure is an efficient way to induce Xe reactivity, especially with oxides, resulting in the formation of covalent Xe-O bonds. Some examples will be given, ranging from stoichiometric compounds to silicate minerals doped in Xe at the % level, the latter being stable at remarkably low P conditions. Xe reactivity with silicates extends to compressed magmas, molten materials that were also shown to react with krypton.

The search for noble gases compounds has for long been fuelled for their high energy storage capacity, but implications in Earth's sciences are also large as the latter rely on noble gases to trace key planetary processes such as atmospheric formation or underground nuclear tests. Therefore, we will finally discuss the implications of heavy noble gases reactivity under P, i.e. at the conditions of planetary interiors, on isotopic fractionation.

## MS15-02 | HIGH-PRESSURE SYNTHESIS AND PROPERTIES OF IRON OXIDES

Ovsyannikov, Sergey (Bayerisches Geoinstitut, Universität Bayreuth, Bayreuth, GER); Bykov, Maxim (Bayerisches Geoinstitut, Universität Bayreuth, Bayreuth, GER); Bykova, Elena (Bayerisches Geoinstitut, Universität Bayreuth, Bayreuth, GER); Glazyrin, Konstantin (Deutsches Elektronen-Synchrotron (DESY), Hamburg, GER); Manna, Rudra (Institute of Physics, University of Augsburg, Augsburg, AUT); Tsirlin, Alexander (Institute of Physics, University of Augsburg, Bayreuth, GER); Cerantola, Valerio (Bayerisches Geoinstitut, Universität Bayreuth, Bayreuth, GER); Kупenko, Ilya (ESRF-The European Synchrotron, Grenoble, FRA); Kurnosov, Alexander (Bayerisches Geoinstitut, Universität Bayreuth, Bayreuth, GER); Kantor, Innokenty (ESRF-The European Synchrotron, Grenoble, GER); Pakhomova, Anna (Deutsches Elektronen-Synchrotron (DESY), Hamburg, GER); Chuvashova, Irina (Bayerisches Geoinstitut, Universität Bayreuth, Bayreuth, GER); Chumakov, Aleksandr (ESRF-The European Synchrotron, Grenoble, GER); Ruffer, Rudolf (ESRF-The European Synchrotron, Grenoble, FRA); McCammon, Catherine (Bayerisches Geoinstitut, Universität Bayreuth, Bayreuth, GER); Dubrovinsky, Leonid (Bayerisches Geoinstitut, Universität Bayreuth, Bayreuth, GER)

Iron oxides are common and fundamentally important materials for natural sciences. In this presentation, we will review a progress on high-pressure high-temperature (HP-HT) synthesis of novel iron oxides, like  $\text{Fe}_4\text{O}_5$ ,  $\text{Fe}_5\text{O}_6$ ,  $\text{Fe}_7\text{O}_9$ ,  $\text{Fe}_5\text{O}_7$ ,  $\text{Fe}_9\text{O}_{11}$ ,  $\text{FeO}_2$ , and others, and present recent results on high-pressure low-temperature behaviour of one of them, namely,  $\text{Fe}_4\text{O}_5$ . We will present the results of combined single-crystal X-ray diffraction, Mossbauer spectroscopy and magnetization measurements, performed on  $\text{Fe}_4\text{O}_5$  samples under high pressure at low temperature. We will show how the applied pressure that tunes the distances between the neighbouring iron atoms can switch the charge-ordering type between the trimers and dimers. We will show that the charge-ordering processes in iron oxides are predetermined not only by spin and charge interactions, but also by “chemical” interactions between the neighbouring iron atoms. We synthesized large single crystals of  $\text{Fe}_4\text{O}_5$  using multi-anvil high-pressure high-temperature synthesis facilities, and the major part of the studies has been done on single crystals. We will report and discuss the first P-T phase diagram of  $\text{Fe}_4\text{O}_5$ . We also discuss some preliminary results for the other iron oxides.

## MS15-03 | THE TRUE STRUCTURAL RELATIONSHIP BETWEEN ZICON AND SCHEELITE STRUCTURE TYPES, AND A NEW POLYMORPH OF ZIRCON

Angel, Ross J. (University of Pavia, Pavia, ITA); Stangarone, Claudia (German Aerospace Centre (DLR), Berlin, GER); Naemi, Waeselmann (University of Hamburg, Hamburg, GER); Mihailova, Boriana (University of Hamburg, Hamburg, GER); Mauro, Principe (University of Torino, Torino, ITA); Alvaro, Matteo (University of Pavia, Pavia, ITA)

Zircon ( $\text{ZrSiO}_4$ ,  $I4_1/amd$ ) is a very common accessory mineral and important ceramic component. Its high-pressure polymorph with a scheelite-type structure, reidite ( $I4_1/a$ ), has been detected in impact structures where it is diagnostic of shock impacts. Because  $I4_1/a$  is a sub-group of  $I4_1/amd$  many authors have assumed that reidite (and scheelite structures in general) can be obtained by a displacive-type distortion of the zircon structure. Careful analysis of the atomic linkages and symmetry elements in the two structure types shows that this is incorrect, and that the transformation between them must be reconstructive and first order. This is consistent with survival of reidite in meteorite craters, and confirmed by our new ab-initio DFT simulations [1].

The DFT simulations also revealed that zircon has a soft phonon mode that triggers a displacive transition near 20 GPa to a previously-unreported  $\text{ZrSiO}_4$  phase with symmetry  $I-42d$ . We have confirmed the occurrence of a soft-mode driven second-order phase transition by in-situ high-pressure Raman spectroscopy [2]. This also showed that reidite starts to form in the sample just after the transition to the new phase. Thus, at room temperature, the first-order activation barrier between zircon and reidite can be overcome via the formation of the new high-pressure phase as an intermediate bridging state.

Supported by the European Research Council (Grant 714936).

[1] Stangarone et al. (2019) *American Mineralogist*, doi: 10.2138/am-2019-6827

[2] Mihailova et al. (2019) *Physics & Chemistry of Minerals*, submitted

## MS15-04 | STRUCTURAL BEHAVIOR OF THE SII CLATHRASIL CHIBAITE AT LOW TEMPERATURES AND HIGH PRESSURES

Scheidl, Katharina (NTNU, Trondheim, NOR); Effenberger, Herta (University of Vienna, Wien, AUT); Yago, Takehiko (University of Tokyo, Tokyo, JPN); Momma, Koichi (National Museum of Nature and Science, Tsukuba, JPN); Miletich, Ronald (University of Vienna, Vienna, AUT)

Clathrasils are built up from a framework of corner-sharing  $[\text{SiO}_4]$ -tetrahedra that entraps guest atoms and molecules in cages. They have gained interest because of their potential application for gas storage and separation [1]. The behavior of the structure of the clathrasil chibaite and the influence of guest components at low temperatures as well as pressures was investigated using single-crystal X-ray diffraction and Raman spectroscopy. Chibaite is isotypic with the sII-gas hydrate characterized by larger  $[5^{12}6^4]$ -cages and smaller  $[5^{12}]$ -cages [2]. The natural sample of this study contains the hydrocarbons  $\text{C}_2\text{H}_6$ ,  $\text{C}_3\text{H}_8$ ,  $i\text{-C}_4\text{H}_{10}$  in both cage types, and additionally  $\text{CH}_4$  molecules only in the small cages. With decreasing temperature to 100 K, the cubic  $Fd\text{-}3m$  room-temperature structure shows a continuous symmetry-lowering transformation to a monoclinic  $A2/n$  structure [3]. High-pressure experiments up to 10.3 GPa were performed in diamond-anvil cells using 4:1 methanol-ethanol mixture, helium and neon as pressure-transmitting media [4]. Compressed in the non-penetrating methanol-ethanol mixture, the  $Fd\text{-}3m$  framework undergoes a first transformation between 1.7 and 2.2 GPa with monoclinic metric and a second between 3.9 and 4.3 GPa with monoclinic or tetragonal metric. Using neon and helium the structure is stiffened during compression. The high-pressure behavior is characterized by a distortion of the lattice without leading to a pressure-induced amorphization.

[1] Navrotsky, A. et al. (2003). *Am. Mineral.* 88, 1612–1614.

[2] Momma, K. et al. (2011). *Nat. Commun.* 2, 196.

[3] Scheidl, K.S. et al. (2018). *IUCrJ* 5, 595-607.

[4] Scheidl, K.S. et al. (2019). *Microporous Mesoporous Mater.* 273, 73-89.

## MS15-05 | CRYSTALLISATION STUDIES OF BIODIESEL AND METHYL STEARATE AT EXTREME CONDITIONS

Liu, Xiaojiao (university of Edinburgh, Edinburgh, GBR)

The widespread use of biodiesel as a renewable fuel offers many potential advantages, but at the same time presents challenges for modern internal combustion engines, particularly for those that involve high-pressure injection of fuel into the combustion chamber. At the typical elevated pressures used in such engines, biodiesel can crystallise and block fuel filters and injection nozzles, thereby causing engine failure. In this study, optical studies and Raman spectroscopy of a typical biodiesel sample contained in a diamond-anvil cell show that biodiesel initially crystallises at ca. 0.2 GPa and then undergoes a series of structural changes on further increase of pressure. On account of the complex composition of biodiesel, this study focused on one of its main components – methyl stearate. Using a combination of Raman spectroscopy, X-ray powder diffraction and neutron powder diffraction, it was shown that methyl stearate exhibits rich polymorphic behaviour when subjected to elevated pressures up to 6.3 GPa. Under non-hydrostatic conditions, pressures as low as 0.1 GPa converted Form V to crystallites of Form III that typically adopt plate-like morphologies. This observation has implications for the pressure-induced crystallisation of biodiesel containing high proportions of methyl stearate because of the potentially serious consequences for blocking of injection nozzles in engines. Four phase transitions over the pressure range of 0.1 GPa to 6.3 GPa were also observed. Form III was recovered on decompression to ambient pressure. High-pressure neutron powder diffraction studies of a perdeuterated sample showed that Form V persisted up to 3.11 GPa.

## MS15-P01 | REDUCING THE BACKGROUND OF ULTRA-LOW TEMPERATURE X-RAY

### DIFFRACTION DATA

McMonagle, Charlie (Newcastle University, Newcastle upon Tyne, GBR); Probert, Michael (Newcastle University, Newcastle upon Tyne, GBR)

The XIPHOS diffraction facility at Newcastle University has been designed to broaden the range of extreme sample environments available in the home laboratory.<sup>1</sup> One of these extreme conditions is the ultra-low-temperature regime, with temperatures as low as 3 K routinely accessible. In order to reach these ultra-low temperatures, the sample is cooled using a three-stage Displex closed-cycle refrigerator. Conventionally this leads to a very intense and complex background from the beryllium sample environment.

A series of recent upgrades have led to a 6-fold reduction in the average intensity and a 15-fold reduction in peak intensity of the background observed for diffraction experiments, opening up new possibilities to look at weakly diffracting samples with a much-improved signal to noise.<sup>2</sup> The upgrades include a magnetically controlled internal beamstop and separate internal collimator that together, completely remove the scattering contribution to the background from the beryllium vacuum chamber. Additionally, a new radiation shield made from flexible graphite further reduces the background and maintains excellent thermal properties to access an ultra-low base temperature, 2.05 K.

This much-reduced background allows us to elucidate the structure and phase behaviour of chemically complex samples by single-crystal X-ray diffraction at these extreme temperatures.

[1] Probert et al. 2010 J. Appl. Cryst. 43, 1415

[2] McMonagle & Probert 2019 J. Appl. Crystallogr. 52, 445

## MS15-P02 | XPRESS: LATEST RESULTS FROM THE NEW DEDICATED HIGH PRESSURE DIFFRACTION BEAMLINE AT ELETTRA

Joseph, Boby (GdR IISc-ICTP Sincrotrone Trieste, Trieste, ITA); Alabarse, Federico (Elettra Sincrotrone Trieste, Trieste, ITA); Lotti, Paolo (Dipartimento Scienze della Terra, Milan, ITA); Merlini, Marco (Dipartimento Scienze della Terra, Milan, ITA); Sarma, Dipankar Das (Indian Institute of Science, Bengaluru, IND); Lausi, Andrea (Elettra Sincrotrone Trieste, TRIESTE, ITA)

With the recent opening of the Xpress beamline the high pressure (HP) diffraction community have a dedicated experimental set up at the Elettra synchrotron facility. Xpress is part of a scientific partnership between India and Italy under a project administered through the IISc Bangalore, and utilize the radiation from a 49 poles, 3.6 Tesla Superconducting Wiggler, to produce a 25 keV monochromatic X-ray beam focused on a large area detector (fastMAR345) for data acquisition in angle dispersive mode.

The beamline allows powder diffraction experiments using a variety of diamond anvil cells (DAC) and is equipped with online ruby fluorescence spectrometer, long working distance microscope, precision microdriller, automatic pneumatic pressure controller, etc. In front of the detector a precision stage enables easy switching between the pressure monitoring ruby fluorescence and the diffraction data collection using finite size (tens of microns in diameter) monochromatic x-ray beam. A commercial gas loading system, an *in house* developed cryogenic gas loader and a LN<sub>2</sub> cryo stream are currently in the advanced stages of commissioning. Very recently, single crystal (SC) XRD measurements under HP were successfully commissioned in a membrane DAC; once further improvements will be implemented, *HP-single crystal* will be available for the users.

We will present recent scientific highlights of the beamline activity performed on both powder and SC under HP, such as pressure-induced amorphisation, pressure-induced phase transition, insertions and synthesis of new nanocomposites.

## MS15-P03 | PRESSURE-INDUCED SPIN TRANSITIONS IN GARNETS

Friedrich, Alexandra (Julius-Maximilians-Universität Würzburg, Würzburg, GER); Koch-Müller, Monika (GFZ Potsdam, Potsdam, GER); Efthimiopoulos, Ilias (GFZ Potsdam, Potsdam, GER); Morgenroth, Wolfgang (Goethe-Universität Frankfurt am Main, Frankfurt am Main, GER); Cott-Garcia, Joelson (University of Minnesota, Minneapolis, USA); Wentzcovitch, Renata M. M. (Columbia University, New York, USA)

Garnets are of high mineralogical interest as they belong to the most common minerals in the Earth's upper mantle. And garnet crystals are used in many types of applications, for example as scintillator crystals, phosphor materials, magnetic storage materials, laser crystals, and lithium batteries.

Here, we present a comparative study of the effect of cation and anion substitution in garnets on pressure-induced electronic (spin-pairing) transitions of 3d-transition-metal cations, i.e.  $\text{Fe}^{3+}$  and  $\text{Mn}^{3+}$ . The structural compression and spin transitions of OH-free manganese garnets  $\text{Ca}_3\text{Mn}_2[\text{SiO}_4]_3$  and blythite,  $\text{Mn}_3\text{Mn}_2[\text{SiO}_4]_3$  have been studied using single-crystal synchrotron X-ray diffraction at PETRA III, Raman spectroscopy, and theoretical calculations based on density functional theory at pressures of up to 75 GPa. Our new results will be compared with our recent results on andradite,  $\text{Ca}_3\text{Fe}_2[\text{SiO}_4]_3$  and tetragonal henritermierite,  $\text{Ca}_3\text{Mn}_2[\text{SiO}_4]_2[\text{O}_4\text{H}_4]$  [1,2], and with literature data on other  $\text{Fe}^{3+}$ -bearing garnets.

Financial support from the DFG (Fr2491/2-1), the BMBF (05K13RF1), Goethe University Frankfurt, and University of Würzburg, Germany, is gratefully acknowledged. Portions of this research were carried out at PETRA III (DESY), a member of the Helmholtz Association. We thank H.-P. Liermann for support.

[1] A. Friedrich et al., Phys. Rev. B **2014**, 90, 094105

[2] A. Friedrich et al., Phys. Rev. B **2015**, 92, 014117

## MS15-P04 | EXPERIMENTAL CHARGE DENSITY DISTRIBUTION IN GROSSULAR UNDER HIGH PRESSURE - A FEASIBILITY STUDY

Gajda, Roman (University of Warsaw, Warszawa, POL); Stachowicz, Marcin (University of Warsaw, Warszawa, POL); Makal, Anna (University of Warsaw, Warszawa, POL); Sutula, Szymon (University of Warsaw, Warszawa, POL); Fertey, Pierre (Synchrotron SOLEIL, Paris, FRA); Wozniak, Krzysztof (Department of Chemistry, University of Warsaw, Warszawa, POL)

We will present details of experimental charge density distribution in a natural garnet mineral called grossular,  $\text{Ca}_3\text{Al}_2(\text{SiO}_3)_4$  under 1GPa pressure. Single crystal, high resolution X-ray data were collected on the CRISTAL beamline at the SOLEIL synchrotron (Paris, France). Grossular crystallises in the cubic Ia-3d space group. A short wavelength (0.41Å) and a special type of Diamond Anvil Cell (DAC) with the opening angle  $110^\circ$  let us collect data up to 0.35Å (with 100% completeness up to 0.45Å). We compared our results with experimental charge densities obtained for grossular at ambient conditions and those obtained for pyrope -  $\text{Mg}_3\text{Al}_2(\text{SiO}_3)_4$  (isostructural with grossular) collected at 30K (Destro et al., 2017) [1]. In the case of grossular, the obtained properties of charge density at the (3, -1) BCPs as well as the net atomic charges are comparable. Our results indicate transfer of charge among ions under high pressure. Up to our knowledge this is the first fully successful determination of quantitative charge distribution in crystal under high pressure accomplished by performing multipole refinement. We will present detailed results of our investigations.

Acknowledgments: This work was supported by the Foundation for Polish Science (FNP) within the “Core Facility for Crystallographic and Biophysical Research to support the development of medicinal products” project.

[1] R. Destro, R. Ruffo, P. Roversi, R. Soave, L. Loconte, LL. Presti, *Acta Cryst.* **B73** (2017) 722-736.

## MS15-P05 | AB INITIO SIMULATION AND X-RAY DIFFRACTION MEASUREMENTS OF DEVIATORIC STRESS IN MINERAL INCLUSIONS

Morana, Marta (University of Pavia, Pavia, ITA); Murri, Mara (University of Pavia, Pavia, AUT); Girani, Alice (University of Pavia, Pavia, ITA); Angel, Ross J. (University of Pavia, Pavia, ITA); Alvaro, Matteo (University of Pavia, Pavia, ITA)

The behaviour of crystals under deviatoric stress is still poorly understood, despite that it plays an important role in reconstructive [1] and symmetry breaking [2] phase transitions. Even simple systems, such as an inclusion of an elastically anisotropic mineral entrapped in an elastically isotropic host, can develop deviatoric stresses. Since the experimental generation and measurement of deviatoric stress is difficult, we first performed *ab initio* hybrid Hartree–Fock/Density Functional Theory calculations to characterize how deviatoric stress affects crystal structures [3]. An ideal candidate for this study is quartz, since it has a simple and well-known structure, whose variation with pressure and temperature has been widely characterised, and it is one of the most common mineral inclusions. We compared the simulation results with X-ray diffraction data collected from a quartz crystal entrapped in a garnet host. Here we discuss how to overcome the experimental challenges related to the collection of intensity data from a crystal entrapped in another one, assess the quality of the results and the agreement between the experiment and the calculation.

[1] B. Richter, H. Stünitz, R. Heilbronner *Journal of Geophysical Research: Solid Earth*. **2016**, 121(11), 8015-8033.

[2] Bismayer, U., Salje, E., & Joffrin, C. *Journal de Physique*. **1982**, 43(9), 1379-1388.

[3] M. Murri, M. Alvaro, R.J. Angel, M. Prencipe, B.D. Mihailova *Physics and Chemistry of Minerals*, **2019**, 46(5), 487-499

## MS15-P06 | STRUCTURE, CRYSTAL CHEMISTRY, AND COMPRESSIBILITY OF IRON-RICH SILICATE PEROVSKITE AT PRESSURES UP TO 95 GPa

Koemets, Iuliia (Bayerischen Geoinstitut, Universität Bayreuth, Bayreuth, GER); Zhaodong, Liu (Jilin University, Changchun, CHN); Wang, Biao (Bayerischen Geoinstitut, Universität Bayreuth, Bayreuth, GER); Koemets, Egor (Bayerischen Geoinstitut, Universität Bayreuth, Bayreuth, GER); McCammon, Catherine (Bayerischen Geoinstitut, Universität Bayreuth, Bayreuth, GER); Katsura, Tomoo (Bayerischen Geoinstitut, Universität Bayreuth, Bayreuth, GER); Dubrovinsky, Leonid (Bayerischen Geoinstitut, Universität Bayreuth, Bayreuth, GER); Hanfland, Michael (European Synchrotron Radiation Facility, Grenoble, FRA); Chumakov, Aleksandr (European Synchrotron Radiation Facility, Grenoble, FRA)

Bridgmanite (Mg, Fe, Al silicate perovskite) is the most abundant mineral in the Earth's lower mantle. We investigated two crystalline iron-rich materials with compositions of  $\text{FeMg}_{0.5}\text{Si}_{0.5}\text{O}_3$  and  $\text{Fe}_{0.5}\text{Mg}_{0.5}\text{Al}_{0.5}\text{Si}_{0.5}\text{O}_3$ , synthesized at 27 GPa and 2000 K using a Kawai-type multi-anvil apparatus and recovered to ambient conditions. We found that as-recovered  $\text{FeMg}_{0.5}\text{Si}_{0.5}\text{O}_3$  has a previously unknown structure that is derived from a corundum (or ilmenite) prototype. On compression above 15 GPa, this phase transformed into a new monoclinic silicate double-perovskite. A characteristic feature of this double-perovskite structure is the presence of two distinct octahedral B-sites; one occupied by Si only, and the other by iron and magnesium. Analysis of compressibility changes of both polyhedra as obtained by single-crystal X-ray diffraction and variation of Mössbauer hyperfine parameter at pressures up to 95 GPa suggest a spin transition of ferric iron at a pressure of ~40 GPa. Thus, our study resolves the long-standing controversy regarding iron behaviour in bridgmanite and its possible impact on the compressibility of the mineral: we found that ferric iron indeed can occupy octahedral site, can undergo spin crossover, and affect compressional behaviour of the material. However, ferric iron does not mix with silicon in octahedra of silicate perovskite. By combining our data on pressure-volume relations of  $\text{Fe}_{0.5}\text{Mg}_{0.5}\text{Al}_{0.5}\text{Si}_{0.5}\text{O}_3$  and published results for Al-rich bridgmanites we estimate the bulk modulus of  $\text{FeAlO}_3$  end-member

## MS15-P07 | TOWARD ONE-POT GREEN SYNTHESIS OF NANOPOROUS CARBON NITRIDES

Dziubek, Kamil (LENS - European Laboratory for Non-Linear Spectroscopy, Sesto Fiorentino, ITA); Fanetti, Samuele (LENS - European Laboratory for Non-Linear Spectroscopy, Sesto Fiorentino, ITA); Nobrega, Marcelo ( Universidade de São Paulo, São Paulo, BRA); Citroni, Margherita (LENS - European Laboratory for Nonlinear Spectroscopy, Sesto Fiorentino, ITA); Sella, Andrea (University College London, London, GBR); McMillan, Paul (University College London, London, GBR); Hanfland, Michael (European Synchrotron Radiation Facility, Grenoble, FRA); Bini, Roberto (LENS - European Laboratory for Nonlinear Spectroscopy, Sesto Fiorentino, ITA)

Extended layered nanoporous structures are promising materials that exhibit intercalation properties of conventional 2D layered phases combined with selective diffusion and encapsulation-release behaviour of 3D porous frameworks. Since the seminal work of Kuhn et al. [1], covalent triazine-based frameworks (CTFs) have gained attention as potential catalysts and gas adsorbents. Conventional synthesis methods of this class of materials at high temperature and ambient pressure require, however, presence of Lewis acid catalysts, such as ZnCl<sub>2</sub> [2]. To avoid the use of environmentally harmful reagents new routes of single-step, “green” synthesis of highly crystalline CTFs are intensively sought. We have investigated 2,4,6-tricyano-1,3,5-triazine, a precursor to H-free 2D nanoporous polymers with 1:1 C:N ratio, at high pressure and high temperature conditions using synchrotron X-ray diffraction and FTIR spectroscopy [3]. The new high pressure phase II of the molecular monomer was identified and its structure determined above 2.4 GPa at room temperature. A tentative phase diagram was established, including the I-II phase boundary and the melting line. Polymerization of the phase II was studied between 4 and 10 GPa in the temperature range 300 to 550 K. XRD and FTIR analysis of the reaction products revealed amorphous material and crystalline layered carbon nitride domains. The reaction kinetics indicates that the structural transformation is driven by structural defects.

[1] P. Kuhn et al. *Angew. Chem. Int. Ed.* **2008**, *47*, 3450

[2] M. J. Bojdys et al. *Adv. Mater.* **2010**, *22*, 2202

[3] S. Fanetti et al. *CrystEngComm* **2019**, DOI: 10.1039/C8CE02154F

## MS15-P08 | THE MICROSCOPIC ORIGIN OF AXIAL NEGATIVE THERMAL EXPANSION AND NEGATIVE LINEAR COMPRESSIBILITY IN ALPHA- AND BETA-PbAlBO<sub>4</sub>

Gogolin, Mathias (University of Bremen, Institute of Inorganic Chemistry and Crystallography, Bremen, GER); Murshed, M. Mangir (University of Bremen, Institute of Inorganic Chemistry and Crystallography, Bremen, GER); Ende, Martin (University of Vienna, Department of Mineralogy and Crystallography, Vienna, AUT); Kremlicka, Thomas (University of Vienna, Department of Mineralogy and Crystallography, Vienna, AUT); Miletich, Ronald (University of Vienna, Department of Mineralogy and Crystallography, Vienna, AUT); Gesing, Thorsten M. (University of Bremen, Institute of Inorganic Chemistry and Crystallography, Bremen, GER)

PbMBO<sub>4</sub>-materials (M = Ga, Al, Fe, Mn, Cr) have attracted scientific attention due to their magnetic properties [1] as well as their temperature [2]- and pressure-dependent [3] behaviors. The compounds crystallize in space group *Pnam* and belong to the mullite-type family of compounds, featuring a trans-type chain of edge sharing octahedral MO<sub>6</sub>-units extending along the *c*-axis. The chains are interconnected in the *ab*-plane by trigonal planar BO<sub>3</sub>- and pyramidal PbO<sub>4</sub>-units. At ~1048 K, the aluminum phase undergoes an irreversible, reconstructive phase transition into the β-PbAlBO<sub>4</sub>-polymorph [4] (space group *Pbcn*). In-situ X-ray diffraction between 13 K and 1000 K show both polymorphs to be stable in this temperature range. Using temperature- and pressure-dependent X-ray diffraction and ab-initio modeling, we investigated the axial negative thermal expansion (ANTE) and negative linear compressibility (NLC) in α- and β-PbAlBO<sub>4</sub> based on single crystal data. The interplay between the Grüneisen functions and the mechanical properties of the systems determine the ANTE. The structural features suggest that the NLC arises from the topology of the polymorphs, which is directed by the stereochemical active lone electron pairs of the Pb<sup>+2</sup> cations.

[1] A.I. Pankrats, et al., *Solid State Phenom.* 215 (2014) 372–377.

[2] T.M. Gesing, et al., *Zeitschrift Für Krist. - New Cryst. Struct.* 227 (2012) 285–286.

[3] P. Kalita, Dissertation, University of Nevada, Las Vegas, 2015.

[4] H. Park, J. Barbier, R.P. Hammond, *Solid State Sci.* 5 (2003) 565–571.

## MS15-P09 | NEW INSIGHTS ON THE HIGH PRESSURE BEHAVIOUR OF THE $\text{GeSe}_x\text{Te}_{1-x}$ SOLID

### SOLUTION

Herrmann, Markus (Research Centre Juelich GmbH, Juelich, GER); Friese, Karen (Research Centre Juelich GmbH, Juelich, GER); Eich, Andreas (Research Centre Juelich, Juelich, GER); Ait Haddouch, Mohammed (Research Centre Juelich, Juelich, GER); Kuepers, Michael (RWTH Aachen University, Aachen, GER); Stoffel, Ralf (RWTH Aachen University, Aachen, GER); Dronskowski, Richard (RWTH Aachen University, Aachen, GER); Glazyrin, Konstantin (DESY, Hamburg, GER); Grzechnik, Andrzej (RWTH Aachen University, Aachen, GER)

Binary chalcogenides of group IV–VI elements, e.g. GeTe, are candidates for optoelectronic and thermoelectric devices as well as for non-volatile phase-change memories. The incorporation of Se into GeTe has a positive influence on many of the desired properties [1]. At atmospheric conditions, GeTe-I is rhombohedral ( $R3m$ ) [2]. Mixed crystals with  $0 < x < 0.52$  are isostructural to GeTe-I, while a hexagonal phase was found for  $0.58 < x < 0.85$  [2,3].

We performed synchrotron diffraction experiments and DFT calculations on  $\text{GeSe}_x\text{Te}_{1-x}$  ( $x=0, 0.2, 0.5, 0.75$ ) at high pressures. In particular, we studied the influence of Se on the stability fields of the phases and the effect of Ge...Ge interactions.

GeTe,  $\text{GeSe}_{0.2}\text{Te}_{0.8}$ , and  $\text{GeSe}_{0.5}\text{Te}_{0.5}$  follow the transition pathway GeTe-I ( $R3m$ )  $\rightarrow$  GeTe-II (FCC)  $\rightarrow$  GeTe-III ( $Pnma$ ) [4]. The structure of the GeTe-III polymorph was solved from single crystal data [4]. In the structure, which is different from earlier reported models, additional Ge...Ge and Se/Te...Se/Te interactions exist. GeTe-III is isostructural to beta-GeSe, a high-pressure and high-temperature polymorph of GeSe. The stabilization of GeTe-III is due to the strengthening of the longer Ge-Te bonds and of GeGe interactions.

[1] Perumal S. et al., *J. Mater. Chem. C* **4**, 7520-7536 (2016).

[2] Onodera A. et al., *Phys. Rev. B* **56**, 7635-41 (1997).

[3] Serebryanaya N.R. et al., *Phys. Lett. A* **197**, 63-66 (1995).

[4] Herrmann M.G. et al., *Acta Cryst. B* **75**, 246-256 (2019).

## MS15-P10 | SQUEEZING THE MOST DATA OUT OF YOUR HIGH-PRESSURE EXPERIMENT

Graf, Jürgen (Incoatec GmbH, Geesthacht, GER); Stürzer, Tobias (Bruker AXS GmbH, Karlsruhe, GER); Ott, Holger (Bruker AXS GmbH, Karlsruhe, GER); Dera, Przemyslaw (University of Hawaii at Manoa, Honolulu, USA); Ruf, Michael (Bruker AXS Inc., Madison, USA); Radcliffe, Paul (Incoatec GmbH, Geesthacht, GER); Michaelsen, Carsten (Incoatec GmbH, Geesthacht, GER)

Within the last decade high pressure studies have received significant increase of interest. Present typical applications range from the investigation of high-pressure polymorphism of solid-state organics as part of the pharmaceutical drug development to the study of rocks and minerals with an applied pressure of up to 50 GPa.

A major challenge in the field of high pressure crystallography is the acquisition of data of sufficient quality and completeness for a successful structure determination. This presentation will be reviewing recent advances in hardware development, such as X-ray sources with radiation harder than Mo-K $\alpha$ , and highlight the latest improvements in software, which help in tackling the problems with data acquisitions in high-pressure experiments.

Using a Bruker D8 VENTURE system, we will be demonstrating the advanced hardware capabilities and processing methods based on selected data, including data from the Indium METALJET X-ray source. Further, we will be showing how to increase the completeness of high-pressure experiments by mounting multiple samples in a diamond anvil cell and measuring and processing data concurrently.

The high flexibility of the D8 VENTURE can be further expanded by adding enhanced features typically only available at synchrotron facilities, e.g. for studying tiny mineral crystals enclosed in diamond anvil cells. These features include highly accurate, motorized sample positioning and the ability to monitor the intensity of the X-ray beam passing through the diamond anvil cell, as well as an extension for online pressure measurements based on ruby fluorescence. This makes the D8 VENTURE system “a little synchrotron at home”.

## MS15-P11 | SYNTHESIS, CRYSTAL STRUCTURES AND THERMAL EXPANSION OF NOVEL LUTETIUM-BARIUM BORATES

Biryukov, Yaroslav (Institute of Silicate Chemistry of the Russian Academy of Sciences, Saint Petersburg, RUS); Bubnova, Rimma (Institute of Silicate Chemistry of the Russian Academy of Sciences, Saint Petersburg, RUS); Filatov, Stanislav (Institute of Earth Sciences, Department of Crystallography, Saint Petersburg State University, Saint Petersburg, RUS)

The search for new RGB phosphors for wLED is of important interest nowadays. Rare- and alkaline-earth borates have attracted the attention of researchers due to luminescence makes them prospective phosphors, scintillators. Five (Lu,Ba)-borates are known:  $\text{LuBa}_3\text{B}_3\text{O}_9$ ,  $\text{LuBa}_3\text{B}_9\text{O}_{18}$  and recently obtained  $\text{Lu}_5\text{Ba}_2\text{B}_5\text{O}_{17}$  (Hermus *et al.*, 2017),  $\text{Lu}_2\text{Ba}_3\text{B}_6\text{O}_{15}$  (Biryukov *et al.*, 2019) and  $\text{Lu}_5\text{Ba}_6\text{B}_9\text{O}_{27}$  (Filatov *et al.*, 2019). Partially substituted by Ce, Yb and Eu, the borates exhibit good and even excellent luminescence ( $\text{Lu}_2\text{Ba}_3\text{B}_6\text{O}_{15}:\text{Ce,Tb}$ ).

This work is devoted to synthesis of  $\text{Lu}_5\text{Ba}_6\text{B}_9\text{O}_{27}$  and  $\text{Lu}_2\text{Ba}_3\text{B}_6\text{O}_{15}$ , its structure determination from single-crystal, powder XRD data, investigation of thermal properties of these borates and  $\text{LuBa}_3\text{B}_9\text{O}_{18}$  using TG, DSC, HTXRD. The  $\text{Lu}_5\text{Ba}_6\text{B}_9\text{O}_{27}$  structure is composed of the  $\text{BO}_3$  triangles, the cubic  $\text{Lu}_2\text{Ba}_3\text{B}_6\text{O}_{15}$  is built from the  $\text{B}_2\text{O}_5$  groups,  $\text{LuBa}_3\text{B}_9\text{O}_{18}$  structure - from the  $\text{B}_3\text{O}_6$  groups. The thermal expansion is considered as a function of not only polyanions contribution but also of cations one.

This work was supported by the Russian Foundation For Basic Research (grant No. 18-29-12106).

## MS15-P12 | ANTIFERROELECTRIC PNMA PHASE: THE MISSING ELEMENT TO UNDERSTAND MORPHOTROPIC PHASE BOUNDARY LEAD-FREE $\text{Na}_{1/2}\text{Bi}_{1/2}\text{TiO}_3$ BASED PIEZOCERAMICS

hinterstein, Manuel (Karlsruher Institut für Technologie (KIT) Institut für Angewandte Materialien (IAM-KWT), Karlsruhe, GER); Haines, Julien (ICGM Université de Montpellier, Montpellier cedex 05, FRA); Hansen, Thomas (Institut Laue Langevin, Grenoble, FRA); Hermet, Patrick (ICGM Université de Montpellier, Montpellier cedex 05, FRA); Rouquette, Jerome (ICGM Université de Montpellier, Montpellier cedex 05, FRA)

$\text{Na}_{1/2}\text{Bi}_{1/2}\text{TiO}_3$  (NBT) perovskite ( $\text{ABO}_3$ ) are of interest due to their role as an end member of lead-free substitutes to replace the commercially dominant  $\text{PbZr}_{1-x}\text{Ti}_x\text{O}_3$ . NBT exhibits two phase transitions with decreasing temperature: from  $Pm-3m$  to  $P4bm$  and then  $R3c/Cc$ . With pressure, NBT is found to transform from  $R3c/Cc$  phase to  $Pnma$ . Here, we report high-pressure neutron diffraction combined with density functional perturbation theory (DFT) calculations on  $(\text{Na}_{1/2}\text{Bi}_{1/2}\text{TiO}_3)_{0.93}-(\text{BaTiO}_3)_{0.05}-(\text{K}_{0.5}\text{Na}_{0.5}\text{NbO}_3)_{0.02}$  which was chosen as i) it shows the  $P4bm$  structure at ambient temperature and ii) it exhibits optimal piezoelectric properties with a morphotropic phase boundary between  $P4bm$  and  $R3c$  phases.

The calculated full phonon dispersion relations obtained at the GGA level on a model  $\text{Na}_{1/2}\text{Bi}_{1/2}\text{TiO}_3$  compound clearly show three instabilities and support a  $P1$  triclinic ground state structure. With pressure, the tetragonal phase first transforms to  $R-3c$  at 2 GPa and then to antiferroelectric (AFE) ordered  $Pnma$  form close to 5 GPa. Large atomic displacement parameters (ADPs) for A-site perovskite atoms in the tetragonal phase are definitely associated to the high-pressure AFE symmetry whereas strong ADPs in the  $R-3c$  phase linked to density functional based calculations suggest a weakly polar  $P1$  phase. The existence of this AFE state permits to understand disagreements about the average structure and, based on group theory, validates the phase transition sequence in  $P-T$  space.

## MS15-P13 | HIGH PRESSURE X-RAY IMAGING AND DIFFRACTION ON THE PSICHÉ BEAMLINE: RECENT RESULTS AND DEVELOPMENTS USING LARGE VOLUME PRESSES

Itié, Jean-Paul (Synchrotron-soleil.fr, Gif-sur-Yvette, FRA); Deslandes, Jean-Pierre (Synchrotron SOLEIL, Gif-sur-Yvette, FRA); Guignot, Nicolas (Synchrotron SOLEIL, Gif-sur-Yvette, FRA); King, Andrew (Synchrotron SOLEIL, Gif-sur Yvette, FRA)

PSICH (Pressure Structure and Imaging by Contrast at High Energy) is a SOLEIL beamline based on a under vacuum multipole wiggler. Using the white beam, both x-ray diffraction and full field tomography can be performed on the beamline, independently or simultaneously on the same sample. The beamline is mainly dedicated to experiments under extreme conditions of pressure combined or not with high temperature using large volume presses (Multi-anvils, Paris Edinburg).

After a quick overview of the geometry of the beamline, the different experimental set-up which can be implemented in the white beam hutch of the beamline will be described, in particular the CAESAR set-up permanently installed on the beamline.

Then I will illustrate the possibilities of the beamline with few examples:

- Determination of the density of amorphous samples and liquids under pressure using pdf and/or 3D imaging
- Synthesis of new materials under high pressure and high temperature
- Observation of the iron  $\alpha - \gamma$  and  $\alpha - \epsilon$  phase transformations by combined 3D tomography and XRD in PE cells

Finally, I will show some recent developments which will improve the quality of the data and the rapidity of the acquisitions allowing some kinetic measurements.

## MS15-P14 | THE INFLUENCE OF [2+2] PHOTODIMERIZATION AND HIGH PRESSURE ON THE STRUCTURAL TRANSFORMATIONS IN CRYSTALS

Galica, Tomasz (Wroclaw University of Science and Technology, Wroclaw, POL); Turowska-Tyrk, Ilon (Wroclaw University of Science and Technology, Wroclaw, POL)

The [2+2] photodimerization in atmospheric pressure conditions has been widely studied by the crystallographic community. However, there are only few examples of experiments conducted at high pressure. Our research shows, on the example of crystals of seven compounds, how pressure influences the crystal structures and how it modifies the ongoing reaction. To induce the [2+2] photodimerization, UV radiation was used. The photoreaction was conducted in a step-by-step manner with the X-ray data collection after every irradiation. This allowed to obtain the structures of partly reacted crystals, *i.e.* the crystals containing both monomer and dimer molecules. The structural transformations and the influence of pressure on them and on the reaction rate were studied by means of monitoring (a) the unit cell parameters, (b) intermolecular geometry and (c) free space volume with the increase of product content. The results for all the compounds were compared with each other. The applied pressure not only modified the crystal lattice, but also restrained the structural changes caused by the photoreaction.

## MS15-P15 | IN-SITU SINGLE CRYSTAL X-RAY DIFFRACTION STUDIES OF PROTON TRANSFER BEHAVIOUR UNDER AN APPLIED ELECTRIC FIELD ON I19, DIAMOND LIGHT SOURCE

Saunders, Lucy (Diamond Light Source, Oxford, GBR); Warren, Mark (Diamond Light Source, Didcot, GBR); Yeung, Hamish (University of Oxford, Oxford, GBR); Simonov, Arkadiy (ETH Zürich, Zürich, CH); Coates, Chloe (University of Oxford, Oxford, GBR); Allan, Dave (Diamond Light Source, Didcot, GBR)

Hydrogen atoms (H-atoms) can exhibit the chemical phenomenon of transfer behaviour when part of a hydrogen bond (HB). This behaviour occurs related to the shape of the potential energy surface for H-atom motion for certain types of hydrogen bonds. Depending on HB characteristics, this transfer may be susceptible to external stimuli, such as temperature or pressure [1]. In ferroelectrics, proton shuttling may occur under an applied electric field facilitating the reversal of material polarity [2] or transitions between electric (ferro-para) states [3]. Materials such as these are of interest offering applications in sensing and data storage.

The electric properties of materials are typically determined from measuring dielectric constants [4] or polarisation-electric field loops [5] whilst structural effects can be elucidated using Bragg peak mapping [6]. In this work, we showcase a new electric field set up on I19, Diamond Light Source (U.K.) for in-situ single crystal X-ray diffraction measurements allowing full structure elucidation under an applied field. We describe the set-up and explore its potential in the study of proton transfer behaviour with the aim of discovering new candidates for electric field applications.

[1] D.M.S.Martins *et al.*, *J.Am.Chem.Soc.*, 2009, **131**, 3884-3893.

[2] I.A. Abronin, I.A.Koval'chuk and V.P.Sakun, *Russ.J.Phy.Chem.B*, 2016, **10**, 357-359.

[3] Z.-S.Yao *et al.*, *J.Am.Chem.Soc.*, 2016, **138**, 12005-12008.

[4] S.Horiuchi *et al.*, *Nat.Mater.*, 2005, **4**, 163.

[5] S.Horiuchi, R.Kumai and Y.Tokura, *J.Am.Chem.Soc.*, 2013, **135**, 4492-4500.

[6] H.Choe *et al.*, *J.Appl.Crystallogr.*, 2017, **50**, 975-977.

## MS15-P16 | OXIDES UNDER EXTREME CONDITIONS: PUSHING THE LIMITS OF NEUTRON

### DIFFRACTION

Capone, Mara ( ISIS STFC, University of Edinburgh, ESS, Didcot, GBR); Ridley, Christopher (ISIS STFC, Didcot, GBR); Funnell, Nicholas (ISIS STFC, Didcot, GBR); Loveday, John (University of Edinburgh, Edinburgh, AUT); Guthrie, Malcolm (European Spallation Source, Lund, SWE); Bull, Craig (ISIS STFC, Didcot, GBR)

The  $\text{LaCo}_x\text{Mn}_{1-x}\text{O}_3$  perovskite series has been widely studied as responses to chemical composition or volume give rise to a variety of electrical and magnetic properties [1]. Volume changes can be induced by the application of pressure, which can be used to study structural-property relationships. High-pressure neutron-diffraction experiments have been performed on  $\text{LaCo}_{0.9}\text{Mn}_{0.1}\text{O}_3$  and  $\text{LaCoO}_3$  powders. Neutron powder diffraction is essential to determine the structure of perovskite-like oxides. The high-pressure structural evolution of  $\text{LaCo}_{0.9}\text{Mn}_{0.1}\text{O}_3$  will be presented [2]. The change in tilting angle and strain has been determined upon pressure. This study complements high-pressure magnetisation measurements, where the Curie temperature shows a strong dependence on applied pressure. A structural study of  $\text{LaCoO}_3$  as a function of pressure and temperature using neutron diffraction will also be presented [3]. This study is of great interest for its unique temperature-dependent electronic properties. The aforementioned experiments have been carried out on the PEARL instrument, the high-pressure-dedicated diffractometer at ISIS, STFC [4]. We are developing new pressure cells for neutron diffraction to extend the maximum achievable pressure at ISIS.

- [1] C. Autret *et al*, 2005, J. Phys, Condens. Matter 17, 1601;
- [2] C. Capone *et al*, 2018, J. Phys. Condens. Matter 30, 035402;
- [3] M. Capone *et al*, 2019, Physica Status Solidi A, 1800736;
- [4] C. Bull *et al*, 2016, High Press. Res. 36, 493.

## MS15-P131 - LATE | THERMAL EXPANSION OF ALLUAUDITE GROUP MINERALS (NICKENICHITE AND CALCIOJHILLERITE)

Shablinskii, Andrey (Grebenshchikov Institute of Silicate Chemistry, Russian Academy of Sciences, St. Petersburg, RUS); Filatov, Stanislav (Dept. of Crystallography, Institute of Earth Sciences, St. Petersburg State University, St. Petersburg, RUS); Vergasova, Lidiya (Institute of Volcanology and Seismology, Russian Academy of Sciences, Petropavlovsk-Kamchatsky, RUS)

The alluaudite group minerals and compounds are prospective materials for cathodes of sodium batteries [1-2].

Specimens of two minerals of this group (nickenichite and calciojhillerite) were collected at Tolbachik Volcano, Kamchatka Peninsula, Russia [3]. The crystal structure consists of chains of  $MO_6$  octahedra connected by the edge, which are parallel [10-1]. The  $AsO_4$  tetrahedra link these chains into layers in the  $ac$  plane. The layers are combined into a framework, containing two types of channels parallel [001].

Thermal expansion of minerals is anisotropic: the maximum one is close to the  $a$  axis, the minimal – to the small diagonal of the parallelogram  $ac$ . The main values of tensors at 25 °C:  $\alpha_{11}=13.7(2)$ ,  $\alpha_{22}=9.0(1)$ ,  $\alpha_{33}=3.2(1)\times 10^{-6}$  °C<sup>-1</sup> for nickenichite;  $\alpha_{11}=13.6(3)$ ,  $\alpha_{22}=9.9(2)$ ,  $\alpha_{33}=2.9(1)$  ×°C<sup>-1</sup> for calciojhillerite. The thermal expansion can be caused by the straightening of the corrugation of layers, and the result is that the channels size is suitable for ionic conductivity increase. Insignificant bending is observed on the temperature dependences of the cell parameters at 300 °C. These temperatures correspond to the beginning of the “order-disorder” process and are consistent with the data on ionic conductivity.

The studies were supported RFBR project №18-29-12106. Experiments were performed at SPSU Research Center for XRD studies.

[1] Ennajeh I., Georges S., Ben Smida Y. et al. RSC Adv. 5 (2015) 38918.

[2] Dridi W., Zid M.F. Acta Cryst. E72 (2016) 1103.

[3] Filatov S.K., Krivovichev S.V., Vergasova L.P. J. Volcanology and Seismology. 12 (2018) 388.

## MS15-P133 - LATE | THERMAL EXPANSION OF ALKALINE-EARTH BORATES

Bubnova, Rimma (Grebenshchikov Institute of Silicate Chemistry, Russian Academy of Sciences, Saint Petersburg, RUS); Yukhno, Valentina (Grebenshchikov Institute of Silicate Chemistry, Russian Academy of Sciences, St. Petersburg, RUS); Krzhizhanovskaya, Maria (Dept. of Crystallography, Institute of Earth Sciences, St. Petersburg State University, St. Petersburg, RUS); Filatov, Stanislav (Dept. of Crystallography, Institute of Earth Sciences, St. Petersburg State University, St. Petersburg, RUS)

Here we present the results of investigation of thermal expansion of Ca-borates ( $\text{Ca}_3\text{B}_2\text{O}_6$ ,  $\text{Ca}_2\text{B}_2\text{O}_5$ ,  $\text{CaB}_2\text{O}_4$ ,  $\text{CaB}_4\text{O}_7$ ) in comparison to that of Mg-, Sr- and Ba-borates [1–4]. Tendency of decrease in the volume expansion as well as high decrease of the melting points is observed with an increase in the  $\text{B}_2\text{O}_3$  content in the  $\text{MO}-\text{B}_2\text{O}_3$  systems ( $\text{M} = \text{Ca}, \text{Sr}, \text{Ba}$ ) as a result of the degree of polymerization increase. Average value of volume expansion increases gradually from 34 (Ca) to 42 (Ba)  $\times 10^{-6} \text{ K}^{-1}$  due to increase of the  $\text{M}^{2+}$  size. In the  $\text{M}_3\text{B}_2\text{O}_6$  ( $\text{M} = \text{Mg}, \text{Ca}, \text{Sr}$ ) stoichiometry,  $\text{Mg}_3\text{B}_2\text{O}_6$  borate expands the weakest ( $\alpha_V = 30 \times 10^{-6} \text{ K}^{-1}$ ).

High anisotropy of the expansion is observed for  $\text{M}_3\text{B}_2\text{O}_6$ ,  $\text{M}_2\text{B}_2\text{O}_5$  (0D) and  $\text{MB}_2\text{O}_4$  (1D) based on the  $\text{BO}_3$  triangles only ( $\text{M} = \text{Ca}$  and  $\text{Sr}$ ): the structure highly expands perpendicular to the  $\text{BO}_3$  planes, i. e. along the direction of the weaker bonds in the crystal structure.  $\text{M}_2\text{B}_2\text{O}_5$  monoclinic polymorphs expand maximally anisotropically due to shear deformations of monoclinic plane.

High-temperature powder X-ray diffraction experiments were performed in Saint-Petersburg State University Research Centre for XRD Studies. The study was supported by the Russian Foundation for Basic Research (No. 18-03-00679).

[1] Filatov S.K. *et al.* Struct. Chem. (2016) **27**, 1663.

[2] Bubnova R. *et al.* Crystals (2017) **7**, 93.

[3] Volkov S. *et al.* Acta Cryst. (2017) **B73**, 1056.

[4] Firsova V.A. *et al.* Glass Phys. Chem. (2019) **45**, 305.

## MS16: Structural Characterization of Functional Materials

---

### MS16-01 | POLYMORPHISM IN SESQUIOXIDES OF LATE GROUP-15: WORK UNDER PRESSURE

Sans, Juan Angel (Technical University of Valencia, Valencia, ESP)

Elements belonging to the group 15 are usually associated to the toxic properties of arsenic. These hazardous elements are chemical wastes of refining metals and contribute to the environmental pollution. The exploitation of these elements in functional materials will partially solve this problem. Thus, the aim of this work will be to study the different polymorphs of sesquioxides formed by group 15 elements (As, Sb and Bi) applying high pressure in order to better understand the intrinsic properties of these materials.

Among all the possible polymorphs,  $\alpha$ -As<sub>2</sub>O<sub>3</sub> crystallizes in a cubic structure with strong molecular character being one of the most compressible solid inorganic compounds. In turn, isostructural  $\alpha$ -Sb<sub>2</sub>O<sub>3</sub> shows two 2<sup>nd</sup>-order phase transitions driven by dynamical instabilities below 10 GPa. The completely different behavior of both compounds with the same structure points out that the lone electron pair effect could play an important role in the presence of slight changes of compressibility. Intermediate symmetric structures such as orthorhombic  $\beta$ -Sb<sub>2</sub>O<sub>3</sub> and tetragonal  $\beta$ -Bi<sub>2</sub>O<sub>3</sub> seem to be more prone to undergo anomalous compressibility. Finally,  $\alpha$ -Bi<sub>2</sub>O<sub>3</sub> crystallizes in a monoclinic structure with the smaller cationic lone electron pair effect.

In summary, this work will show some guidelines in the stability of sesquioxide polymorphs and how the stereochemically active lone electron pair distribution affects the stability of the different structures, paying special attention on the intermediate symmetric structures where the most striking results have been observed.

## MS16-02 | IN SITU METHODS FOR THE ANALYSIS OF FUNCTIONAL MATERIALS

Weidenthaler, Claudia (Max-Planck-Institut für Kohlenforschung, Mülheim an der Ruhr, GER)

Monitoring materials under non-ambient conditions opens up possibilities to gain detailed insights how materials behave under reaction conditions. The variety of analytical tools which are nowadays available for *in situ* or operando studies is as wide as the types of reactions which can be investigated. The combination of diffraction methods with spectroscopy enables deep insights into structural but also compositional changes during crystallization or chemical reactions. It will be shown that the use of in-house diffraction equipment can provide detailed insight into structure and microstructure changes. *In situ* diffraction data contain not only useful information on the averaged crystal structures but also on changes of local structures. The talk we will focus mainly on the design of *in situ* diffraction experiments performed under variable temperatures (between 100 K and 1000 K), elevated gas pressures, adjustable reaction gas atmospheres, or mechanochemical reaction conditions. The materials which will be presented cover hydrogen storage materials as well as inorganic catalysts, or materials used for electrochemical applications. Hydrogenation studies performed with in-house diffractometers at variable temperatures and hydrogen pressures require the construction of tailor-made sample environments. Reactions with ammonia as hydrogen carrier are challenging due to experimental restrictions. Temperature dependent crystallization studies of Pt-based electrocatalysts from the precursors to the alloys represent a combination of crystal structure refinement and atomic pair distribution analysis.

## MS16-03 | IMPACT OF INTENSE ELECTRIC FIELDS ON THE STRUCTURE OF CENTROSYMMETRIC RELAXOR FERROELECTRIC $\text{Sr}_{0.85}\text{Pr}_{0.15}\text{TiO}_3$

Cecchia, Stefano (University of Milan, Milan, ITA); Cabassi, Riccardo (CNR-IMEM, Parma, ITA); Allieta, Mattia (University of Milan, Milan, ITA); Coduri, Mauro (ESRF - The European Synchrotron, Grenoble, FRA); Giacobbe, Carlotta (ESRF - The European Synchrotron, Grenoble, FRA); Scavini, Marco (University of Milan, Milan, ITA)

Crystallography under electric field (EF) has been recently applied to reveal macroscopic and microscopic structural response of ferroelectric functional materials to intense EF. Here we focus on the effect of applied EF on the structure of a relaxor ferroelectric oxide. While in classic ferroelectrics clear signatures of polar distortion instabilities allow straightforward interpretation of diffraction data in terms of increased electric dipole moment, the centrosymmetric structure of relaxor ferroelectrics inhibits long-range polarization. However, their susceptibility to distortion under EF points to local polar fluctuations and structural changes.

We present the case of Pr-doped strontium titanate ( $\text{Sr}_{0.85}\text{Pr}_{0.15}\text{TiO}_3$ ). Its structure shows high-temperature stabilization of the centrosymmetric antiferrodistortive (AFD) tetragonal phase observed in  $\text{SrTiO}_3$  below 105 K. The structural modifications induced by applied EF were studied by synchrotron high-resolution diffraction combined with Pair Distribution Function analysis. EF induces inhomogeneous strain and preferential orientation. Concomitant increases of tetragonal strain and octahedral  $\text{TiO}_6$  tilting angle do not break the initial long-range centrosymmetry. Conversely, PDF reveals that Ti is off-centered within its octahedral cage already at zero field, forming polar regions spanning up to 2 nm. The electric field enhances polarization within the polar nanoregions with no effect on their size, suggesting that they are pinned to charged defects introduced by Pr-doping. The large tetragonal strain found at the local scale may contribute to the ordering of the tilting angle at larger scales. This may imply a coupling between the local ferroelectric and the long-range AFD instabilities.

## MS16-04 | STRUCTURAL CONTROL OF THERMOMECHANICAL PROPERTIES OF MONOCLINIC RARE-EARTH CALCIUM OXOBORATES

Münchhalfen, Marie (Ruhr University Bochum, Bochum, GER); Schreuer, Jürgen (Ruhr University Bochum, Bochum, GER); Reuther, Christoph (Freiberg University of Mining and Technology, Freiberg, GER); Mehner, Erik (Freiberg University of Mining and Technology, Freiberg, GER); Stöcker, Hartmut (Freiberg University of Mining and Technology, Freiberg, GER)

Monoclinic rare-earth calcium oxoborates (*RCOB*),  $RCa_4O(BO_3)_3$  recently gathered interest as candidates for high-temperature piezoelectric sensing applications since they combine favorable properties like high melting point at around 1770 K, no reported structural phase transitions, high piezoelectric sensitivity and high electric resistivity. Since the *RCOB* structure offers different possibilities for cation substitution, tuning of physical properties is principally possible.

Large single crystals of *RCOB* ( $R = \text{Er, Y, Dy, Gd, Sm, Nd, La}$ ) were grown from melt using the Czochralski method. Their structural properties were studied at ambient conditions on as cast and on annealed and subsequently quenched samples using X-ray diffraction methods. Dilatometry and resonant ultrasound spectroscopy were employed to investigate their thermo- and electromechanical properties between 100 K and 1473 K.

Substitution of rare earth cations with larger size leads to a decrease in the bulk modulus, whereas the maximum value of the piezoelectric effect increases. Contrary to the reported lack of phase transitions, the investigated physical properties undergo reproducible discontinuities between 900 K and 1300 K which are characteristic for a glass-like transition. Structural investigations indicate a correlation with dynamic disorder of  $R$  and  $\text{Ca}$  on the independent cation sites at higher temperatures. The transition temperature as well as the specific type of disorder are both related to size of the rare earth ion.

Acknowledgments: The authors gratefully acknowledge financial support of the DFG (PAK921/1, SCHR761/4: Structure/property relationships and structural instabilities of high-temperature piezoelectrics of the oxoborate family).

## MS16-05 | MEAD, SALT, AND SUNSHINE: CATION DISTRIBUTION IN CZTSE, CFTS, AND CZSISE

Többens, Daniel (Helmholtz-Zentrum Berlin (HZB), Berlin, GER); Gurieva, Galina (Helmholtz-Zentrum Berlin, Berlin, GER); Niedenzu, Sara (Helmholtz-Zentrum Berlin, Berlin, GER); Schuck, Götz (Helmholtz-Zentrum Berlin, Berlin, GER); Zizak, Ivo (Helmholtz-Zentrum Berlin, Berlin, GER); Schorr, Susan (Helmholtz-Zentrum Berlin, Berlin, GER)

Multiple Edge Anomalous Diffraction (MEAD) [1] has been applied to various quaternary sulfosalts belonging to the adamantine compound family in order to validate the distribution of copper, zinc, and iron cations in the structure. Semiconductors from this group of materials are promising candidates for photovoltaic applications. Their properties are strongly dependent on point defects, in particular related to cation order-disorder. However,  $\text{Cu}^{+1}$ ,  $\text{Zn}^{2+}$ , and  $\text{Fe}^{2+}$  have very similar scattering factors and are all but undistinguishable by normal X-ray diffraction. Anomalous diffraction utilizes the dependency of the atomic scattering factors  $f$  and  $f'$  from the energy of the radiation, especially close to the element-specific absorption edges. In the technique called MEAD individual Bragg peaks are tracked over an absorption edge. The intensity changes depending on the structure factor can be highly characteristic for Miller indices selected for a specific structural problem, but require very exact measurements. Beamline KMC-2 [2] at synchrotron BESSY II, Berlin has been recently upgraded for this technique. Anomalous X-ray powder diffraction and EXAFS complement the data.

[1] B. A. Collins *et al.*: *Physical Review B* **92**, 224108 (2015)

[2] Helmholtz-Zentrum Berlin für Materialien und Energie: *J Large-scale research facilities*, **2**, A49 (2016)

## MS16-P01 | SHORT-RANGE STRUCTURE OF Zr AND Pd BULK METALLIC GLASSES PREPARED DURING THE MELTING AND COOLING PROCESS

Frison, Ruggero (Empa, Swiss Federal Laboratories for Materials Science and Technology, Center for X-Ray Analytics, Dübendorf, CH); Dommann, Alex (Empa, Swiss Federal Laboratories for Materials Science and Technology, Center for X-ray Analytics, Dübendorf, CH); Neels, Antonia (Empa, Swiss Federal Laboratories for Materials Science and Technology, Center for X-ray Analytics, Dübendorf, CH)

Bulk metallic glasses (BMGs) represent a class of materials with superior mechanical properties that combine a high mechanical strength (about 2 GPa) and a 5 – 10 times higher elastic strain limit (1.5 – 2 %) in comparison with conventional metals [1,2]. BMGs undergo, however, catastrophic failure when deforming beyond the elastic strain limit. The macroscopic brittleness is the result of strain localization in shear bands. For the improvement of BMG formation and processing, a thorough understanding of the crystallization kinetics is required as well as refined models of crystal nucleation from the undercooled liquid.

By means of in-situ X-ray total scattering experiments, we obtained statistically reliable data on atomic pair-pair correlation functions that is about the local structure of the Zr and Pd based BMG systems, which allowed us to estimating the bond length, the average coordination number, and the free volume, a parameter that correlates the structure with the glass forming ability [3] and mechanical properties [4]. We correlated the results about the local structure with complementary tomographic scans, allowing the pore structures of the BMG to be visualized, and with measurements on mechanical properties, thus providing a multi-scale physical picture of the investigated BMG system.

[1] W.H. Wang, et al., *Materials Science and Engineering R: Reports*, 44(2), 45-89, (2004).

[2] M. Mohr, et. al., *NPJ Microgravity* 2019, 2019, 5(1), 4, 1-8.

[3] Q. Hu, et. al., *J. Appl. Phys.* **109**, 053520 (2011).

[4] J. Tan, et al., *Appl. Phys. Lett.* **98**, 151906 (2011).

## MS16-P02 | PURE GYROTROPIC FERROELASTIC PHASE TRANSITIONS IN THE MATERIALS

### PbMXO<sub>4</sub> (M = BA, SR; X=SI,GE): A NEW PIEZOELECTRIC FAMILY

Prugovecki, Stjepan (Malvern Panalytical B.V., Almelo); Nenert, Gwilherm (Malvern Panalytical B.V, Almelo); Zhang, Weiguo (University of Houston, Huston, USA); Halasyamani, Shiv (University of Huston, Huston, USA)

Gyrotropic phase transitions are characterized by the appearance of a spontaneous optical activity [1]. The appearance of such activity is very common in ferroelectric materials. In such materials, the optical activity is a secondary order parameter and is coupled to the primary order parameter which is the electrical polarization. However, only very rare examples are known of a pure gyrotropic phase transition.

In this contribution, we have investigated materials belonging to the BaNdGaO<sub>4</sub> structural type (space group P2<sub>1</sub>2<sub>1</sub>2<sub>1</sub>), of general formula PbMXO<sub>4</sub> (M= Sr, Ba; X = Si, Ge) using powder X-ray diffraction as function of temperature, second harmonic generation and piezoelectric properties. We present extensive studies on PbMGeO<sub>4</sub> and preliminary results on the Si doped systems. PbSrGeO<sub>4</sub> shows a 2<sup>nd</sup> order type phase transition towards a Pnma structure with metrically hexagonal phase. On the contrary, PbBaGeO<sub>4</sub> exhibits a first order phase transition, similarly to (C<sub>5</sub>H<sub>11</sub>NH<sub>3</sub>)<sub>2</sub>ZnCl<sub>4</sub>, however with a phase competition between the high and low temperature phases over almost 200°C.

Second harmonic generation and investigation of the piezoelectric properties demonstrated that this family is a new playground for new non-linear optical materials and identify the BaNdGaO<sub>4</sub> structural type as a new source for pure gyrotropic materials.

[1] C. Konak, V. Kopsky, F. Smutny; J. Phys. C: Solid State Physics 11, 2493 (1978)

[2] S. Prosandeev, I. A. Kornev, L. Bellaiche; Phys. Rev. Lett. 107, 117602 (2011)

## MS16-P03 | STRUCTURE DESIGN OF NOVEL $\text{Ba}_{3-x}\text{Sr}_x\text{TeO}_6$ DOUBLE PEROVSKITES AND THE EFFECT OF TEMPERATURE AND COMPOSITION ON STRUCTURE STABILITY

EL BACHRAOUI, Fatima (University Mohammed VI polytechnic / University Hassan 1, Benguerir, MAR); TAMRAOUI, Youssef (University Mohammed VI polytechnic, Benguerir, MAR); LOUHI, Said (University Hassan 1, Settlat, MAR); SAADOUNE, Ismael (University Mohammed VI polytechnic / Cadi Ayyad University, Marrakech, MAR); ALAMI, Jones (University Mohammed VI polytechnic, Benguerir, MAR); LAZOR, Peter (Uppsala University, Uppsala, SWE); MANOUN, Bouchaib (University Hassan 1 / University Mohammed VI polytechnic, SETTAT, MAR)

Double perovskite structure typically has the chemical formula  $\text{A}_2\text{BB}'\text{O}_6$ . Depending on the elements residing at A and B sites, different crystalline structures are possible. Fundamental understanding of the structure stability and phase transitions of these materials, under different synthesis conditions, is very important for optimizing the physical properties [1, 2].

In the present study, the mechanisms of self-doping together with continuous composition modulation in the  $\text{Ba}_{3-x}\text{Sr}_x\text{TeO}_6$  ( $0 \leq x \leq 3$ ) system are investigated. The structure stability and phase transition of compounds are studied using X-ray diffraction, and Raman spectroscopy at ambient and elevated temperatures. At ambient temperature, a systematic structure transition ( $I41/a \rightarrow R-3m \rightarrow R-3 \rightarrow R-3m \rightarrow C1$ ) was determined, with  $x$  increasing from 0 to 3. At elevated temperatures (up to 570 °C) all structures tend to merge to the single cubic phase  $Fm-3m$ , indicating an expanded bonding length and a greater atomic thermal motion. The optical properties of the  $\text{Ba}_{3-x}\text{Sr}_x\text{TeO}_6$  ( $0 \leq x \leq 3$ ) system were part of the paper objective in investigating the substitution effect on the optical response. The optical properties of the compounds were significantly dependent to the symmetry change in the system and a shrink in the band gap energy values was observed as the amount of the strontium increase.

[1] Nielsen KK, Engelbrecht K, Andersen K. 2012;(May 2014). doi:10.1063/1.3695338

[2] Tamraoui Y, Manoun B, Mirinioui F, et al. J Mol Struct. 2017;1131.

## MS16-P04 | PEROVSKITE $\text{BaTiO}_3$ DOPED WITH PYROCHLORE BISMUTH ZINC NIOBATE - A NEW PEROVSKITE RELAXOR FERROELECTRIC BZN-BT

Thomas, Pamela (University of Warwick, Coventry, GBR); Marshall, Jessica (University of Warwick, Coventry, GBR); Walker, David (University of Warwick, Coventry, GBR)

The novel perovskite lead-free ferroelectric relaxor system  $\text{Bi}_{1-y}(\text{Zn}_{1/3} \text{Nb}_{2/3})_x\text{O}_3\text{-Ba}_y\text{Ti}_{(1-x)}\text{O}_3$  (BZN-xBT), has been investigated in a range of compositions from  $x=0$  to  $x=0.2$  using x-ray powder diffraction, SEM, dielectric and piezoelectric measurements. Studies of bulk-ceramic samples revealed a maximum in the piezoelectric coefficient  $d_{33}$  of  $120 \text{ pC N}^{-1}$  at  $x=0.038$  together with a coercive field of  $E_c = 9.3 \text{ kV cm}^{-1}$ . Powder x-ray diffraction studies in the temperature range from 295K to 20K show this system having considerable polar phase coexistence with the highest  $d_{33}$  correlating with dominance of the monoclinic phase at room temperature. The tetragonal perovskite structure characteristics of BT at room temperature disappears between  $x=0.06$ - $0.07$ .

Low-temperature x-ray powder diffraction studies in the range 295-20K indicate a BT-like sequence of phase transitions from tetragonal-orthorhombic-rhombohedral for  $x=0$  to  $x=0.04$ . Beyond  $x=0.04$ , the rhombohedral phase no longer appears. Appearance of a potential Morphotropic Phase Boundary (MPB) is signalled by the collapse of the tetragonal  $c_T/a_T$  ratio near  $x=0.045$ , which ratio then shows relative invariance with temperature over the whole interval. Above  $x=0.07$ , after the tetragonal phase has been eliminated at room temperature, BZN-BT appears as essentially an almost invariant mixture of monoclinic (Cm) and orthorhombic (Amm2) phases at all temperatures measured,

Piezoelectric coefficients showed a rapid decline for  $x > 0.039$  at 295K. For  $0.045 < x < 0.08$ , the materials are lossy dielectrics ( $T_m \sim 295\text{K}$ ) and potentially candidate electrocalorics.

## MS16-P05 | ENVIRONMENTAL EFFECT ON TITANIUM ALLOY Ti6242S IN AIR BETWEEN 500 AND 700 °C

Kalienko, Maksim (Ural Federal University, Ekaterinburg, RUS)

After a long period at high temperature (>500°C) titanium alloys present some embrittlement in the form of absence of surface thermal stability. The environmental behavior of Ti6242S alloy was studied in air between 500 and 700 °C by optical microscopy, scanning electron microscopy, microhardness measurements and X-ray diffraction. The X-ray diffraction analysis was used to study the effect of the oxygen solid solution on the lattice parameters of Ti6242S alloy near the oxide/metal interface. It was found that unit cell lattice parameters of oxygen enriched layer depend on exposure time and temperature. These results indicate that the oxidation mechanism depends on the oxide scale structure and oxygen diffusion process.

## MS16-P06 | FORBIDDEN/NON-FORBIDDEN BRAGG REFLECTIONS STUDY UNDER PHASE TRANSITIONS AND EXTERNAL INFLUENCES

Ovchinnikova, Elena (M.V.Lomonosov Moscow State University, Moscow, RUS); Dmitrienko, Vladimir (A.V. Shubnikov Institute of Crystallography, FSRC "Crystallography and Photonics" RAN, Moscow, RUS); Zchornak, Matthias (Inst. of Experimental Physics IEP, TU Bergakademie Freiberg TUBAF, Freiberg, GER); Oreshko, Alexey (M.V.Lomonosov Moscow State University, Moscow, RUS); Kozlovskaya, Ksenia (M.V.Lomonosov Moscow State University, Moscow, RUS)

A method has recently been developed that demonstrates a record sensitivity to atomic displacement, which uses a study of the energy dependence near the absorption edges of weak Bragg reflections [1]. In this method, the anisotropic properties of resonant X-ray scattering are neglected. However, the resonant anisotropic contribution to the scattering amplitude always exists, although it is small compared with charge scattering.

We propose to use polarization analysis to study the resonant scattering of  $\sigma$ -polarized radiation into  $\pi$ -polarization in allowed reflections. The  $\sigma$ - $\pi$  channel is not forbidden in resonant X-ray scattering close to the absorption edges, in contrast to the conventional Thomson scattering. The study of this scattering channel can provide additional information when studying phase transitions and the effects of external influences on crystals. For example, in [1], the applied electric field caused a phase transition in  $\text{SrTiO}_3$  from the phase with cubic symmetry  $\text{Pm}\bar{3}\text{m}$  to the phase of an MFP with symmetry  $\text{P}4\text{mm}$ . In the studied reflection 007 there is no scattering channel  $\sigma$  -  $\pi$ , but it exists, for example, in reflections  $h0l$ . In the  $\text{Pm}\bar{3}\text{m}$  space group, this is ensured only by dipole-quadrupole resonance scattering, but in the MFP phase, a stronger dipole-dipole resonant  $\sigma$ - $\pi$  scattering channel is possible. Therefore, this phase transition can be observed as a jump in the reflection intensity using  $\sigma$ -polarized synchrotron radiation and a polarization analyser.

This work is supported by the grant DFG-RFBR n. 19-052-12029.

[1] C. Richter, et al., Nature Communications. V. 9, p. 178 (2018).

## MS16-P07 | CRYSTAL STRUCTURE AND DEHYDRATION BEHAVIOR OF $\text{Ag}^+$ -EXCHANGED LEVYNE

Cametti, Georgia (University of Bern, Bern, CH); Scheinost, Andreas (The Rossendorf Beamline at the European Synchrotron Radiation Facility (ESRF), Grenoble, FRA); Churakov, Sergey (Bern University, Bern, CH)

The crystal structure and dehydration behavior of a natural zeolite, levyne, exchanged with  $\text{Ag}^+$  was investigated by combining *in situ* Single Crystal X-ray Diffraction (SCXRD), X-ray Absorption Spectroscopy (XAS) and Molecular Dynamics (MD) simulations.

At room temperature, structure solution indicated the space group  $R-3m$ . The latter corresponds to the space group of the natural levyne-Ca. However, in contrast to the pristine material,  $\text{Ag}^+$ -levyne is not twinned by merohedry. The  $\text{Ag}^+$  ions are highly disordered on partially occupied sites distributed along the three-fold axis and in the middle of the 8-membered ring window of the *lev* cage. The analysis of pseudo-radial distribution function calculated from XAS data and MD simulations shows that silver is on average coordinated by five oxygen with distances between 2.44 and 2.80 Å.

The thermal stability was investigated by SCXRD from 25 to 400°C. The dehydration starts at 50°C. At 100°C the space group changes from  $R-3m$  to  $R-3$ . At 250°C new sites, close to the tetrahedral sites T1 and T3, appear, indicating the onset of the rupture of the T1-O2-T3 and T1-O3-T3 connections forming the double six-ring cage. At 300°C the percentage of the broken bridges converge to 13% and the new links T1B-OB1-T3B and T1B-OB2-T3B form. Differently from the natural levyne-Ca no additional T-O-T connection breaks up to 300°C. From 350°C to 400°C the intensity of the reflections significantly dropped and only the cell parameters were extracted. The total unit-cell volume contraction in the investigated temperature range is 4%.

## MS16-P08 | LATTICE CONSTANTS PREDICTION AND THERMOCHEMISTRY OF HEXAHALOMETALLATE $A_2MX_6$

Hadda, Krarcha (Primalab univ batna1, Batna, DZA)

In this study we describes the attention of lattice parameters of hexahalometallate  $A_2MX_6$  salts in cubic structure  $Fm\bar{3}m$ . Mail parameters received from recent experimental studies are investigated for 87 compounds to obtain a linear prediction formula depending on ionic radius and electronegativity of constituents. A good agreement between the experimental and predicted lattice constants is found with an average error less than 1.6 % only. First principles calculations of enthalpies of formation is presented using GGA approximations.

It was shown that the lattice constant is a linear function of the Enthalpy of formation

## **MS16-P09 | INVESTIGATION OF PHYSICAL PROPERTIES OF EQUIATOMIC SILVER-RARE EARTH COMPOUNDS Ag-Re (RE=Nd, Ce, Gd) FROM FIRST PRINCIPLES CALCULATIONS.**

Abdelhak, Ferroudj (LEPCM laboratory, batna, DZA)

Density functional theory (DFT) within generalized gradient approximation (GGA) pseudo-potentials and plane waves basis VASP (Vienna ab initio Software Package) are used to investigate physical properties of silver-rare earth equiatomic binary alloys Ag-Re (Re=Gd, Nd, Ce). Elastic properties have been computed and showed that these compounds have the strongest alloying ability and structural stability. A much better agreement was achieved between the mechanical properties calculated results and the reported experimental data.

## MS16-P10 | $\text{LiTaO}_3$ DEFECT STRUCTURES BY MEANS OF FORBIDDEN REFLECTIONS

Nentwich, Melanie (TU Bergakademie Freiberg, Freiberg, GER); Weigel, Tina (TU Bergakademie Freiberg, Freiberg, GER); Zschornak, Matthias (TU Bergakademie Freiberg, Freiberg, GER); Richter, Carsten (Leibniz-Institut für Kristallzüchtung, Berlin, AUT); Köhler, Thomas (TU Bergakademie Freiberg, Freiberg, GER); Mehner, Erik (TU Bergakademie Freiberg, Freiberg, GER); Novikov, Dmitri (DESY, Hamburg, GER); Meyer, Dirk C. (Tu Bergakademie Freiberg, Freiberg, GER)

A wide range of optical and electrical applications of lithium tantalate  $\text{LiTaO}_3$  (LTO) is closely related to its defect chemistry. Most of the defects are correlated with Li deficiency in congruent  $\text{Li}_{1-5x}\text{Ta}_5\text{O}_3$  (C-LTO). Near stoichiometric (NST-LTO) samples can be grown by the double-crucible Czochralski method with larger effort. Here, we present an investigation of C- and NST-LTO in dependence of temperature using *Resonant X-ray Diffraction* (RXD) at "forbidden" reflections, giving insights into their defect chemistry. In literature, several intrinsic defect models have been suggested [10.1103/PhysRevMaterials.2.013804], which will be correlated with the energy and azimuthal dependence of the RXD.

Resonant X-ray diffraction offers powerful characterization techniques to study atomic displacements [10.1038/s41467-017-02599-6] and the local electronic structure of selected atomic positions in crystals [10.1002/crat.201300430]. In particular spectra of "forbidden" reflections only exist in the vicinity of absorption edges due to the anisotropy of electronic transitions. These "forbidden" reflections are highly sensitive to displacements of the resonant atom and, hence, to defects and vibrations. Temperature dependence allows for separation of contributions to the reflection intensity induced by thermal motion and by point defects. The obtained spectra can be modelled from first principles, using the structural information of stoichiometric LTO lattice and defect models. The "forbidden" reflections of stoichiometric LTO have no contributions of the electronic dipole transitions, therefore transitions of higher order need to be considered, the calculation of which are theoretically highly sophisticated. For instance, FDMNES can calculate these contributions and, hence, allows the numeric modelling of the experimental data.

## MS16-P11 | MORINGA OLEIFERA WASTE AS DOPANTS FOR S, N, C-TiO<sub>2</sub> PHOTOCATALYSTS

### DEVELOPMENT

AGBAHOUNGBATA, Marielle Yasmine (University of Zurich, Zürich, CH); LINDEN, Anthony (University of Zurich, Zürich, CH)

Titanium dioxide (TiO<sub>2</sub>), finds a wide range of applications in environmental remediation such as air/surfaces sanitization, wastewater treatment, due to its photocatalytic properties. However, one of the main shortcomings of TiO<sub>2</sub> is its wide band gap which restrains its use to UV light. Therefore, the development of TiO<sub>2</sub> materials with enhanced visible light activity is important for using solar energy as the light source during the photocatalytic process. This is often the result of electronic structure engineering of materials through doping. An effective way is to dope TiO<sub>2</sub> with non-metal elements such as carbon (C), sulphur (S), nitrogen (N), fluorine (F), etc., especially the incorporation of multiple dopants (codoping) which was found to be an efficient strategy for improving TiO<sub>2</sub> visible light activity [1].

On the other hand, it is known that Moringa oleifera seeds contain some chemical compounds rich in carbon, nitrogen and sulphur [2]. Usually, after oil extraction, the seed residues become a waste. In this study, several compounds have been isolated from Moringa oleifera residues. Those, which contain carbon, nitrogen and sulphur have been used for TiO<sub>2</sub> codoping. Several techniques, especially X-ray diffraction, were used to characterise the obtained S, N, C-TiO<sub>2</sub> photocatalysts. The results showed that Moringa oleifera waste could be valorised as dopant to develop a simple and efficient method for the preparation of novel TiO<sub>2</sub> based photocatalysts.

[1] J.A. Rengifo-Herrera, Sol. Energy 84 (2010) 37

[2] Amelia P. Guevara, Mutation Research 440 (1999) 181–188

## MS16-P12 | MORPHOLOGICAL ANALYSIS OF THE MIGRATION-INDUCED FIELD-STABILIZED POLAR PHASE IN $\text{SrTiO}_3$ WITH SCANNING X-RAY DIFFRACTION MICROSCOPY

Weigel, Tina (TU Bergakademie Freiberg, Freiberg, GER); Richter, Carsten (European Synchrotron Radiation Facility (ESRF), Grenoble, FRA); Nentwich, Melanie (TU Bergakademie Freiberg, 09599, GER); Mehner, Erik (TU Bergakademie Freiberg, 09595, GER); Zschornak, Matthias (TU Bergakademie Freiberg, 09599, GER); Meyer, Dirk C. (Tu Bergakademie Freiberg, Freiberg, GER)

Dielectric strontium titanate  $\text{SrTiO}_3$  (STO) is a perovskite material with space group  $Pm-3m$ . During application of an electric field oxygen vacancies migrate to the cathode and oxygen ions to the anode. Slowly, the anode side of the STO crystal transforms into a tetragonal phase, the migration-induced field-stabilized polar (MFP) phase. The MFP phase shows polar properties, as piezoelectricity and pyroelectricity, in contrast to cubic STO. This indicates structural changes due to the electric field. We refined the structure of the MFP, in the same type as  $\text{PbTiO}_3$  and  $\text{BaTiO}_3$  with space group  $P4mm$ . The new lattice is a highly strained state of STO, with a strain of  $\sim 1\%$  in field direction. Polar displacements play an important role for the formation of the tetragonal disorder, but the specifics of the forming- and collapsing-process of the polar phase is yet unknown. To gain further insight into these processes, we used Scanning X-ray Diffraction Microscopy to analyse the strain field and morphology of the MFP phase at the Beamline ID01 of the European Synchrotron Radiation Facility. We examined STO crystals in the unformed state, during electroformation with the appearing MFP phase, and after formation. The results will give a better understanding of the thickness dependence of the strain and the metastable character of the polar phase after switching the voltage off. Hopefully, the conclusions are transferable to other strain-driven phase-transitions and their impact on the crystal structure as well as related material properties.

## MS16-P13 | HOW DIFFERENT DO DIFFRACTION PATTERNS OF THE SAME SUBSTANCE HAVE TO BE TO INDICATE POLYMORPHISM?

Glowka, Marek (Lodz University of Technology, Lodz, POL)

Theoretically, any difference in a crystal of the compound results in changes in its diffraction pattern (diffractogram in the powder sample). The differences may be related either to the arrangement of atoms within a crystal (called structure) or to experimental conditions. Some experimental conditions also change the structure, i.e. temperature.

The basic relations between the structure and diffraction patterns are as follows:

1. Bragg's angles of diffraction maxima depend on averaged dimensions of all unit cells within the studied crystal;
2. The intensities of maxima depend on the electron density of respective diffracted  $hkl$  family planes;
3. The width of maxima depends on experimental conditions and on the structure itself.

It has to be mentioned that the X-rays wave "see" atoms frozen in their accidental positions as atoms' vibrations have much lower frequencies. As a result, the diffraction pattern reflects "space-averaged" structure, which is presented as the "time-averaged" one. In practice, there are no two identical diffraction patterns, not only of the same substance but even of the same sample. So, if one of the main methods to distinguish polymorphs is diffraction, when are we allowed to "discover" a new polymorph basing on comparison of diffractograms as we usually do?

In the case of API (Active Pharmaceutical Ingredient) the discovery of a new polymorph may be rewarded by a patent. Therefore, the title question is a very serious one and in the presentation I will demonstrate, how difficult the answer is.

## MS16-P135 - LATE | SYNTHESIS AND STRUCTURAL CHARACTERIZATION OF NEW SALTS CONTAINING 2-AMINO-3-METHYLPYRIDINIUM CATIONS

Bednarchuk, Tamara (Institute of Low Temperature and Structure Research Polish Academy of Sciences, Wrocław, POL)

Ionic compounds with nitrogen containing heterocycles and organic acids are characterized by a great structural diversity, interesting physicochemical properties and potential applications, such as ferroic or nonlinear optical materials. In this context, four new salts containing 2-amino-3-methylpyridinium cations were prepared and structurally characterized.

The structure of the bis(2-amino-3-methylpyridinium) bis(hydrogen succinate) succinic acid monohydrate crystal belongs to a triclinic system with  $P-1$  space group and with  $a = 5.239(3)$ ,  $b = 8.360(3)$ ,  $c = 16.907(5)$  Å,  $\alpha = 84.86(3)$ ,  $\beta = 82.29(3)$ ,  $\gamma = 74.43(3)^\circ$ ,  $V = 705.8(5)$  Å<sup>3</sup>,  $Z = 2$ .

The structure of the bis(2-amino-3-methylpyridinium) succinate succinic acid crystal was solved in the monoclinic system in the  $C2/c$  space group with  $Z = 4$  and  $a = 14.805(4)$ ,  $b = 5.497(3)$ ,  $c = 27.126(7)$  Å,  $\beta = 101.60(3)^\circ$ , and  $V = 2162.5(14)$  Å<sup>3</sup>.

A crystal of 2-amino-3-methylpyridinium hydrogen adipate monohydrate crystallizes in the noncentrosymmetric space group  $P2_1$  with  $a = 5.474(3)$ ,  $b = 17.532(5)$ ,  $c = 7.362(3)$  Å,  $\beta = 102.08(3)^\circ$ ,  $V = 690.9(5)$  Å<sup>3</sup>,  $Z = 2$ .

The single crystals of the compound of 2-amino-3-methylpyridinium D,L-tartrate crystallizes in triclinic system with  $P-1$  space group with  $a = 7.210(3)$ ,  $b = 9.269(3)$ ,  $c = 10.741(4)$  Å,  $\alpha = 80.87(3)$ ,  $\beta = 78.51(3)$ ,  $\gamma = 88.69(3)^\circ$ ,  $V = 694.5(5)$  Å<sup>3</sup>,  $Z = 2$ .

Precise structural analysis of the abovementioned crystal structures, including 3D Hirshfeld surfaces and 2D fingerprint plots, will be presented at the conference.

### MATERIALS

Giménez Marqués, Mónica (Instituto de Ciencia Molecular, paterna, ESP); Gómez Muñoz, Iván (Universidad de Valencia, Instituto de Ciencia Molecular, Paterna, ESP); Morant Giner, Marc (Universidad de Valencia, Instituto de Ciencia Molecular, Paterna, ESP); Forment Aliaga, Alicia (Universidad de Valencia, Instituto de Ciencia Molecular, Paterna, ESP)

Metal-Organic Frameworks or MOFs are crystalline porous solids that have been largely studied over the past two decades. Compared to classical porous systems (*e.g.*, porous carbon, mesoporous silica, and zeolite), MOFs possess a vast chemical versatility that provides them with unique properties such as large surface areas with tunable pore size and ample chemical functionalities.

Even more interesting is the variety of MOFs that possess the ability to respond to external stimuli such as solvent, gas pressure or temperature [1]. These flexible or breathing MOFs are capable of adapting their structure, resulting in dynamic characteristics that make them appealing in applications such as gas separation, controlled drug delivery, sensors and catalysis. The implementation of these flexible MOFs in functional devices has been hampered by their poor processability, since they have been typically obtained in the form of polycrystalline powders. A plausible solution for their practical use is their miniaturization in the form of nanoparticles, which, however, has been less explored.

We will first present a general protocol for the synthesis of nanostructured flexible MOFs using a microwave-based synthesis which permits to obtain 50 nm particle size of the material. Then, we will show how it is possible to exploit their surface characteristics to combine them with 2D materials presenting interesting electrical properties. In particular, we have developed a procedure to obtain a composite material based on exfoliated nanosheets of MoS<sub>2</sub> [2], and a flexible nanostructured MOF.

[1] C. Serre, C. Mellot-Draznieks, S. Surblé et al *Science* **2007**, *315*, 1828–1832.

[2] M. Morant-Giner, R. Sanchis-Gual, J. Romero et al *Adv. Funct. Mater.* **2018**, *28*, 1–11

## MS17: Pressure and Mechanical Stress Induced Phase Transition and...

---

### MS17-01 | DYNAMIC COMPRESSION OF MATERIALS AT PRESSURES OF EARTH'S INTERIOR USING THE dDAC

Marquardt, Hauke (University of Oxford, Oxford, GBR)

Phase transitions play a central role for the structure and dynamics of Earth deep mantle. Here, I will discuss results of high-pressure experiments where we employ a diamond-anvil cell driven by a piezoelectric actuator (dynamic DAC) to dynamically compress Earth materials across phase transitions that are expected to occur in Earth's lower mantle. I will present results of two types of experiments, where (a) materials are compressed over a wide range of compression rates (up to about 1 TPa/s) and (b) the pressure (stress) imposed on the sample material is oscillated around a mean pressure. In our experiments, we monitor the elastic and structural response of the materials by time-resolved in-situ x-ray diffraction at the Extreme Conditions Beamline (ECB) at PETRA III, DESY, Germany. I will discuss the implications of our results for understanding Earth's deep interior and highlight some possible future directions.

## MS17-02 | HIGH-PRESSURE POLYMORPHS OF ORGANIC COMPOUNDS WITH INTERACTIONS INVOLVING NITROGEN ATOMS

Olejniczak, Anna (Adam Mickiewicz University, Poznan, POL)

High-pressure can significantly influence the formation, transformations and properties of materials. Organic materials are attractive due to their easy production and disposal. Their structures and properties are often dominated by weak intermolecular interactions. They can be rearranged or broken at high pressure, and at the same time new types of intermolecular interaction can be formed. Weak intermolecular forces involving nitrogen atoms and their transformation at high-pressure conditions are particularly interesting, because they can form various interactions, such as hydrogen bonds, which play a significant role in biology, chemistry or medicine. Varied thermodynamic conditions can be required for the synthesis of new materials, their transformations or the formation of solvates. The new polymorphs and solvates usually have different properties than those of neat compounds.

Nitrogen atoms are presented in many important compounds, for example in 1,4-diazabicyclo[2.2.2]octane salts, exhibiting ferroelectric or relaxor properties; methylamines, which are widely used in organic chemistry and industry; urea, which is one of the most common chemical and biological compound, widely used in chemical practice and in industry, mainly for the production of fertilizers or pharmaceuticals; thiourea, which can be used as dyes, plant protection agents, pesticides, corrosion inhibitors; and high-nitrogen-contents compounds, which can be the components of medical drugs or exhibit explosive properties. The compression experiments on the nitrogen rich compounds will be presented.

## MS17-03 | CRYSTAL STRUCTURE COMPRESSION AND PRESSURE-INDUCED POLYMERIZATION OF ARENE-PERFLUOROARENE CO-CRYSTALS LEADING TO COLUMNAR HYDROFLUOROCARBONS

Friedrich, Alexandra (Julius-Maximilians-Universität Würzburg, Würzburg, GER); Collings, Ines E. (European Synchrotron Radiation Facility, Grenoble, FRA); Dziubek, Kamil (European Laboratory for Nonlinear Spectroscopy (LENS), Sesto Fiorentino (FI), ITA); Fanetti, Samuele (European Laboratory for Nonlinear Spectroscopy (LENS), Sesto Fiorentino (FI), ITA); Radacki, Krzysztof (Julius-Maximilians-Universität Würzburg, Würzburg, GER); Ruiz-Fuertes, Javier (Universidad de Cantabria, Santander, ESP); Pellicer-Porres, Julio (Universitat de València, Burjassot, ESP); Hanfland, Michael (European Synchrotron Radiation Facility, Grenoble, FRA); Sieh, Daniel (Julius-Maximilians-Universität Würzburg, Würzburg, GER); Bini, Roberto (European Laboratory for Nonlinear Spectroscopy (LENS), Sesto Fiorentino (FI), ITA); Clark, Stewart J. (University of Durham, Durham, GBR); Marder, Todd B. (Julius-Maximilians-Universität Würzburg, Würzburg, GER)

The arene-perfluoroarene interaction is a robust supramolecular synthon, which is used for the development of highly oriented, stacked  $\pi$ -systems [1]. We investigated the structural compression of 1:1 arene-perfluoroarene co-crystals, naphthalene:octafluoronaphthalene (NOFN) and anthracene:octafluoronaphthalene (AOFN), using single-crystal synchrotron X-ray diffraction. Our study shows the remarkable pressure stability of the crystal structures and hence of the parallel arene-perfluoroarene stacking arrangement up to 20 and 25 GPa for NOFN and AOFN, respectively, at which they show pressure-induced phase transitions, irreversible on decompression. Increasing pressure leads, predominantly, to reduction of the interplanar  $\pi$ -stacking separations, which are strongly compressed at the phase transitions. This indicates the pressure-induced breakdown of  $\pi$ - $\pi$  stacking via polymerization and formation of  $\sigma$ -bonded high-pressure phases. Complementary high-pressure infra-red spectroscopy measurements and quantum mechanical computations based on density-functional theory using CASTEP [2] confirm the pressure-induced polymerization and the formation of columns of  $\sigma$ -bonded hydrofluorocarbons along the arene-perfluoroarene  $\pi$ -stacking direction as well as the one-dimensionality of the chemical reactions. Structural models for the fully polymerized phases of NOFN and AOFN are presented, which are in agreement with experimentally determined unit cell parameters.

The authors thank the ESRF for synchrotron beamtime. Financial support from ESRF, LASERLAB-EUROPE (grant 654148, EU's Horizon 2020 program), the Spanish MINECO (Juan de la Cierva Program, grant IJCI-2014-20513), and University of Würzburg is greatly appreciated. The UK Archer supercomputer was used (grant EPSRC EP/P022782/1).

[1] J.C. Collings et al. *New J. Chem.* **2001**, *25*, 1410

[2] S.J. Clark et al. *Z. Kristallogr.* **2005**, *220*, 567

## MS17-04 | PRESSURE INDUCED PHASE TRANSITION IN $\text{CoSO}_4 \cdot \text{H}_2\text{O}$

Ende, Martin (Institut für Mineralogie und Kristallographie, Wien, AUT); Loitzenbauer, Michael (Institut für Mineralogie und Kristallographie, Wien, AUT); Matzinger, Philipp (Institut für Mineralogie und Kristallographie, Wien, AUT); Meusbürger, Johannes (Institut für Mineralogie und Kristallographie, Wien, AUT); Talla, Dominik (Institut für Mineralogie und Kristallographie, Wien, AUT); Miletich, Ronald (Institut für Mineralogie und Kristallographie, Wien, AUT); Wildner, Manfred (Institut für Mineralogie und Kristallographie, Wien, AUT)

Kieserite-type  $\text{CoSO}_4 \cdot \text{H}_2\text{O}$  is one of the endmember compositions of the monohydrate sulphate series, most recently discussed as an astrophysically important mineral group apart from rare terrestrial occurrences such as of cobaltkieserite. As sulphates significantly influence melting equilibria on the icy moons of Saturn and Jupiter and possibly lead to subsurface oceans and cryovolcanism [1,2], their investigation in our solar system receives growing attention [e.g. 3]. Hence, knowledge of respective and related mineral phases and their high-pressure behavior seems to be crucial. Even though the high-pressure behavior of sulphate minerals in higher hydration stages has already been subjected to numerous studies, the compression information for the low-hydrated phases is still limited.

Synthetic single crystals were studied by means of in-situ high-pressure XRD and Raman spectroscopy using an ETH-type diamond-anvil cell. During the pressure increase most notably a Raman band around  $50 \text{ cm}^{-1}$  (ambient pressure) and a second one around  $280 \text{ cm}^{-1}$  revealed a structural phase transition around 2 GPa. The subsequent XRD investigations revealed that  $\text{CoSO}_4 \cdot \text{H}_2\text{O}$  undergoes a compression-induced change of symmetry from monoclinic to a triclinic high-pressure polymorph. The space group seems to change directly from  $C2/c$  into  $P-1$ .

[1] Kargel J. S. (1991) *Icarus*, **94**, 368-390.

[2] McCord T. B., Hansen G. B., Hibbits C. A. (2001) *Science*, **292**, 1523-1525.

[3] Wang A., Freeman J. J., Jolliff B. L. (2009) *J. Geophys. Res.*, **114**, E04010.

## MS17-05 | PRESSURE-INDUCED POLYMERIZATION AND ELECTRICAL CONDUCTIVITY OF A POLYIODIDE

Macchi, Piero (University of Bern, Bern, CH); Poreba, Tomasz (Paul Scherrer Institute, Villigen, CH); Ernst, Michelle (University of Bern, Bern, CH); Casati, Nicola (Paul Scherrer Institute, Villigen, CH)

The tetra-ethyl ammonium di-iodo triiodide  $[\text{C}_8\text{H}_{20}\text{N}][\text{I}_3](\text{I}_2)_2$  is an organic polyiodide salt in which a progressive addition of the electrophilic iodine molecules to the nucleophilic triiodide anion occurs.<sup>1</sup> Compression leads initially to mono-anionic hepta-iodide units and eventually to the polymerization which forms a 3D anionic network. Although the structural changes appear to be continuous, the electrical conductivity changes dramatically above 10 GPa, as the system displays a semiconductive behaviour, whereas at ambient pressure it is a dielectric. The electronic features of the “pre-reactive state” and the polymerized state are revealed by the computed electron and energy density distributions. The formation of the new bonds of course triggers the conductivity, however it is interesting that this occurs only when specific features of electron density and energy densities are observed.

[1] T. Poreba, M. Ernst, D. Zimmer, P. Macchi, N. Casati *Angew. Chem., Int. Ed. Engl.*, **2019**, in the press.

## MS17-P01 | SYMMETRY LOWERING IN NATROCHALCITE $\text{NaCu}_2(\text{H}_3\text{O}_2)(\text{SO}_4)_2$ UNDER PRESSURE.

Ende, Martin (Institut für Mineralogie und Kristallographie, Wien, AUT); Giester, Gerald (Institut für Mineralogie und Kristallographie, Wien, AUT); Kurz, Maditha (Institut für Mineralogie und Kristallographie, Wien, AUT); Miletich, Ronald (Institut für Mineralogie und Kristallographie, Wien, AUT)

Natrochalcite compounds, currently discussed as an anode material for Li-/Na-ion batteries [1], exhibit hydrogen-bond lengths that are among hydrogen-bearing solids some of the shortest ones reported so far [2]. Furthermore, at high-pressure the formation of an extremely short single-well no-barrier hydrogen bond is possible.

At ambient pressure the space group of natrochalcite is  $C2/m$  [3]. The XRD measurements performed between 0.4 and 10 GPa showed the Bravais lattice centering to remain and the continuous decrease of the hydrogen bonds, respectively their O...O distances. However, the Raman spectra show clear changes in the  $\text{SO}_4$  bending region. Furthermore, all the oxygen atoms of the  $\text{SO}_4$ -tetrahedron clearly show higher isotropic displacement parameters compared to the only oxygen not involved in this polyhedron. The acceptor oxygen for the longer hydrogen bond, shrinks about 0.18(2) Å until 10 GPa and shows the strongest displacement starting at ambient pressure up to 10 GPa, when refined in  $C2/m$ .

Since all the oxygens of the  $\text{SO}_4$ -tetrahedron are shared with Na-polyhedra it is very likely that at least for these polyhedra the symmetry is lowered above 2 GPa. Due to the preserved C-centering only two space groups are reasonable then,  $Cm$  and  $C2$ .

[1] Liu Z., Zhou H., Ang S. S., Zhang J.-J., (2016) *Electrochim. Acta*, **211**, 619-626.

[2] Krickl R., Wildner M., (2007) *Eur. J. Mineral.*, **19**, 805-816.

[3] Giester G., Zemann J. (1987) *Z. Kristallogr.*, **179**, 431-442

## MS17-P02 | STRUCTURE–MAGNETIC PROPERTY CORRELATIONS IN METAL–FORMATE FRAMEWORKS AT HIGH PRESSURE

Collings, Ines (Empa, Dübendorf, CH); Manna, Rudra Sekhar (Indian Institute of Technology Tirupati, Tirupati, IND); Tsirlin, Alexander A. (Augsburg University, Augsburg, GER); Bykov, Maxim (University of Bayreuth, Bayreuth, GER); Bykova, Elena (University of Bayreuth, Bayreuth, GER); Hanfland, Michael (ESRF, Grenoble, FRA); Gegenwart, Philipp (Augsburg University, Augsburg, GER); van Smaalen, Sander (University of Bayreuth, Bayreuth, GER); Dubrovinsky, Leonid (University of Bayreuth, Bayreuth, GER); Dubrovinskaia, Natalia (University of Bayreuth, Bayreuth, GER)

Magnetic metal–organic frameworks (MOFs) have attracted increasing interest due to their capabilities of coupling magnetism with other properties, such as ferroelectricity, porosity, and optical activity [1]. The structural flexibility and responsive nature of MOFs mean that significant changes in their magnetic properties could be achieved upon their exposure to external stimuli. However, few guidelines exist to tune and improve their magnetic properties. High-pressure investigations are particularly useful as they allow changes in the magnetic properties to be related to structural variations without additional electronic effects that are present upon chemical substitutions.

The family of protonated amine or ammonium templated metal formates display a range of interesting physical properties, such as ferroelectricity, antiferromagnetism, multiferroicity, and have a rich chemical diversity. Here, we investigate the structural and magnetic properties of ammonium metal formates [2],  $[\text{NH}_4][\text{M}(\text{HCOO})_3]$ , for  $\text{M} = \text{Mn}^{2+}$ ,  $\text{Fe}^{2+}$ ,  $\text{Ni}^{2+}$ , at high pressure up to 2.5 GPa and low-temperature conditions by use of single-crystal X-ray diffraction and magnetisation measurements. We find that the overall magnetic behaviour of each phase upon compression was not only dependent on the structural distortions but also on the electronic configuration of the metal cation [3].

[1] G. Rogez *et al.*, *Angew. Chem. Int. Ed.* **2010**, 49, 1921–1923.

[2] G.-C. Xu *et al.*, *J. Am. Chem. Soc.* **2011**, 133, 14948–14951.

[3] I. E. Collings *et al.*, *Phys. Chem. Chem. Phys.* **2018**, 20, 24465–24476.

## MS17-P03 | PRESSURE-INDUCED MODIFICATION OF MOLECULAR AGGREGATION IN CRYSTALS OF BENZOCAINE

Patyk-Kazmierczak, Ewa (Adam Mickiewicz University, Poznan, POL); Kazmierczak, Michal (Adam Mickiewicz University, Poznan, POL); Katrusiak, Andrzej (Adam Mickiewicz University, Poznan, POL)

Benzocaine (BZC), a local anaesthetic and one of the best known representative of biologically active esters of 4-aminobenzoic acid, is an Active Pharmaceutical Ingredient (API) of many commercially available drugs. Unfortunately, its water solubility of 0.131 mg/ml makes it unsuitable for enteral administration. Solubility of an API is an important aspect affecting properties and application of a final drug product. It strongly depends on intermolecular interactions present in the solid form of a given compound, making analysis of H-bonding pattern crucial for investigation of crystal properties. It was shown that BZC exhibits specific tendency for molecular aggregation and H-bonding pattern formation, common to all three polymorphs of BZC reported so far (Sinha & Pattabhi, 1987; Lynch & McClenaghan, 2002; Chan *et al.*, 2009). In order to induce changes in BZC aggregation and synthons hierarchy a series of high-pressure experiments was performed. Pressure has proven to induce a phase transition in crystals of BZC, introducing its new polymorph. Herein, we present a thorough analysis and comparison of intermolecular interactions and molecular packing for all four polymorphs of BZC.

[1] Chan, E. J., Rae, A. D. & Welberry, T. R. (2009). *Acta Crystallogr. B.* **65**, 509–515.

[2] Lynch, D. E. & McClenaghan, I. (2002). *Acta Crystallogr. Sect. E Struct. Rep. Online.* **58**, o708–o709.

[3] Sinha, B. K. & Pattabhi, V. (1987). *J. Chem. Sci.* **98**, 229–234.

## MS17-P04 | EFFECT OF PRESSURE ON SLIT CHANNELS IN HYDRATE OF SODIUM SALT OF GUANINE: A LINK TO NUCLEOBASE INTERMOLECULAR INTERACTIONS

Gaydamaka, Anna (Novosibirsk State University, Novosibirsk, RUS); Arkhipov, Sergey (1Novosibirsk State University, Boreskov Institute of Catalysis SB RAS, Novosibirsk,, RUS); Zakharov, Boris (Novosibirsk State University, Boreskov Institute of Catalysis SB RAS, Novosibirsk, RUS); Seryotkin, Yuriy (Novosibirsk State University, V.S. Sobolev Institute of Geology and Mineralogy SB RAS, Novosibirsk, RUS); Boldyreva, Elena (Novosibirsk State University, Boreskov Institute of Catalysis SB RAS, Novosibirsk, RUS)

The studies of the biological and biomimetic objects are important not only for fundamental science but also for the design of drugs and materials.

The crystal structure of a hydrate of the sodium salt of guanine ( $2\text{Na}^+ \cdot \text{C}_5\text{H}_3\text{N}_5\text{O}^{2-} \cdot 7\text{H}_2\text{O}$ ) [1] was studied using single-crystal X-ray diffraction and Raman spectroscopy up to  $\sim 2.5$  GPa, after what the structure collapsed and the diffraction pattern disappeared. On increasing pressure, the distances between the double walls of the slit channels formed by the guanine moieties became more equal, the longer one shortening and the shorter one expanding. The topology of the  $\text{Na}^+$  - water intra-channel infinite clusters was preserved, although these clusters got distorted on compression. Among several types of the  $\text{NH}\dots\text{O}$  and  $\text{OH}\dots\text{O}$  hydrogen bonds, only two practically did not change with increasing pressure, namely the  $\text{OH}\dots\text{O}$  and the  $\text{NH}\dots\text{O}$  bonds connecting the guanine walls with the intra-channel water molecules. A possible relation to the interactions in the ion channels with the walls formed by the guanine species in biological systems is discussed.

**Acknowledgements:** The work was supported by the Russian Ministry of Science and High Education (project AAAA-A19-119020890025-3)

[1] D. Gur, L. Shimon, *Acta Cryst. E*, 2015, E71, pp. 282-283.

## MS17-P05 | Ex-situ study of the pressure induced decomposition of iron nitride

### Fe<sub>4</sub>N

Wetzel, Marius H. (TU Bergakademie Freiberg, Institute of Materials Science, Freiberg, GER); Rabending, Tina (TU Bergakademie Freiberg, Institute of Materials Science, Freiberg, GER); Schwarz, Marcus R. (TU Bergakademie Freiberg, Institute of Inorganic Chemistry, Freiberg, GER); Leineweber, Andreas (TU Bergakademie Freiberg, Institute of Materials Science, Freiberg, GER)

Although the instability of the iron nitride  $\gamma'$ -Fe<sub>4</sub>N with respect to high pressure seems well established, only few studies exist which focus on the influence of pressure upon phase equilibria resulting from its transformation [1].

In this study, samples of  $\gamma'$ -Fe<sub>4</sub>N powder have been exposed to pressures between 2-13 GPa and temperatures between 300-900°C in a multi-anvil press. For ex-situ study, the samples were quenched to room temperature and subsequently decompressed to atmospheric pressure. Microstructure and phase composition have been analysed by means of electron backscatter diffraction and X-ray diffraction analysis. N contents of the phases have been determined from lattice parameter data.

Our results show that both phase composition and microstructure of samples containing more than 8 at% N can be retained at ambient conditions, thus facilitating ex-situ analysis. Moreover, our data indicate a pressure induced decomposition of  $\gamma'$  nitride into a low-N  $\gamma$ -type solid solution and a high-N  $\epsilon$  nitride. At 400°C and 4 GPa  $\gamma'$  nitride is still observed whereas above 6 GPa it decomposed into  $\gamma$  solid solution and  $\epsilon$  nitride. At 13 GPa  $\gamma'$  nitride was found to transform into other phases for all treatment temperatures between 400 and 900°C.

The acquired phase constitution data were cast into a partial Fe-N pressure-temperature-composition phase diagram and provide insight into the pressure dependent evolution of the phase equilibria and potential transition reactions related with the decomposition of  $\gamma'$  nitride.

[1] Litasov et al., *J. Geophys. Res. Solid Earth* 2017, **122**, 3574.

## MS17-P06 | PHASE TRANSFORMATIONS OF (RS)-2-CHLOROMANDELIC ACID IN THE SOLID STATE: FROM RACEMIC COMPOUND TO CONGLOMERATE UNDER MECHANICAL FORCE

LIU, JIE (Laboratoire de Chimie des Polymeres, Brussels, BEL); Liu, Guangfeng (Laboratoire de Chimie des Polymeres, Brussels, BEL); Geerts, Yves (Laboratoire de Chimie des Polymeres, Brussels, BEL)

(RS)-2-Chloromandelic acid being chiral compound can exist as a racemic compound or a conglomerate. And the phase transition occurs between the polymorphic racemic compounds and conglomerate. It is of importance to study the phase transformations especially in the solid state, which is beneficial for the pharmaceutical factories to control the polymorphs very well. The transition from metastable racemic compounds to conglomerate under the application of grinding was disclosed. The metastable racemic compounds, form  $\beta$ , were prepared by recrystallization from the melt of commercially available racemic compounds Form  $\alpha$ . The form  $\beta$  can be stable for days in air without additional forces. However, the crystals of form  $\beta$  transforms to crystalline conglomerate quickly when the mechanical force (e.g. grind) was applied.

## MS17-P07 | PHASE TRANSITIONS OF COPPER(I) IODIDE COMPOUNDS UNDER HIGH PRESSURE

Gonzalez-Platas, Javier (Universidad de La Laguna, La Laguna, ESP); Aguirrechu-Comeron, Amagoia (Universidad de La Laguna, La Laguna, ESP); Rodriguez-Mendoza, Ulises R. (Universidad de La Laguna, La Laguna, ESP); Lavin della Ventura, Victor (Universidad de La Laguna, La Laguna, ESP); Conesa-Egea, Javier (Universidad Autonoma de Madrid, Madrid, ESP); Amo-Ochoa, Pilar (Universidad Autonoma de Madrid, Madrid, ESP)

Copper(I) iodide compounds can exhibit interesting mechanochromic and thermochromic luminescent properties with important technological applications. Mainly due to their large variety of structural configurations where CuI has the capability to form clusters with different dimensionality as rhomboid dimers, cubane, or staircase ladders [1-2]. It does a large variety of Cu...Cu interactions giving attractive photoluminescence properties. Therefore, it could be interesting to explore new properties if we were able to control these interactions by applying external stimuli as temperature, grinding or pressure. We have done Xray diffraction and luminescence experiments under high pressure at room temperature and then we have performed the isothermal equation of state (EoS) for both compounds [3]. For CuICl<sub>2</sub>Py (1D staircase) we observe an isosymmetric phase transition of first order at 6GPa while for (CuI)<sub>2</sub>(Quin) (2D staircase) the phase transition is more subtle. It is a phase transition of second order around 3.5GPa. All these changes have been confirmed also in luminescence properties under pressure that we will show in the poster session.

[1] Q. Benito, I. Maurin, T. Cheisson, G. Nocton, A. Fargues, A. Garcia, C. Martineau, T. Gacoin, J.-P. Boilot, and S. Perruchas *Chem. - A Eur. J.*, 2015, 21, pp. 5892–5897

[2] A. Aguirrechu-Comerón, R. Hernández-Molina, P. Rodríguez-Hernández, A. Muñoz, U. R. Rodríguez-Mendoza, V. Lavín, R. J. Angel, and J. Gonzalez-Platas, *Inorg. Chem.* 2016, 55, 7476-, vol. 55, no. 15, pp. 7476–7484.

[3] J. Gonzalez-Platas, M. Alvaro, F. Nestola, and R. Angel, *J. Appl. Crystallogr.*, 2016, 49, 1377–1382.

## MS18: Materials for Energy Storage and Conversion

---

### MS18-01 | ELECTROCHEMICAL ENERGY STORAGE BEYOND LITHIUM

Ehrenberg, Helmut (Karlsruher Institut für Technologie, Eggenstein-Leopoldshafen, GER)

Electrochemical energy storage beyond lithium is highly relevant for sustainable energy technology. New electrode concepts are needed for the intercalation of larger monovalent ( $\text{Na}^+$ ,  $\text{K}^+$ ) or multivalent ions ( $\text{Mg}^{2+}$ ). One example for a promising Na-ion battery is presented based on symmetrical NASICON-structured  $\text{Na}_2\text{VTi}(\text{PO}_4)_3$  electrodes [1]. Operando synchrotron diffraction and absorption spectroscopy unravel the underlying sodium storage and charge compensation mechanisms. Model systems for multivalent-ion insertion are also hybrid batteries with two mobile metal ions in the electrolyte, where Mg is plated at the negative electrode, while Li- or Na-ions are inserted at the positive electrode [2, 3]. Recent results on the working mechanisms in such hybrid batteries are revealed by operando synchrotron diffraction and ex situ XPS. Appropriate material combinations for Mg-batteries with insertion-type positive electrodes and sufficiently high cell voltages are still lacking. For example,  $\text{V}_2\text{O}_5$  works only with unstable electrolytes in contact with Mg-metal and steel housing. The Mg-insertion mechanism was therefore investigated for a full cell with  $\text{Mg}_x\text{Mo}_6\text{S}_8$  as a suitable negative electrode [4].

This work contributes to research performed at CELEST (Center for Electrochemical Energy Storage Ulm-Karlsruhe) and was funded by the German Research Foundation (DFG) under Project ID 390874152 (POLiS Cluster of Excellence).

[1] Wang, D. et al., Nature Communications 2017, 8, 15888.

[2] Bian, X. et al., Mater. Chem. A 2017, 5, 600.

[3] Fu, Q. et al., Electrochim. Acta 2018, 277, 20.

[4] Fu, Q. et al., J. Am. Chem. Soc. 2019, 141, 2305.

## MS18-02 | ORDER-DISORDER TRANSITIONS IN BATTERY ELECTRODES STUDIED BY OPERANDO X-RAY SCATTERING

Ravnsbæk, Dorthe (University of Southern Denmark, Odense M, DNK)

Development of novel electrode materials for intercalation type batteries have in the past focused on highly crystalline materials with the capability to retain long-range order during cycling. However, recent years have seen an increased interest for disordered materials, e.g. with the discovery of multiple high capacity electrodes based on disordered rock-salt structures or even completely amorphous materials exhibiting higher capacities than their crystalline counterparts.[1] Furthermore, it was recently showed by Ceder et al that long-range order is not a prerequisite for maintaining percolating intercalation pathways.[2] Still very little is known about the structural mechanisms behind order-disorder transitions induced by ion-intercalation or about ion-storage mechanisms in disordered materials.

Using a combination of operando synchrotron X-ray diffraction and total scattering (with pair distribution function analysis), we have studied a series of disordered and amorphous electrode materials such as nano-rutile  $\text{TiO}_2$ ,  $\text{V}_2\text{O}_5$ , and various MnOx-polymorphs [4]. This allows us to map out the structural evolution during battery charge and discharge at the atomic- and nano-scale, and begin to understand the ion-storage mechanisms in such materials. In this presentation, we will focus on results which demonstrate the different types of order-disorder phenomena (e.g. topotactic, reconstructive, domain size reduction) and ion-storage mechanisms (e.g. solid solution, two-phase transition) we have encountered.

[1] J. Lee et al., Nature 2018, 556, 185-190.; E. Uchaker et al., J. Mater. Chem. A 2014, 2, 18208-18214.

[2] J. Lee et al., Science 2014, 343, 519-522.

[3] C. K. Christensen et al., Chem. Mater. (2019) DOI: 10.1021/acs.chemmater.8b04558.

## MS18-03 | DEFECTS, DISORDER AND ELECTROCHEMISTRY IN PHOSPHATE-BASED METAL-ION BATTERY CATHODES

Abakumov, Artem (Skolkovo Institute of Science and Technology, Moscow, RUS)

Formation and annihilation of defects is an intrinsic and inseparable part of alkali cation (de)intercalation from positive electrodes (cathodes) for metal-ion batteries. Here we discuss antisite disorder in the olivine-structured  $\text{LiFePO}_4$ , 3D framework or layered  $\text{A}_2\text{MPO}_4\text{F}$  ( $\text{A} = \text{Li, Na}$ ,  $\text{M} = \text{transition metal}$ ). We demonstrate that the bonding of the alkali metal cations to the semi-labile oxygen atoms is an important factor affecting electrochemical activity of alkali cations in the polyanion structures. Such semi-labile oxygens are not included into the  $\text{M}(\text{O,F})_6$  octahedra, being tetrahedrally coordinated by one P and three alkali cations and forming localized  $\text{sp}^3$ -hybridized states. Upon alkali cation deintercalation these oxygens experience severe undercoordination, causing an energy penalty for removing the alkali cations located in the proximity of such semi-labile oxygens. The importance of this semi-labile oxygens stems from their influence on the (de)intercalation mechanism, diffusion barriers and antisite defect formation. Dependence of the deintercalation potential of different alkali cation sites on the proximity to the semi-labile oxygens, charge compensation mechanism through the antisite Li/M disorder and associated changes in the deintercalation mechanism will be discussed. For  $\text{LiFePO}_4$  we establish the relation between antisite Li/Fe disorder and chemical substitution in the polyanion sublattice leading to unusual “hydrotriphylite”-type solid solutions, altering the crystal structure and electrochemical capacity. The work was supported by RFBR (grant 17-03-00370).

## MS18-04 | CRYSTAL GROWTH AND STRUCTURAL AND ELECTROCHEMICAL PROPERTIES OF GARNET-TYPE LITHIUM ION CONDUCTING OXIDES

Kataoka, Kunimitsu (National Institute of Advanced Industrial Science and Technology, Tsukuba, JPN); Akimoto, Junji (National Institute of Adv. Ind.Sci. & Tech., Tsukuba, JPN)

Lithium ion batteries are required improvement in safety and high energy density, because of wide applications from small-sized electrical devices to large-sized power sources. Especially, all solid state Li-ion batteries (LIB) using solid oxide electrolyte have attracted attention as next-generation batteries without inflammable organic liquid electrolytes. Among many candidates of Li-ion conducting oxide materials as solid electrolyte for all solid state LIB, the garnet-type  $\text{Li}_7\text{La}_3\text{Zr}_2\text{O}_{12}$  is most suitable because of both high Li-ion conductivity and wide electrochemical potential window. We recently focused on the Ta-substituted  $\text{Li}_7\text{La}_3\text{Zr}_2\text{O}_{12}$  materials having a relatively higher Li-ion conductivity at room temperature. We synthesized sintered body and single crystal samples of  $\text{Li}_{6.5}\text{La}_3\text{Zr}_{1.5}\text{Ta}_{0.5}\text{O}_{12}$  [1-3], and determined precise structural and electrochemical properties. A relationship between the detailed Li-ion arrangement in the garnet structure and the Li-ion conductivity will be presented.

This study was supported by the Advanced Low Carbon Technology Research and Development Program (ALCA-SPRING) from Japan Science and Technology Agency (JST).

[1] H. Hamao, K. Kataoka, N. Kijima J. Akimoto, *J. Ceram. Soc. Jpn.*, **124** (2016) 678.

[2] K. Kataoka and J. Akimoto, *ChemElectroChem*, **5** (2018) 2551.

[3] K. Kataoka, H. Nagata, J. Akimoto, *Scientific Reports*, **8** (2018) 9965.

## MS18-05 | STRUCTURAL INSIGHTS INTO METHANATION CATALYSTS FROM MOF-PRECURSORS VIA PDF

Prinz, Nils (University of Bayreuth, Bayreuth, GER); Schwensow, Leif (Ruhr University Bochum, Bochum, GER); Kleist, Wolfgang (Ruhr University Bochum, Bochum, GER); Zobel, Mirijam (University of Bayreuth, Bayreuth, GER)

The conversion of CO<sub>2</sub> to methane using H<sub>2</sub> from water electrolysis is a promising approach to tackle the challenge of long-term energy storage based on energy from renewable resources. Because of fluctuations in the H<sub>2</sub> supply due to dynamic changes in wind and solar energy, a highly stable catalyst, which resists H<sub>2</sub> dropouts, is needed for the methanation reaction. Supported Ni nanoparticles are typical catalysts, yet prone to deactivation by surface oxidation or sintering under fluctuating conditions [1]. Catalysts derived from metal-organic framework (MOF) precursors via thermal decomposition are promising materials due to the fine dispersion of active centres [2]. We have synthesized Ni(BDC)(PNO) MOFs (BDC=benzene-1,4-dicarboxylate, PNO=pyridine-N-oxide), which were thermally converted into stable methanation catalysts consisting of Ni clusters or nanoparticles on a carbonaceous, amorphous support. With pair distribution function (PDF) analysis of total scattering data we target the structural transitions from the crystalline MOF to the nanostructured catalyst, since the PDF is a histogram of interatomic distances and, in contrast to traditional crystallographic approaches, does not require crystallinity within the sample to refine its structure. Both lab and synchrotron PDF data show that the structure of the Ni nanoparticles as well as of the carbonaceous support depend on temperature and atmosphere (reducing, inert) of the thermal decomposition. Structural insight into these mechanistic steps of catalyst formation will allow a future targeted design of catalysts from MOF precursors.

[1] B. Mutz et al., *Catalysts* **2017**, *7*, 279

[2] R. Lippi et al., *J. Mater. Chem. A* **2017**, *5*, 12990

## MS18-06 | INCREASE YOUR ENERGY WITH XRD

Welzmler, Simon (Thermo Fisher Scientific, Ecublens, CH)

Due to humanity's growing use of energy, it is crucial to enhance the capabilities in both, production and storage of environmentally sustainable electricity. The usage of the sun as unlimited power source requires the design of highly efficient photovoltaic materials to convert light into usable electrical energy. Currently there are three predominantly used materials for thin film solar cells (Cadmium telluride CdTe, amorphous silicon, Copper Indium Gallium Telluride CIGS). Such solar cells are more cost efficient compared to bulk solar cells (crystalline silicon) as the required amount of material is very low. Nevertheless, they still exhibit lower cell efficiencies due to less mature upscaling compared to crystalline silicon based solar cells. Anyways, the latter materials are still intensively investigated to enhance their properties, usually by chemical substitution and designing the interfaces of the solar cell layers.

The crystallographic structure of multi-functional inorganic and hybrid organic-inorganic thin films (nano-meter scale) has to be characterized by GIXRD (grazing incidence XRD). This is important as electronical and optical properties strongly depend on the structure of compounds.

Another variable in designing thin film materials for various applications is the thickness, roughness and density of certain layers. One technique for determining these properties in (multi)-layers up to ~100nm is X-ray reflectometry (XRR), which is based on the interference between X-rays reflected on different layers in the material. In contrast to XRR, which requires perfectly homogeneous samples, X-ray fluorescence spectroscopy (XRF) is also able to determine the thickness of (multi)-layer films by using a fundamental parameter approach in both wavelength-dispersive and energy-dispersive XRF.

## MS18-P01 | PRUSSIAN BLUE ANALOGUES AS CATHODE MATERIAL IN LOW COST AQUEOUS BATTERIES

Kjeldgaard, Solveig (Aarhus University, Aarhus, DNK); Najbjerg Skov, Lasse (Aarhus University, Aarhus N, DNK); Brummerstedt Iversen, Bo (Aarhus University, Aarhus, DNK); Bentien, Anders (Aarhus University, Aarhus, DNK)

In order to increase the use of sustainable energy sources like solar and wind, new solutions in terms of energy storage are needed to overcome their highly intermittent nature. For battery technologies to be relevant for grid-scale storage, the electrode materials must be low cost, environmentally benign, have high energy efficiency and long cycle life. Because of the requirement for cheap electrode materials, the choice of elements are limited to earth abundant transition metals such as iron, manganese, zinc and copper.

In this work, eight Prussian blue analogues (PBAs) are investigated as cathode material in large-scale, low cost aqueous batteries. Prussian blue analogues are a large family of transition metal hexacyanoferrates with the general structural formula  $A_xM[Fe(CN)_6]$ , where A is a cation and M is a transition metal. PBAs are practically insoluble and are structurally very stable towards insertion/extraction of ions, why they have very good cycling capabilities. PBAs can be used in aqueous electrolyte with a wide range of insertion ions. Here, PBAs with M: Fe, Mn, Zn and Cu are synthesized in both the oxidized and reduced form. The structural differences and similarities are discussed and the electrochemical performance is evaluated using cyclic voltammetry.

## MS18-P02 | TAILORED EXOLUTION OF METAL NANOPARTICLES: STRUCTURAL AND CHEMICAL CHARACTERISATION OF DOPED PEROVSKITES BY XPS AND XRD

Raschhofer, Johannes (TU Wien, Wien, AUT); Lindenthal, Lorenz (TU Wien, Wien, AUT); Popovic, Janko (TU Wien, Wien, AUT); Ruh, Thomas (TU Wien, Wien, AUT); Rameshan, Raffael (TU Wien, Wien, AUT); Nenning, Andreas (TU Wien, Wien, AUT); Opitz, Alexander (TU Wien, Wien, AUT); Rameshan, Christoph (TU Wien, Wien, AUT)

Perovskite-type oxides are a large class of materials with many interesting properties, including piezo- and pyroelectricity, mixed ionic-electronic conductivity and high catalytic activity. There is a wide range of applications, e.g. the use as sensors or electrode materials in solid oxide fuel cells. Their chemical formula is  $ABO_3$ , with two different cations A (bigger) and B (smaller). The ideal structure is cubic, but it is often distorted as can be seen for  $NdFeO_3$ . The high versatility is due to the possibility of adjusting the properties by choosing different elements for the cations. Doping of the cation sites opens up an even larger matrix for materials design.

Different perovskite-type oxides will be synthesised and characterised. These perovskites are promising catalyst materials for several energy related reactions, such as the water gas shift reaction, water splitting or the CO oxidation. Another recently shown outstanding property is the exsolution of metal nanoparticles from perovskites under reducing conditions. This surface modification can change the catalytic activity and selectivity of the perovskite surface completely.

Starting with  $La_xCa_{1-x}FeO_3$ , perovskites with different cation species and dopant amounts will be investigated, choosing the most promising. X-ray diffraction (XRD) allows structural determination, while X-ray photoelectron spectroscopy (XPS) gives chemical information of the surface. A focus will be on the stability and reducibility of the synthesized perovskites, as this is crucial for nanoparticle exsolution. Only in an ideal metastable window, controlled formation of metal nanoparticles can be achieved.

## MS18-P03 | PHASE EVOLUTION DURING PEROVSKITE FORMATION - INSIGHT FROM PDF ANALYSIS

Hua, Xiao (University of Oxford, oxford, GBR)

The recent introduction of organometal halide perovskites to solar cells has significantly enhanced the power conversion efficiency of alternative photovoltaic devices, revolutionizing the development of photovoltaic technologies. To produce perovskite thin films with high device performances, various fabrication methodologies have been developed leading to thin films with different surface structures and crystal morphologies. Tremendous efforts have been devoted to characterizing macro- and microscopic structures within these films to better understand the processing-property-performance relationship. However, their atomic structure and its influence on device performance remains poorly understood. To this end, we employed pair distribution function analysis of X-ray total scattering data to obtain crystallographic and compositional information of methylammonium-lead-iodide (MAPbI<sub>3</sub>) thin films. This analysis revealed a presence of two near-amorphous intermediate phases with local structures that share subtle but significant correlations with the PbI<sub>2</sub> precursor and the desired perovskite phase. The structure transformation from these intermediates to the perovskite deviates from the intuitive belief where the molecular cations get inserted between the sheets of layered PbI<sub>2</sub> upon the crystallization of perovskite. The knowledge offers critical insight into the perovskite formation pathway and reveals an important link between the short-range structure of the thin films and their corresponding device performance.

## MS18-P04 | AB-INITIO STUDY OF OXYGEN ADSORPTION ON PdZn(111) SURFACE

Otani, Yusuke (Kagoshima University, Kagoshima, JPN); Yamaguchi, Kotaro (Kagoshima University, Kagoshima, JPN); Nozawa, Kazuki (Kagoshima University, Kagoshima, JPN)

Pd is highly active for the decomposition of methanol, but it becomes active for methanol steam reforming when alloying with Zn [1, 2]. A close connection between the catalytic property and the d-band structure was pointed out, and it is confirmed that PdCd, showing very similar d-band structure with PdZn, exhibits comparable catalytic property with PdZn [2, 3]. The change in the d-band structure, namely, leads to the change in the catalytic property. This change in the d-band structure was also clearly demonstrated by electronic structure calculations based on the density functional theory (DFT) [4]. However, a different origin of the change in the catalytic property was proposed for the isostructural intermetallic compound NiZn, and it was concluded that the desegregation of the NiZn surface by Zn oxidation is essential [5]. Needless to say, understanding the mechanism of the change in the catalytic property is important, thus, we are carrying out plane-wave DFT calculations to investigate the effect of oxidation on the electronic structure of PdZn. In this presentation, we will discuss the optimal structure of oxygen-adsorbed PdZn(111) surface.

[1] N. Iwasa et al., *Appl. Catal.* **125**, 145 (1995).

[2] A.P. Tsai et al., *J. Phys. Soc. Jpn.*, **73**, 3270 (2004).

[3] A. P. Tsai et al., *Acc. Chem. Res.* **50**, 2879 (2017).

[4] K. Nozawa et al., *J. Phys. Soc. Jpn.*, **80**, 064801 (2011).

[5] M. Friedrich et al., *J. Phys. Chem. C*, **116**, 14930 (2012).

## MS18-P05 | COMBINATION OF EXAFS AND XRD FOR STUDIES OF THE ORTHORHOMBIC-TETRAGONAL PHASE TRANSFORMATION IN $\text{MAPbI}_{3-x}\text{Cl}_x$ PEROVSKITES

Schuck, Götz (Helmholtz-Zentrum Berlin für Materialien und Energie GmbH, Berlin, GER); Többens, Daniel M. (Helmholtz-Zentrum Berlin für Materialien und Energie GmbH, Berlin, GER); Lehmann, Frederike (Helmholtz-Zentrum Berlin für Materialien und Energie GmbH, Berlin, GER); Schorr, Susan (Helmholtz-Zentrum Berlin für Materialien und Energie GmbH, Berlin, GER)

Research interest has increasingly focused on hybrid perovskites  $\text{MABX}_3$  like  $[\text{CH}_3\text{NH}_3]^+$  (MA), B = Pb and X = I or Cl as a future photovoltaic material. In QENS studies it could be shown that chlorine substitution has a large influence on the rotational dynamics of the MA molecule in  $\text{MAPbI}_{3-x}\text{Cl}_x$  perovskites. The QENS results show that chlorine substitution in the low temperature orthorhombic phase leads to a weakening of the hydrogen bridge bonds (these bonds connect the MA molecules with the  $[\text{PbX}_6]^-$  octahedra host structure) since the characteristic relaxation times of  $\text{C}_3$  rotation at 70 K in  $\text{MAPbCl}_3$  (135 ps) and  $\text{MAPbI}_{2.94}\text{Cl}_{0.06}$  (485 ps) are much shorter than in  $\text{MAPbI}_3$  (1635 ps).[1] The structural counterpart to the changes in the MA molecule dynamics caused by the chlorine substitution is the influence of the chlorine substitution on the tilting and distortion of the  $[\text{PbX}_6]^-$  octahedra in the orthorhombic-tetragonal phase transformation temperature range. By a combination of EXAFS Pb L3 edge investigations (local structure) and XRD (long-range order) the influence of the chlorine substitution on the distortions of the  $[\text{PbX}_6]^-$  octahedra was investigated. The temperature dependent XAFS measurements as well as the temperature dependent XRD measurements were performed at KMC-2 at Bessy II.

[1] G. Schuck, F. Lehmann, J. Ollivier, H. Mutka, S. Schorr, J. Phys. Chem. C (2019), DOI: 10.1021/acs.jpcc.9b01238.

## MS18-P06 | SYNTHESIS AND CRYSTAL CHARACTERIZATION OF A NEW LAYERED ACIDIC DIPHOSPHATE METALLATE

HAMDI, Najlaa (University Sidi Mohamed Ben Abdelah, FES, MAR); OURSAL, Rachid (USMBA, FES, MAR); CHAOUCH, Souad (USMBA, FES, MAR); EL BALI, Brahim (UMP, Oujda, MAR); LACHKAR, Mohammed (USMBA, Fes, MAR)

The hydrated hydrazinium hemicobalt hydrogenodiphosphate  $[(\text{H}_2\text{O})_2\text{Co}_2(\text{N}_2\text{H}_5)_2(\text{HP}_2\text{O}_7)_2]$  has been synthesized using wet chemistry. The structure was obtained by single crystal X-ray diffraction. It crystallizes in the triclinic system (S.G: P-1). The crystal packing consists in a three dimensional network made by layers parallel to bc plane of  $\text{CoO}_6/\text{CoN}_2\text{O}_4$  octahedra sharing four vertices with  $\text{HP}_2\text{O}_7$  double tetrahedra. The protonated hydrazine molecules interact with the inorganic moiety via covalent bonding and also through establishing hydrogen bonds on N atoms. The diphosphate group shows bent eclipsed conformation which was confirmed by infrared spectroscopy. The dehydrogenation of the crystal structure takes place into one step corresponding to the departure of hydrazine ligands and water molecules.

## MS18-P07 | FIRST-PRINCIPLES STUDY OF OXYGEN ADSORPTION STRUCTURE ON Ni<sub>3</sub>Al(210)

### SURFACE

Yamaguchi, Kotaro (Kagoshima University, Kagoshima, JPN); Nozawa, Kazuki (Kagoshima University, Kagoshima, JPN)

Recently, it was reported that Ni<sub>3</sub>Al is highly active for hydrogen production from methanol and methane, and its catalytic performance is considered to be attributed to the selective oxidation and hydroxylation of Al and the formation of metallic Ni particles at low oxygen partial pressures [1,2]. In order to reveal the details of the initial oxidation process, we are studying the stable adsorption structure of oxygen on the Ni<sub>3</sub>Al (210) surface using the first-principles calculation based on the density functional theory. For low coverage surfaces (0.25 and 0.5 ML), the most stable adsorption site is a pseudo-threefold hollow site surrounded by two Al atoms and Ni atom, implying partial oxidation of surface Ni. Although the atomic arrangement of surface atoms and the adsorbed oxygen atom of the most stable adsorption structure is very similar to the reported most stable adsorption structure on the NiAl (110) surface [3], the oxidation behavior of the surface Ni atom may disagree with the recent experiment, which did not observe the sign of the Ni oxidation at the initial stage of the oxidation process [4]. We will also discuss the electronic structure of the surface atoms and stable adsorption structures taking into account the exchange of atoms between different atomic layers.

[1] Y. Xu et al., *Intermetallics* **13**, 151-155(2005)

[2] Y. Ma et al., *Catal.Lett.* **112**, 31-36(2006)

[3] A. Y. Lozovoi, *Phys. Rev. Lett.*, **85**, 610-613 (2000).

[4] Y. Xu et al., *Appl. Surf. Sci.*, **39**, 18-23(2017).

## MS18-P08 | STRUCTURE AND THERMOELECTRIC CHARACTERIZATION OF LITHIUM-SUBSTITUTED BISMUTH PALLADIUM OXIDE

Nguyen, Hong Hai (Helmholtz-Zentrum Berlin für Materialien und Energie, Berlin, GER); Hoffmann, Jan-Ekkehard (Helmholtz-Zentrum Berlin für Materialien und Energie, Berlin, GER); Habicht, Klaus (Helmholtz-Zentrum Berlin für Materialien und Energie, Berlin, GER); Fritsch, Katharina (Helmholtz-Zentrum Berlin für Materialien und Energie, Berlin, GER)

Over the last decades, thermoelectric (TE) oxides have gained increasing interest as potential materials for the direct conversion of waste heat into electricity for applications in the mid- to high temperature range up to 1200°C. To overcome a major drawback of oxides - a typically low electrical conductivity  $\sigma$  - the use of square planar structural motifs has recently been theoretically proposed based on an inverse band structure design approach [1] and, in combination with stereo-chemically active lone-electron pairs on heavy constituent atoms, the system  $\text{Bi}_2\text{PdO}_4$  has been proposed as a promising TE oxide [2]. The material is predicted to display an intrinsically low thermal conductivity and good electrical properties, specifically a high power factor  $\text{PF}=\sigma S^2$  attainable upon hole doping. In this talk, I will present experimental work on the synthesis of polycrystalline and bulk samples of  $\text{Bi}_2\text{PdO}_4$  and Li-substituted  $\text{Bi}_2\text{Pd}_{1-x}\text{Li}_x\text{O}_4$  and report on their structural characterization by means of powder X-ray and high-resolution neutron diffraction measurements. I will further discuss the results of our macroscopic characterization of the TE properties which show that the experimental validation of theoretical predictions is a crucial step towards a better understanding and proper design of novel TE materials.

[1] E.B. Isaacs and C. Wolverton, Chem. Mater. 2018, 30, 1540-1546

[2] J. He et al., Chem. Mater. 2017, 29, 2529-2534

## MS18-P09 | DETERMINATION OF HOST AND DOPANT ION DISTRIBUTION IN $\text{Mg}_2\text{Si}_{1-x}\text{Sn}_x$

### THERMOELECTRIC MATERIALS BY ELECTRON CHANNELING

Delimitis, Andreas (University of Stavanger, Stavanger, NOR); Hansen, Vidar (University of Stavanger, Stavanger, NOR); Symeou, Elli (University of Cyprus, Nicosia, CYP); Kyratsi, Theodora (University of Cyprus, Nicosia, CYP); Minde, Mona Wethrus (University of Stavanger, Stavanger, NOR); Taftø, Johan (University of Oslo, Oslo, NOR)

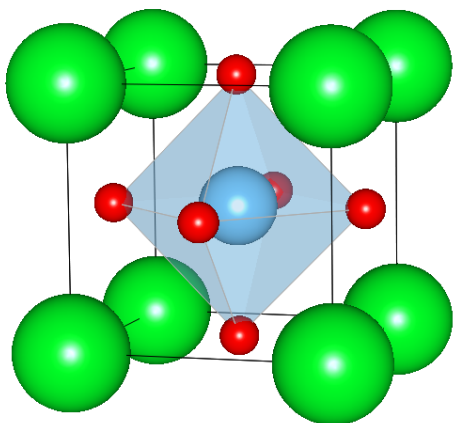
Detailed structure studies by electron microscopy methods have been widely exploited due to the unique capabilities electrons provide. Precise identification of atomic positions is feasible by employing spectroscopy techniques in an analytical transmission electron microscope. In this aspect, methods such as energy dispersive X-ray spectroscopy (EDS) are utilised, under strong channelling conditions, where the yield of element characteristic X-ray emission can be modified and manipulated, dependent upon crystallographic directions of the incident beam. These channelling effects are powerful in determining atomic site locations in crystals and techniques such as ALCHMI (Atom Location by Channeling Enhanced Microanalysis) have been developed and evaluated.

Structural analyses employing electron channelling have a recent focus in systems for renewable technologies and energy harvesting, such as thermoelectric (TE) materials. TEs based on  $\text{Mg}_2\text{Si}_{1-x}\text{Sn}_x$  have gained increased interest, due to inexpensive production costs, abundance and a toxic nature of raw materials, especially for power generation applications within the intermediate temperature range (500–900 K). Synthesis of  $\text{Mg}_2\text{Si}_{1-x}\text{Sn}_x$  in nanocrystal morphologies, often coupled by incorporation of dopants in their host matrix is exploited, with a scope to efficiently reduce thermal conductivity, particularly for Sn-rich or Bi doped Si-rich compounds. Previous studies confirmed the multiplicity of phases in this system, however, the precise distribution of host and dopant ions location is still controversial. Application of the electron channelling technique is therefore more than essential in order to accurately determine and refine their structural characteristics. Experimental outcomes will be demonstrated and discussed.

## MS18-P10 | STRUCTURAL MODIFICATION OF PEROVSKITES BY TAILORED EXSOLUTION FOR ENHANCED CATALYTIC ACTIVITY

Rameshan, Raffael (Technische Universität Wien, Wien, AUT); Rameshan, Christoph (Technische Universität Wien, Wien, AUT); Ruh, Thomas (Technische Universität Wien, Wien, AUT); Nennung, Andreas (Technische Universität Wien, Wien, AUT); Opitz, Alexander (Technische Universität Wien, Wien, AUT); Rameshan, Christoph (Technische Universität Wien, Wien, AUT); Rameshan, Raffael (Technische Universität Wien, Vienna, AUT)

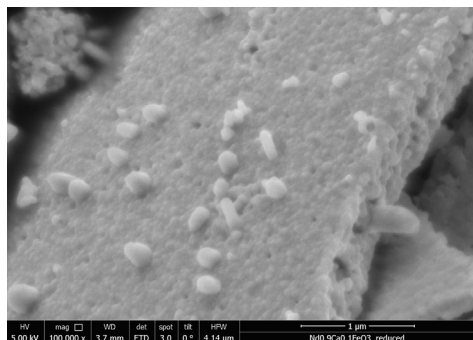
Perovskites provide a dynamic structure, where induced oxygen vacancies can trigger the formation of nanoparticles on the surface. The process of nanoparticle formation can thus be controlled and reversed by choosing a suitable chemical potential of the gas phase or by polarization (i.e. applying voltage to the system) of the perovskite.



Using a lab-based near ambient pressure X-ray photoelectron spectrometer (NAP-XPS) that is specially designed for investigations of electro-catalytic systems under realistic operating conditions combined with in-situ X-ray diffraction spectroscopy (XRD), scanning electron microscopy (SEM) and energy dispersive X-ray spectroscopy (EDX) we provide first results on the effect of exsolution on water gas shift (WGS) and reverse WGS reaction.

**Acknowledgement.** This work has received funding from the European Research Council (ERC) under the European Union's Horizon 2020 research and innovation programme (grant agreement n° 755744 / ERC - Starting Grant TUCAS).

[1] K. Momma and F. Izumi, "VESTA 3 for three-dimensional visualization of crystal, volumetric and morphology data," J. Appl. Crsallogr., 44, 1272-1276 (2011).



## MS18-P11 | BAND GAP DEPTH PROFILE OF $\text{Cu}(\text{In}_{1-x}\text{Ga}_x)\text{Se}_2$ ABSORBING LAYER IN THIN-FILM SOLAR CELL BY GLANCING INCIDENCE X-RAY DIFFRACTION

KIM, YONG-IL (Institute, Daejeon, KOR); KIM, KI-BOK (Institute, Daejeon, KOR)

Absorbing materials of the thin-film solar cells need a direct band gap and a very high absorption coefficient for visible light because the solar cells convert sunlight into electricity by exciting electrons in the absorbing layer using the photons of light from the sun. Hence,  $\text{Cu}(\text{In,Ga})\text{Se}_2$  (CIGS) has attracted attention as one of the absorbing materials due to its a direct band gap with a high absorption coefficient. One of the main factors that determine the performance of the solar cells is the band gap of the absorbing material. The present work investigates in-depth lattice parameters of the CIGS absorbing layer using a glancing incidence X-ray diffraction (GIXRD) because the band gaps of materials depend on the lattice parameters. As the glancing incident angle increases, the  $a$  and  $c$  lattice parameters changed from 5.7776(3) to 5.6905(2) Å and 11.3917(3) to 11.2114(2) Å, respectively. These variations were due to the compositional gradients of the CIGS absorbing layer. The behavior of the unit-cell volume variations was similar to the compositional depth profiles of In or Ga using energy dispersive X-ray analysis. The band gap of the CIGS absorbing layer based on the in-depth analysis of the lattice parameters refined using GIXRD data was in the range of 1.222 to 1.532 eV. This approach, estimating the relative contents of In or Ga occupied in the same lattice sites from the refinement of the lattice parameters with GIXRD provides the band gap depth profile of the absorbing layer under the unit-cell volume follows Vegard's law.

## MS18-P12 | IN-SITU CARBONATION OF SrO AT 298 K AND CONTROLLED HUMIDITY FOR THERMOCHEMICAL ENERGY STORAGE

Gravogl, Georg (University of Vienna, Vienna, AUT); Lengauer, Christian (University of Vienna, Vienna, AUT); Knoll, Christian (TU Wien, Vienna, AUT); Müller, Danny (TU Wien, Vienna, AUT); Weinberger, Peter (TU Wien, Vienna, AUT); Miletich, Ronald (University of Vienna, Vienna, AUT)

In this work the carbonation behavior of SrO under humid conditions was studied through *in-situ* pXRD measurements at room temperature conditions (298K) with respect to investigate the potential for thermochemical energy storage (TCES).

The experiments were performed on a PANalytical X'Pert Pro diffractometer in Bragg-Brentano geometry using  $\text{CuK}\alpha_{1,2}$ . An Anton Paar XRK 900 reaction chamber was used monitoring *in-situ* the reaction. In order to investigate the carbonation in the presence of  $\text{H}_2\text{O}$  saturated conditions the  $\text{CO}_2$  was previously passed through an external moisturizer.

The study reveals a remarkable carbonation behavior of SrO. As SrO is very hygroscopic it transforms almost immediately to  $\text{Sr}(\text{OH})_2$  when getting into contact with the moistened  $\text{CO}_2$ . It consecutively hydrates yielding  $\text{Sr}(\text{OH})_2 \cdot \text{H}_2\text{O}$ . Parallel to this hydration a slow continuous carbonation reaction starts which is followed by a significantly accelerated carbonation step after the  $\text{SrCO}_3$  phase reached an amount of 10 wt%. This fast carbonation completes the full conversion into  $\text{SrCO}_3$  within a short time interval.

We conclude, that the reaction starts at the surface of the particles thus forming a carbonate layer, which retards the  $\text{CO}_2$  diffusion into the core of the particles. This is the presumable reason for the slow reaction kinetics at the beginning of the carbonation process. At a certain point the comparatively fast transformation of  $\text{Sr}(\text{OH})_2 \cdot \text{H}_2\text{O}$  into  $\text{SrCO}_3$  starts, which can be explained by the formation of micro-cracks and microstructural changes including fragmentation of the particles.

## MS18-P13 | LOCAL STRUCTURE OF GLASS-CERAMIC SODIUM SULFIDIC SOLID STATE

### ELECTROLYTES

Fritsch, Charlotte (Karlsruhe Institute of Technology, Eggenstein-Leopoldshafen, GER); Stepien, Dominik (Karlsruhe Institute of Technology, Eggenstein-Leopoldshafen, GER); Hansen, Anna-Lena (Karlsruhe Institute of Technology, Eggenstein-Leopoldshafen, GER); Indris, Sylvio (Karlsruhe Institute of Technology, Eggenstein-Leopoldshafen, GER); Knapp, Michael (Karlsruhe Institute of Technology, Eggenstein-Leopoldshafen, GER); Ehrenberg, Helmut (Karlsruhe Institute of Technology, Eggenstein-Leopoldshafen, AUT)

Sodium thiophosphates are promising candidates for the use as solid state electrolytes in sodium batteries. [1] These classes of materials is derived from its lithium equivalents with the recently well-described stoichiometries  $\text{Li}_3\text{PS}_4$  and  $\text{Li}_7\text{P}_3\text{S}_{11}$ . [2] Sodium thiophosphates show a more diverse formation of crystalline phases, occurring in different symmetries, compared to their lithium equivalents. The presence of the different crystalline phases has to be studied more thoroughly in order to find relations between the local structure and sodium ion conductivity.

Different sodium thiophosphate glassy ceramics (50-90%  $\text{Na}_2\text{S}:\text{P}_2\text{S}_5$ ) were synthesized by mechanical milling. Dependent on the ratio of the reagents, the mixtures showed a different amorphisation behaviour, resulting in the formation of different properties such as sodium ion mobility. The local structure of the amorphous *as synthesized* samples was investigated with NMR and pdf technique. In addition to that, the samples were heated to observe the crystallization behaviour of the amorphous glasses.

For the first time, the synthesis of  $\text{Na}_8\text{P}_2\text{S}_9$  and  $\text{Na}_9\text{PS}_7$  with 80% and 90%  $\text{Na}_2\text{S}$  is described. Different characterization methods such as Raman,  $^{31}\text{P}$ -,  $^{23}\text{Na}$ -NMR and pdf provided information on how the electronic and crystallographic structure of these samples differs from the other phases.

[1] M. Tatsumisago, A. Hayashi, Int. J. Appl. Gl. Sc., 5 (2014).

[2] H. Stöffler et al., J. Phys. Chem. C, 123 (16), (2019).

## **MS18-P14 | NEW METHOD FOR ELECTROMECHANICAL LOSSES EVALUATION OF THE ELECTROSTRICTIVE ENERGY EFFICIENCY: EXPERIMENTS AND MODELING**

Farhan, Rida (Faculty of Sciences Ben M'Sik Hassan II University, Casablanca, Morocco, Casablanca, MAR)

Converting vibrations to a practical form of energy have been the subject of many late surveys. The concluding purpose is to convert ambient vibrations to achieve low-power consumption devices, such as microelectromechanical systems and wireless sensors, which have restricted existence duration that would need costly maintenance. The techniques used to convert vibrations into electrical energy comprise: piezoelectric elements, electromagnetic devices or electrostatic systems. Electroactive polymers have been most used as smart material for sensing in last year's. Electromechanical applications are actually concentrated on energy harvesting, including the development of wireless portable electronic equipment autonomous and specific actuators such as artificial muscles. The aim of this work is the identification of electromechanical conversion losses by electrostrictive polymers using the Fast Fourier Transform (FFT) analysis. These losses are due mainly to the variation of the electrical and mechanical parameters exciting the electrostrictive polymer. In order to estimate this dissipated energy, an evaluation by FFT has been performed. In this context, an analytical model will be detailed and the theoretical results will be compared with the experimental results. Good agreement have been found between the two approaches.

Keywords: Electrostrictive polymer, electromechanical losses, FFT analysis, energy conversion

## MS18-P15 | THERMOCHROMIC LEAD-FREE HALIDE DOUBLE PEROVSKITES

Ning, Weihua (Linköping university, Linköping, SWE); Gao, Feng (Linköping university, Linköping, SWE)

Lead-free halide double perovskites with diverse electronic structures and optical responses, as well as superior material stability show great promise for a range of optoelectronic applications. However, their large bandgaps limit their applications in the visible light range such as solar cells. In this work, an efficient temperature-derived bandgap modulation, that is, an exotic fully reversible thermochromism in both single crystals and thin films of Cs<sub>2</sub>AgBiBr<sub>6</sub> double perovskites is demonstrated. Along with the thermochromism, temperature-dependent changes in the bond lengths of Ag–Br ( $R_{\text{Ag-Br}}$ ) and Bi–Br ( $R_{\text{Bi-Br}}$ ) are observed. The first-principle molecular dynamics simulations reveal substantial anharmonic fluctuations of the  $R_{\text{Ag-Br}}$  and  $R_{\text{Bi-Br}}$  at high temperatures. The synergy of anharmonic fluctuations and associated electron–phonon coupling, and the peculiar spin–orbit coupling effect, is responsible for the thermochromism. In addition, the intrinsic bandgap of Cs<sub>2</sub>AgBiBr<sub>6</sub> shows negligible changes after repeated heating/cooling cycles under ambient conditions, indicating excellent thermal and environmental stability. This work demonstrates a stable thermochromic lead-free double perovskite that has great potential in the applications of smart windows and temperature sensors. Moreover, the findings on the structure modulation-induced bandgap narrowing of Cs<sub>2</sub>AgBiBr<sub>6</sub> provide new insights for the further development of optoelectronic devices based on the lead-free halide double perovskites.

## MS18-P16 | INFLUENCE OF Fe DOPING ON THE CRYSTAL STRUCTURE, ELECTRONIC STRUCTURE AND SUPERCAPACITANCE PERFORMANCE OF BIRNESSITE WITH HIGH AREAL MASS LOADING

Liu, Hao (China University of Geoscience (Beijing), Beijing, CHN); Liao, Libing (China University of Geosciences (Beijing), Beijing, CHN); Gu, Wenlong (China University of Geosciences (Beijing), Beijing, AUT); Lv, Guocheng (China University of Geosciences (Beijing), Beijing, CHN); Mei, Lefu (China University of Geosciences (Beijing), Beijing, CHN)

The supercapacitance performance of birnessite is greatly hindered by poor electrical conductivity, especially when the areal mass loading of the active materials is high enough for practical application. Heterogeneous atom doping is an effective way for improving the supercapacitance performance of birnessite. Herein, we mainly investigate the influence of Fe doping on the crystal structure, electronic structure and capacitance performance of birnessite in detail by combining the experiments and theoretical calculations/simulations. It is found that Fe atoms mainly substitute the central trivalent Mn in  $[\text{MnO}_6]$  octahedral after doping without changing the crystalline phase of birnessite. Meanwhile, the particle size and surface area of Fe-doped birnessite continuously increase with the increase of the content of Fe dopant. On the other hand, the electronic conductivity of the doped birnessite firstly increases and then decreases with the increase of the Fe content due to the reduced indirect band gap and the increased number of the boundary/grain interfaces. Based on these results, the influences of Fe doping on the supercapacitance performance of birnessite electrode with very high areal mass loading of  $\sim 10\text{-}12 \text{ mg cm}^{-2}$  are elaborately discussed related to morphology, structure, electrical conductivity, and ion diffusion properties.

## MS18-P17 | THE INFLUENCES OF MG INTERCALATION ON THE STRUCTURE AND SUPERCAPACITIVE BEHAVIOURS OF MoS<sub>2</sub>

Liao, Libing (China University of Geosciences (Beijing), Beijing, CHN); Liu, Hao (China University of Geoscience (Beijing), Beijing, CHN); Chen, Bochao (China University of Geosciences (Beijing), Beijing, CHN); Lv, Guocheng (China University of Geosciences (Beijing), Beijing, CHN); Mei, Lefu (China University of Geosciences (Beijing), Beijing, CHN)

Metallic 1T MoS<sub>2</sub> greatly benefits the application of MoS<sub>2</sub> in many fields, such as electrochemical energy storage systems, due to its considerably higher conductivity as compared to semiconducting 2H MoS<sub>2</sub>. Alkali metals, such as Li, Na and K, are always used to prepare 1T MoS<sub>2</sub> through intercalation of alkali metal ions into the interlayer of 2H MoS<sub>2</sub>. Nevertheless, the properties of MoS<sub>2</sub> with alkali-earth metals as guest in the interlayer are rarely investigated and the influences of these guest ions on the polymorphs of MoS<sub>2</sub> have not been known. Herein, we introduced hydrated Mg ions as the guest into MoS<sub>2</sub> nanosheets, which leads to enlarged interlayer spacing of 1.144 nm as compared to pristine MoS<sub>2</sub> and restacking MoS<sub>2</sub>. Moreover, the 1T phase concentration after the introduction of hydrated Mg ions was as high as ~90%. Consequently, as supercapacitor electrode, the specific capacitance of the MoS<sub>2</sub> with Mg guest ions was greatly improved as compared to the restacking MoS<sub>2</sub> or pristine MoS<sub>2</sub> counterparts at different discharging/charging rates. Both the energy densities and power densities of the MoS<sub>2</sub> with Mg guest ions electrode were therefore superior to the other two electrodes.

## MS18-P18 | THE SURFACE PHASE DIAGRAM OF $\text{La}_{0.8}\text{Sr}_{0.2}\text{MnO}_3$ IN STM

Riva, Michele (Institute of Applied Physics - TU Wien, Wien, AUT); Franceschi, Giada (Institute of Applied Physics - TU Wien, Wien, AUT); Schmid, Michael (Institute of Applied Physics - TU Wien, Wien, AUT); Diebold, Ulrike (Institute of Applied Physics - TU Wien, Wien, AUT)

Solid oxide fuel cells produce clean electricity by electrochemically oxidizing a fuel. This entails reduction of oxygen at the cathode's surface and its incorporation in the device. The rate of oxygen reduction and incorporation reactions at the cathode's surface is currently limiting the device efficiency. In most commercial applications, the cathode material is  $\text{La}_{0.8}\text{Sr}_{0.2}\text{MnO}_3$  (LSMO). Investigating the influence of the LSMO surfaces on its performance requires establishing models for its surface structures. To this end, we have combined PLD with *in-situ* surface science techniques to grow and investigate epitaxial, single-crystalline LSMO(110) films on  $\text{SrTiO}_3$ (110).

We observe a rich variety of composition-related surface reconstructions that compensate for the LSMO(110) bulk polarity. We show that we can control these structures by tuning the surface composition, e.g., via deposition of defined amounts of the constituents. By performing the deposition experiments at fixed temperature and pressure, we establish a composition phase diagram at fixed oxygen chemical potential ( $\mu_{\text{O}}$ ).

We then investigate the stability of these structures over a variety of  $\mu_{\text{O}}$ s by annealing the samples at oxygen pressures ranging from 0.2 mbar to UHV. The (La,Sr)-rich (1×1) structure is exceptionally stable, and stays unaltered upon annealing at all temperatures and pressures. The Mn-rich surfaces laterally separate into Mn-poor (1×1) areas and new Mn-richer structures, preserving the overall surface stoichiometry. We investigate this behaviour in detail and establish a surface phase diagram as a function of both,  $\mu_{\text{O}}$  and cation chemical potentials.



## Ms18-P19 | COMBINATION OF DATA MINING AND DFT MODELING OF $\text{Ag}^+$ -CONDUCTIVITY IN S(SE)-CONTAINING INORGANIC COMPOUNDS

Morkhova, Yelizaveta (Samara Center for Theoretical Materials Science, Samara, RUS)

Now the Li-batteries meet problems of large-scale production: they are unsafe and expensive due to depletion of natural resources. Replacement of the Li conductors with new high-conductive substances is a great challenge for materials science. One of the solutions is the processing of large amounts of structural data to mine prospective ion conductors. We use fast database screening by means of ToposPro program package [1], which we have designed for modeling of ion conductivity. We have adopted Voronoi approach to explore  $\text{Ag}^+$ -ion migration in S(Se)-containing compounds and selected 826 ternary and quaternary Ag and S(Se)-containing compounds from the last ICSD. The 91 S- and 42 Se-containing structures were found, which possess 1D, 2D or 3D  $\text{Ag}^+$ -ion migration maps.

Out of them, 87 compounds have not been examined before as  $\text{Ag}^+$ -ion conductors and can be recommended for experimental testing. Further, we estimated the migration energies for 13 compounds by the NEB method within the DFT approach and found a good agreement with the experimental conductivity for  $\text{Ag}_4\text{P}_2\text{S}_6$ ,  $\text{AgCrS}_2$  and  $\text{Ag}_3\text{PS}_4$ . Such combination of fast crystallochemical and precise DFT methods can serve as an effective prediction scheme to search for new fast-ion conductors.

[1] Vladislav Blatov, Alexander Shevchenko, Davide Proserpio // *Cryst. Growth Des.* 2014. V. 14.7. P. 3576-3586.



## MS19: Quantum Materials

---

### MS19-01 | ORBITAL MOLECULES IN OXIDES

Attfield, J. Paul (University of Edinburgh, Edinburgh, GBR)

Orbital molecules are weakly bonded clusters of transition metal ions within an orbitally ordered solid [1]. The importance of these quantum states has become apparent in recent years following the discovery of ‘trimeron’ orbital molecules in the ground state of magnetite ( $\text{Fe}_3\text{O}_4$ ) [2]. Determination of the full superstructure below the famous Verwey transition at 125 K showed that  $\text{Fe}^{2+}/\text{Fe}^{3+}$  charge ordering occurs with a pronounced orbital ordering of  $\text{Fe}^{2+}$  states that leads to localization of electrons in the linear, three-Fe trimers. Recent results on orbital molecule orders in doped magnetites including natural samples will be presented [3]. Vanadium oxides also provide many examples of orbital molecule orders, associated with NTE (negative thermal expansion) in the orbital polymer material  $\text{V}_2\text{OPO}_4$ . [4] Persistence of large orbital molecules to high temperatures is discovered in the spinels  $\text{AlV}_2\text{O}_4$  [5] and the new analog  $\text{GaV}_2\text{O}_4$  [6]. Electronic phase separation driven by trimeron formation has recently been reported in  $\text{CaFe}_3\text{O}_5$  [7]. Finally, some recent results revealing the origin of the Verwey transition will be presented [8]

- [1] J. P. Attfield, *APL Materials* 2015, **3**, 041510.
- [2] M.S. Senn, J.P. Wright, J.P. Attfield, *Nature* 2012, **481**, 173.
- [3] G. Perversi, et al, *Chem. Comm.* 2016, **52**, 4864.
- [4] E. Pachoud, et al, *J. Am. Chem. Soc.* 2018, **140**, 636.
- [5] A. J. Browne; et al. *Phys Rev Mat* 2017, **1**, 052003.
- [6] A. J. Browne; et al. *Inorg. Chem.* 2018, **57**, 2815.
- [7] K. H. Hong, et al *Nature Comm.* 2018, **9**, 2975.
- [8] G. Perversi, et al, submitted.

## MS19-02 | TORQUE MAGNETOMETRY, A TOOL FOR MAGNETIC CRYSTALLOGRAPHY IN THIN FILMS OF FRUSTRATED MAGNETS

Beekman, Christianne (Florida State University, Tallahassee, USA)

Geometrically frustrated systems have an incompatibility between the lattice geometry and the magnetic interactions, resulting in macroscopically degenerate ground-state manifolds. In pyrochlore titanates (such as  $\text{Ho}_2\text{Ti}_2\text{O}_7$ ), large single ion anisotropy leads to a highly degenerate two-in/two-out spin ice state. Degeneracy is lifted when magnetic fields are applied, leading to transitions between various spin textures that depend on the direction of the field, and to emergent excitations equivalent to magnetic monopoles. There is an enticing potential of harnessing these monopoles, as information carriers; to realize these thin films are required. I will demonstrate the applicability of torque magnetometry in probing specific spin textures hosted by the spin ice state, and the transient states associated with transitions between them. High quality single crystals and thin films have been measured at temperatures down to 20 mK in applied fields up to 11 T. Sample rotation allowed for application of magnetic fields along various crystallographic directions of the samples. Utilizing reported results from neutron scattering as a starting point I have developed a phenomenological model that describes the anisotropic magnetic phase diagram of the bulk spin ice. This sensitive technique is highly suitable for thin film characterization; hence, this paves the way to compiling temperature-field phase diagrams, detailing thin film spin ice physics as a function of film thickness and strain.

C.B. acknowledges support from the National Research Foundation, grant NSF DMR-1847887. The National High Magnetic Field Laboratory is supported by National Science Foundation through NSF DMR-1157490 / DMR-1644779, and the State of Florida.

## MS19-03 | CRYSTAL GROWTH INVESTIGATIONS OF LITHIUM IRIDATE, $\text{Li}_2\text{IrO}_3$ , AND LITHIUM RUTHENATES, $\text{Li}_2\text{RuO}_3$ AND $\text{Li}_3\text{RuO}_4$

Kerkhoff, Linda (Section Crystallography, Institute of Geology and Mineralogy, University of Cologne, Köln, GER); Becker, Petra (Section Crystallography, Institute of Geology and Mineralogy, University of Cologne, Köln, GER)

Recently, lithium ruthenates,  $\text{Li}_2\text{RuO}_3$  and  $\text{Li}_3\text{RuO}_4$ , and the  $\text{Li}_2\text{IrO}_3$ -modifications attracted considerable attention with exhibiting unconventional magnetism[1-3].

The structures of the three modifications of  $\text{Li}_2\text{IrO}_3$  ( $\alpha$ -,  $\beta$ - and  $\gamma$ - $\text{Li}_2\text{IrO}_3$ [4-6]) and  $\text{Li}_2\text{RuO}_3$ [7] consist of a honeycomb-like network, while the main structural components of  $\text{Li}_3\text{RuO}_4$  are zigzag chains[8]. The need for high-quality single crystals for further investigations turns all compounds into subjects of crystal growth efforts, which are complemented by DTA and powder-XRD.

Single crystals are grown from the gaseous phase. A modified setup after [9] was realised, in which educts are separated by spacers with spikes, acting as preferred nucleation sites. The place of crystallisation depends on the position of the chemical equilibrium. Moreover,  $\text{Li}_2\text{IrO}_3$ -modifications show preferred growth conditions. For the first time, the applicability of this setup for the growth of  $\text{Li}_3\text{RuO}_4$  is shown.

Currently, single crystals of  $\alpha$ - $\text{Li}_2\text{IrO}_3$ (1mm),  $\beta$ - $\text{Li}_2\text{IrO}_3$ (0,5mm),  $\text{Li}_2\text{RuO}_3$ (0,6mm) and  $\text{Li}_3\text{RuO}_4$ (0,1mm) can be grown successfully.

- [1] Jackeli & Khaliullin, *Phys.Rev.Lett.*, **102**,017205(2009)
- [2] Chaloupka et al., *Phys.Rev.Lett.*, **105**,027204(2010).
- [3] Manuel et al., *Phys.Rev.B*, **84**,174430(2011).
- [4] O'Malley et al., *J.Solid State Chem.*, **181**,1803–1809(2008).
- [5] Biffin et al., *Phys.Rev.B*, **90**,205116(2014).
- [6] Modic et al., *Nat.Comm.*, **5**,4203(2014).
- [7] Kobayashi et al., *Solid State Ionics*, **82**,25-31(1995).
- [8] Alexander et al., *J.Mater.Chem.*, **13**,2612-2616(2003).
- [9] Freund et al., *Scientific reports*, **6**,35362(2016).

## MS19-04 | CRYSTAL STRUCTURE AND ISOTOPE EFFECT IN QUANTUM LIQUID $\text{H}_3\text{LiIr}_2\text{O}_6$

Gibbs, Alexandra (ISIS Neutron and Muon Source, Didcot, GBR); Takayama, Tomohiro (University of Stuttgart, Stuttgart, GER); Takagi, Hidenori (Max Planck Institute for Solid State Research, Stuttgart, GER)

The search for realisations of the Kitaev model on a honeycomb lattice has recently led to the discovery of  $\text{H}_3\text{LiIr}_2\text{O}_6$ , lacking long-range order down to 50 mK and displaying experimental signatures consistent with a spin liquid ground state. Although the Ir-O network and its distortions are fundamental to the bond-dependent interactions on the honeycomb lattice, theoretical work suggests the inter-layer hydrogen and its ordering is crucial to understanding the intriguing behaviour of  $\text{H}_3\text{LiIr}_2\text{O}_6$ . Upon deuterium substitution, the antiferromagnetic couplings are enhanced but the liquid state remains robust. Structural studies to date have relied on X-ray diffraction which is unable to locate hydrogen / deuterium ions in the presence of heavy iridium, requiring the intuiting of possible positions based on crystal chemistry and knowledge of similar layered materials. Recently we have used the isotope effect on  $\text{H}_3\text{LiIr}_2\text{O}_6$  to study the effect of the inter-layer species. In addition, we have taken advantage of recent developments in the use of  $^{193}\text{Ir}$  enrichment. The structures of  $\text{H}_3\text{}^7\text{Li}^{193}\text{Ir}_2\text{O}_6$  and  $\text{D}_3\text{}^7\text{Li}^{193}\text{Ir}_2\text{O}_6$  have been elucidated using high resolution neutron diffraction, allowing the crucial determination of the hydrogen/deuterium positions and studies of disorder. The results of these detailed structural studies and their link to the isotope effect on physical properties will be discussed within the context of recent theoretical work and future materials design.

## MS19-05 | STRUCTURE AND MAGNETIC PHASES IN THE $\text{Cs}_2\text{CuCl}_{4-x}\text{Br}_x$ MIXED SYSTEM

van Well, Natalija (University Bayreuth, Bayreuth, GER); Eisele, Claudio (Laboratory of Crystallography, University of Bayreuth, Bayreuth, GER); Ramakrishnan, Sitaram (Laboratory of Crystallography, University of Bayreuth, Bayreuth, GER); Shang, Tian (Laboratory for Multiscale materials experiments, Paul Scherrer Institute, Villigen, GER); Medarde, Marisa (Laboratory for Multiscale materials experiments, Paul Scherrer Institute, Villigen, CH); Cervellino, Antonio (Swiss Light Source (SLS), Paul Scherrer Institute, Villigen, CH); Skoulatos, Markos (Heinz Maier-Leibnitz Zentrum (MLZ), Technische Universität München, Garching bei München, GER); Georgii, Robert (Heinz Maier-Leibnitz Zentrum (MLZ), Technische Universität München, Garching bei München, GER); Pedersen, Björn (Heinz Maier-Leibnitz Zentrum (MLZ), Technische Universität München, Garching bei München, GER); van Smaalen, Sander (Laboratory of Crystallography, University of Bayreuth, Bayreuth, GER)

The  $\text{Cs}_2\text{CuCl}_{4-x}\text{Br}_x$  mixed system is very rich in structural and magnetic phases, which can be separated by their tetrahedral/octahedral  $\text{Cu}^{2+}$  environment. For the tetrahedral one, neutron diffraction investigation of the magnetic phase diagram of  $\text{Cs}_2\text{CuCl}_{4-x}\text{Br}_x$  provides detailed information about the influence of a specific Br concentration on the magnetic structure [1]. For the octahedral one, the compounds are typical quasi 2-D antiferromagnets. The realisation of the new tetragonal phase of  $\text{Cs}_2\text{CuCl}_4$  is possible using specific crystal growth conditions at a temperature below 281K. For the structure investigation, synchrotron powder diffraction was used. The susceptibility measurements of it show similar magnetic behaviour like the tetragonal  $\text{Cs}_2\text{CuCl}_{2.9}\text{Br}_{1.1}$ ,  $\text{Cs}_2\text{CuCl}_{2.5}\text{Br}_{1.5}$  and  $\text{Cs}_2\text{CuCl}_{2.2}\text{Br}_{1.8}$  and present consistent results for typical quasi 2-D antiferromagnets [2]. The structure analysis down to 4K for  $\text{Cs}_2\text{CuCl}_{2.2}\text{Br}_{1.8}$  shows no phase transition and the tetragonal symmetry  $I4/mmm$ , being the same at room temperature. However, the new neutron single crystal diffraction investigation presents a very small orthorhombic distortion (subgroup relationship). Several magnetic reflections corresponding to the propagation vector  $k = (0, 0, 0)$  are observed for this compound below the magnetic phase transition at  $T_N = 11.3\text{K}$  confirming its antiferromagnetic nature.

[1] Natalija van Well et al., Annalen der Physik, 530,1800270 (2018)

[2] P.T. Cong et al., IEEE Transactions on Magnetics 50, 2700204 (2014)

## MS19-P01 | HIGH-PRESSURE SYNTHESIS, CRYSTAL STRUCTURE, AND MAGNETIC PROPERTIES OF $\text{Ba}_3\text{CuOs}_2\text{O}_9$

Chen, Jie (National Institute for Material Science, Tsukuba, JPN); Feng, Hai L. (Max Planck Institute for Chemical Physics of Solids, Dresden, GER); Matsushita, Yoshitaka (National Institute for Materials Science (NIMS), Tsukuba, JPN); Belik, Alexei A. (National Institute for Material Science, Tsukuba, JPN); Yoshihiro, Tsujimoto (National Institute for Material Science, Tsukuba, JPN); Katsuya, Yoshio (National Institute for Material Science, Sayo, JPN); Tanaka, Masahiko (National Institute for Material Science, Sayo, AUT); Li, Man-Rong (Sun Yat-sen University, Guangzhou, CHN); Liang, Hongbin (Sun Yat-sen University, Guangzhou, CHN); Zheng, Lirong (Institute of High Energy Physics, Beijing, CHN); Yamaura, Kazunari (National Institute for Material Science, Tsukuba, JPN)

The triple perovskite  $\text{Ba}_3\text{CuOs}_2\text{O}_9$  crystallizes into an orthorhombic structure (Cmcm) and shows a manifest antiferromagnetic transition at 47 K [1], while it crystallizes into a hexagonal structure ( $P6_3/mmc$ ) when treated under a high-pressure and high-temperature condition (typically 6 GPa and 1100 °C). The change of structure gains a 1.3% increase in structural density. The hexagonal phase was quenched at ambient condition and the magnetic and electrical properties were investigated via measurements of the ac and dc magnetic susceptibilities, electrical resistivity, and specific heat capacity. The data indicated that the magnetic transition temperature increased to 290 K by the structure change. We discuss details of the magnetic and electrical properties of the newly synthesized hexagonal  $\text{Ba}_3\text{CuOs}_2\text{O}_9$ .

[1] H. L. Feng and M. Jansen *J Solid State Chem.* **258**, 776 (2018).

## MS19-P02 | SELF-ASSEMBLY OF OCTANUCLEAR COMPLEXES CONTAINING TETRA- AND PENTACOORDINATE Co(II) CENTERS

Nemec, Ivan (CEITEC BUT, Brno, CZE)

In this work we report on synthesis, crystal structures, spectroscopic and magnetic properties of octanuclear Co(II) complexes, which were prepared by self-assembly of Co(II) perchlorates or tetrafluoroborates with neocuproine in alcoholic solutions (MeOH or PhOH) and in the presence of aliphatic triamines. The resulting molecular structures contain alcoholate and carbonate bridging ligands and each Co(II) metal center is coordinated by neocuproine ligand. Remarkably, all the central atoms are tetra- or pentacoordinate and aliphatic triamines do not coordinated the Co(II) atoms.

Magnetic properties of the prepared compounds were investigated by magnetometry and EPR spectroscopy. It was revealed that magnetic exchange interactions are of antiferromagnetic nature. The experimental investigations were supported by BS-DFT and CASSCF theoretical calculations.

## MS19-P03 | MAGNETISM IN DOUBLE PEROVSKITES $\text{Ba}_2\text{CrMoO}_6$

BOUADJEMI, Bouabdellah (University of Mostaganem, Algeria, MOSTAGANEM, DZA); BOUADJEMI, Bouabdellah (University of Mostaganem 27000, Algeria, Mostaganem, DZA); MATOUGUI, Mohamed ( University of Mostaganem, Algeria, MOSTAGANEM, DZA); HOUARI, Mohamed (University of Mostaganem, Algeria, MOSTAGANEM, DZA); BENTATA, Samir (University of Mascara, Algeria, MASCARA, DZA); LANTRI, Tayeb (University of Mostaganem, Algeria, MOSTAGANEM, DZA); HAID, Slimane ( University of Mostaganem, Algeria, MOSTAGANEM, DZA)

Cubic  $\text{Ba}_2\text{CrMoO}_6$  double perovskite (see Fig.1) is studied using the full potential linearized augmented plane wave (FP-LAPW) method within the frame work of density functional theory (DFT). The structural, electronic and magnetic properties are calculated by using the GGA approximation, GGA+U and MBJ-GGA. Density of states and band structure results reveal a half-metallic ferromagnetic ground state for this component. The mBJ calculations yield a better energy-gap than the GGA and GGA+U methods. Our results make the  $\text{Ba}_2\text{CrMoO}_6$  double perovskite to be a promising candidate for the spintronic application.

## MS20: Combined Approaches for Structure Characterization of Complex...

---

### MS20-01 | COMBINED ANALYSIS OF STRUCTURE AND STRAIN IN ENGINEERING MATERIALS BY NEUTRON AND SYNCHROTRON X-RAY DIFFRACTION, AND ELECTRON MICROSCOPY

Korsunsky, Alexander (University of Oxford, Oxford, GBR)

Heterogeneous multi-scale nature commonly observed in advanced engineered and natural materials are the subject of active experimental and modelling research. Key ideas will be introduced for materials and tissues such as human dentine and enamel, nickel-base superalloys, and materials for Li-ion battery cathodes.

Structure and processes in battery cathodes were considered using combined techniques. Damage during cyclic charging develops from the atomic lattice scale to nano-, micro- and macro-scale. Recent results will be overviewed:

1. *Operando* X-ray absorption spectroscopy (XANES, EXAFS) of Mn, Co and Ni atomic environment evolution during (dis)charging reveals 'staged', partially reversible nature [1].
2. *Operando* synchrotron X-ray diffraction analysis of unit cell dimension and phase transformation in  $\text{Li}(\text{Mn,Co,Ni})\text{O}_2$  reveals the origins of anisotropic lattice straining [2].
3. TOF-SIMS quantitative nanoscale mapping of Li distribution in mixed transition metal oxide cathodes reveals the presence of Li "hot spots" and "trapping" causing local strains and strain gradients [3].
4. Analytical solutions for Li concentration and stress in secondary spherical particles in cathodes during charging/discharging [4].
5. Progressive fragmentation of secondary active material particles in cyclic charging under lithiation-induced inter-granular strains [5].
6. Nano- to micro-scale FIB-SEM serial sectioning tomography of Li battery cathodes for visual evidence of active material fragmentation [6].

[1] Kim TH et al., 2016

[2] Song BH et al., PCCP, 2016

[3] Song BH et al., NanoEnergy 2015

[4] Korsunsky AM, Sui T, Materials & Design, 2015

[5] Sun GH et al., Extreme Mechanics Letters, 2016

[6] Song BH et al., J Mater Chem A, 2015

## MS20-02 | X-RAY CHARACTERIZATION OF MORPHOLOGY AND STRUCTURE OF MATERIALS AT MULTIPLE LENGTH SCALES

Zschech, Ehrenfried (Fraunhofer IKTS Dresden, Dresden, GER)

High-resolution 3D characterization of materials and structures is needed in materials research and development. Currently, two types of laboratory-based XCT setups, micro XCT in projection geometry with a resolution of about 1 micrometer and nano XCT with focusing X-ray lenses with a resolution down to < 100 nanometers, are available commercially for nondestructive 3D inspection of medium and small sized objects, as well as object interiors and materials' microstructure components. Because of their ability to reveal structural characteristics, materials' microstructure and flaws, such as cracks and pores, or local composition and density differences, they are potential techniques for imaging of micro- und nano-structured objects. Examples for high-resolution X-ray imaging will be shown: Crack propagation in composites and failure localization in microchips, morphology of porous or skeleton materials and interior of biological objects.

Perspectives of high-resolution XCT for nondestructive 3D imaging of materials will be provided. Potential and limits of these XCT techniques for nondestructive evaluation of geometrical features, materials' microstructure and flaws will be discussed. Perspectives to overcome two major limitations of state-of-the-art nano XCT tools, i.e. the necessity of sample preparation (typically less than 50 mm thickness, depending on the material composition, if 8 keV photons are used) and low sample throughput, will be given. A novel tool concept for X-ray microscopy at high photon energies, using advanced X-ray sources with high flux and the option of multi-energy photons, and of advanced X-ray optics with high efficiency at photon energies > 10 keV, will be presented.

## MS20-03 | CHARACTERIZATION OF APERIODIC BI-BASED LAYERED OXIDES THIN FILMS BY TEM MULTISCALE APPROACHES

Boullay, Philippe (CRISMAT - CNRS UMR 6508, Caen, FRA); Li, Leigang (School of Materials Engineering, West Lafayette, USA); Lu, Ping (Sandia National Laboratories, Albuquerque, USA); Jian, Jie (School of Materials Engineering, West Lafayette, USA); Pérez, Olivier (CRISMAT - CNRS UMR 6508, Caen, FRA); Wang, Haiyan (School of Materials Engineering, West Lafayette, USA)

Using strain engineering, metastable phases can be stabilized in the form of thin films. Besides their intrinsically small diffracting volume, these films are clamped onto a thick crystalline substrate that significantly complicates their analysis by X-ray diffraction methods and usually prevents any structure determination of unknown complex phases stabilized in the form of thin films. In this contribution we will show that the combination of multiscale approaches in a transmission electron microscope is a powerful tool to provide structural information using imaging, spectroscopy and 3D electron diffraction methods even for artificially grown layered composite structures (LCS).

We present here two novel Bi-based LCS prepared by pulsed laser deposition from  $\text{Bi}_2\text{AlMnO}_6$  (BAMO) [1] and  $\text{Bi}_2\text{NiMnO}_6$  (BNMO) [2] targets. Both LCS are composed of alternative layer stacking of two sub-lattices along the film growth direction where the sub-lattice 1 consists of a  $(\text{A}/\text{Mn})\text{O}_6$  octahedral slab with  $\text{A} = \text{Al}$  or  $\text{Ni}$  and the sub-lattice 2 consists of a  $\text{Bi}_2\text{O}_3$  slab (Fig. 1). The sub-lattice 2 presents a stacking disorder whose origin can be understood based on a local structure inspection by STEM-HAADF imaging. In terms of properties, these new materials possess tunable physical properties including robust room-temperature ferromagnetism and unique optical properties [1,2].

[1] L. Li, P. Boullay et al., *Nano Lett.* 17 (2017) 6575-6582.

[2] L. Li, P. Boullay et al., *Materials Today Nano* (2019) accepted.

## MS20-04 | ORIENTATIONAL DISORDER IN MONOMETHYL-QUINACRIDONE INVESTIGATED BY RIETVELD REFINEMENT, PAIR-DISTRIBUTION FUNCTION ANALYSIS AND LATTICE-ENERGY MINIMISATIONS

Schmidt, Martin U. (Goethe-Universität, Frankfurt a.M., Frankfurt am Main, GER); Schlesinger, Carina (Goethe Universität, Frankfurt am Main, GER); Hammer, Sonja M. (Goethe-Universität, Frankfurt am Main, GER)

The crystal structure of the poorly crystalline, organic red pigment 2-monomethyl-quinacridone ( $C_{21}H_{14}N_2O_2$ ) was solved from X-ray powder diffraction data. The structure solution led to a crystal structure in  $P-1$  with  $Z = 1$ , with a molecule on the inversion centre. Correspondingly, the molecule, which itself has no inversion symmetry, must be orientationally disordered on two orientations, with a disorder of  $CH_3$  versus H. The disorder and the local structure were investigated using various ordered structural models in  $P1$  and  $P-1$ ,  $Z = 1, 2$ , and 4. All models were analysed by three approaches: Rietveld refinement, fit to the pair-distribution function (PDF), and lattice-energy minimisation.

All Rietveld refinements with *TOPAS V4* [1] converged with acceptable  $R$ -values. All fits to the PDF using *TOPAS V6* [2] were quite reasonable. The lattice-energies of the optimised structures using the *DREIDING* [3] force field were within a range of  $6 \text{ kJ mol}^{-1}$ . In all methods there were small, but significant differences between the various structural models. In conclusion, all methods favour a statistical orientational disorder with a preferred antiparallel orientation of molecules in neighbouring chains. [4]

[1] Coelho A. A., *TOPAS-Academic 4.1*, Coelho Software, **2007**, Brisbane.

[2] Coelho A. A. *J. Appl. Cryst.* **2018**, 51, 210-218.

[3] Mayo S. L., Olafson B. D., Goddard III W. A., *J. Phys. Chem.*, **1990**, 94, 8897.

[4] Schlesinger, C., Hammer, S. M., Schmidt, M. U., submitted.

## MS20-05 | SMALL-ANGLE SCATTERING STUDY FOR DEVELOPING ALKALINE DURABLE IMIDAZOLIUM-BASED GRAFTED ANION EXCHANGE MEMBRANES FOR Pt-FREE FUEL CELLS

Zhao, Yue (National Institutes for Quantum and Radiological Science and Technology, Takasaki, JPN)

Anion-exchange membranes (AEMs) have been regarded as an alternative to proton-exchange membranes (PEMs) in energy conversion devices, due to the advantage of saving expensive platinum catalysts. However, neither the molecular design nor the property understanding is sufficient for developing AEMs capable of practical fuel cell applications. It is crucial to thoroughly study the current AEMs in terms of their chemical/microscopic structures and membrane properties. We recently developed new grafted AEMs by radiation-induced grafting method, where imidazolium and styrene monomers were grafted into poly(ethylene-co-tetrafluoroethylene) (ETFE) base films. We have discovered the correlations between suitable membrane properties and morphologies using small-angle scattering technique. Our results show that: 1) semi-crystalline feature conserved from the base film offers good mechanical properties; 2) a clear micro-phase separation between conducting phase composed of graft polymers and water, and non-conducting phase promotes the conductivity; 3) a homogeneous conducting phase is more alkaline stable than a heterogeneous conducting phase, and the ion transport in the homogeneous phase is more efficient. This study contributes to a better understanding of the interplay between the structure and properties of the anion-exchange membranes that should make it possible to rationally design membranes with optimal properties.

## MS20-P01 | DISCOVERY OF COMPLEX METAL OXIDE MATERIALS BY RAPID PHASE IDENTIFICATION AND STRUCTURE DETERMINATION

Li, Jian (Stockholm University, Stockholm, SWE); Sun, Junliang (Perking University, Beijing, CHN)

The discovery of new inorganic functional materials is of fundamental importance in synthetic and materials science. In the past, the discovering new materials relied on a slow and serendipitous trial-and-error process, especially in the well-studied oxide systems. Here, we presented a strategy to shorten the period of discovery of new complex metal oxide materials by rapid phase identification and structure determination with 3D electron diffraction (ED) techniques, which do not require pure samples or single crystal growth. With such strategy, three new complex metal oxide materials ( $\text{BiTi}_{0.855}\text{Fe}_{1.145}\text{O}_{4.93}$ ,  $\text{BiTi}_4\text{FeO}_{11}$  and  $\text{BiTi}_2\text{FeO}_7$ ) were discovered in the simple ternary  $\text{Bi}_2\text{O}_3$ - $\text{Fe}_2\text{O}_3$ - $\text{TiO}_2$  system. To our best knowledge, it is the first time to discover three new complex metal oxide materials with new structure types in a single study of ternary metal oxide system. The structures of new materials were refined by combining powder X-ray diffraction (PXRD) with powder neutron diffraction (PND). The most striking feature in this system is that  $\text{BiTi}_{0.855}\text{Fe}_{1.145}\text{O}_{4.93}$  presents edge-shared five-coordinated iron/titanium polyhedra. In addition, another new phase  $\text{BiTi}_4\text{GaO}_{11}$ , which is isostructural with  $\text{BiTi}_4\text{FeO}_{11}$ , can be obtained when replacing Fe in  $\text{BiTi}_4\text{FeO}_{11}$  with Ga. This method for developing new materials is available to all fields in chemistry and material chemistry where the limiting factors are impurity, submicrometer-sized crystals, etc.

## MS20-P02 | SYNTHESIS AND STRUCTURE DETERMINATION OF SCM-15: A 3D LARGE PORE ZEOLITE WITH INTERCONNECTED STRAIGHT 12×12×10-RING CHANNELS

Luo, Yi (Stockholm University, Stockholm, SWE); Smeets, Stef (Stockholm University, Stockholm, SWE); Wang, Zhendong (Sinopec Shanghai Research Institute of Petrochemical Technology, Shanghai, CHN); Sun, Junliang (Stockholm University, Stockholm, SWE); Yang, Weimin (Sinopec Shanghai Research Institute of Petrochemical Technology, Shanghai, CHN)

SCM-15 (Sinopec Composite Material No. 15), the first zeolite containing a 3-dimensional channel system with interconnected 12-, 12-, and 10-ring channels, has been synthesized using 4-pyrrolidinopyridine as organic structure-directing agent (OSDA) [1]. Its structure has been determined by combining single-crystal electron diffraction (SCED) and synchrotron powder X-ray diffraction (SPXD) data. The complete framework structure of SCM-15 was determined directly using direct method (by *SHELXS*) based on SCED data, [2] as well as the rough locations of guest molecules such as OSDA and F<sup>-</sup> ions and framework atoms such as Ge. The more accurate framework structure and the locations of OSDA, F<sup>-</sup> ions, and Ge atoms were then obtained by refining the structure against the SPXD data. It was found that the results obtained from SCED data show good consistency with those from SPXD data, indicating the good reliability of the results from SCED data.

The determined structure demonstrates that the framework of SCM-15 is related to a class of frameworks (FOS-5, ITQ-7, PKU-16, ITQ-26, ITQ-21, Beta polymorph B, and SU-78B) that can be built from similar chains which are connected by shared 4-ring or d4r units. Six topologically reasonable 3D large or extra-large pore hypothetical zeolites are then predicted based on the relationship between those frameworks.

[1] Y. Luo, S. Smeets, Z. Wang, J. Sun, W. Yang, *Chem. -Eur. J.* 2019, 25, 2184-2188.

[2] G. M. Sheldrick, *Acta Crystallogr. A*, 2008, 64, 112-122.

## MS20-P03 | RAMAN AND SURFACE ANALYSIS STUDIES OF $(\text{CuGaSe}_2)_{0.8}(\text{CuAlSe}_2)_{0.2}$ SINGLE CRYSTALS

Rywkin, Shanti (BMCC, City University of New York, New York, USA); Korzun, Barys (BMCC, City University of New York, New York, USA); Adam, Jonathan (BMCC, City University of New York, New York, USA); Li, Tai-De (ASRC, City University of New York, New York, USA)

Chalcopyrite ternary compounds - Copper Gallium Selenide ( $\text{CuGaSe}_2$ ) and Copper Aluminum Selenide ( $\text{CuAlSe}_2$ ), belong to the I-III-VI<sub>2</sub> group of semiconductors that exhibit a wide band gap and are extensively studied as active elements in optical filters and as absorbing materials in solar cells. To optimize their properties, it is necessary to control their surface characteristics. To this end, the structure and chemical modification of the surfaces of single crystals of the  $(\text{CuGaSe}_2)_{1-x}(\text{CuAlSe}_2)_x$  system, with  $x = 0.20$ , grown by chemical vapor transport (CVT), were studied using confocal Raman spectroscopy (CRS), scanning electron microscopy (SEM), energy dispersive spectroscopy (EDS) and X-ray photon electron spectroscopy (XPS). The surface of the crystal was characterized at room temperature, before and after alkali etching, and after  $\text{Ar}^+$  sputtering. After scanning with a 532 nm laser and a 20x objective lens, Raman maps showed that areas corresponding to iodide related compounds at  $123 \text{ cm}^{-1}$  and at  $141 \text{ cm}^{-1}$  were concentrated in the crevices and uneven surfaces of the crystal. Additional bands such as the split of the  $A_1$  mode at  $184 \text{ cm}^{-1}$  was also observed. These bands were no longer visible after chemical etching and  $\text{Ar}^+$  sputtering, and a more uniform surface was obtained. This data was confirmed with SEM-EDS and XPS studies. CRS combined with additional surface studies are proving to be useful tools for the surface characterization of these compounds.

## MS20-P04 | UNIVERSAL ALGORITHM FOR PREDICTION OF NEW CLEAVAGE PLANES IN SINGLE CRYSTALS

Vaknin, Uriel (Tel Aviv University, Tel Aviv, ISR); Sherman, Dov (Tel Aviv University, Tel Aviv, ISR); Gorfman, Semën (Tel Aviv University, Tel Aviv, ISR)

Cleavage describes the tendency of crystals to break along specific lattice planes. Acquiring information about cleavage is essential for the investigation of mechanical properties such as fracture energy, plasticity and strength. Although cleavage planes are commonly known for some simple materials (e.g. (110) and (111) for silicon), such information about arbitrary crystals is not available. There are no simple computational methods to predict cleavage planes in single crystals, apart from visual inspection of three-dimensional structures using programs like CrystalMaker or VESTA. Developing such methods may contribute to the understanding of physical and mechanical properties of crystals.

This work aims to develop an algorithm and computer program for automatic inspection of crystal structures and prediction of likely cleavage planes for specific structures. This algorithm enumerates all the possible lattice planes (by listing their Miller indices) and counts intersected atoms / bonds for every plane and its position along the related crystallographic direction. We modelled atoms by thermal ellipsoids / probability density functions (PDFs) derived from their atomic displacement parameters (ADPs), which are commonly available from X-ray diffraction experiment. We modelled bonds by virtual atoms (bond charges) at their anticipated Wyckoff positions and empirical PDFs, accounting for bond strength and extension.

We tested our algorithm on simple inorganic crystal structures such as  $\alpha$ -SiO<sub>2</sub>, LiNbO<sub>3</sub> and CaF<sub>2</sub>. Our algorithm can be used for fast and intuitive prediction of cleavage planes to be further approved by rigorous and time-consuming density functional theory calculations.

## MS20-P05 | POWDER XRD STRUCTURE DETERMINATION OF NANOSTRUCTURED, DISORDERED $\text{MoS}_2$ -ETHYLENEDIAMONIUM LAYERED COMPOUND AND MOLECULAR MODELING OF ITS DEPROTONATION REACTIONS

Goloveshkin, Alexander (A.N. Nesmeyanov Institute of Organoelement Compounds of Russian Academy of Sciences, Moscow, RUS); Ushakov, Ivan (A.N. Nesmeyanov Institute of Organoelement Compounds of Russian Academy of Sciences, Moscow, RUS); Korlyukov, Alexander (A.N. Nesmeyanov Institute of Organoelement Compounds of Russian Academy of Sciences, Moscow, RUS); Lenenko, Natalia (A.N. Nesmeyanov Institute of Organoelement Compounds of Russian Academy of Sciences, Moscow, RUS); Golub, Alexandre (A.N. Nesmeyanov Institute of Organoelement Compounds of Russian Academy of Sciences, Moscow, RUS)

Unusual, metallic 1T-molybdenum disulfide monolayers showing prospect for application in electrocatalysis can be stabilized by their incorporation into heterolayered systems with organic cations. For these disordered nanomaterials, we recently developed an original approach allowing structure analysis and evaluation of the layers cohesion energy from PXRD data and molecular modeling [1-3]. Here we report an application of this combined approach for new  $\text{MoS}_2$  compound, which contains protonated ethylenediamine (EDA) molecules and therefore cation- $\text{MoS}_2$  hydrogen bonding network. By quantifying the binding interaction strength we found that the  $\text{NH}\dots\text{S}$  hydrogen bonds have the greatest contribution to the total energy of the specific interactions between organic and inorganic layers (80% of the total energy). By comparison of the energetic characteristics provided by PW-DFT-d calculations for the assembled structure and its “delaminated” and “deprotonated” models, the cohesion energy and behavior of the compound under deprotonation conditions were evaluated. The results show that the compound is stable against deprotonation in the absence of  $\text{O}_2$ , while participation of  $\text{O}_2$  makes possible partial deprotonation leading to  $(\text{EDAH}^+)_{1/6}(\text{MoS}_2)^{1/6-}$  [4].

This work was supported by the RFBR grant 16-29-06184-ofi-m.

[1] Goloveshkin A.S. et al., *RSC Adv*, **2015**, *5*, 19206–19212.

[2] Goloveshkin A.S. et al., *Langmuir*, **2015**, *31*, 8953–8960.

[3] Bushmarinov I.S. et al., *J. Phys. Chem. Lett.*, **2016**, *7* (24), 5162–5167.

[4] Ushakov I.E. et al., *Cryst. Growth Des.*, **2018**, *18*, 5116-5123.

## MS20-P100 - LATE | EFFECT OF THE SIDE-CHAIN ON THE TOPOLOGY OF COORDINATION POLYMERS OF COPPER(II) WITH AMINO ACIDS

Smokrovic, Kristina (Department of Chemistry, Faculty of Science, University of Zagreb, Zagreb, HRV); Đilovic, Ivica (University of Zagreb, AUT); Matkovic-Calogovic, Dubravka (University of Zagreb, Faculty of Science, Department of Chemistry, Zagreb, HRV)

Over the past few decades the development of highly porous 3D coordination polymers (CP) has been of great interest, especially those derived from biodegradable and nontoxic compounds. Most of the well-known porous CPs are derived from carboxylic acids and prepared using mechanochemical or solvothermal routines.[1] That means that the structural characterization of prepared materials is usually done by X-ray powder diffraction, since growing single crystals of the right size and quality can be difficult.

Although they are easily available and provide a way of incorporating a chiral element in the structure, 3D CPs derived from amino acids are not well studied, with the exception of materials derived from aspartic acid. [1, 2] Another reason that makes amino acids attractive building blocks for the preparation of such compounds is the great variability in solubility caused by the side-chain functional groups. Because of these reasons, we have decided to research the effect of the side-chain on the topology of the CPs with copper(II) and using 4,4'-bipyridine as a bridging ligand.

Novel CPs of copper(II) and 4,4'-bipyridine with L-alanine, L-proline, L-threonine and D- and L-valine were synthesized and structurally characterized using single crystal diffraction datasets from in-house and synchrotron instruments. Interlocked, helical cation chains are common motifs present in all of the crystal structures, with large, solvent accessible voids. All of the prepared compounds are isostructural, except for polymers derived from L-proline. Amino-acids with large side-chains produce 2D CPs with a distorted honeycomb topology, without the large solvent accessible voids.

Acknowledgments:

This work has been funded by the Croatian Science Foundation (project no. IP-2014-09-4274). The experimental data was collected at Elletra Sincrotrone Trieste.

- [1] Barrio, J. P., Rebilly, J., Carter, B., Bradshaw, D., Bacsá, J., Ganin, A. Y., Park, H., Trewin, A., Vaidhyanathan, R., Cooper, A. I., Warren, J. E., Rosseinsky, M. J., (2008.) *Chem. Eur. J.*, 14, pp 4521-4532.  
[2] Vaidhyanathan, R., Bradshaw, D., Rebilly, N., Barrio, J. P., Gould, J. A., Berry, N. G., Rosseinsky, M. J., (2006) *Angew. Chem.*, 118, pp 6645-6649.

## MS21: Modern Quantum Crystallography

---

### MS21-01 | POSSIBLE QUANTUM CRYSTALLOGRAPHY SOLUTIONS FOR N-REPRESENTABLE ONE-ELECTRON REDUCED DENSITY MATRICES RECONSTRUCTION

Gillet, Jean-Michel (CentraleSupélec Université Paris Saclay, Gif sur Yvette, FRA); Gueddida, Saber (Université de Lorraine, Nancy, FRA); de Bruyne, Benjamin (CentraleSupélec Université Paris Saclay, Gif sur Yvette, FRA); Yan, zeyin (Southern University of Technology, Shenzhen, CHN); Kibalin, Iuri (CEA, LLB, Saclay, FRA); Souhassou, Mohamed (Université Lorraine, Nancy, FRA); Claiser, Nicolas (Université de Lorraine, Nancy, FRA); Lecomte, Claude (Université de Lorraine, Nancy, FRA); Cortona, Pietro (CentraleSupélec Université Paris Saclay, Gif sur Yvette, FRA); Gillon, Beatrice (CEA LLB, Saclay, FRA)

One of the goals of Quantum Crystallography is to study to what extent experimental tools of crystallography such as X-ray, electron, neutron diffraction, in their polarized and non-polarized versions can be used to gain better access to fundamental quantum properties such as the N-electron wavefunction.

In recent years, our collaboration has developed methods to extend the range of scattering experiments to gain access to better one-electron reduced density matrices which fulfill N-representability conditions. Two such possible approaches will be described in the cases of spin-resolved and charge-only 1-RDM for model systems. The purpose is to assess the quality of a 1-RDM reconstruction using coherent-elastic and incoherent-inelastic pseudo-experimental data and critically compare the result to the original, periodic ab-initio derived, 1-RDM standard reference.

## MS21-02 | ELECTRON CONFIGURATION AND ELECTRONEGATIVITY OF THE ATOMS UNDER COMPRESSION

Rahm, Martin (Chalmers University of Technology, Gothenburg, SWE); Cammi, Roberto (University of Parma, Parma, ITA); Ashcroft, N. W. (Cornell, Ithaca, USA); Hoffmann, Roald (Cornell, Ithaca, USA)

The ground state configuration of atoms is fundamental to the structure of the periodic table. Electronegativity is central for rationalizing chemical bonding, and in particular polarity and charge transfer [1]. Can the use of these atomic descriptors be extended to also predict chemistry at high pressures? To answer this question, we use a quantum mechanical model [2] to compress single atoms in a nonreactive, isotropic and neon-like environment. The effects of compression are here evaluated in a pressure range between 0 to 300 GPa for 93 atoms. Configurational transitions,  $s \rightarrow p$ ,  $s \rightarrow d$ ,  $s \rightarrow f$  and  $d \rightarrow f$  are shown to be an essential chemical and physical consequence of compression. Our study confirms that the filling of energy levels in compressed atoms more closely follows the hydrogenic *aufbau* principle, where the ordering is determined by the principal quantum number. Magnetism is predicted to both increase and decrease with pressure, depending on which atom is considered. However, Hund's rule is never violated for single atoms in the considered pressure range. Drastic changes, and reordering, of electronegativity is calculated, which lead to predictions of changing chemistry and the possibly for polarity-inverted (red-ox) alloys. This extension of atomic reference data assists the working of chemical intuition at extreme pressure and can act as a guide to both experiments and computational efforts.

[1] M. Rahm, T. Zeng, R. Hoffmann, J. Am. Chem. Soc. 141 (2019) 342-351.

[2] R. Cammi, B. Chen, M. Rahm, J. Comp. Chem. 39 (2018) 2243-2250

## MS21-03 | INTERACTIONS BETWEEN STEREO CHEMICALLY ACTIVE LONE PAIRS IN $\text{MnSb}_2\text{O}_4$

Tolborg, Kasper (Aarhus University, Aarhus, DNK); Gatti, Carlo (CNR-ISTM, Milano, ITA); Brummerstedt Iversen, Bo (Aarhus University, Aarhus, DNK)

Stereo chemically active lone pairs are usually treated as text book examples of non-bonding effects and occur in post-transition metal compounds, in which the post-transition metal is in an oxidation state of two lower than its main group number. These oxidation states are found in many technologically important materials, but their structural chemistry is quite intriguing, since the ability to form a lone pair does not always lead to asymmetric coordination. This has been shown to arise from the lone pairs not being chemically inactive, but rather arising from hybridization with the anion valence states.

We here report density functional theory calculations on structurally intriguing  $\text{MnSb}_2\text{O}_4$ , in which the presumed lone pairs on antimony seem to point directly towards each other, suggesting strong interactions between lone pairs. Based on analysis of chemical bonding through orbital based and real space descriptors, we establish the presence of stereo chemically active lone pairs on antimony, and show that they are formed through a similar mechanism to those in binary post-transition metal chalcogenides.

The lone pairs interact through a void space in the structure and are shown to minimize their mutual repulsion by introducing a deflection angle. This deflection angle increases significantly with decreasing Sb-Sb distance introduced by simulating high pressure. This shows the highly destabilizing nature of the lone pair interactions. The chemical bonding in the material is dominated by polar covalent interactions with both significant contributions from charge accumulation in the bonding regions and charge transfer.

## MS21-04 | QUANTUM CRYSTALLOGRAPHY FOR MACROMOLECULES: THE HAR-ELMO

### METHOD

Malaspina, Lorraine (University of Bremen, Bremen, GER); Wieduwilt, Erna (CNRS & University of Lorraine, Metz, FRA); Grabowsky, Simon (University of Bremen, Bremen, GER); Genoni, Alessandro (CNRS & University of Lorraine, Metz, FRA)

Hirshfeld Atom Refinement (HAR) is undoubtedly one of the emerging methods of modern Quantum Crystallography [1,2]. Strongly based on tailor-made quantum chemistry calculations, the technique uses only X-ray diffraction data to obtain the positions of hydrogen atoms with precision and accuracy that are usually achieved through neutron diffraction experiments [3].

Since nowadays more and more high-resolution X-ray diffraction data for macromolecules are available, HAR could be exploited also to successfully refine crystallographic structures of proteins. Nevertheless, its extension to large systems is hampered by the fact that the HAR requires a quantum chemical calculation for each iteration of the refinement, with a consequent increase of the computational cost as larger molecules are investigated.

To circumvent the problem, HAR has been coupled with the recently constructed databanks of Extremely Localized Molecular Orbitals [4], which allow fast and reliable reconstructions of wavefunctions and electron densities of polypeptides and proteins.

In this presentation, the results of the first HAR-ELMO refinements will be shown. In particular, after illustrating preliminary tests performed on small systems, the first applications of the new technique to polypeptides and proteins will be presented and discussed.

[1] D. Jayatilaka, B. Dittrich, *Acta Cryst. A* **2008**, *64*, 383.

[2] S. Capelli, H.-B. Bürgi, B. Dittrich, S. Grabowsky, D. Jayatilaka, *IUCrJ* **2014**, *1*, 361.

[3] M. Woińska, S. Grabowsky, P. M. Dominiak, K. Woźniak, D. Jayatilaka, *Sci. Adv.* **2016**, *2*, e1600192.

[4] B. Meyer, A. Genoni, *J. Phys. Chem. A* **2018**, *122*, 8965.

## MS21-05 | SPIN-RESOLVED ATOMIC ORBITAL MODEL REFINEMENT FOR COMBINED CHARGE AND SPIN DENSITY ANALYSIS: APPLICATION TO THE PEROVSKITE

Lecomte, Claude (Universite de Lorraine, Vandoeuvre-les-Nancy, FRA)

A new model was developed in order to refine spin-resolved atomic orbitals from combined charge and spin density studies. This new algorithm allows the simultaneous refinement against x-ray diffraction and polarized Neutron diffraction data, giving access to spin-resolved electron densities. This atomic orbital model is applied to the perovskite. The radial Extension, orientation and population of outer atomic orbitals for each atom are calculated. The interaction term between  $Ti^{3+}$ ,  $Y^{3+}$  cations and  $O_2^-$  ligands is estimated. A comparison of the refinement qualities obtained by means of the orbital and multipole models, respectively, is presented.

## MS21-P01 | STRUCTURAL INVESTIGATIONS ON BRIDGING STIBINIDENE COMPLEXES WITH CU-K $\beta$ -RADIATION: A COMPARISON

Rummel, Lena (University of Regensburg, Regensburg, GER); Bodensteiner, Michael (University of Regensburg, Regensburg, GER); Balázs, Gábor (University of Regensburg, Regensburg, GER); Scheer, Prof. Dr. Manfred (University of Regensburg, Regensburg, GER)

The bridging pentelidene complexes  $[\text{Cp}^*\text{E}\{\text{W}(\text{CO})_5\}_2]$  ( $\text{Cp}^*$  = pentamethylcyclopentadienyl,  $\text{E} = \text{P}, \text{As}$ ) have been a subject of interest in our group for almost 20 years and thus their reaction behavior towards nucleophiles such as phosphines [1-2] and nitriles [3] has been investigated thoroughly. In contrast, since their discovery in 1978 [4], trigonal-planar stibinidene complexes have not been investigated much [5]. Therefore, the stibinidene complex  $[\text{ClSb}\{\text{Cr}(\text{CO})_5\}_2(\text{thf})]$  has been used as starting material in the reaction with several nucleophiles. The structural investigations on the products have been carried out by single crystal X-ray diffraction using Mo-K $\alpha$ -, Cu-K $\alpha$ - as well as Cu-K $\beta$ -radiation. Additionally, we are about to use values from theoretical calculations of these complexes to see if structure factors can be obtained. The results are compared and discussed.

[1] M. Stubenhofer, C. Kuntz, G. Balázs, M. Zabel, M. Scheer, *Chem. Commun.* 2009, 1745 - 1747.

[2] M. Stubenhofer, C. Kuntz, M. Bodensteiner, A. Y. Timoshkin, M. Scheer, *Organometallics* 2013, 32, 3521-3528.

[3] M. Seidl, R. Weinzierl, A. Y. Timoshkin, M. Scheer, *Chem. Eur. J* 2016, 22, 5484-5488.

[4] G. H. J. von Seyerl, *Angew. Chem.* 1978, 90, 911-912.

[5] B. P. J. a. M. S. Michael Schiffer, *Z. anorg. allg. Chem.* 2000, 626, 2498-2504.

## MS21-P02 | ELECTRON DENSITIES OF MOLECULAR CRYSTALS FROM POWDER X-RAY

### DIFFRACTION

Svane, Bjarke (Aarhus University, Aarhus C, DNK); Brummerstedt Iversen, Bo (Aarhus University, Aarhus, DNK)

Detailed knowledge of the nature of the chemical bonding is a prerequisite for understanding the physical and chemical properties of materials. This information is best available in the electron density (ED). Virtually all experimental ED distributions are determined from structure factors extracted from single crystal X-ray diffraction, since this has been regarded the optimal way to obtain data of the highest quality. However, our recent work has shown that data obtained from powder X-ray diffraction (PXR) can exceed the data quality from single crystal diffraction [1-5].

I aim to determine ED distributions and atomic displacement parameters (ADPs) of molecular materials from highly accurate PXR data using the well-known Hansen-Coppens multipole modelling [6]. Structure factors are obtained from Rietveld refinement to partition intensity between overlapping reflections. The modelling is improved using aspherical approximate atomic scattering factors. The better model will lead to more accurate intensity extraction, which can then be used in a subsequent full ED refinement using the multipole method. This is of critical importance if the PXR method to obtain EDs is to be extended from small unit cell inorganic solids to molecular crystals with severe peak overlap.

- [1] N. Bindzus et al. (2014), *Acta Cryst. A*
- [2] T. Straasø et al. (2014), *J. Synchrotron Rad.*
- [3] N. Wahlberg et al. (2015), *J. Phys. Chem.*
- [4] K. Tolborg et al. (2017), *Acta Cryst. B*
- [5] M. R. V. Jørgensen et al. (2014), *IUCrJ*
- [6] Hansen, N. K. & Coppens, P. (1978). *Acta Cryst. A*

## MS21-P03 | ACCURATE EXPERIMENTAL CHARGE DENSITY DATA: TIPS & TRICKS FOR DATA COLLECTION & PROCESSING

Ott, Holger (Bruker AXS GmbH, Karlsruhe, GER); Ruf, Michael (Bruker AXS Inc., Madison, WI, USA); Kaercher, Joerg; Adam, Martin (Bruker AXS GmbH, Karlsruhe, GER)

A number of recent hardware developments enable scientists working in Quantum Crystallography to collect best ever crystallographic data in shorter time and with utmost convenience. High-brilliance sources, such as the first generation of diamond cooled microfocus sources (I $\mu$ S DIAMOND) and the METAJET providing Indium Ka radiation go along with large active area, mixed-mode photon counting pixel array detectors (PAD) [1] for highest system efficiency.

Despite of all efforts for automation, next to a carefully selected crystal planning and execution of the experiment are of crucial importance. To gain best results from the individual hardware components experimentalists ideally have a certain level of experience and carefully stick to the rules of Good Crystallography Practice (GCP).

This presentation will provide tips & tricks proven to make the charge density research more efficient. These include hints to optimize the instrument performance, but also GCP aspects. The presentation will also highlight recent improvements of the software suites, such as the APEX3 package, with a focus on special options particularly important to the field.[2]

[1] Genoni, L. Bučinský, N. Claiser, J. Contreras-García, B. Dittrich, P. M. Dominiak, E. Espinosa, C. Gatti, P. Giannozzi, J.-M. Gillet, D. Jayatilaka, P. Macchi, A. Ø. Madsen, L. Massa, C. F. Matta, K. M. Merz, P. N. H. Nakashima, H. Ott, U. Ryde, K. Schwarz, M. Sierka, S. Grabowsky, Chem. Eur. J. 2018, 24, 10881.

[2] APEX3, Bruker AXS GmbH., 2019.

## MS21-P102 - LATE | NON-SPHERICAL FORM FACTORS AND CRYSTALLOGRAPHIC REFINEMENT

Midgley, Laura (Durham University, Durham, GBR)

Standard crystallographic refinement relies on tabulated form factors [1] – carefully calculated and confirmed functions derived from single-atom electron densities. These spherical form factors have been used for decades, but are necessarily an approximation to the true form factors. My recent work has focused on the viability of using alternative form factors of improved accuracy, such as from quantum mechanical calculations.

In its simplest iteration, the form factor is the Fourier transform of the electron density associated with a particular atom. In the standard tables, this electron density is taken as a spherically symmetric function around an atom, leading to a spherically symmetric form factor dependent only on the magnitude of the vector  $h^*+kb^*+lc^*$ . However, in reality, bonding and other factors lead to an electron density which is influenced by its neighbours – that is, the atoms of the whole molecule affect the electron density, and thus, in turn, the form factor.

In this contribution, I cover the theoretical backing behind the use of such form factors, consider the information required, and discuss the adjustments and considerations made to the crystallographic refinement process needed to properly employ this information. Additionally, I will mention further investigations needed into the limits of viability of these form factors, the limits of inaccuracy of the model under which they become less accurate than standard spherical approximations.

[1] International tables for crystallography. Vol. C. Mathematical, physical and chemical tables, Bryan, RF

## MS22: Structure-Property Relationships via Charge Density Methods

---

### MS22-01 | 'PANCAKE' BONDING - A CHARGE DENSITY PERSPECTIVE

Haynes, Delia (Stellenbosch University, Stellenbosch, ZAF)

The 1,2,3,5-dithiadiazolyls ( $R\text{-CNSSN}^\bullet$ , hereafter DTDA), a family of thiazyl radicals, have been the focus of much investigation due to their potential as building blocks for magnetic and conducting materials. [1] However, these molecules tend to dimerise in the solid state *via* a spin-pairing interaction known as 'pancake bonding', a two-electron multi-centre interaction between  $\pi$ -radicals [2]. This dimerization renders the resulting materials diamagnetic. Much effort has been devoted to overcoming this interaction to produce magnetic materials.

In order to gain a deeper understanding of pancake bonding, experimental charge density analysis has been carried out on a number of DTDA homodimers, heterodimers and monomers. [3] These data, as well as various computational results, are assessed to probe the nature of the pancake bonds in DTDA.

[1] D. A. Haynes, *CrystEngComm*, 2011, **13**, 4793-4805.

[2] H. Z. Beneberu, Y.-H. Tian and M. Kertesz, *Phys. Chem. Chem. Phys.*, 2012, **14**, 10713-10725; Cui, H. Lischka, H. Z. Beneberu and M. Kertesz, *J. Am. Chem. Soc.*, 2014, **136**, 12958-12965; K. Preuss, *Polyhedron*, 2014, **79**, 1-15.

[3] S. Domagała, K. Kości, S. W. Robinson, D. A. Haynes and K. Wozniak, *Cryst. Growth Des.*, 2014, **14**, 4834-4848; S. Domagała and D. A. Haynes, *CrystEngComm*, 2016, **18**, 7116-7125; A. B. Voufack, N. Claiser, A. B. Dippenaar, C. Esterhuysen, D. A. Haynes, C. Lecomte and M. Souhassou' *manuscript in preparation*.

## MS22-02 | ELUCIDATING THE MECHANISMS OF SINGLE MOLECULE MAGNETS USING DIFFRACTION METHODS

Overgaard, Jacob (Department of Chemistry, Aarhus University, Aarhus C, DNK); Damgaard-Møller, Emil (Department of Chemistry, Aarhus University, Aarhus C, DNK); Andreasen Klahn, Emil (Department of Chemistry, Aarhus University, Aarhus C, DNK)

Single-molecule magnets (SMM) are special molecules, which are able to preserve an induced magnetization after the removal of an external magnetizing field. Such tiny magnets have potential technological applications in e.g. spin-based electronics. The functionality of these materials relies on strong magnetic anisotropy caused by orbital angular momentum. Both lanthanide-based [1] as well as more abundant transition-metal based SMMs exist, and the origin of the magnetic properties in the two types are slightly different. In this talk, I will show how X-ray and neutron diffraction studies of SMMs add valuable insight into the properties of SMMs.

Firstly, I will show selected results of experimental charge density (CD) studies of transition-metal based SMMs, from which we are able to extract quantitative magnetic properties such as that described using the zero-field splitting parameter. Secondly, I use CD studies of two dysprosium SMMs to experimentally confirm the predicted oblate shape of the valence density while also indicating the mixed nature of the ground state [2]. Finally, I will show how polarized neutron single crystal data can lead to quantitative knowledge of the local susceptibility tensor in related dysprosium-compounds [3].

[1] K. R. Meihaus, J. R. Long, *J. Am. Chem. Soc.* **2013**, *135*, 17952-17957.

[2] C. Gao, A. Genoni, S. Gao, A. Soncini, S.-D. Jiang, J. Overgaard, *submitted*.

[3] E. A. Klahn, C. Gao, B. Gillon, A. Gukasov, X. Fabreges, R. O. Piltz, S. D. Jiang, J. Overgaard, *Chemistry* **2018**, *24*, 16576-16581.

## MS22-03 | ELECTRON DENSITIES OF TWO NONAPEPTIDES FROM INVARIOM APPLICATION

Luger, Peter (Free University Berlin, Berlin, GER); Dittrich, Birger (Heinrich-Heine-University, Düsseldorf, GER)

The invariom formalism and the related database of aspherical scattering factors were introduced more than a decade before. Like other database approaches the invariom formalism relies on Richard Bader's transferability concept of atomic or submolecular fragments. Since transferability was originally examined for single amino acids and later for oligopeptides, invariom applications on oligo- and polypeptides became of early interest. We report here an invariom study on the rare case of two nonapeptides where very accurate X-ray data sets to  $(\sin\theta/\lambda)_{\max} = 0.61 \text{ \AA}^{-1}$  were published [1]. The compounds

Cyclo (Val-Leu-Pro-**Ile**-Leu-Leu-Leu-Val-Leu) (I); CSD code LETPIM;

Cyclo (Val-Leu-Pro-**Ala**-Leu-Leu-Leu-Val-Leu) (II); CSD code LETHIE

were identified as candidates for development as potential anti-cancer drugs. They differ only in residue 4, Ile in (I) and Ala in (II). The structures are free of disorder, a favorable (but not essential) provision for invariom treatment. It was therefore a task of a few mouseclicks to generate and refine an invariom based electron density and to derive results. Focus was directed to discuss molecular surfaces like electrostatic and Hirshfeld surfaces. Both nonapeptides are composed exclusively of non-polar amino acid residues. Consequently the outer electrostatic potential surfaces show mostly positive regions, negative potential is seen in the interior of the cyclic peptides. Since the anti-tumor potency is reduced for the Ala peptide (II), the question how the exchange at residue 4 influences the electron density, will be examined.

[1] Bioorg. Med. Chem. 26 (2018), 609-622.

## MS22-04 | THE ROLE OF ELECTROSTATIC INTERACTIONS IN IFIT PROTEINS COMPLEXED WITH RNA WITH DIFFERENT 5' END PREDICTED BY THE UBDB+EPMM METHOD

Budniak, Urszula (Department of Chemistry, CNBCh, University of Warsaw, Warsaw, POL); Dominiak, Paulina (Department of Chemistry, CNBCh, University of Warsaw, Warsaw, POL)

My project is focused on IFITs proteins (Interferon-induced proteins with tetratricopeptide repeats) which are expressed in cells infected by viruses. By binding foreign RNA they prevent synthesis of viral proteins in human host cell. IFIT1, IFIT2 and IFIT5 bind different forms of RNA: with triphosphate group or cap at 5' end of RNA. Calculated electrostatic interactions in selected complexes of IFIT1 and IFIT5 proteins with RNA will allow to compare the results with experimental values of binding affinity.

One of the more advanced methods to calculate electrostatic energy is University at Buffalo Pseudoatom DataBank (UBDB) together with Exact Potential Multipole Method (EPMM). UBDB enables reconstruction of charge density for macromolecules in quantitative manner. By UBDB+EPMM approach, which takes also charge penetration effects into account, it is possible to compute electrostatic energies with similar accuracy as with quantum chemistry methods, but much faster. Energy calculations are based on the structures of IFIT5 proteins with pppRNA and IFIT1 with different 5' end of RNA deposited in PDB. I want to verify the hypothesis of the lack of influence of RNA sequence on interaction energy in IFIT-RNA complexes. Moreover, I examine how modifications at 5' end of RNA alter interaction strength.

Project is financed from the grant PRELUDIUM11 of National Science Centre, Poland nr 2016/21/N/ST4/03722.

[1] Abbas, Y. M. et al. (2017) PNAS 114(11), E2106-E2115.

[2] Jarzembska, K. N. & Dominiak, P. M. (2012) Acta Cryst. A68, 139–147.

[3] Volkov A et al. (2004) Chem. Phys. Lett. 391, 170–175.

## MS22-05 | USING CRYSTAL STRUCTURE, AN IMPROVED ELECTROCHEMICAL METHOD AND COMPUTATIONAL DFT STUDIES TO UNDERSTAND THE MEDICINAL PROPERTIES OF CELASTRACEAE SPECIES OF PLANTS

Caruso, Francesco (Vassar College, Poughkeepsie, USA); Belli, Stuart (Vassar College, Poughkeepsie, USA); Singh, Manrose (Vassar College, Poughkeepsie, USA); Berinato, Molly (Vassar College, Poughkeepsie, USA); Chavez, Haydee (Universidad Nacional San Luis Gonzaga, Ica, PER); Rossi, Miriam (Vassar College, Poughkeepsie, USA)

Members of the *Celastraceae* family all over the world have remarkable medicinal properties. We describe the results of diverse experimental and computational methodologies on two members of this family to understand their pharmacological activity. First, we focus on celastrol, a triterpenoid extracted from *Tripterygium wilfordii* Hook F., a perennial vine of *Celastraceae* family (Chinese name "lei gong teng"). This plant (and compound) is often used in traditional medicine as a remedy for inflammatory and autoimmune diseases. We describe features from the crystal structure of the molecule, and together with results of computational docking and DFT studies, attempt to elucidate celastrol's biological activities on a molecular level. Additionally, our research focuses on determining the antioxidant effectiveness of pure celastrol using a recently improved voltammetry method with a rotating ring-disk electrode (RRDE). This method tests the reactivity of celastrol towards the superoxide radical anion. This is particularly interesting as the superoxide radical is produced by the body under oxidative stress and is considered a damaging species. Next, the results of similar electrochemistry experiments to detect the antioxidant reactivity of an ethanolic extract of leaves from a related member of the medically rich *Celastraceae* family, the *Maytenus octogona* tree, with superoxide radical are described.

## MS22-P01 | 3D -VISUALIZATION AND -PRINTING OF MOLECULAR SURFACES

Hübschle, Christian (Lehrstuhl für Kristallographie, Universität Bayreuth, Bayreuth, GER)

Molecular and other crystal structures are often complex. A three dimensional visualization can help in understanding them and optimizing the applied model to fit the experimental data. A visualization on screen is nice, but some times touching a physical model is a step further to get into the details of some structure properties. Recent Version of *MoleCoolQt*<sup>1</sup> can not only visualize density iso-surfaces, Hirshfeld surfaces and Voronoi-polyhedra, it is also possible to export three dimensional surfaces in file formats that are suitable for 3D-printers.

[1] C. B. Hübschle and B. Dittrich. *J. Appl. Cryst.* (2011). **44**, 238-240.

## MS22-P02 | EVALUATION OF COVALENT BOND DENSITY IN MOLECULAR CRYSTALS USING SIMPLIFIED VIRTUAL SCATTERING CENTERS

Nazarenko, Alexander (State University of New York, College at Buffalo, Buffalo, USA)

Here we address a 'gray area' of good quality structures with 0.5-0.8 Å resolution, which show visible deviation from IAM but are not satisfactory for experimental charge density calculations. The suggested methodology follows the well-known virtual atom method. Virtual scattering centers (VSC) are placed at fixed calculated positions between C, N, and O atoms with 'occupancies' being different for single, double, aromatic, and triple bonds. Scattering is approximated by a single Gaussian which can be justified by a small value of correction. VSCs are treated as isotropic; multiplication of scattering Gaussian by Debye-Waller factor yields one Gaussian function to describe both effects (no deconvolution of vibrations and charge density). The number of introduced parameters can be as low as one (for overall occupancy of the VSC part of the structure). Alternatively, each bond can be treated separately (number of additional parameters is roughly equal to the number of bonds). An attempt was made to handle S-C, S-O, and C-H bonds and various types of lone pairs. A number of organic and element-organic molecules were tested. When it was possible, charge density calculations (MoPro) and/or HART calculations (Tonto) were performed using the same experimental data. Visible improvement of fitting characteristics was achieved, especially for the molecules with aromatic fragments. After removing residual bond density from the Fourier difference map, other sources of deviation such as disorder and experimental and data processing errors can be addressed.

## MS22-P03 | PHASE TRANSITIONAL BEHAVIOR AND CHARGE DENSITY STUDY OF DRUG

### METHIMAZOLE

Fayzullin, Robert R. (Arbuzov Institute of Organic and Physical Chemistry, FRC Kazan Scientific Center, Russian Academy of Sciences, Kazan, RUS); Zakharychev, Dmitry V. (Arbuzov Institute of Organic and Physical Chemistry, FRC Kazan Scientific Center, Russian Academy of Sciences, Kazan, RUS); Saifina, Alina F. (Arbuzov Institute of Organic and Physical Chemistry, FRC Kazan Scientific Center, Russian Academy of Sciences, Kazan, AUT); Shteingolts, Sergey A. (Arbuzov Institute of Organic and Physical Chemistry, FRC Kazan Scientific Center, Russian Academy of Sciences, Kazan, AUT); Lodochnikova, Olga A. (Arbuzov Institute of Organic and Physical Chemistry, FRC Kazan Scientific Center, Russian Academy of Sciences, Kazan, AUT)

In this study, phase transitional behavior and electron density distribution in the crystals of drug methimazole were carefully investigated. The compound presents rich polymorphic diversity, where among all the phase transitions a peculiar, previously unknown, solid-state process was discovered, which can be especially important for the dosage form and storing of the active pharmaceutical ingredient. This phase transition is characterized by the exceptional features, such as the  $\lambda$ -shaped contour of the DCS curve, practical absence of thermal hysteresis, the low integral value of configurational heat capacity and existence of "heating memory". The nature of this process was revealed and it can be considered to be the 2nd order phase transition controlled by the cooperative effect. Charge density analysis for the phase existing at low temperature was performed. For the system with two molecules in the asymmetric cell, distribution of the electron density around sulfur atoms was studied, topological characteristics of the N–H $\cdots$ S hydrogen bonds, including local source function, were described.

This work was financially supported by the Russian Science Foundation (Grant № 17-13-01209).

## MS22-P04 | ASSEMBLY, CRYSTAL STRUCTURES AND (NON)LINEAR OPTICAL PROPERTIES OF MULTICOMPONENT MATERIALS CONTAINING SULFONAMIDES

Wojnarska, Joanna (Jagiellonian University, Krakow, POL); Gryl, Marlena (Jagiellonian University, Krakow, POL); Seidler, Tomasz (Jagiellonian University, Krakow, POL); Stadnicka, Katarzyna (Jagiellonian University, Faculty of Chemistry, Cracow, POL)

The constant progress observed in photonics introduces the need for new, more efficient materials. Often, research in materials science focuses on organic crystalline phases as they can possess large and fast responses to the electromagnetic field. The growing demand for innovative ideas motivates scientists to test new molecules as useful components of functional materials.

In this work, we present crystalline phases containing sulfonamides with potential applications in optical devices. Sulfonamides were selected as useful building blocks because many of them possess large values of (hyper)polarizabilities. Additionally, due to their widespread usage in drugs, they are easily accessible and thoroughly examined. The chosen sulfonamide molecules were co-crystallized with selected co-formers to ensure the required polar symmetry necessary for large nonlinear optical properties of even order. The obtained materials were studied using both theoretical and experimental methods. Intermolecular interactions and their influence on molecular assembly were analysed using Bader's QTAIM theory [1] as well as NCI index [2]. The linear (birefringence) and nonlinear optical (second harmonic generation) properties of obtained materials were predicted using the Local Field Theory approach [3] and compared with the experimentally measured responses. The performed analysis of material properties and the arrangement of molecules in crystal architecture enables us to obtain and discuss the structure-property relationship.

[1] R. Bader, *Atoms in Molecules: A Quantum Theory*, Oxford University Press, USA, 2003.

[2] J. Contreras-García et.al, *J. Chem. Theory Comput.*, 2011, 7, 625-632.

[3] T. Seidler et. al. *J. Phys. Chem. C*, 2016, 120, 4481-4494.

## MS22-P05 | CHARGE DENSITY ANALYSIS OF A SERIES OF 4-METHYLTHIOSTILBENE

### DERIVATIVES

Kubicki, Maciej (Adam Mickiewicz University, Poznan, POL); Stefanski, Tomasz (Adam Mickiewicz University, Poznan, POL); Korzanski, Artur (Adam Mickiewicz University, Poznan, POL); Dutkiewicz, Zbigniew (Poznan University of Medical Sciences, Poznan, POL)

The microtubular system with its dynamic nature characterized by the polymerization and depolymerization of  $\alpha,\beta$ -tubulin heterodimers, is essential in a variety of cellular processes, including cell division. Because of this function microtubules are one of the significant and more successful molecular target for designing of new active molecules possessing anticancer activity. Among this group of compounds chalcones (1,3-diphenylprop-2-en-1-on derivatives) represent a promising class of compounds with a simple structure, taking the possibility of structural modifications that improve their anticancer properties. Our successful investigation on novel inhibitors of tubulin polymerization from group of combretastatin A-4 thioderivatives [1] prompted us to extend our research on chalcone scaffold.

In the course of these studies, a series of stilbene derivatives, bearing methylthio group at position 4 of one phenyl rings and different number and positions of methoxy groups connected with the second phenyl ring, has been synthesized and structurally characterized. The influence of the substituents on the geometry and electron density distribution was studied by means of the charge density analysis, based on the high-resolution X-ray diffraction studies for well-diffracted crystals as well as on the transfer of the multipolar parameters, obtained from this analysis, to the samples of lesser quality. Multipolar Hansen-Coppens model was applied for building of electron density distribution, and the Atoms-In-Molecules approach for analysis of intra- and intermolecular interactions.

The study was supported by National Science Center Poland (Grant No. 2015/17/B/ST4/03701)

[1] Stefański, T. et al. *Eur. J. Med. Chem.* 2018, 144, 797-816

## MS22-P06 | INSIGHTS INTO THE ORIGIN OF MAGNETIC ANISOTROPY IN LINEAR IRON COMPLEXES FROM THE EXPERIMENTAL ELECTRON DENSITY

Thomsen, Maja K. (Dept. of Chemistry and iNANO, Aarhus University, Aarhus C, DNK); Nyvang, Andreas (Dept. of Chemistry, Aarhus University, Aarhus C, DNK); Walsh, James P. S. (Dept. of Chemistry, Northwestern University, Evanston, Illinois, USA); Bunting, Philip C. (Dept. of Chemistry, University of California, Berkeley, California, USA); Long, Jeffrey R. (Dept of Chemistry & Chemical and Biomolecular Engineering & Materials Sciences Division, University of California, Berkeley, California, USA); Neese, Frank (Dept. of Molecular Theory and Spectroscopy, Max Planck Institut für Kohlenforschung, Mülheim an der Ruhr, GER); Atanasov, Michael (Dept. of Molecular Theory and Spectroscopy, Max Planck Institut für Kohlenforschung, Mülheim an der Ruhr, GER); Genoni, Alessandro (Université de Lorraine and CNRS, Laboratoire de Physique et Chimie Théoriques (LPCT), UMR CNRS 7019, Metz, FRA); Overgaard, Jacob (Dept. of Chemistry, Aarhus University, Aarhus C, DNK)

In 2013, Zadrozny *et al.* [1,2] discovered zero-field slow magnetic relaxation and hysteresis for the linear iron(II) complex  $[\text{Fe}(\text{C}(\text{SiMe}_3)_2)]^-$ , which has one of the largest spin-reversal barriers reported for mononuclear transition-metal single-molecule magnets. Theoretical calculations suggested that the magnetic anisotropy is due to pronounced stabilization of the iron  $3d_z^2$  orbital in this complex compared to the neutral iron(II) complex  $\text{Fe}(\text{C}(\text{SiMe}_3)_2)$  [3]. Experimental support for this interpretation has however remained lacking. In the present study[4], we have determined the experimental electron density from high-resolution single-crystal X-ray diffraction data in  $[\text{Fe}(\text{C}(\text{SiMe}_3)_2)]^-$  and  $\text{Fe}(\text{C}(\text{SiMe}_3)_2)$ , which shows that the  $d_z^2$  orbital is indeed more populated in  $[\text{Fe}(\text{C}(\text{SiMe}_3)_2)]^-$  than in  $\text{Fe}(\text{C}(\text{SiMe}_3)_2)$ . This can be interpreted as arising from a greater stabilization of the  $d_z^2$  orbital in  $[\text{Fe}(\text{C}(\text{SiMe}_3)_2)]^-$  than in  $\text{Fe}(\text{C}(\text{SiMe}_3)_2)$ , thus providing unprecedented experimental evidence for the origin of magnetic anisotropy in  $[\text{Fe}(\text{C}(\text{SiMe}_3)_2)]^-$  and the corresponding slow magnetic relaxation.

[1] Zadrozny, J. M.; Xiao, D. J.; Atanasov, M.; Long, G. J.; Grandjean, F.; Neese, F.; Long, J. R. *Nat. Chem.* **2013**, *5*, 577–581.

[2] Zadrozny, J. M.; Xiao, D. J.; Long, J. R.; Atanasov, M.; Neese, F.; Grandjean, F.; Long, G. J. *Inorg. Chem.* **2013**, *52*, 13123–13131.

[3] Atanasov, M.; Zadrozny, J. M.; Long, J. R.; Neese, F. *Chem. Sci.* **2013**, *4*, 139–156.

[4] Thomsen, M. K.; Nyvang, A.; Walsh, J. P. S.; Bunting, P. C.; Long, J. R.; Neese, F.; Atanasov, M.; Genoni, A.; Overgaard, J. *Inorg. Chem.* **2019**, *58*, 3211–3218.

## MS22-P07 | QUINOID DIANION FORMING A LONE-PAIR PI-HOLE CONTACT

Vukovic, Vedran (CRM2, Université de Lorraine, Vandoeuvre-lès-Nancy, FRA); Jelsch, Christian (CRM2, Université de Lorraine, Vandoeuvre-lès-Nancy, FRA); Wenger, Emmanuel (CRM2, Université de Lorraine, Vandoeuvre-lès-Nancy, FRA); Molcanov, Krešimir (Institut Ruder Boškovic, Zagreb, HRV)

Lone pair (lp)··· $\pi$  interactions are quite rare and little studied type of  $\pi$ -hole interactions. They consist of a close contact which occurs between a lone pair and a  $\pi$ -hole of a planar ring. So far, the only studied examples involved aromatic rings, usually electron-depleted. Our study of lithium 2,5-dihydroxyquinonate DMSO solvate ( $\text{Li}_2\text{DHQ}\cdot\text{DMSO}$ ) is thus the first instance of a lp··· $\pi$  contact with (a) a non-aromatic and (b) an anionic ring. Distances between the sulphur atom and the ring centroid is 3.46 Å, and the closest S···C distance is only 3.25 Å, significantly shorter than the sum of van der Waals radii (3.66 Å).

This unprecedented interaction has been studied by X-ray charge density, to gain more insight into its nature. Topology of electron density revealed a bond critical point (3,-1) between the sulphur and a carbon atom of the ring (S1···C2) with maximum electron density of 0.066(2) e Å<sup>-3</sup>. These results are reproduced well by theoretical computations (periodic DFT in Crystal14, B3LYP/6-31G(d,p)); the same critical point is found with almost the same electron density value (0.063 e Å<sup>-3</sup>).

These results point out to an attractive interaction between the lone pair of the non-planar sulphur atom and the  $\pi$ -system of quinoid dianion.

## MS22-P08 | UNDERSTANDING OF CHROMIC PHENOMENA: THE EXAMPLES OF VIOLURIC ACID

### - AMINO ACID BASED SALTS AND CO-CRYSTALS

Rydz, Agnieszka (Jagiellonian University, Faculty of Chemistry, Cracow, POL); Gryl, Marlena (Jagiellonian University, Faculty of Chemistry, Cracow, POL); Krawczuk, Anna (Jagiellonian University, Faculty of Chemistry, Cracow, POL); Stadnicka, Katarzyna (Jagiellonian University, Faculty of Chemistry, Cracow, POL)

The color-changing effects play important role in modern technologies, thus chromic materials find enormous applications in thermal printing, optical data storage, biosensor development etc. In crystalline phases, several chromic effects, such as termochromism, piezochromism or crystallochromism can be observed.

Crystallochromic phenomena are well described for single-component crystals in which  $\pi\cdots\pi$  interactions between molecules are responsible for their absorption properties. In multicomponent materials, evaluation of the color source is more complicated. Our previous study [1] showed that violuric acid (VA) can form colored organic salts which led to formation of red and violet crystals. It has to be pointed out, that in those systems no  $\pi\cdots\pi$  interactions can be found. In order to examine ability of VA to form colored co-crystals and salts in the presence or absence of  $\pi\cdots\pi$  interactions, we have chosen amino acids as cocrystallization components. Due to variety of interactions formed by amino acids we can investigate color changes analyzing possible  $\pi\cdots\pi$  interactions and hydrogen bonds.

Here we present a set of crystalline phases containing violuric acid and selected amino acids. The color phenomenon for those materials is studied using experimental and theoretical methods including X-Ray diffraction, UV-Vis spectroscopy, Fingerprint plots [2] and Non-Covalent Interaction index [3]. This study allowed us to find correlation between crystal packing features and absorption properties of obtained crystalline phases.

[1] Gryl, *et al.* (2019). *IUCrJ*, 6, 2.

[2] Spackman, *et al.* (2002). *CrystEngComm*, 4, 378–392.

[3] Contreras-García, *et al.* (2011). *J. Chem. Theory Comput.* 7, 625-632.

## MS22-P09 | POLYMORPHISM AND THE ROLE OF F...F INTERACTIONS IN CRYSTAL PACKING OF FLUORINATED TOSYLATES

Korlyukov, Alexander (A.N.Nesmeyanov Institute of Organoelement Compounds of Russian Academy of Sciences, Moscow, RUS); Arkhipov, Dmitry (A.N.Nesmeyanov Institute of Organoelement Compounds of Russian Academy of Sciences, Moscow, RUS); Volodin, Alexander (INEOS, Moscow, RUS)

The peculiarities of interatomic interactions formed by fluorine atoms were studied in four tosylate derivatives  $p\text{-CH}_3\text{C}_6\text{H}_4\text{OSO}_2\text{CH}_2\text{CF}_2\text{CF}_3$  and  $p\text{-CH}_3\text{C}_6\text{H}_4\text{OSO}_2\text{CH}_2(\text{CF}_2)_n\text{CHF}_2$  ( $n = 1, 5, 7$ ) using X-ray diffraction and quantum chemical calculations (Arkhipov *et al.*, 2019). Compounds  $p\text{-CH}_3\text{C}_6\text{H}_4\text{OSO}_2\text{CH}_2(\text{CF}_2)_n\text{CHF}_2$  ( $n = 1, 5$ ) were crystallized in several polymorph modifications. Analysis of intermolecular bonding was carried out using QTAIM approach, NCI method and energy partitioning scheme implemented in Crystal Explorer program (CE-B3LYP/6-31G(d,p)). All compounds are characterized by crystal packing of similar type and the contribution of intermolecular interactions formed by fluorine atoms to lattice energy is raised along with the increase of their amount. The energy of intra- and intermolecular F...F interactions is varied in range 0.5–13.0 kJ/mol. Total contribution of F...F interactions to lattice energy does not exceed 40%. Crystal structures of studied compounds are stabilized mainly by C-H...O and C-H...F weak hydrogen bonds. The analysis of intermolecular interactions and lattice energies in polymorphs of  $p\text{-CH}_3\text{C}_6\text{H}_4\text{OSO}_2\text{CH}_2(\text{CF}_2)_n\text{CHF}_2$  ( $n = 1, 5$ ) has shown that most stabilized ones are characterized by the least contribution of F...F interactions.

The study was financially supported by Russian Science Foundation (grant 18-73-00339).

[1]Arkhipov, D. E., Lyubeshkin, A. V., Volodin, A. D. & Korlyukov, A. A. (2019). *Crystals*. **9**, 242.

## MS23: Aperiodic and Modulated Structures

---

### MS23-01 | CHEMICAL VS CONFORMATIONAL ENTROPIES AT THE INCOMMENSURATE AND LOCK-IN PHASE TRANSITIONS OF MORPHOLINIUM TETRAFLUOROBORATE

Noohinejad, Leila (Deutsches Elektronen-Synchrotron DESY, Hamburg, GER)

I will give an introduction to ferroelectric molecular crystals [1]. Ferroelectric crystals are pyroelectric crystals that exhibit reversible polarisation. Most applications of ferroelectric materials involve inorganic compounds, such as lead zirconate titanate, barium titanate and layered perovskites. The field of molecular ferroelectrics has started to gain interests only recently. Molecular ferroelectrics can be classified in two groups: pure organic hydrogen bonded supramolecular chains with a polar space group form one class of ferroelectric materials another series of molecular ferroelectrics belong to H-bonded hybrid organic-inorganic assemblies. Inorganic backbones are formed by strong covalent or ionic metal–halogen bonds to form an extended framework. Morpholinium tetrafluoroborate,  $[\text{C}_4\text{H}_{10}\text{NO}]^+[\text{BF}_4]^-$ , belongs to a class of ferroelectric compounds  $\text{ABX}_4$ . However,  $[\text{C}_4\text{H}_{10}\text{NO}]^+[\text{BF}_4]^-$  does not develop ferroelectric properties because the incommensurate phase below  $T_{c,I} = 153$  K is centrosymmetric with superspace group  $\text{Pnam}(\delta_1 00)00s$  and  $\delta_1 = 0.42193(12)$  at  $T = 130$  K; the threefold superstructure below  $T_{c,II} = 117\text{--}118$  K possesses the acentric but non-ferroelectric space group  $\text{P2}_12_12_1$ . Switching the modulation wavevector from incommensurate along  $a^*$  towards along  $c^*$  imposes first-order character onto the transition II–III. Phase transition mechanism is discussed based on crystal structures. The difference in configurational entropy between the disordered and incommensurate phases has been computed from the structure models. These features show that the order–disorder contribution is only a minor contribution to the transition entropy and that other factors, such as conformational changes, play a larger role in the phase transitions.

[1] Noohinejad, L., Aperiodic Molecular Ferroelectric Crystals, PhD Thesis, University of Bayreuth. 2016

## MS23-02 | EVIDENCING OF CHARGE DENSITY WAVE INSTABILITIES IN EVEN MEMBERS OF THE MONOPHOSPHATE TUNGSTEN BRONZES FAMILY

Duverger-Nédellec, Elen (Charles University, Faculty of Math. & Phys., DCMP, Praha 2, CZE); Kolincio, Kamil (Laboratoire CRISMAT, UMR 6508 CNRS, Caen CEDEX 4, FRA); Hervé, Laurence (Laboratoire CRISMAT, UMR 6508 CNRS, Caen CEDEX 4, FRA); Pautrat, Alain (Laboratoire CRISMAT, UMR 6508 CNRS, Caen CEDEX 4, FRA); Pérez, Olivier (Laboratoire CRISMAT, UMR 6508 CNRS,, Caen CEDEX 4, FRA)

The MonoPhosphate Tungsten Bronzes (MPTB) family,  $(\text{PO}_{2,4}(\text{WO}_3)_{2m})$ , can be described as a regular intergrowth of  $\text{PO}_4$  tetraedra layers and of corner-sharing- $\text{WO}_6$  octaedra slabs, with a thickness depending on the  $m$  parameter. This family, discovered in the late 70s, was extensively studied until the end of the 90s for their potential Charge Density Wave (CDW) instabilities. According to Peierls theory, a transition toward a CDW state is characterized by an anomaly in the transport measurements accompanied by the appearance of structural modulations. Modulated structures were actually observed for all the MPTB members. However, only members with  $m \leq 6$  show resistivity anomalies similar to the anomalies expected for classical CDW instabilities. These observations lead to the questioning of the nature of the structural transitions observed for the members with  $m > 6$ . In 2000, first MPTB modulated structures were solved, revealing the formation of tungsten clusters on the centre of the  $\text{WO}_3$  slabs for the  $m=4$  member, identified by the authors as the structural signature of the CDW. To know if this characteristic is generalizable to all the MPTB members presenting CDW states, a structural study of the  $m=6$  member is proposed. A complete study, from resistivity measurements to structural resolutions, of the  $m=8$  and 10 members will be then presented to evidence if their structural transitions originate from a CDW instability and if the CDW observed in the  $m \leq 6$  members is preserved when the value of  $m$  increases.

## MS23-03 | MULTIDIMENSIONAL APERIODIC STRUCTURES FROM BGU

Ben-Abraham, Shelomo (Ben-Gurion University of the Negev, Beer Sheba, ISR)

I present an overview of multidimensional deterministic aperiodic structures which I constructed together with my collaborators, mainly my own students. First I present the octagonal two-color Ben-Abraham-Gähler structure constructed by maximal covering of the plane by two octagonal patches. It serves to interpret the structure of the octagonal MnSiAl quasicrystal found by Kuo et al. and investigated by electron crystallography by Hovmöller et al. It is an infinite layer structure with layers alternating in color reflecting the physical structure where alternating layers are antiphases of each other. Next I show our multidimensional generalizations of the Paperfolding and Period doubling sequences. In the sequel I present the Color coding of the chair tiling in arbitrary dimension and the multidimensional Brick tiling (my generalization of the table tiling) as well as its color coding. The latter has a singular continuous part in its Fourier spectrum. Finally I show my two newest structures: The Crossed cube structures – generalizations of the Crossed square tiling whose singular continuous Fourier spectrum is equivalent to that of the non-Pisot squiral tiling. At last I present the multidimensional generalization of the Golay-Rudin-Shapiro sequence whose Fourier spectrum is essentially absolutely continuous.

## MS23-04 | THE 1D MODULATED STRUCTURE OF THE MIXED-VALENT CHAIN SULFIDO FERRATE $K_{7.09}[FeS_2]_4$

Röhr, Caroline (Universität Freiburg, Institut für Anorganische und Analytische Chemie, Freiburg, GER); Stüble, Pirmin (Universität Freiburg, Freiburg, GER); Schwarz, Michael (Universität Freiburg, Freiburg, GER)

The series of alkaline (A) sulfido ferrates  $A_{1+x}[Fe^{III}_{1-x}Fe^{II}_xS_2]$  starts ( $x=0$ ) with the longest-known pure ferrates(III)  $A[FeS_2]$ , which contain linear chains of edge-sharing  $[FeS_4]$  tetrahedra [1]. The recently prepared pure ferrate(II),  $Na_2[FeS_2]$  ( $x=0$ , [2]), which likewise contains linear tetrahedra chains, completes the series. In-between ( $0.33 < x < 0.75$ ), several mixed-valent ferrates with always buckled chains of edge-sharing tetrahedra are reported: This encompasses the long-known salts  $A_3[FeQ_2]_2$  with an equiatomic  $Fe^{II}/Fe^{III}$  ratio ( $x=0.5$ , [1]) and the complex monoclinic structures of  $Rb_4[FeS_2]_3$  ( $x=0.33$ ) and  $K_7[FeS_2]_4$  ( $x=0.75$ ) [3]. Herein we present the 1D modulated structure of  $K_{7.09}[Fe^{II,III}S_2]_4$  (space group  $C222(00\gamma)00s$ ,  $a=1363.87(5)$ ,  $b=2487.23(13)$ ,  $c=583.47(3)$  pm,  $q=0,0,0.444$ ,  $R1=0.0767$ ,  $x=0.773$ ), in which the position modulation of the  $[FeS_2]$  chain (i.e. its undulation) and the surrounding  $K^+$  cations is associated with an occupation modulation of two of the five cation sites. In the case of the new rubidium ferrate  $Rb_7[FeS_2]_5$  ( $x=0.4$ ) and its isotopic mixed Rb/Cs-analog, the shape of the tetrahedra chain is again commensurable resulting in a monoclinic structure with a large  $a$  lattice parameter. In all mixed-valent chain compounds, the buckling of the chains is evidently controlled by the local coordination of the changing number of alkali cations with different sizes, but not by an Fe charge ordering.

[1] P. Stüble, C. Röhr, Z. Anorg. Allg. Chem., 643, 1462 (2017) and references therein.

[2] P. Stüble, S. Peschke, D. Johrendt, C. Röhr, J. Solid State Chem., 258, 416 (2018).

[3] M. Schwarz, M. Haas, C. Röhr, Z. Anorg. Allg. Chem., 639, 360 (2013).

## MS23-05 | NEW TOOLS IN JANA2006/JANA2020 TO STUDY AND CHARACTERIZATION OF PI-PI STACKING OF INCOMMENSURATE MODULATED STRUCTURES: $\alpha$ & $\beta$ -Mn(DMP)Cl<sub>2</sub>

Poupon, Morgane (Fyzikální ústav AV CR, v. v. i., Prague 8, CZE); Dušek, Michal (Fyzikální ústav AV CR, v. v. i., Prague 8, CZE); Petříček, Václav (Fyzikální ústav AV CR, v. v. i., Prague 8, CZE); Abbasi Tyula, Yunes (Lorestan University, Khoramabad, IRN)

Understanding packing and interactions inside solids is important knowledge for crystal engineering aiming to build new desired compounds with specific physical and chemical properties [1], as well as for understanding properties such as luminescence [2]. Two important interactions in organic, organometallic or protein structures are highlighted: hydrogen bonding [3] and  $\pi$  interactions ( $\pi$ -anion,  $\pi$ -cation and  $\pi$ - $\pi$ -stacking) [4]. Both types of interaction are characterised by specific distances and angles, which can be easily determined and visualized using graphic software such as Diamond[5] or Mercury[6] for 3D structures. However, in case of modulated structure (3+1)D, this visualisation and interpretation is not so straightforward. In this contribution, we describe new tools developed for Jana2006/Jana2020 software in order to find and visualize  $\pi$ - $\pi$ -stacking in (3+1)D modulated structures. The improvement of the  $\pi$ - $\pi$  stacking visualization allowed us to understand the difference between two new polymorphs,  $\alpha$  and  $\beta$ -Mn(dmp)Cl<sub>2</sub>, which we use as a case study.

- [1] Desiraju, G.R.: J. Am. Chem. Soc. 135, 9952–9967 (2013).
- [2] Harrowfield, J.M., & al. Eur. J. Inorg. Chem. 2006, 389–396 (2006).
- [3] Steiner, & al. Chem. Int. Ed. 41, 48–76 (2002).
- [4] Martinez, C.R., & al. Chem. Sci. 3, 2191–2201 (2012).
- [5] Brandenburg, K.: DIAMOND. Crystal Impact GbR, Bonn, Germany (1999)
- [6] Macrae, C.F., & al. J. Appl. Crystallogr. 41, 466–470 (2008).

## MS23-P01 | CORRECTION FOR PHONONS, PHASONS AND MULTIPLE SCATTERING IN QUASICRYSTALS

Strzalka, Radoslaw (AGH University of Science and Technology, Krakow, POL)

In modern crystallography of quasicrystals and aperiodic systems a proper diffraction data treatment and structure refinement are still a challenge. In this presentation new approach to corrective terms to diffraction data for phonons and phasons will be discussed within a statistical method (or average unit cell method) of diffraction and structure investigation of aperiodic systems. Both phenomena, i.e. thermal vibrations and phasonic flips of atoms, are well reflected in the shape of the statistical distribution of atomic positions in the aperiodic tiling, which makes it possible to model phonons and phasons at the stage of constructing a structure factor. In this sense, corrective terms (Debye-Waller factors) for phonons and phasons become additive terms to the structure factor with a small number of parameters to fit (for phasons it will be a probability of flips of a given kind) [1]. Also a new approach to multiple scattering effect treatment will be discussed. It is based on the Rossmanith theory and considers a redistribution of peak intensities among all reflections with a given probability (the probability parameter is to be fitted). New corrections are tested against model quasiperiodic systems and real quasicrystals [2].

[1] J. Wolny, I. Buganski, P. Kuczera, R. Strzalka, *J. Appl. Cryst.* **49**, 2106 (2016).

[2] I. Bugański, R. Strzalka, J. Wolny, *Acta Cryst. A* **75**, 352 (2019).

## MS23-P02 | THE REAL SPACE REFINEMENT OF THE ICOSAHEDRAL QUASICRYSTAL

Buganski, Ireneusz (AGH University of Science and Technology, Krakow, POL); Wolny, Janusz (AGH University of Science and Technology, Krakow, POL); Takakura, Hiroyuki (Faculty of Engineering, Hokkaido University, Sapporo, JPN)

The icosahedral quasicrystal (i-QC) is an aperiodic crystal exhibiting an icosahedral symmetry. The state-of-art of the i-QC structure solution is the Takakura's model, vastly used for numerous quasicrystals with Tsai cluster and recently, Mackay cluster. The model, proposed for the i-CdYb is set in a 6D space, where atoms are grouped in three domains, called occupation domains, extended along the 3D perpendicular space. In addition to the occupation domain of the cluster atoms, there are the interstitial atoms to be modelled. The third known type, the Bergman-type, frequently found in ZnMg alloys, was never successfully refined with the cluster approach.

To find the structure of i-ZnMgTm, we have chosen a different approach. We have resigned from the cluster-based model and focus on a real space structure refinement based on the decoration of the Ammann-Kramer-Neri tiling. With the *Supeflip* software we obtained an *ab initio* structure solution which served to find a unique decoration of two golden rhombohedra with an edge length of 24.1 Å. To reduce the number of parameters during a refinement, the asymmetric part of each rhombohedron was used. The refinement concluded with  $R=9.7\%$ , which is one of the best results among obtained for an icosahedral quasicrystal.

After the model was refined, we were able to confirm the existence of three occupations domain by lifting the structure to a 6D space. The similarity to the simple decoration model is found.

## MS23-P03 | FROM A SINGLE SLIT TO PERIODIC, MODULATED AND QUASIPERIODIC CRYSTALS

### — A NEW APPROACH TO THE DIFFRACTION ANALYSIS OF APERIODIC SYSTEMS

Wolny, Janusz (AGH University of Science and Technology, Kraków, POL)

Over a hundred years old diffraction analysis of periodic crystals encountered serious difficulties when trying to describe diffraction patterns of aperiodic systems. In order to restore periodicity in the direct space, a multidimensional approach is commonly used. In the multidimensional description, both the periodic direct space lattice and the symmetrically equivalent periodic reciprocal space lattice are defined, which allows the use of well-known classical methods of crystallography. The problem is the lack of the universality of this approach. For each case, one needs to redefine both the dimension of the space used and the so-called atomic surface in additional dimensions. The problem is complicated even for simple model structures. In addition, there are many model structures which does not become periodic in any space with a finite number of dimensions. We encounter even greater difficulties when describing the dynamics of multidimensional systems. Thus, an attempt was made to describe any structure using only physical space (3D), abandoning the concept of a direct and reciprocal lattices with associated symmetry elements. This method uses the properties of the Fourier transform and is based on calculating the appropriate probability distributions of the positions of the atoms relative to the reference lattice. Ultimately, this leads to the expression of a structural factor in the form of a multimodal Fourier transform of probability distributions. The paper will present examples of the application of this method to describe diffraction patterns of selected systems: a single slit case, periodic and quasiperiodic crystals, including modulated structures.

## MS23-P04 | WILL PdPb CONFIRM THE PREDICTION THAT ITS STRUCTURE IS MODULATED?

Folkers, Laura (Centre for Analysis and Synthesis, Lunds Universitet, Lund, SWE); Lidin, Sven (Lund University, Lund, SWE)

Recently, crystals of PdPb were successfully grown. Preliminary room temperature data shows a triclinic modulated structure with a q-vector ( $1/2$  0.245  $1/2$ ) similar to that of AuIn at room temperature.

The structure of AuIn was elucidated not long ago, showing its structural changes with temperature [1]. Interest in AuIn grew since it proved harder to grow single crystals from this material than expected and since its differential scanning calorimetry (DSC) data shows one solidification peak but two melting peaks. With the DSC data at hand, growth of a single crystal was possible and temperature dependent diffraction data could be obtained. This data revealed that AuIn, believed to be of the TII type [2], actually only shows the TII structure above the temperature of 443°C and at lower temperatures undergoes a Peierls type like distortion before becoming incommensurate [1].

PdBi emerges to be a similar case, with atomic positions of the reported high temperature phase structure corresponding to the TII type structure [3]. Also the DSC measurement shows the same behaviour as for AuIn. As expected, a synchrotron study of PdBi shows that the structure transforms from a commensurate super structure, via an incommensurate structure, to a disordered structure between room temperature and 300°C.

[1] Folkers, Simonov, Wang, Lidin, *InorgChem.*, **57**, (2018), 2791.

[2] Schubert, Rösler, Kluge, Anderko, Härle, *Naturwissenschaften*, **40**, (1953), 34

[3] Zhuravlev, *Zhurnal Eksperimental'noi i Teoreticheskoi Fiziki*, **5**, (1957), 1064.

## MS23-P05 | CRYSTAL STRUCTURE OF INCOMMENSURATELY MODULATED $\beta$ -NaBrF<sub>4</sub>

Ivlev, Sergei (Philipps-Universität Marburg, Marburg, GER); Petříček, Václav (Institute of Physics ASCR, Prague, CZE); Conrad, Matthias (Philipps-Universität Marburg, Marburg, GER); Karttunen, Antti (Aalto University, Aalto); Kraus, Florian (Philipps-Universität Marburg, Marburg, GER)

Bromine trifluoride, BrF<sub>3</sub>, can act as a Lewis acid in the reactions involving certain fluorides and can form compounds known as tetrafluoridobromates(III),  $M(\text{BrF}_4)_n$ , where  $M$  is a cation. These compounds are renowned for their strong oxidizing and fluorinating properties, which define several possible applications for them, such as quantitative analysis of noble metals in natural ores, urban mining, and bromination of organic substrates.

Recently in our report on the crystal structure of sodium tetrafluoridobromate(III) [1] we suggested that another modification of NaBrF<sub>4</sub> may exist, which was deduced from a few additional reflections in its powder X-ray diffraction pattern. At the time of the publication we could neither unambiguously index those reflections, nor find the conditions which would allow us to obtain the other modification phase-pure. Here we will present the results of our further investigations on the nature of the previously unknown phase, which has been found to be a new incommensurately modulated polymorph modification of sodium tetrafluoridobromate(III),  $\beta$ -NaBrF<sub>4</sub>.

[1] S. I. Ivlev, R. V. Ostvald, F. Kraus, *Monatsh. Chem.* **2016**, *147* (10), 1661–1668. DOI: 10.1007/s00706-016-1799-2.

## MS23-P06 | ON THE PUZZLING CASE OF SODIUM SACCHARINATE 1.875-HYDRATE: STRUCTURE DESCRIPTION IN (3+1)-DIMENSIONAL SUPERSPACE

Rekis, Toms (University of Bayreuth, Bayreuth, GER); Schönleber, Andreas (University of Bayreuth, Bayreuth, GER); van Smaalen, Sander (University of Bayreuth, Bayreuth, GER)

Sodium Saccharinate hydrate is an artificial sweetener. Despite its extensive use in the food industry, its structure has been first reported relatively recently [1,2]. The reason for that may be the unusual complexity of this solid phase. It comprises a large unit cell in  $P2_1/n$  space group with  $Z'=16$ . However, a considerable pseudosymmetry can be noted hinting that this high- $Z'$  structure can be described in a higher dimensional space.

In this study superspace approach has been used to describe Sodium Saccharinate 1.875-hydrate structure in (3+1)-dimensional superspace. Reconstruction of the  $hkl$  planes in the reciprocal space indicates for an 8-fold substructure in a base-centered lattice. Examination of the raw diffraction data has revealed commensurability of this modulated structure which has been later proven also during the refinement. The structure has been described in the superspace group  $C2/c(0, \frac{3}{4}, 0)_s0$  with  $Z'=2$ . Unit cell parameter  $b$  is  $\frac{1}{4}$  of that of the supercell structure in  $P2_1/n$ . The other parameters being equal to those of the 3-dimensional structure description. In addition to positional modulation there is also a complex occupational modulation present in a crenel function fashion.

[1] Naumov P., Jovanovski, G., Grupce, O., Kaitner, B., Rae, A. D., Ng, S. W. *Angew. Chem. Ed.*, 2005, 44, 1251

[2] Banerjee, R., Bhatt, P. M., Kirchner, M. T., Desiraju, G. R. *Angew. Chem. Ed.*, 2005, 44, 2515

## MS23-P07 | MODULATED STRUCTURE IN $\text{Ni}_2\text{MnGa}_{0.95}\text{In}_{0.05}$ SHAPE-MEMORY ALLOY

Cejpek, Petr (Charles University, Prague, CZE); Doležal, Petr (Charles University, Prague, CZE); Opletal, Petr (Charles University, Prague, CZE)

Magnetic shape memory alloys related to  $\text{Ni}_2\text{MnGa}$  are intensively studied because of their promising properties and possible applications as micro-pumps or actuators. Their physical properties, structure and transition temperature are strongly dependent on composition and various doping.

To study abovementioned compositional dependence,  $\text{Ni}_2\text{MnGa}_{0.95}\text{In}_{0.05}$  single crystal was grown by Bridgman method. It was examined with x-ray diffraction (XRD) at low temperatures and with the magnetisation measurement. High-temperature cubic phase (austenite) undergoes transition to premartensite at 215 K and the transition to tetragonal martensite occurs around 100 K. In the low-temperature martensite, the twin variants (100) and (001) were clearly distinguishable in the XRD. The satellite diffractions were observed as well.

The presence of the satellite diffraction spots is connected to the modulation of atomic positions in the structure. The positions of the satellites imply the 10M type of the modulation with the corresponding modulation vector  $\mathbf{q}=(0.4, 0.4, 0.4)$ .

The satellite maxima are visible also above the temperature of martensitic transformation and even above the temperature of premartensitic transformation. This implies that the modulation in the sample occurs stepwise already before the transformation. Theoretical simulations of the satellite intensity show that the intensity increase should correspond to the increase of the modulation amplitude.

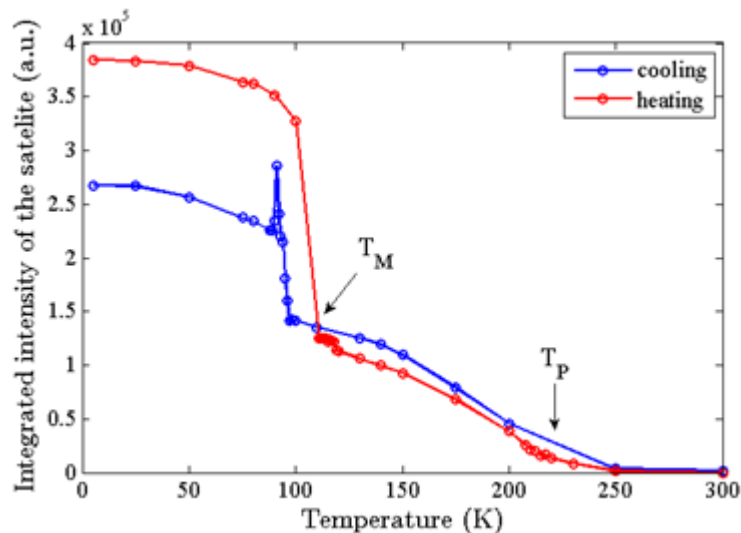


Figure 1: Temperature dependence of the integrated intensity of satellite diffraction maxima 4.4 0.4 0.  $T_M$  shows the temperature of martensitic transformation,  $T_P$  shows the temperature of premartensitic transformation.

## MS23-P08 | NOVEL APPROACH TO STRUCTURE DETERMINATION OF COMPLEX PROTEIN SYSTEM HYP-1/ANS

Smietanska, Joanna (AGH University of Science and Technology, Kraków, POL); Sliwiak, Joanna (Center for Biocrystallographic Research, Institute of Bioorganic Chemistry, Polish Academy of Sciences, Poznan, POL); Jaskolski, Mariusz (Center for Biocrystallographic Research, Institute of Bioorganic Chemistry, Polish Academy of Sciences, Poznan, POL); Gilski, Miroslaw (Center for Biocrystallographic Research, Institute of Bioorganic Chemistry, Polish Academy of Sciences, Poznan, POL); Dauter, Zbigniew (Synchrotron Radiation Research Section, MCL, National Cancer Institute, Argonne National Laboratory, Argonne IL, USA); Strzalka, Radoslaw (AGH University of Science and Technology, Krakow, POL); Wolny, Janusz (Faculty of Physics and Applied Computer Science, AGH University of Science and Technology, Kraków, POL)

Newly discovered modulated crystal structure in organic systems, and still uncommon, require a deeper investigation. No exact and detailed solution of such systems has not been done up-to-date. One possibility is to use an approximation of commensurate modulation which enables constructing a supercell, extending to the case, where translational symmetry (periodicity) is recovered, and simplify the analysis. An assumption of commensurateness of the modulation is, however, questionable and rather unverifiable. The goal of our project is to use a novel, original statistical method of structural modeling which enables a refinement based on the average unit cell with (commensurate or incommensurate) modulation without unclear assumption of commensurateness and supercell approach. Our model system is a pathogenesis-related protein (Hyp-1) complex with fluorescent probe 8-anilino-1-naphthalene sulfonate (ANS) which is a unique example of macromolecular system with modulated crystal structure. Previous studies have shown that Hyp-1/ANS complexes are tetartohedral twinned and crystallized in an asymmetric unit cell containing repetitive motif of four protein molecules arranged with 7-fold noncrystallographic repetition along c axis of the C2 space group. This commensurate structure modulation demands description of structure in highly expanded unit cell with 28 unique protein molecules inside. The Hyp-1/ANS structure was solved by molecular replacement and refined using maximum-likelihood targets with reliability factor  $R_{\text{free}}$  of 27%. Our approach involves development of the original software, re-integration of raw data and multidimensional analysis used to build the structure model and perform the refinement for significant improvement of results.

## MS23-P09 | INCOMMENSURATELY MODULATED STRUCTURES IN THE SERIES $RETe_{2-\delta}$

Poddig, Hagen (Technische Universität Dresden, Dresden, GER); Doert, Thomas (Technische Universität Dresden, Dresden, GER)

Rare earth metal polychalcogenides  $REX_{2-\delta}$  ( $X = S, Se, Te$ ;  $0 \leq \delta \leq 0.2$ ) comprise puckered  $[REX]$  double layers and planar  $[X]$  layers, the latter being subject to modulations due to electronic reasons and chalcogen defects [1].

The main reflections of all  $RETe_{2-\delta}$  crystals correspond to an average  $ZrSSi$  type (space group  $P4/nmm$ ) with unit cell with cell dimensions of  $a \approx 440$  to  $450$  pm and  $c \approx 910$  to  $920$  pm. Satellite positions, however, vary with  $\delta$ . The structures of  $RETe_{1.9}$  ( $RE = La, Pr, Nd$ ) compounds can be described in the tetragonal superspace group  $P4/n(\alpha\beta 1/2)00(-\beta\alpha 1/2)00$  with modulation vectors  $q_1 \approx (0.26, 0.32, 1/2)$  and  $q_2 \approx (-0.32, 0.26, 1/2)$ , whereas  $LaTe_{1.8}$  is orthorhombic, superspace group  $Pmmn(\alpha\beta 1/2)000(-\alpha\beta 1/2)000$  as its modulation vectors  $q_1 = (0.275, 0.31, 1/2)$  and  $q_2 = (-0.275, 0.31, 1/2)$  are incompatible with fourfold rotational symmetry.

The Te layers of the  $RETe_{1.9}$  compounds show a displacive and occupational modulation, forming an array of vacancies,  $Te_2^{2-}$  anions and linear  $Te_3^{4-}$  anions. For  $LaTe_{1.8}$ , the modulation in the Te layers is more pronounced with a variety of different Te anions.

[1] T. Doert, C. J. Müller: Binary Polysulfides and Polyselenides of Trivalent Rare-Earth Metals, in: *Reference Module in Chemistry, Molecular Sciences and Chemical Engineering*, Elsevier, **2016**.

## MS24: Magnetic Order: Methods and Properties

---

### MS24-01 | A SYMMETRY MOTIVATED APPROACH FOR ENUMERATING MAGNETOELECTRIC COUPLINGS IN PEROVSKITES

Senn, Mark (University of Warwick, Coventry, GBR)

A group-theoretical approach is used to enumerate the possible couplings between magnetism and ferroelectric polarization in the parent Pm-3m perovskite structure. It is shown that third-order magnetoelectric coupling terms must always involve magnetic ordering at the A and B sites which either transforms both as R-point or both as X-point time-odd irreducible representations (irreps). For fourth-order couplings it is demonstrated that this criterion may be relaxed allowing couplings involving irreps at X-, M- and R-points which collectively conserve crystal momentum, producing a magnetoelectric effect arising from only B-site magnetic order. In this case, exactly two of the three irreps entering the order parameter must be time-odd irreps and either one or all must be odd with respect to inversion symmetry. It is possible to show that the time-even irreps in this triad must transform as one of:  $X_1^+$ ,  $M_{3,5}^-$  or  $R_5^+$ , corresponding to A-site cation order, A-site antipolar displacements or anion rocksalt ordering, respectively. This greatly reduces the search space for type-II multiferroic perovskites. Similar arguments are used to demonstrate how weak ferromagnetism may be engineered and a variety of schemes are proposed for coupling this to ferroelectric polarization. By considering the literature, suggestions are given of which avenues of research are likely to be most promising in the design of novel magnetoelectric materials.

## MS24-02 | SPIRAL SPIN-LIQUID, MULTI-STEP ORDER AND THE EMERGENCE OF A VORTEX-LIKE STATE IN $\text{MnSc}_2\text{S}_4$

Zaharko, Oksana (Laboratory for Neutron Scattering and Imaging, Villigen, CH); Gao, Shang (RIKEN Center for Emergent Matter Science, Wako, Saitama, JPN); Kaur, Guratinder (Laboratory for Neutron Scattering and Imaging, Villigen, CH); Rosales, Diego (CONICET, La Plata, ARG); Go'mez, Flavia (CONICET, La Plata, ARG); Cabra, Daniel (CONICET, La Plata, ARG); Tsurkan, Vladimir (Lehrstuhl für Experimentalphysik V, Augsburg, GER)

$\text{MnSc}_2\text{S}_4$  spinel with magnetic  $\text{Mn}^{2+}$  ions forming the diamond lattice is an excellent model material for study magnetic frustration conceiving exotic states such as spiral spin liquid, competing long-range ordered phases and triple-q state in applied magnetic fields [1]. Neutron diffuse scattering gives direct experimental evidence for the existence of the spiral spin liquid ( $T_{N1}=2.2 \text{ K} < T < T_{cw}=23 \text{ K}$ ), which was predicted to occur in the  $J_1$ - $J_2$  model on the diamond lattice, when the ratio between the ferromagnetic first and antiferromagnetic second neighbour couplings is  $|J_2/J_1| > 0.125$  [2]. Neutron single crystal diffraction unravels three long-range ordered phases supplanting each other on temperature lowering ( $T_{N1}=2.2 \text{ K}$ ,  $q_1=3/4 \ 3/4 \ 0$ ;  $T_{N2}=1.75 \text{ K}$ ,  $q_2=3/4+d \ 3/4-d \ 0$ ;  $T_{N3}=1.6 \text{ K}$ ,  $q_3=q_1$ ) and, from the field variation of intensities of the different  $q_3$  arms discloses the triple-q state. With Monte Carlo simulations we scrutinize further details of the spin Hamiltonian, i.e. the third neighbour coupling, single ion anisotropy and exchange anisotropy and establish that this set of parameters indeed stabilizes the lattice of dense topological objects akin to skyrmions [3].

[1] S. Gao, O. Zaharko, V. Tsurkan, et al. *Nature Physics*, 13, 157 (2016).

[2] D. Bergman, J. Alicea, E. Gull, S. Trebst, L. Balents, *Nature Physics* 3, 487 (2007).

[3] S. Gao, D. Rosales, V. Tsurkan, O. Zaharko, et al. in preparation.

## MS24-03 | HIGH SYMMETRY DICTATES A VORTEX MAGNETIC STRUCTURE FOR THE MYSTERIOUS HIDDEN ORDER IN URu<sub>2</sub>Si<sub>2</sub>

Dmitrienko, Vladimir E. (A.V. Shubnikov Institute of Crystallography, FSRC “Crystallography and Photonics” RAS, Moscow, RU); Chizhikov, Viacheslav A. (A.V. Shubnikov Institute of Crystallography, FSRC “Crystallography and Photonics” RAS, Moscow, RU)

For more than 30 years, there were tremendous research efforts to understand the mysterious Hidden Order (HO) in the heavy-fermion compound URu<sub>2</sub>Si<sub>2</sub> [1].

To solve this enigma, we suppose that there is no spatial symmetry breaking at the HO transition temperature and solely the time-reversal symmetry breaking emerges owing to unusual magnetic ordering [2]. As a result of its high *4/mmm* symmetry, each uranium atom is a *three-dimensional* magnetic vortex; its intra-atomic magnetization  $\mathbf{M}(\mathbf{r})$  is intrinsically noncollinear, so that its dipole, quadrupole, and toroidal magnetic moments vanish, thus making the vortex “hidden”. The first nonzero magnetic multipole of the uranium atom is the toroidal quadrupole. In the unit cell, two uranium atoms can have either the same or opposite signs of their vortex magnetization  $\mathbf{M}(\mathbf{r})$ ; this corresponds to either *ferrovortex* or *antiferrovortex* structures with *I4/mmm* or *PA/mmm* magnetic space groups, respectively.

Our first-principles calculations (DFT with the spin-orbit interaction) show that the vortex magnetic order of URu<sub>2</sub>Si<sub>2</sub> is rather strong [2]: the total absolute magnetization  $|\mathbf{M}(\mathbf{r})|$  is about 0.9 Bohr magneton per U atom. The vortex structure provides a very unusual form factor of magnetic neutron scattering, calculated both for *ferrovortex* and *antiferrovortex* structures [2]. We will also discuss other systems with similar unusual vortex order.

This work was supported RFBR Project No.19-52-12029.

[1] J.A.Mydosh, P.M.Oppeneer, Rev. Mod. Phys. **83**, 1301(2011).

[2] V.E.Dmitrienko, V.A.Chizhikov, Phys. Rev. **B98**, 165118(2018).

## MS24-04 | MAGNETIC INVERSION SYMMETRY BREAKING AND SPIN REORIENTATION IN $Tb_2MnNiO_6$ : A POLAR STRONG FERROMAGNET

Garcia-Muñoz, Jose Luis (Institut de Ciència de Materials de Barcelona, ICMAB-CSIC, Bellaterra, ESP); Blasco, Javier (Instituto de Ciencia de Materiales de Aragón, ICMA-CSIC–Universidad de Zaragoza, Zaragoza, ESP); Zhang, Xiaodong (Institut de Ciència de Materials de Barcelona, ICMAB-CSIC, Bellaterra, ESP); Romaguera, Arnau (Institut de Ciència de Materials de Barcelona, ICMAB-CSIC, Bellaterra, ESP); Fabelo, Oscar (ILL-Institut Laue Langevin, Grenoble, FRA)

We present a description and comprehensive study on four successive magnetic transitions in ferromagnetic  $Tb_2MnNiO_6$  double perovskite, investigated by neutron diffraction. In the ground state ( $P2_1'$ ), the moments of magnetic A and B sites order according to different non-polar magnetic modes (*irreps*) of the paramagnetic phase. But the coupling between them generates an overall polar symmetry which makes this oxide potentially multiferroic (and therefore ferromagnetic and ferroelectric) in its ground state. Its macroscopic magnetization is large ( $5 \mu_B/f.u$ ) and not related to a weak ferromagnetic (wFM) component induced by Dzyaloshinskii–Moriya (DM) interaction. In addition, a sharp and severe spin reorientation of the ferromagnetic transition-metal moments has been observed which opens the door to the magnetic switching of the ferroelectric state in this perovskite, and conversely to the control of the magnetization direction by electrical fields applied parallel to  $b$ . We also anticipate that in this material the direction of the magnetization (towards  $c / a$ ) could be used as the key to switch the polar/non-polar (ferroelectric/antiferroelectric) transformation.

Acknowledgments: This work was financially supported by Spanish MINECO (MAT2015-68760-C2-2 and SEV- 2015-0496).

- [1] J.M. Perez-Mato *et al*, Annu. Rev. Mater. Res. 45, 217 (2015).
- [2] B.J. Campbell *et al*, J. Appl. Crystallogr. 39, 607 (2006).
- [3] J.L. Garcia-Muñoz *et al*, submitted.

## MS24-05 | SUPERSPACE MAGNETIC STRUCTURE AND TOPOLOGICAL CHARGES IN WEYL SEMIMETAL CeAlGe

Puphal, Pascal (Paul Scherrer Institut, Villigen, CH); Pomjakushin, Vladimir (Paul Scherrer Institut, Villigen, CH); Gawryluk, Dariusz (Paul Scherrer Institut, Villigen, CH); Keller, Lukas (Paul Scherrer Institut, Villigen, CH); Pomjakushina, Ekaterina (Paul Scherrer Institut, Villigen, CH); White, Jonathan S. (Paul Scherrer Institut, Villigen, CH)

A recent first principles theoretical calculations have predicted that the members of the chiral RAlGe (R = Pr, Ce) system (I41/md space group) can be new magnetic Weyl semimetals [1]. The successful single crystal growth of CeAlGe and bulk magnetic characterizations have been recently reported [2]. Here we present the results of the single crystal and powder neutron diffraction studies of CeAlGe [3]. We have found that the one of the most symmetric solutions for the magnetic structure in a superspace magnetic group results in the interesting topological spin textures, which will be discussed.

[1] G. Chang, B. Singh, S.-Y. Xu, G. Bian, S.-M. Huang, C.-H. Hsu, I. Belopolski, N. Alidoust, D. S. Sanchez, H. Zheng, H. Lu, X. Zhang, Y. Bian, T.-R. Chang, H.-T. Jeng, A. Bansil, H. Hsu, S. Jia, T. Neupert, H. Lin, and M. Z. Hasan, *Physical Review B* 97 (2018).

[2] P. Puphal, C. Mielke, N. Kumar, Y. Soh, T. Shang, M. Medarde, J. S. White, and E. Pomjakushina, *Physical Review Materials* (2019).

[3] P. Puphal et al, to be published (2019).

## MS24-P01 | STRUCTURAL DISORDER AND MAGNETIC CORRELATIONS DRIVEN BY OXYGEN

### DOPING IN $\text{Nd}_2\text{NiO}_{4.11}$

Maity, Sumit Ranjan (Paul Scherrer Institute, Villigen PSI, CH); Ceretti, Monica (CNRS-University Montpellier, Montpellier, FRA); Keller, Lukas (Paul Scherrer Institute, Villigen PSI, CH); Schefer, Jürg (Paul Scherrer Institute, Villigen PSI, CH); Shang, Tian (Paul Scherrer Institute, Villigen PSI, CH); Pomjakushina, Ekaterina (Paul Scherrer Institute, Villigen PSI, CH); Meven, Martin (Aachen University and Jülich Centre for Neutron Science, Garching bei München, GER); Sheptyakov, Denis (Paul Scherrer Institute, Villigen PSI, CH); Cervellino, Anonio (Paul Scherrer Institute, Villigen PSI, CH); Paulus, Werner (CNRS-University Montpellier, Montpellier, FRA)

The interplay of chemical doping, structural and electronic complexity in layered Ruddlesden-Popper type non-stoichiometric oxides ( $\text{Ln}_2\text{MO}_{4+\delta}$ ) is an exciting field of solid state research as this can trigger for example oxygen mobility at room temperature. The complexity of these compounds is both, a challenge and an opportunity to control many active degrees of freedom such as charge, spin and orbital ordering for tailoring new dedicated materials for technological applications.

$\text{Nd}_2\text{NiO}_{4+\delta}$  is a promising compound showing oxygen mobility close to room temperature. Here we present our results on the  $\text{Nd}_2\text{NiO}_{4+\delta}$  phase with moderate oxygen doping level  $\delta \approx 0.11$ . By means of X-ray and neutron diffraction as well as macroscopic methods we investigated the structural degree of oxygen order as well as the magnetic ordering phenomena in the temperature range of 2-300 K. This study [1] revealed that the excess oxygen atoms are disordered and, in addition, introduce strong disorder to the apical oxygen site. This favors oxygen diffusion close to room temperature. The magnetic order phenomena at low temperature have been investigated, revealing a region of coexistence of commensurate and incommensurate long-range magnetic order. The possible origin of the incommensurate phase is discussed and the magnetic phase diagram is proposed.

[1] S. Maity et al., submitted to Phy. Rev. Materials

## MS24-P02 | OXYGEN ORDER CORRELATION TO THE INCOMMENSURATELY MODULATED

### MAGNETIC STRIPES AND THEIR INTERACTION IN 214-TYPE $\text{Pr}_{2-x}\text{Sr}_x\text{NiO}_{4+\delta}$

Maity, Avishek (IPC, University of Goettingen, Goettingen, GER); Dutta, Rajesh (IFK, RWTH Aachen University, Aachen, GER); Masicano, Anna (ICGM, University of Montpellier, Montpellier, FRA); Ceretti, Monica (ICGM, University of Montpellier, Montpellier, FRA); Bossak, Alexie (The European Synchrotron-ESRF, Grenoble, FRA); Paulus, Werner (ICGM, University of Montpellier, Montpellier, FRA)

Magnetic stripes in 214-type nickelates  $\text{La}_{2-x}\text{Sr}_x\text{NiO}_{4+\delta}$  have been investigated intensively in last two decades as several theoretical and experimental studies suggest strong spin fluctuation in between the stripes give rise to the unconventional superconductivity in the isostructural high- $T_c$  cuprates. Though no superconductivity has been found in  $\text{La}_{2-x}\text{Sr}_x\text{NiO}_{4+\delta}$ , much of the attention has been given to the understanding of exotic quantum phenomena at low temperature of magnetically ordered  $\text{Ni}^{2+}$  ions for different hole concentrations mostly obtained by Sr-doping [1]. What still remains poorly investigated is the electronically equivalent O-doped compounds where the interstitial oxygen (Oint) gets ordered in a very long range even at RT. To study the effect of Oint ordering we have chosen  $\text{Pr}_2\text{NiO}_{4+\delta}$  to be the perfect model system as it accommodates very large amount of Oint ( $0 < \delta < 0.25$ ) [2] compared to the others. From several synchrotron and neutron scattering measurements on a series of O-doped and O/Sr co-doped compounds, our study suggests that the RT-oxygen ordering plays a critical role to influence the discommensuration [3] of the magnetic stripes leading to a mix checker board and stripe ordering occurring at low temperature. Depending on the oxygen order modulation for different O-doping concentration we find the underlying spin-microstructure gets modified and hence their exchange interaction.

[1] Freeman et. al. PRB 71, 174412 (2009).

[2] Ceretti et. al. Inorg. Chem., 57, 4657–4666 (2018).

[3] Kajimoto et. al. Phys. Rev. B 67, 014511 (2003).

## MS24-P03 | REVISITING THE MAGNETIC STRUCTURE OF $R_{1/3}Sr_{2/3}FeO_3$ (R = LA, PR, ND) BY NEUTRON POWDER AND SINGLE CRYSTAL DIFFRACTION COMBINED WITH SPHERICAL POLARIMETRY

Li, Fei; Pomjakushin, Vladimir; Sibille, Roman; Rössli, Bertrand; Pomjakushina, Ekaterina (Paul Scherrer Institute, Villigen, CH)

We present our study of a magnetic structure in  $R_{1/3}Sr_{2/3}FeO_3$  (R = La,Pr,Nd) system, which is interesting because it has a metal-insulator (MI) transition concomitantly with the magnetic ordering. In our previous paper [1] we have shown that the neutron powder diffraction data can be equally well fitted by two different magnetic space groups, namely a canted helical model  $P3_221$  and a collinear arrangement of the Fe-spins  $C2/c$ . The latter model supports the charge ordering, implying that it is responsible for MI-transition. We show that the neutron single crystal diffraction and spherical polarimetry experiments performed on crystals with R=La were able to resolve the above issue, giving the definitive preference to  $C2/c$  [2].

[1] F.Li *et al.*, Phys.Rev. B 97, 174417 (2018)

[2] F.Li *et al.*, to be published

## MS24-P04 | MAGStREX: MAGNETIC STRUCTURES THROUGH RESONANT X-RAY SCATTERING

Bereciartua, Pablo J. (Deutsches Elektronen-Synchrotron (DESY), Hamburg, GER); Francoual, Sonia (Deutsches Elektronen-Synchrotron (DESY), Hamburg, GER); Mardegan, Jose R. L. (Deutsches Elektronen-Synchrotron (DESY), Hamburg, GER); Sears, Jennifer (Deutsches Elektronen-Synchrotron (DESY), Hamburg, GER); Rodríguez-Carvajal, Juan (Institut Laue Langevin, Grenoble, FRA); Picca, Frédéric-Emmanuel (Synchrotron SOLEIL, Gif-sur-Yvette, FRA)

Synchrotron radiation has succeeded in determining the magnetic structure of many different materials in a microscopic scale. If the energy of the incident beam is tuned to the absorption edge of one of the elements of the sample, a resonant effect appears with a significant enhancement of the diffracted signal. Resonant X-ray Magnetic Scattering (RXMS) technique is based on this principle, which makes possible to distinguish the magnetic ordering of atoms of different species [1]. RXMS also allows studying materials that are difficult to be studied by neutron diffraction due to large neutron absorption of some elements.

At beamline P09 of PETRA III (DESY) different types of experiments to study magnetic phases through RXMS are currently available, as well as other experimental resources [2]. However, the analysis of the collected data to determine the magnetic structure is complicated and there is no specific software dedicated to this technique. Here we present an ongoing project to develop the software called MagStReX (**M**agnetic **S**tructures through **R**esonant **X**-ray Scattering), a program to facilitate the planning of a RXMS experiment, as well as to carry out the analysis of the data obtained in these experiments. An overview of the RXMS technique and the experiments mentioned above will be presented, together with the current status and the future development of MagStReX.

[1] C. Vettier, Eur. Phys. J. Special Topics 208, 3 (2012)

[2] J. Stempfer, S. Francoual, *et al.*, *J. Synchrotron Rad.* **20**, 541 (2013)

## MS24-P05 | UNDERSTANDING AND TUNING MAGNETISM OF MESOSCOPIC HOLLOW OXIDE SPHERE BY SURFACE ENGINEERING

Hsu, Pei-Kai (Department of Materials Science and Engineering, National Taiwan University of Science and Technology, Taipei, TWN); Chen, Hong-Jie (National Taiwan University of Science and Technology, Taipei, TWN); Tseng, Eric Nestor (National Taiwan University of Science and Technology, Taipei, TWN); Sasniati, Popi (National Taiwan University of Science and Technology, Taipei, TWN); Chen, ShihYun (National Taiwan University of Science and Technology, Taipei, TWN); Gloter, Alexandre (Laboratoire de Physique des Solides, Université Paris Sud, Paris, FRA)

In this study, magnetism of mesoscopic hollow ceria spheres was revealed. Hollow microspheres were synthesized by spray pyrolysis and then undergone various post process, including surface treatment and annealing. At first, TEM observations show that the synthesized hollow spheres have a diameter of 50 nm to 2  $\mu\text{m}$  and a shell thickness of about 30 to 40 nm. Raman spectroscopy and STEM/EELS analysis indicated that the defects were mainly oxygen vacancy ( $V_{\text{O}}$ ) and the reduced cerium ( $\text{Ce}^{3+}$ ). Both were found to concentrate in the surface layer of about 2 nm and the distribution trend was independent of the size of the hollow sphere. After the post treatment, the size, porosity, and defect concentration of the shell changed. However, the distribution of defect keeps the same, it still concentrated in the range of 2 nm from the surface. Magnetic measurement demonstrated that synthesized hollow ceria spheres were ferromagnetic at room temperature. Unusual size effect on magnetism was noted in present hollow spheres as comparing to nanoparticle and bulk systems. The value of saturation magnetization ( $M_s$ ) of the large spheres (larger than 800 nm) is an order of magnitude higher than that of the small ones. After post treatment,  $M_s$  could be further enhanced. The highest saturation magnetization was obtained in the sample subjected to react with  $\text{HNO}_3$  for 15 minutes, which was attributed to the optimized surface state. At last, the structure-magnetism dependence observed in present study will be discussed by the giant orbital paramagnetic model.

## MS24-P06 | PROBING THE MAGNETIC GROUND-STATES OF RARE-EARTH COMPOUNDS BY SINGLE CRYSTAL NEUTRON DIFFRACTION

Henriques, Margarida (Institute of Physics, Prague, CZE); Ouladdiaf, Bachir (Institute Laue-Langevin, Grenoble, FRA); Gorbunov, Denis (Hochfeld-Magnetlabor Dresden, Dresden, GER); Andreev, Alexander (Institute of Physics, Czech Academy of Sciences, Prague, CZE)

New materials exhibiting complex physical behaviors related to magnetism may play a paramount role in future technologies. Such systems often require detailed analysis of their crystalline and magnetic structures in the ground states and/or when submitted to multi-extreme conditions.

Laue diffraction can probe large reciprocal space areas, imaging the rich physics frequently found in these systems, manifested as incommensurability, diffuse scattering and magnetoelastic effects. The characterization of the magnetic phases can be completed with higher resolution data from monochromatic diffraction.

In rare-earth-based intermetallic compounds, the oscillatory character of the RKKY (Ruderman-Kittel-Kasuya-Yosida) exchange causes competing interactions which often frustrate magnetic moments. It is the case of the compounds belonging to the families  $R_3\text{Ru}_4\text{Al}_{12}$  ( $R$  is a rare-earth element),  $R_2\text{Co}_3\text{Al}_9$  and  $R\text{Fe}_5\text{Al}_7$ . They display multiple spontaneous and induced phase transitions and complex magnetic structures that provide an opportunity to study the interplay among magnetic frustration, exchange interactions, and magnetic anisotropy. Here, we will present studies of the magnetic ground states using the neutron Laue diffraction combined with monochromatic neutron diffraction.

The Ho atoms in  $\text{Ho}_3\text{Ru}_4\text{Al}_{12}$  form a kagome lattice and their magnetic ordering below the Néel temperature is not complete. Furthermore, Laue diffraction images taken in the antiferromagnetic state indicate that the magnetic structure needs to be described by two independent propagation vectors. Similarly, the  $\text{TmFe}_5\text{Al}_7$  compound exhibits an incommensurate magnetic ground state and the propagation vector is determined from the Laue data despite the very weak magnetic scattering and the presence of a large twin crystal on the sample.

## MS24-P104 - LATE | MAGNETIC TEXTURES IN NON-MAGNETIC SYSTEMS

Wolpert, Emma (University of Oxford, Oxford, GBR); Goodwin, Andrew (University of Oxford, Oxford, GBR)

Magnetic textures have become of increasing interest in condensed matter physics due to the discovery of non-topologically trivial magnetic textures such as skyrmions. Experimentally observing new skyrmions proves a challenge as the chemical conditions needed lead to a small pool of available candidates. Here we look at the possibility of creating analogues of magnetic textures in non-magnetic materials by replacing the magnetic dipoles with non-magnetic quadrupoles and switching the magnetic field for a strain field. Through Monte Carlo simulations, we explore the possibility of producing analogues of magnetic textures by coupling these quadrupoles hosted within a chiral framework to a strain field and measuring the behaviour on varying strain and temperature. This opens up the field to new ways of creating non-topologically trivial textures that could potentially be less restrictive than chiral magnets.

## MS25: Electron Crystallography as a Tool for Structure Solution and Refinement

---

### MS25-01 | STRUCTURE DETERMINATION OF NANO-PRECIPTATES IN METALLIC ALLOYS USING ELECTRON CRYSTALLOGRAPHY METHODS

Meshi, Louisa (Ben Gurion University of the Negev, Beer Sheva, ISR)

Aluminides is an interesting class of materials which contain wide variety of structural complexity from simple cubes with several atoms/unit cell to quasicrystals and complex metallic alloys with hundreds atoms/unit cell. Aluminides usually appear as nanosized particles dispersed in metallic matrices. Traditional X-ray diffraction methods cannot be used for characterization of such structures due to the lack of single crystals and overlapping and/or broadening of powder diffraction peaks. Thus, Electron Crystallography (which is a combination of electron imaging and diffraction methods for solution of atomic structure of materials) is sometimes the only viable tool for this purpose due to stronger (than X rays) interaction with matter. The uniqueness in structure solution of complex aluminides` structures is in lack of chemical reasonability since interatomic distances and angles vary. Thus, special methods for verification of correctness of proposed atomic model should be used. This is even more problematic, when the solution is done basing on electron diffraction (ED) data which is noisy. Atomic structures of novel complex aluminides revealed in the Th-Ni-Al and Nd-Re-Al systems were solved using ED tomography method. Verification methods used in current research included comparison of in zone ED patterns and high resolution transmission electron micrographs to simulated (constructed based on suggested atomic model). It is interesting to note that atoms in the studied structures are situated in flat and puckered layers. This structural feature occurs in many A-T-Al aluminides (where T=transition metal and A=actinide/lanthanide), serving as additional verification of correctness of the proposed models.

## MS25-02 | ELECTRON CRYSTALLOGRAPHY IS A POWERFUL AND FEASIBLE EXTENSION TO EVERY X-RAY FACILITY

Gruene, Tim (University of Vienna, Wien, AUT)

Structure determination from crystal diffraction plays an important role in chemistry and biology. X-rays has been the main radiation source. X-ray crystallography has been well developed for many decades and also set standards for validation and data storage for other fields of interest. X-ray crystallography is limited by sample size. Typically a few micrometer in every dimension are to lower limit for structure determination (unless access to free electron lasers is available). Electron crystallography overcomes this size limit.

As long as the sample is crystalline, with a few dozen of unit cells in each direction, it can produce a diffraction pattern through electron radiation. With the latest demonstration, that even the chirality of organic compounds can be determined, electron crystallography has become a fully independent companion of X-ray crystallography [1]. I am going to present how we set up an electron diffractometer simply by mounting an EIGER hybrid pixel detector to a transmission electron microscope, and how we calibrated the instrument to meet the requirements of a typical X-ray facility [2]. While our work focused on chemical compounds [3], I will also share my experience considering the application of electron crystallography with respect to structural biology, including possible phasing scenarios.

[1] Brazda et.al, Science (2019), 364, 667-669

[2] Heidler et.al, Acta Crystallogr. (2019), D75, 458-466

[3] Gruene et.al, Angew. Chemie Int. Ed. (2018), 57, 16313-16317

## MS25-03 | HOW CAN WE DIRECTLY SEE THE MOLECULE ARRAY IN 3D PROTEIN CRYSTAL UNDER TEM?

Shintake, Tsumoru (OIST Graduate University, Onna, Okinawa, JPN)

The author discusses on basic physics Bragg diffraction, and propose a new sheme to caputure images under TEM. This technique will directly provide real image of molecules in 3D crystal, and thus suitable to analyze sub-micron-size protein crystals like Micro-ED, even with high mosaic spread, or disordered. The author will also discuss on practical liminations.

## MS25-04 | SERIAL PROTEIN CRYSTALLOGRAPHY IN A S/TEM

Bücker, Robert ; Hogan-Lamarre, Pascal ; Kassier, Günther ; Mehrabi, Pedram ; Schulz, Eike (Max Planck Institute for Structure and Dynamics of Matter (MPSD), Hamburg, GER); Miller, R. J. Dwayne (Max Planck Institute for the Structure and Dynamics of Matter, Hamburg, GER)

Serial crystallography, where diffraction snapshots of a large ensemble of randomly oriented crystals are taken, evades the cumulative damage inherent to rotation diffraction techniques. This approach has facilitated the use of sub-micron crystals in latest-generation X-ray sources, making large classes of small, radiation-sensitive systems such as recalcitrant protein crystals or nano-porous materials amenable to crystallographic structure solution [1]. On the other hand, electron radiation provides the advantage of a more favorable ratio of elastic scattering to damaging energy deposition by three orders of magnitude over X-rays, enabling another viable path to study such small, sensitive crystals, using transmission electron microscopes (TEMs) [2].

We present a new scheme for high-speed, low-dose protein nano-crystallography in a scanning TEM (S/TEM), which combines the benefits of both serial and electron approaches in order to achieve ultimate dose efficiency, while providing a high level of automation and ease of operation. Combining automated real-space mapping of protein crystal positions and morphologies with hardware-synchronized beam positioning and diffraction detection using a hybrid-pixel camera, diffraction snapshots from hundreds of crystals can be acquired per second, at a hit rate exceeding 60%.

Results on lysozyme and granulin samples are presented, both of which were solved at a resolution better than 2Å using mostly standard X-ray software, along with a thorough discussion of the data acquisition and analysis pipeline.

[1] Chapman *et al.*, Nature 470, 73 (2011)

[2] Shi *et al.*, eLife 2, e01345 (2013)

## MS25-05 | USING ARCIMBOLDO'S FRAGMENT-BASED MR FOR SOLVING MICROED DATA FROM MACROMOLECULAR STRUCTURES

Millán Nebot, Claudia Lucía (Institut de Biologia Molecular de Barcelona, Barcelona, ESP); Borges, Rafael (Institut de Biologia Molecular de Barcelona, Barcelona, ESP); Richards, Logan (UCLA-DOE Institute, Los Angeles, USA); Miao, Jennifer (UCLA-DOE Institute, Los Angeles, ESP); Rodríguez, José (UCLA-DOE Institute, Los Angeles, USA); Usón, Isabel (Institut de Biologia Molecular de Barcelona, Los Angeles, USA)

The proof of principle of protein structure determination using MicroED (micro electron diffraction) from sub-micron sized 2D protein crystals was established with lysozyme in 2013, for which molecular replacement (MR) was performed for phasing. Since that milestone, a number of different cases with resolution ranging from 3.2-1.0 Å have been solved. For atomic resolution, *ab-initio* methods, relying only on the measured intensities, were used for phasing. For lower resolutions, MR has been the phasing method of choice, but it requires a model.

ARCIMBOLDO performs fragment-based MR with PHASER, using as models either secondary structure elements, or libraries of small local folds or fragments from a distant homolog. Such small accurate fragments produce many solutions from which only a few are correct, but density modification and mainchain autotracing with SHELXE allows the completion and discrimination of correct substructures. For non-atomic resolutions but better than 3 Å, this method has been successful in many X-ray structure determinations.

Recently, we are adapting ARCIMBOLDO to work with electron scattering factors and using our model fragments, a number of MicroED datasets can be solved. In this work we will discuss the results of these cases and the current and future developments in our software for dealing with MicroED data.

[1] Rodriguez JA *et al.* (2017). *Curr Opin Struct Biol.* 46: 79-26.

[2] Millan, C, *et al.* (2015). *IUCrJ* 2, 95-105.

[3] McCoy, AJ, *et al.* (2007). *J Appl Crystallogr* 40: 658-674.

[4] Sheldrick, GM (2010). *Acta Crystallogr D Biol Crystallogr* 66: 479-485.

## MS25-P01 | ELECTRON CRYSTALLOGRAPHY FOR STUDYING MOF-INTERCALATED GUESTS

samperisi, laura (Stockholm University, Stockholm, SWE)

Immobilization of target molecules in MOFs has allowed interesting structures to be determined using X-ray single crystal diffraction [1;2]. However, one of the most important parameters that determine the data quality is the ratio of guest to host, which is strongly influenced by the concentration of the target molecule in the crystal and the dimensions of the crystalline host [1]. Electrons interact with matter  $10^4\times$  more strongly than X-rays. Thus, electron diffraction can be used to study crystals  $10^8\times$  smaller by volume than X-ray diffraction. Electron microscopy is the only method capable of acquiring imaging and diffraction data from the same sample volume. Moreover, the development of continuous rotation electron diffraction (cRED) has enabled very fast data collection, allowing multiple datasets to be rapidly collected from a large number of crystals. For these reasons we expect that electron crystallography can be used to solve structures of MOF-intercalated guests present in small quantities in the host complex. Working toward this goal, we prepared a Zn-based MOF that has already been used for target molecule immobilization [1],  $[(\text{ZnI}_2)_3(2,4,6\text{-tris(4-pyridyl)triazine})_2\cdot x(\text{solvent})]_n$ , and solved and refined its structure using cRED and standard X-ray crystallographic software (XDS, SHELX). Data were collected on a JEOL2100 LaB<sub>6</sub> under cryogenic conditions using an ASI Timepix hybrid detector. An atomic model of the structure is presented.

[1] Hoshino, M. et al. (2016). IUCrJ, 3, 139–151

[2] Lee, S. et al. (2016). Science 353 (6301), 808-811

## MS25-P02 | DATA PROCESSING OF 3D PRECESSION ELECTRON DIFFRACTION DATA

Palatinus, Lukas (Institute of Physics of the Czech Academy of Sciences, Prague, CZE); Brázda, Petr (Institute of Physics of the CAS, Prague 8, CZE)

3D electron diffraction (3D ED) has become popular recently as novel, powerful methods have been developed for structure solution and structure refinement from such data. A number of protocols have been devised for data collection. One of them is the combination of step-wise data collection with precession electron diffraction technique (PED). This technique has a number of advantages. It provides intensities well suitable for kinematical structure refinement and it is so far the only method providing data suitable for dynamical refinement. While data collected without PED can be processed by many programs including those developed for X-ray diffraction data, PED data have specific features that require special treatment.

The main specific feature of 3D ED with PED is the unique rocking curve of the reflections, which has two maxima and resembles the back of a camel. The shape of the rocking curve can be estimated by analyzing the data and determining the crystal mosaicity. Once the shape is known, the reflection intensity can be accurately extracted. Moreover, the orientation of each frame can be determined with accuracy better than  $0.1^\circ$ , allowing for the correction of possible crystal rotation during the data collection and consequently allowing for a better determination of lattice parameters and better intensity extraction.

The specifics of processing of PED data will be described and its benefits will be illustrated on several examples ranging from accurate determination of lattice parameters, through the structure solution of an extremely beam-sensitive material to the determination of absolute configuration of chiral molecules.

## MS25-P03 | AUTOMATED ELECTRON DIFFRACTION: 3D STRUCTURE DETERMINATION WITH SUB-ÅNGSTRÖM RESOLUTION

Roslova, Maria (Stockholm University, Stockholm, SWE); Smeets, Stef (Delft University of Technology, Delft); Wang, Bin (Stockholm University, Stockholm, SWE); Thersleff, Thomas (Stockholm University, Stockholm, SWE); Hu, Hongyi (Stockholm University, Stockholm, SWE); Zou, Xiaodong (Stockholm University, Stockholm, SWE)

Electron diffraction (ED) is a well-known technique for 3D structure determination of solids, which is especially advantageous for the study of micro- and nanocrystals. Several software-based methods for automated collection of 3D ED data have been developed, however, until now many automation packages were optimized for specific microscopes available in the labs that created the software. A new custom DigitalMicrograph (DM) script InsteaDMatic has been developed to facilitate rapid semi-automated electron diffraction data acquisition on our Themis Z microscope with a Gatan One View CCD camera. The InsteaDMatic communicates to both the microscope and camera via DM interfaces, and thus can in principle be directly used in all microscopes with a Gatan CCD camera, where the hardware communications are by default already set up by the DM software.

Benefiting from InsteaDMatic, we collected high-quality data on randomly-oriented crystals of ZSM-5 zeolite down to 50-100 nm in size. The method delivers up to 0.8 Å resolution data, suitable for “ab-initio” crystal structure analysis by XDS and SHELX-97 software. Positions of the Si and O atoms in ZSM-5 can be determined within an accuracy of more than 0.1 Å. Thus, the development of the cross-platform software makes cRED with a sub-ångström resolution available for all microscopes utilizing the DM software.

## MS25-P04 | DEDICATED ELECTRON SOURCE FOR SERIAL ELECTRON CRYSTALLOGRAPHY

Hogan-Lamarre, Pascal (University of Toronto, Toronto, CAN); Khazai, Nariman (University of Toronto, Toronto, CAN); Bücken, Robert (Max Planck Institute for the Structure and Dynamics of Matter, Hamburg, GER); Kassier, Günther (Max Planck Institute for the Structure and Dynamics of Matter, Hamburg, GER); Miller, R.J.Dwayne (University of Toronto, Toronto, CAN)

Work in electron-based macromolecular structure determination has grown in importance with the recent developments in rotation electron crystallography [1]. It was recently shown that serial electron crystallography (serialED) can be implemented within an electron microscope (TEM) to recover structures from nanocrystalline inorganic molecules [2]. This raises questions on the applicability of serialED to organic macromolecules. Such materials present challenges, notably in terms of dose sensitivity and beam quality. Moreover, TEMs have their own limitations: spatial constraints forbid large-travel high-precision stages or equipment for dynamics triggering.

We present the design of a dedicated electron beamline for serialED in development. A Schottky field emitter filtered by a 50- $\mu\text{m}$  aperture creates a highly-coherent beam. Sub- $\mu\text{s}$  pulses are generated through pulsing of the extraction potential and beam blanking. Properties of the beamline are explored through particle-tracking simulations based on realistic representations of the optics from finite-element methods. Macromolecular structures determination in a high-current regime is discussed: considering a fluence threshold of 5  $\text{e}/\text{\AA}^2$ , simulations show that a repetition rate of the order of 100 Hz is achievable.

Data processing is explored in a proof-of-principle experiment within a TEM. Using softwares developed for x-ray diffraction, such as CrystFEL<sup>4</sup> and CCP4, the structures of hen-egg lysozyme, and granulovirus are recovered at a resolution of 2  $\text{\AA}$  and 1.8  $\text{\AA}$ , respectively.

[1] D.Shi *et al.*, *eLife*, (2013).

[2] S.Smeets *et al.*, *J. Appl. Cryst* **51**, (2018).

[3] T.A.White *et al.*, *J. Appl. Cryst* **45**, (2012).

## MS25-P05 | CONTINUOUS ROTATIONAL ELECTRON DIFFRACTION METHOD FOR STRUCTURE

### DETERMINATION OF SMALL ORGANIC MOLECULES

Ge, Meng (Stockholm University, Stockholm, SWE); Huang, Zhehao (Stockholm University, Stockholm, SWE); Zou, Xiaodong (Stockholm University, Stockholm, SWE)

The properties of a material are well related to their structures. X-ray diffraction method is the most commonly used technique for structure determination of crystalline materials. Compared with X-ray, electrons have much shorter wavelength and much stronger interaction with atoms in the crystal. Therefore, electron crystallography can effectively determine the structures of nano- and micron-sized crystals. In recent years, 3D electron diffraction techniques are used for structure determination of various types of complex structures such as zeolites and metal-organic frameworks (MOFs). However, some materials are sensitive to the high energy of electrons which will lead to structural distortion. Here we use the continuous rotation electron diffraction (cRED) method developed in our group to investigate the crystal structure of a small molecule. During the cRED data acquisition, the goniometer is continuously rotated at a constant speed. The typical collection time of cRED data is less than 5 mins which makes it possible to study electron beam sensitive materials. We demonstrate that by using cRED we could determine the structure of a small organic molecule, which is nano-crystal and highly beam sensitive. The unit cell parameters and space group were determined from 3D reciprocal space, and the structure was solved by using Shelx. All the atoms were found directly.

## MS25-P06 | LOW DOSE ELECTRON DIFFRACTION TOMOGRAPHY (LD-EDT) SOLVES THE STRUCTURE OF A NEW $(\text{Na}_{2/3}\text{Mn}_{1/3})_2\text{Mn}_3\text{Ge}_3\text{O}_{12}$ PHASE SYNTHESIZED AT HIGH PRESSURE AND HIGH TEMPERATURE

Kodjikian, Stéphanie (Université Grenoble Alpes and CNRS - Institut Néel, Grenoble, FRA); Klein, Holger (Université Grenoble Alpes and CNRS - Institut Néel, Grenoble, FRA); Mangin, Thomas (Université Grenoble Alpes and CNRS - Institut Néel, Grenoble, FRA); Darie, Céline (Université Grenoble Alpes and CNRS - Institut Néel, Grenoble, FRA); Legendre, Murielle (Université Grenoble Alpes and CNRS - Institut Néel, Grenoble, FRA); Ding, Lei (Université Grenoble Alpes and CNRS - Institut Néel, Grenoble, FRA); Colin, Claire V. (Université Grenoble Alpes and CNRS - Institut Néel, Grenoble, FRA); Goujon, Céline (Université Grenoble Alpes and CNRS - Institut Néel, Grenoble, FRA); Bordet, Pierre (Université Grenoble Alpes and CNRS - Institut Néel, Grenoble, FRA)

Our team has recently developed the LD-EDT method [1], which makes it possible to study the crystallographic structure of sensitive materials that are very promising in many fields (medical, energy, etc.), but from which one cannot obtain single crystals large enough for X-ray diffraction. The LD-EDT method, based on electron diffraction tomography, eliminates all periods of irradiation of the sample except those actually used for data acquisition. It therefore uses the minimum dose ( $< 1$  electron/Å<sup>2</sup>). In addition, the LD-EDT method ensures that the diffracting volume of the crystal remains the same at all stages, which leads to particularly reliable data.

We present here the structure solution of a new sodium compound, discovered in a polyphase powder, synthesized under high pressure and high temperature in the framework of expanding the range of germanium-based compounds in the pyroxene family. Since it is well known that sodium migrates or vaporizes under the electron beam, we decided to apply the new LD-EDT method to acquire the diffracted intensities without damaging the crystals. The structure was solved by direct methods:  $(\text{Na}_{2/3}\text{Mn}_{1/3})_2\text{Mn}_3\text{Ge}_3\text{O}_{12}$  crystallizes in a  $(Ia-3d)$  garnet-like cubic structure, with a cell parameter of 12.0 Å. The refinement against X-ray powder diffraction data revealed a mixed Na/Mn occupancy on one site.

[1] Stéphanie Kodjikian and Holger Klein, *Ultramicroscopy* 200 (2019) 12-19

## MS25-P07 | DYNAMICAL STRUCTURE REFINEMENT FROM DATA OBTAINED WITH A DOSE OF LESS THAN $1 \text{ e}^-/\text{\AA}^2$

Klein, Holger (Institut Néel, Grenoble, FRA); Kodjikian, Stéphanie (Institut Néel, Grenoble, FRA)

Solving the structures of beam sensitive materials is one of the current challenges in crystallography. This challenge is even bigger when it comes to the refinement of their structures. The fact that it is notoriously difficult for many beam sensitive materials to grow large single crystals doesn't make it easier. As a consequence, in certain material classes like metal-organic frameworks (MOF) many compounds have been synthesized but stay in the drawer because they lack a suitable structure investigation method.

Electron diffraction is the most sensible choice in these cases. Not only can we exploit single crystals that are a million times smaller than in X-ray diffraction, but for the same amount of useful signal the dose can also be three to four orders of magnitude lower. On this basis we recently developed the low-dose electron diffraction tomography (LD-EDT) that is optimized for dose by eliminating all periods of irradiation except those actually used for data acquisition.

In this contribution we show that the data quality of LD-EDT is suitable for dynamical refinement of the structures even when the total dose used for data acquisition is less than  $1 \text{ electron} / \text{\AA}^2$ . We present the results of the refinements of complex oxides as well as MOF.

## MS25-P08 | REFINEMENT OF ORGANIC CRYSTAL STRUCTURE WITH MULTIPOLAR ELECTRON

### SCATTERING FACTORS

Gruza, Barbara (CNBCh, Department of Chemistry, University of Warsaw, Warszawa, POL); Chodkiewicz, Michal (CNBCh, Department of Chemistry, University of Warsaw, Warszawa, POL); Krzeszczakowska, Joanna (CNBCh, Department of Chemistry, University of Warsaw, Warszawa, POL); Dominiak, Paulina (CNBCh, Department of Chemistry, University of Warsaw, Warszawa, POL)

Electron diffraction (ED) is based on scattering of electron beam on electrostatic potential. This recently fast advancing method allows to obtain crystal structures of nanocrystals at atomic resolutions, for both small and macro- molecules [1,2]. However, for this purpose, it is necessary to use proper scattering factors [3]. Different models, already known for x-ray diffraction, can be implemented for ED.

In this study, we present comparison of refinements of IAM and TAAM (Transferable Aspherical Atom Model) with parameters of multipolar model with Hansen-Coppens formalism taken from UBDB [4]. For both models are used electron scattering factors implemented in DiSCaMB library [5] and interfaced with Olex2[6]. The TAAM accounts for the fact that atoms in molecules bear partial charge and are not spherical. Refinements are performed against experimental electron structure factors [1] and theoretical electron structure factors computed in Crystal14 [7]. Results show the possibilities and limitations of the TAAM method. We discuss e.g. improvement of fitting statistics (R1), anisotropic displacement parameters and hydrogen atoms positions obtained from refinements of TAAM instead of IAM.

Support of this work by the National Centre of Science (Poland) through grant OPUS No.UMO-2017/27/B/ST4/02721 is gratefully acknowledged.

[1] ACS Cent. Sci. 2018, 4, 1587;

[2] Angew. Chem, Int. Ed. 2018, 57, 16313

[3] IUCrJ 2018, 5, 348

[4] Acta Cryst 2019, A75, 398.

[5] J. Appl. Cryst. 2018, 51, 193.

[6] J. Appl. Cryst. 2009, 42, 339.

[7] Int. J. Quantum Chem. 2014; 114, 1287.

## MS25-P09 | STRUCTURE OF A NOVEL R2-LIKE LIGAND-BINDING OXIDASE REVEALED BY ELECTRON DIFFRACTION

Xu, Hongyi (Stockholm University, Stockholm, SWE); Lebrette, Hugo (Stockholm University, Stockholm, SWE); Clabbers, Max (Stockholm University, Stockholm, SWE); Zhao, Jingjing (Stockholm University, Stockholm, SWE); Griese, Julia ; Zou, Xiaodong (Stockholm University, Stockholm, SWE); Högbom, Martin (Stockholm University, Stockholm, SWE)

Electron diffraction (ED) has in recent years shown to be a promising method for protein structure determination when only micron-sized three-dimensional crystals are available that are beyond what can be resolved by conventional macromolecular X-ray crystallography (MX). However, up until now ED had only been applied to refine known protein structures that were already solved previously by MX. Here, we present the first unknown protein structure – a novel R2lox metalloenzyme – solved using ED. Despite encountering preferential orientation of the plate-like crystals, low signal-to-noise ratio, and a highly viscous sample environment, the structure could successfully be solved by molecular replacement using a search model of only 35% sequence identity. The resulting electrostatic scattering potential map at 3.0Å resolution was of sufficient quality to allow accurate model building and refinement. Our results illustrate that ED has the potential to become a widely applicable technique for structural biology, complementing MX when crystal volume is the limiting factor in structure elucidation.

## MS25-P10 | MICROED, FAST AND FURIOUS

Raaijmakers, Hans (Thermofisher, Eindhoven)

Small molecule electron diffraction may be as old as electron microscopes, but made its popular debut only last year, thanks to teams from PSI [1] and UCLA-Caltech [2]. The new method, called microED, allows researchers to perform crystallographic analysis at the atomic level from simple powders composed of only nanocrystals – and much quicker than ever before. MicroED gives researchers the opportunity to characterize newly synthesized compounds “on the fly,” meaning they can gather important details about a sample throughout its creation, potentially guiding the chemical development process. For the first time ever, a team lead by Tim Gruene at the Paul Scherrer Institut was able to show the power of this technique using a commercially-available capsule of a painkiller. Using MicroED, they were able to separate out and characterize one single crystal of the main active ingredient, paracetamol. This technique isn’t just limited to small molecules; peptide samples that were previously considered too unstructured to crystallize can now be analyzed as well [3].

Moving forward, this method, using cryo-EM instrumentation already at our fingertips, will provide structural insight at unparalleled speeds and with higher resolution images. We have created a workflow to make microED fast and easy, and easily accessible to all users. This workflow does also support macromolecular MicroED.

[1] Tim Gruene et al., *Angew. Chem. Int. Ed.* 2018, 57, 1 – 6

[2] CG. Jones, Tamir Gonen et al,

[https://chemrxiv.org/articles/The\\_CryoEM\\_Method\\_MicroED\\_as\\_a\\_Powerful\\_Tool\\_for\\_Small\\_Molecule\\_Structure\\_Determination/7215332](https://chemrxiv.org/articles/The_CryoEM_Method_MicroED_as_a_Powerful_Tool_for_Small_Molecule_Structure_Determination/7215332)

[3] Shi et al. *eLife* 2013;2:e01345, [https://cryoem.ucla.edu/uploads/image/pdfs/2013\\_shi.pdf](https://cryoem.ucla.edu/uploads/image/pdfs/2013_shi.pdf)

## MS25-P106 LATE | EXPLORATION OF BRAGG IN-LINE ELECTRON HOLOGRAPHY AS A POSSIBLE TOOL FOR CRYSTAL STRUCTURE DETERMINATION

Cassidy, Cathal (OIST, Onna, JPN); Latychevskaia, Tatiana (Paul Scherrer Institute & University of Zurich, Villigen, CH); Shintake, Tsumoru (OIST, Onna, JPN)

We have been exploring a hybrid crystal imaging scheme in TEM, acquiring deeply defocused images such that individual Fourier components in the image are spatially separated (which we term “Bragg in-line holography”). Interference between the reference beam and each individual “Bragg beam” results in an internal 2-beam interference pattern in each individual Bragg image. Previously (ECM31) we presented first experimental results on MgO nanocubes, confirming the presence of lattice information in each individual Bragg image. In the meantime, we have performed further simulations, and begun experimental efforts on (cryo-prepared) organic crystals. We include selected examples of recent simulation work below.

## MS25-P108 LATE | ON THE DESIGN OF A DEDICATED ELECTRON DIFFRACTOMETER

Hovestreydt, Eric (ELDICO Scientific AG, Villigen, CH); Santiso-Quinones, Gustavo (ELDICO Scientific, Villigen, CH); Steinfeld, Gunther (ELDICO Scientific, Villigen, CH)

Electron Diffraction (ED) as such has been around since the early days of Electron Microscopy. Since Transmission Electron Microscopes (TEMs) are available with accelerating powers of 200 to 300 kV and 2D detectors have become fast enough, Electron Crystallography really took off.

So far, ED has been done in TEMs that are modified, resulting in challenging experiments and limited datasets, yet, structures could be obtained from samples in the range of merely tens of nanometers, that were unsolvable with either conventional or even synchrotron X-ray radiation.

For some reason, no dedicated Electron Diffractometer has been available commercially so far. Data quality would greatly benefit from a TEM setup that focuses on the diffraction capability over imaging and allowing for faster and more complete datasets.

We will present a possible Electron Diffractometer design for Electron Crystallography from the point-of-view of X-ray Crystallography and indicate improvements over present TEM-based as well as X-ray instruments. It is envisioned, that preliminary results will also be presented.

[1] [www.eldico-scientific.com](http://www.eldico-scientific.com)

## MS26: Complex Metallic Alloys: Periodic and Non Periodic

---

### MS26-01 | SOME RECENT ADVANCES IN THE SURFACE SCIENCE OF COMPLEX METALLIC ALLOYS

McGrath, Ronan (University of Liverpool, Oxford Street, Liverpool, GBR)

Complex metallic alloys present unique challenges and opportunities in surface science, both for preparation of clean surfaces and for epitaxial studies.

Studies of three Ag-In-RE(100) (RE=Yb,Gd,Tb) approximants illustrate a variety of surface behaviours when prepared in ultra-high-vacuum conditions [1] from flat surfaces to multiple faceting; I will discuss the origin these behaviours in terms of surface atomic bonding.

In recent work, we demonstrated that C<sub>60</sub> molecules adsorbed on this surface at room temperature form a Fibonacci square grid – the first physical manifestation of a prediction made in 2002 by Lifshitz [2]. In this case the C<sub>60</sub> molecules bond preferentially to Mn atoms in the surface layer, which are arranged in the Fibonacci square grid geometry [2].

In a further study, the adsorption of Pb atoms on the 3-fold surface of the icosahedral Ag-In-Yb quasicrystal proceeds in an unusual way; instead of layer-by-layer growth as was observed on the five-fold surface [3], the atoms form quasicrystalline Pb nanoclusters by mimicking the structure of the underlying substrate. I will discuss whether this is long-sought evidence for "cluster stability" in quasicrystals.

[1] S. Hars, H. R. Sharma, J. A. Smerdon, T. P. Yadav, A. Al-Mahboob, J. Ledieu, V. Fournée, R. Tamura, and R. McGrath, *Phys. Rev. B* 93 (2016) 205428

[2] S. Coates, J.A. Smerdon, R. McGrath & H. R. Sharma, *Nature Communications* 9 (2018) 3435.

[3] S. Coates, S. Thorn, R. McGrath and H.R. Sharma, in preparation.

## MS26-02 | THE POWER OF ANALOGY IN PHYSICS: FROM FARADAY WAVES THROUGH SOFT MATTER TO COMPLEX METALLIC ALLOYS

Lifshitz, Ron (Raymond and Beverly Sackler School of Physics & Astronomy, Tel Aviv, ISR)

As early as 1985, Landau free-energy models [1-3] and density-functional mean-field theories [4] were introduced in an attempt to explain the stability of quasicrystals, with only partial success if any. It is only in recent years, that great progress has been made in understanding the thermodynamic stability of quasicrystals in such simple isotropic classical field-theories. Much of this has happened thanks to insight from the experimental observation of quasicrystalline order in diverse systems ranging from fluid dynamics to soft condensed matter. The key to unlocking the stability puzzle was in the realization that more than a single length scale was required, but more importantly in figuring out how to introduce these multiple scales into the models, and identifying the remaining requirements [5,6]. We and others have since managed to produce Landau and other mean-field theories with a wide range of quasicrystals as their minimum free-energy states, and have also confirmed some of these theories using molecular dynamics simulations with appropriately designed interparticle potentials [7-14]. I shall give a quick overview of the quasicrystals that can be stabilized in these theories—in systems of one or two types of particles, in two and in three dimensions—and attempt to identify a trend that might be emerging in going from Landau theories to more realistic density-functional mean-field theories. It remains an open question whether this trend may eventually lead to understanding the stability of quasicrystals in complex metallic alloys.

This research is supported by Grant No. 1667/16 from the Israel Science Foundation.

- [1] P. Bak, Phys. Rev. Lett. 54, 1517 (1985).
- [2] N.D. Mermin, S.M. Troian, Phys. Rev. Lett. 54, 1524 [Erratum on p. 2170] (1985).
- [3] P.A. Kalugin, A.Yu. Kitaev, L.C. Levitov, JETP Lett. 41, 145 (1985).
- [4] S. Sachdev, D.R. Nelson, Phys. Rev. B 32, 4592 (1985).
- [5] R. Lifshitz, H. Diamant. Phil. Mag. 87, 3021 (2007).
- [6] R. Lifshitz, D. Petrich, Phys. Rev. Lett. 79, 1261 (1997).
- [7] K. Barkan, H. Diamant, R. Lifshitz, Phys. Rev. B 83, 172201 (2011).
- [8] A.J. Archer, A.M. Rucklidge, E. Knobloch, Phys. Rev. Lett. 111, 165501 (2013).
- [9] K. Barkan, M. Engel, R. Lifshitz, Phys. Rev. Lett. 113, 098304 (2014).
- [10] C. V. Achim, M. Schmiedeberg, and H. Löwen, Phys. Rev. Lett. 112, 255501 (2014).
- [11] P. Subramanian, A.J. Archer, E. Knobloch, A.M. Rucklidge, Phys. Rev. Lett. 117, 075501 (2016).
- [12] S. Savitz, M. Babadi, R. Lifshitz, IUCrJ 5, 247 (2018).
- [13] M.C. Walters, P. Subramanian, A.J. Archer, R. Evans, Phys. Rev. E 98, 012606 (2018).
- [14] S. Savitz, R. Lifshitz, "Self-assembly of body-centered icosahedral cluster crystals", in preparation (2019).

## MS26-03 | NUCLEATION AND GROWTH OF TENFOLD TWINS OF NiZr DURING NON-EQUILIBRIUM SOLIDIFICATION

Hornfeck, Wolfgang (Academy of Sciences of the Czech Republic, Prague, CZE)

Understanding the solidification of metals and alloys is of utmost importance in metallurgy and materials science, since it ideally allows for a purposeful microstructure design, which itself is governing the properties of a technologically used material. However, while some metallic systems are well-understood in this sense, this is not true in general. In particular, for many alloys crystal structures are as complex as microstructures and the interplay between both levels of structural hierarchy appears as mostly uncharted territory.

Here, we report on the homogeneous nucleation of a single quasicrystalline seed from the undercooled melt of glass-forming NiZr and its continuous growth into a tenfold twinned dendritic microstructure. Observing a series of crystallization events on electrostatically levitated NiZr confirms homogeneous nucleation. Mapping the microstructure with electron backscatter diffraction suggests a unique, distortion-free structure merging a common structure type of binary alloys with a spiral growth mechanism resembling phyllotaxis. A general geometric description, relating all atomic loci, observed by atomic resolution electron microscopy, to a pentagonal Z module, explains how the seed's decagonal long-range orientational order is conserved throughout the symmetry breaking steps of twinning and dendritic growth.

## MS26-04 | THEORETICAL STUDY OF SINGLE-ELEMENT QUASI-PERIODIC THIN FILMS FORMED ON Ag-IN-Yb QUASICRYSTAL

Nozawa, Kazuki (Kagoshima University, Kagoshima, JPN); Makoshi, Kenji (University of Hyogo, Hyogo, JPN); Ishii, Yasushi (Chuo University, Tokyo, JPN)

Developments in the preparation and understanding of the surfaces of Quasicrystals (QCs) enable us to use QCs as a template of the epitaxial growth of the quasi-periodic thin films, and we recently reported the first successful fabrication of three-dimensional quasi-periodic Pb thin film using the Ag-In-Yb QC as a template [1]. It was confirmed that Pb film grown on the QC template forms a three-dimensional quasi-periodic structure. But, more surprisingly, the accumulated Pb occupy the absent rhombic triacontahedral sites, which is a structural building unit of the substrate QC, created by the crystal truncation of the substrate QC at the surface. Recent theoretical advances in the structure of the quasi-periodic thin film of Bi [2], Sb and Ag [3] obtained using the first-principles calculations based on the density functional theory will be discussed.

[1] H.R. Sharma, K. Nozawa, J.A. Smerdon, P.J. Nugent, I. McLeod, V.R. Dhanak, M. Shimoda, Y. Ishii, A.P. Tsai, and R. McGrath *Nat. Commun.* **4**, 2715 (2013).

[2] K. Nozawa and Y. Ishii, *J. Phys. Conf. Ser.*, **809**, 012018 (2017).

[3] K. Nozawa, *Proceedings of International Scientific Conference on Engineering and Applied Sciences 2018*, 197 (2018).

## MS26-05 | THREE DIMENSIONAL LOCAL ATOMIC CONFIGURATIONS OF DECAGONAL AlNiCo QUASICRYSTAL STUDIED BY X-RAY FLUORESCENCE HOLOGRAPHY

de Boissieu, Marc (CNRS, Univ. Grenoble Alpes, Saint Martin d'Hères, FRA); Stelhorn, J.R (Photon Science, Hamburg, GER); OSOKAWA, S (Kumamoto University, Kumamoto, JPN); Kimura, K (Nagoya Institute of Technology, Nagoya, JPN); Hayashi, K. (Nagoya Institute of Technology, Nagoya, JPN); Gille, P. (LMU, Munich, GER); Tsai, A. P. (IMRAM, Sendai, JPN); Mihalkovic, M. (Slovak Academy of Science, Bratislava, SVK); Boudet, N. (Univ. Grenoble Alpes, CNRS, Institut Néel, Grenoble, FRA); Blanc, N. (Univ. Grenoble Alpes, CNRS, Institut Néel, Grenoble, FRA); Beutier, G. (Univ. Grenoble Alpes, CNRS, Simap, Saint Martin d'Hères, FRA)

Decagonal quasicrystal are characterised by a periodic stacking of quasiperiodic planes [1]. In this study, we apply the x-ray fluorescence holography (XFH) technique [2] to explore atomic configurations in two different decagonal quasicrystal with respective compositions equal to  $Al_{73}Co_{15}Ni_{12}$  (Co-rich) and  $Al_{72}Co_9Ni_{19}$  (Ni-rich). The measurements have been carried out on large single grain samples, above the Ni and Co edge. The XFH experiment allowed the reconstruction of the average 3D local environment around Co and Ni atoms.

This study is particularly interesting since the two quasicrystals do present significant differences: whereas the Co-rich decagonal phase displays a large amount of x-ray diffuse scattering even on the half integer layers, the Ni-rich one has a limited amount of diffuse scattering.

The results are compared with current atomic model using the tiling decoration proposed in [3].

[1] Janssen, T., Chapuis, G. & de Boissieu, M. (2007, second edition 2018). *Aperiodic Crystals. From modulated phases to quasicrystals*. Oxford: Oxford University Press.

[2] K. Hayashi et al., J. Phys.: Condens. Matter **24**, (2012) 093201

[3] M. Mihalkovic, M. Widom and C.L. Henley, Phil. Mag. **91** (2010) 2557-66

## MS26-P01 | PECULIARITIES OF SOLID SOLUTIONS WITH NATL-TYPE STRUCTURE IN LI-ZN-X (X=AL,GA,IN) SYSTEMS

Dmytriv, Grygoriy (Ivan Franko National University of Lviv, Lviv, UKR); Pavlyuk, Volodymyr (Ivan Franko National University of Lviv, Lviv, UKR); Ehrenberg, Helmut (Karlsruhe Institute of Technology, Eggenstein-Leopoldshafen, GER)

Li-Zn-X (X=Al,Ga,In) systems are characterized by forming of solid solutions across LiZn-LiX section with NaTl-type structure. This is expected, because all binary compounds of this section have the same structure type which, only differences in the lattice parameters:  $a = 6.209 \text{ \AA}$  for LiZn,  $a = 6.3757 \text{ \AA}$  for LiAl,  $a = 6.195 \text{ \AA}$  for LiGa and  $a = 6.786 \text{ \AA}$  for LiIn. Main task of our research was to compare these solid solutions.

As expected from the very close lattice parameters of LiZn and LiGa binary compounds, continuous solid solution  $\text{Li}(\text{Zn}_{1-x}\text{Ga}_x)$  is formed in the Li-Zn-Ga system. A peculiarity of this solid solution is that only very small shifts of lattice parameters are observed within the full composition range. The difference of lattice parameters of LiZn and LiAl binary compounds is not very high. Nevertheless, the change of lattice parameters within the continuous solid solution  $\text{Li}(\text{Zn}_{1-x}\text{Al}_x)$  are more pronounced. In contrast, the difference of lattice parameters of LiZn and LiIn binary compounds is very big and no continuous solid solution  $\text{Li}(\text{Zn}_{1-x}\text{In}_x)$  is formed for the Li-Zn-In system. Instead a two phase region was clearly observed along the LiZn-LiIn quasibinary cut at the composition  $\text{Li}(\text{Zn}_{0.75}\text{In}_{0.25})$ . Both limited solid solutions crystallize in the NaTl-type structure, but have different lattice parameters:  $6.4111(1) \text{ \AA}$  for the solid solution  $\text{Li}(\text{In}_{1-x}\text{Zn}_x)$  ( $x=0.75$ ) and  $6.3250(1) \text{ \AA}$  for the solid solution  $\text{Li}(\text{Zn}_{1-x}\text{In}_x)$  ( $x=0.25$ ).

## MS26-P02 | CHEMICAL BONDING AND STRUCTURAL COMPLEXITY IN KNOWN INTERMETALLIC COMPOUNDS $o\text{-Al}_{13}\text{Co}_4$ AND $\text{Al}_{2.75}\text{Ir}_2$

grin, Yuri (Max-Planck-Institut für Chemische Physik fester Stoffe, Dresden, GER)

Investigations on binary compounds of transition metals with aluminum have a long-time history. The crystal structure of  $o\text{-Al}_{13}\text{Co}_4$  was reinvestigated 35 years after the first report about the phase [1,2]. The recent crystal structure redetermination reveals a strong disorder in parts of the unit cell. High-resolution diffraction and TEM experiments show a very complex atomic arrangement obviously deviating from the translational symmetry [3]. The similar situation is found also for the phase  $\text{Al}_{2.75}\text{Ir}$  first discovered [4] and much later structurally described [5]. Crystal structure reinvestigation revealed an extremely complex crystallographic picture of two modifications with the LT phase being orthorhombic with doubling of the previous cubic unit cell [6]. The reasons for such complexity may be found in the chemical bonding within the crystal structures characterized by an interplay of the strongly polar and non-polar, two-center and multi-center interactions.

[1] R. C. Hudd, W.H. Taylor, *Acta Crystallogr.* 15, 441 (1962).

[2] Yu. Grin, U. Burkhardt, M. Ellner, K. Peters, *J. Alloys Compds.* 206, 243 (1994).

[3] P. Simon, I. Zelenina, W. Carrillo-Cabrera, U. Burkhardt, M. Feuerbacher, P. Gille, Yu. Grin, unpublished results (2019).

[4] R. Ferro, R. Capelli, R. Marazza, S. Delfino, A. Borsese, G. B. Bonino, *Atti Accad. Naz. Lincei, Cl. Sci. Fis. Mat. Nat. Rend.* 45, 556 (1968).

[5] Yu. Grin, K. Peters, U. Burkhardt, K. Gotzmann, M. Ellner, *Z. Kristallogr.* 212, 439 (1997).

[6] Yu. Prots, J. Kadok, M. Schmidt, M. Coduri, V. Fournée, J. Ledieu, Yu. Grin, unpublished results (2019).

## MS26-P03 | NEW CA/MG/ZN INTERMETALLICS OF ONE INTERGROWTH FAMILY.

Köhler, Katharina (Albert-Ludwigs-Universität Freiburg, Freiburg, GER); Röhr, Caroline (Albert-Ludwigs-Universität Freiburg, Freiburg, GER)

Ternary intermetallic compounds  $A_xM_yM'_z$  of the title family formed between one of the heavier alkaline-earth metals Ca, Sr, or Ba (A) and Li/Zn and Li/Al respectively ( $M, M'$ ) show a remarkable series of related structures at an  $M/A$  ratio between 3.8 and 5.3 [1,2]. They can be arranged into an intergrowth series deduced from the three structure types  $Ba_2Li_{4.2}Al_{4.8}$  [1],  $Th_6Mn_{23}$  and  $EuMg_{5+x}$ .

In the system Ca/Mg/Zn (cf. also [4]) two new ternary phases of the title family were obtained (starting from elements, weighed under argon atmosphere in Ta tubes,  $T_{max}=900^\circ C$ ). The structure of  $Ca_9Mg_{14}Zn_{25}$  ( $P6_3/mmc$ ,  $a=939.06(2)\text{pm}$ ,  $c=2528.71(9)\text{pm}$ ,  $V=1931.15(11)\cdot 10^6\text{pm}^3$ ,  $Z=2$ ,  $Sr_3Mg_{13}$ -type [3]) and  $Ca_6Mg_8Zn_{15}$  ( $Fm-3m$ ,  $a=1330.46(7)\text{\AA}$ ,  $V=2355.1(4)\cdot 10^6\text{pm}^3$ ,  $Z=4$ ,  $Th_6Mn_{23}$ -type) are closely related to the  $Th_6Mn_{23}$ - and the  $EuMg_{5+x}$ -type.

[1] U. Häussermann, M. Wörle, R. Nesper, *J. Am. Soc.* **118**, 11789-11797 (1996).

[2] Q. Lin, R. Zhu, G. J. Miller, *Inorg. Chem.* **55**, 5041-5050 (2016).

[3] J. Erassme, H. Lueken, *Acta Crystallogr.* **43B**, 244-250 (1987).

[4] K. Köhler, C. Röhr, *Z. Anorg. Allg. Chem.*, **645**, 219-232 (2019).

## MS27: Structural Dynamics, Disorder and Physical Properties

---

### MS27-01 | COMBINING DIFFUSE AND INELASTIC SCATTERING IN THE EXPLORATION OF PHASE TRANSITIONS

BOSAK, Alexei (ESRF, Grenoble, FRA)

Diffuse x-ray scattering (DS) and inelastic x-ray scattering (IXS) complement each other in the studies of lattice dynamics and static or slowly changing correlated disorder. Fast mapping of the reciprocal space with high momentum resolution allows the identification of regions of interest, which can be further explored in more detail by energy-resolved IXS experiment. Unambiguous attribution of DS features as inelastic or (quasi)elastic can immediately provide valuable insights on the behaviour of the system; rapid and efficient screening of temperature (pressure, field, etc.) response becomes available.

We present the results obtained at ESRF by tandem use of IXS and diffraction/diffuse scattering beamlines for the selection of first- and second-order phase transitions related to the phonon softening or displacement disorder. The considered examples include the ferroic perovskites and strongly correlated systems with charge density waves, where electron-phonon coupling is essential.

## MS27-02 | RECENT DEVELOPMENTS IN THE USE OF SINGLE CRYSTAL DIFFUSE SCATTERING TO STUDY MATERIALS PROPERTIES

Rosenkranz, Stephan (Argonne National Laboratory, Lemont, USA); Krogstad, Matthew (Argonne National Laboratory, Lemont, USA); Osborn, Raymond (Argonne National Laboratory, Lemont, USA)

Many physical properties of crystalline materials are strongly enhanced or driven by local disorder and short-range correlations. Examples include ionic conduction, thermoelectricity, relaxor behavior, unconventional superconductivity, and many more. Obtaining a microscopic understanding of such disorder requires accurate measurements of the total scattering comprising both Bragg peaks from the long-range average order and diffuse scattering from deviations from that average, which includes short-range correlations as well as extended short-range order resulting from defect-defect interactions. Single-crystal diffuse scattering hence offers a powerful probe of the many unusual physical phenomena that are driven by complex disorder, but its use has been limited by the experimental challenge of collecting data over a sufficiently large volume of reciprocal space and the theoretical challenge of modeling the results. However, recent instrumental advances now allow the efficient measurement over the large three-dimensional volume of reciprocal space, with sufficient resolution to separate diffuse from Bragg scattering and sufficient dynamic range to include both simultaneously, that is necessary to accurately test models of complex disorder, whether obtained by the use of phenomenological potentials or short-range-order parameters or by *ab initio* methods. Computational advances furthermore enable rapid transformation of large volumes of reciprocal space data into three-dimensional pair-distribution functions that provide model-independent images of nanoscale disorder in real space.

Here, we discuss recent developments of neutron and x-ray diffuse scattering techniques and present results on a variety of phenomena including relaxor ferroelectricity, cation ordering in electrode materials, nematic correlations in iron-based superconductors, and charge density wave correlations.

## MS27-03 | UNDERSTANDING TWO-DIMENSIONAL POLYMERISATION USING BRAGG AND DIFFUSE X-RAY SCATTERING

Weber, Thomas (ETH Zurich, Zürich, CH); Hofer, Gregor (ETH Zurich, Zürich, CH); Simonov, Arkadiy (ETH Zurich, Zürich, CH); Kröger, Martin (ETH Zurich, Zürich, CH); Schlüter, Dieter (ETH Zurich, Zürich, CH)

Two-dimensional polymers are topologically exceptional macromolecules. One approach for synthesising such graphene-analogue polymeric material is the single-crystal-to-single-crystal polymerization method, where the monomers are pre-oriented in a layered 'reactive packing'. In this packing, the polymerization may be triggered by light and it can be reversed by heat treatment or illumination with light of a different wavelength. In this contribution we will present a detailed study of the polymerization and depolymerization mechanisms of a two-dimensional polymer based on Bragg and diffuse scattering. The latter was achieved with the 3D-DeltaPDF method using the program Yell.

We could identify the most important factors that made such a complex non-destructive transformation possible. It was found that the incorporated solvent molecules buffer the local strain induced by polymerization through a complex chain of movements. As a result, the accumulated global strain remains small enough to essentially maintain the single crystal state during a complete polymerization/depolymerization cycle. Of particular importance for the understanding of two-dimensional polymers is the development of the connectivity between molecules. The combination of reaction kinetics with real structure information as obtained from diffuse scattering, enabled the development of a polymerisation propagation model. It was found that both, polymerization and depolymerization are self-impeding processes, which lead to a more uniform spatial distribution of the polymer bonds in the intermediate structures than island models. As a result, polymerization-induced strain does not accumulate locally, but is distributed more evenly over the crystal and allows to preserve the integrity of the single-crystalline state.

## MS27-04 | SUB-MESOSCALE OXYGEN ORDERING IN NON-STOICHIOMETRIC OXYGEN ION CONDUCTOR $\text{Pr}_2\text{NiO}_{4+\delta}$

Paulus, Werner (University of Montpellier, Montpellier, FRA); Dutta, Rajesh (Institute of Crystallography, RWTH Aachen University and JCNS, FZ Jülich at Heinz Maier-Leibnitz Zentrum (MLZ), Garching bei München, GER); Maity, Avishek (Institute for Physical Chemistry | Georg-August-University of Goettingen Outstation at Heinz Maier-Leibnitz Zentrum (FRM II), Garching bei München, GER); Marsicano, Anna (University of Montpellier, Montpellier, FRA); Ceretti, Monica (CNRS Institut Charles Gerhardt UMR 5253, Montpellier, FRA); Bosak, Alexei (ESRF, Grenoble, FRA)

Non-stoichiometric oxides can undergo important variations in the oxygen stoichiometry, enabling to tune physical and chemical properties. Combining neutron diffraction, inelastic neutron scattering and *ab initio* lattice dynamics calculations, we have recently evidenced the importance of lattice dynamics, i.e. soft phonon modes, triggering low temperature oxygen mobility in Brownmillerite type  $(\text{Ca}/\text{Sr})\text{Fe}/\text{CoO}_{2.5}$  and Ruddlesden Popper type oxides, e.g.  $(\text{Pr}/\text{Nd})_2\text{NiO}_{4+\delta}$ . [1-4]. This new concept has technological relevance for the optimization of oxygen membranes and electrolytes in SOFCs.

We report here on single-crystal synchrotron diffraction experiments on non-stoichiometric  $\text{Pr}_2\text{NiO}_{4+\delta}$ , uncovering unprecedented oxygen ordering up to the sub meso-scale. Complex oxygen ordering is established during a topotactic solid-state reaction already proceeding at ambient temperature, following small oxygen release. The resulting 3D-incommensurate modulated structure is described in terms of modulation vectors and related twin domain structures. Melting of the oxygen ordering around 365°C strongly amplifies the oxygen mobility, evidenced by  $^{18}\text{O}/^{16}\text{O}$  oxygen isotope exchange, and associated with phonon softening manifested in a pronounced increase of thermal diffuse scattering. Our results thus strengthen the idea of a phonon assisted oxygen diffusion mechanism, which can be more generally applied to understand cooperative diffusion mechanisms.

[1] Paulus, W., et al., J. Am. Chem. Soc, 2008. 130(47): p. 16080-16085.

[2] Perrichon, A., et al., J. Phys. Chem. C, 2015. 119(3): p. 1557-1564.

[3] M. Ceretti et al. J. Mater. Chem. A, 3, 42 (2015) p21140-48.

[4] M. Ceretti et al., InorganicChemistry, 2018, 57 (8), pp.4657-4666.

## MS27-05 | PHASE TRANSITIONS IN ZR-RICH LEAD ZIRCONATE-TITANATE STUDIED BY SINGLE CRYSTAL DIFFUSE AND INELASTIC X-RAY SCATTERING

Andronikova, Daria (Ioffe Institute, St. Petersburg, RUS); Bronwald, Iurii (Peter the Great St. Petersburg Polytechnic University, St. Petersburg, RUS); Bosak, Alexei (European Synchrotron Radiation Facility, Grenoble, FRA); Chernyshov, Dmitry (Swiss-Norwegian Beam Lines at the European Synchrotron Radiation Facility, Grenoble, FRA); Filimonov, Alexey (Peter the Great St. Petersburg Polytechnic University, St. Petersburg, RUS); Vakhrushev, Sergey (Ioffe Institute, St. Petersburg, RUS)

Lead zirconate-titanate ( $\text{PbZr}_{1-x}\text{Ti}_x\text{O}_3$ , PZT) is a piezoelectric perovskite material, which possesses ferroelectric as well as antiferroelectric properties. Thanks to high piezoelectric coefficient PZT is broadly used in many electronic devices [1].

For PZT with  $0 < x < 0.06$  antiferroelectric phase is stable at room temperature. This phase has an orthorhombic structure resulting from antiparallel displacements of lead ions and opposite rotations of  $\text{ZrO}_6$  octahedra for the neighboring layers of paraelectric cubic perovskite structure [2]. Thus, phase transition into the antiferroelectric phase is associated with condensation of two phonon modes with different symmetry. In paraelectric phase dielectric measurements [3] revealed critical divergence of dielectric constant, which could be associated with ferroelectric mode instability in Brillouin zone center. There is ferroelectric intermediate phase in-between the antiferroelectric and paraelectric phases. Electron diffraction indicates that the intermediate phase has incommensurate modulated structure [4], however, the symmetry of this phase is still not well understood.

To study microscopic mechanism resulting in PZT phase transitions the measurements of single crystal diffuse and inelastic X-ray scattering in PZT with  $0.007 < x < 0.04$  have been performed. In the present contribution, the relevant critical dynamics accompanying phase transitions in Zr-rich PZT will be discussed using obtained results.

Andronikova D. acknowledges support by Russian President Grants No. SP-3762.2018.5

[1] Haertling G. H. JACS, 82, 4, 1999

[2] Fujishita H. et.al., JPSJ, 53,1 1984

[3] Roleder K. et.al. Phase Transitions, 71, 287, 2000

[4] Watanabe S. et.al. PRB, 66, 2002

## MS27-P01 | STRUCTURAL AND PHYSICAL PROPERTIES OF A 2,2';6',2''-TERPYRIDINE DERIVATIVE IN THE SOLID STATE PHASE TRANSITION BEHAVIOR

Chen, Yan-An (Department of Molecular Science and Engineering, National Taipei University of Technology, Taipei, TWN); Yang, Chia-Wei (Department of Molecular Science and Engineering, National Taipei University of Technology, Taipei, TWN); Chen, Bo-Hao (National Synchrotron Radiation Research Center, Hsinchu, TWN); Chuang, Yu-Chun (National Synchrotron Radiation Research Center, Hsinchu, TWN); Lee, Jey-Jau (National Synchrotron Radiation Research Center, Hsinchu, TWN); Wen, Yuh-Sheng (Institute of Chemistry, Academia Sinica, Taipei, TWN); Hsu, I-Jui (Department of Molecular Science and Engineering, National Taipei University of Technology, Taipei, TWN)

Materials with solid-solid phase transition characters have attracted intensive attentions due to their potential applications in data storage, sensing, and signal processing. In this work, the solid to solid phase transitions of 4'-(2-Furyl)-2,2':6',2''-terpyridine (ftpy) was characterized by variable temperature of powder x-ray diffractions (PXRD) and differential scanning calorimetry (DSC). Two different polymorphs of  $\alpha$ -ftpy and  $\beta$ -ftpy were obtained by different synthetic strategies. The colorless single crystal of  $\alpha$ -ftpy is crystallized in P  $2_1/c$  space group with cell constants  $a = 10.395(1) \text{ \AA}$ ,  $b = 13.195(1) \text{ \AA}$ ,  $c = 11.376(1) \text{ \AA}$ , and  $\beta = 105.457(3)^\circ$ , but the celadon powder of  $\beta$ -ftpy is crystallized in P  $2_1/n$  space group with cell constants  $a = 10.6142(1) \text{ \AA}$ ,  $b = 35.4639(2) \text{ \AA}$ ,  $c = 3.8687(4) \text{ \AA}$ , and  $\beta = 91.671(2)^\circ$ . The structure of  $\beta$ -ftpy is determined by simulated annealing algorithm in real space. In comparison with packing structures of both polymorphs, the shortest  $\pi$ - $\pi$  interaction distances are  $\sim 3.9 \text{ \AA}$  and  $\sim 3.3 \text{ \AA}$  for  $\alpha$ -ftpy and  $\beta$ -ftpy, respectively. A DSC study of powder  $\beta$ -ftpy shows that an endothermic event occurs at  $\sim 148.6 \text{ }^\circ\text{C}$ . The variable-temperature PXRD studies of  $\beta$ -ftpy indicate that  $\alpha$ -ftpy appears at  $\sim 398 \text{ K}$ , and the phase transform is complete at  $\sim 408 \text{ K}$ . However, the  $\alpha$ -ftpy cannot transform back to  $\beta$ -ftpy by further cooling experiments. In the study of luminescence characters of both polymorphs at solid state, both display the maximum intensity of emission peak at 403nm with absolute quantum yield 4.9% and 3.8% for  $\alpha$ -ftpy and  $\beta$ -ftpy, respectively.

## MS27-P02 | NEW RADIATION-INDUCED PHASE OF MAPbI<sub>3</sub> - AN UNEXPECTED SURPRISE OF SYNCHROTRON EXPERIMENTS.

Minns, Jake (University of Kent at Canterbury, Canterbury, GBR)

The last decade of photovoltaic research has been dominated by the rise of organic-inorganic hybrid perovskites (OHPs). Of all OHP variants MAPbI<sub>3</sub> has received the most attention from the photovoltaic community, this compound is composed of an organic cation, methylammonium (MA), within a post transition metal halide framework, lead iodide. These materials promise low-cost solution-processing with power conversion efficiencies approaching that of single-crystalline silicon devices at 23.7%. In spite of this OHP devices are yet to be proven commercially viable, this is in large part due to the chemical instability of the material under ambient conditions. This instability has been attributed to the volatile nature of the organic cation, uptake of H<sub>2</sub>O, and formation of I<sub>2</sub>.

One of the ways to improve the stability is to look for a more stable polymorphic modification that would retain the same photovoltaic properties. Single-crystal and powder synchrotron diffraction studies reveal a radiation-induced phase not reported before. Surprisingly though, a new phase was observed to emerge from the diffuse scattering after prolonged exposure to the synchrotron beam, the development of this phase appears to be correlated with the intrinsic diffuse scattering present in MAPbI<sub>3</sub>. This new phase has since been stabilized through post synthesis treatment of MAPbI<sub>3</sub>. Our observations show that X-ray radiation may be also considered as one more tool to engineer functional photovoltaic perovskites.

## MS27-P03 | LOCAL ORDER IN CO AND MN PRUSSIAN BLUE ANALOGUES, THE 3D- $\Delta$ PDF

### ANALYSIS.

Simonov, Arkadiy (ETH Zurich, Zürich, CH); Boström, Hanna (Uppsala University, Uppsala, SWE); Goodwin, Andrew (University of Oxford, Oxford, GBR)

Prussian Blue Analogues is a family of materials with the general formula  $M'[M''(\text{CN})_6]_{1-x} \cdot \text{H}_2\text{O}$  where  $M'$  and  $M''$  are transition metals. These materials are currently actively investigated due to their interesting stimuli-dependent magnetic, electronic and optical properties.

These materials are disordered, since in order to achieve the charge balance, the site containing the hexacyanometallate group  $[M''(\text{CN})_6]$  is partially vacant. This disorder is important for physical properties, since it defines the internal flexibility of the structure. Up until now, only qualitative models of disorder were proposed [1-2].

In this work we will present the quantitative investigation of local correlations between the vacancies in single crystals of two members of the Prussian blue analogue family:  $\text{Mn}[\text{Co}(\text{CN})_6]_{2/3} \cdot \text{H}_2\text{O}$  and  $\text{Co}[\text{Co}(\text{CN})_6]_{2/3} \cdot \text{H}_2\text{O}$ . The crystals show a very similar ordering pattern on the  $[M''(\text{CN})_6]$  groups and vacancies, however the manganese version contains additional diffuse scattering features which are associated with the correlated displacements of the  $[M''(\text{CN})_6]$  columns.

[1] Bhatt, P., Thakur, N., Mukadam, M.D., Meena, S.S. and Yusuf, S.M. (2013), *J. Phys. Chem. C*, 117(6), 2676-2687

[2] Chernyshov, D. and Bosak, A. (2010), *Phase. Trans.*, 83(2), 115-122

## MS27-P04 | ENDOHEDRAL METALLOFULLERENE CRYSTALS: PLAYING WITH DISORDERS

Liu, Fupin (IFW-Dresden, Dresden, GER); Popov, Alexey A. (IFW-Dresden, Dresden, GER)

Endohedral metallofullerenes (EMFs) are fullerenes encapsulating metal ions or clusters [1]. These molecules are interesting for their characteristic structures and potential applications in the fields of energy conversion, biomedicine, and molecular magnets. One of the great challenges for studying these molecules is the structural elucidation. Because of the round shape of the molecule, crystals of EMF frequently suffered severe disorder. Co-crystallization with structural complementary molecules such as nickel octaethylporphyrin could reduce the disorder [2,3,4], otherwise, functionalizing the fullerene cages with functional groups may also reduce the disorder by restraining the rotation of the fullerenes in the crystal lattice [5]. The dynamics of the encapsulated species is a very interesting topic when we froze the movement of the fullerene cage. Recently, we observed the movement of the two encapsulated Dy ions in  $C_{80}$  fullerene cage via variable temperature X-ray diffraction studies [6]. In this contribution, the disorder problem frequently encountered in EMF crystals as well as the successful observation of the movement of encapsulated two Dy ions will be discussed.

1. A. A. Popov et al., Chem. Rev. 2013, 113, 5989-6113.
2. F. Liu et al., J. Am. Chem. Soc. 2016, 138, 14764-14771.
3. F. Liu et al., Angew. Chem. 2017, 129, 1856-1860.
4. D. S. Krylov et al., Phys. Chem. Chem. Phys. 2018, 20, 11656-11672.
5. F. Liu et al., Nat. Commun. 2017, 8, 16098.
6. F. Liu et al., Nat. Commun. 2019, 10, 571.

## MS27-P05 | CORRELATION OF HIGH-RESOLUTION X-RAY DIFFRACTION WITH MECHANICAL EXPERIMENTS AND FINITE ELEMENT ANALYSIS

Dommann, Alex (Empa, St. Gallen, CH); Neels, Antonia (Empa, Dübendorf, CH); Schifferle, Andreas (Helbling Technik AG, Aarau, CH)

A concept for the investigation of mechanically loaded MEMS materials on an atomic level is introduced combining high-resolution X-ray diffraction (HRXRD) measurements with finite element analysis (FEA) and mechanical testing. In situ HRXRD measurements were performed on tensile loaded single crystal silicon (SCSi) specimens by means of profile scans and reciprocal space mapping (RSM) on symmetrical (004) and (440) reflections. A comprehensive evaluation of the rather complex X-ray diffraction and scattering features was enabled by the correlation of measured with simulated, 'theoretical', patterns. These simulated patterns were calculated by a specifically developed simple and fast approach based on continuum mechanical considerations [1]. Qualitative and quantitative analysis confirmed the admissibility and accuracy of the presented method. In this context, the [001] Poisson's ratio was determined providing an error of less than 1.5% with respect to the analytical prediction [2].

Consequently, the introduced procedure contributes to further going research of weak scattering being related to strain and defects in crystalline structures and therefore supports investigations on materials and devices failure mechanisms.

[1] "Where is the limit? Yield strength improvement in silicon micro-structures by surface treatments" A. Schifferle, T. Bandi, A. Neels, A. Dommann, *Phys. Status Solidi A* 213, 2016, 102–107.

[2] "In situ MEMS testing: correlation of high-resolution X-ray diffraction with mechanical experiments and finite element analysis" A. Schifferle, A. Dommann, A. Neels, *Science and Technology of Advanced Materials* (2017) 18(1), 219–230.

## MS27-P06 | THE BENEFITS OF CU-K<sub>β</sub> RADIATION IN ELUCIDATING THE MOLECULAR STRUCTURE OF POLYPNICTOGEN CATIONS

Riesinger, Christoph (University of Regensburg, Regensburg, GER); Duetsch, Luis (University of Regensburg, Regensburg, GER); Bodensteiner, Michael (University of Regensburg, Regensburg, GER); Scheer, Prof. Dr. Manfred (University of Regensburg, Regensburg, GER)

Cationic polypnictogen frameworks, which are not completely saturated with organic substituents, are a relatively rare class of compounds, with metal fragment stabilised  $[P_{10}]^{2+}$ , [1]  $[E_4]^{2+}$  (E = Pnictogen) [2] and the homoleptic  $[P_9]^+$  being some of the most prominent representatives [3]. In depth crystallographic studies of compounds containing such species are often hampered by the presence of so called WCAs (WCA = weakly coordinating anion) which are needed for their stabilisation. One of the least coordinating, yet crystallographically often problematic WCAs is the  $[TEF]^-$  anion ( $[TEF]^- = [Al(OC(CF_3)_3)_4]^-$ ). Its sphere-like topology can lead to very high degrees of disorder within the Perfluorptertbutyl – groups which often cannot be resolved properly by using standard wavelengths. Compared to Cu-K<sub>α</sub> radiation, Cu-K<sub>β</sub> radiation has the advantage of a better resolution limit (0.72 Å), while still allowing for relatively high intensity measurements compared to Mo-K<sub>α</sub> radiation. Thus, utilisation of Cu-K<sub>β</sub> radiation is beneficial for the X-ray crystallographic investigation and allows a better structural solution of compounds containing highly disordered WCAs such as  $[TEF]^-$ . This will be demonstrated by a comparison of X-ray crystallographic data of compounds of the general formulae  $[Cp''Ni(\eta^3-P_4R_2)][TEF]$  obtained by using Cu-K<sub>α</sub>, Cu-K<sub>β</sub> and Mo-K<sub>α</sub> radiation.

[1] M. V. Butovskiy, G. Balazs, M. Bodensteiner, E. V. Peresykina, A. V. Virovets, J. Sutter and M. Scheer, *Angew. Chem. Int. Ed.* 2013, 52, 2972 – 2976.

[2] L. Dütsch, M. Fleischmann, S. Welsch, G. Balazs, W. Kremer, and M. Scheer, *Angew. Chem. Int. Ed.* 2018, 57, 3256 – 3261.

[3] T. Köchner, T. A. Engesser, H. Scherer, D. A. Plattner, A. Steffani, and I. Krossing, *Angew. Chem. Int. Ed.* 2012, 51, 6529 – 6531.

## MS27-P07 | UNIQUE PROPERTIES OF GEOINSPIRED NANOTUBES AS WATER NANOCONTAINER

MONET, Geoffrey (Université Paris Saclay, Orsay, FRA); CHAI, Ziwei (Beijing Computational Science Research Centre, Beijing, CHN); PAINEAU, Erwan (CNRS, Orsay, FRA); LIU, Li-Min (Beijing Computational Science Research Centre, Beijing, CHN); TEOBALDI, Gilberto (Daresbury laboratory, Daresbury, GBR); ROLS, Stéphane (Institut Laue-Langevin, Grenoble, FRA); LAUNOIS, Pascale (CNRS, Orsay, FRA)

Clay-like imogolite nanotubes (INT) are ideal platforms for studying the novel properties of confined molecules. Compared to the well-known carbon nanotubes (CNT), they own well defined diameter. Moreover, the molecular affinity of their inner cavity is tunable. Such properties confer to these tubular structures a wide range of potential applications, from filtration to depollution of water.

X-ray and inelastic neutron scattering techniques are used here, in combination with simulations, to investigate structural and dynamical properties at the nanoscale. We performed inelastic neutron scattering (INS) experiments to study hydrated geo-inspired alumino-germanate imogolite nanotubes (Ge-INT) [1], whose structure is first determined thanks to X-ray scattering [1,2]. INS experiments coupled to ab-initio molecular dynamics simulations reveal a unique structure of the water layer adsorbed inside Ge-INT. To the best of our knowledge, it differs from that of any kind of two-dimensional water. We show that the dynamics of INT and water are strongly interrelated, so that hydrated Ge-INT can be considered as a different system from dry Ge-INT. A well-defined translation vibrational mode of water molecules with respect to the nanotube wall is also observed. Finally, the evolution of mean square displacements of water molecules as a function of temperature is found to differ markedly in Ge-INT and in CNT, in which water slips without friction, which is attributed to the peculiar bonding of water molecules with germanol groups.

[1] G. Monet et al., in preparation

[2] G. Monet et al., Nature Comm., 9, 2033 (2018)

## MS27-P110 - LATE | TOWARDS PHASE TRANSITION IN COCRYSTALS OF ALLYLAMINE WITH ALIPHATIC ALCOHOLS

Nowosielska, Bernadeta (University of Warsaw, Faculty of Chemistry, Czocharlski Advanced Crystal Engineering Laboratory, Warsaw, POL); Cyranski, Michal (University of Warsaw, Faculty of Chemistry, Czocharlski Advanced Crystal Engineering Laboratory, Warsaw, POL); Boese, Roland (University of Warsaw, Faculty of Chemistry, Czocharlski Advanced Crystal Engineering Laboratory, Warsaw, POL); Dobrzycki, Lukasz (University of Warsaw, Faculty of Chemistry, Czocharlski Advanced Crystal Engineering Laboratory, Warsaw, POL)

Alcohols and amines can be considered as excellent cocrystal forming agents. This is due to compatibility of the intermolecular interactions where both compounds can act as hydrogen bond donor and/or acceptor. In such structures different energy-efficient structural motifs as isolated oligomers (0D), ribbons (1D), layers (2D) etc. can be expected. The aim of the research was to investigate cocrystallization of allylamine with selected aliphatic alcohols (methanol, ethanol, 1-propanol, 2-propanol, cyclobutanol, 1-butanol, *tert*-butanol), analyze structural motifs and check dynamic of the molecules in the obtained systems. The examined mixtures are liquid at ambient conditions, therefore, a laser-assisted *in situ* crystallization method directly on the goniometer of the single crystal diffractometer was used [1].

Among obtained cocrystals those with methanol, ethanol and 1-propanol contain molecules arranged in layers with L4(4)8(8) motif [2] of hydrogen bonds. In systems with other alcohols formation of 1D ribbons of hydrogen-bonded molecules are observed. Change of the crystal architecture can be attributed to the larger size of aliphatic group of the alcohols acting as a steric hindrance what is clearly visible in disordered structure with *tert*-butanol. Here a discrepancy between the size of cocrystal components lead to reversible order-disorder phase transition at lower temperatures with fragmentation of hydrogen bond chains, turning crystal architecture to 0D.

The research was supported by the National Science Center in Poland (Grant SONATA BIS 6 NCN, 2016/22/E/ST4/00461).

[1] R. Boese, *Z. Kristallogr.*, **2014**, 229, 595-601.

[2] L. Infantes, S. Motherwell, *CrystEngComm*, **2002**, 4, 454-461.

## MS28: Dynamics and Disorder Probed by Diffuse Scattering

---

### MS28-01 | CHALLENGES IN MEASUREMENT AND INTERPRETATION OF SCATTERING FROM PROTEIN CRYSTALS

Meisburger, Steve (Cornell University, Ithaca, USA); Case, David (Rutgers University, Piscataway, USA); Ando, Nozomi (Cornell University, Ithaca, USA)

The collective motions of proteins are important for function, yet these motions are a challenge to observe experimentally. Intriguingly, when such motions occur in protein crystals, they leave distinctive fingerprints in the scattering between the Bragg peaks. The nascent field of "crystallography beyond Bragg" aims to extract information of biological relevance from this diffuse signal. However, both measurement and interpretation have been challenging. In this talk, I will discuss these challenges and our recent findings on the total scattering from proteins crystals.

## MS28-02 | BEYOND THE AVERAGE BRAGG STRUCTURE - DYNAMICS, DISORDER AND DIFFUSE SCATTERING

Bürgi, Hans-Beat (Universities of Zürich and Bern, Zürich, CH)

No real crystal shows the periodicity and symmetry implied by its space group. The deviations from this idealized model are static and dynamic. The former encompass atomic positional and substitutional disorder, either in the body or near the surfaces of the mosaic blocks or in both; they cause disorder diffuse scattering below and between the Bragg reflections. Dynamic disorder is due to the omnipresent atomic vibrations and causes the temperature dependent thermal diffuse scattering (TDS). Intensities of diffuse scattering depend on the degree of deviations from symmetry and are generally weaker than Bragg intensities because they are smeared out over the whole of reciprocal space. Multiple atomic positions, occupation factors and atomic displacement parameters derived from Bragg diffraction represent averages over the entire crystals and the time of the diffraction experiment. Diffuse scattering contains information on local structure. Powder diffraction-type, 1D data are interpreted from 1D Pair Distribution Functions (PDFs), single crystal diffuse scattering from 3D PDFs which are related to the Patterson function of a disordered crystal. Alternatively, 3D diffuse scattering is modeled with Monte Carlo-type (MC) models of local order. Examples will show how to distinguish static and dynamic disorder from temperature dependent Bragg experiments, how to develop local pictures of occupational disorder from 3D PDFs and how to characterize local structural deformations with MC models. The examples will also delineate the large uncharted territory in the area of crystal dynamics, disorder and diffuse scattering.

## MS28-03 | A DISORDERED SUPERSPACE APPROACH TO UNDERSTAND HIGHLY STRUCTURED DIFFUSE SCATTERING

Schmidt, Ella Mara (Friedrich-Alexander-Universität Erlangen-Nürnberg, Erlangen, GER); Neder, Reinhard B. (Friedrich-Alexander-Universität Erlangen-Nürnberg, Erlangen, GER)

Single crystal diffuse scattering is generally interpreted using correlation parameters, that describe probabilities for certain configurations on a local scale. If the diffuse maxima are at a general position in reciprocal space many parameters are needed to simulate a short range ordered structure in direct space, which reproduces the observed diffuse maxima.

In the field of incommensurate crystallography a (3+d)-dimensional approach is taken to describe satellite reflections in reciprocal space, that cannot be indexed with integer (h,k,l) . A 3-dimensional aperiodic crystal structure is periodic in (3+d)-dimensional superspace and the atomic positions and/or occupancies of the 3D structure are described by modulation functions.

A perfectly periodic superspace gives rise to sharp satellite reflections. In order to describe broadend satellite reflections we introduce disorder into superspace. By introducing phase domains in the superspace structure we can generate structures that give rise to diffuse maxima at any position in reciprocal space with an arbitrary width [1]. The disordered superspace approach also allows for a straight forward simulation of a disordered structure using only few parameters.

The compound ThAsSe shows highly structured diffuse planes at  $\mathbf{G} \pm 0.14 \langle 110 \rangle^* \pm \epsilon \langle 110 \rangle^* \pm \eta [001]^*$  with  $\epsilon$  and  $\eta$  essentially continuous [2]. The observed extinction conditions and the sharp diffuse rods can be interpreted directly using the disordered superspace approach. The diffuse planes in reciprocal are reproduced from a computational model crystal that was build using the disordered superspace approach.

[1] Schmidt, E.M. and Neder, R.B. submitted.

[2] Withers, R.L. et al. Solid State Chemistry, 177 (2004) 701-708.

## MS28-04 | THE SECRET LIFE OF MOFs' FUNCTIONAL GROUPS: SHOULD WE TRUST RANDOM DISORDER?

Canossa, Stefano (Delft University of Technology, Delft); Gonzalez Nelson, Adrian (Delft University of Technology, Delft); Rega, Davide (Delft University of Technology, Delft); van der Veen, Monique (Delft University of Technology, Delft); Bürgi, Hans-Beat (Universität Bern, Bern, CH); Pei, Xiaokun (UC Berkeley, Berkeley, USA); Yaghi, Omar (UC Berkeley, Berkeley, USA)

The practice of endowing metal–organic frameworks (MOFs) with novel functionalities by adding chemical groups to their backbone is one of the key strategies to achieve better performances [1]. One of the simplest approaches in this regard is to employ functionalised ligands (*linkers*) in the final coordination network [2]. Since the functional groups often decrease the linkers' symmetry without affecting the framework connectivity, they usually occupy alternative positions with similar energy minima and thus occupancy values. Importantly, the assumption of their random distribution should be considered a misguided approximation as it excludes any relevant interaction between adjacent groups or with the framework itself. In this context we present the case studies of ZIF-90 [3] and NO<sub>2</sub>-MIL-53(Al) [4], whose linker disorder revealed to be strongly correlated or even crystallographic order upon symmetry breaking. Total scattering single crystal XRD analysis afforded corrected structural models showing important differences from the random disorder-based ones with consequences on relevant features such as pores opening, presence of dipole moments and availability of metal sites. These findings highlight the importance of local order of framework components in functionalised MOFs and the possible risks of trusting random disorder models.

[1] H. Furukawa et al., *Science*, 2013, **341**, 1–12.

[2] W. Lu et al., *Chem Soc Rev*, 2014, **43**, 5561–5593.

[3] O. M. Yaghi et al., *J. Am. Chem. Soc.*, 2008, **130**, 12626–12627.

[4] G. Férey et al., *Chem. Commun.*, 2003, **0**, 2976–2977.

## MS28-05 | UNRAVELING LOCAL CORRELATIONS IN HEAVILY DISORDERED FERROELECTRIC

### $\text{Sr}_x\text{Ba}_{1-x}\text{Nb}_2\text{O}_6$

Pasciak, Marek (Institute of Physics of the Czech Academy of Sciences, Prague, CZE); Ondrejko, Petr (Institute of Physics of the Czech Academy of Sciences, Prague, CZE); Welberry, Richard (Research School of Chemistry, Australian National University, Canberra, AUS); Kulda, Jiri (Institut Laue-Langevin, Grenoble, FRA); Kopecky, Milos (Institute of Physics of the Czech Academy of Sciences, Prague, CZE); Kub, Jiri (Institute of Physics of the Czech Academy of Sciences, Prague, CZE); Buixaderas, Elena (Institute of Physics of the Czech Academy of Sciences, Prague, CZE); Hlinka, Jiri (Institute of Physics of the Czech Academy of Sciences, Prague, CZE)

When it comes to structural complexity,  $\text{Sr}_x\text{Ba}_{1-x}\text{Nb}_2\text{O}_6$  has it all. There is occupational disorder of Sr and Ba cations with additional vacant positions in the unfilled tetragonal tungsten bronze structure. Dynamical chains of relative Nb-O<sub>6</sub> displacements are present at high temperatures and gain transverse correlation when going through the ferroelectric phase transition to form domains. Whether the transition is 'normal' or 'diffuse' depends on the Sr content with the latter appearing for  $x \geq 0.6$ . On top of that there is an incommensurate modulation which mainly involves rotations of oxygen octahedra; their amplitude being again dependent on the Sr/Ba ratio. This abundance of local disruptions to the long range order is reflected in the reciprocal space being very richly populated with diffuse scattering.

In this work we combine neutron pair distribution function [1] and X-ray diffuse scattering analysis [2] – both for the range of concentrations and temperatures – with multi-scale simulations. First-principles molecular dynamics is used for the understanding of the structure and its dynamics at short distances and provides a basis for atomistic model development. This in turn is instrumental in 3D diffuse scattering analysis. All this information allows us to explore the interrelation between the mentioned local-structure modes and their contribution to the diffuse transition characterized by large dielectric susceptibility over a broad range of temperatures.

[1] M. Paściak et al., *Phys. Rev. B* **99**, 104102 (2019).

[2] M. Paściak et al., *Phase Transitions* **91**, 969 (2018).

## MS28-P01 | SOLVING THE DISORDERED STRUCTURE OF BETA-CU<sub>2</sub>SE USING THE THREE-DIMENSIONAL DIFFERENCE PAIR DISTRIBUTION FUNCTION

Roth, Nikolaj (Center for Materials Crystallography, Department of Chemistry, Aarhus University, Aarhus, DNK)

High-performing thermoelectric materials such as Zn<sub>4</sub>Sb<sub>3</sub> and clathrates have atomic disorder as the root to their favorable properties. Cu<sub>2-x</sub>Se is an intensely studied, cheap and non-toxic high performance thermoelectric material with highly peculiar transport properties, which must be related to the crystal structure. Attempts to solve the crystal structure of the room temperature phase, β-Cu<sub>2-x</sub>Se, have been unsuccessful since 1936. So far, all studies have assumed that β-Cu<sub>2-x</sub>Se has a three-dimensional periodic structure, but here we show that the structure is ordered only in two dimensions while it is disordered in the third dimension with a near random stacking sequence. Using the three-dimensional difference pair distribution function (3D-ΔPDF) method for diffuse single crystal X-ray scattering, we solve the structure of the two-dimensional ordered layer and show that there are two modes of stacking disorder present, which give rise to an average structure with higher symmetry. The present approach allows for a direct solution of structures with disorder in some dimensions and order in others, and can be thought of as a generalization of the crystallographic Patterson method. The 3D-ΔPDF gives an intuitive method for structural solution of disordered systems without the need for reverse Monte-Carlo simulations or energy minimization calculations. The local and extended structure of a solid determines its properties and Cu<sub>2-x</sub>Se represents an example of a high-performing thermoelectric material where the local atomic structure differs significantly from the average periodic structure observed from Bragg crystallography.

## MS28-P02 | LOCAL DIPOLE FORMATION IN IV-VI SEMICONDUCTORS

Holm, Kristoffer (Aarhus University, Aarhus C, DNK); Roth, Nikolaj (Aarhus University, Aarhus C, DNK); Brummerstedt Iversen, Bo (Aarhus University, Aarhus, DNK)

IV-VI semiconductors exhibit a wide range of useful physical properties leading to applications as e.g. thermoelectric materials, optoelectronic materials, and much more. In the present work, the correlated local dipole formation of IV-VI semiconductors is investigated using both qualitative 3D- $\Delta$ PDF analysis and quantitative local structure refinements against the diffuse scattering intensities. Such analysis allows for a deeper understanding of these local order phenomena, which are considered to be highly correlated with the physical properties of the materials.

## MS28-P03 - CANCELLED | UNDERSTANDING STRUCTURAL DISORDER IN NICKEL CYANIDE USING 1D STATISTICAL MECHANICAL MODELS

Wolpert, Emma (University of Oxford, Oxford, GBR); Simonov, Arkadiy (University of Oxford, Oxford, GBR); Goodwin, Andrew (University of Oxford, Oxford, GBR)

1D statistical mechanical models have been used to understand materials behaviour in condensed matter physics. Naturally much of the focus so far has been on electronic and magnetic behaviour. Yet, it has long been known that the 1D Ising model is also relevant to the structural behaviour of some surprisingly simple bulk phases [1,2]. In our work, we look at extending the relevance of 1D statistical mechanical models and structural behaviour by looking at the case of structural disorder in the layered inorganic solid  $\text{Ni}(\text{CN})_2$ . Using Monte Carlo simulations we explore the interactions between neighbouring layers using two different 1D statistical mechanical models: the 1D Ising model, and a 1D chain of interacting quaternions. Through X-ray powder diffraction patterns [3], we show that the continuous degrees of freedom of the latter model reproduces the key diffuse features of the experimental pattern remarkably well in a way the discrete Ising model cannot. Thus, we show that the energy of the local interaction between neighbouring layers can be related to that of a 1D chain of interacting quaternions. Using this model, we are able to relate the behaviour of  $\text{Ni}(\text{CN})_2$  layers to a spin  $\frac{1}{2}$  chain that interacts via the Heisenberg XXZ model.

[1] S. Ramasesha and C. N. R. Rao, *Philos. Mag.* **34** (1977), 827-833.

[2] M. K. Uppal, S. Ramasesha and C. N. R. Rao. *Acta Cryst. A* **36** (1980), 356-361.

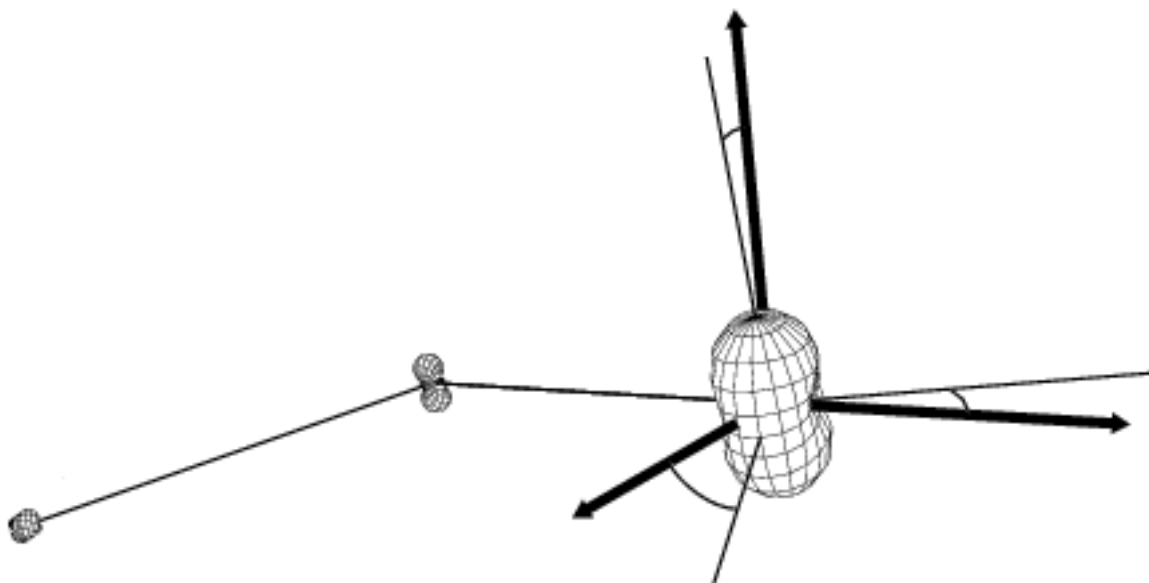
[3] S. J. Hibble *et al.*, *Angew. Them. Int. Ed.*, **46**, 7116-7118 (2007)

## MS29: Accurate Treatment of Hydrogen Atoms

---

### MS29-01 | MODELLING OF HYDROGEN ATOMS IN CRYSTALLOGRAPHY – AN OVERVIEW

Madsen, Anders Østergaard (University of Copenhagen, Copenhagen, DNK)



Hydrogen is the most abundant element in the universe, and - because of the role of water - the most abundant element in living matter. Most organic molecules have a skin of - often labile - hydrogen atoms which thereby facilitate the interactions between molecules, as well as determine properties like charge and pH.

Because of its light mass, its polarizability and the fact that only one electron is associated to the atom, it is a difficult atom to model, seen with a crystallographer's eyes. Yet there are more than a million crystal structures containing hydrogen in the structural databases.

I will present an overview of how crystallographers have modeled hydrogen atoms historically, but will especially put focus on the state of the art - and try to sketch what is appearing in the horizon.

## MS29-02 | INFLUENCE OF A HYDROGEN BOND ON OPTICAL PROPERTIES OF MATERIALS

Krawczuk, Anna (Jagiellonian University, Faculty of Chemistry, Cracow, POL)

The correlation between the crystal structure and physical properties of a given material has long been a subject of many studies. One of the key features of designing efficient multifunctional materials is to use specific building blocks and/or synthons in order to increase a desired effect in a certain crystallographic direction. For example, to obtain efficient optical devices it is necessary to use highly polarizable functional groups which will form strong hydrogen bonds and promote high optical effect, e.g. high refractive index. It is thus crucial to get a precise information on the influence of hydrogen bonds on the group polarizabilities which in turn should give an answer which hydrogen bonds will mostly contribute to the physical effect. This in turn could be very helpful for the crystal engineering purpose when designing new optically effective materials.

## MS29-03 | STRUCTURE SPECIFIC RESTRAINTS FOR LEAST-SQUARES REFINEMENT FROM TIGHT BINDING QUANTUM CHEMISTRY

Dittrich, Birger (Novartis Pharma, Basel, CH); Müller, Peter (MIT Department of Chemistry, Cambridge, USA)

Disordered crystal structures [1] can cause problems in a statistical post analysis as performed as part of solid-form selection in the pharmaceutical industry [2]. Underlying challenges posed by disorder are inaccurate atomic positions in a crystal structure. Their determination is especially difficult when atoms with disordered split sites are closer to each other than the resolution of a single-crystal diffraction experiment. While non-hydrogen atom positions can usually be resolved, the situation is even more difficult for hydrogen-atom positions due to their scattering power [3], especially when these are rotationally disordered. This asks for a “quantum-chemical aide” [4]. We have therefore extended the functionality of the program Baerlauch [5] to read/write input/output files of the dispersion-corrected tight-binding program XTB [6]. The output of Baerlauch cluster computations then (among other results) provides bond distance and bond angle restraints for use in classical independent-atom model refinements e.g. with SHELXL. Results of this generally applicable workflow to optimize crystal structures (or only their hydrogen atoms) are presented.

[1] Müller, P., et al. (2006). *Crystal Structure Refinement: A Crystallographer’s Guide to SHELXL*. New York, Oxford University Press.

[2] Galek, P. T. A., et al. (2009). *CrystEngComm* 11(12): 2634.

[3] Dittrich, B., et al. (2017). *Chem. Eur. J.* 23, 4605-4614.

[4] Deringer, V. L., et al. (2012). *Cryst. Growth Des.* 12: 1014-1021.

[5] Dittrich, B., et al. (2012). *Acta Cryst. A* 68: 110-116.

[6] Grimme, S., et al. (2017). *J Chem Theory Comput* 13(5): 1989-2009.

We acknowledge helpful discussions with A. Udvarhelyi and T. Wager

## MS29-04 | HYDROGEN POSITIONS IN SMALL ORGANIC MOLECULES DETERMINED BY 3D ELECTRON DIFFRACTION

Lightowler, Molly (Stockholm University, Stockholm, SWE)

Understanding the distribution of hydrogen atoms is an essential part of any crystal structure analysis. However, the localization of hydrogen atoms is often hindered by their small scattering power. The vast majority of structures are identified through X-ray crystallography, yet this technique is limited to micrometre-sized crystals and since X-rays only interact weakly with matter, acquiring a strong-enough signal to unveil fine structural details, such as hydrogen positions, is often impossible. 3D electron diffraction has shown to be powerful in structure determination of nano- and micron-sized organic crystals. Hydrogen positions in nanocrystals could be revealed as a result of the stronger interaction of electrons with matter and the use of dynamical refinement. We report the structures and direct localization of hydrogen atoms in nanocrystalline, small organic molecules, using 3D electron diffraction and only kinematic approximation. Hydrogen positions were found in structures from three individual molecules ( $\beta$ -glycine, sucrose and ABTC). Every hydrogen position was determined within the structure of  $\beta$ -glycine, whilst only certain hydrogen positions were found in sucrose and ABTC. The results demonstrate that the ability to locate hydrogens depends upon their environment within the structure. The flexible hydrogens, with varying positions averaging out over the crystal, cannot be determined, whilst the rigid hydrogens, e.g. those that are hydrogen bonded or aryl hydrogens, are easier to locate. The results demonstrate that 3D electron diffraction can achieve determination of fine structural details from single crystals of small organic molecules with nanosized dimensions.

## MS29-05 | ANISOTROPIC HYDROGEN ATOMS IN CHARGE DENSITY ANALYSIS

Herbst-Irmer, Regine (Universität Göttingen, Göttingen, GER); Köhler, Christian (Universität Göttingen, Göttingen, GER); Lübben, Jens (Universität Göttingen, Göttingen, GER); Krause, Lennard (Aarhus University, Aarhus, DNK); Hoffmann, Christina (Oak Ridge National Laboratory, Oak Ridge, USA); Stalke, Dietmar (Universität Göttingen, Göttingen, GER)

In our recent experimental charge density studies, we noticed residual density close to hydrogen positions that could be modelled as anisotropic displacement. To justify this treatment, we collected neutron data for two benchmark structures and compared the derived anisotropic hydrogen displacement parameters to our refined parameters against the X-ray data, results obtained from the *SHADE*-server [1], the software *APD-Toolkit* [2] and from *HARt* [3]. The smallest deviations from the neutron values were achieved by the refinement of anisotropic hydrogen displacement parameters against the X-ray data. With that, the refinement of bond-directed quadrupole parameters turned out to be important. The main discrepancies were observed for hydrogen atoms that are attached to carbon atoms that were refined with Gram-Charlier coefficients. Furthermore, we investigated also the free refinement of the C-H bond distances after anisotropic refinement of the hydrogens. While *HARt* yields the most reliable C-H bond distances, it overestimated the hydrogen anisotropic displacement parameters [4].

[1] Madsen, A. Ø. & Hoser, A. A. (2014). *J. Appl. Cryst.* 47, 2100–2104.

[2] Lübben, J., Bourhis, L. J. & Dittrich, B. (2015). *J. Appl. Cryst.* 48, 1785–1793.

[3] Fugel, M., Jayatilaka, D., Hupf, E., Overgaard, J., Hathwar, V. R., Macchi, P., Turner, M. J., Howard, J. A. K., Dolomanov, O. V., Puschmann, H., Iversen, B. B., Bürgi, H.-B. & Grabowsky, S. (2018). *IUCrJ.* 5, 32–44.

[4] Köhler, C.; Lübben, J.; Hoffmann, C., Krause, L.; Herbst-Irmer, R. & Stalke, D. (2019). *Acta Cryst.* B75, in production.

## MS29-P01 | KOALA - ROUTINE H-ATOM DETERMINATIONS BY LAUE NEUTRON DIFFRACTION

Edwards, Alison (Australian Centre for Neutron Scattering, Lucas Heights, AUS); Piltz, Ross (Australian Centre for Neutron Diffraction, Lucas Heights, AUS)

KOALA entered the ANSTO neutron beam user program in 2009 following the example of VIVALDI at the ILL which proposed relatively rapid neutron diffraction studies of molecular crystals ( $0.1\text{mm}^3$  minimum crystal volume) for which a broad range of determination constitutes “accuracy”. In some instances, the presence or absence of a hydrogen nucleus constitutes an accurate result and this can, where necessary, be achieved via a relatively low resolution determination from specimens of limited crystallinity. In other cases, exact hydrogen atom positions are sought for comparison with methods seeking to extend the utility of X-ray diffraction in cases such as quantum crystallographic refinement or purely theoretical methods. Two major enhancements to our operation of KOALA have been the implementation of a COBRA cryostream to facilitate the handling of samples which are air and moisture sensitive and to speed sample change; and the creation of a user friendly data reduction procedure which facilitates timely presentation of the neutron structure determination with the full chemical study. The achievements with KOALA demonstrate that the promise of VIVALDI was achievable and there is no reason why VIVALDI or a similar Laue instrument could not be successfully made available at a reactor source, capitalising on the development initiated at the ILL.

## MS29-P02 | ON PRECISION AND ACCURACY OF X-RAY AND NEUTRON DIFFRACTION RESULTS FOR SINGLE CRYSTALS OF GLYCINE

Sutula, Szymon (Department of Chemistry, University of Warsaw, Warsaw, POL); Malinska, Maura (Department of Chemistry, University of Warsaw, Warsaw, POL); Canadillas-Delgado, Laura (Institut Laue-Langevin, Grenoble, FRA); Fabelo-Rosa, Oscar (Institut Laue-Langevin, Grenoble, FRA); Wozniak, Krzysztof (Department of Chemistry, University of Warsaw, Warsaw, POL)

In our work, we aim at characterization and estimation of precision and accuracy of single crystal X-ray and neutron results obtained for high-quality crystals of  $\alpha$ -glycine. As expected, the shorter the wavelength, the better resolution, and one can refine the structure of glycine with more details. That is why we used MoK $\alpha$ , AgK $\alpha$  and X-ray synchrotron radiation for our measurements. Even more, we also have obtained the structural data with neutron single wavelength radiation as relative diffraction lengths for hydrogen atoms are much higher in neutron diffraction than the corresponding atomic scattering factors in the case of X-ray diffraction. For those two distinct radiation sources, we collected the data at different temperatures ranging from 90 K to 295 K. Afterwards, we used different resolution limits ranging from full possible for each source down to 0.5  $\text{\AA}^{-1}$ . Finally, the fourth differentiating factor was the model used for refinement. We applied the simple IAM (Independent Atom Model) with isotropic treatment of hydrogen atoms, IAM with anisotropic thermal motion for hydrogen atoms, MM (Multipole Model) and finally a model allowing for the anharmonic motion for hydrogen atoms. What we find the most interesting, is the dependence of ADPs of all atoms within the glycine molecule on the resolution of the collected data. We would like to present detailed comparison of results from different techniques and different sources and interesting relation regarding thermal motion and finally ask a question, what should the standards of nowadays structure experiments look like.

## MS29-P03 | COMPARISON OF DIFFERENT STRATEGIES FOR MODELLING HYDROGEN ATOMS IN CHARGE-DENSITY ANALYSES

Köhler, Christian (University of Göttingen, Göttingen, GER); Lübben, Jens (University of Göttingen, Göttingen, GER); Krause, Lennard (Aarhus University, Aarhus, DNK); Hoffmann, Christina (Oak Ridge National Laboratory, Oak Ridge, USA); Herbst-Irmer, Regine (University of Göttingen, Göttingen, GER); Stalke, Dietmar (University of Göttingen, Göttingen, GER)

The quality of five approximation methods to model anisotropic displacement parameters (ADPs) for hydrogen atoms was investigated in a comparative study based on two model compounds [1]. Hydrogen atom parameters and structural properties derived from our collected neutron data sets of these compounds were compared with those obtained from the SHADE-server [2], the software APD-Toolkit [3], the results from Hirshfeld atom refinement conducted in the OLEX2 GUI (HART) [4], and the results of anisotropic hydrogen refinement within XD2016 [5]. Surprisingly, the refinement of anisotropic hydrogen displacement parameters against the X-ray data yielded the smallest deviations from the neutron values. The refinement of bond-directed quadrupole parameters turned out to be vital for the quality of the resulting ADPs [6].

[1] Köhler, C., Lübben, J., Krause, L., Hoffmann, C., Herbst-Irmer, R., Stalke, D. (2018). *Acta Cryst. B*, B75, in production.

[2] Madsen, A. Ø. & Hoser, A. A. (2014). *J. Appl. Cryst.* 47, 2100–2104.

[3] Lübben, J., Bourhis, L. J. & Dittrich, B. (2015). *J. Appl. Cryst.* 48, 1785–1793.

[4] Fugel, M., Jayatilaka, D., Hupf, E., Overgaard, J., Hathwar, V. R., Macchi, P., Turner, M. J., Howard, J. A. K., Dolomanov, O. V., Puschmann, H., Iversen, B. B., Bürgi, H.-B. & Grabowsky, S. (2018). *IUCrJ.* 5, 32–44.

[5] Volkov, A., Macchi, P., Farrugia, L. J., Gatti, C., Mallinson, P. R., Richter, T. & Koritsanszky, T. (2016). XD2016.

[6] Roversi, P. & Destro, R. (2004). *Chem. Phys. Lett.* 386, 472–478.

## MS29-P04 | TAAM: A RELIABLE AND USER FRIENDLY TOOL FOR HYDROGEN ATOM LOCATION USING X-RAY DIFFRACTION DATA

Chodkiewicz, Michal (University of Warsaw, Department of Chemistry, Warsaw, POL); Jha, Kunal (Biological and Chemical Research Centre, Department of Chemistry, University of Warsaw, Warsaw, POL); Gruza, Barbara (Biological and Chemical Research Centre, Department of Chemistry, University of Warsaw, Warsaw, POL); Dominiak, Paulina (Biological and Chemical Research Centre, Department of Chemistry, University of Warsaw, Warsaw, POL)

The use of TAAM (Transferable Aspherical Atom Model) – a multipole model based approach - instead of spherical atom model in the structure refinement against X-ray data largely improves the X-H bond lengths.[1] A new method called Hirshfeld Atom Refinement (HAR) was shown to allow for accurate and precise estimation of the X-H bond lengths in small molecule by Woinska et. al.[2]. However, the computation cost for HAR is much higher than the TAAM refinement. The applicability of TAAM in determining the X-H bond lengths with accuracy comparable to neutron data was reinvestigated on the 81 organic molecule datasets used by Woinska et. al. A library called DiSCaMB has been developed to facilitate integration of the aspherical atom model into refinement programs.[3] The structures were refined using TAAM via DiSCaMB integrated with locally modified version of Olex2[4] and the X-H bond lengths thus obtained have been categorized and compared with the averaged neutron lengths as defined by Allen and Bruno.[5] The model related statistics comparison between IAM, HAR and TAAM will be highlighted.

Support of this work by the National Centre of Science (Poland) through grant OPUS No.UMO-2017/27/B/ST4/02721 is gratefully acknowledged.

[1] Bąk, J. M. *et al.* ActaCryst.A **2011**,67,141-153.

[2] Wońska, M. *et al.* Sci. Adv. **2016**, 2, e160019

[3] Chodkiewicz, M. L; *et al.* J. Appl. Cryst. **2018**, 51, 193–199

[4] Dolomanov, O.V. *et. al.* J. Appl. Cryst. **2009**, 42, 339-341.

[5] Allen, F. H; Bruno, I. J. Acta Crystallogr, **2010**, B66, 380–386.

## MS29-P05 | COMPARISON OF X-RAY WAVEFUNCTION REFINEMENT AND MULTIPOLE REFINEMENT BASED ON THE ENERGETIC ANALYSIS OF THE CRYSTAL STRUCTURES OF 2-HYDROXY-8-X-QUINOLINE DERIVATIVES (X = Cl, Br, I, S-Ph)

Woinska, Magdalena (Department of Molecular Physiology and Biological Physics, University of Virginia, Charlottesville, POL); Wanat, Monika (Biological and Chemical Research Centre, Department of Chemistry, University of Warsaw, Warsaw, POL); Taciak, Przemyslaw (Department of Drug Chemistry, Faculty of Pharmacy, Medicinal University of Warsaw, Warsaw, POL); Pawinski, Tomasz (Department of Drug Chemistry, Faculty of Pharmacy, Medicinal University of Warsaw, Warsaw, POL); Minor, Wladek (Department of Molecular Physiology and Biological Physics, University of Virginia, Charlottesville, USA); Wozniak, Krzysztof (Biological and Chemical Research Centre, Department of Chemistry, University of Warsaw, Warsaw, POL)

This study compares two methods of high-resolution X-ray data refinement – multipole refinement (MM) and X-ray wavefunction refinement (XWR) – applied to data sets collected for crystals of four quinoline derivatives substituted by Cl, Br, I atoms and the -S-Ph group. Problems such as refinement of hydrogen positions (unrestrained vs restrained to average neutron distances) and ADPs (unrestrained vs estimated with SHADE2), anharmonic thermal motion refinement and the influence of rejection of weak reflections for data of varying quality are investigated. Bond lengths and angles are verified against the values obtained in the course of dispersion-corrected periodic DFT geometry optimization. Hydrogen ADPs are compared, based on the similarity index (Spackman), whereas for the anharmonic refinement, the number of non-zero Gram-Charlier coefficients and probability density function are analysed. Another aspect of the presented study are energetic investigations, comprising dimer interactions, cohesive and geometrical relaxation energy. Formation of similar crystal structures of the Cl and Br derivatives is governed by halogen bonds and the N-H...O hydrogen bonds, the latter also present in the -S-Ph derivative. For the crystal lattice of the I compound, in which molecules interacting via halogen bonds are arranged in slabs, interlayer interaction energies were calculated. To extend the analysis of dimer interactions and investigate the contribution of electrostatic and dispersive terms, energy frameworks were generated. The results show superiority of XWR over MM in terms of refinement of hydrogen positions, comparable performance in the energetic aspect and the importance of refinement based on the full set of reflections.

## MS30: Chirality and Polarity in Crystals

---

### MS30-01 | SOLID-STATE CHIRAL RESOLUTION VIA METAL COMPLEXATION

Grepioni, Fabrizia (University of Bologna, Bologna, ITA)

Spontaneous chiral resolution upon ionic co-crystals (ICCs) formation is observed reacting the amino acid histidine or proline with lithium halides. The  $\text{Li}^+$  cations selectively link to molecules of the same chirality, forming enantiopure chains, resulting in a chiral resolution process in the solid-state *via* conglomerate formation.

One possible reason for chiral preference in lithium ICCs could be the tetrahedral geometry around the lithium cations, which favours the coordination of molecules of the same handedness. Complexation of enantiopure *S*-etiracetam (levetiracetam) and of racemic *RS*-etiracetam to zinc in the form of their  $\text{ZnCl}_2$  salts has also been investigated, as zinc is known to favour tetrahedral coordination. By varying the stoichiometric ratio it is possible to “switch” reversibly from a stable racemic compound to a conglomerate. Co-crystallization with metal ions favouring tetrahedral coordination can thus be successfully used to obtain chiral selectivity and conglomerate formation from racemic compounds.

[1] D. Braga, L. D. Esposti, K. Rubini, O. Shemchuk and F. Grepioni, *Cryst. Growth Des.*, 2016, **16**, 7263-7270.

[2] O. Shemchuk, L. Degli Esposti, F. Grepioni and D. Braga, *CrystEngComm*, 2017, **19**, 6267-6273

[3] O. Shemchuk, L. Song, K. Robeyns, D. Braga, F. Grepioni and T. Leyssens, *Chem. Commun.*, 2018, **54**, 10890-10892.

[4] L. Song, O. Shemchuk, K. Robeyns, D. Braga, F. Grepioni, and T. Leyssens, *Cryst.Growth Des.*, 2019, DOI:10.1021/acs.cgd.9b00136

## MS30-02 | ELECTRON CRYSTALLOGRAPHY FOR DETERMINING THE HANDEDNESS OF CHIRAL CRYSTALS

Oleynikov, Peter (ShanghaiTech University, Shanghai, CHN); Ma, Yanhang (ShanghaiTech University, Shanghai, CHN); Terasaki, Osamu (ShanghaiTech University, Shanghai, CHN)

The atomic level chirality study of a sub-  $\mu\text{m}$ -sized crystal is a difficult task due to the lack of efficient and reliable characterization methods. Here, we propose two novel and practical electron crystallography approaches of characterization for determining the handedness of chiral zeolite nanocrystals [1]. The handedness is evaluated either by (i) the comparison of two aligned high-resolution transmission electron microscope images taken along 2 different zone axes of the same nanocrystal by tilting it around its screw axis, or (ii) the analysis of intensity asymmetry for a Bijvoet pair of reflections in a single precession electron-diffraction pattern. The image alignment is performed using gold nanoparticle markers; depending on the tilt direction the observable shift between the two projections leads to the correct space group assignment. The asymmetry in the diffraction spots intensities is analyzed by quantitative comparison with calculated dynamical electron diffraction patterns. Both approaches provide new elegant ways for the handedness determination of small, chiral crystals.

[1] Y.H. Ma, P. Oleynikov, O. Terasaki. Electron Crystallography for Determining the Handedness of Chiral Crystals. *Nature Materials*. 16(7) (2017) 755-759.

## MS30-03 | ABSOLUTE CONFIGURATION OF PHARMACEUTICAL MOLECULES DETERMINED FROM A NANOCRYSTAL BY ELECTRON DIFFRACTION

Brazda, Petr (Institute of Physics of the Czech Academy of Sciences, Prague 8, CZE); Palatinus, Lukas (Institute of Physics of the Czech Academy of Sciences, Prague, CZE); Babor, Martin (University of Chemistry and Technology, Prague, Prague, CZE)

Crystallographic analysis plays an important role in the development and characterization of new pharmaceutical substances. An essential part of a complete structure analysis is determination of absolute configuration of chiral molecules. If an organic molecular crystal forms only micro- or nanocrystals, ab initio crystal structure determination becomes an extreme challenge. An important breakthrough in the structure analysis of micro- and nanocrystalline pharmaceutical materials has been made recently [1] by the employment of electron diffraction tomography (EDT) techniques, though the absolute structure determination has not been tackled yet. A limiting factor for structure determination of organic molecular crystals is the radiation damage. Ab initio structure determination by electron diffraction has so far been limited to compounds that maintain their crystallinity after a dose of  $1 \text{ e}^- \text{ \AA}^{-2}$  or more. We present a complete structure analysis of a pharmaceutical cocrystal of sofosbuvir and L-proline, which is about one order of magnitude less stable. Data collection on multiple positions of a crystal and an advanced intensity integration procedure enabled us to solve the structure ab initio. We further show that dynamical diffraction effects are strong enough to permit unambiguous determination of the absolute structure of material composed of light scatterers [2].

[1] L. Palatinus, et al., *Science* 10.1126/science.aak9652 (2017); T. Gruene et al., *Angew. Chem. Int. Ed.* 10.1002/anie.201811318 (2018); C. G. Jones et al., *ACS Cent. Sci.* 10.1021/acscentsci.8b00760 (2018)

[2] Brázda et al., *Science* accepted (2019)

## MS30-04 | OPTICAL RESOLUTION OF 2- AND 4-CHLOROMANDELIC ACIDS WITH CYCLOHEXYLETHYLAMINE RESOLVING AGENT—CRYSTAL STRUCTURES OF THE DIASTEREOMERS AND THE DOUBLE SALT

Bereczki, Laura (Hungarian Academy of Sciences Research Centre for Natural Sciences, Budapest, HUN); Zodge, Amit (Budapest University of Technology and Economics, Budapest, HUN); Holczbauer, Tamás (Hungarian Academy of Sciences Research Centre for Natural Sciences, Budapest, HUN); Körösi, Márton (Budapest University of Technology and Economics, Budapest, AUT); Székely, Edit (Budapest University of Technology and Economics, Budapest, HUN); Bombicz, Petra (Hungarian Academy of Sciences Research Centre for Natural Sciences, Budapest, HUN)

Racemic mandelic acid can efficiently be resolved with cyclohexylethylamine. From this starting point, cyclohexylethylamine can be considered as an eligible resolving agent for 2- and 4-chloromandelic acids. Both target compounds are important pharmaceutical and agrochemical intermediates and are utilized in enantiopure form. In spite of this, the resolution experiments showed that neither of the chloromandelic acids can be resolved with cyclohexylethylamine. In both cases, the double salt (containing the racemic chloromandelic acid and the resolving agent in optically pure form) will crystallize. The attainable enantiomeric excess is practically zero. In the cases of the optical resolutions of 2- and 4-chloromandelic acids with cyclohexylethylamine resolving agent, the crystal structures of both diastereomers and the double salt have been determined by single crystal X-ray diffraction and compared. The structural background of the formation of the double salt has been explored. The physico-chemical properties of the diastereomers and the double salt have been correlated with the structures.

The crystal structure of the less soluble diastereomer had in both cases high symmetry and crystal density. The more soluble diastereomer had in both cases the least dense structure, more than one ion pair in the asymmetric unit and eventually disordered molecular fragments. The shortest hydrogen bond interactions were formed in the structures of the double salts corresponding to a lower solubility and higher melting enthalpy as compared to the diastereomers.

## MS30-05 | HIGHLY VERSATILE METAL-ORGANIC FRAMEWORKS

Shimon, Linda (Weizmann Institute of Science, Rehovot, ISR); di Gregoria, Maria Chiara (Weizmann Institute of Science, Rehovot, ISR); Houben, Lothar (Weizmann Inst. of Science, Rehovot, ISR); Lahav, Michal (Weizmann Inst. of Science, Rehovot, ISR); van der Boom, Milko (Weizmann Institute, Rehovot, ISR)

The relationship between crystallization conditions, crystal structure and properties is a pivotal point in modern chemistry both for the investigation of fundamental aspects and for material design. The interest spans from the macro- to the nanoscale, and across the gamut of natural, laboratory-made, organic and inorganic systems.

In our study, we investigate the factors affecting the size and morphology of self-assembled metal-organic frameworks (MOFs). In general, micro-nano crystals grown by modulator-free synthesis are polydispersed in size, exhibit non-homogeneous shape or simple polyhedral morphologies, usually reflecting the underlying geometry of the crystallographic structure. We developed an approach that results in the formation of monodispersed crystals with a large variability of morphologies, while keeping the crystallographic structure nearly identical. No templates or modulators are used. The crystals generated include rare polyhedral shapes, hollow structures and unique morphologies not classifiable according to conventional rules. Interestingly, we prepared morphologically highly complex crystals from achiral components that exhibits single crystallinity and chirality at both the molecular structure and crystal morphology. The work provides new fundamental insights in the growth of uniform and chiral crystals, opening up opportunities for their use as 3D objects for nanotechnological applications.

## MS30-P01 | FEATURES OF CRYSTAL FORMATION OF CHIRAL DERIVATIVES OF 1,5-DIHYDRO-2H-PYRROLE-2-ONE

Saifina, Alina (Arbuzov Institute of Organic and Physical Chemistry, FRC Kazan Scientific Center, Russian Academy of Sciences, Kazan, RUS); Lodochnikova, Olga (Arbuzov Institute of Organic and Physical Chemistry, FRC Kazan Scientific Center, Russian Academy of Sciences, Kazan, RUS); Samigullina, Aida (Arbuzov Institute of Organic and Physical Chemistry, FRC Kazan Scientific Center, Russian Academy of Sciences, Kazan, RUS); Gubaidullin, Aidar (Arbuzov Institute of Organic and Physical Chemistry, FRC Kazan Scientific Center, Russian Academy of Sciences, Kazan, RUS)

1,5-Dihydro-2H-pyrrol-2-ones represent an important class of five-membered nitrogen-containing heterocycles. Their structural moiety is found in different natural molecules and synthesized compounds having a wide range of biological activities. Among the compounds of this class, substances with antimicrobial, anti-inflammatory, antitumor, analgesic, antiviral, nootropic, antiaggregant and other types of biological activities have been found.

We have studied series of halogen derivatives of 1,5-dihydro-2H-pyrrol-2-ones. The presence of a chiral center in the studied compounds leads to the formation of three types of crystals: racemates, conglomerates and solid solutions with a different composition. All types of crystals were studied by single-crystal, powder X-Ray diffraction and DSC methods. It was found, that crystallization of conglomerates in a high-symmetric crystal systems (as opposed to racemic crystals) is a characteristic feature of the compounds under investigation.

The classical hydrogen bonds between the hydroxyl and carboxyl groups leads either to the formation of a centrosymmetric H-dimers or to H-bonded chains in the crystals. Powder diffraction and DSC studies have shown that during the melting of racemic crystals the processes of racemate melting, followed by the formation of a conglomerate from a supercooled solution and its further melting are observed. The reasons for such phase transitions in the crystals are discussed. The conclusion about the greater thermodynamic stability of highly symmetric conglomerates derived on the basis of the study of the rapid crystallization of compounds from various solvents by powder diffraction.

The studies were financially supported by the Russian Science Foundation (grant no. 17-13-01209).

## MS30-P02 | ABSOLUTE STRUCTURE ASSIGNMENT THROUGH INTERPLAY OF X-RAY DIFFRACTION AND EBSD

Borrmann, Horst (Max-Planck-Institut für Chemische Physik fester Stoffe, Dresden, GER); Burkhardt, Ulrich (Max-Planck-Institut für Chemische Physik fester Stoffe, Dresden, GER); Winkelmann, Aimo (Laser Zentrum Hannover, Hannover, GER)

Various classes of compounds have gained strong interest in solid state sciences with respect to particular properties which are linked to the absence of a center of symmetry in the crystal structure. A prominent case are compounds adopting the B20 or FeSi type structure, respectively. Reliable characterisation of particular physical properties requires single crystals of adequate size and quality. However, it is of utmost importance to assure that crystals under investigation are single domain, i.e. twins by inversion have to be excluded rigorously. The universal approach introduced by the late Howard Flack is well established though has its weaknesses in cases of very simple but highly symmetric structures. For larger single crystals there exists no reliable method to obtain a proper set of Bragg intensities.

This contribution presents an approach in confirming the absolute structure of a larger single crystal via a combination of X-ray diffraction and Electron Backscatter Diffraction (EBSD) methods. A small but representative piece is extracted from the large crystal using Xe-ions in a Focused Ion Beam (FIB) micromachining setup. This particular crystallite allows for an entire structure determination including the assignment of the absolute structure. Finally, this structural model is used to map the entire crystal applying EBSD methods at high spatial resolution.

## MS30-P03 | CRYSTALLIZATION-INDUCED STEREOISOMERIC RECOGNITION AND STEREOCHEMICAL TRANSFORMATIONS OF CHIRAL ORGANIC MOLECULES: ROLE OF SUPRAMOLECULAR SYNTHONS

Lodochnikova, Olga (A.E. Arbuzov Institute, Kazan, RUS)

Supramolecular chemistry developed in 1970s, following on from and elaborating the ideas of organic chemistry, and borrowing some key concepts from it. One of the most complete and successful examples thereof is the concept of supramolecular synthon. The history of stereochemistry, in turn, goes back more than one and a half centuries. Two aspects of stereochemistry are commonly distinguished: Static and dynamic. The concept of stereochemistry was also quite successfully extended to the supramolecular area in the sense of a field of chemistry that studies the mutual arrangement of structural blocks within complex associates. In other words, currently, the basic area of stereochemistry, namely static stereochemistry, has been adapted to the supramolecular area.

At the same time, accumulating much information on various supramolecular associates formed through hydrogen bonds or other intermolecular interactions in a different and complex manner requires transferring the ideology and the basic concepts of dynamic stereochemistry to the supramolecular area. Just as classical dynamic stereochemistry considers the spatial features of reaction behaviors, so supramolecular dynamic stereochemistry will focus on the spatial features of binding molecules in associates via intermolecular interactions. The time is ripe for introducing the concept of stereochemical transformation, that is amplifying the stereochemical specifications of a molecule at the stage of forming some intricate supramolecular associates. The driving force of stereochemical transformation is usually the tendency to forming one or another stable supramolecular synthon.

This work was financially supported by the Russian Science Foundation (grant No 17-13-01209).

## MS30-P04 | UNEXPECTED POLYMORPHIC BEHAVIOR OF FOUR RACEMIC 3-PYRROLIN-2-ONE DERIVATIVES

Gerasimova, Daria (A.E. Arbuzov Institute of Organic and Physical Chemistry, Kazan, RUS); Fayzullin, Robert R. (Arbuzov Institute of Organic and Physical Chemistry, FRC Kazan Scientific Center, Russian Academy of Sciences, Kazan, RUS); Saifina, Alina (A.E. Arbuzov Institute of Organic and Physical Chemistry, Kazan, RUS); Vandyukova, Irina (A.E. Arbuzov Institute of Organic and Physical Chemistry, Kazan, RUS); Kurbangalieva, Almira (A.M. Butlerov Chemical Institute, Kazan (Volga region) Federal University, Kazan, RUS); Lodochnikova, Olga (A.E. Arbuzov Institute of Organic and Physical Chemistry, Kazan, RUS)

Polymorphism of organic, especially chiral, compounds is of great interest and value for modern crystallography, physical chemistry, process, and patent law. Since the free energy of different polymorphs of the same substance is different, all their physicochemical properties are different, that is, melting point, solubility, stability, hygroscopicity, pharmacodynamic and pharmacokinetic properties, and so on. Therefore, bioactive substances are particularly attractive from the point of view of guided polymorph search. In this abstract, we reported crystallization and heterogeneous equilibria and transitions of four racemic N-substituted 4-arylsulfanyl-3-chloro-5-hydroxy-3-pyrroline-2-ones consisting an unsaturated  $\gamma$ -lactam ring that is an important pharmacophore group. As a result, in this series of compounds, a unique “conglomerate-conglomerate” polymorphic pair and a pair of packing polymorphs were found. All individual crystalline phases were studied by means of single crystal and powder X-ray diffractions. Their phase behavior was carefully investigated using heat flux differential scanning calorimetry, temperature-resolved solid-state vibration spectroscopy and hot-stage microscopy.

This work was financially supported by the Russian Science Foundation (grant No 17-13-01209).

## MS30-P05 | SEPARATION AND RESOLUTION OF METHYLCYCLOHEXANONES BY ENCLATHRATION WITH DEOXYCHOLIC ACID

Bouanga Boudiombo, Jacky Sorrel (University of Cape Town, Cape Town, ZAF); Nassimbeni, Luigi (University of Cape Town, Cape Town, ZAF); Bourne, Susan (University of Cape Town, Cape Town, ZAF)

Molecular selectivity by host-guest procedures is a method which can be applied to the separation of enantiomers. The resolution of methycyclohexanones (MCH) by enclathration has been studied using a variety of chiral hosts<sup>1,2</sup>. For the analysis reported here, deoxycholic acid (DCA) was used as a host to separate and resolve the different isomers of (MCH) whose normal boiling points range from 162 to 169°C. Competition experiments of these isomers resulted in a preference of DCA towards 2MCH with the following trend 2MCH>3MCH>4MCH. This trend was then confirmed by differential scanning calorimetry results. Additionally, DCA resolved 2MCH by enclathrating the *S*-conformer, but 3MCH remained unresolved. However, competition experiments of rac-2MCH/rac-3MCH resulted in both guests been resolved yielding to (*S*)-conformers, this suggested that 2MCH had a templating effect on the final structures. This was then proven along a selectivity curve of 2MCH vs 3MCH with 2MCH mole fraction varying from 0 to 1. This is shown in figure 1.

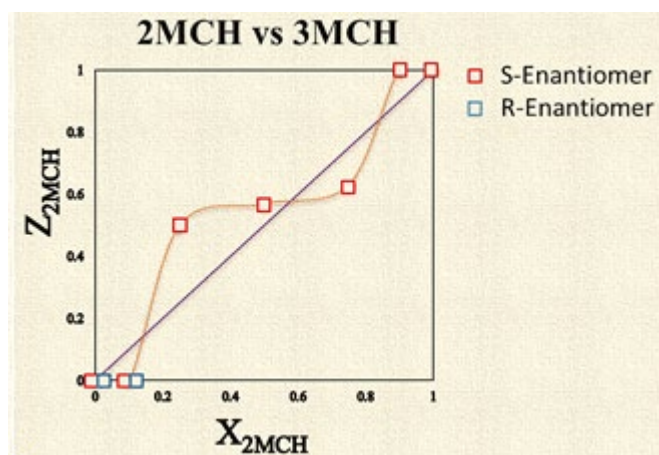


**Figure 1.** Competition experiment of 2MCH vs 3MCH with *S*-enantiomer represented in red while the *R*-enantiomer is represented in blue.

[1] Weber, E.; Reutel, C.; Foces-Foces, C.; Llamas-Saiz, A. L. J. Alanine-derived hosts comprising a roof-shaped carbonimide framework. Synthesis, inclusion formation and X-ray crystal structures of racemic and optically resolved free hosts, and their crystalline complexes with 3-methylcyclohexanone. *Soc. Perkin Trans.2* 1994, 1455-1461.

[2] Batai, E.; Nassimbeni, L.R.; Weber, E. Inclusion compounds of a borneol dumb-bell host with methylcyclohexanones and 2-butanols: structures and resolutions. *CrystEngComm*. 2015, 17, 4205-4209.

## MS30-P06 | PECULIARITIES OF SUPRAMOLECULAR ORGANIZATION IN CENTRIC, ACENTRIC AND CHIRAL KETONES WITH VINYLACETYLENE FRAGMENTS

Voronova, Evgeniia (INEOS RAS, Moscow, RUS); Ushakov, Ivan (INEOS RAS, Moscow, RUS); Aleshin, Dmitry (INEOS RAS, Moscow, RUS); Vologzhanina, Anna (INEOS RAS, Moscow, RUS); Golovanov, Alexandr (Togliatti State University, Togliatti, RUS)

Crystal structures of a series of 1,5-diarylpentenones and cyclic ketones with vinylacetylene fragments were studied. These compounds are prospective for application in non-linear optics, and nearly half of them crystallize in acentric and chiral space groups. Full Interaction Maps were used to understand the features of their supramolecular organization [1,2]. Besides, topological features of isolated molecules and intermolecular contacts were studied by means of the theoretical charge density studies [1]. Studies have shown that molecular planarity does not affect crystal chirality, while electronic and steric factors govern the formation of chiral chains, and acentric crystals for all the homologues of (E)-1,5-diarylpent-1-en-4-in-3-ones. Energies of intermolecular interactions were found to correlate with melting temperatures of compounds. The charge density distribution in isolated molecules allows predicting the supramolecular organization of such compounds that can be useful in the development of new materials with nonlinear optical properties. Mutual disposition of olefin fragments in some ketones satisfy criteria needed to allow a photoinitiated cycloaddition reactions to occur. Thus, effect of irradiation on some compounds was studied using  $^1\text{H}$  NMR technique.

The study was supported by the Russian Science Foundation (grant 17-13-01442).

[1] E. D. Voronova, A. A. Golovanov, K. Yu. Suponitsky, I. V. Fedyanin, A. V. Vologzhanina, *Cryst. Growth Des.* **2016**, 16, 3859–3868.

[2] E. D. Voronova, A. A. Golovanov, I. S. Odin, M. A. Anisimov, P. V. Dorovatovskii, Y. V. Zubavichus, A. V. Vologzhanina *Acta Cryst.* **2018**, C74, 1674–1683.

## MS30-P112 - LATE | STRUCTURAL SIMILARITIES OF 2D AND 3D WATER FRAMEWORKS IN 3,3-DIMETHYL-2-BUTYLAMINE, TERT-AMYLAMINE AND AZEPANE HYDRATES

Rzepinski, Patryk (University of Warsaw, Warsaw, POL); Dobrzycki, Lukasz (University of Warsaw, Warsaw, POL); Cyranski, Michal (University of Warsaw, Warsaw, POL); Boese, Roland (University of Warsaw, Warsaw, POL)

The presence of water molecules in the structure can play an important role in the stability and property of the crystals. However the resulting structure is still hard to predict. Herein we present crystalline hydrates of racemic mixture of 3,3-dimethyl-2-butylamine (**1**), chiral (S)-3,3-dimethyl-2-butylamine (**1\***), *tert*-amylamine (**2**) and azepane (**3**). All these phases were grown under ambient pressure using IR laser assisted *in situ* method.

Amines (**1**), (**1\***) and (**2**) forms dihydrates. These structures crystallize in different space groups. Moreover dihydrate of (**1\***) undergoes reversible  $P2_1 \leftrightarrow P1$  phase transition. Nevertheless all these crystal structures contain the same water layers denoted as L4(4)8(8) composed of 4- and 8-membered rings. With a moderate water amount (**3**) forms trihydrate containing L4(6)5(7)6(8) [2] layered water motif. In addition all these amines form hydrates with higher amount of water. In the case of (**1\***), (**2**) and (**3**) undecahydrate with the same 3D water framework topology is observed. These structures contain channels occupied by the amine interacting with H<sub>2</sub>O species. In these structures empty 4<sup>3</sup>5<sup>6</sup> cages are also present. Surprisingly the amine (**1**) which is a racemate of (**1\***) behaves differently and crystallizes as heksadekahydrate. Here the amine is trapped in large 6<sup>8</sup>5<sup>10</sup> water cages but unlike in clathrate hydrates forms strong hydrogen bonds with H<sub>2</sub>O.

## MS31: Responsive Materials & Structural Dynamics in Crystal...

---

### MS31-01 | MECHANICAL PROPERTIES OF MOLECULAR CRYSTALS: THE BIGGER PICTURE

Naumov, Pance (New York University Abu Dhabi, Abu Dhabi, ARE)

Mechanically reconfigurable molecular crystals—ordered materials that can adapt to variable operating and environmental conditions by deformation, whereby they attain motility or perform work—are quickly shaping up a new research direction in materials science, crystal adaptronics. Properties such as elasticity, superelasticity and ferroelasticity that are normally related to inorganic materials, and phenomena such as shape-memory and self-healing effects which are well established for soft materials, are increasingly reported for molecular crystals, yet their mechanism, quantification, and relation to the crystal structure in organic crystals are not immediately intelligible to the chemistry and materials science research communities. This lecture will provide a condensed topical overview of the elastic, superelastic and ferroelastic molecular crystals, emerging new classes of materials that bridge the gap between the soft matter and inorganic materials. The occurrence and detection of these unconventional properties, and the underlying structural features of the related molecular materials will be discussed and highlighted together with selected prominent recent examples.

## MS31-02 | DYNAMIC MOFs WITH BREATHING-DEPENDENT REDOX BEHAVIOR

Minguez Espallargas, Guillermo (ICMol, University of Valencia, Paterna, ESP); Souto, Manuel (ICMol, University of Valencia, Paterna, ESP); Vicent-Morales, Maria (ICMol, University of Valencia, Paterna, ESP)

Flexible or “breathing” Metal-Organic Frameworks (MOFs) involving changes in their physical and structural properties upon an external stimulus are an interesting class of crystalline materials due to their range of potential applications including chemical sensors.[1] Recently, we have reported the use of a tetrathiafulvalene (TTF)-based ligand and trimeric Fe<sub>3</sub>O SBUs to yield a highly stable MOF, namely **MUV-2**, with non-interpenetrated hierarchical crystal structure and an enhanced catalytic activity.[2] This MOF shows a continuous breathing behaviour with a reversible swelling upon solvent adsorption, which affects the planarity of the TTF linkers. This breathing behaviour directly impacts on its electrochemical properties and thus opens the way for the development of new electrochemical sensors.[3] On the contrary, the interpenetrated analogue, **MUV-2-i**, shows a reduced breathing capacity.[4]

[1] A. Schneemann, V. Bon, I. Schwedler, I. Senkowska, S. Kaskel and R. A. Fischer, *Chem. Soc. Rev.*, 2014, **43**, 6062.

[2] M. Souto, A. Santiago-Portillo, M. Palomino, I. Vitorica-Yrzebal, B. J. C. Vieira, J. C. C. Waerenborgh, S. Valencia, S. Navalon, F. Rey, H. Garcia and G. Minguez Espallargas, *Chem. Sci.*, 2018, **9**, 2413.

[3] M. Souto, J. Romero, J. Calbo, I. J. Vitorica-Yrzebal, J. L. Zafra, J. Casado Cordón, E. Ortí, A. Walsh and G. Minguez Espallargas, *J. Am. Chem. Soc.*, 2018, **140**, 10562.

[4] M. Vicent-Morales, I. J. Vitorica-Yrzebal, M. Souto, G. Minguez Espallargas, *CrystEngComm* 2019, **21**, 3031.

## MS31-03 | ENERGY STUDIES OF SINGLE CRYSTAL TO SINGLE CRYSTAL TRANSFORMATIONS IN CYCLIC PEPTOIDS

Tedesco, Consiglia (University of Salerno, Fisciano, ITA); Macedi, Eleonora (University of Salerno, Fisciano, ITA); Pierri, Giovanni (University of Salerno, Fisciano, ITA); De Riccardis, Francesco (University of Salerno, Fisciano, ITA); Izzo, Irene (University of Salerno, Fisciano, ITA)

Biological processes rely on the control of the dynamic behaviour of biomolecules: the intrinsic flexibility of proteins enables accurate guest recognition and specific substrate conversion. Cyclic peptoids are cyclic *N*-substituted polyglycines, as peptidomimetic compounds they feature useful biological activities and novel chemical properties both in solution and in the solid state [1].

Recently, we reported that a cyclic hexapeptoid strategically decorated by propargyl and methoxyethyl side chains undergoes a reversible single-crystal to single-crystal transformation upon guest release/uptake. The transformation consists in a drastic conformational change, where two propargyl side chains move by 113° and form a CH- $\pi$  zipper, which reversibly opens and closes, allowing for guest sensing [2]

We continued the structural characterization of cyclic hexapeptoids [4] and discovered new solid state transformations either triggered by temperature changes or by guest molecules [3].

Here we will report the results of *in-situ* X-ray crystallography, conformational energy studies and energy framework analysis of cyclic peptoids.

These findings highlight that the solid state assembly of the macrocycles determines their solid state dynamic behaviour and pave the way to the design and synthesis of artificial systems able to mimic biological functions.

[1] Tedesco, C., Erra, L., Izzo, I. & De Riccardis, F. (2014). *CrystEngComm*, 16, 3667-3687.

[2] Meli, A. et al. (2016). *Angew. Chem. Int. Ed. Engl.*, 55, 4679-4682.

[3] Macedi, E. et al. (2017). *CrystEngComm*, 19, 4704-4708.

[4] Tedesco, C. et al. (2017). *Acta Cryst. B*73, 399-412.

## MS31-04 | INSIGHTS FROM HIGH-PRESSURE CRYSTALLOGRAPHY AND X-RAY CHARGE

### DENSITY ANALYSIS INTO MECHANICAL FLEXIBILITY OF METAL-ORGANIC COMPLEX CRYSTALS

Thomas, Sajesh (Aarhus University, Aarhus 8000, DNK); Worthy, Anna ( Queensland University of Technology, Brisbane, AUS); Eikeland, Espen Zink (Aarhus University, Aarhus 8000, DNK); Grosjean, Arnaud (University of Western Australia, Perth, AUS); Spackman, Mark A (University of Western Australia, Perth, AUS); McMurtrie, John C. (Queensland University of Technology, Brisbane, AUS); Clegg, Jack K. (The University of Queensland, St Lucia, Queensland, AUS); Brummerstedt Iversen, Bo (Aarhus University, Aarhus, DNK)

Crystal engineering studies have provided insights into unusual mechanical phenomena such as crystal bending and shearing - based on anisotropy of intermolecular interactions in crystals. However, as more and more complex and anomalous cases of flexible crystals are being discovered, it demands for quantitative approaches to understand the structural origin and mechanism of such properties. In recent reports, we have shown the utility of novel computational tools and experimental charge density analysis to understand these properties [1,2]. In this presentation, I will discuss the application of high-pressure crystallography using diamond anvil cell (DAC) in understanding the structural changes occurring in flexible molecular crystals upon a homogeneous pressure. We propose that the structural changes at varying pressures can provide valuable information on the intermolecular structural dynamics involved in the mechanism of flexibility in such crystals. The example of an elastically flexible crystal formed by a Copper (II) complex will be discussed, with a focus on the structural changes at molecular and intermolecular level -observed between ambient to high pressures ( $10^{-4}$  -15 GPa). The role of some unusual 'sigma-hole' interactions/bonds in guiding the flexible property of this crystal has been unravelled by synchrotron X-ray charge density model and computational analysis.

[1] M. J. Turner, S. P. Thomas, M. W. Shi, D. Jayatilaka, M. A. Spackman, *Chem. Commun.*, **51**, 3735 (2015).

[2] S. P. Thomas, M. W. Shi, G. A. Koutsantonis, D. Jayatilaka, A. J. Edwards, M. A. Spackman, *Angew. Chem. In. Ed.* **56**, 8468 (2017).

## MS31-05 | SINGLE-CRYSTAL TO SINGLE-CRYSTAL TRANSFORMATIONS IN SPIN-CROSSOVER COMPOUNDS. AN INCREDIBLE ZOOLOGY!

GUIONNEAU, Philippe (University of Bordeaux, Pessac, FRA); MARCHIVIE, Mathieu (University of Bordeaux, Pessac, FRA); TAILLEUR, Elodie (University of Bordeaux, Pessac, FRA); GUO, Wenbin (University of Bordeaux, Pessac, FRA); ROSA, Patrick (CNRS, Pessac, FRA); CHASTANET, Guillaume (CNRS, Pessac, FRA)

**Stimuli** like pressure, light and temperature induce a drastic **response of spin-crossover crystals** with modifications of colors, electrical and magnetic properties as well as **significant volume variations** (up to 15 %) offering a wide range of potential applications going from sensors to electronic devices. **Crystallography** plays a key role since the interplay between the structural properties and the transition features (temperature(s), abruptness, light-induced response ...) is clearly demonstrated. [1] If focusing on molecular compounds, the spin-crossover phenomenon is often reversible in the solid state with encountered situations going from partial conversion to hysteretic transitions. The combination of the structural response with the stimulus and many other events (polymorphism, structural transition, loss of solvent ...) **results in an incredible zoology of the observed structural responses**. The later are going from impressive negative thermal expansion to intricate phase diagrams, reversible bond breaking, finger-pushed transitions or guest-driven transitions for example. X-ray diffraction allows to describe all these behaviors and, in return, the spin-crossover field offers a great opportunity to push the frontiers of structural investigations [1, 2]. Based on 20 years of experience in the crystallography of spin-crossover materials, we will present an overview of such structural zoology.

[1] (a) P. Guionneau, *Dalton Trans.* **2014**, 43, 382 (b) E. Collet, P. Guionneau, *C. R. Chimie*, **2018**, 1133

[2] (a) Elodie Tailleur et al. *Chem. Eur. J.*, **2018**, 24, 14495 – 14499 (b) S. Lakhroufi et al. *Phys. Chem. Chem. Phys.*, **2016**, 18, 28307

## MS31-P01 | STRUCTURAL ANALYSIS AND IR-SPECTROSCOPY OF A NEW ANILINIUM HYDROGENSELENITE HYBRID COMPOUND: A SUBTLE STRUCTURAL PHASE TRANSITION

takouachet, Radhwane (Abbes Laghrour Khenchela University, Khenchela, DZA); Benali-Cherif, Rim (Abbes Laghrour Khenchela University, Khenchela, DZA); Bendeif, El-Eulmi (Laboratoire de Cristallographie, Résonance Magnétique et Modélisations CRM2, Lorraine university, Nancy, FRA); Benali-Cherif, Nourredine (Bouira University, Bouira, DZA)

The hybrid compounds have been extensively studied over the last few decades for their specific properties and potential applications. These compounds display a wide range of molecular interactions network, from strong ionic and hydrogen bonding to weak van der Waals contacts. The asymmetric unit of this compound consists of two anilinium organic cations, two hydrogenselenite anions and one water molecule.

The temperature dependent structural investigation reveals that the studied compound undergoes a subtle non-centrosymmetric to centrosymmetric structural phase transition. At room temperature the crystal structure is non-centrosymmetric and is characterized by an important disorder in the organic part. By decreasing the temperature to 100K the organic cation is less disordered and the rotation angle of the aromatic rings changes. As a consequence, the low temperature structure becomes centrosymmetric. The infrared spectra recorded on cooling and heating the sample in the temperature range of 300–9K support this analysis.  $\text{NH}_3$  is significantly affected by the temperature change. This effect results, when cooling the sample below 140K, in the appearance of a new vibrational band corresponding to the  $(\text{NH}_3)$ -wagging modes at  $705\text{cm}^{-1}$ . The phenomenon is completely reversible and the new vibrational band disappears upon heating the sample above 140K. Moreover, the  $\nu(\text{C-N})$ -stretching and the  $(\text{NH}_3)$ -scissoring modes are also affected by the temperature variation as can be seen in the spectral ranges of  $1250\text{--}1400\text{cm}^{-1}$  and  $1610\text{--}1635\text{cm}^{-1}$ .

## MS31-P02 | TRIETHYLPHOSPHINE AS A MOLECULAR GEAR — PHASE TRANSITIONS IN FERROCENYL–ACETYLIDE–GOLD(I)

Makal, Anna (University of Warsaw, Faculty of Chemistry, Warsaw, POL)

Molecular materials undergoing single-crystal-to-single-crystal (SCSC) phase transitions are of great interest to science and industry. Their spectroscopic, photoelectric, mechanic or gas-storage properties can be switched by controlled pressure or temperature changes without destroying crystallinity, while their mechanisms, vital for understanding the processes and for materials design, can be probed by means of systematic structural studies.

A sequence of two such discontinuous phase transitions has been observed for a ferrocenyl–acetylide–gold(I) complex with triethylphosphine, by means of a multi-temperature single-crystal X-ray diffraction. Three distinct phases have been identified. The high-temperature and low-temperature phases share the same space group  $Pbca$ , whereas the intermediate phase is in the  $Pb21a$  subgroup of  $Pbca$ .

In all phases molecules of form well defined double layers, with  $PEt_3$  groups interlocking in planes perpendicular to  $[001]$ . On the molecular level, both phase transitions involve almost uniquely a conformational change of triethylphosphine: a gear-like rotation around the  $P–Au$  axis.

The mechanism of these transitions may be imagined as initiated by a rotation of a single  $PEt_3$  group in a double layer (a single gear movement), followed by adjacent phosphines adjusting their conformations as a result of steric strain. These structural changes are sequential, occurring layer-wise and involving approximately every other layer in the crystal lattice.

The sequence of phase transitions results in a noticeable contraction of the crystal cell volume with temperature. The mechanism resembles the concerted rotation of the rigid  $Fe(CN)_6$  octahedra underlying extreme compressibility of  $LnFe(CN)_6$  under pressure.

## MS31-P03 | PHOTOCRYSTALLOGRAPHIC INVESTIGATIONS OF NEW NICKEL(II) NITRO COMPLEXES

Kutniewska, Sylwia Ewa (University of Warsaw, Warsaw, POL); Borowski, Patryk (University of Warsaw, Warsaw, POL); Kaminski, Radoslaw (University of Warsaw, Warsaw, POL); Jarzemska, Katarzyna (University of Warsaw, Warsaw, POL)

The design of solid-state materials, properties of which can be modified in a controllable way, is among challenges of modern materials science. Understanding of the physicochemical processes occurring in photoactive materials under light stimuli requires detailed knowledge of the related changes at different structural levels. In this contribution we present a photocrystallographic study of selected nickel(II) nitro complexes. Our investigations are focused on finding relationships between the material's structure features (crystal packing, intermolecular interactions, crystal lattice stability) and its behaviour (photoswitching properties - conversion percentage, structural changes' nature) when exposed to LED light, as the analysed compounds may undergo the photo-induced nitro group isomerisation. All of the studied complexes exist as a nitro isomer (Ni-N(O)<sub>2</sub>) in the ground state and all of them switch to the nitrito form (Ni-O-NO) upon LED light irradiation. So far, compound 1 appeared to be the most promising photoswitchable system among the series. The IR spectroscopy results indicate in this case the 100% conversion level from the nitro ground-state form to the nitrito isomer after exposure to the 590nm LED light at 180K, while the metastable state exists up to around 240K. For the compound 2 similar photoisomerisation conditions were observed. After irradiation using the 660nm wavelength at 160K about 100% conversion was achieved. In turn, the crystal structure of 3 contains two complex molecules in ASU, out of which only one undergoes photoisomerisation, however, with a somewhat lower conversion level.

The authors thank the NCN (2017/25/N/ST4/02440) and the WCSS (grant No.285).

## MS31-P04 | PROBING SPIN CROSSOVER IN NOVEL METAL ORGANIC COMPLEXES

Musselle-Sexton, Jake (Newcastle University, Newcastle, GBR); Probert, Michael (Newcastle University, Newcastle, GBR); Sellars, Jonathan (Newcastle University, Newcastle, GBR)

Spin Crossover is a phenomenon in which metals  $d^4$ - $d^7$  can undergo electronic spin transitions between high and low spin states under the influence of external stimuli such as temperature pressure and light[1]. These systems have the potential to be used as molecular switches which leads to the requirements for room temperature thermal hysteresis.

In the work presented a library of 1,2,4-triazole ligands based on abpt (4-amino-1,2,4-triazole-3,5-bipyridyl) with various electron withdrawing and donating properties has been produced and complexed [2]. Using a sequence of metals, solvents and counter ions to expand the variety of complexes available to test changes across similar systems and the effect they have on any transition energies.

Multiple metal complexes have been produced and the structures via single crystal crystallography under differing conditions to probe for the spin transition phenomena.

Another serendipitous discovery from this work includes an unprecedented room temperature ligand migration for one of the triazole systems in the presence of iron(II) bis-isothiocyanate [3]. This system produced multiple solvates that were shown to display solvato-chromism [4].

[1] P. Gutlich, *Eur. J. Inorg. Chem.*, **2013**, 581-591.

[2] H. E. Mason, W. Li, M. A. Carpenter, M. L. Hamilton, J. A. K. Howard and H. A. Sparkes, *New J. Chem.*, **2016**, *40*, 2466–2478

[3]. J. A. Kitchen, D. S. Larsen and S. Brooker, *Chem. Asian J.*, **2010**, *5*, 910-918

[4] A. Marini, A. Muñoz-Losa, A. Biancardi, and B. Mennucci, *J. Phys. Chem.B*, **2010**, *114*, 51, 17128-17135

## MS31-P05 | STRUCTURAL AND COMPUTATIONAL STUDIES OF A SERIES OF NEW PHOTOSWITCHABLE NICKEL NITRO COMPLEXES

Borowski, Patryk (Department of Chemistry University of Warsaw, Warsaw, POL); Kutniewska, Sylwia (1Department of Chemistry, University of Warsaw,, Warsaw, POL); Kaminski, Radoslaw (1Department of Chemistry, University of Warsaw,, Warsaw, POL); Jarzemska, Katarzyna Natalia (1Department of Chemistry, University of Warsaw,, Warsaw, POL)

Transition-metal switchable complexes, thanks to the specific interactions and presence of molecular fragments that can exist in multiple isomeric forms, resulting in their interesting properties. Hence, the current study was devoted to a series of photoactive Ni(II) 8-aminoquinoline and pyridine complexes, which contain the NO<sub>2</sub> group bound to the nickel centre. The photoisomerisation reaction may undergo in the solid state under certain conditions. Understanding of the process' mechanism is a key step towards conscious development of photoswitchable materials.

The six presented complexes were examined crystallographically and computationally. They all crystallise in the centrosymmetric space groups belonging to the monoclinic and triclinic crystal systems. The crystals are stabilised majorly by  $\pi$ -stacking interactions and the C-H...O hydrogen-bond-like contacts involving the nitro species. The effect of small modifications of a molecular structure (e.g. introduction of the methyl substituent) on the crystal packing and intermolecular interactions was investigated. According to the Hirshfeld surface and reaction cavity analysis, there should be enough space in the crystal lattice to enable efficient switching between the NO<sub>2</sub> group coordination modes.

The intermolecular interactions were characterised energetically, especially these involving the nitro ligand. Additionally, the stability of different linkage isomers of the studied complexes was examined both for isolated molecule DFT calculations and employing the QM/MM approach. Both approaches prove that *endo*-nitrito isomer is more thermodynamically stable than the *exo*-analogue. The photoswitchable properties were confirmed by the photocrystallographic experiments.

Thanks the PRELUDIUM grant (2017/25/N/ST4/02440) of the NCN in Poland and The WCSS (grant No. 285)

## MS31-P06 | PRESSURE-INDUCED POLYMERIZATION AND ELECTRICAL CONDUCTIVITY OF A POLYIODIDE

Poreba, Tomasz (Paul Scherrer Institute, Villigen, CH)

Polyiodides represent one of a few classes of compounds that can form extensive inorganic homoatomic polymeric networks. Furthermore, polyiodide compounds exhibit useful redox properties, as well as electrical conductivity uncommon for nonmetals. Therefore, they have found technical applications in electronic and electrochemical devices such as batteries, fuel cells, dye-sensitized solar cells, optical devices, etc. We investigated the response of tetraethylammonium di-iodine triiodide (TEAI) for compression, using powder and single-crystal X-ray diffraction, electrical conductivity, and first principle calculations. We report the high-pressure structural characterization of TEAI in which a progressive addition of iodine to triiodide groups occurs. Compression leads to the initial formation of discrete hepta-iodide units, followed by polymerization to a 3D anionic network. Although the structural changes appear to be continuous, the insulating salt becomes a semiconducting polymer just above 10 GPa. The features of the pre-reactive state and the polymerized state are revealed by analysis of the computed electron and energy densities. The unusually high electrical conductivity can be explained with the formation of new bonds. These features make TEAI a tunable pressure-sensitive electric switch. Structural studies at high pressure can rationalize the synthesis and search for the future organic and hybrid semiconductors based on polyiodides and other iodine-rich compounds. This includes structures with the soft I...I contacts, which are the most prone for charge transport across the crystal under increased pressure.

## MS31-P07 | BREATHING METAL-ORGANIC FRAMEWORKS BASED ON FLEXIBLE INORGANIC BUILDING UNITS

Grape, Erik (Stockholm University, Stockholm, SWE); Rooth, Victoria (Stockholm University, Stockholm, SWE); Xu, Hongyi (Stockholm University, Stockholm, SWE); Willhammar, Tom (Stockholm University, Stockholm, SWE); Inge, Andrew Ken (Stockholm University, Stockholm, SWE)

Bismuth is a fairly inexpensive heavy metal and its compounds generally have low toxicity (i.e. significantly less than NaCl) and have been used as active pharmaceutical ingredients (APIs) for centuries. Despite these features, few nanoporous metal-organic frameworks (MOFs) have been built using bismuth cations. Our ongoing investigations on bismuth-MOFs have repeatedly shown framework flexibility. Typically, the breathing effect in MOFs (the reversible opening and closing of the framework as a response to its environment) is permitted by a flexible range of bond angles between the metal cation and the ligand. Through a combination of electron diffraction [1-3] and X-ray powder diffraction, we established that different mechanisms are responsible for the dynamic features in bismuth-based systems.

We have recently developed a new MOF, SU-100, containing  $\text{Bi}_2\text{O}_{12}$  inorganic building units (IBUs). Unlike most other breathing MOFs, flexibility of SU-100 is largely attributed to deformations of the IBU made possible by the flexible coordination geometry around the Bi(III) cations. We have also developed novel pseudo-polymorphs of the API bismuth subgallate [4], one of which is a breathing MOF. Two types of metal-ligand interactions are observed, strong and rigid chelation, as well as weaker interactions which give rise to framework flexibility.

[1] Nannenga, B.L. *et al.* (2014) *Nat. Methods*, **11**, 927-931.

[2] Gemmi, M. *et al.* (2015) *J. Appl. Crystallogr.* **48**, 718-727.

[3] Cichocka M.O. *et al.* (2018) *J. Appl. Crystallogr.* **51**, 1652-1661.

[4] Wang, Y. *et al.* (2017) *Chem. Commun.*, **53**, 7018-7021.

## MS31-P08 | CONFORMATIONAL SWITCHING IN SINGLE CRYSTALS OF A CALIX[4]RESORCINARENE

Mirzaei, Saber (Marquette University, Milwaukee, USA); Timerghazin, Qadir (Marquette University, Milwaukee, USA); Lindeman, Sergey (Marquette University, Milwaukee, USA)

Freshly crystallized O,O-dipropyl-4-methyl-calix[4]resorcinarene has a boat conformation with -OPr groups oriented perpendicular to the benzene rings because of sterical hindrances. At slow cooling, a single-crystal-to-single-crystal phase transition takes place around 240K with inversion of orientation of some -OPr groups and mutual shift of the molecules in the crystal. Further cooling to 100K results in complete ordering of the originally heavily disordered alkyl chains. Also, after few days in the mother liquor, the crystals of the original boat conformer redissolve and form crystals of a chair conformer.

## MS31-P09 | WAVELENGTH-SELECTIVE PHOTOISOMERISATION OF NO AND NO<sub>2</sub> LIGANDS

Schaniel, Dominik (Université de Lorraine & CNRS, Vandoeuvre-les-Nancy, FRA); Casaretto, Nicolas (Université de Lorraine & CNRS, Vandoeuvre-les-Nancy, FRA); Bendeif, El-Eulmi (Université de Lorraine & CNRS, Vandoeuvre-les-Nancy, FRA); Sébastien, Pillet (Université de Lorraine & CNRS, Vandoeuvre-les-Nancy, FRA)

In the last few years we have studied a number of complexes containing the photoswitchable ligands NO and NO<sub>2</sub> [1-4]. On the examples of [RuX(NO)<sub>2</sub>(PR<sub>3</sub>)<sub>2</sub>]BF<sub>4</sub> (PR<sub>3</sub> = PPh<sub>3</sub>, PCyp<sub>3</sub>, Pcy<sub>3</sub>; X=Cl, Br, I) and [Rh(NO)(NO<sub>2</sub>)<sub>2</sub>(Bu<sup>t</sup><sub>2</sub>PH)<sub>2</sub>] we will demonstrate how the combination of photocrystallography and infrared spectroscopy allows for structural characterization of the photoinduced linkage isomers (PLI) as well as deducing a general scheme for their generation. Furthermore, we will discuss the possibility of selectively addressing one or the other ligand for generation of a NO or NO<sub>2</sub> linkage isomer by choosing appropriate excitation wavelengths.

[1] Casaretto, N., Pillet, S., Bendeif, E.-E., Schaniel, D., Gallien, A.K.E., Klüfers, P. & Woike, T. (2015). IUCrJ, 2, 35-44.

[2] Casaretto, N., Pillet, S., Bendeif, E.-E., Schaniel, D., Gallien, A.K.E., Klüfers, P. & Woike, T. (2015). Acta Crystallographica, B71, 788-797.

[3] Casaretto, N., Fournier, B., Pillet, S., Bendeif, E.-E., Schaniel, D., Gallien, A.K.E., Klüfers, P. & Woike, T. (2016). CrystEngComm, 18, 7260-7268.

[4] Schaniel, D., Bendeif, E.-E., Woike, T., Böttcher, H.-C., Pillet, S. (2018). CrystEngComm, 20, 7100-7108.

## MS31-P10 | PHOTOINITIATED [2+2] CYCLOADDITION REACTIONS OBSERVED IN D-METAL(II) MALONATES WITH N,N'-CONTAINING LINKERS

Vologzhanina, Anna V. (A. N. Nesmeyanov Institute of Organoelement Compounds of RAS, Moscow, RUS); Volodin, Alexander (INEOS, Moscow, RUS); Zorina-Tikhonova, Ekaterina N. (N. S. Kurnakov Institute of General and Inorganic Chemistry of RAS, Moscow, RUS); Sidorov, Aleksei A. (N. S. Kurnakov Institute of General and Inorganic Chemistry of RAS, Moscow, RUS); Chistyakov, Alexandr S. (N. S. Kurnakov Institute of General and Inorganic Chemistry of RAS, Moscow, RUS); Eremenko, Igor L. (A. N. Nesmeyanov Institute of Organoelement Compounds of RAS, Moscow, RUS)

Solid-state photocycloaddition reactions are known as a path to cyclobutane derivatives that proceeds without any solvents or catalysts. We aimed to rationalize the solid-state synthesis of cyclobutane derivatives from coordination compounds with olefins fixed in reactive positions by metal atoms. Information about coordination modes of malonate anions ( $An^{2-}$ ), metal environment,  $M^{II} : An : L$  ratio, and underlying nets of complexes was extracted from the CSD. The most abundant composition, connectivity and periodicity of complexes obtained from  $M^{II} : An^{2-} : L : H_2O$  reaction mixtures were quantitatively estimated. Newly obtained complexes realize highly probable compositions,  $M^{II}$  environment and ligand connectivities [1]. The majority of these complexes also have one of the predicted architectures. The effect of the precursor on the composition and dimensionality of the net was investigated.

Some of complexes underwent photoinitiated homocycloaddition reactions to one of two 1,2,3,4-tetrakis(4-pyridyl)cyclobutane isomers via  $2D \rightarrow 2D$ ,  $3D \rightarrow 3D$  or  $0D \rightarrow 1D$  transformations of complexes. Besides, the first diastereoselective solid-state cross-cycloaddition reaction afforded a racemic mixture of two enantiomers of an unsymmetrical (1*R*,2*S*,3*S*)-substituted cyclobutane derivative in high yield [2].

This work was supported by the Russian Science Foundation (grant 17-13-01442).

[1] E. N. Zorina-Tikhonova, et al. *IUCrJ* **2018**, *5*, 293.

[2] A. D. Volodin, et al. *ChemCommun.* **2018**, *54*, 13861.

## MS31-P11 | MOLECULAR SWITCHES IN NANOCONTAINERS

Diskin-Posner, Yael (Weizmann Institute, Rehovot, ISR); Shimon, Linda (Weizmann Institute, Rehovot, ISR); Samanta, Dipak (Weizmann Institute, Rehovot, ISR); Hanopolskyi, Anton (Weizmann Institute, Rehovot, ISR); Klajn, Rafal (Weizmann Institute, Rehovot, ISR)

Molecular switches, entities that can be toggled between two or more forms upon exposure to an external stimulus, such as light, often require conformational freedom to isomerize. Confining these molecules to volumes only slightly larger than the molecules themselves can alter their properties. Molecular switching events often entail a conformational change that require the confining cage to be flexible enough to adapt to the shape of the guest and allow it enough freedom to successfully switch between the different conformers. In the absence of the cage the photoswitching can be either suppressed or the guest can be excluded from the solubilizing medium.

A very flexible, and adapting to accommodate cage synthesized from triimidazole ligand and Pd(TMEDA)(NO<sub>3</sub>)<sub>2</sub>receptor [1]. The crystals of the cage containing methyl orange and pyrazol are very sensitive to the cryo protectant and undergo a single crystal to single crystal transformation. Even after cage conformational changes and the shifting of guest molecules inside, the crystals still diffract and allow a full single crystal X-ray structure analysis. The crystal structure unit cell volume is relatively large and contains a cage, one or two guest and numerous counter ions and solvent molecules.

These newly synthesized materials are a novel type of information storage medium in which messages could be written and erased in reversible fashion using light.

[1] Samanta D., Mukherjee S., Patil Y.P. & Mukherjee P.S.; *Chem. -A Eur. J.* **18**, 12322-12329 (2012)

## MS31-P12 | DYNAMIC, BREATHING, WATER-STABLE, MIXED-LIGAND ZN(II) METAL-ORGANIC FRAMEWORKS WITH DIFFERING WATER AND VAPOUR SORPTION PROPERTIES

Oliver, Clive L. (University of Cape Town, Rondebosch, ZAF)

Metal-organic frameworks (MOFs) consist of 1-periodic, 2-periodic or 3-periodic metal-organic coordination networks and have attracted widespread attention for their porosity and potential applications in separation chemistry, catalysis, molecular sensing and gas storage.[1] Firstly, we report a partially-fluorinated, 2-periodic MOF,  $[Zn(hfipbb)(bpt)]_n \cdot n(C_3H_7NO)_2 \cdot n(H_2O)$  where  $H_2hfipbb$  = 4,4'-(hexafluoroisopropylidene)bis(benzoic acid) and  $bpt$  = 4-amino-3,5-bis(4-pyridyl)-1,2,4-triazole. This framework undergoes single-crystal-to-single-crystal in solvent exchange with ethanol, dichloromethane and diacetamide, respectively. The solvent-induced 'breathing' of the 2-periodic frameworks results in potential void spaces varying from 15.2-35.4%. In addition, we report the synthesis of a pair of isorecticular mixed-ligand MOFs,  $[Zn(\mu_2-ia)(\mu_2-bpe)]_n \cdot nDMF$  and  $[Zn(\mu_2-mia)(\mu_2-bpe)]_n \cdot n(C_3H_7NO)$ , where  $ia$  = isophthalate,  $mia$  = 5-methoxyisophthalate and  $bpe$  = 1,2-bis(4-pyridyl)ethane. Both structures exhibit entanglement of a pair of neighbouring frameworks to form 2-periodic, 2D bilayers. Despite a lower void space, one of the activated MOFs exhibits significantly higher sorption of carbon dioxide at 195 K, illustrating that small changes in functional groups, even in structurally similar MOFs, may have a large effect on sorption properties.

[1] Zhou, H.; Long, J. R.; Yaghi, O. M. Introduction to Metal-Organic Frameworks. *Chem. Rev.* **2012**, *112*, 673-674.

[2] Chatterjee, N. and Oliver, C.L., *Cryst. Growth Des.* **2018**, *18*, 7570-7578.

[3] Gcwensa, N., Chatterjee, N., Oliver, C.L., *Inorg. Chem.* **2019**, *58*, 2080-2088.

## MS31-P13 | EXCEPTIONALLY FLEXIBLE COORDINATION POLYMERS OF Cd(II)

Pisacic, Mateja (University of Zagreb, Zagreb, HRV); Đaković, Marijana (University of Zagreb, Zagreb, HRV)

Molecular crystals have for a long been considered as brittle, inelastic, and incapable of enduring application of even relatively insignificant mechanical stress without losing their integrity. But recently, there has been a number of examples where crystals can respond to external mechanical stimuli.[1] It was shown that macroscopic mechanical behavior of crystalline material is mostly determined by the strength and geometry of supramolecular interactions as well as their mutual arrangement in a 3-D architecture.

Recently, we have for the first time reported on a class of coordination polymers of cadmium(II) with halopyrazine ligands that display tunable elastic responses to applied mechanical force.[2] To refine our understanding of this unusual phenomenon of metal-organic crystalline materials, here we report on a similar class of coordination polymers of cadmium(II) with pyrazine ligands bearing amide functionalities, capable of forming desired supramolecular topologies that allow us correlation of slight structural changes with a mechanical response. The crystals have also shown excellent elastic response to applied external stimuli that was quantified and structural changes in bent crystals were mapped.

[1] A. Worthy, A. Grosjean, M. C. Pfrunder, Y. Xu, C. Yan, G. Edwards, J. K. Clegg, J. C. McMurtrie, *Nat. Chem.* **10** (2018) 65-69.

[2] M. Đaković, M. Borovina, M. Pisačić, C.B. Aakeröy, Ž. Soldin, B.-M. Kukovec, I. Kodrin, *Angew. Chem. Int. Ed.* **57** (2018) 14801-14805.

## MS31-P14 | THERMO- / MECHANO- MECHANICALLY RESPONSIVE COCRYSTALS DURING SINGLE-CRYSTAL-TO-SINGLE-CRYSTAL PHASE TRANSITIONS

Liu, Guangfeng (Laboratoire de Chimie des Polymères, Brussels, BEL); Jie, Liu (Université Libre de Bruxelles, BEL); Xutang, Tao (Université Libre de Bruxelles, BEL); Qichun, Zhang (Université Libre de Bruxelles, BEL)

Molecular cocrystals, especially charge-transfer co-crystals, have been found to exhibit distinct optical, electrical and magnetic properties, but they can also show mechanically responsive behaviors under a thermo-, mechano-, or photo- stimulation [1]. However, in this field, understanding structure-property relationships are still lacking. Thus, we utilized a series of *in situ* techniques (i.e., optical microscope, XRD, AFM and TEM) to observe the thermo- / mechano- responsive behaviors and single-crystal-to-single-crystal phase transitions in cocrystals and coordination polymers. Some interesting phenomena were found during these experiments, including mechano-mechanically responsive oriented single-crystal-to-single-crystal phase transitions in 8-hydroxyquinoline-Based cocrystals ( $\text{CuQ}_2\text{-TCNQ}$ , and  $\text{PdQ}_2\text{-TCNQ}$ ) [2]; self-healing behavior in thermo-mechanically responsive coronene-TCNB cocrystals [3]; and nanoparticles-mediated migration and oriented attachment during a crystallization process in  $[\text{Ni}(\text{quinolone-8-thiolate})_2]$  ( $[\text{Ni}(\text{qt})_2]$ ) [4] The results indicated that molecular cocrystal is an excellent research platform for studying the mechanically responsive crystalline material.

[1] a) P. Naumov, et. al., Chem. Rev. 2015, 115, 12440-12490, b) G. Liu, et.al., Angew. Chem., Int. Ed. 2018, 57, 1928-1932.

[2] a) G. Liu, et.al., J. Am. Chem. Soc. 2014, 136, 590-593, b) G. Liu, et.al., Chem. Asian J. 2016, 11, 1682-1687.

[3] G. Liu, et.al., 2017, Angew. Chem., Int. Ed. 56, 198-202.

[4] G. Liu, et.al., J. Am. Chem. Soc. 2015, 137, 4972-4975.

## MS31-P15 | SEPARATION OF ISOMERS BY HOST-GUEST CHEMISTRY: POLYMORPHISM, RESOLUTIONS AND TEMPLATING.

Nassimbeni, Luigi (University of Cape Town, Rondebosch, ZAF)

Separation by enclathration is a useful technique when the compounds to be separated have similar physico-chemical properties, as often occurs with isomers. The Werner host  $\text{Ni}(\text{NCS})_2(4\text{-phenylpyridine})_4$  has been employed to separate 1- and 2- methyl-naphthalenes. The crystals formed from a methanol-solution change colour from purple to blue, with a concomitant change to a new polymorph. The kinetics of this process have been studied. A second study deals with the separation of methylcyclohexanones with the chiral host deoxycholic acid. Competition experiments between 2-methyl- and 3-methyl- cyclohexanones result in (S)-2-methylcyclohexanone predominating and acting as a template throughout the selectivity profile of the 2-methyl- and 3-methyl(rac)-cyclohexanones.

## MS31-P16 | STRUCTURE / REACTIVITY RELATIONSHIPS FROM DETAILED REACTION MECHANISMS

Roodt, Andreas (Univ of the Free State, Bloemfontein, ZAF); Mokolokolo, Pennie P (Univ of the Free State, Bloemfontein, ZAF); Alexander, Orbett T (Univ of the Free State, Bloemfontein, ZAF); Kama, Dumisani V (Univ of the Free State, Bloemfontein, ZAF); Brink, Alice (Univ of the Free State, Bloemfontein, AUT); Schutte Smith, Marietjie (Univ of the Free State, Bloemfontein, ZAF)

This presentation addresses some fundamental issues of importance in selected process reactions currently employed or with potential scope to be implemented (in industry). Different processes were chosen and include examples from homogeneous catalysis, radiopharmaceutical models, with some comment aimed at environmental issues.

Extracts of key points to be discussed include the following:

The first reaction involves the basic oxidative addition of substrates to catalyst models, a *fundamental* process in many a homogeneous catalytic cycle [such as hydroformylation, hydrogenation, carbonylation and others] [1,2]. It will highlight complex (modified) characteristics, substrate behavior and knowledge thereof in predicting outcomes within the process.

A next reaction to be discussed involves *theranostic* models in radiopharmacy and how intimate mechanistic understanding is critical for basic design of agents, whether it is only for diagnostics, or only for therapy, or for both [3]. Some expanded aspects of detailed mechanisms, also of importance in metal beneficiation and green chemistry will be further presented [4].

[1] S. Warsink, P.D.R. Kotze, J.M. Janse van Rensburg, J.A. Venter, S. Otto, E. Botha, A. Roodt. *European Journal of Inorganic Chemistry* **2018**, 32, 3615.

[2] M.V. Dobrynin, C. Pretorius, D.V. Kama, A. Roodt, V.P. Boyarskiy, R.M. Islamova. Rhodium(I)-catalysed cross-linking of polysiloxanes conducted at room temperature. *Journal of Catalysis* **2019**, 372, 193.

[3] A. Frei, P.P. Mokolokolo, R. Bolliger, H. Braband, M.S Tsosane, A. Brink, A. Roodt, R. Alberto. *Chemistry-A European Journal* **2018**, 24, 10397.

[4] M. Schutte-Smith, A. Roodt, H.G. Visser. *Dalton Transactions* **2019**, 48, 9984.

## MS32: New Insights into Non-Covalent Bondings & Tetrel, Pnictogen, Chalcogen...

---

### MS32-01 | CHALCOGEN BONDING IN CRYSTAL ENGINEERING

Resnati, Giuseppe (Politecnico di Milano, Milano, ITA); Scilabra, Patrick (Politecnico di Milano, Milano, ITA); Terraneo, Giancarlo (Politecnico di Milano, Milano, ITA)

The distribution of the electron density in bonded atoms of Groups 14-18 of the Periodic Table is anisotropic and regions of depleted electron density, named  $\sigma$ -holes, are present opposite to the covalent bonds formed by these elements [1]. The electrostatic potential at the atomic surface of these regions is frequently positive and attractive interactions with donors of electron density are formed. Group 16 elements typically form two covalent bonds and can thus have two positive  $\sigma$ -holes interacting with nucleophiles. According to a recent IUPAC Recommendation, these interactions are named chalcogen bond (ChB), in analogy with the halogen bond (HaB), pnictogen bond (PnB), and the tetrel bond (TtB), the analogous interactions between nucleophiles and Group 17, 15, and 14 elements. It will be described how the ChB can be strong enough to function as an effective and robust tool in crystal engineering [2]. Sulfur, selenium, and tellurium can all form ChBs in crystalline solid, the tendency to give rise to close contacts with nucleophiles increasing with the polarizability of the chalcogen. A particular attention will be given to chalcogen containing azoles and their derivatives due to the relevance of these moieties in biosystems and molecular materials.

[1] Cavallo G., Metrangolo P., Pilati T., Resnati G., Terraneo G. (2014) *Cryst. Growth Des.* 14, 2697–2702.

[2] Scilabra P., Terraneo G., Resnati G., (2018) *Acc. Chem. Res.* In press.

## MS32-02 | INTERACTIONS INVOLVING 13-17 GROUPS' ELEMENTS ACTING AS THE LEWIS ACID CENTRES – COMPARISON WITH THE HYDROGEN BOND

Grabowski, Slawomir (University of the Basque Country and Donostia International Physics Center (DIPC), Donostia - San Sebastian, ESP)

The elements of 14th-17th Groups are often characterized by areas of positive electrostatic potential and they act as the Lewis acid centres in interactions labelled as the  $\sigma$ -hole bonds [1]. Numerous elements in planar molecular fragments may also act as the Lewis acid centres through  $\pi$ -holes. In general,  $\pi$ -hole bonds are the corresponding interactions, while these are triel bonds for 13th Group elements) [2]. The above mentioned interactions possess numerous properties similar to those of the hydrogen bond; there is the electron charge transfer from the Lewis base unit to the Lewis acid one. The centre that is characterized by  $\sigma$ -hole or  $\pi$ -hole losses its electron charge as a result of complexation. The strength of these interactions, including hydrogen bonds, increases if the distance between Lewis acid - Lewis base units decreases; the latter effect is connected with the increase of the covalent character of interaction and with the increase of polarization effects. The mechanisms of these interactions are the same or at least they are very similar one to each other. It is important that structural motifs in crystals of species linked by these interactions are also very similar between themselves [2,3].

[1] P. Politzer, J.S. Murray, T. Clark, *Phys. Chem. Chem. Phys.*, 2013, 15, 11178-11189.

[2] S. J. Grabowski, *Phys. Chem. Chem. Phys.*, 2017, 19, 29742-29759.

[3] E. Parisini, P. Metrangolo, T. Pilati, G. Resnati, G. Terraneo, *Chem. Soc. Rev.*, 2011, 40, 2267-2278.

## MS32-03 | CAN MEP VALUES BE USED TO PREDICT THE SUPRAMOLECULAR CONNECTIVITY IN THE CRYSTAL STRUCTURE?

Borovina, Mladen (Department of Chemistry, Faculty of Science, University of Zagreb, Zagreb, HRV); Kodrin, Ivan (Department of Chemistry, Faculty of Science, University of Zagreb, Zagreb, HRV); Đaković, Marijana (Department of Chemistry, Faculty of Science, University of Zagreb, Zagreb, HRV)

Research based on Margaret Etter's Rules [1] has shown that hydrogen and halogen bond donor-acceptor pairings follow a hierarchy based on their strengths which can be correlated with calculated molecular electrostatic potential (MEP) values. Studies conducted on organic systems have shown that it is possible to predict the donor-acceptor pairing if the difference in MEP values is significant. It still remains to be determined if insights obtained for organic systems can be used in a tandem with metal centers.

We have shown in our previous work that MEP values can be used to rationalize the supramolecular connectivity in the metal-organic setting for both hydrogen [2] and halogen [3] bonds. We have also shown that it is possible to use MEP values to predict the supramolecular connectivity in 2,4-pentanedionate (acac)-based complexes ( $\text{Ni}^{\text{II}}$ ,  $\text{Co}^{\text{II}}$ ,  $\text{Cu}^{\text{II}}$ ), equipped with the lactam moiety [4]. The goal of our current research is to determine if it is possible to use MEP values to predict the supramolecular connectivity in systems displaying more conformational freedom. To assess this hypothesis, we used acac-based complexes of  $\text{Co}(\text{II})$  and  $\text{Ni}(\text{II})$  with small heterocyclic ligands equipped with the amide functionality, and here we are reporting on the results.

[1] M. C. Etter, *Acc. Chem. Res.* **23** (1990) 120–126.

[2] M. Đaković et al.; *IUCrJ* **5** (2018) 13–21.

[3] M. Borovina, I. Kodrin, M. Đaković, *CrystEngComm*, **20** (2018) 539–549.

[4] M. Borovina, I. Kodrin, M. Đaković, *Cryst. Growth Des.*, **19** (2019) 1985–1995.

## MS32-04 | PHOSPHORUS CAN DO MORE: P-P STACKING OF PLANAR AROMATIC P5-RINGS

Peresytkina, Eugenia (University of Regensburg, Regensburg, GER); Virovets, Dr. Alexander (University of Regensburg, Regensburg, GER); Scheer, Prof. Dr. Manfred (University of Regensburg, Regensburg, GER)

The directed non-bonding interactions play an important role in modern supramolecular chemistry. Concerning phosphorus, so-called pnictogen bonding is usually mentioned in this context [1]. However, cyclic polyphosphorus ligands open new perspectives for the supramolecular chemistry. Since many years we have been using pentaphosphaferrocenes [ $\text{Cp}^{\text{R}}\text{Fe}(\eta^5\text{-P}_5)$ ] ( $\text{Cp}^{\text{R}}=\eta^5\text{-C}_5\text{R}_5$ , R=Me,  $\text{CH}_2\text{Ph}$ , etc.) as building blocks to obtain coordination polymers and giant supramolecules [2-5]. The X-ray diffraction studies proved that  $\text{cyclo-P}_5^-$  planar aromatic ligand of the pentaphosphaferrocene is capable of the  $\pi$ - $\pi$  stacking interactions with the other aromatic  $\pi$ -systems. The interplanar spacing of 3.5-3.8 Å, parallel arrangement of the aromatic fragments as well as  $^{31}\text{P}$  MAS-NMR data show the presence of intermolecular interaction. These interactions influence the orientation of the guest molecules in the central cavities of the supramolecules [2-4] and the crystal packing in the coordination polymers [5].

Financial support from the ERC grant ADG 339072 is gratefully acknowledged. The research was partly done at the light source PETRA III at DESY.

- [1] L. Brammer (2017) *Faraday Discuss.* **203**, 485.
- [2] E. Peresytkina, et al (2016) *Structure and Bonding* **174**, 321.
- [3] E. Peresytkina, et al (2018) *Chem.-A Eur. J.*, **24**, 2503.
- [4] H. Brake, et al (2019) *Chem. Sci.* **10**, 2940.
- [5] M. Elsayed Moussa, et al (2018) *Eur. J. Inorg. Chem.*, 2689.

## MS32-05 | SUPRAMOLECULAR SYNTHONS ORIENTATION RULE IN THE CRYSTALS OF BENZODIAZEPINES, QUINOXALINES AND BENZIMIDAZOLES AS A PREDICTIVE TOOL IN THE MATERIAL DESIGN

Gubaidullin, Aidar (Arbuzov Institute of Organic and Physical Chemistry, FRC Kazan Scientific Center, Russian Academy of Sciences, Kazan, RUS); Samigullina, Aida (Arbuzov Institute of Organic and Physical Chemistry, FRC Kazan Scientific Center, Russian Academy of Sciences, Kazan, RUS)

Creation of new materials and pharmaceuticals based on heterocyclic compounds require the development of the predictive aspect in the description of their structure in the crystalline state. An empirical rule connecting the type and dimension of supramolecular structures (arising due to non-covalent interactions) with their orientation in the unit cell of the crystal has been first formulated. The latter based on the analysis of new series of benzodiazepines, benzimidazoles and quinoxalines with a wide variation of the substituents. According to the rule, the one-dimensional supramolecular structures are oriented predominantly in the crystals along the smallest unit cell parameter, and two-dimensional layers – along two smallest parameters. The analysis of structural data from CSD for all known titled compounds confirm the versatility of the founded rule, which is associated with the orienting effect of the most pronounced structure-forming interactions in the unit cells. This rule of thumb is also observed in the case of the absence of classical hydrogen bonds in the crystal, as well as in crystals of racemic and enantiopure samples, and various polymorphic modifications, and, probably, is of a more general character, not limited only to the classes of compounds studied by us. This makes it possible not only to predict the supramolecular structure and crystal packing of the benzodiazepines and benzimidazoles, and also to expand the opportunities for targeted design of new nitrogen-containing heterocyclic compounds with desired properties.

This work was partially financially supported by the Russian Scientific Foundation (grant No 17-13-01209).

## MS32-P01 | IN SITU PXRD MONITORING THE MECHANOSYNTHESIS OF METAL-ORGANIC HALOGEN-BONDED COCRYSTALS

Lisac, Katarina (Department of Chemistry, Faculty of Science, University of Zagreb, Zagreb, HRV); Germann, Luzia S. (Max Planck Institute for Solid-State Research, Stuttgart, GER); Etter, Martin (Deutsches Elektronen-Synchrotron (DESY), Hamburg, GER); Dinnebier, Robert E. (Max Planck Institute for Solid-State Research, Stuttgart, GER); Friscic, Tomislav (McGill University, Montreal, QC, CAN); Cincic, Dominik (Department of Chemistry, Faculty of Science, University of Zagreb, Zagreb, HRV)

In the last decade, in situ powder X-ray diffraction (PXRD) monitoring of mechanochemical reactions has become a prominent technique for studying the course and mechanisms of organic and metal-organic solid formation [1]. Following our previous study on mechanochemical syntheses of metal-organic halogen-bonded cocrystals [2], in this work we have investigated mechanosynthesis of cocrystals containing  $\text{CoCl}_2\text{bzpy}_2$  (bzpy = 2-benzoylpyridine) and a halogen bond donor, 1,4-diiidotetrafluorobenzene (14tfib), by in situ PXRD. First, we performed experiments in solution, and have unexpectedly obtained three different products: two cocrystals with different metal-organic unit isomers,  $\text{trans}-(\text{CoCl}_2\text{bzpy}_2)(14\text{tfib})_2$  and  $\text{cis}-(\text{CoCl}_2\text{bzpy}_2)(14\text{tfib})_2$ , and a cocrystal of 1:1 stoichiometry,  $\text{cis}-(\text{CoCl}_2\text{bzpy}_2)(14\text{tfib})$ . In order to determine whether single phases could be prepared, mechanosynthesis of obtained cocrystals was studied by in situ PXRD using synchrotron X-ray radiation. Three different liquid-assisted grinding experiments were monitored: grinding of  $\text{CoCl}_2\text{bzpy}_2$  and 14tfib in the 1:2 molar ratio, one-pot grinding of  $\text{CoCl}_2 \cdot 6\text{H}_2\text{O}$ , bzpy and 14tfib in the 1:2:2 molar ratio and grinding of  $\text{CoCl}_2\text{bzpy}_2$  and 14tfib in the 1:1 molar ratio. All three monitored reactions revealed presence of a cocrystal with cis isomer as an intermediate and fast conversions to a final, thermodynamically more stable product,  $\text{trans}-(\text{CoCl}_2\text{bzpy}_2)(14\text{tfib})_2$ , in less than 10 min. Single crystal X-ray diffraction experiments reveal that dominant supramolecular interactions in all obtained solids are  $\text{I} \cdots \text{Cl}$  halogen bonds. In the trans- cocrystal halogen bonds form 2D networks while in cis-cocrystals 1D chains are formed.

[1] T. Frišćić et al., *Nat. Chem.*, 2013, **5**, 66.

[2] K. Lisac and D. Cinčić, *CrystEngComm.*, 2018, **20**, 5955.

## MS32-P02 | EFFICIENT RECOGNITION OF STEROIDS BY PLANAR AROMATIC MOLECULES: A NOVEL BIOMOLECULAR RECOGNITION MOTIF AND ITS POTENTIAL APPLICATIONS

Topic, Filip (McGill University, Montreal, QC, CAN); Friscic, Tomislav (McGill University, Montreal, QC, CAN)

Traditionally, functional groups attached to the backbone of steroid molecules were seen as the key factors in their molecular recognition and, consequently, their physiological function. However, a systematic study of the cocrystals of steroids with electron-rich, planar aromatic molecules (arenes) by our group has recently revealed the  $\alpha\cdots\pi$  interaction: a previously undescribed interaction mode of steroids involving the  $\alpha$ -face of a steroid and the  $\pi$ -electron system of aromatic molecules. Progesterone was found to reliably engage in  $\alpha\cdots\pi$  interaction with various arenes, whereas other steroids studied so far suggest a strong dependence of this interaction on the fine structural details of the steroid backbone. This mimics the steroid behavior in the biological systems, where small structural differences give rise to significantly different biological functions.

We set out to pursue the cocrystallization of progesterone with a variety of polyaromatic hydrocarbons and heterocycles using the mechanochemical solid-state screening methods developed in our group. Furthermore, we sought to expand the set of steroid cocrystal formers towards biologically and pharmaceutically relevant adrenosterone (a weak androgen), cholest-4-en-3-one (metabolite of cholesterol), exemestane (anticancer drug) and levonorgestrel (used in birth control), all of which exhibit a degree of structural similarity with progesterone. Finally, we investigated the possibility of combining the  $\alpha\cdots\pi$  interaction with known interactions such as hydrogen and halogen bonding to engineer increasingly complex molecular solids.

This presentation will outline our initial findings, which confirm the reliability of the  $\alpha\cdots\pi$  interactions and establish its applicability to steroid molecules beyond progesterone.

## MS32-P03 | INFLUENCE OF THE BASICITY OF HALOGEN BOND ACCEPTORS ON STOICHIOMETRY OF COCRYSTALS WITH 1,3,5-TRIIODO-2,4,6-TRIFLUOROBENZENE

Bedekovic, Nikola (Faculty of Science, University of Zagreb, Zagreb, HRV); Stilinovic, Vladimir (Faculty of Science, University of Zagreb, Zagreb, HRV); Cincic, Dominik (Faculty of Science, University of Zagreb, Zagreb, HRV)

Perfluorinated halogenobenzenes are group of halogen bond donors that include a wide range of compounds with different number of donor atoms, what ultimately allows to synthesize halogen bonded cocrystals with various stoichiometries and crystal packing motifs [1]. In many crystal structures can be observed that molecules that are potential donors of more halogen bonds, participate in bonding with a smaller number of donor atoms [2]. Related to our previous research [3], in this study we have prepared cocrystals of 1,3,5-triiodo-2,4,6-trifluorobenzene (**titfb**) with a series of organic nitrogen bases with different basicities to investigate the influence of the basicity, sterics and topology of halogen bond acceptors to form cocrystals with 3:1 stoichiometry. Out of the 12 used compounds, 3 the most basic acceptors form cocrystals of 3:1 stoichiometry, 2 moderate bases gave cocrystals with 2:1 stoichiometry, while the 7 cocrystals with weak bases have one acceptor bonded to **titfb** molecule. These preliminary results indicate that along with the efficiency of crystal packing, also basicity of the halogen bond acceptor is an important factor in the supramolecular synthesis of compounds with high acceptor:donor ratio [4].

[1] Metrangolo *et. al.*, *Chem. Rev.* **116** (2016) 2478 – 2601.

[2] M. E. van der Boom *et. al.*, *Cryst. Growth Des.* **7** (2007) 386 – 392.

[3] Bedeković *et. al.*, *New J. Chem.* **42** (2018) 10584 – 10591.

[4] W. Bruce *et. al.*, *Cryst. Growth Des.* **10** (2010) 3710 – 3720.

## MS32-P04 | TOWARDS THE LINEAR [S2X]+ SYSTEMS: METAL COMPLEXES AND HALOGEN BONDING

Valkonen, Arto (University of Jyväskylä Department of Chemistry, Jyväskylä); Happonen, Lauri (University of Jyväskylä Department of Chemistry, Jyväskylä); Rissanen, Kari (University of Jyväskylä Department of Chemistry, Jyväskylä)

Halogen bonding (XB) has been defined as a noncovalent interaction between electropositive halogen region and electronegative atom. This rather well established interaction has shown recent importance in many fields of chemistry, like in supramolecular chemistry and molecular recognition. Halonium ions ( $X^+$ ) as donors of that interaction have provided a novel linear functionality, in which two acceptor molecules are bound by two parallel halogen bonds on opposite sides of the central halogen donor ( $X^+$ ). Recently, one of our interests and aim has been the preparation such systems with Sulphur acceptor ligands. These  $S \cdots X^+ \cdots S$  XB systems are much harder to prepare and control than better known  $N \cdots X^+ \cdots N$  systems due to several reasons, like instability of organic Sulphur compounds, two separate acceptor sites of S atom and multivalent behavior of S and X (also Ag) atoms. Although,  $N \cdots X^+ \cdots N$  systems can be obtained via  $N \cdots Ag^+ \cdots N$  complexes, the corresponding route to obtain  $S \cdots X^+ \cdots S$  systems has not been shown, so far, to be possible. To research the preparation of  $S \cdots X^+ \cdots S$  systems and potential utilization of  $Ag^+$  intermediates we have prepared a series of  $S \cdots Y^+ \cdots S$  ( $Y = Ag, Au, I, \dots$ ) complexes for structural characterization. The current presentation sums up the results of these investigations.

## MS32-P05 | INSIGHTS INTO WEAK C-H...F-C INTERACTIONS IN C<sub>6</sub>F<sub>6</sub>:C<sub>6</sub>H<sub>6-N</sub>MEN CO-CRYSTALS USING VARIABLE TEMPERATURE CRYSTALLOGRAPHY TO FOLLOW MOLECULAR DYNAMICS

Cockcroft, Jeremy (UCL, London, GBR)

The development of modern X-ray instrumentation (new sources and detectors) combined with modern software is enabling problems to be tackled in the laboratory that were inconceivable several years ago. One can now solve structures from tiny single-crystals selected from polycrystalline sample in a matter of minutes, e.g. routinely using a “What is This?” approach in CrysAlisPro on a Supernova diffractometer. Combining this with variable temperature PXRD and DSC data has permitted structures to be solved from “single-crystals” that no “self-respecting crystallographer” would have dared touch in the past, for example, structures from broken crystals or ones with high mosaic spread as a consequence of phase transitions.

This talk will present examples of how a daring and patient approach to in-situ crystallography has enabled a detailed understanding of co-crystal adducts formed from C<sub>6</sub>F<sub>6</sub> with a variety of methyl-substituted benzenes across a wide range of temperature and through several phase transitions. In terms of the parent adduct C<sub>6</sub>F<sub>6</sub>:C<sub>6</sub>H<sub>6</sub>, it enabled 25 year old powder neutron data to be analysed extensively. Earlier this year, we solved the structures of both the toluene and p-xylene adducts from SXD data despite PXRD data showing the existence of an apparently highly-destructive transition from 6-fold disorder to 2-fold disorder and then to an ordered state for the former. The talk will demonstrate how software such as CrysAlisPro and ShelXT can be used to tackle these challenging systems in order to enable a deeper understanding of these systems and their phase transitions.

## MS32-P06 | IDENTIFICATION OF NON-COVALENT INTERACTIONS BY HIRSHFELD SURFACE AND ENERGY FRAMEWORKS IN CHALCONE-FLAVANONE ISOMERS

Malecka, Magdalena (University of Lodz, Faculty of Chemistry, Lodz, POL); Checinska, Lilianna (University of Lodz, Faculty of Chemistry, Lodz, POL); Biernacka, Marta (University of Lodz, Faculty of Chemistry, Lodz, POL); Kupcewicz, Bogumila (Collegium Medicum in Bydgoszcz of Nicolaus Copernicus University in Torun, Bydgoszcz, POL)

Chalcones and flavanones are members of flavonoid class, which is one of the most important family of natural products. Chalcones and their derivatives have displayed numerous synthetic applications and have attracted much interest due to their multitarget and broad-spectrum biological activities. They exhibit, among others, antioxidant, antimicrobial, cancer-preventive activity, neuroprotective and hepatoprotective effects.

*ortho*-Hydroxychalcone and flavanone are examples of a molecular switching, these molecules are capable of predictable and reversible conformational changes. Such compounds have become increasingly desirable targets for organic synthesis.

The aim of the study is to analyze non-covalent interactions via Hirshfeld surface approach and pairwise model energy calculations together with energy frameworks visualization for 7 pairs chalcone-flavanone isomers. What is more the electron structure descriptors are also examined in order to find relationship between energetic parameters and structural descriptors.

## MS32-P07 | INTERMOLECULAR HEAD-TO-HEAD INTERACTIONS OF CARBONYL AND THIOCARBONYL GROUPS

Shteingolts, Sergey A. (Arbuzov Institute of Organic and Physical Chemistry, FRC Kazan Scientific Center, Russian Academy of Sciences, Kazan, RUS); Fayzullin, Robert R. (Arbuzov Institute of Organic and Physical Chemistry, FRC Kazan Scientific Center, Russian Academy of Sciences, Kazan, RUS)

In this study, we report unusual head-to-head carbonyl–carbonyl and thiocarbonyl–thiocarbonyl interactions explored for crystalline  $\beta$ -hydroxyketones and drug thiamazole, respectively. Three studied  $\beta$ -hydroxyketones display an ability to form dimensionally different crystal formative motifs ranging from 1D to 3D. Despite the structural differences, primarily in intermolecular interactions, the studied ketones are arranged by the same bicyclic hydrogen-bonded twelve-membered supramolecular synthon, where the  $C=O\cdots O=C$  contact plays a key role. Thiamazole molecules form an analogous  $C=S\cdots S=C$  contact, but observed outside the cyclic  $N-H\cdots S$  bonded supramolecular synthon. These unusual interactions along with all the others that are present in the crystal structures, for instance, classical H-bonds, were investigated by means of quantum-topological analysis of the calculated and experimental electron densities.

This work was financially supported by the Russian Science Foundation (grant No. 17-13-01209).

## MS32-P08 | INTERMOLECULAR CHALCOGEN...HALOGEN INTERACTION IN ORGANIC MOLECULAR CRYSTALS

Kazmierczak, Michal (Adam Mickiewicz University, Poznan, POL); Katrusiak, Andrzej (Adam Mickiewicz University, Poznan, POL)

Interactions between chalcogen and halogen atoms are one of the least investigated type of  $\sigma$ -hole bonding in crystals. The focus of academia is shifted to much frequently occurring halogen and chalcogen bonds. Although, structures where formation of chalcogen...halogen contact is possible are relatively common, there is always probability of creation of competing halogen...halogen or chalcogen...chalcogen contacts in such structures. Axiomatic impossibility to avoid this competition, makes chalcogen...halogen interactions less frequent and as a result harder to investigate. Nevertheless, datamining of the Cambridge Structural Database [1,2] allowed us to reveal group of organic molecular crystals with governing chalcogen...halogen interactions. For this population understanding the nature of this cohesion force is crucial for explaining process of molecular aggregation.

[1] Bruno, I. J., Cole, J. C., Edgington, P. R., Kessler, M., Macrae, C. F., McCabe, P., Pearson, J. & Taylor, R. (2002). *Acta Crystallogr. B.* **58**, 389–397.

[2] Groom, C. R., Bruno, I. J., Lightfoot, M. P. & Ward, S. C. (2016). *Acta Crystallogr. Sect. B Struct. Sci. Cryst. Eng. Mater.* **72**, 171–179.

## MS32-P09 | NON-COVALENT BONDING IN ORGANIC CRYSTALS: A COMBINED X-RAY AND DFT STUDY

Voronina, Julia (N.S.Kurnakov Institute of General and Inorganic Chemistry RAS; A.E.Arbusov Institute of Organic and Physical Chemistry RAS, Moscow, RUS)

The study of non-covalent interactions is an actual problem for both chemists and biologists, materials scientists, physicists and pharmacologists. Such interest is explained by an important role of non-covalent interactions both in the formation of structures of compounds and in biological, biochemical processes, processes of molecular recognition and self-assembly. One of the most relevant areas today is the search and study of structure – property correlations the identification of which allows us to significantly expand our understanding of the flow of various processes and to regulate them. The most widely studied and described non-covalent interactions are of course the hydrogen bonds, however, interest in weaker and much less studied interactions has recently increased.

In this work, using high-resolution X-ray diffraction analysis and DFT calculations performed for a series of crystals of biologically active organic molecules, we analyzed weak non-covalent interactions such as H-bonds, stacking interactions and Lp..pi (cyclic and non-cyclic) one. Their effect on the electronic, molecular and crystal structure of studied compounds, as well as the propensity of related compounds to form certain non-covalent interactions, is discussed in details. Obtained results are important from the fundamental point of view and as a contribution to crystal engineering concept.

The X-ray measurements were performed using shared experimental facilities supported by IGIC RAS state assignment. The work was done with the financial support of the Russian Science Foundation (project #17-13-01209).

## MS32-P10 | STRUCTURAL LANDSCAPE OF Cu(II) COORDINATION COMPOUNDS WITH ISOMERS AND DERIVATIVES OF CYCLIC TRIIMIDAZOLE

Melnic, Elena (Institute of Applied Physics, Chisinau, MDA); Kravtsov, Victor (Institute of Applied Physics, Chisinau, MDA); Lucenti, Elena (Istituto di Scienze e Tecnologie Molecolari - Consiglio Nazionale delle Ricerche and INSTM UdR,, Milano, ITA); Cariati, Elena (INSTM-UdR Milano, Dipartimento di Chimica, Università degli Studi di Milano, Milano, ITA); Forni, Alessandra (Istituto di Scienze e Tecnologie Molecolari del CNR(ISTM-CNR),INSTM-UdR, Milano, ITA); Fonari, Marina (Institute of Applied Physics, Chisinau, MDA)

The interest in functional coordination compounds is motivated by their potential applications in materials science associated with properties of both inorganic and organic constituents. The cyclic triimidazo[1,2- $\alpha$ :1',2'-c:1'',2''-e][1,3,5] triazine,  $L_1$ , emissive in the solid state due to stacking interactions and formation of H-aggregates, was documented as a multidentate ligand capable to assemble Cu(I) halide coordination networks with emissive and NLO behaviour (Licenti *et al.*, 2017; 2019). Starting from copper(II) nitrate or acetate salts and four triimidazole ligands including  $L_1$ , its positional isomer, triimidazo[1,2- $\alpha$ :1',2'-c:1'',5''-e][1,3,5]triazine,  $L_2$ , and two isomeric pyridine-substituted derivatives,  $L_3$  and  $L_4$ , eight Cu(II) compounds are reported: four mono- ( $[Cu(L_2)_4(NO_3)_2]\cdot dmf$ , **1**,  $[Cu(L_2)_4(NO_3)_2]\cdot CH_3CN$ , **2**,  $[Cu(L_2)_2(CH_3COO)_2]$ , **3**,  $[Cu(L_4)_2(NO_3)_2(H_2O)_2]\cdot H_2O$ , **4**), two dinuclear ( $[Cu_2(L_1)_2(CH_3COO)_4]$ , **5**, and  $[Cu_2(L_3)_2(CH_3COO)_4]$ , **6** complexes, and two 1D coordination polymers, ( $\{[Cu_2(L_2)(CH_3COO)_4]_2 [Cu_2(L_2)(CH_3COO)_4 H_2O] 2(H_2O)\}_n$ , **7**, and  $\{[Cu(L_3)(NO_3)_2]\}_n$ , **8**). The Cu(II) atom in **1-4** has either  $N_4O_2$  or  $N_2O_4$  square-bipyramidal coordination cores. Complexes **5-6** include paddle-wheel acetate dimers capped by  $L_1$  or  $L_3$  in axial positions. In the zigzag-like coordination polymer **7** the acetate paddle-wheel dimers, interlinked by bridging  $L_2$  ligand, coordinate via axial positions to Cu(II) atoms by different N-binding sites, being associated in the crystal with discrete  $[Cu_2(L_2)(CH_3COO)_4 H_2O] 2(H_2O)$  dinuclear units. In **8**,  $L_3$  coordinates the metal atom in a chelate mode, while nitrate anions coordinate the metal in a chelate and bidentate bridging modes. The ligands' stacking motifs are traced and discussed. Studies on the emissive properties of selected compounds are currently underway.

**Acknowledgments:** The financial support from bilateral Moldova/Italy project 18.80013.16.03.03/It and ASM-CNR 2018-2019 project is acknowledged.

## MS32-P11 | SOLID STATE STRUCTURE OF PHARMACEUTICALLY IMPORTANT COUMARIN DERIVATIVES FROM IN HOUSE COLLECTED XRPD DATA

Bényei, Attila (University of Debrecen, Debrecen, HUN); Pogácsás, Ákos (University of Debrecen, Debrecen, HUN); Eszenyi, Tibor (Alkaloida R&D Ltd., Tiszavasvári, HUN); Báthori, Nikoletta (Cape Peninsula University of Technology, Cape Town, ZAF)

O-heterocycles show biological activities and coumarin derivatives are known as active pharmaceutical ingredients (APIs) and as antioxidants. Acenocoumarol is an anticoagulant Vitamin K antagonist. Pharmaceutical companies are relentlessly interested in the solid state structure of APIs as they are formed, *i.e.* as powders. Structure determination from X-ray powder diffraction pattern is more difficult than extracting structure from single crystal data (SCXRD). The main problem of this method, often called *ab initio* structure determination, is the inherent loss of data compared to SCXRD. Fortunately, modern X-ray sources, detectors and software resources open new possibilities to solve such difficult problems even using *in house* collected powder diffraction data and minimal sample manipulation. Powder patterns were collected using a Bruker D8 Venture diffractometer equipped with Photon II detector and dual (Mo and Cu) INCOATEC I $\mu$ S 3.0 microsource using Cu K $\alpha$  radiation. The sample was acenocoumarol powder. After indexing it turned out, that the unit cell dimensions are highly unusual, one unit cell axis was rather long. Use of the DASH package, part of the CSD software made it possible to index and integrate the pattern as well as solve and refine the structure. The results suggests, that intramolecular nucleophile addition occurred and a new derivative was formed. By extending the methodology compounds of similar chemical structures such as Trolox were also investigated. Analysis of non covalent interactions will also be reported.

### Acknowledgement

The research was supported by the EU and co-financed by the European Regional Development Fund under the projects GINOP-2.3.2-15-2016-00008, GINOP-2.3.3-15-2016-00004.

## MS32-P12 | EXAMINATION OF THE INTERMOLECULAR AUOPHILIC INTERACTIONS IN THE CRYSTALS OF THE $(\text{ArCOC}=\text{C})(\text{PET}_3)\text{Au}$ AND $[(\text{ArCOC}=\text{C})_2\text{Au}]-[\text{Au}(\text{PET}_3)_2]^+$ COMPLEXES.

Pawledzio, Sylwia (Biological and Chemical Research Centre, Department of Chemistry, University of Warsaw, Warsaw, POL); Makal, Anna (Biological and Chemical Research Centre, Department of Chemistry, University of Warsaw, Warsaw, POL); Wozniak, Krzysztof (Biological and Chemical Research Centre, Department of Chemistry, University of Warsaw, Warsaw, POL)

Due to their specific luminescence [1] or catalytical [2] properties, the chemistry of gold(I) complexes is of great research interest. Apart from that, in some of their supramolecular architectures, aurophilic interactions [3] could be found. The occurrence of these interactions is, among others, strongly related to the relativistic effects and the strength of these interactions is comparable to the strength of hydrogen bonds. Therefore, these interactions compete with other secondary interactions in the crystal packing and could be easily overruled by steric effects [4].

Recently, Głodek *et al.* [1] reported the synthesis of a new type of title complexes. The structures were determined by the X-ray diffraction and their luminescence properties were described.

Herein, we would like to extend the characterization of these complexes and examine the ligand-scrambling influence on their supramolecular architectures. It appears that the steric effects play a decisive role in the crystal packing and aurophilic interactions were only found in the crystal structure of  $[(\text{ArCOC}\equiv\text{C})_2\text{Au}]^-[\text{Au}(\text{PET}_3)_2]^+$ . Therefore, in this study we would like to present a comprehensive comparison of the supramolecular architecture, intermolecular interactions and energy band gaps in these complexes.

[1] Głodek, M. *et al.*, *Dalton Trans.* **47**, 6702–6712 (2018).

[2] Liu, L.-P. & B. Hammond, G., *Chemical Society Reviews* **41**, 3129–3139 (2012).

[3] Bardají, M. & Laguna, A., *Journal of Chemical Education* **76**, 201–203 (1999).

[4] Angermaier, K. & Schmidbaur, H., *Chemische Berichte* **127**, 2387–2391 (1994).

## MS32-P13 | EFFECT OF LOCALIZED NON-BONDING/REPULSIVE INTERACTIONS ON DISTRIBUTION OF ELECTRON DENSITY IN PI-CONJUGATED SYSTEMS

Lindeman, Sergey (Marquette University, Milwaukee, USA)

Putting a local sterical pressure on conjugated pi-bonds can cause the electron density to flow away from the point where the pressure was applied onto less sterically hindered areas of the pi-system. Particularly, such in-plane inter-orbital repulsions are the origin of "Mills-Nixon effect" resulting in benzene rings with localized double bonds (Kekule's structure). An extensive analysis of both own and literature structural data reveals that short intramolecular contacts perpendicular to the plane of the benzene ring have the same effect. The list includes Kekule's structure formation in tripod arene metal pi-complexes along with some 1,3,5-substituted benzene cages and sterically overcrowded organic molecules. The examples of the out-of-plane contacts resulting in the pi-electron depletion for a sole pi-bond are much more numerous. The finding allows for intelligent engineering of pi-electron density distribution in electrophilic substrates.

## MS32-P14 | HYPERVALENT CHALCOGEN-CHALCOGEN HETEROPENTALENES AND THEIR CHARGE TRANSFER ADDUCTS

Levendis, Demetrius (Molecular Sciences Institute, Johannesburg, ZAF); Levendis, Demetrius (Molecular Sciences Institute, Johannesburg, ZAF); Reid, David (University of the Witwatersrand, Johannesburg, ZAF)

The bonding or nonbonding interactions between atoms in molecules are one of the most central concepts in chemistry. In this paper, we consider two types of nonbonding interactions; hypervalent chalcogen---chalcogen and charge-transfer interactions.

For the interaction between sulfur atoms a wide range of S---S distances has been observed. These range from covalent disulfide bonds (2.03(2) Å), hypervalent bonds between sulfur atoms in thiathiophthenes or in bicyclic heteropentalenes (2.42 (5) Å, which we report here), so-called pancake bonds (3.02 (5) Å, for example in dithiadiazolyls) as well as Van der Waals S---S interactions (many shorter than the sum of the Van der Waals radii, 3.60 Å).

Charge-transfer complexes (CTs) have been known for decades. In this work we also investigate the use of substituted heteropentalenes, such as dithia-6-azapentalene, together with strong aromatic donors, such as trinitrobenzene, to generate a new class of charge-transfer adducts showing electrostatic potential complementarity.

Here we report the structures of five new 1,6a-dithia- or diseleno -6-azapentalenes containing hypervalent bonds between two chalcogen atoms, charge-transfer adducts of two of them with 1,3,5-trinitrobenzene and an analysis of the intra- and inter-nonbonding interactions. DFT calculations of different conformers of the heteropentalenes show that the *cis* form is more stable than the *trans* form by about 60 kJ/mol due to the hypervalent S---S interaction.

**Keywords:** charge-transfer complex, heteropentalene, hypervalent bond

## MS32-P15 | SELENOUREAS AS BUILDING BLOCKS IN BINARY AND TERNARY COCRYSTALS

Grguric, Toni (Division of Organic Chemistry and Biochemistry, Ruder Boškovic Institute, Zagreb, HRV); Ward, Jas S. (University of Jyväskylä, Department of Chemistry, Nanoscience Center, Jyväskylä); Rissanen, Kari (University of Jyväskylä, Department of Chemistry, Nanoscience Center, Jyväskylä); Džolic, Zoran (Division of Organic Chemistry and Biochemistry, Zagreb, HRV)

A halogen bond is an attractive non-covalent interaction between an electrophilic region in a covalently bonded halogen atom and a Lewis base and recently it took a prominent role in supramolecular synthesis [1]. Oxygen and nitrogen atoms were predominantly used as acceptors of halogen bond, although there are few examples of heavier atoms such as S, P, As, Sb as acceptors [2].

In recent paper, thioureas were utilized in construction of ternary cocrystal [3]. Giving that bonding nature of sulfur and selenium should be similar; we selected selenoureas as potential candidates in construction of binary and ternary cocrystals. It is known that selenium atoms can act as a hydrogen bond acceptor or even a chalcogen bond donor, but there are only few examples of selenium atom as a halogen bond acceptor.

Cocrystallization of selenoureas and different perfluorohalocarbons with 18-crown-6 led to formation of ternary cocrystals in which molecules of selenoureas formed 2:1 discrete complex with 18-crown-6 via N–H···O hydrogen bonds, while formed aggregates were further connected via I···Se halogen bonds forming 2D or 3D networks.

Acknowledgement: This work has been fully supported by Croatian Science Foundation under the project IP-2016-06-5983.

[1] G. Cavallo, P. Metrangolo, R. Milani, T. Pilati, A. Priimägi, G. Resnati, G. Terraneo, *Chem. Rev.*, 2016., **116**, 2478–2601.

[2] K. Lisac, F. Topić, D. Cinčić, T. Friščić *et. al.*, *Nature Communications*, 2019, **10**, Article number: 61.

[3] F. Topić, K. Rissanen, *J. Am. Chem. Soc.*, 2016, **138**, 6610-6616..

## MS32-P16 | INTERPLAY BETWEEN OCCURRENCE FREQUENCIES OF CHARGED AND NEUTRAL BASE PAIRS IN SMALL MOLECULE CRYSTALS

Cabaj, Malgorzata (University of Warsaw, Department of Chemistry, Biological and Chemical Research Centre, Warsaw, POL); Dominiak, Paulina (University of Warsaw, Department of Chemistry, Biological and Chemical Research Centre, Warsaw, POL)

We searched Cambridge Structural Database for structures containing one of the nucleobases – adenine, guanine, hypoxanthine, thymine, uracil or cytosine – and then made an extensive survey concerning the base pairs they formed. The nucleobases behaved mostly in accordance to their pKa values - hypoxanthine, thymine and uracil did not form any base pairs with protonated molecules, whereas adenine, guanine and cytosine did form charged base pairs. It is interesting that we did not find any statistically important differences between the bonds lengths of charged and neutral base pairs, which suggests that factors like higher-order structure and presence of other molecules in the crystal structure are important enough to outweigh electrostatic repulsion between two cations. The charge of the molecules comes mainly from additional protons located in the molecule ring, which heavily affects their ability to form particular base pairs – it can enable, prevent or not affect the formation at all. It is worth to note that although protonation may enable the formation of new base pair, it does not favor such base pairs. Although there are visible trends in the nucleobases behavior, we found a few structures with base pairs formed from differently protonated molecules or behaving in an unexpected way.

## MS32-P114 - LATE | 2D MATERIALS IN ELECTRON MICROSCOPE

Singh, Rajendra (University of Vienna, Vienna, AUT)

Two dimensional materials are the ideal sample for transmission electron microscopy due to their intrinsically thin structure. These materials also allow to study the electron irradiation effects to individual atoms. Displacement cross section is a measure of the probability for displacing an atom by scattering event and is fully determined by the material dependent displacement threshold energy. It already has been measured for the pristine graphene structure, and we are currently extending the work for the undercoordinated atom at a single vacancy. Transmission electron microscopy also allows the measurement of the corrugation in 2D materials electron diffraction, which is practically impossible to do with any other technique. In our current work involves expanding this study to 2D materials beyond graphene and to van der Waals heterostructures.

## MS32-P116 - LATE | MOLECULAR INTERACTION IN HYDRATES OF 4-METHYLPYPERIDINE AND 4-CHLOROPYPERIDINE

Socha, Pawel (Faculty of Chemistry, University of Warsaw, Warsaw, POL); Dobrzycki, Lukasz (Faculty of Chemistry, University of Warsaw, Warsaw, POL); Cyranski, Michal K. (Faculty of Chemistry, University of Warsaw, Warsaw, POL); Boese, Roland (Faculty of Chemistry, University of Warsaw, Warsaw, POL)

Piperidine is an aliphatic, heterocyclic amine consisting of a six-membered ring. The crystal structure of the amine is known [1]. Our previous research shown that piperidine tends to form several crystalline hydrates with different amounts of water [2]. Importantly, the hydrates with high concentration of water have very similar structures to gas clathrates [3].

The aim of this research was to investigate the impact of the substituent in the piperidine ring on the hydrate formation and to analyze the architecture of obtained structures. Hydrates were grown at ambient pressure, directly on the single crystal diffractometer using IR laser supported *in situ* method [4]. As a result the following phases were obtained: hemihydrate and trihydrate for 4-methylpiperidine and monohydrate and trihydrate for 4-chloropiperidine. Interestingly, both trihydrates have the same L4(6)5(7)6(8) [5] water-layer motif and both melt around 263 K. However, amine-water hydrogen bonds in these crystals are different. Moreover, in the 4--chloropiperidine hydrate halogen-halogen interactions can be found. Among analyzed piperidine derivatives no high water content systems similar to clathrate hydrates were observed what can be attributed to inappropriate shape and size of the investigated molecules.

[1] A.Parkin, I.D.H. Oswald, S.Parsons, *Acta Crystallogr.*, **2004**, B60, 219-227.

[2] Ł.Dobrzycki, P.Socha, A.Ciesielski, R.Boese, M.K.Cyrański, *Cryst. Growth Des.*, **2019**, 19, 1005–1020.

[3] E.D. Sloan, "*Clathrate Hydrates of Natural Gases*", Marcel Dekker, New York, USA, **1990**.

[4] R.Boese, *Z. Kristallogr.*, **2014**, 229, 595–601.

[5] L.Infantes, S.Motherwell, *CrystEngComm*, **2002**, 4, 454–461.

## MS33: Tuning Crystalline Frameworks and Their Applications Through Structural Design...

---

### MS33-01 | UNDERSTANDING THE STRUCTURE-DERIVED FUNCTION OF METAL-ORGANIC FRAMEWORKS AND THEIR APPLICATION IN SEPARATIONS

Asgari, Mehrdad (EPFL Valais, SB-ISIC-LFIM, Sion, CH); Kochetygov, Ilia (EPFL Valais, SB-ISIC-LFIM, Sion, CH); Hudson, Matthew (National Institute of Standards and Technology, Center for Neutron Research, Gaithersburg, USA); Long, Jeffrey R. (Dept of Chemistry & Chemical and Biomolecular Engineering & Materials Sciences Division, University of California, Berkeley, California, USA); Brown, Craig (National Institute of Standards and Technology, Center for Neutron Research, Gaithersburg, USA); Queen, Wendy (EPFL, Sion, CH)

Separations consume an estimated 10-15% of global energy. With the expectation that energy consumption will increase with population growth and the implementation of large-scale carbon capture efforts, there is intensive focus on developing new adsorbents. This feat is difficult, as the differences in the molecules of interest, such as CO<sub>2</sub> and N<sub>2</sub>—the main components in post-combustion flue gas, are minimal. As such, separations require tailor-made adsorbents with molecule specific chemical interactions on their internal surface. One such solution, metal-organic frameworks (MOFs), are constructed by metal-ions or metal-ion clusters that are interlinked by organic ligands. Their unprecedented internal surface areas promote the adsorption of large quantities of guests. Further, the molecular nature of the organic ligands allows structural tunability, the introduction of multifunctional properties, and a modular approach to their design. As such, MOFs offer unmatched opportunities to achieve optimal efficiencies in many separations. New MOFs are regularly reported; however, to develop better materials in a timely manner, the interactions between guests and the internal MOF surface must first be understood. In this presentation, studies focused on understanding the structure-derived function of MOFs will be presented. Particular emphasis will be placed on applying *in-situ* x-ray and neutron diffraction techniques to elucidate small-molecule interactions in several MOF families that undergo extensive chemical substitution. The latter can provide a platform to test the efficacy and accuracy of developing computational methodologies in slightly varying chemical environments, a task that is necessary for their evolution into viable, robust tools for screening hypothetical materials.

## MS33-02 | MODULATED SELF-ASSEMBLY OF HARD AND SOFT POROUS CRYSTALS

Forgan, Ross (University of Glasgow, Glasgow, GBR)

Metal-organic frameworks (MOFs) are network materials comprised of organic ligands connected by metal ion clusters into multidimensional structures that often have permanent porosity. Their chemically addressable structures, combined with their ability to store large quantities of small molecules within their pores, have led to applications in gas storage, heterogeneous catalysis, sensing, and drug delivery, amongst others. Coordination modulation, the addition of monomeric modulators to synthetic mixtures, can tune particle size from nanometres to centimetres, through capping of crystallites (decreasing size) or coordinative competition with ligands (increasing size).

The talk will cover the development of our own modulation techniques for a range of MOFs, describing the versatility of modulation in controlling phase purity and physical properties such as interpenetration, defectivity, and porosity. Our techniques provide access to high quality single crystals of many different MOFs, allowing the subsequent characterisation of their mechanical properties, flexibility upon guest uptake, molecular sponge-like behaviour, single-crystal to single-crystal postsynthetic modification, and the development of fluorescent sensors.

## MS33-03 | RULES FOR DESIGNING ROD METAL-ORGANIC FRAMEWORKS: A TOPOLOGICAL APPROACH

Vaganova, Ekaterina (Samara Center for Theoretical Materials Science (SCTMS), Samara University, Samara, RUS); Alexandrov, Eugeny (Samara Center for Theoretical Materials Science (SCTMS), Samara University, Samara, RUS); Blatov, Vladislav A. (Samara Center for Theoretical Materials Science (SCTMS), Samara State Technical University, Samara, RUS); Proserpio, Davide (Dipartimento di Chimica, Università degli Studi di Milano, Milano, ITA)

We present a comprehensive geometrical-topological taxonomy of 1869 metal-organic frameworks with rod secondary building units (rod MOFs) retrieved from the Cambridge Structural Database. First taxonomy of Rod MOFs was presented in [1]. Our new classification was performed with automatic tools implemented in the ToposPro program package (<https://topospro.com/>). As a result, a knowledge database that contains information on geometrical and topological properties of the MOFs and building units (ligands, linkers and rods) was created. A number of descriptors were identified for ligands (chemical formula, molecular graph, coordination mode), rods (rings, points of extension, topological type, shape), linkers (chemical formula, molecular graph, coordination number) and frameworks (rods orientations, underlying nets). Rod MOFs were arranged according to their complexity (the number and type of constituent components and value of numerical descriptors) and a number of correlations between descriptors were identified.

We have shown that these rules are useful for screening and designing rod MOFs, in particular, chemically and mechanically stable crystalline materials with „breathing“ behavior upon adsorption.

The authors are grateful to the Russian Science Foundation (grant No. 18-73-10116) and Russian Foundation for Basic Research (grant No. 17-57-10001) for financial support.

[1] Schoedel A., Li M., Li D., O’Keeffe M., Yaghi O. M. Chem. Rev., 2016, 116, 12466

## MS33-04 | THE CRYSTALLINE SPONGE METHOD: PITFALLS, CHALLENGES AND SOLUTIONS

de Gelder, Rene (Radboud University, Nijmegen); de Poel, Wester (Radboud University, Nijmegen); Tinnemans, Paul (Radboud University, Nijmegen); Duchateau, Alexander L.L. (DSM Biotechnology Center, Delft); Honing, Maarten (Maastricht University, Maastricht); Rutjes, Floris P.J.T. (Radboud University, Nijmegen); Vlieg, Elias (Radboud University, Nijmegen)

The crystalline sponge (CS) method promises the elucidation of the (absolute) structure of molecules using single-crystal X-ray diffraction and eliminates the need for crystals of the target compound. The target compound is absorbed into a porous host crystal and by applying single-crystal X-ray diffraction to the host-guest complex, structure elucidation of the target compound becomes possible. There are, however, important factors that limit the successful application of the CS method: there is no universal sponge that can host every possible target compound, ordering of guest molecules inside the host framework is rather unpredictable, instability of the crystalline sponges limits the range of molecules that can be investigated and guest exchange may affect the quality of the host-guest crystals.

In this contribution we present our experience with the CS method and attempts to solve the problems mentioned. Powder X-ray diffraction provides a direct view on incorporation of ordered guest molecules and was used to determine the optimal and/or minimal soaking time. Enantiomeric pairs were found to order inside the channels of the host framework when a racemic guest instead of an enantiopure compound is used. Stable MOF hosts based on f-block metals make application of the CS method to a wider array of guests and solvents possible. Cooperative ordering, selective ordering, and joint disorder were observed, dependent on the specific combinations and ratios of guest compounds. Our results show that the CS method still needs a lot of development before it will become generally applicable and accepted by the crystallographic community.

## MS33-05 | EXPLORING THE DYNAMIC GAS ADSORPTION BEHAVIOUR OF A FAMILY OF COORDINATION POLYMERS THROUGH *IN SITU* DIFFRACTION TECHNIQUES

Roseveare, Thomas (The University of Sheffield, Sheffield, GBR); Warren, Mark (Diamond Light Source, Oxfordshire, GBR); Thompson, Stephen (Diamond Light Source, Oxfordshire, GBR); Brammer, Lee (The University of Sheffield, Sheffield, GBR)

Coordination polymers consist of inorganic coordination nodes connected by organic linkers. The construction of these frameworks leads to crystalline materials with void space present for the inclusion of gaseous and solution-phase guests. Typically these materials are considered to be rigid networks, but a growing number of materials have demonstrated dynamic behaviour in response to external stimuli. Typically, dynamic behaviour is inferred by complementary techniques. For example, isothermal gas adsorption studies often result in stepped isotherms or hysteresis suggesting a dynamic structural change. Without *in situ* structural studies, however, it is not possible to definitively show that a stepped adsorption isotherm is due to dynamic structural behaviour of the material. The development of gas cells has made these *in situ* diffraction experiments more accessible, with control of the pressure dosing allowing for recording structural data over a full pressure range.

The work presented focuses on a family of one-dimensional coordination polymers  $[\text{Cu}_2(4\text{-Xbz})_4(\text{pyz})]_n$ , where bz=benzoate, X=F, Cl, Br or I and pyz=pyrazine). Prior work on this family of coordination polymers demonstrated, by volumetric gas adsorption, that they display guest inclusion properties dependent on the halogen present on the benzoate ligand. This work, therefore, sought to better understand how these polymers changed as a function of increasing gas pressure by conducting *in situ* single-crystal and powder synchrotron diffraction studies at Diamond Light Source. This work also explored how functionalising the pyrazine linker affects the uptake properties by using both volumetric gas adsorption and *in situ* diffraction techniques.

## MS33-P01 | TUNABLE POLAR LINKER DYNAMICS IN METAL-ORGANIC FRAMEWORKS

Gonzalez-Nelson, Adrian (Delft University of Technology, Delft); Simenas, Mantas (Vilnius University, Vilnius, LTU); van der Veen, Monique (Delft University of Technology, Delft)

Among the numerous interesting properties of metal–organic frameworks (MOFs), the rotational flexibility afforded by the organic linkers is especially captivating, and has been shown to drastically impact gas adsorption/separation.<sup>1</sup> The use of linkers with polar side groups is particularly interesting, since the dynamics of the resulting rotors could in principle be controlled by an external electric field.<sup>2</sup> Nevertheless, few studies of functionalized linker mobility are available,<sup>3</sup> and the techniques that have been used lack specificity, amounting to an incomplete understanding of the type of motions and the effect of different functionalities. In this work, we present the first comprehensive characterization of linker rotation dynamics in the amino- and nitro-functionalized forms of the renowned MOF MIL-53.

A combined experimental-computational study including broadband dielectric spectroscopy and density functional theory showed that the amine-functionalized linkers are mostly static within the framework, while the nitro-functionalized linkers undergo rotational motions. Both behaviors differ drastically from the dynamics observed in unfunctionalized MIL-53, where phenylene rings perform complete rotations about their axis. The functionalization of MOF linkers thus proves to be an effective strategy to tune their framework dynamics, which could provide a handle to tune several properties of practical importance for future applications.

[1] Yan et al. *JACS* 139, 13349 (2017).

[2] Namsani & Yazaydin O. *Mol. Syst. Des. Eng.* 3, 951 (2018).

[3] Damron et al. *Angew. Chemie* 57, 8678 (2018). Devautour-Vinot et al. *Chem. Mater.* 24, 2168 (2012). Morris et al. *J. Mol. Struct.* 1004, 94–101 (2011). Winston et al. *Phys. Chem. Chem. Phys.* 10, 5188–5191 (2008).

## MS33-P02 | POLARIZED FLUORESCENCE HARVESTED FROM FULLERENES LOADED IN NON-CENTROSYMMETRIC Ni-MOF

Vasylevskiy, Serhii (University of Fribourg, Fribourg, CH); Raffy, Guillaume (Université de Bordeaux, Talence, FRA); Bassani, Dario (Université de Bordeaux, Talence, FRA); Fromm, Katharina (University of Fribourg, Fribourg, CH)

At this ECM-32 we will present a new functional Ni-MOF (Ni(II) metal-organic framework) capable to uptake fullerenes from the solution mixture. The crystal structure of the new Ni-MOF revealed hexagonal channels with sufficient pores size that can accommodate guests such as  $C_{60}$  and  $C_{70}$  inside. However, crystallographically those guests cannot be seen due to high disorder and random distribution in the 1D channels of Ni-MOF, therefore approach of confocal laser scanning microscopy (CLSM) was utilized to visualize and characterize spectroscopically the uptake of  $C_{60}$  and  $C_{70}$  into the pores of Ni-MOF with selective excitation of the crystals of Ni-MOF (Figure 1). Results show that new Ni-MOF has relatively selective uptake of the  $C_{70}$  in comparison to  $C_{60}$ . Results have been evaluated by emission from the single crystals, as well as by lifetime. In addition, the study of polarization of the light harvested from  $C_{60}$  and  $C_{70}$  in the channels indicates that the guests are located close to each other forming excimer emission. Also, evaluation of the selectivity of uptake of the guests was performed using HPLC of the destroyed Ni-MOF. These new results are very promising for producing a new generation of hybrid MOFs for new ultra high surface area materials for uptake energetically valuable gases e.g.  $H_2$ ,  $CH_4$ ,  $CO_2$ .

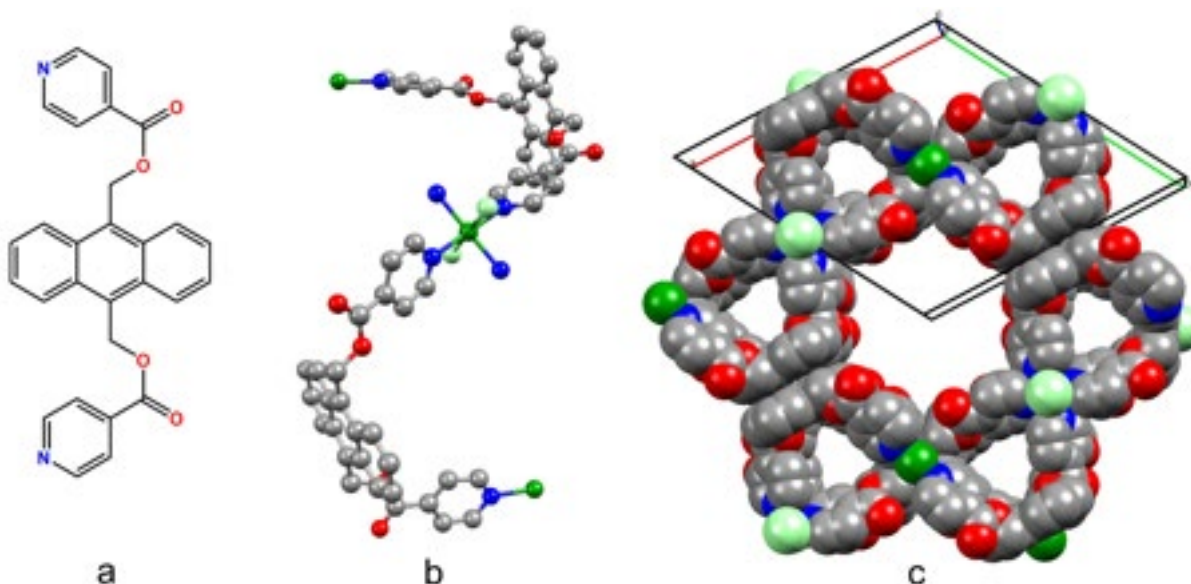


Figure 1. (a) Ligand used to synthesize the Ni-MOF (1), (b, c) functional groups bending, view along the c-axis in the crystal structure

## MS33-P03 | HETEROCYCLIC LIGANDS FOR WATER SORPTION IN METAL–ORGANIC FRAMEWORKS: A STRUCTURAL STUDY USING THE RIETVELD METHOD

Wharmby, Michael (Deutsches Elektronen Synchrotron (DESY), Hamburg, GER); Reinsch, Helge (Christian-Albrechts-Universität Kiel, Kiel, GER); Lenzen, Dirk (Christian-Albrechts-Universität Kiel, Kiel, GER); Wahiduzzaman, Mohammad (Université Montpellier, Montpellier, FRA); Maurin, Guillaume (Université Montpellier, Montpellier, FRA); Stock, Norbert (Christian-Albrechts-Universität Kiel, Kiel, GER)

The application of metal-organic frameworks (MOFs) as water sorbents for de-/humidification and water production applications has grown in popularity in recent years. MOFs constructed from high-valence metals, such as  $Zr^{4+}$  or  $Cr^{3+}$ , have demonstrated good stability under operating conditions (i.e. repeated ad-/desorption cycles under hydrothermal conditions), with a number of  $Al^{3+}$ -based MOFs showing even better stability and water sorption performances. For instance, aluminium isophthalate [ $Al(OH)(O_2C-C_6H_4-CO_2)$ ], also known as CAU-10 (CAU=Christian-Albrechts-Universität), [1] has achieved at least 10,000 water sorption cycles [2]. By replacing the isophthalate unit with structurally similar heterocyclic linker molecules (i.e. 2,6- and 3,5-pyridinedicarboxylic acids or furandicarboxylic acid), three new coordination compounds were obtained, the structures of which were refined by the Rietveld method [3,4]. Two of these have extended 3d-networks and demonstrate promising water sorption properties: CAU-10-pydc and MIL-160 (MIL=Materiaux Institut Lavoisier) [5]. Interestingly both compounds show a displacive phase transition on ad-/desorption of water, which has also been fully characterised. For MIL-160, DFT calculations were used to confirm the locations of water molecules determined during Rietveld refinement. DFT and Rietveld derived sites are in excellent agreement.

[1] H. Reinsch, *et al.*, *Chem. Mater.* **2012**, *25*, 17–26.

[2] D. Frohlich, *et al.*, *J. Mater. Chem. A* **2016**, *4*, 11859–11869.

[3] M. Wahiduzzaman, *et al.*, *Eur. J. Inorg. Chem.* **2018**, *2018*, 3626–3632.

[4] M. T. Wharmby, N. Stock, *Z. Anorg. Allg. Chem.* **2018**, *644*, 1816–1825.

[5] A. Cadiau, *et al.*, *Adv. Mater.* **2015**, *27*, 4775–4780.

## MS33-P04 | SYNTHESIS AND CHARACTERIZATION OF NEW LANTHANIDE MOFs USING A SEMI-FLEXIBLE BIS-IMIDE LIGAND.

González Chávez, Fernando (Universidad Autónoma Metropolitana, Ciudad de México, MEX)

Metal-Organic Frameworks (MOFs) synthesized with lanthanide ions (LMOFs) has been less explored than the MOFs obtained with transition metals, probably because the rationalization of the synthesis of LMOFs is harder due to the variability in the coordination number and flexibility in the coordination geometry. However, the intrinsic properties of the lanthanide ions make attractive the research and its use in the building of new LMOFs because of its potential applications such as sensors, catalyst, magnetism, among others.

In this work we report five isostructural 2D LMOFs, obtained through the solvothermal reaction of the ligand 2,2'-(1,3,5,7-tetraoxo-5,7-dihydropyrrolo[3,4-f]isoindole-2,6(1H,3H)-diyl)dipropionic acid[1] and hydrate nitrate salts of Pr, Eu, Tb, Er, and Tm. The single X-ray diffraction showed that the materials are isostructural and crystallized in triclinic P-1 space group. The lanthanide ions are octacoordinated with 8 oxygens, three from the solvent (DMF) and five from the ligands. Two lanthanide ions are bridged by four carboxylates from the ligands giving place to the SBU. Each SBU is joined by ligands in such a way that 1D chains are obtained. These chains are transversally joined through another ligand resulting in a 2D MOF. The Eu and Tb material showed the characteristics red and green emissions when were excited under UV light. Their emission was enhanced almost four and three times respectively after a partially activation procedure.

[1] Joarder, B., et al., Guest-Responsive Function of a Dynamic Metal–Organic Framework with a  $\pi$  Lewis Acidic Pore Surface. *Chemistry – A European Journal*, 2014. **20**(47): p. 15303-15308.

## MS33-P05 | NOBLE GAS ADSORPTION IN MFU-4L FRAMEWORKS WITH DIFFERENT METAL ATOMS

Magdysyuk, Oxana (Diamond Light Source, Didcot, GBR)

The detailed xenon/krypton gas adsorption and *in situ* X-ray powder diffraction measurements on seven different frameworks with MFU-4l structure [1] under different temperatures and pressures allowed following step-by-step the formation of the first and second adsorption layers in large and small cavities of these frameworks and identification of different structural factors favouring the noble gas adsorption through increasing the isosteric heat of adsorption, as well as precise interpretation of the shape of experimental adsorption isotherms.

Structural investigations revealed the sequence of filling of multiple adsorption sites (up to 10 crystallographically independent positions) in two sequential adsorption layers and formation of quasi-solid structure by adsorbed Xe and Kr atoms (stabilised by van der Waals interaction) above their boiling temperature. The distances between adsorbed Xe or Kr atoms in the cavities are very close to the distances in the solid Xe and Kr, respectively. Our research also revealed that the pore geometry have a critical influence on the noble gas adsorption and can strongly influence the involvement of open metal sites and polarizable linkers into the process of Xe and Kr adsorption.

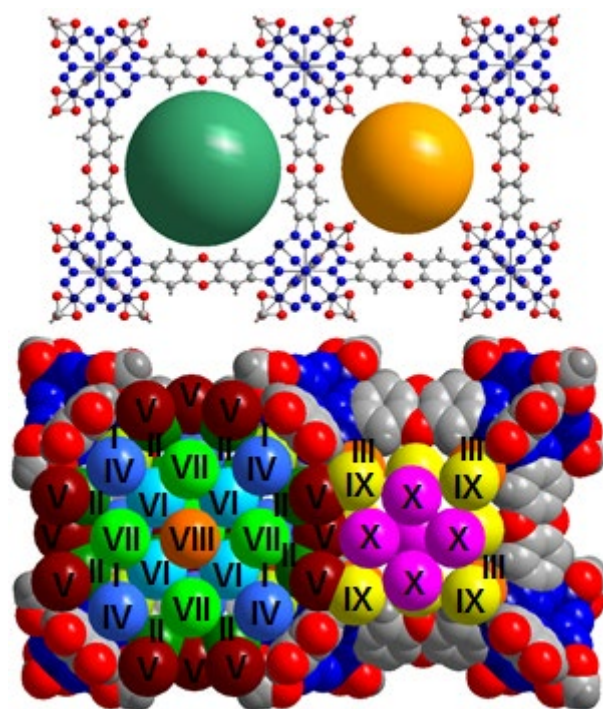


Fig. 1. (top) Crystal structure of MFU-4l framework with two types of alternating cavities: large and small cavities; (bottom) generalized structure of MFU-4l with all 10 positions of Xe atoms occupied (van der Waals radii for all atoms; crystallographically independent positions of Xe atoms are labelled from I to X). Unlabelled atoms: oxygen (red), nitrogen (blue), carbon and hydrogen (gray).

[1] D. Denysenko et al. *Chem. Eur. J.*, **17**, 1837 (2011)

## MS33-P06 | CONTROLLED RELEASE OF NATURAL ESSENTIAL OILS FROM MICROPOROUS METAL-ORGANIC FRAMEWORK

Mazzeo, Paolo Pio (University of Parma, Parma, ITA); Balestri, Davide (University of Parma, Parma, ITA); Carraro, Claudia (University of Parma, Parma, ITA); Perrone, Roberto (University of Parma, Parma, ITA); Fornari, Fabio (University of Parma, Parma, ITA); Bianchi, Federica (University of Parma, Parma, ITA); Careri, Maria (University of Parma, Parma, ITA); Pelagatti, Paolo (University of Parma, Parma, ITA); Bacchi, Alessia (University of Parma, Parma, ITA)

Hollow molecular structures capable of guest inclusion represent an area of raising interest and lie at the forefront of the modern supramolecular chemistry. After the work on the crystalline sponge method by Fujita, MOFs have been considered as good candidate to confine molecular species even in a post-synthetical procedure due to the fine tuning of their properties, such as porosity and framework flexibility.

We focused on the preparation of porous MOFs that can include a number of organic molecules of nutraceutical interest, (i.e. essential oils, EOs), with the final aim of storing them into the framework and subsequently releasing them in a controlled manner. EOs are natural compounds with strong antibacterial attributes, nevertheless, several of their physical-chemical properties – e.g. high volatility, distinct flavour, low thermal and photo-stability – sometimes hampers their direct use as pure substances. These problems can be overcome including them within the crystalline framework of a properly functionalized MOF.

In particular, we report on the stepwise structural evolution of nanoconfined supramolecular aggregates of pure EO or mixtures of different EOs along the whole loading process inside the cavities of a novel flexible MOF (PUM168, Parma University Material); furthermore, we correlated this phenomenon to the structural reorganization of the host framework, elucidating the dynamic interplay between the container and the content. Finally we investigated the stimulated extrusion of the included guests by head-space GC-MS analyses.

This paves the way to the development of functional materials with potential applications in sensing or in the controlled release of chemicals.

## MS33-P07 | LARGE PORE MOFs AS CATALYTIC NANOREACTORS

Vande Velde, Christophe (University of Antwerp, Antwerpen, BEL); Fucci, Rosa (University of Antwerp, Antwerpen, BEL); Cool, Pegie (University of Antwerp, Wilrijk, BEL)

The development of innovative environmentally friendly catalysts is of crucial importance for the establishment of a new sustainable chemical industry. The immobilization of the catalysts on a support can solve problems of selectivity and activity. We propose a scaffold based on Metal Organic Frameworks (MOFs). Under appropriate conditions they can be assembled into a porous material on which we can immobilize catalyst, making possible its recovery/reuse at the end of the process. The advantages of MOFs as scaffolds are clear: uniform, reproducible and controllable manufacture and the possibility of engineering the linkers, in order to control and personalize the whole network structure. These proposed nanoreactors will be designed and synthesized according to modular principles (based on isorecticular synthesis<sup>[1]</sup>). The desired MOFs will have specific characteristics to be used as scaffold for catalyst: pore size in the mesopores range ( $\geq 6\text{nm}$ ), 1-D hexagonal channel structures to help the diffusion of reactants/products<sup>[2]</sup> and easy/fast/cheap to synthesize organic linkers. (Figure 1). The library of long star-shaped linkers will be used for Zr-, La-, In- and Ga-based MOFs in order to obtain the desired 1-D channel topology.

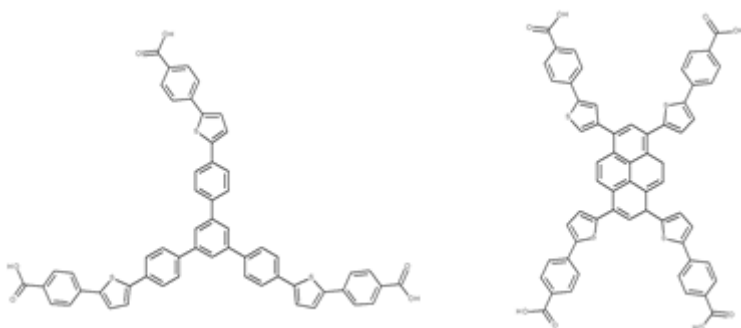


Figure 1. Novel and long linkers for mesoporous 1-D hexagonal MOFs.

[1] Deng, H.; et al. *Science* 2012, 336 (6084), 1018-1023

[2] Čejka, Morris, Nachtigall; *RSC Catalysis Series No. 28* (2017)

[3] Yabo Li et al. *J. Org. Chem.* 2014, 79, 2890–2897

## MS33-P08 | ABOUT THE POLYMORPHISM OF TWO ANTI-INFLAMMATORY DRUGS WITHIN

### THIN FILMS

Kaltenegger, Martin (Laboratoire de Chimie Polymères, Université Libre de Bruxelles, Bruxelles, BEL); Werzer, Oliver (Institute of Pharmaceutical Sciences, University of Graz, Graz, AUT); Resel, Roland (Institute of Solid State Physics, Graz University of Technology, Graz, AUT); Geerts, Yves (Chimie des Polymères, Université Libre de Bruxelles, Bruxelles, BEL)

Investigations on polymorphism play an important role in different fields like materials science, pharmaceuticals etc. Specifically, the capability of different molecules to form polymorphic structures in the vicinity of surfaces appears to be essential in finding new structures of distinct properties. In pharmaceuticals, new polymorphs would for instance affect the bioavailability or shelf-life-time. The present work investigates two anti-inflammatory drugs in thin films: the pro-drug nabumetone and the chiral S-naproxen. Both molecules were dissolved in different solvents allowing thin films fabrication techniques like spinning or drop casting. The X-ray diffraction experiments reveal that nabumetone exists either in form 1 or form 2. Here the concentration as well as the processing speed are the selection criteria; large concentration and slow processing favor the formation of the stable form 1 with standing molecules while lower concentration and faster processing reveals form 2 with the molecules lying on the substrate surface. However, the less stable form 2 recrystallized within 2 months into form 1.

For S-naproxen, mainly form 1 appeared independent from the concentration and the processing speed with upright standing molecules. Only the usage of chlorobenzene resulted in the formation of a new polymorph. The results allow to conclude that nabumetone is more affected by the processing than is the S-naproxen. Nabumetone changes its interaction with the surface so that in form 2 molecules tend to stronger interactions, and the molecules lie down. For S-naproxen the solvent-drug-interaction is more relevant rather than the kinetics like in the case of nabumetone.

## MS33-P09 | PRIOR EVALUATION OF GUEST EXCHANGE IN CRYSTALLINE FRAMEWORK USING PRELIMINARY DIFFRACTION DATA

Hoshino, Manabu (RIKEN, Saitama, JPN); Nakanishi-Ohno, Yoshinori (The University of Tokyo, Tokyo, JPN); Hashizume, Daisuke (RIKEN, Saitama, JPN)

The demand for accurate structure determination of guest molecule in crystalline host framework is rapidly increasing nowadays [1]. Sufficient guest exchange in crystalline framework is a crucial step to achieve definitive structural characterization of a guest molecule by crystal structure analysis. However, degree of guest exchange in a grain of crystal specimen is hardly evaluated until finishing X-ray diffraction data collection and structural analysis with spending a lot of time.

Here we show an analytical methodology for evaluation of guest exchange in crystalline framework using a small preliminary diffraction data. In this methodology, Bayesian inference is adopted for statistically estimating an intrinsic parameter, which represents thermal nature peculiar to a guest molecule, in diffraction data. Just applying this methodology to a few hundreds of diffraction data covering a possibly-wide resolution range for sample screening, guest molecules in crystalline frameworks were successfully distinguished.

Since efficiency of guest exchange is related to unique characters in crystal (e.g., grain size, surface conditions, and crystallinity), crystal specimens are usually nonuniform in degree of guest exchange. We will propose this methodology as a fundamental technology to select the promising crystal for accurate structural characterization of guest molecule in crystalline framework.

[1] M. Hoshino, A. Khutia, H. Xing, Y. Inokuma, M. Fujita, *IUCrJ*, 3, 139-151 (2016).

## MS33-P10 | MECHANOCHEMISTRY AND ELECTRON CRYSTALLOGRAPHY: A WINNING COMBINATION FOR THE DISCOVERY OF NEW METAL-ORGANIC MATERIALS

Lanza, Arianna (Istituto Italiano di Tecnologia, Pisa, ITA); Guagnini, Francesca (Università di Parma , Parma, ITA); Marchetti, Danilo (Università di Parma, Parma, AUT); Righi, Lara (Università di Parma , Parma, ITA); Massera, Chiara (Università di Parma , Parma, ITA); Dal Canale, Enrico (Università di Parma , Parma, ITA); Gemmi, Mauro (Istituto Italiano di Tecnologia, Pisa, ITA)

Mechanochemistry is emerging as a promising environmental-friendly strategy for the preparation of new organic and metal-organic materials in the form of molecular crystals, salts, cocrystals as well as polymeric and framework structures.

This approach drastically reduces the use of solvents and excess reagents in the synthetic process and potentially allows to achieve high conversion while minimizing energy consumption and chemical waste. Moreover, mechanochemical synthesis can allow the formation of products, polymorphs and topologies different from what is obtained with solution methods.

The structural characterization of such new materials is typically complicated by the small crystallite size and multiple twinning induced by the grinding process and the nucleation in almost solvent-free conditions. Conventional single-crystal XRD is therefore not applicable in such cases and also powder methods are extremely challenging, especially in case of large unit cells, low symmetry, severe peak broadening and, not least, because of the difficulty of obtaining pure phases.

In this contribution we will show how the most recent developments in electron crystallography allow successful indexing and structure solution of new mechanochemically synthesized organic and metal-organic materials with different dimensionalities, and even porous structures, overcoming their typical beam sensitivity. In particular, a 1D coordination polymer based on Zn and pyridinedicarboxylate could be expanded by the incorporation of pyridine-based polytopic ligands in the mechanochemical synthesis, obtaining higher dimensional topologies and porous structures. A challenge for electron diffraction is the localization and identification of guest molecules, aiming to a complete characterization of the sorption-desorption properties of these promising framework materials.

## MS33-P11 | ENHANCED SELECTIVITY FOR CO<sub>2</sub> IN MIXED-LIGAND BIS(PYRAZOLATE) ZN(II) MOFs THROUGH DILUTION OF FUNCTIONALIZATION: A STRUCTURAL AND TEXTURAL STUDY

Vismara, Rebecca (Università degli Studi dell'Insubria, Como, ITA); Tuci, Giulia (Istituto di Chimica dei Composti Organometallici, Sesto Fiorentino, ITA); Tombesi, Alessia (Università di Camerino, Camerino, ITA); Di Nicola, Corrado (Università di Camerino, Camerino, ITA); Giambastiani, Giuliano (Istituto di Chimica dei Composti Organometallici, Sesto Fiorentino, ITA); Chierotti, Michele Remo (Università di Torino, Torino, ITA); Bordignon, Simone (Università di Torino, Torino, ITA); Gobetto, Roberto (Università di Torino, Torino, ITA); Pettinari, Claudio (Università di Camerino, Camerino, ITA); Rossin, Andrea (Istituto di Chimica dei Composti Organometallici, Sesto Fiorentino, ITA); Galli, Simona (Università degli Studi dell'Insubria, Como, ITA)

In the past century, the global temperature rose by 0.7 K. CO<sub>2</sub> concentration in the atmosphere, contributing by more than 60% to global warming, overcame 410 ppm in 2019. MOFs are a potential alternative to all-inorganic materials in applications requiring gas adsorption. Their performances can be optimized using one properly functionalized ligand or a mixture therefrom.

The four mixed-ligand MOFs Zn-H/NO<sub>2</sub>, Zn-H/NH<sub>2</sub>, Zn-NO<sub>2</sub>/NH<sub>2</sub> and Zn-H/NO<sub>2</sub>/NH<sub>2</sub>, synthesized employing 4,4'-bipyrazole, 3-nitro-4,4'-bipyrazole and 3-amino-4,4'-bipyrazole, were characterized in the solid state. Their crystal structures were assessed by PXRD, they are isorecticular to the end-members Zn-H [1], Zn-NO<sub>2</sub> [2] and Zn-NH<sub>2</sub> [3], showing a 3-D open frameworks with 1-D square/rhombic channels. The ligand stoichiometric ratio was determined independently, with an excellent agreement, by <sup>13</sup>C CP/MAS solid-state NMR and PXRD. DSC and PXRD, upon application of the Vegard law, confirmed the formation of solid solutions. The four MOFs are thermally stable (T<sub>dec</sub> = 708-726 K) and, as proved by variable-temperature PXRD, show permanent porosity. N<sub>2</sub> adsorption at 77 K revealed BET surface areas in the range 400-600 m<sup>2</sup>/g. CO<sub>2</sub> adsorption capacity, isosteric heat of adsorption (Q<sub>st</sub>) and CO<sub>2</sub>/N<sub>2</sub> selectivity (at 1 bar and 298 K), were compared with those of their end-members. The amino-decorated compounds show higher Q<sub>st</sub> values and better selectivity vs. the nitro-tagged analogues; moreover, tag "dilution" is beneficial compared to the end-members.

[1] C.Pettinari et al. *Inorg.Chem.* 2012, 51, 5235-5245.

[2] N.Mosca et al. *Chem.Eur.J.* 2018, 24, 13170-13180.

[3] R.Vismara et al. *Inorg.Chem.Front.* 2019, 6, 533-545.

## MS33-P12 | SERIAL-MOF: DEVELOPING SERIAL CRYSTALLOGRAPHY METHODS FOR MOF

### NANO-CRYSTALS

De Zitter, Elke (Synchrotron Soleil, Gif-sur-Yvette, FRA); Savko, Martin (Synchrotron Soleil, Gif-sur-Yvette, FRA); Jeangerard, Damien (Synchrotron Soleil, Gif-sur-Yvette, FRA); Tissot, Antoine (Institut des Matériaux Poreux de Paris IMAP, Paris, FRA); Marot, Jerome (Institut Lavoisier de Versailles, Versailles, FRA); Cadot, Emmanuel (Institut Lavoisier de Versailles, Versailles, FRA); Serre, Christian (Institut des Matériaux Poreux de Paris IMAP, Paris, FRA); Shepard, William (Synchrotron Soleil, Gif-sur-Yvette, FRA)

Metal-organic frameworks (MOFs) form a class of porous materials made from metal cores linked together by organic moieties and have diverse functionalities. With the ease of metal node alteration and (post)modification of the organic linkers, the MOF-research field permits the development towards tailor-made solutions to various problems in the field of gas separation, catalysis, energy storage, etc.

Due to their small crystal sizes and high metal content, the structural study of MOFs has been mainly limited to powder diffraction and electron microscopy which do not allow detailed structural investigations. As MOFs form the research topic of an ever increasing number of researchers, new and more powerful methods need to be developed and standardized for the structural study of these porous materials. Here, we show how serial synchrotron crystallography (SSX) provides an answer for this demand. Using ZIF-8 and MIL-100(Fe) crystals of sizes ranging from the sub-micrometer to tens of micrometers, we show different fixed-target strategies for successful crystal delivery, data collection and data processing at the microfocus beamline PROXIMA 2A at SOLEIL. These proof-of-principle studies demonstrate how SSX can overcome hurdles such as small crystal size and radiation sensitivity in the structure determination of small molecules and porous materials – making this strategy accessible to researchers from a broader range research areas.

## MS33-P13 | CRYSTAL ENGINEERING MEETS STEREOCHEMISTRY: INVESTIGATIONS OF THE CRYSTAL STRUCTURES AND RESULTING PROPERTIES OF COPPER COMPOUNDS FEATURING TARTARIC ACID

Kremer, Marius (Institute of Inorganic Chemistry, RWTH Aachen, Aachen, GER); Englert, Ulli (Institute of Inorganic Chemistry, RWTH Aachen, Aachen, GER)

Crystallisation of copper tartrate with TMEDA (Tetramethylethylenediamine) as co-ligand was performed. The experiment was carried out with all available Enantiomers and Diastereomers of tartaric acid (*D*, *L*, *meso*, *rac.*). New crystal structures were found for all resulting compounds. The physical properties of the new materials were investigated, and several different synthetic routes and stoichiometric combinations of the reactants were explored. While most of the obtained compounds crystallise as one-dimensional chain polymers, a discrete trinuclear compound could be obtained for meso tartaric acid. The properties of the new compounds differ significantly from the plain copper tartrate in certain regards. The solubility in Water is drastically increased, for example. Further research could provide new materials for possible industrial or medical applications.

## MS33-P14 | CONSTRUCTING EXTENDED BISMUTH(III) STRUCTURES USING TRIDENTATE ORGANIC LINKERS

Senior, Levi (University of Zurich, Zürich, CH); Linden, Tony (University of Zurich, CH)

Reticular chemistry entails a ‘building block’ approach to developing porous compounds that extend infinitely in 1-3 dimensions [1]. Primarily approached using transition-metal-based nodes, less has been developed around metals with more flexible coordination geometries, such as bismuth.

Bismuth is a non-toxic metal element of known medicinal value – currently used to treat gastrointestinal problems. A small range of metal-organic framework (MOF) materials has been developed through the employment of the same carboxylate-based linkers as used to produce *d*-block-based MOFs [2]. Few instances of polymeric bismuth complexes utilising non-carboxylate organic linking ligands have been reported to date.

We are exploring the structural chemistry of extended bismuth-based frameworks primarily through the tridentate 2,6-pyridinedicarboxylic acid (PDC) backbone as an organic linking moiety [3]. The crystal structures of several Bi-PDC-based coordination polymers are presented and shown to possess a consistent coordination environment from which multidimensional frameworks evolve. A node consisting of bismuth bound by two tridentate PDC moieties is apparent, capable of forming a Bi<sub>2</sub>O<sub>2</sub> cluster through carboxylate bridging interactions. Through this, rigid, charge-neutral frameworks might be constructed in a predictable manner.

[1] H. Furukawa, K. E. Cordova, M. O’Keeffe, O. M. Yaghi, *Science*, 2013 **341**, 6149

[2] G. Wang, Y. Liu, B. Huang, X. Qin, X. Zhang, Y. Dai, *Dalton Trans*, 2015, **44**, 16238-16241

[3] HL. Gao, L. Yi, B. Zhao, XQ. Zhao, P. Cheng, DZ. Liao, SP. Yan, *Inorg. Chem.* 2006, **45**(15), 5980-5988

## MS33-P15 | COORDINATION POLYMERS AND SOLVATOMORPHS – COPPER COMPLEXES WITH AMINO ACIDS AND 2,2'-BIPYRIDINE

Vušak, Darko; Ležaić, Katarina (Faculty of Science, University of Zagreb, Zagreb, HRV); Prugovečki, Biserka (Faculty of Science, University of Zagreb, Zagreb, HRV); Matković-Calogović, Dubravka (Faculty of Science, University of Zagreb, Zagreb, HRV)

Copper complexes with amino acids and heterocyclic bases are interesting systems in crystal engineering due to versatility of noncovalent interactions (hydrogen bonds,  $\pi$ -interactions), which are responsible for different architectures. These type of complexes are also used in medicine, enantioselective synthesis and for molecular recognition.

As part of our investigation of porous materials, coordination polymers and solvatomorphism in copper–amino acidato systems, we report 4 new structures of copper complexes with 2,2'-bipyridine (bpy) and L-alanine (ala), L-valine (val) and L-threonine (thr):  $[\text{Cu}(\text{ala})(\text{H}_2\text{O})(\text{bpy})]_2\text{SO}_4 \cdot 2.5\text{H}_2\text{O}$  (**1**),  $[\text{Cu}(\text{ala})(\text{H}_2\text{O})(\text{bpy})]_2\text{SO}_4 \cdot 2\text{H}_2\text{O}$  (**2**),  $[\text{Cu}(\text{val})(\text{H}_2\text{O})(\text{bpy})]_2\text{SO}_4 \cdot 2\text{H}_2\text{O}$  (**3**), and  $[\text{Cu}(\text{thr})(\text{H}_2\text{O})(\text{bpy})]_2\text{SO}_4 \cdot 4\text{H}_2\text{O}$  (**4**). In cations of mononuclear complex **4** the copper(II) ion is pentacoordinated by *N,O*-donating thr ligand and *N,N'*-donating bpy ligand in the basal plane and an apically coordinated water molecule with close  $\text{C}=\text{O} \cdots \text{Cu}$  contact at unoccupied axial position. 1D coordination polymers **1–3** contain complex cations with Cu(II) ions octahedrally coordinated by didentate ala or val, bpy and carboxyl oxygen atom. **1–4** form infinite double chains through  $\pi$ -interactions of the neighbouring bpy rings, which are interconnected by  $\text{O}-\text{H} \cdots \text{O}$  hydrogen bonds. Water molecules of crystallization are located in pockets between double chains, and, with sulfate ions, serve as hydrogen bond bridges between adjacent chains through  $\text{O}-\text{H} \cdots \text{O}$  and  $\text{N}-\text{H} \cdots \text{O}$  hydrogen bonds.

## MS33-P16 | GIANT SUPRAMOLECULES AS MOLECULAR CONTAINERS

Virovets, Alexander (University of Regensburg, Regensburg, GER); Peresykina, Dr. Eugenia (University of Regensburg, Regensburg, GER); Scheer, Prof. Dr. Manfred (University of Regensburg, Regensburg, GER)

One of the most outstanding areas in the modern coordination chemistry is the rational design of giant supramolecules built up from metal ions connected to each other *via* polytopic ligands resulting in large hollow cages. The systematic approach to the synthesis of hollow supramolecules developed in our group is the coordination of  $\text{Cu}^+$  and  $\text{Ag}^+$  cations to phosphorus atoms of the pentaphosphaferrocenes,  $[\text{Cp}^{\text{R}}\text{Fe}(\eta^5\text{-P}_5)]$  ( $\text{Cp}^{\text{R}}=\eta^5\text{-C}_5\text{R}_5$ ,  $\text{R}=\text{Me}$  ( $\text{Cp}^*$ ),  $\text{CH}_2\text{Ph}$  ( $\text{Cp}^{\text{Bn}}$ ), etc.) [1-3]. The central cavity of these pentaphosphaferrocene-based supramolecules (reaching 0.60–1.35 nm) can include various guest molecules like metastable  $\text{P}_4$  and  $\text{As}_4$ , various neutral and anionic metallocenes and triple-decker complexes, or cage molecules. The hosting supramolecules can often be adjusted to the size, shape and charge of the guest molecules. Moreover, the usage of  $\text{AgSbF}_6$ ,  $[\text{Cp}^*\text{Fe}(\eta^5\text{-P}_5)]$  and  $\text{N}\equiv\text{C}(\text{CH}_2)_n\text{C}\equiv\text{N}$  ( $n=5\text{-}12$ ) linkers allowed us to obtain coordination polymers with giant supramolecular nodes encapsulating  $[\text{Cp}^*\text{Fe}(\eta^5\text{-P}_5)]$  and  $\text{P}_4$  molecules or  $\text{SbF}_6^-$  anion.

Financial support from the ERC grant ADG 339072 is gratefully acknowledged. The research was partly done at the light source PETRA III at DESY.

[1] E. Peresykina, et al (2016) *Structure and Bonding* **174**, 321.

[2] H. Brake, et al (2019) *Chem. Sci.* **10**, 2940.

[3] E. Peresykina, et al (2018) *Chem.-A Eur. J.*, **24**, 2503.

## MS33-P17 | DIRECT STRUCTURE DETERMINATION OF VOLATILE ODOR COMPOUNDS VIA CRYSTALLINE SPONGE METHOD

Kikuchi, Takashi (Rigaku Corporation, Tokyo, JPN)

Three-dimensional structure determination of odor compounds leads to elucidating cause of natural odor and developing artificial flavors or aromas. Single crystal X-ray analysis (SCX), the most powerful tool to determine 3D molecular structure, has rarely been applicable to odor compounds, because they are usually gaseous or volatile liquid compounds, which never crystallize under ambient conditions. Recently, Fujita's group reported that incorporation of analyte compound in a porous coordination polymer, crystalline sponge (CS), enabled SCX of a sub-microgram scale of non-crystalline compounds. Here we present direct 3D structure analysis of volatile odor compounds contained in daily commodities, foods, and aroma oils by SCX assisted by the CS method. Several drops of lime-flavored kitchen detergent were sealed in a capped vial besides a small vial containing one CS crystal and the vial was kept for 1 day at room temperature. The resultant crystal afforded good X-ray diffraction, and structure analysis directly revealed the 3D structure of a compound absorbed in the pore of CS, d-limonene. Although the detergent sample and the CS crystal were spatially separated, vapor of the odor compound diffused into CS to form the inclusion complex. Interestingly, only d-limonene was selectively incorporated in CS from the flavor mixture containing several other terpenoids, presumably because of majority rule or best affinity to the CS pore. We have also tested food samples, wasabi and garlic, and mint oils, and achieved direct structure elucidation of the volatile odor compounds.

## MS33-P19 | COMPLEXATION STUDIES OF CHIRAL CYCLOHEXYLHEMICUCURBIT[N]URIL TO METALLOPORPHYRINS IN SOLID-STATE

Truong, Khai-Nghi (University of Jyväskylä, Jyväskylä); Ustrnul, Lukáš (Tallinn University of Technology, Tallinn, EST); Kaabel, Sandra (Tallinn University of Technology, Tallinn, EST); Aav, Riina (Tallinn University of Technology, Tallinn, EST); Rissanen, Kari (University of Jyväskylä, Jyväskylä)

The main building blocks of living organisms consist of chiral species. On a daily basis, chiral molecules are conventionally used and produced by pharmaceutical, food, agrochemical, perfume, and cosmetics industries. As a result, chiral waste becomes an extremely important issue. These chiral compounds can be ecologically hazardous due to their high biological activity creating a global pollution problem to the environment. Due to the wide distribution of chiral waste, there is a critical need of systems able of stereospecific recognition. Our current EU-project called *INITIO*, INnovative chemical sensors for enantioselective detection of chiral pollutants, is working on the development of low-cost, portable chemical sensor devices which are reliable, sensitive and capable of fast, simple and real-time *in situ* and on site analysis for sensing and discrimination of chiral molecules. The main components of our chiral sensing materials consist of (hemi)cucurbituril and porphyrin derivatives. The deposition of these materials later onto transducer surfaces will allow for testing and validating the new chemical sensor devices with enantiomeric pairs of model analytes.

Here, we report the first complexation products obtained from the reaction of two chiral macrocycles, namely (*all-R,R*)-cyclohexylhemicucurbit[6]uril (cycHC[6]) and (*all-R,R*)-cyclohexylhemicucurbit[8]uril (cycHC[8]), with various metalloporphyrin derivatives in a dichloromethane/methanol solvent mixture.

## MS33-P20 | SYNTHESIS AND CRYSTAL STRUCTURE OF A NEW BIMETALLIC PLATINUM COMPLEX $[\text{Pt}_2(\mu\text{-H})(\mu\text{-PPH}_2)2\text{Br}_2(\text{PPh}_3)_2]$

OUIS, Sakina (Université Mentouri Constantine ALGERIA, Constantine, DZA)

Transition metal hydrides play a central role in many homogeneous catalytic reactions (Bertolasi et al., 1993), they are very important in hydrogenation or hydroformylation. Their characterization is commonly carried out by NMR spectroscopy, X-Ray analysis or neutron diffraction (Ciriano et al., 1978). Hydrides of Pt(II) are the most numerous (Leoni et al., 1995) of any transition metal hydride group; In addition to the presence of the hydride ligand, the complexes invariably have a coordinated phosphine, the pure complexes are usually both air stable and kinetically inert (Roundhill., 1978). We report here the synthesis and structural analysis of a new hydrodo bridged diplatinum complex  $[\text{Pt}_2(\mu\text{-H})(\mu\text{-PPH}_2)2\text{Br}_2(\text{PPh}_3)_2]$ .

The title compound is composed of a triangle formed by two platinum atoms and one phosphorus (P2), the coordination sphere of each platinum is completed with a terminal phosphine (P1, P3) and two bromides (Br1, Br2).

## MS33-P118 - LATE | STABILITY OF NON-TOXIC GAMMA-CYCLODEXTRIN-BASED METAL-ORGANIC FRAMEWORK IN VARIOUS SOLVENTS

Krukle-Berzina, Kristine (Latvian Institute of Organic Synthesis, Riga, LVA); Belyakov, Sergey (Latvian Institute of Organic Synthesis, Riga, LVA); Mishnev, Anatolijs (Latvian Institute of Organic Synthesis, Riga, LVA); Shubin, Kirill (Latvian Institute of Organic Synthesis, Riga, LVA)

Metal-organic frameworks (MOFs) have been known for decades, and they continuously have gained interest because of their potential application in the fields of medicine and pharmacology for drug storage, delivery and controlled release. For use in healthcare applications MOFs need to be toxicologically acceptable to human. Such kind of edible MOFs can be easily obtained from readily available components, e.g.  $\gamma$ -cyclodextrin ( $\gamma$ -CD) and potassium hydroxide.  $\gamma$ -CD has been used to prepare biocompatible and non-toxic MOFs due to the presence of -OCCO- binding groups in the primary and secondary faces, which can be readily used to form complexes with alkali and alkaline earth metal ions.

In this study  $\gamma$ -CD-based metal ( $K^+$ ) MOF ( $\gamma$ -CD-MOF-1) was synthesized as described in [1] and its stability in various solvents was verified by single-crystal X-ray structure analysis. Symmetry changes of the examined crystals from cubic to orthorhombic was observed in diethyl ether, dichloromethane (DCM) and toluene. The symmetry of the  $\gamma$ -CD-K crystal is lowered. Major changes of the sample crystals occurred in DCM and toluene, where two  $\gamma$ -CD molecules are bonded by 4 potassium cations, whereas in  $\gamma$ -CD-MOF-1 8 potassium cations are bonded to one  $\gamma$ -CD molecule. Thereby  $\gamma$ -CD tori arrangement in crystal structure is different if compared to  $\gamma$ -CD-MOF-1 and the ( $\gamma$ -CD)<sub>6</sub> cubes are not observed in these crystals. Meanwhile, packing similarity to the mother crystal along the *a* direction is maintained.

[1] Smaldone, R. A.; et al. Metalorganic frameworks from edible natural products. *Angew. Chemie - Int. Ed.* **2010**, 49, 8630–8634.

## MS33-P120 - LATE | THE CRYSTALLINE SPONGE METHOD FOR THE STRUCTURAL DETERMINATION OF NON-CRYSTALLINE COMPOUNDS USING METAL ORGANIC FRAMEWORK

Habib, Faiza (University College London, London, GBR)

The crystalline sponge method [1,2] allows the absolute structural determination of non-crystalline compounds such as powder, amorphous solid, liquid, volatile matter or oily state. It involves using a porous framework material such as metal-organic frameworks (MOFs) as crystalline sponge, into which non-crystalline compounds in the solution can be soaked and arrange themselves in a regular pattern with the help of specific interactions between MOF pores and the guests. Thus, allowing molecular structure determination of non-crystalline compounds along with the framework via single crystal X-ray diffraction.

We are focused on structure determination of terpenoids into the pores of  $[[\{ZnI_2\}_3(\text{tris}(4\text{-pyridyl})\text{-}1,3,5\text{-triazine})_2 \cdot x(\text{solvent})_n]$  MOF or crystalline sponge. In this work, we present two novel inclusion compounds with geraniol and  $\beta$ -damascone in the pores  $[[\{ZnI_2\}_3(\text{tris}(4\text{-pyridyl})\text{-}1,3,5\text{-triazine})_2 \cdot x(\text{solvent})_n]$  crystalline sponge along with the experimental details and showing guest-host interactions.

[1] Y. Inokuma, S. Yoshioka, J. Ariyoshi, T. Arai, Y. Hitora, K. Takada, S. Matsunaga, K. Rissanen and M. Fujita, *Nature*, 2013, **501**, 262–262.

[2] M. Hoshino, A. Khutia, H. Xing, Y. Inokuma and M. Fujita, *IUCrJ*, 2016, **3**, 139–151.

## MS33-P122 - LATE | USING METAL ORGANIC FRAMEWORKS TO DETERMINE THE CRYSTAL STRUCTURES OF NON-CRYSTALLINE COMPOUNDS

Lunn, Richard (University College London, London, GBR); Tocher, Derek (UCL Department of Chemistry, London, GBR); Sidebottom, Philip (Syngenta, Kealott's Hill International Research Centre, Berkshire, GBR); Montgomery, Mark (Syngenta, Kealott's Hill International Research Centre, Berkshire, GBR); Keates, Adam (Syngenta, Kealott's Hill International Research Centre, GBR); Carmalt, Claire (GBR)

Publication of the crystalline sponge (CS) method by Fujita *et al.* in 2013<sup>1</sup> provided a major advancement in the structural elucidation of non-crystalline compounds using single crystal X-ray diffraction. This method involves soaking a metal-organic framework (MOF) in a solution of the target compound, the target can then enter the MOF pores where it is ordered and held in place by host-guest intermolecular interactions. The most commonly used crystalline sponge,  $\{[\text{ZnX}_2]_3(\text{TPT})_2\} \cdot x(\text{solvent})\}_n$  (TPT = 2,4,6-Tri(4-Pyridyl)-1,3,5-triazine), is limited by the size ( $8 \times 5 \text{ \AA}^2$ ) and the hydrophobic nature of the pores, therefore, alternative MOFs are needed to overcome these limitations.

In this work, novel inclusion complexes of a fungicide and herbicide are reported within the pores of the host  $\{[\text{ZnBr}_2]_3(\text{TPT})_2\} \cdot x(\text{CHCl}_3)\}_n$ . Additionally, simple aromatic compounds were successfully encapsulated into a copper-based MOF which was investigated as a crystalline host due to the hydrophilic nature of the MOF, suitable pore sizes ( $24 \text{ \AA} \times 9.6 \text{ \AA}$  and  $12.7 \text{ \AA} \times 12.7 \text{ \AA}$ ) and low symmetry space group ( $P2_1/c$ ).

# MS34: Computer Simulation of Molecular Interactions and Crystal Structures

---

## MS34-01 | TOWARDS THE DESIGN OF MOLECULAR MATERIALS

Brandenburg, Gerit (Heidelberg University, Heidelberg, GER)

New technologies are made possible by new materials, and until recently new materials could only be discovered experimentally. However, quantum mechanical approaches are now integrated to many design initiatives in academia and industry, underpinning efforts such as the computational crystal structure prediction (CSP [1]). The latest CSP blind test revealed two major remaining challenges:[2] (i) Dealing with a vast search space, in particular for molecules with increased flexibility. (ii) Crystal polymorphs are often separated by just a few kJ/mol, exceeding the accuracy of density functional approximations (DFAs). Cost-effective electronic structure methods will be presented that gain up to four orders of magnitude in computational speed compared to traditional DFAs and are suited for optimizing a huge number of putative crystal structures [3]. Promising applications to the CSP of pharmaceutical-like molecules have been demonstrated recently [4]. On the other hand, recent developments in Quantum Monte-Carlo make it feasible to molecular crystals and we are now able to predict static lattice energies with potentially sub-chemical accuracy [5].

[1] S.L. Price, *JGB, Molecular Crystal Structure Prediction*; Elsevier Australia, **2017**, 333-364.

[2] A.M. Reilly, et al. *Acta. Cryst. B* **2016**, 72, 439.

[3] E. Caldeweyher, *JGB, J. Phys.: Condens. Matter* **2018**, 30, 213001.

[4] L. Iuzzolino, P. McCabe, S.L. Price, *JGB, Faraday Discuss.* **2018**, 211, 275.

[5] A. Zen, *JGB*, J. Klimeš, A. Tkatchenko, D. Alfè, A. Michaelides, *Proc. Natl. Acad. Sci. USA* **2018**, 115, 1724.  
gerit-brandenburg.de

## MS34-02 | TOWARDS CRYSTAL STRUCTURE SOLUTION OF ORGANIC COMPOUNDS BY FIT TO THE PAIR DISTRIBUTION FUNCTION WITHOUT PRIOR KNOWLEDGE OF SPACE GROUP AND LATTICE PARAMETERS

Prill, Dragica (Goethe University Frankfurt am Main, Frankfurt am Main, GER); Schlesinger, Carina (Goethe University Frankfurt am Main, Frankfurt am Main, GER); Habermehl, Stefan (Goethe University Frankfurt am Main, Frankfurt am Main, GER)

Local structures in crystalline, nanocrystalline and amorphous compounds can be investigated using pair distribution functions (PDFs). However, the fit of structural models to the PDF curve has rarely been done for organic compounds. In our previous research, the method developments for structure determination from PDF were successful with determination of molecular position and orientation starting from random values [1]. Experimental lattice parameters and space group have been given as an input. For many nanocrystalline organic compounds the space group and lattice parameters are unknown. Therefore, a global procedure in which the lattice parameters, the space group, the molecular position and orientation are determined from PDF-Data has been developed [2]. The calculations initiate with a large set of random starting structures in various space groups using FIDEL Software [3]. The space groups have been chosen according to the space group frequency [4]. The optimisation of lattice parameters starts from random values within the sensible range. The ranges are chosen depending on the size of the investigated molecule and space group in which the calculations are performed. The optimisation calculations have been carried out using TOPAS Software [5].

[1] D. Prill et al., *Acta Cryst. A*, 2015, 72, 62.

[2] D. Prill, C. Schlesinger, S. Habermehl, *in preparation*.

[3] S. Habermehl et al., *Acta Cryst. B*, 2014, 70, 347.

[4] E. Pidcock et al., *Acta Cryst. B*, 2003, 59, 634.

[5] A. A. Coelho, *J. Appl. Cryst.*, 2018, 51, 210.

## MS34-03 | CLPDYN: A CHEAP AND RELIABLE TOOL FOR MOLECULAR DYNAMICS STUDIES OF ORGANIC MOLECULES IN CONDENSED PHASE

Lo Presti, Leonardo (Università degli Studi di Milano, Milano, ITA); Gavezzotti, Angelo (Università degli Studi di Milano, Milano, ITA)

We present CLPdyn, a freely available code intended to perform Molecular Dynamics simulations of organic molecules in condensed phase.[1–3] CLPdyn can handle both continuous phases (liquids, crystals) and finite-size clusters (liquid droplets, nanoparticles), and exploits the thoroughly tested Coulomb-London-Pauli atom-atom intermolecular potential[4,5]. The implementation relies on standard MD algebra, but also includes new algorithms, specifically designed to deal with isolated clusters, to (i) suppress net overall translational and rotational momenta, (ii) handle the evaporation of molecules from the cluster surface, and (iii) measure the amount of residual symmetry from the number and kind of isometries present in the cluster. Application to organic solvents (benzene, chloroform, methanol and pyridine) [2] and crystals spanning very different intermolecular recognition patterns (maleic/succinic anhydrides, alanine/glutamic acid, methylurea, 1,4-cyclohexadiene and methyl-2-amino-5-hydroxybenzoate) [3], shows that CLPdyn reliably reproduces macroscopic thermodynamic quantities, and highlights the effect of the relative strengths of intermolecular forces on rotational correlation times, self-diffusion coefficients and pair distribution functions. Possible applications of CLPdyn to the molecular-level study of non-equilibrium solution chemistry, including the early stages of crystal nuclei formation, are also discussed.

[1] A. Gavezzotti, CLPdyn, Monte Carlo and Molecular Dynamics modules, Description and user manual, [www.angelogavezzotti.it](http://www.angelogavezzotti.it) (2018).

[2] A. Gavezzotti, L. Lo Presti, *New J. Chem.*, 2019,43, 2077-2084.

[3] A. Gavezzotti, L. Lo Presti, in preparation

[4] A. Gavezzotti, *New J. Chem.* 2011, 35, 1360–1368.

[5] A. Gavezzotti and L. Lo Presti, *Crystal Growth Des.* 2016, 16, 2952–2962.

## MS34-04 | COMPUTATIONAL PROTOCOL FOR SIMULATING THE ANISOTROPIC LATTICE EXPANSION IN ORGANIC CRYSTALS

Ienco, Andrea (CNR-ICCOM, Sesto Fiorentino, ITA); Paoli, Paola (Department of Industrial Engineering, University of Florence, Florence, ITA); Rossi, Patrizia (Department of Industrial Engineering, University of Florence, Florence, AUT)

The anisotropic lattice expansion is a different variation of one crystallographic axis respect the other ones. In a temperature dependent X-Ray Powder Diffraction experiment, the anisotropic lattice expansion can be visualized as a significant shift of a set of peaks while others practically did not move. As a consequence, the anisotropic expansion could lead wrong conclusions on the purity and/or composition of a crystalline phase.

We observed anisotropic lattice expansion for metoprolol succinate salt ( metoprolol = ( $\pm$ )-1-isopropylamino-3-[4-(2-methoxy-ethyl)-phenoxy]-propan-2-ol) salt. For the related and structural close, metoprolol tartrate salt no such behavior was found. [1] Moreover also the metoprolol free base is subject to anisotropic expansion while the related betaxolol, with similar solid state arrangement and very small structural difference, expands isotropically. [2]

In this work, we show that semiempirical HF-3c method [3] is able to reproduce the experimental observations at a reasonable computational cost within the standard error in reproducing crystal structures. [4] Our protocol could help to shed some light on the anisotropic lattice expansion in organic crystals and to rationalize the factor responsible for the phenomenon.

[1] P. Paoli, P. Rossi, E. Macedi, A. Ienco, L. Chelazzi, G. L. Bartolucci, B. Bruni *Cryst. Growth Des.* 2016, 16, 789.

[2] P. Rossi, P. Paoli, L. Chelazzi, L. Conti, A. Bencini *Acta Cryst.* 2019, C75, 87.

[3] R. Sure, S. Grimme *J. Comput. Chem.* 2013, 34, 1672.

[4] M. Cutini, B. Civalleri, M. Corno, R. Orlando, J. G. Brandenburg, L. Maschio, P. Ugliengo *J. Chem. Theory Comput.* 2016, 12, 3340.

## MS34-05 | ANALYSING AROMATIC INTERACTIONS: CLARITY OUT OF COMPLEXITY

Sovago, Ioana (Cambridge Crystallographic Data Centre, Cambridge, GBR); Wood, Peter (Cambridge Crystallographic Data Centre, Cambridge, AUT); McCabe, Patrick (Cambridge Crystallographic Data Centre, Cambridge, AUT); Pulido, Angeles (Cambridge Crystallographic Data Centre, Cambridge, GBR); Stevens, Joanna (Cambridge Crystallographic Data Centre, Cambridge, GBR)

The fundamental understanding of crystal structures and the structural drivers for stability is a key topic within chemical crystallography, as well being critical in an industrial context, particularly for the pharmaceutical and agrochemical industries. Here at the CCDC, we have been developing a suite of structure-based methods to help scientists better understand their crystal forms; to assess the stability and predict likely outcomes.

Currently, the community's solid form analysis methods focus mostly on analysing the quantity and quality of hydrogen bonds. This has been shown as a reasonably reliable indicator of solid form stability in systems where hydrogen bonding is present and dominant. There are, however, many solid forms where hydrogen bonds do not dominate, or are missing entirely. In these cases, the ability to analyse additional types of interactions is needed to rapidly provide a more holistic assessment of a crystal structure. Aromatic interactions are known to be another important interaction type for solid form stability and particularly so when hydrogen bonds are weaker, or not present.

We have developed a method to visualise and assess the strength of aromatic interactions in the context of a crystal structure, without needing to manually measure any geometric parameters. Using a sophisticated machine-learning approach, trained on high-level DFT-D3 energy calculations of benzene-benzene dimers, we can score phenyl ring-ring interactions quickly just from the observed geometry. The addition of effective assessment of phenyl-phenyl interactions to our solid form analysis toolbox takes us a big step closer towards more complete understanding of solid forms.

## MS34-P01 | CRYSTAL STRUCTURE AND HIRSHFELD SURFACE ANALYSIS OF 1,3,4-THIADIAZOL DERIVATIVE

TABTI, Charef (UNIVERSITY OF MOSTAGANEM, MOSTAGANEM, DZA)

1,3,4-thiadiazol derivative has been synthesized. Its structural properties were investigated using density functional theory (DFT) by employing B3LYP with 6-311G (d,p) basis set. Its crystalline structure was determined using X ray diffraction data. The theoretical results from DFT are in good agreement with the X ray diffraction. A good agreement with the structure determined from the single crystal measurements was found. Hirshfeld surface analyses (HS) and spectral analysis using IR, RMN-<sup>1</sup>H and RMN-<sup>13</sup>C were performed. The frontier molecular orbitals (HOMO and LUMO) were simulated. They showed a small energy gap which confirms that charge transfer takes place. Electrostatic potential (MEP) surface was simulated demonstrating the existence of reactive sites in the title molecule. Nonlinear optical (NLO) behavior of the examined molecule was investigated by the determination of the electric dipole moment  $\mu$ , the polarizability  $\alpha$  and the hyperpolarizability  $\beta$  using the B3LYP method.

## MS34-P02 | USE OF CRYSTAL STRUCTURE PREDICTION TO DESIGN TEMPLATE

### CRYSTALLIZATION EXPERIMENTS OF NITROBENZOIC ACID DERIVATIVES

Berzinš, Agris (University of Latvia, Riga, LVA); Actinš, Andris (University of Latvia, Riga, LVA)

Crystal structure prediction of ansoivates and monohydrates of three 2-substituted 4-nitrobenzoic acids were used to obtain information about the theoretical crystal structure energy landscape. Substituents included in the study were chlorine (2C4NBA), methyl (2Me4NBA) and hydroxyl (2OH4NBA). The obtained structure landscapes were analysed by searching for structures isostructural to the experimental crystal structures of the studied derivatives. This analysis for ansoivates clearly showed that most of such isostructural structures are present in the generated landscapes with part of the structures being energetically competitive or even more stable than the experimentally obtained polymorphs of the respective compound. In monohydrate landscape of 2Me4NBA isostructural phase to the only experimentally obtained monohydrate (2C4NBA monohydrate) was present, while the obtained landscape of 2OH4NBA monohydrates suggested that the obtained landscape is incomplete and doesn't contain all relevant structures. Crystallization experiments in the presence of seed crystals of the other compounds have been initiated to evaluate whether the predicted structures are experimentally accessible. The attempts to crystallize monohydrates of 2Me4NBA and 2OH4NBA in absence and presence of seeds of 2C4NBA monohydrate were unsuccessful.

Crystal structure prediction was performed using CrystalPredictor and lowest energy structures were optimised with CrystalOptimizer. This research was carried out at UCL in the laboratory of Prof. Sally Price. The research was funded by the European Regional Development Fund, within the Project activity 1.1.1.2 "Post-doctoral Research Aid" (project no. 1.1.1.2/VIAA/1/16/195).

## MS34-P03 | POLYMORPHISM OF R-ENCENICLINE HYDROCHLORIDE: ACCESS TO THE HIGHEST NUMBER OF STRUCTURALLY CHARACTERIZED POLYMORPHS USING DESOLVATION OF VARIOUS SOLVATES

Kons, Artis (University of Latvia, Riga, LVA); Berzinš, Agris (University of Latvia, Riga, LVA); Rekis, Toms (University of Bayreuth, Bayreuth, GER)

R-encenicline ((R)-7-chloro-N-quinuclidin-3-yl)benzo[b]thiophene-2-carboxamide) hydrochloride (Enc-HCl) a partial, selective agonist of the  $\alpha$ -7 nicotinic acetylcholine receptor which was developed for the treatment of cognitive deficits in schizophrenia and Alzheimer's disease. Here, we report an experimental, structural and computational study of neat polymorphs of Enc-HCl. In solid form screening numerous solvates including hydrates have been obtained, and their desolvation produced twelve neat polymorphs and for ten of them crystal structures were determined. The crystal structures of precursor solvates/hydrates were found to be structurally similar and related to those of desolvated phases, which was consistent with the observed phase transitions among the related pairs. In addition, a comparison of the thermodynamic stability of polymorphs were performed using differential scanning calorimetry data and solvent mediated slurry-bridging experiments. The energy ranking of ten polymorphs were obtained by DFT calculations with different functionals and/ or dispersion correction methods.

## MS34-P04 | DFT STUDIES OF STRUCTURAL, ELECTRONIC AND MAGNETIC PROPERTIES OF INP AND $\text{In}_{0.75}\text{X}_{0.25}\text{P}$ (WHERE X=Cr, Mn & Fe)

Kaur, Kirandish (Panjab University, Chandigarh, Muktsar, IND); Sharma, Dr. Suresh (DAV College, Abohar, Abohar, IND)

We investigate the structural, Electronic, Magnetic and Elastic properties of  $\text{Ga}_{1-x}\text{Cr}_x\text{P}$ ,  $\text{Ga}_{1-x}\text{Mn}_x\text{P}$  and  $\text{Ga}_{1-x}\text{Fe}_x\text{P}$  diluted Magnetic Semiconductor ( $x=0.25$ ) in Zinc Blende (B3) phase. The calculations have been performed using Density functional theory as implemented in the Spanish Initiative for Electronic Simulations with Thousands of Atoms code using local density approximation as exchange-correlation (XC) potential. The study of electronic structures and magnetic properties show that doping of Cr/Mn/Fe transition metal atom in GaP results the induction of ferromagnetism and develops a half metallic (HM) gap at fermi level with 100% spin polarization. The calculated values of s-d exchange constant  $N_0\alpha$  and p-d exchange constant  $N_0\beta$  indicate the magnetic nature of these compounds. These compounds are predicted to good candidate for spintronic applications. Calculated results are in good agreement with previous theoretical and experimental data.

## MS34-P05 | HOW TO CORRECTLY SAMPLE UNIT CELLS IN COMPUTER SIMULATIONS OF CRYSTAL STRUCTURES

Kurlin, Vitaliy (University of Liverpool, Liverpool, GBR)

All computer simulations of crystal structures choose unit cells (non-rectangular boxes) that define periodic arrangements of atoms or molecules. The 6 parameters (3 edge-lengths and 3 angles) of these unit cells are often randomly chosen. However, very different parameters can define identical (or nearly identical) crystal lattices.

The underlying problem is the existence of infinitely many unit cells (or primitive bases) for any periodic lattice. Hence a random choice of cell parameters can often produce very similar lattices and also miss large regions in the space of all lattices.

A classical approach to the ambiguity of a cell representation is to consider Niggli's reduced cell. Our first result is a new simpler definition of Niggli's reduced cell and a validation algorithm with necessary and sufficient conditions for reduced cells. Our second result justifies that the Voronoi cell of a lattice is geometrically stable with respect to well-defined distances on lattices. Though a Voronoi cell can be more complicated than a parallelepiped, the geometric parameters of this cell continuously change under atomic perturbations.

The main contribution is an explicit description of the space of all lattices by continuous parameters, which allows one to visualize regions that were under-sampled when unit cells are chosen. We are also extending this continuous parameterization of the space of all lattices to the space of all crystals based on a given chemical composition. Parts of this work are done in collaboration with the groups of Andrew Cooper and Matthew Rosseinsky at the Materials Innovation Factory, Liverpool.

## MS34-P06 | A COMBINED THEORETICAL AND EXPERIMENTAL INVESTIGATION INTO THE HIGH THROUGHPUT SCREENING OF COCRYSTAL COFORMERS

Braun, Doris (University of Innsbruck, Innsbruck, AUT); Adjiman, Claire (Imperial College London, London, GBR); Pantelides, Costas (Process Systems Enterprise Limited, London, GBR); Sugden, Isaac (Imperial College London, London, GBR)

The CrystalPredictor [1,2] and CrystalOptimizer [3] codes have explored crystallographic space successfully in several CSP investigations in recent years, including in CCDC [4] blind tests. Recent advances in CrystalPredictor [5], give significant increases in global search stage efficiency, whilst the capacity of LAM databases to reuse quantum mechanical calculations for the same molecule, allows for QM accuracy in conformation, intramolecular energy and molecular electrostatics, at forcefield cost.

Exploiting these advances, we present a high throughput cocrystallisation study into 4 API's, combined with 10 cofomers. Having performed a standard, neat, CSP study on each of the molecules, assessing the energy of potential cocrystals of the API and any of the cofomers becomes an almost trivial task, through judicious use of LAM databases. Comparing the energies of the cocrystals, versus the combined single crystal energies, allows the user to predict which cofomer can crystallise with the API.

Cocrystallisation experiments were also performed between the API's and cofomers; comparisons will be made to assess the accuracy, as well as demonstrate the capacity for the technique to be taken up into standard pharmaceutical development workflows.

- [1] M. Habgood, *et. al.*, J Chem Theory Comput **11**, 1957 (2015).
- [2] I. Sugden, *et. al.*, Acta Crystallogr B **72**, 864 (2016).
- [3] A. V. Kazantsev, *et. al.*, J Chem Theory Comput **7**, 1998 (2011).
- [4] A. M. Reilly, *et. al.*, Acta Crystallogr B **72**, 439 (2016).
- [5] I. Sugden, *et. al.*, Acta Crystallogr B (*Accepted*).

## MS34-P07 | DEVELOPMENT OF ACCURATE AND EFFICIENT AB INITIO POTENTIALS FOR EFFECTIVE CRYSTAL STRUCTURE PREDICTION

Bowskill, David (Imperial College London, London, GBR); Sugden, Isaac (Imperial College London, London, GBR); Pantelides, Constantinos (Imperial College London, London, GBR); Adjiman, Claire (Imperial College London, London, GBR)

Recent blind tests organised by the CCDC have highlighted the growing capabilities of crystal structure prediction (CSP) for increasingly complex systems, but what is often considered a success in a blind test does not always provide sufficient information to complement experimental solid-form screening efforts in an effective way. Despite the requirement for efficient methods, the use of computationally expensive periodic density functional theory (DFT) calculations has become a staple for many practitioners of CSP. Although this typically achieves greater accuracy, the computational cost may often be prohibitively large for the study of systems of industrial relevance particularly in the early stages of product development.

In this study, we investigate the role of parameter estimation and adaptive force fields in the development of bespoke *ab initio* potentials. The proposed methodology aims to improve the reliability of existing force field models used commonly in CSP to be competitive in accuracy with much more expensive DFT calculations. These improvements are facilitated through the rigorous construction of training sets from theoretical calculations. The application of these training sets vastly increases the abundance of available data. In addition, comparison with experimentally derived training sets demonstrates large discrepancies which can mainly be attributed to high experimental uncertainties and mischaracterised free energy corrections. Beyond this, by taking cues from successful developments in DFT dispersion corrections over recent years, we aim to use these training sets to develop tailored *ab initio* potentials that incorporate the effects of the molecular environment into the potential seamlessly whilst retaining parameter transferability.

## MS34-P08 | UNDERSTANDING OF CHOLESTEROL TRANSPORT IN NPC FAMILY PROTEIN: A COMPUTATIONAL STUDY

YOON, HYEJIN (Seoul National University, Seoul, KOR); Jang, Soonmin (Sejong University, Seoul, KOR); Jeong, Hyunah (Sejong University, Seoul, AUT); Joo, EunSook (Jeju National University, Jeju, KOR); Lee, Hyung Ho (Seoul National University, Seoul, KOR)

Even though there has been significant progress of understanding the dietary cholesterol exchange in cellular environment, many of the details still remains unclear. The transmembrane protein NPC1 inside lysosome plays one of the major roles in cholesterol transport mediated by NPC2. Meanwhile, NPC1L1 (Niemann-Pick type C1 like 1), which is related to the dietary cholesterol absorption process in small intestine, shares sequence homology with NPC1. However, unlike NPC1, NPC2 is not involved in cholesterol internalization with NPC1L1. The structure of N-terminal domain (NTD) of NPC1 in complex with cholesterol (PDB id: 3GKH and 3GKI) was known while only cholesterol free NTD (PDB id: 3QNT) is known for NPC1L1. It is noted that the whole cryo-EM structure of NPC1 is determined (PDB id: 3JD8).

We compared the NPC1L1 and NPC1 in complex with cholesterol with molecular docking followed by molecular dynamics study for better understanding of these underlying behavior. The NTD molecular dynamics simulation shows different structural and dynamical features. The difference in cholesterol internalization mechanism between NPC1 and NPC1L1 might be closely related to these structural and dynamical characteristics. We believe the current study can provide better understanding of cholesterol absorption/re-absorption process via NPC1 and NPC1L1 and their difference with atomic detail.

## MS34-P09 | AFFINITY PREDICTIONS FOR COCRYSTALS' DESIGN: COMPUTATIONAL VS. EXPERIMENTAL RESULTS.

ROCA PAIXAO, Luisa (University of Lille, Villeneuve-d'Ascq, FRA); CORREIA, Natalia T. (University of Lille, Villeneuve-d'Ascq, FRA); DANEDE, Florence (University of Lille, Villeneuve-d'Ascq, FRA); Affouard, Frederic (University of LILLE, VILLENEUVE D'ASCQ, FRA)

Lately, in order to enhance aqueous solubility, dissolution rate, hygroscopicity or bioavailability of poorly water soluble pharmaceutical molecules, the design of functional molecular materials using cocrystallization has attracted increasing interest. Cocrystals are multicomponent materials composed of neutral chemical species present in the same crystal lattice in a certain stoichiometric ratio and assembled via weak interactions such as van der Waals, hydrogen, halogen or  $\pi$ - $\pi$ . Pharmaceutical cocrystals usually refer to the combination of two APIs (active pharmaceutical ingredients) or one API and another small molecule that form a homogeneous crystalline single-phase system. Cocrystallization can be obtained by many techniques such as crystallization from solution, neat and liquid-assisted grinding, among many others. Using those techniques is usually considered a time consuming approach as it requires the experimental screening of a large number of chemicals. In the present study, calculations have been performed to estimate energetic affinity between an API and a large set of small organic molecules of pharmaceutical interests. Computational results were directly compared to the experimental ones, including all the literature data. Thus, the validity of the computational tool aiming to shorten the cocrystal design has been assessed.

This project has received funding from the Interreg 2 Seas programme 2014-2020 co-funded by the European Regional Development Fund under subsidy contract 2S01-059\_IMODE.

## MS35: From Synthon Engineering to Property Engineering

---

### MS35-01 | SYNTHONS: THROUGH THE LOOKING-GLASS, AND WHAT WE HAVE YET TO FIND THERE

Bucar, Dejan-Kresimir (University College London, London, GBR)

This presentation will critically evaluate the concepts, theories, and ideas underpinning modern crystal engineering efforts, with a view to stimulating a constructive, community-wide conversation about the current state of the art [1]. Some of our recent efforts to further develop existing guidelines for the design of molecular cocrystals and solid solutions will also be discussed, along with a brief description of an alternative and underused method for the preparation of novel cocrystals [2].

[1] M. K. Corpinot, D.-K. Bučar, *Cryst. Growth Des.* **2019**, 19, 1426-1453.

[2] S. J. Diez, M. D. Eddleston, M. Arhangelskis, M. Milbled, M. J. Müller, A. D. Bond, D.-K. Bučar, W. Jones, *Cryst. Growth Des.* **2018**, 18, 3263–3268.

## MS35-02 | FLEXIBLE CRYSTALLINE COORDINATION POLYMERS WITH TUNABLE RESPONSES TO MECHANICAL STIMULI

Đaković, Marijana (University of Zagreb, Zagreb, HRV)

Nowadays, we are witnessing a change in perceiving crystals, from stationary to more responsive objects. Crystals have been found to move, jump, flex or even explode as a response to a number of external stimuli like heat or irradiation, [1] but very recently it has been observed for a bunch of organic crystals [2] and a sole 0-D metal-complex [3] that they can be adaptive even to external mechanical force.

Recently, by targeting structural features common to both of these classes, we have managed to impart flexibility to crystalline coordination polymers for the first time.[4] Our 1D polymers of cadmium(II) were capable of displaying exceptional mechanical elasticity in response to the application of external pressure. More importantly, we have shown that the extent of the mechanical responses of our materials could be controlled by manipulating the strength and influence of intermolecular interactions. Here, we are showing that by introducing small and controllable structural changes we can dial-in both the nature of extent of flexibility of our materials.

[1] P. Naumov, S. Chizhik, M.K. Panda, N.K. Nath, E. Boldyreva, *Chem. Rev.* **115** (2015) 12400-12490.

[2] C.M. Reddy, M.T. Kirchner, R.C. Gundakaram, K.A. Padmanabhan, G.R. Desiraju, *Chem. Eur. J.* **12** (2006) 2222-2234.

[3] A. Worthy, A. Grosjean, M.C. Pfrunder, Y. Xu, C. Yan, G. Edwards, J.K. Clegg, J.C. McMurtrie, *Nat. Chem.* **10** (2018) 65-69.

[4] M. Đaković, M. Borovina, M. Pisačić, C.B. Aakeröy, Ž. Soldin, B.-M. Kukovec, I. Kodrin, *Angew. Chem Int. Ed.* **57** (2018) 14801-14805.

## MS35-03 | CRYSTALLIZATION OF CHIRAL 2,4-DINITROPHENYL PYRIDOXINE DERIVATIVES IN «NO ZONK» GROUPS: REGULARITY OR RANDOMNESS?

Samigullina, Aida (A.E. Arbuzov Institute of Organic and Physical Chemistry, FRC Kazan Scientific Center, Russian Academy of Sciences, Kazan, RUS); Garipov, Marsel (Kazan Federal University, Kazan, RUS); Lodochnikova, Olga (A.E. Arbuzov Institute of Organic and Physical Chemistry, FRC Kazan Scientific Center, Russian Academy of Sciences, Kazan, RUS); Gubaidullin, Aidar (A.E. Arbuzov Institute of Organic and Physical Chemistry, FRC Kazan Scientific Center, Russian Academy of Sciences, Kazan, RUS)

Materials with nonlinear optical properties are widely used in medicine, computer and laser technology, photonics and optoelectronics. At present more attention is paid to researching the new classes of compounds and establishing the features of their molecular and crystalline structure for designing the NLO-materials.

Recently we have demonstrated that the 2,4-dinitrophenyl pyridoxine with achiral center crystallizes in the noncentrosymmetric space group  $Pca2_1$  regardless of the used solvent and its crystals exhibit nonlinear optical properties. In this work, we report the investigating of the structural analogs of this compound, the chirality of which were varied by changing the type of substituents. It was found, that even in the presence of the chiral center in the molecules of 2,4-dinitrophenyl pyridoxine derivatives, there is a tendency for their crystallization not in the Zonk group, but in the centrosymmetric space groups. And even in the case of isopropyl substituted derivative crystallization in  $P212121$  space group, in the independent part of the unit cell is an enantiomeric pair, so that the compound crystallizes as a pseudo-racemate. At the same time, compounds of this series with an achiral center in molecules tend to form crystals in non-centrosymmetric groups, and this is one of the requirements for obtaining crystals with potential nonlinear-optical properties. The geometry of the molecules, the peculiarities of intermolecular interactions and their relationship with the crystallographic parameters of the crystals are discussed.

This work was financially supported by the Russian Science Foundation (grant No 17-13-01209)

## MS35-04 | DIRECT PROPORTIONALITY BETWEEN STRUCTURAL FEATURES AND PROPERTY IN MULTICOMPONENT CRYSTALS OF SALICYLIC ACID

Nyamayaro, Kudzanai (Cape Peninsula University of technology, Cape Town, ZAF); Hearshaw, Meredith (Cape Peninsula University of technology, Cape Town, ZAF); Bathori, Nikoletta (Cape Peninsula University of Technology, Cape Town, ZAF)

Crystal engineering involves the manipulation of intermolecular interactions to design functionalised crystalline materials and has proved to be an effective tool for the modification of physicochemical properties of active pharmaceutical ingredients (APIs).

Our aim was to systematically influence the rate of dissolution of a highly soluble API using crystal engineering principles. Salicylic acid (SA) was employed to form multicomponent crystals with a series of selected cinchona alkaloids: quinine (QUIN), quinidine (QUID), cinchonine (CINC), cinchonidine (CIND), N-benzylquininium chloride (NBQUIN), N-benzylcinchonidinium chloride (NBCIND) and N-benzylcinchoninium chloride (NBCINC). These compounds were selected because of their ability to form strong intermolecular interactions with the API, i.e. salts; and because of their size and flexibility that allow them to shield the API's polar groups and thus limit the access of the solvent molecules during dissolution.

The resulting novel crystalline forms were found to be salts, and were characterised using single crystal X-ray diffraction, powder X-ray diffraction, differential scanning calorimetry and thermogravimetric analysis. The dissolution profiles of the salicylate salts, measured from an aqueous medium using high performance liquid chromatography-mass spectroscopy, show a significant decrease in the rate of dissolution of SA. Subsequently, Hirshfeld surface analysis was used as a tool for quantitative and qualitative comparison of the crystal structures. Crystal morphology studies showed that the clear disparity in the rate of dissolution between the unsubstituted cinchona alkaloid salicylates and the N-benzyl substituted cinchona alkaloid salicylates can be attributed to the presence of more faces that are covered by hydrophobic groups in the latter.

## MS35-05 | SURFACE PROPERTIES OF ORGANIC CRYSTALS BASED ON A QUANTUM CHEMICAL TREATMENT OF CRYSTAL FACETS

Van de Velde, Jasper (University of Antwerp, Antwerp, BEL); Blockhuys, Frank (University of Antwerp, Antwerp, BEL)

The differences in reactivity of the different facets of a crystal to solute and/or solvent molecules is a rich source of information in the development of new materials based on small organic molecules for technological or pharmaceutical applications. Indeed, many macroscopic crystal properties such as morphology, interfacial stability, growth direction and speed, polarity, sticking propensity, wetting etc. are directly related to the susceptibility of the crystal facets to other molecular moieties during the crystallization process. In turn, controlling these properties is important for downstream unit processes associated with *e.g.* pharmaceutical product manufacture, such as filtration, granulation and compression.

A computational treatment of different crystal facets of materials ranging from small pharmaceuticals to large organic oligomers for optical applications, was performed at the level of DFT under Periodic Boundary Conditions. In the case of solute probe molecules, in which the attachment of solvated molecules to the crystal structure is simulated, an approach based on strong intermolecular synthons was used. In the case of solvent probes, in which the wetting and solubility of the crystal is central, a free relaxation mechanism was applied. The interactions between different probe molecules and the crystal surfaces results in energy profiles that can be directly linked to the growth direction of the crystal and hence the morphological importance of the different crystal facets. Although it is not a dynamic simulation of the crystallization process, this thermodynamic description allows a relatively fast screening of a large number of interactions on the surface.

## MS35-P01 | MONONUCLEAR COBALT, NICKEL AND COPPER COMPLEXES WITH GLYCINAMIDE: STRUCTURAL PROPERTIES AND BIOLOGICAL ACTIVITY

Prugovecki, Biserka (University of Zagreb, Zagreb, HRV); Vušak, Darko (University of Zagreb, Zagreb, HRV); Smrecki, Neven (University of Zagreb, Zagreb, HRV); Kralj, Marijeta (Ruder Boškovic Institute, Zagreb, HRV); Uzelac, Lidija (Ruder Boškovic Institute, Zagreb, AUT); Matkovic-Calogovic, Dubravka (University of Zagreb, Zagreb, HRV)

Glycinamide (**HL**) is the simplest amino acid amide, cheap and available and easily synthesized. In the CSD there are only six structures containing the glycinamide fragment: glycinamide hydrochloride, two rhodium complexes, a bimetallic (Mn, Cr) ferrimagnet, a ruthenium complex and an iridium complex. As a part of our ongoing research on investigation of metal complexes with amino acids and their derivatives, we report synthesis, solid-state characterization and antiproliferative activity of cobalt, nickel and copper complexes with glycinamide. In the cobalt(II) and nickel(II) complexes  $[M(H_2O)_2(HL)_2]X_2$  ( $M = Co, Ni$ ;  $X = Cl, Br/Cl, I$ ), the metal(II) cation is octahedrally coordinated by two glycinamide molecules in a *cis*-fashion and by two water molecules. In  $[CuCl_2(HL)_2]$  and  $[CuBr_{1.3}Cl_{0.7}(HL)_2]$  the octahedral coordination environment around the Cu(II) ions consists of two *N,O*-bidentate glycinamide ligands in a *trans*-fashion and two halide ions.  $[Co(H_2O)_2(HL)_2]Cl_2$  and  $[CuCl_2(HL)_2]$  showed moderate antiproliferative activity and selectivity towards MCF-7 cell lines.

The research was supported by the Croatian Science Foundation, project "Essential metal ions in Helicobacter pylori proteins and model complexes structure and function/property" (HRZZ-IP-2014-09-4274).

## MS35-P02 | PHASE TRANSITIONS ASSOCIATED WITH CONFORMATIONAL CHANGES OF LIGAND AND ANION REORIENTATION TRIGGER NORMAL AND REVERSE SPIN CROSSOVER

Kusz, Joachim (University of Silesia, Chorzów, POL); Weselski, Marek (University of Wrocław, Wrocław, POL); Książek, Maria (University of Silesia, Chorzów, POL); Mess, Pamela (University of Wrocław, Wrocław, POL); Bronisz, Robert (University of Wrocław, Wrocław, POL)

Spin crossover (SCO) in octahedral complexes of  $3d^4$ - $3d^7$  metal ions affects structure of materials because is connected with shortening of Fe-ligand distances at about  $0.2\text{\AA}$ . An occurrence of phase transition can trigger reverse SCO depending on high spin  $\rightarrow$  low spin (HS  $\rightarrow$  LS) transition upon elevation of temperature. Thus structural properties of the material are a crucial factor responsible for occurrence of spin crossover in normal or reverse mode.

Taking into account uncommon properties of ebbtr system [1] we have decided to use trifluoromethanesulfonate anion which can be a source of structural lability. The crystal of  $[\text{Fe}(\text{ebbtr})_2(\text{CH}_3\text{CN})_2](\text{CF}_3\text{SO}_3)_2 \times 4\text{CH}_3\text{CN}$  is composed from polymeric layers and area between them is occupied by anions and noncoordinated acetonitriles. At 270K the Fe-N distances are characteristic for HS form. Lowering of temperature triggers HS  $\rightarrow$  LS transition, however structural phase transition at 220K involves reversal of direction of SCO and leads to formation of superstructure ( $\mathbf{q} = 1/3\mathbf{a}^* + 1/3\mathbf{b}^* - 1/3\mathbf{c}^*$ ) with Fe-N bond distances characteristic for HS form. During further cooling there occurs subsequent structural phase transition which results in vanishing of superstructure and formation of LS form. In the heating mode two structural phase transitions occurs again, however they are shifted to higher temperatures which results in two types of hysteresis loops: "normal" and "reverse".

[1] M. Weselski, M. Książek, D. Rokosz, A. Dreczko, J. Kusz, R. Bronisz, *Chem. Commun.*, **2018**, 54, 3895.

## MS35-P03 | LUMINESCENT [Os(Cl)(Co)(P^P)(Pbi)] COMPLEXES

Kamecka, Anna (Institute of Chemistry, Faculty of Sciences, Siedlce, POL); Kapturkiewicz, Andrzej (Institute of Chemistry, Faculty of Sciences, Siedlce, AUT); Suwinska, Kinga (Faculty of Mathematics and Natural Sciences, Warsaw, POL)

A series of [Os(Cl)(CO)(P^P)(pbi)] complexes have been synthesized and characterized using FT-IR,  $^1\text{H}$  NMR, and  $^{31}\text{P}$  NMR spectroscopy. Their molecular structures have been confirmed by means of X-ray diffraction studies. For each of the studied bidentate phosphines (P^P = *cis*-1,2-bis(diphenylphosphino)ethene – dppv, 1,2-bis(diphenylphosphino)ethane – dppe, 1,2-bis(diphenylphosphino)benzene – dppb) the applied synthesis procedure has afforded in preparation of two isomers with pseudo-octahedral coordination of the osmium(II) ion. Each of *cis*-[Os(Cl)(CO)(P^P)(pbi)] show intense green emissions attributable to the excited triplet state of pbi ligand, whereas yellow emissions from the excited *trans*-[Os(Cl)(CO)(P^P)(pbi)] exhibit slight metal-to-ligand charge transfer character (from Os(Cl)(CO)(P^P) fragment to pbi ligand). The investigated complexes are generally well emissive with emission quantum yields up to 0.45 and emission lifetimes in the range of 10-100 ns. Only the yellow emissive *trans*-[Os(Cl)(CO)(dppv)(pbi)] exhibits remarkably different photophysical behaviour despite that all three *trans*-[Os(Cl)(CO)(P^P)(pbi)] isomers emit in the same spectral region. In the view of DFT/TD-DFT results this has been explained by the presence of an additional excited dark state possessing distinct charge transfer character (from Os(Cl)(CO)(pbi) fragment to dppv ligand).

In this paper the crystal structures of the [Os(Cl)(CO)(P^P)(pbi)] complexes are presented.

## MS35-P04 | STRUCTURAL STUDIES OF THE HOST-GUEST COMPLEXES OF CARBOXYLATED PILLAR[N]ARENES

Butkiewicz, Helena (Institute of Physical Chemistry Polish Academy of Sciences, Warsaw, POL); Kosiorek, Sandra (Institute of Physical Chemistry Polish Academy of Sciences, Warsaw, POL); Danylyuk, Oksana (Institute of Physical Chemistry Polish Academy of Sciences, Warsaw, POL); Sashuk, Volodymyr (Institute of Physical Chemistry Polish Academy of Sciences, Warsaw, POL)

"Pillar[n]arenes, first reported by Ogoshi in 2008 [1], are highly symmetrical pillar-shaped compounds composed of n hydroquinone units. They also have many hydroxyl groups on both rims. These features and their rigid hydrophobic, electron-rich cavity make them great candidates as host molecules for various electron-deficient or cationic guests. My project focuses on water soluble pillar[n]arenes substituted by carboxyl groups (CPA[n]). Under basic conditions, there are negatively charged carboxylate centers, making the CPA[n] to act as receptors for cations in water. Moreover, these carboxyl groups are located at the terminal positions of flexible aliphatic chains, so they can adjust to the size and shape of guest molecules. Here we want to present X-ray structure of the carboxylic acid substituted pillar[5]arene in the form of its host-guest complexes with viologen derivatives. These studies provide new information on the formation of the host-guest complexes of CPA[n] with viologen derivatives, the interactions responsible for their formation and the aggregation of the molecules in the crystal lattice. In a broader perspective it may have potential applications in drug delivery and molecular recognition systems.

[1] T. Ogoshi, S. Kanai, S. Fujinami, T. Yamagishi, Y. Nakamoto; J. Am. Chem. Soc., 2008, 130, 15, 5022–5023"

## MS35-P05 | GRAPH-SET ANALYSIS AND NON-LINEAR OPTICAL PROPERTIES OF SALTS OF L-ARGININE HOMOLOGUE

Rejnhardt, Piotr (Institute of Low Temperature and Structure Research Polish Academy of Science, Wroclaw, POL); Daszkiewicz, Marek (Institute of Low Temperature and Structure Research Polish Academy of Science, Wroclaw, POL)

Salts of L-arginine have wide applications in medicine, such as: treatment of hepatic and renal disorders or reducing blood cholesterol [1]. They have also potential application as an energy converter in optics, because the L-arginine salts crystallize without a centre of symmetry. We present five new compounds based on the arginine homologue, (S)-2-amino-3-guanidinopropanoic acid (AmGP), as potential new functional materials:  $(\text{H}_2\text{AmGP})\text{Cl}_2$  (**1**),  $(\text{HAmGP})\text{Cl}$  (**2**),  $(\text{H}_2\text{AmGP})(\text{NO}_3)_2$  (**3**),  $(\text{H}_2\text{AmGP})_2(\text{H}_2\text{O})(\text{NO}_3)_4$  (**4**),  $(\text{H}_2\text{AmGP})\text{Br}_2$  (**5**). Generally, most important parts of AmGP molecule in SHG context are carboxyl and guanidinium functional groups as they possess delocalized p electrons. In the AmGP molecule, these groups are less separated to each other, and therefore higher values of hyperpolarizability  $\beta$  is expected for AmGP molecule in comparison to L-arginine. SHG measurements shows that the monochloride salt has 2.4 times better SHG response than KDP. What is more, (S)-2-amino-3-guanidiniumpropanoic acid monochloride has 8 times better SHG response than L-argininium monochloride [2]. Analysis of molecular structure reveals that conformation of the organic cation varies in presented compounds and the greatest difference occurs in  $(\text{HAmGP})\text{Cl}$  (**2**). This fact can be associated with enhancement of SHG signal for this compound.

[1] M Walser - US Patent 4,320,146, 1982

[2] D. Kalaiselvi, Rangasamy Mohan Kumar, R. Jayavel, Crystal Research and Technology, 2008, 43:851

## MS35-P06 | NOVEL COORDINATION COMPOUNDS FOR BIOLOGICAL APPLICATIONS

García-Granda, Santiago (University Oviedo - CINN, Oviedo, ESP); Abdelbaky, Mohammed S. M. (University Oviedo - CINN, Oviedo (Asturias), ESP); Direm, Amani (Université Abbes Laghrour, Khenchela, DZA); Moeini, Keyvan (Payame Noor University, Tehran, IRN)

The interaction of transition metal ions with biological molecules provides one of the most promising class of coordination chemistry. The biological activity of such class makes them the fascinating candidate for biomedical uses. Imidazole occurs in most proteins as part of the side chain of histidine and constitutes a binding site for various transition metal to form imidazole based complexes that display a variety of pharmacological effects, including antitumor, superoxide dismutase and catecholase activities [1]. On the other hand, Schiff bases ligands and their complexes show interesting biological effects such as anticancer antimicrobial and urease inhibitory activates. Herein, and in order to contribute to the study of these systems, Schiff bases imidazole based complexes with different metal ions are presented. The resulting compounds have been structurally characterized and their biological activates were investigated. They have shown remarkable anticancer, antimicrobial and antifungal inhibition activities, which have been predicted by exploring the computational chemical reactivity of the these complexes [2]

**Keywords:** Coordination networks; imidazole-based copper complexes; topological analysis; Ab-initio calculations; magnetic properties; biological properties.

**Acknowledgements:** The financial support from Université Abbes Laghrour Khenchela, Algeria, Spanish MINCIU (MAT2016-78155-C2-1-R,), Principality of Asturias (GRUPIN14-060/GRUPIN-IDI/2018/000170) and FEDER is acknowledged.

[1] G. Tabbi, W.L. Driessen, J. Reedijk, R. P. Bonomo, N. Veldman, A.L. Spek, *Inorg Chem*, 36(6),1997,1168-1175

[2] A. Direma, M.S.M. Abdelbaky, K. Sayın, A. Cornia, O. Abosedo, S. García-Granda, *Inorg. Chim. Acta* 478, 2018, 59-70

## MS35-P07 | NOVEL SCHIFF BASE-METAL COMPLEXES; SYNTHESIS, CRYSTAL STRUCTURE AND BIOLOGICAL ACTIVITY

S. M. Abdelbaky, Mohammed (University of Oviedo, Oviedo, ESP); Ahmed Osman, Doaa (University of Oviedo, Oviedo, ESP); Moeini, Keyvan (Payame Noor University, Tehran, IRN); García Granda, Santiago (University of Oviedo, Oviedo, ESP)

Schiff base metal complexes occupy an important role in the development of the chemistry of chelate systems due to the fact that especially these with NO donor atoms, such systems closely resemble metallo-proteins and used to form polynuclear complexes with interesting structural motifs. Schiff base ligands and their complexes show interesting pharmacological effects such as anticancer, antimicrobial, antibacterial, and urease inhibitory activities [1]. Herein, we reported the synthesis of three schiff base metal complexes. All compounds were characterized by X-ray diffraction, NMR and elemental analysis. Additionally, the *in vitro* activities of all compounds against the human leukemia cell line K562 were investigated by evaluation of IC50 values and mode of cell death (apoptosis). The experiments revealed that the cytotoxicity of the studied complexes is higher or comparable with the cisplatin.

Keywords: Schiff base; Anticancer; K562 cell line; Docking study

Acknowledgements: Spanish MINECO (MAT2016-78155-C2-1-R,), Gobierno del Principado de Asturias (GRUPIN-IDI/2018/000170) and FEDER are acknowledged.

[1] N. K. Chaudhary, P. Mishra. *Bioinorg. Chem. Appl* 2017, 1-13

## MS35-P08 | TWO COMPOSITE Mn(II)-SQUARATE-DPE SUPRAMOLECULAR NETWORKS SHOWING INTERESTING WATER HYSTERESIS PHENOMENON IN WATER VAPOR AD-/DE-SORPTION ISOTHERMS

Wang, Chih-Chieh (Department of Chemistry, Soochow University, Taipei, TWN)

Assembly of two Mn(II)-squarate supramolecular networks, including composite two-dimensional (2D)  $[\text{Mn}(\text{Hdpe})(\text{C}_4\text{O}_4)_{0.5}(\text{H}_2\text{O})_3][\text{Mn}(\text{C}_4\text{O}_4)_2(\text{H}_2\text{O})_2]$  (**1**) and  $[\text{Mn}(\text{Hdpe})_2(\text{H}_2\text{O})_4][\text{Mn}(\text{C}_4\text{O}_4)_2(\text{H}_2\text{O})_2]_2 \times 8\text{H}_2\text{O}$  (**2**) ( $\text{C}_4\text{O}_4^{2-}$  (squarate = dianion of 3,4-dihydroxycyclobut-3-ene-1,2-dione ( $\text{H}_2\text{C}_4\text{O}_4$ ); dpe = 1,2-bis(4-pyridyl)ethane), associated with monodentate *anti*- $\text{Hdpe}^+$  ligands, have been synthesized and structurally characterized by single-crystal X-ray diffraction studies. Compound **1** is a [2D plus 2D] tri-layered composite polythreading network, composed of one 2D cationic  $[\text{Mn}(\text{Hdpe})(\text{C}_4\text{O}_4)_{0.5}(\text{H}_2\text{O})_3]^{2+}$  metal-organic framework (MOF) and two 2D anionic  $[\text{Mn}(\text{C}_4\text{O}_4)_2(\text{H}_2\text{O})_2]^{2-}$  MOFs, with the penetration of the monoprotonated *anti*-form  $\text{Hdpe}^+$  ligands dangling above and below the 2D Mn(II)-(m<sub>1,2,3,4</sub>-C<sub>4</sub>O<sub>4</sub>) layer in the 2D cationic  $[\text{Mn}(\text{Hdpe})(\text{C}_4\text{O}_4)_{0.5}(\text{H}_2\text{O})_3]^{2+}$  MOFs into the square-grid windows of two 2D Mn(II)-(m<sub>1,3</sub>-C<sub>4</sub>O<sub>4</sub>) layers in the anionic  $[\text{Mn}(\text{C}_4\text{O}_4)_2(\text{H}_2\text{O})_2]^{2-}$  MOFs. Compound **2** is a [0D plus 2D] bi-layered composite polythreading network composed of a cationic  $[\text{Mn}(\text{Hdpe})_2(\text{H}_2\text{O})_4]^{2+}$  monomer and a 2D layered anionic  $[\text{Mn}(\text{C}_4\text{O}_4)_2(\text{H}_2\text{O})_2]^{2-}$  MOF, with the penetration of the monoprotonated *anti*-form  $\text{Hdpe}^+$  ligands in the cationic  $[\text{Mn}(\text{Hdpe})_2(\text{H}_2\text{O})_4]^{2+}$  monomers into the square-grid windows of two 2D Mn(II)-(m<sub>1,3</sub>-C<sub>4</sub>O<sub>4</sub>) layers in the anionic  $[\text{Mn}(\text{C}_4\text{O}_4)_2(\text{H}_2\text{O})_2]^{2-}$  MOF. Both of the 2D composite polythreading networks in **1** and **2** are further extended to their 3D supramolecular architectures *via* the combination of intermolecular hydrogen bonds and p-p stacking interactions. Compounds **1** and **2** both exhibit interesting hysteresis phenomenon in water vapor ad-/de-sorption isotherms with chemisorption on the Mn(II) sites found in **1** and **2** and physisorption of water chains found in **2**. The de/re-hydration procedures by cyclic TG analysis and powder X-ray diffraction measurements of **1** and **2** evidence reversible sponge-like water de-/ad-sorption property associated with a dynamic structural transformation.

## MS35-P09 | NEW HETEROBIMETALLIC COMPLEXES OF Cu(II) AND Mn(II) WITH CYCLAM

### DERIVATIVES

Kuchár, Juraj (Pavol Jozef Šafárik University in Košice, Košice, SVK); Samolová, Erika (Pavol Jozef Šafárik University in Košice, Košice, SVK)

Nowadays, magneto-thermal effects become relevant not only by solving fundamental problems in solid physics, but also for the technological applications. One such phenomenon is the magnetocaloric effect that can be used in the thermal study of compound's magnetic properties, or for practical use, for example in magnetic refrigerators. There are several ferrimagnets in which the magnetocaloric effect was observed and also it was found that one-dimensional ferrimagnets under external magnetic field can pass to spin-liquid state (Luttinger spin liquid) and such transition can be technologically attractive [1, 2]. It is well known that systems based on one-dimensional bimetallic chains with Cu(II) and Mn(II) atoms ordered in alternating manner should show ferrimagnetic behavior [3].

Important step in the preparation of mentioned complexes is the selection of ligands, as they significantly influence the formation of chains and their arrangement in the crystal structure. We have undertaken study of a copper(II) compounds with central atom coordinated by the N-derivatives of cyclam (1,4,8,11-tetraazacyclotetradecane) and with Mn(II) atom that is tetracoordinated by chloride ligands. Such arrangement allows the formation of bimetallic chains with paramagnetic atoms bridged by chlorido ligand. Further details on the syntheses, characterizations and X-ray structure analysis of prepared compounds will be given.

The financial support for this work that was given by the VEGA agency (1/0063/17) is acknowledged.

[1] P. Konieczny et al., *Inorg. Chem.*, 56 (2017) 2777.

[2] J. Strečka, T. Verkholyak, *J. Low Temp. Phys.* 187 (2017) 712.

[3] Y. Pei et al., *Inorg. Chem.*, 26 (1987) 138.

## MS35-P10 CANCELLED | HYDROTHERMAL SYNTHESIS, CRYSTAL STRUCTURE AND LUMINESCENT PROPERTIES OF A NEW PRASEODYMIUM COORDINATION POLYMER

Bemmerad, Belkacem University of Bejaia, Bejaia, ALG)

The complex,  $[\text{Pr}(\text{glu})(\text{Hglu})(\text{phen})]\cdot 2\text{H}_2\text{O}$  (glu = glutarate, Hglu = hydrogen glutarate, phen = 1,10-phenanthroline) has been synthesized from hydrothermal reaction of  $\text{PrCl}_3$ , glutaric acid and 1,10-phenanthroline.

The compound crystallizes in the triclinic system. The  $\text{Pr}^{3+}$  is nine-coordinated and possesses an N2O7 environment surrounded by two nitrogen atoms from a chelating phen molecule, three oxygen atoms from two Hglu ligands and four oxygen atoms from glu ligands. The Pr-O and Pr-N bond lengths vary from 2.41 to 2.73 Å and from 2.64 to 2.72 Å, respectively.

One carboxylate group, of the glutarate ligand, is in bidentate mode and other bridges two Pr(III) ions, with Pr...Pr distance of 4.0475(2) Å forming 1D chain along a-axis. While in the hydrogen glutarate ligand, one carboxylate groups coordinates to Pr(III) in chelates/bridging tridentate and the other carboxylate groups are not coordinated. Lattice water molecules are stabilized in the crystal by hydrogen bonding with the uncoordinated carboxylate group of Hglu ligand.

The emission spectrum of the complex in solid state is composed of nine emission peaks: at 477-505, 516-550, 580-635, 645, 680, 698 and 730 nm; for the intrinsic transitions of Pr(III) corresponding to the f-f transition. emitting red orange light with CIE coordinates (0.56, 0.37).

## MS35-P11 | STRUCTURAL AND COMPUTATIONAL STUDY OF QUINOLINE-BASED CHALCOGENSEMICARBAZONES

Klisuric, Olivera (University of Novi Sad, Faculty of Sciences, Novi Sad); Armakovic, Sanja (University of Novi Sad, Faculty of Sciences, Novi Sad); Armakovic, Stevan (University of Novi Sad, Faculty of Sciences, Novi Sad); Markovic, Sanja (University of Belgrade, Faculty of Chemistry, Belgrade); Todorovic, Tamara (University of Belgrade, Faculty of Chemistry, Belgrade); Portalone, Gustavo (Sapienza University of Rome, Department of Chemistry, Rome, ITA); Filipovic, Nenad (University of Belgrade, Faculty of Agriculture, Belgrade)

Chalcogensemicarbazones are condensation products between semicarbazide and its sulphur and selenium isosters with carbonyl compounds with a broad spectrum of biological activities [1-3]. In this work the X-ray structural investigation of library of six chalcogensemicarbazones has been complemented with computational study of their global and local reactive properties, within the framework of density functional theory (DFT). Among other information, DFT calculations helped us to locate the most reactive sites of studied molecules and to identify their sensitivity towards the oxidation. Investigated compounds have been also checked for their optoelectronic properties, due to the fact that they share certain structural similarity with molecules that have exhibited potentially important properties for the area of organic electronics. Pharmacokinetic properties have been assessed by the analysis of frequently employed drug likeness parameters.

Part of this study was conducted within the project funded by the Provincial Secretariat for Higher Education and Scientific Research, Autonomous Province of Vojvodina (project No. 142-451-2362/2018-01).

- [1] Calcaterra, V., et al., Phenolic thio- and selenosemicarbazones as multi-target drugs. *Eur J Med Chem*, 2015. 94: p. 63-72.
- [2] Todorovic, T.R., et al., (Chalcogen)semicarbazones and their cobalt complexes differentiate HL-60 myeloid leukaemia cells and are cytotoxic towards tumor cell lines. *MedChemComm*, 2017. 8(1): p. 103-111.
- [3] Filipović, N.R., et al., Pro-apoptotic and pro-differentiation induction by 8-quinolinecarboxaldehyde selenosemicarbazone and its Co(III) complex in human cancer cell lines. *MedChemComm*, 2016. 7(8): p. 1604-1616.

## MS35-P12 | NEW TITANIUM CALIX[N]ARENE-BASED SCAFFOLDS AS ANTI-TUMOUR AGENTS.

Elsegood, Mark (Loughborough University, Loughborough, GBR)

There is a drive to develop new anti-tumour agents based on metals other than platinum. Some recently made Ti salen complexes have been shown to outperform cis-platin.<sup>1</sup> We present a range of new Ti calix[n]arene [n = 4, 6, 8] complexes and, for some examples, report on toxicity testing against tumour cell line U87. We have also investigated the deliberate hydrolysis of such species to track their chemistry under physiological conditions.<sup>2</sup>

Our synthetic and structural studies have developed and characterised a range of new Ti(IV) scaffolds including: (1) monometallic, calix[4]arene-based; (2) dimetallic, with OH<sup>-</sup>/Cl<sup>-</sup> bridges, calix[4]arene-based; (3) Ti<sub>4</sub> ladders encapsulated by calix[8]arene; (4) more exotic architectures, including: up to 8 Ti<sup>4+</sup> ions, an example with non-coordinated polyiodide ions, and a rare example with a disiloxane (from grease) bridge over a Ti<sub>4</sub> ladder.

Variation of the halogen in the starting material, and carried through into the products, leads to some common scaffolds, namely the Ti<sub>4</sub> ladders, but also some insights into reaction pathways via the isolation of key intermediates and/or secondary products. This leads to an appreciation of the variety possible in such systems, and hence the degree of control required to generate the desired products.

[1] A. Tzubery & E. Y. Tshuva, *Inorg. Chem.*, 2011, 50, 7946-7948.

[2] D. M. Miller-Shakesby, S. Nigam, D. L. Hughes, E. Lopez-Estelles, M. R. J. Elsegood, C. J. Cawthorne, S. J. Archibald, and Carl Redshaw, *Dalton Trans.*, 2018, 47, 8992-8999.

## MS35-P13 | EXPLORING THE LIMITS OF IODONIUM (I<sup>+</sup>) FORMATION

Ward, Jas (University of Jyväskylä, Jyväskylä)

The occurrence of halonium ions (halogen atoms in the 1+ oxidation state) has been known for some time and exist as linear two-coordinate complexes stabilised by appropriate nucleophilic ligands. Halonium species can be straightforwardly synthesised by cation exchange of the analogous Ag(I) complex with an elemental halogen (Br<sub>2</sub>, I<sub>2</sub>), though as the reactivity increases as you go up group 17, examples of Iodonium (I<sup>+</sup>) complexes in the solid-state are most prevalent. However, given their intrinsic reactivity, with species like [I(pyridine)<sub>2</sub>][BF<sub>4</sub>] even being sold commercially as reagents, the number of halonium complexes studied in the solid-state is still quite small. Studies investigating the links between halonium formation, steric considerations of the nucleophilic ligands, or the identity of the counterion are also largely absent in the literature. Understanding the conditions which favour/disfavour halonium formation would greatly aid in the future development of this area of research.

Herein we report the solid-state structures of two-coordinate Ag(I) complexes possessing a range of different common counterions, all of which were synthesised for their potential to be converted into the analogous halonium species. Those successfully converted into the analogous iodonium complexes, and the reasons thereof, will also be discussed.

## MS35-P14 | CRYSTAL STRUCTURE AND SELF-ASSEMBLY OF PILLAR[N]PYRIDINIUMS

Danylyuk, Oksana (Institute of Physical Chemistry Polish Academy of Sciences, Warsaw, POL); Rosa, Bartłomiej (Institute of Organic Chemistry Polish Academy of Sciences, Warsaw, POL); Butkiewicz, Helena (Institute of Physical Chemistry Polish Academy of Sciences, Warsaw, POL); Kosiorek, Sandra (Institute of Physical Chemistry Polish Academy of Sciences, Warsaw, POL); Boinski, Tomasz (Institute of Organic Chemistry Polish Academy of Sciences, Warsaw, POL); Szumna, Agnieszka (Institute of Organic Chemistry Polish Academy of Sciences, Warsaw, POL); Sashuk, Volodymyr (Institute of Physical Chemistry Polish Academy of Sciences, Warsaw, POL)

Macrocyclic host molecules are important multidentate toolboxes in modern supramolecular chemistry. Depending on their size, shape and electronic properties macrocycles found many useful applications in diverse host-guest transport systems, sensing, extraction, catalysis *etc.* Very recently, the new class of cationic macrocycles, pillar[n]pyridiniums P[n]P, has been synthesized and introduced into supramolecular arena. [1] Pillar[n]pyridiniums are cyclic oligomers consisted of pyridinium units linked through nitrogen and *para* carbon with methylene bridges. The open cylindrical cavity surrounded by cationic electron-deficient pyridinium units provide a highly potential platform for anion recognition and anion-induced self-assembly. Moreover, the simple structure, straightforward synthesis and good aqueous solubility are attractive advantages of these novel macrocyclic hosts.

We would like to present structural aspects and solid state self-assembly features of these inherently cationic macrocycles. Particularly, the conformational properties in the solid state (rigidity *versus* flexibility of the macrocyclic skeleton), the binding of different anionic guests, main non-covalent interactions involved in the molecular recognition and self-assembly processes with anions will be discussed.

[1] S. Kosiorek, B. Rosa, T. Boinski, H. Butkiewicz, M. P. Szymanski, O. Danylyuk, A. Szumna, V. Sashuk, *Chem Commun.*, **53** (2017) 13320; S. Kosiorek, H. Butkiewicz, O. Danylyuk, V. Sashuk, *Chem Commun.*, **54** (2018), 6316.

## MS35-P15 | CRYSTAL STRUCTURES AND TOPOLOGICAL ANALYSIS OF Ag(I) COMPLEXES WITH 1,4-HETERODISUBSTITUTED CYCLOHEXANES

Marjanovic, Ivana (University of Novi Sad Faculty of Sciences, Novi Sad); Klisuric, Olivera (University of Novi Sad Faculty of Sciences, Novi Sad); Filipovic, Nenad (University of Belgrade Faculty of Agriculture, Belgrade); Todorovic, Tamara (University of Belgrade Faculty of Chemistry, Belgrade); Vulic, Predrag (University of Belgrade Faculty of Mining and Geology, Belgrade); Ristic, Predrag (University of Belgrade Faculty of Chemistry, Belgrade); Gulea, Michaela (Laboratoire d'Innovation Thérapeutique, UMR 7200, Université de Strasbourg Faculté de Pharmacie, Illkirch Cedex, FRA); Donnard, Morgan (Laboratoire d'Innovation Moléculaire et Applications, UMR 7042, CNRS, ECPM, Université de Strasbourg, Strasbourg, FRA)

Silver nitrate and silver perchlorate were combined with thiomorpholine-4-carbonitrile (**L1**) and piperazine-1,4-dicarbonitrile (**L2**) to observe the effect of small structural changes in used ligands on the final structures. Reactions with **L1** yield  $\{[Ag(L1)_2](NO_3)]_n$  (**1**) and  $\{[Ag(L1)_2](ClO_4)]_n$  (**2**), while **L2** reactions produce  $\{[Ag(L2)_2](NO_3) \times H_2O]\}_n$  (**3**) and  $\{[Ag(L2)_2](ClO_4)]_n$  (**4**). The XRPD investigation indicates that the samples **1–4** correspond to the single-phase X-ray powder patterns in accordance with the structural model obtained by SCXRD. Topological analysis suggests that **1** and **2** are two-dimensional structures that have a **sql** underlying topology, while **3** and **4** are three-dimensional metal-organic frameworks with **dia** underlying nets. In **3**, the MOF comprises five interpenetrating networks related by 6.67 Å translations along the [100] direction (interpenetration class Ia) [1]. In **4**, there are two crystallographically different Ag(I) ions. The first one builds two interpenetrating networks related by 12.61 Å translations along the [100] direction (interpenetration class Ia) [1]. The second Ag(I) ion gives four interpenetrating networks related both by 12.61 Å translations along the [100] direction and by an inversion centre (interpenetration class IIIa) [1].

[1] Baburin I.A, Blatov V.A. Carlucci L, Ciani G. & Proserpio D. M. (2005). *J. Solid State Chem.* 178, 2452-2474

## MS35-P16 | A LAMELLAR STRUCTURE EXHIBITING NANO-MORPHOLOGICAL REVERSIBILITY, DISASSEMBLY-AND-SELF-ASSEMBLY CRYSTALLIZATION INTO NOVEL COORDINATION POLYMERS

Hung, Ling-I (National Tsing Hua University, Hsinchu, TWN); Chen, Pei-Lin (National Tsing Hua University, Hsinchu, TWN)

A hybrid organic-inorganic two-dimensional layer structure with functional carboxylic acid ( $-\text{COOH}$ ) groups protruding on both sides of zincophosphate sheets is prepared for the first time. The interior  $-\text{COOH}$  groups allow the hybrid sheets to stack tightly via strong hydrogen bonds to form a sturdy supramolecular network characteristic of extraordinary thermal stability. The supramolecular solid could exhibit tunable wettability via a facile mechano-chemical reaction, which is enabled by the  $-\text{COOH}$  groups exposed on the solid surface. We also observed an intriguing reversible lamella-to-nanorod transformation presumably initiated and prompted by surface and interior  $-\text{COOH}$  groups collectively. To investigate the reactivity of such a solid toward organic bases, we immersed the supramolecular network in solutions of bipyridyl alkanes and observed from the solutions two novel zinc coordination polymer compounds crystallized, demonstrating a unique disassembly-and-self-assembly process.

## MS35-P17 | CRYSTALLOGRAPHIC EVIDENCE FOR AGGREGATION PATTERNS OF TWO CYCLIC TRIIMIDAZOLE PHOSPHORS IN Zn(II) AND Cd(II) COMPLEXES

Kravtsov, Victor (1 Institute of Applied Physics, Chisinau, MDA); Bold, Victor (1 Institute of Applied Physics, Chisinau, MDA); Chisca, Diana (1 Institute of Applied Physics, Chisinau, MDA); Lucenti, Elena (2 Istituto di Scienze e Tecnologie Molecolari del CNR(ISTM-CNR), Milano, Italy; 3 INSTM-UdR Milano, Italy, Milano, ITA); Cariati, Elena (3 INSTM-UdR Milano, Italy; 4 Dipartimento di Chimica, Università degli Studi di Milano, Milano, ITA); Forni, Alessandra (2 Istituto di Scienze e Tecnologie Molecolari del CNR(ISTM-CNR), Milano, Italy; 3 INSTM-UdR Milano, Italy, Milano, ITA); Fonari, Marina (1 Institute of Applied Physics, Chisinau, MDA)

Design of materials with ligand-centered emission from a highly emissive ligand with the use of optically inactive metal ions Zn(II) and Cd(II) allows tuning the ligands stacking and influences on the lifetime, quantum yield and stability of emitters. Generally,  $d^{10}$  metal complexes show no emission originating from MLCT/LMCT excited states, since these ions are in a stable oxidation state. Otherwise,  $d^{10}$  metals have flexible coordination numbers, providing the diversity of coordination arrays. Furthermore, these metals compete with platinum group compounds in view of their low cost and availability. Depending on the ligand structure and the nature of the metal core, bright luminescent materials can be prepared and used in LEDs. Under consideration are complexes obtained from Zn/Cd perchlorates, tetrafluoroborates, nitrates, and acetates by successive substitution aqua ligands in the metals' coordination cores by the photophysically active triimidazo[1,2- $\alpha$ :1',2'- $c$ :1'',2''- $e$ ][1,3,5] triazine ( $L_1$ ), which displays crystallization-induced and mechanochromic emission due to H-aggregation, and its positional isomer, triimidazo[1,2- $\alpha$ :1',2'- $c$ :1'',5''- $e$ ][1,3,5]triazine ( $L_2$ ). The reactions resulted in coordination of one, two or six phosphor molecules to the metal centers. Ligands' association patterns represent the stacking dimers in salt-cocrystals  $[M(H_2O)_6](An)_2(L_1)_2$  ( $M=Zn, Cd, An=[BF_4]^-, [ClO_4]^-, [NO_3^-]$ ); infinite stacks in the mononuclear complexes  $[Zn(H_2O)_3(L_1)(NO_3)](NO_3)$ ,  $[Cd(L_1)_2(H_2O)_2(NO_3)_2]$ ,  $[Cd(L_2)_2(NO_3)_2(H_2O)]$ ,  $[Zn(L_2)_2(CH_3COO)_2]$ ,  $[Cd(L_2)_2(CH_3COO)_2(Im)] \cdot H_2O$  with either one or two ligand molecules coordinated to the metals, and stacking layers in the salt-cocrystal  $[Zn_3(CH_3COO)_6(H_2O)_2](L_1)_2$ , where the ligands arrangement similar to that in pure phase. The reported complexes give examples of isomorphs, polymorphs, and isostructural compounds.

**Acknowledgments:** Authors thank the bilateral Moldova/Italy project 18.80013.16.03.03/It and ASM-CNR 2018-2019 project for financial support.

## MS35-P18 | CRYSTAL STRUCTURES OF CHOLESTEROL BASED PHOTO-SWITCHABLE MESOGENIC DIMERS. STRONGLY BENT MOLECULES VERSUS AN INTERCALATED STRUCTURE.

Pruszkowska, Kamila (University of Warsaw, Warsaw, POL); Zep, Anna (University of Warsaw, Warsaw, POL)

Liquid crystals, being the unique compounds combining the properties of two states of matter – anisotropy of the solid state and fluidity of the liquids, have always been an important class of functional materials [1].

Here we present our studies in the area of self-assembly of liquid crystalline materials. The subject of research is a homologue series of bent-shaped mesogenic dimers with different length of a terminal alkoxy chain. The photosensitivity of mesogenic molecules gives possibility for manipulating the structure of liquid crystalline phase by light. Compound with the shortest alkoxy tail exhibits heliconical twist-bend nematic phase ( $N_{tb}$ ). Elongation of the terminal alkoxy chain prevents formation of  $N_{tb}$  phase, for compounds with longer tail instead of  $N_{tb}$  phase, SmA is observed, which is rather unique for bent-shaped dimeric mesogens.

Crystal structures presented here shed new light on possible molecular conformation and arrangement of molecules in liquid crystalline phase. We have shown that, in addition to the model of intercalated molecules, special attention should be paid to the model of strongly bent molecules. New model of molecular packing of bent-shaped dimers with flexible linker in SmA phase is proposed [2].

The studies presented here show that insightful crystal structure analysis allows future design of liquid crystalline materials with the strictly required properties.

[1] Q. Li, Nanoscience with Liquid Crystals: From Self-Organized Nanostructures to Applications, Springer, Heidelberg, 2014.

[2] A.Zep, K.Pruszkowska, Ł.Dobrzycki, K.Sektas, P.Szałański, P.H.Marek, M.K.Cyrański and R.R.Sicinski, CrystEngComm, 2019, DOI: 10.1039/C9CE00013E.

## MS35-P19 | CUBE VS DIMER: PECULIARITIES OF CRYSTAL STRUCTURE OF $\text{Cu}_2\text{I}_2$ - AND $\text{Cu}_4\text{I}_4$ -COMPLEXES OF 10-(ARYL)PHENOXARSINES AND 10-(ARYL)PHENARSAZINES

Dobrynin, Alexey (A.E. Arbuzov Institute of Organic and Physical Chemistry FRC KazSC RAS, Kazan, RUS); Galimova, Milyausha (A.E. Arbuzov Institute of Organic and Physical Chemistry FRC KazSC RAS, Kazan, RUS); Musina, Elvira (A.E. Arbuzov Institute of Organic and Physical Chemistry FRC KazSC RAS, Kazan, RUS)

The complexes of copper (I) halides have been of great interest due to the large variety of their photophysical properties associated with the ability of copper (I) halides to form various types of structures [1]. The composition and structure of the complexes depend on the geometry and steric factors of the ligand, type of solvent and ligand to metal ratio [2]. It is known that the  $\text{Cu}_4\text{I}_4$  clusters with various pnictogen ligands demonstrate luminescent properties [3,4].

Cubic complexes exhibit intense green solid-state luminescence under UV irradiation.

This report is devoted to analysis of crystal structure of Cu (I) iodide complexes of 10-(aryl)phenoxarsines and 10-(aryl)phenarsazines with a tetrameric (cubic)  $\text{Cu}_4\text{I}_4$ -core and dimeric  $\text{Cu}_2\text{I}_2$ -core.

[1] Q. Benito, X. F. LeGoff, G. Nocton, A. Fargues, A. Garcia, A. Berhault, S. Kahlal, J.-Y. Saillard, C. Martineau, J. Trebosc, T. Gacoin, J.-P. Boilot, S. Perruchas. *Inorg. Chem.*, 2015, 54, 4483-4494.

[2] P. Bartos, P. Taborsky, M. Necas. *Phosphorus Sulfur and Silicon and the Related Elements*, 2016, 191, 645-647.

[3] S. Perruchas, C. Tard, X.F. Le Goff, A. Fargues, A. Garcia, S. Kahlal, J.-Y. Saillard, T. Gacoin, JP Boilot. *Inorg. Chem.*, 2011, 50, 10682–10692.

[4] W.V. Taylor, U.H. Soto, V.M. Lynch, M.J. Rose. *Inorg. Chem.*, 2016, 55, 3206-3208.

This work was financially supported by the Russian Science Foundation (grant No 17-13-01209).

## MS35-P20 | CORRELATION BETWEEN STRUCTURAL STUDIES AND THIRD ORDER NLO

### PROPERTIES OF THREE NEW SEMI-ORGANIC COMPOUNDS

Benali-Cherif, Rim (Abbes Laghrour Khenchela University, khenchela, DZA); Takouachet, Radhwane (Abbes Laghrour Khenchela University, Khenchela, DZA); Bendeif, El-Eulmi (Laboratoire de Cristallographie, Résonance Magnétique et Modélisations (CRM2) Université de Lorraine, Nancy, FRA); Benali-Cherif, Nourredine (Akli Mohand Oulhadj-Bouira, University, Bouira, DZA)

The study of semi-organic compounds has been of growing interest for a few years. In addition to their fundamental interest in the nature of the bonds occurring between inorganic anions and organic cations, these compounds also have remarkable physico-chemical and optical properties. Recently, the variety of semi-organic hybrid crystals has been developed for NLO applications. The combination of organic compounds, especially amino acids with mineral acids, gives rise to new hybrid crystals with strong NLO properties. Semi-organic compounds play an important role in cell metabolism; they intervene in transfer of energy because of their richness in hydrogen bonds.

Measurement of nonlinear third order electrical susceptibilities was performed for three new compounds by the THG technique. Fig. 1 shows the intensity of the THG signal as a function of the angle of incidence, it exhibits the same behavior as the silica.

**Table 01.** Experimental values of nonlinear susceptibility of the third order.

Compounds	Chemical structure	Space group	$\chi_{33}^{(3)}$ [ $\text{m}^2\text{V}^{-2}$ ] $10^{-22}$
ortho ammonium benzoic acid hydrogenselenite ( <i>o</i> -AAB) <sup>+</sup> , (HSeO <sub>3</sub> ) <sup>-</sup>		P 2 <sub>1</sub> , chiral	96,3
meta-ammonium benzoic acid hydrogenselenite ( <i>m</i> -AAB) <sup>+</sup> , (HSeO <sub>3</sub> ) <sup>-</sup>		P 2 <sub>1</sub> /n, achiral	67,7
para-ammonium benzoic acid hydrogenselenite ( <i>p</i> -AAB) <sup>+</sup> , (HSeO <sub>3</sub> ) <sup>-</sup>		P -1, achiral	43,2

The values are stronger than that of silica. The largest value is observed for the first compound, =  $9,63 \times 10^{21} \text{ m}^2/\text{V}^2$  due to the increase in charge transfer and the large number of hydrogen bonding which increases the dipole moment of the compound.

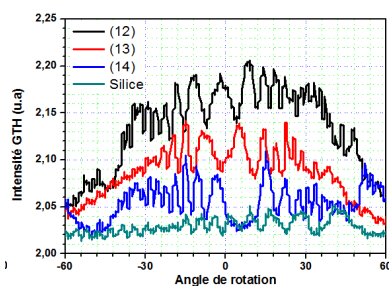


**Figure 1.** Intensity of the third harmonic for the three samples

These optical measurements revealed different optical behaviors of the three compounds studied. Several structural parameters affect the physical and optical properties of these materials such as: atomic arrangement, intra- and intermolecular interactions, crystal symmetry and electron density distribution.

## MS35-P21 | FILLING THE GAPS: WHAT NEW POLIMORPHS OF ACETILPYRENE TELL US ABOUT THE FLUORESCENCE OF PYRENE DERIVATIVES

Tchon, Daniel (University of Warsaw, Faculty of Chemistry, Warsaw, POL); Makal, Anna (University of Warsaw, Faculty of Chemistry, Warsaw, POL); Trzybinski, Damian (University of Warsaw, Biological and Chemical Research Centre, Warsaw, POL)

Policyclic Aromatic Hydrocarbons (PAHs) have been shown to feature interesting electronic and optical properties, which showcase them as one of the most potent synthons for modern material design. The compounds are easily modified by the means of chemical substitution, which allows to use them in a wide range of applications, from conducting metal-organic frameworks to luminescent bio-markers.

Partly because of the presence of large  $\pi$ -conjugated systems, PAHs are known to form various aggregates, whose spectroscopic properties tend to depend significantly on individual molecules' environment. Luminescence of even the simplest compound such as pyrene undergoes a significant modifications whenever a formation of  $\pi$ -dimers is possible, i.e. in concentrated solution or solid state. The following trend is preserved in its derivatives.

In the course of our studies, two new polymorphs of acetylpyrene (AP) have been found and their structures have been characterised. In contrast to the already known crystal form AP-Cc, which features no  $\pi$ -stacking and exhibits very weak luminescence in the solid state, two new-found polymorphs denoted AP-P2<sub>1</sub> and AP-P2<sub>1</sub>/c feature strong aggregation of aromatic rings, which reflects in their sharp colours when exposed to ultraviolet. While the individual differences between two new forms are very small, they impact on the electronic structure of AP heavily enough so that individual crystals of these forms are easily distinguishable under UV light with a naked eye.

This study was financially supported by the National Science Centre Poland (NCN) based on decision DEC-2015/17/B/ST4/04216.

## MS35-P22 | MEDIUM CHAIN LENGTH (MCL)-PHA-BASED NANOCOMPOSITES FOR BIOMEDICAL APPLICATIONS: SYSTEM EVALUATION THROUGH XRD

Malagurski, Ivana (Faculty of Technology and Metallurgy, University of Belgrade, Belgrade); Frison, Ruggero (Swiss Federal Laboratories for Materials Science and Technology, Center for X-Ray Analytics, Dübendorf, CH); Maurya, Anjani (Swiss Federal Laboratories for Materials Science and Technology, Center for X-Ray Analytics, Dübendorf, CH); Nikodinovic-Runic, Jasmina (Institute of Molecular Genetics and Genetic Engineering, University of Belgrade, Belgrade); Babu, Ramesh (AMBER Centre, Trinity College Dublin,, Dublin); O`Connor, Kevin (BEACON SFI Bioeconomy Research Centre and School of Biomolecular and Biomedical Science, University College Dublin, Belfield, Dublin 4); Neels, Antonia (Swiss Federal Laboratories for Materials Science and Technology, Center for X-Ray Analytics, Dübendorf, CH)

Medium-chain polyhydroxyalkanoates (mcl-PHA) are flexible, elastomeric polymers produced by wide range of bacteria as intercellular storage of carbon and energy. They represent attractive components in biomaterial design because they are biocompatible, biodegradable and can be obtained using variety of carbon sources including waste streams [1]. However, being semi-crystalline, all mcl-PHAs are characterized by low melting temperature and poor tensile strength which can interfere with processing methods and wider biomedical application. Simple way to improve mcl-PHAs properties is to incorporate a nanophase within biopolymer to obtain nanocomposites. Nano-sized constituents interact with biopolymer more intimately affecting in turn the obtained nanocomposite properties as well as functionality. Among inorganic nanofillers, TiO<sub>2</sub> nanostructures with high aspect ratio (*e.g.* nanofibers) have unique properties that support osteogenic phenotype which makes them suitable for bone tissue engineering [2].

The aim of this study was to synthesize novel mcl-PHA-based nanocomposites for potential biomedical applications. The effects of nanophase incorporation on the obtained nanocomposites structural properties, namely phases, nano-sizes and crystallinity, are evaluated by X-ray diffraction techniques [3]. The relationship between nanocomposites structure and corresponding mechanical and thermal properties is investigated. In addition, functionality in terms of cytotoxic effect against normal human fibroblasts is evaluated.

[1] Rai, R. et al. *Biomacromolecules*, **2011**, (12), 2126-2136.

[2] Wang, X.; Gittens, R. A.; Song, R.; Tannenbaum, T.; Olivares-Navarrete, R.; Schwartz, Z.; Chen, H.; Boyan, B. D. *Acta Biomater.* **2012**, (8), 878-885.

[3] Maurya, A. et al. *Nanoscale*, **2019**, 11(15), 7176-7187.

## MS35-P23 | STRUCTURAL AND VIBRATIONAL STUDY OF NEW 2-ETHYLANILINIUM PHOSPHITE (C<sub>8</sub>H<sub>12</sub>N)H<sub>2</sub>PO<sub>3</sub>

ZERRAF, Soufiane (Hassan University of Casablanca, Morocco, Casablanca, MAR)

Chemical preparation, crystal structure and vibrational study are reported for a new 2-ethylanilinium phosphite (C<sub>8</sub>H<sub>12</sub>N)H<sub>2</sub>PO<sub>3</sub>. This organic cationic phosphate was synthesized by the action of phosphoric acid on an aqueous solution of Dimethylamine, (C<sub>8</sub>H<sub>12</sub>N)H<sub>2</sub>PO<sub>3</sub> crystallizes in the triclinic system with centric space group P-1. Its unit-cell dimensions are  $a = 4.6042(2) \text{ \AA}$ ,  $b = 10.3863(4) \text{ \AA}$ ,  $c = 10.7848(5) \text{ \AA}$ ,  $\alpha = 90.115(3)^\circ$ ,  $\beta = 97.878(3)^\circ$ ,  $\gamma = 98.462(3)^\circ$ ,  $Z = 2$  and  $V = 505.18(4) \text{ \AA}^3$ . The crystal structure was refined down to  $R = 0.0362$ ,  $R_w = 0.0495$  for 1989 reflections satisfying criterion  $I \geq 2\sigma(I)$ .

The vibrational study using IR absorption spectroscopy shows the presence of bands characterized by the vibrations of the H<sub>2</sub>PO<sub>3</sub><sup>-</sup> ion in the structure.

## MS35-P24 | SUPRAMOLECULAR ASSEMBLIES OF COPPER(II) COMPLEXES: SUPRAMOLECULAR SYNTHON TRANSFERABILITY AND MAGNETIC PROPERTIES

Penic, Nikolina (Department of Chemistry, Faculty of Science, University of Zagreb, Zagreb, HRV)

In the pursuit of new technologies there is exigency for novel materials with desired physical and chemical properties. Despite the fact that metal-based crystalline solids provide an access to properties that are typically unavailable or difficult to achieve in metal-free settings (i.e. magnetic or optical). Hydrogen and halogen bonds have proven to be invaluable crystal engineering tools and their use in the design of organic systems has already been well documented, but introduction of metal cations and charge-balancing entities into metal-free solids commonly disrupt well established connectivity of the key functional groups. Therefore, our aim is to study transferability of supramolecular synthons from organic to metal-organic systems, and to correlate supramolecular connectivity of metal-based building units with a number of bulk crystal properties, in particular magnetic and mechanical.

For that purpose, we prepared a series of 1-D halide coordination polymers of copper(II) with the amine and amide derivatives of pyridine, pyrazine and pyrimidine. The targeted octahedral geometry was achieved for all structurally described complexes,  $[\text{CuCl}_2(2\text{-NH}_2\text{pz})_2]_n$ ,  $[\text{CuCl}_2(2\text{-pyz})_2]_n$ ,  $[\text{CuCl}_2(4\text{-pym})_2]_n$  and  $[\text{CuBr}_2(4\text{-pym})_2]_n$ , as well as the desired connectivity via N-H...O/N interactions. It was found that the halide ions do not have disruptive effect on the supramolecular motif  $C(4)$ , which remained preserved as in purely organic systems. Antiferromagnetic spin chain behaviour, described by Bonner-Fischers model, was observed for all prepared complexes. Also, impact of the counter ion and Cu-X...Cu angles on superexchange interaction is observed.

## MS35-P25 | REVEALING MECHANICAL PLASTIC BENDING IN COORDINATION POLYMER CRYSTALS

BHATTACHARYA, BISWAJIT (BAM Federal Institute for Materials Research and Testing, Berlin, GER); Michalchuk, Adam A. L. (BAM Federal Institute for Materials Research and Testing, Berlin, GER); Emmerling, Franziska (BAM Federal Institute for Materials Research and Testing, Berlin, GER)

Crystalline molecular materials with mechanical flexibility are promising for technological development. While a growing number of mechanically flexible crystalline molecular materials are being reported,<sup>1</sup> they remain scarce. At present, most discoveries are serendipitous, as limited design strategies are currently known. Amongst these strategies Desiraju *et. al.* suggested that elastic materials must contain herringbone structures.<sup>2</sup> For plastic crystals, the so-called 'shape-synthon' strategy has been developed, in which weak non-covalent interactions are introduced into structures to facilitate mobility of molecules.<sup>3</sup> This includes formation of slip planes. Generally, these models have performed very well at predicting and rationalizing the mechanical properties of new materials. Recently, however, a family of one-dimensional covalent networks (coordination polymers; CPs) has been described, which show mechanical elasticity. With drastically different structural chemistry, these systems do not seem to adhere to the currently established rules. Herein, we present the first such system: a plastically bendable crystal of a 1D CP,  $[\text{Zn}(\text{m-Cl})_2(\text{3,5-Cl}_2\text{Py})_2]_n$  (where 3,5-Cl<sub>2</sub>Py = 3,5-dichloro pyridine). This CP crystallizes in a tetragonal, and can therefore be bent over two major faces to acute angles without fracturing. We conducted bending and indentation experiments to quantify the mechanical properties of the CP crystal. This was complimented by Vibrational (Raman and Terahertz) spectroscopy and theoretical calculations for deeper understanding of molecular level structural deformation.

[1] Acc. Chem. Res., 2018, 51, 2957–2967.

[2] Angew. Chem. Int. Ed., 2015, 54, 2674–2678.

[3] J. Am. Chem. Soc., 2016, 138, 13561–13567.

[4] Angew. Chem., 2018, 130, 15017–15021.

## MS35-P26 | ORGANIC COCRYSTALS WITH MECHANICALLY INTERLOCKED ARCHITECTURES: UNPRECEDENTEDLY STIFF AND HARD WITH ELASTIC FLEXIBILITY

Dey, Somnath (Institute of Crystallography, RWTH Aachen University, Aachen, GER); Das, Susobhan (Department of Chemical Sciences, Indian Institute of Science Education and Research (IISER) Kolkata, Mohanpur, IND); Reddy, C. Malla (Department of Chemical Sciences, Indian Institute of Science Education and Research (IISER) Kolkata, Mohanpur, IND)

Mechanical properties of molecular crystals and their limits of adaptability have attracted tremendous interest among researchers in the recent years. Recent nanoindentation experiments revealed that certain molecular crystals with strong hydrogen bond networks can be as stiff as 44 GPa while theoretical predictions show these values exceeding 100 GPa [1]. However, the very presence of strong H-bonds deters any macroscopic flexibility which is also a key determining factor of candidacy for potential applications. On the other hand, mechanically flexible crystals which comprise overwhelmingly weaker interactions are mostly known to be significantly softer (up to ~18 Gpa).

Here we report an exceptional mechanical stiffness (~78 GPa) and unprecedentedly high hardness (~7 GPa) in an elastically bendable organic cocrystal [caffeine, 4-chloro-3-nitrobenzoic acid and methanol (1:1:1) [2]]. These values are comparable to certain low-density metals and counter intuitive considering the current knowledge. Spatially resolved atomic level studies reveal that (i) mechanically interlocked weak hydrogen bond networks separated by dispersive interactions gives rise to such unprecedented elasticity and hardness; (ii) The bent crystals significantly conserve the overall energy by efficient redistribution of stress; (iii) Perturbations in weak hydrogen bonds are compensated by strengthened  $\pi$ -stacking. Further, we report for the first time a remarkable stiffening (~11%) and hardening (~100%) in the elastically bent crystal. Hence, mechanically interlocked architectures provide an unexplored route to reach new mechanical limits and adaptability in organic crystals.

[1] Angew. Chem. Int. Ed. 2015, 54, 13566 –13570

[2] Angew. Chem. Int. Ed. 2012, 51, 10319 –10323

## MS35-P27 | ENGINEERING OF SUPRAMOLECULAR COORDINATION SPHERES FOR SELECTIVE FULLERENE BINDING AND FUNCTIONALISATION

Holstein, Julian (TU Dortmund University, Dortmund, GER); Chen, Bin (TU Dortmund University, Dortmund, GER); Horiuchi, Shinnosuke (TU Dortmund University, Dortmund, GER); Hiller, Wolf (TU Dortmund University, Dortmund, GER); Clever, Guido (TU Dortmund University, Dortmund, GER)

We present a modular self-assembly system based on a new low-molecular-weight binding motif, appended by two palladium(II)-coordinating units of different steric demands, to either form a  $[\text{Pd}_2\text{L}^1_4]^{4+}$  cage or an unprecedented  $[\text{Pd}_2\text{L}^2_3(\text{MeCN})_2]^{4+}$  bowl (with  $\text{L}^1 = \text{pyridyl}$ ,  $\text{L}^2 = \text{quinoliny}$  donors). The former was used as a selective induced-fit receptor for  $\text{C}_{60}$ . The latter, owing to its more open structure, also allows binding of  $\text{C}_{70}$  and fullerene derivatives. By exposing only a fraction of the bound guests' surface, the bowl acts as fullerene protecting group to control functionalization, as demonstrated by exclusive monoaddition of anthracene. Supramolecular crystals of these systems are extremely volatile to solvent loss. Crystal quality was preserved by immediate flash cooling in liquid nitrogen and subsequent cryogenic sample handling and storage. For this study, six structures were successfully characterized by single-crystal X-ray diffraction using macromolecular synchrotron beamline P11, DESY. Challenges in structural modelling related to highly flexibility and disorder in the structures were addressed by carefully adapted macromolecular refinement protocols.

## MS35-P28 | EVALUATION OF TRENDS IN A SERIES OF HALOGENATED ISOPHTHALAMIDES

Osman, Islam Ali (Dublin City University, Dublin); Gallagher, John F (Dublin City University, Dublin)

A series of halogenated isophthalamides (**X-DIPs**; **X** = halogen) has been synthesised and characterised by conventional spectroscopic techniques and single crystal X-ray diffraction. The series builds on previous studies of the crystal structures of benzamides and carboxamides together with their physicochemical properties, especially melting point analyses. Structural comparisons are made with results obtained from conformational analyses (potential energy scans) and modelled minima correlated with crystal structure data.

Structures in the **X-DIP** series preferentially adopt either the *anti/anti*- or *syn/anti* molecular conformations. In **Br-DIP**, molecules aggregate *via* reciprocal N-H...N and C-H...N interactions about inversion centres forming molecular pairs [graph sets  $R^2_2(7)$ ,  $R^2_2(20)$ ]. **Br-DIP** pairs connect by N-H...O and C-H...O interactions that cumulatively aggregate into a one molecule wide sheet (~20 Å wide) and parallel with the *bc* plane. Strong intermolecular interactions within the sheet involve both amides and pyridines (N-H...O=C; N-H...N), together with C-H...O/N interactions. Two sheets form per unit cell intersecting at  $x = 0, 0.5$ . The sheet surface contains Br atoms interspersed regularly as an array with five shortest Br...Br distances from 4.1 to 5.1 Å. Sheets link by Br...Br halogen bonding with shortest Br...Br = 3.6197(17) Å. Two other Br...Br contacts span the sheet interface at 3.8534(14) Å and 3.8988(16) Å. The sheet surface does not contain any other type of intermolecular interaction and one can surmise that sheets can glide over one another easily and may explain the observed twinning.

## MS35-P29 | INSIGHTS INTO THE MOLECULAR ARRANGEMENTS OF SUBSTITUTED HYDROXYPYRIDINE CARBOXYLIC ACIDS

May, Nóra V. (Research Centre for Natural Sciences, Hungarian Academy of Sciences, Budapest, HUN); Gál, G. Tamás (Research Centre for Natural Sciences, Hungarian Academy of Sciences, Budapest, HUN); Di Marco, Valerio B. (Department of Chemical Sciences, University of Padova, Padova, ITA); Bombicz, Petra (Research Centre for Natural Sciences, Hungarian Academy of Sciences, Budapest, HUN)

Exploring the secondary interactions is important to the development of new pharmaceutical therapies by understanding the interactions at drug binding site, in protein-protein interactions and also in drug encapsulation and targeted release mechanism. Hydroxypyridinecarboxylic acids (HPC) have been proposed recently as potential chelating agents for Fe(III) and Al(III) due to their favourable properties which include low toxicity, no redox activity and high complex stability. A series of mono- and dimethyl, hydroxy-ethyl and carboxy-ethyl substituted HPCs have been crystallized and the crystal structures have been determined by single crystal X-ray diffraction. The non-covalent interactions and molecular arrangements have been studied to investigate the electrostatic and steric effect of H-donor and  $\pi$ -acceptor substituents to the molecular self-assembly. The position of the hydroxyl proton involved in an intramolecular hydrogen bond with the carboxylate oxygen inform us about the electron distribution on the oxygen donor atoms and about the aromaticity of the pyridine ring. This is important because this proton is replaced by the metal ion during the action of chelation therapy. The main secondary interactions ( $\pi\cdots\pi$ , C-O $\cdots\pi$ , C-H $\cdots$ O, N-H $\cdots$ O) have been identified with which synthon arrangements are preserved in the crystals of different substituents.

These results could give a deeper understanding of intermolecular interactions and their effect on the arrangement of molecules in the solid phase influenced by addition of H-donor and acceptor substituents.

Acknowledgements: This work was supported by the National Research, Development and Innovation Office through OTKA K115762, K124544 and by the J. Bolyai Research Scholarship of the HAS (N. V. M.).

## MS35-P30 | HALOGENATION DICTATES ARCHITECTURES AND PROPERTIES OF AMYLOID

### PEPTIDES

Terraneo, Giancarlo (Politecnico di Milano, Milano, ITA); Pizzi, Andrea (Politecnico di Milano, Milano, ITA); Pigliacelli, Claudia (Aalto University, Espoo); Baldelli Bombelli, Francesca (Politecnico di Milano, Milano, ITA); Metrangolo, Pierangelo (Politecnico di Milano, ITA)

Besides pathological roles in many diseases, *e.g.*, Alzheimer's, Parkinson's, Creutzfeldt–Jakob, and Huntington's, amyloid peptide architectures have found many other non-biological applications such as forming highly ordered nanomaterials. Together with their biocompatibility and the ease of production, amyloidogenic peptides show a very versatile polymorphic behavior yielding a broad range of hierarchical structures, such as tapes, ribbons, fibers, nanoparticles, and nanotubes. Subtle variations in the experimental conditions, peptide sequence or its chemical functionalization may impact the self-assembly pathway and, consequently, the resulting nanostructures. Here we report that depending on the number, position, and nature of the halogen atoms introduced into either one or both phenylalanine benzene rings of the amyloid  $\beta$  peptide-derived core-sequences such as DFNKF (H<sub>2</sub>N-Asp-Phe-Asn-Lys-Phe-COOH) and KLVFF (H<sub>2</sub>N-Lys-Leu-Val-Phe-Phe-COOH), different architectures and properties are obtained in a controlled manner [1].

[1] Pizzi, A., Demitri, N., Terraneo, G. & Metrangolo, P. (2018). *CrystEngComm*. **20**, 5321–5326.

[2] Pizzi, A., Pigliacelli, C., Gori, A., Ikkala, O., Demitri, N., Terraneo, G., Castelletto, V. & Hamley, I. W. (2017). *Nanoscale*. 9805–9810.

## MS35-P31 | DESIGN OF COCRYSTALS BASED ON ESSENTIAL OILS WITH A PALETTE OF DIFFERENT PROPERTIES

Bacchi, Alessia (University of Parma, Parma, ITA); Carraro, Claudia (University of Parma, Parma, ITA); Mazzeo, Paolo Pio (University of Parma, Parma, ITA); Pelagatti, Paolo (University of Parma, Parma, ITA)

Cocrystals are multicomponent crystalline materials made by different chemical entities in stoichiometric ratio: designing a cocrystal requires a thorough knowledge of the possible interactions between the molecular partners. We present cocrystals containing liquid natural essential oils (EO), designed to tune the oil release profile at different environmental conditions. Appropriate supramolecular synthons between the EO molecule and suitable coformers provide a stable intermolecular network for the EO and increase the melting point stabilizing the liquid ingredient in a solid form. These supramolecular interactions also determine many fundamental physical properties of the material, e.g. solubility, hygroscopicity, thermal stability, density and mechanical strength. Thus cocrystallization offers great opportunities to create a palette of materials with empowered characteristics for processing, performance and shelf-life. We present the design of a library of cocrystals combining eugenol (extracted from clove buds and leaves), carvacrol (extracted from oregano) and thymol (the main component of thyme) with phenazine and hexamethylenetetramine to scan the range of properties that can be varied by pairing each EO with a different coformer. Coformers have been selected as rigid molecules acting as H-bond acceptors. The six EO/coformer combinations resulted in six prototype cocrystals, which were fully characterized in terms of physical properties and in-vitro biological activities and compared with the pure EO. We show that these cocrystals span a broad range of properties, thus extending the applicability of these materials in various circumstances which might need different responses to external conditions, such as high or low ambient temperature, short term or long term release.

## MS35-P32 | HIERARCHICAL DESIGN OF LIPID-POLYMER COMPOSITE NANOFIBERS: THE INTERPLAY OF MULTISCALE STRUCTURES AND BIOFUNCTIONS

Sadeghpour, Amin (Empa, Swiss Federal Laboratories for Materials Science and Technology, Center for X-Ray Analytics, St. Gallen, CH); Tien, Nguyen-Dung (Empa, Swiss Federal Laboratories for Materials Science and Technology, Center for X-Ray Analytics, St. Gallen, CH); Maurya, Anjani Kumar (Empa, Swiss Federal Laboratories for Materials Science and Technology, Center for X-Ray Analytics, St. Gallen, CH); Fortunato, Giuseppino (Empa-Swiss Federal Laboratories for Materials Science and Technology, Laboratory for Biomimetic membranes and Textiles, St. Gallen, CH); Dommann, Alex (Empa, Swiss Federal Laboratories for Materials Science and Technology, Center for X-Ray Analytics, St. Gallen, CH); Rossi, René M. (Empa-Swiss Federal Laboratories for Materials Science and Technology, Laboratory for Biomimetic membranes and Textiles, St. Gallen, CH); Neels, Antonia (Empa, Swiss Federal Laboratories for Materials Science and Technology, Center for X-Ray Analytics, Dübendorf, CH)

The unique features of lyotropic liquid crystalline cubic particles (cubosomes) originate from their thermodynamically stable hierarchical arrangement of molecules in nanoscale. Their function as drug delivery systems is correlated with the complex structural reorganisation in response to variations of biophysical conditions [1]. Moreover, polymer electrospinning is a versatile technique to produce sub-micron sized interconnected fibers which offers a noble solid substrate for uptake of nanoparticles for wide range of applications in biomedical domain [2,3]. Our recent work has been focused on the fabrication and characterisation of novel smart nanofibers based on polymer-lipid cubosome composites, Qfibers.

In this contribution, we present our latest achievements on the design of novel Qfibers and understanding their multiscale structural variations, mainly by small and wide angle X-ray diffraction techniques. The interplay between cubosomes and polymers over electrospin processing and after fabrication and under different external mechanical/environmental conditions will be discussed. Electron microscopy and micro-CT techniques will also be linked to scattering/diffraction analysis. Eventually, the structural responses will be briefly communicated along with the functional behaviour i.e. kinetics of drug release.

[1] Rajabalaya, R.; Musa, M. N.; Kifli, N.; David, S. R. *Drug Des. Dev. Ther.* **2017**, *11*, 14.

[2] Guex, A. G.; Weidenbacher, L.; Maniura-Weber, K.; Rossi, R. M.; Fortunato, G. *Macromol. Mater. Eng.* **2017**, *302*, (10), 8.

[3] Maurya, A. K.; Weidenbacher, L.; Spano, F.; Fortunato, G.; Rossi, R. M.; Frenz, M.; Dommann, A.; Neels, A.; Sadeghpour, A. *Nanoscale* **2019**, *11*, (15), 7176-7187.

## MS35-P33 | NEW SYNTHONS IN SUPRAMOLECULAR CHEMISTRY OF SHORT BIOLOGICALLY

### ACTIVE PEPTIDES

Bojarska, Joanna (Technical University of Lodz, Łódź, POL); Wolf, Wojciech (Technical University of Lodz, Łódź, POL); Zabrocki, Janusz (Technical University of Lodz, Łódź, POL); Kaczmarek, Krzysztof (Technical University of Lodz, Łódź, POL); Remko, Milan (Remedika, Bratislava, SVK)

Oligopeptides have been attracting an increasing interest due to their applications in anticancer therapy, drug delivery or as supramolecular biofunctional materials. Simple biomolecules in bio-systems, whose architecture is controlled by non-covalent interactions, have an input in understanding of bio-systems. Supramolecular interactions in a precise co-operation just like virtuosos play a symphony of *life*. Rational design of smart bio-materials should be based on thorough knowledge on interactions, what is still challenging. The concept of supramolecular synthons is useful in small supramolecules study and helps to understand the ligand binding in the protein-active-sites. This work focuses on introducing new bio-synthons, viewed in a holistic way at the supramolecular landscape, based on our research or from the CSD/PDB. We revealed that weak interactions ( $\pi\cdots\pi$ , C-H $\cdots\pi$ , a lone pair $\cdots\pi$ , etc.) play a vital role in synthons creation. Interplay of them leads to cooperativity. In particular, fluorenylmethoxycarbonyl (Fmoc) participates in bio-synthons *via* C-H $\cdots$ O( $\pi$ ), C-Br(I) $\cdots\pi$  interactions. Peptides modified by Fmoc are used as hydrogelators or inhibitors in therapies of Alzheimer`s diseases, while presence of cyclopropyl in APIs, similar to proline, increases bio-activity. The cyclopropyl has ability (due to C-C bonds character) to formation of  $\pi$ -<sub>cyclopropyl</sub> $\cdots$ H-C synthon. We highlight relevance of proline-based synthons and synthon methodology in study of APIs/biomaterials polymorphism. The results will contribute to the development of supramolecular chemistry of biomolecules, which has a bright future ahead in interpretation of bio-phenomena, advanced therapeutic approaches.

Participation financed by National-Science-Centre, Poland, 2018/02/X/ST4/02237.

## MS35-P34 | CONTROLLING THE SALT-COCRYSTAL CONTINUUM AND pK<sub>a</sub> RULE: THE MULTI-DRUG IONIC-COCRYSTALS OF LAMATRIGINE AND VALPROIC ACID

Lusi, Matteo (University of Limerick, Limerick); Kavanagh, Oisín (University of Limerick, Limerick)

The rational design of molecular crystals requires that the structure and properties of a crystallization product could be successfully predicted from the knowledge of the structures and properties of its molecular components. Such goal is still to come and synthetic crystallographers must rely to practical rules of thumb to increase chances of success in their endeavours. One of such rule uses the difference in pK<sub>a</sub> between interacting molecules to predict whether the product of a cocrystallization forms a salt or a cocrystal. The rule is less reliable for values of  $\Delta pK_a$  comprised between 0 and 3 and such behaviour is explained by the concept of a continuum between salt and cocrystals.

Here the multi-drug ionic cocrystal between Lamatrigine and Valproic acid is reported. The new form has increased solubility and mechanical properties over the starting materials and a stoichiometry that is indicated in the treatment of epilepsy. Moreover, crystal structure and computational analysis reveal that the ionization of the aminopyridinium-carboxilate synthon depends on ancillary H-bond donors. Ultimately, such multi-molecular synthon explains the salt-cocrystal continuum and the limits of the pK<sub>a</sub> rule.

## MS35-P35 | EFFECT OF CRYSTALLIZATION CONDITIONS ON DIURETIC CLOPAMIDE AND ITS COPPER(II) COMPLEXES

Gál, Gyula Tamás (Hungarian Academy of Sciences Research Centre for Natural Sciences, Budapest, HUN); May, Nóra V. (Hungarian Academy of Sciences Research Centre for Natural Sciences, Budapest, HUN); Trif, László (Hungarian Academy of Sciences Research Centre for Natural Sciences, Budapest, HUN); Bombicz, Petra (Hungarian Academy of Sciences Research Centre for Natural Sciences, Budapest, HUN)

Clopamide (4-chloro-N-2,6-dimethylpiperidin-1-yl)-3-sulfamoylbenzamide) is an active pharmaceutical ingredient (API) categorized as a thiazide-like diuretic and is used against hypertension and oedema. The carbonyl oxygen and the piperidine nitrogen of the clopamide molecule are able to coordinate to metal centres. The sort of coordination of the bioligand to metal ions can affect their biological properties. Despite of its medical application the structure of the clopamide molecule or any of its metal complexes has not been published so far.

Our primary aim was to reveal the single crystal structure of clopamide. The outcome of several successful crystallization experiments allowed us to harvest single crystals of a series of clopamide containing compounds. It has opened up the way to determine how far the molecular conformation and the packing arrangement – isostructurality - can be preserved in respond to chemical changes to enrich the knowledge on the aspects which contribute to the development of materials with specific properties.

We have studied the free ligand and its copper(II) complexes under different conditions (pH, solvent, counter ion) applying different techniques (single crystal X-ray diffraction (SXRD), electron paramagnetic resonance (EPR) spectroscopy, and thermoanalytical methods).

SXRD was used to determine the crystal structure of the free ligand and of the *bis*-ligand copper complexes obtained under different crystallization conditions. We succeeded to determine the crystal structure of both clopamide hemihydrate (C2/c) and anhydrous clopamide (P2<sub>1</sub>/n). The *bis*-ligand copper(II) complexes of clopamide have been crystallized from different pH's and solvents.

## MS35-P36 | MULTICOMPONENT CRYSTAL FORMATION OF BACLOFEN WITH ACIDS AND BASES

Malapile, Ramokone (Cape Peninsula University of Technology, Cape Town, ZAF); Nassimbeni, Luigi (University of Cape Town, Cape Town, ZAF); Bathori, Nikoletta (Cape Peninsula University of Technology, Cape Town, ZAF)

Amino acids are used often as coformers in cocrystallisation experiments due to the coexistence of a carboxylic acid/carboxylate and a primary amine/ammonium moiety in their molecular structure. Extensive investigations often focus on the  $\alpha$ -amino acids because of their biological importance and abundance in naturally occurring proteins and, rather less interest has been shown towards the  $\beta$  or  $\gamma$ -amino acids [1]. Baclofen (BAC, (*RS*)-4-amino-3-(4-chlorophenyl)butanoic acid), a  $\gamma$ -amino acid is an active pharmaceutical ingredient that is in the focus of interest in the South African pharmaceutical research because of its possible use in treatment of soft drug addictions and early stage of alcoholism. We have previously used BAC to form multicomponent crystals with a series of organic acids and concluded that  $\gamma$ -amino acids, such as BAC, are promising crystal engineering tools because of their structural flexibility and hydrogen bonding properties [2].

Seven multicomponent crystals of BAC were formed with both acidic and basic coformers to investigate the synthon formation of BAC when it is in protonated or deprotonated form. The crystal structure, thermal analysis and powder X-ray analysis of the multicomponent crystals are presented and conformation and protonation properties of the baclofen moiety are discussed.

**Keywords:** pharmaceuticals, multicomponent crystals, crystal engineering

[1] E. V. Boldyreva, Crystalline amino acids, in *Models, mysteries and magic of molecules*, ed. J. C. A. Boyens and J. F. Ogilvie, Springer, Dordrecht, 2008, pp. 167–192.

[2] N. B. Báthori and O. E. Y. Kilinkissa, *CrystEngComm* **2015**, *17*, 8264-8272.

## MS35-P37 | STRUCTURALLY DIVERSE MANGANESE(III) - SALPN COMPLEXES WITH BRIDGING

### FORMATE LIGAND

Schoeller, Martin (Department of Inorganic Chemistry, Institute of Inorganic Chemistry, Technology and Materials, Slovak University of Technology, Bratislava, SVK); Moncol, Jan (Department of Inorganic Chemistry, Institute of Inorganic Chemistry, Technology and Materials, Slovak University of Technology, Bratislava, SVK)

A series of formate-bridged manganese(III) complexes derived from Schiff based obtained by the condensation of 5-bromo-salicylaldehyde, 5-chloro-salicylaldehyde, 3,5-dibromo-salicylaldehyde or 3,5-dichloro-salicylaldehyde and 1,3-diaminepropane have been synthesized and characterized using single-crystal X-ray crystallography in the cases of  $[\text{Mn}(5\text{-Brsalpn})(\text{HCO}_2)]_n$  (1),  $[\text{Mn}(5\text{-Clisalpn})(\text{HCO}_2)]_n$  (2),  $[\text{Mn}(3,5\text{-Br}_2\text{salpn})(\text{HCO}_2)]_n$  (3),  $[\text{Mn}(3,5\text{-Cl}_2\text{salpn})(\text{HCO}_2)]_n$  (4) and  $[\text{Mn}(3,5\text{-Br}_2\text{salpn})(\text{HCO}_2)(\text{MeOH})] \cdot 2\text{MeOH}$  (5).

## MS35-P38 | THE PHOTODIMERIZATION OF SCHIFF BASES: BENZOPHENONE AZINE CRYSTALS AND THEIR WEAK C-H... $\pi$ INTERACTIONS

Smith, Mark (University of South Africa, Johannesburg, ZAF); Lemmerer, Andreas (University of the Witwatersrand, Johannesburg, ZAF)

Four benzophenone azines were synthesized through a photodimerization process. The crystals are constructed through weak C-H... $\pi$  packing interactions, with additional  $\pi$ ... $\pi$  stabilization in two of the crystals. The four intermediates of the photodimerization process were also crystallized and their crystal structures are discussed. The packing of three of these intermediates involves weak C-H...O interactions. The crystal structure of di-isoniazid azine, an expected by-product of the photodimerization process, is also described.

### DIOLS

Cichowicz, Grzegorz (University of Warsaw, Warszawa, POL); Dobrzycki, Lukasz (University of Warsaw,, Warsaw, POL); Boese, Roland (University of Warsaw, Warsaw, POL); Cyranski, Michal (University of Warsaw, Warsaw, POL)

Simple amines and alcohols are usually used as “building blocks” in supramolecular synthesis, solvents, ligands or cocrystallization agents. Variety of applications originates in presence of functional groups able to participate in strong hydrogen bonds. As both hydroxyl and amine moieties are complementary, designing new cocrystals of such compounds can lead to complex structures with large diversity of crystal architectures.

Cocrystals of primary monoalcohols and amines exhibits a topology similar to allotropic form of gray arsenic - layers build by six-membered ring-shaped with chair conformation. In order to obtain complex three-dimensional motifs, cocrystallizations of linear aliphatic diamines and diols with different chain length were performed. Most of them are liquids at ambient condition, therefore an IR laser supported *in situ* crystallization method has been applied. In most of obtained phases containing saturated diols characteristic layers composed of six-membered, ring-shaped hydrogen bond motif is present. However, in some phases, like in the case of 1,5-diaminopentane with 1,5-pentanediol cocrystal, this motif does not occur, what is associated with a conformational change of both molecules. These structures contain molecules arranged in 1D columns instead. Relatively small change in shape of a molecule may affect the final structure. Indeed, cocrystallization of unsaturated 1,4-but-2-enediol with 1,4-diaminobutane and 1,6-diaminohexane resulted in formation of incommensurately modulated phases.

The National Science Center in Poland (Grant SONATA BIS 6 NCN, 2016/22/E/ST4/00461) is gratefully acknowledged for financial support.

## MS35-P126 - LATE | HYBRID POLYOXOMOLYBDATE SYSTEMS BASED ON RATIONALLY DESIGNED ASYMMETRIC CARBOHYDRAZONES

Rubicic, Mirta (Department of Chemistry, Faculty of Science, University of Zagreb, Zagreb, HRV); Topic, Edi (Department of Chemistry, Faculty of Science, University of Zagreb, Zagreb, HRV); Pisk, Jana (Department of Chemistry, Faculty of Science, University of Zagreb, Zagreb, HRV); Vrdoljak, Višnja (Department of Chemistry, Faculty of Science, University of Zagreb, Zagreb, HRV)

The hydrazone functional group is a universal building block incorporated in a wide spectrum of organic and inorganic compounds [1]. Its stability, modularity and subsequent structural versatility along with the acid-base properties makes hydrazones applicable as *e.g.* molecular switches, sensors or as anion receptors. Moreover, the adaptability of hydrazones *via E/Z* isomerisation, designates them as pervasive ligands for the construction of extended metal-organic assemblies, like metal-organic grids or hybrid metal-organic systems. In this family, especially stimulating are bis-hydrazones, as they extend the scope of the (mono)hydrazone counterparts. Carbohydrazones, in particular offer, besides increment in a number of hydrazone linkages, a possibility of asymmetric design, while providing systems with two different subunits varying in coordinating behaviour and acid-base properties.

Here we unveil an interesting coordination and anion receptor scenarios offered by asymmetric carbohydrazones bearing hydroxyaryl and pyridyl moieties. It was established that under appropriate conditions, such carbohydrazones can act as cations, as multifunctional ligands or as a combination thereof. While the first scenario led to corresponding polyoxomolybdate (POM) salts, in the second case discrete dinuclear complexes formed. The last option refers to hybrid POMs, where charged dioxomolybdenum(VI) complexes adopted a role of cations. Whereas dioxomolybdenum(VI) complexes have their structures determined by chelating hydroxyaryl subunit, structures of POM salts are shaped by competition between the relevant hydrogen bonds involving both ligand subunits.

[1] X. Su, I. Aprahamian, *Chem. Soc. Rev.* **43** (2014) 1963.

This work has been fully supported by Croatian Science Foundation under the project IP-2016-06-4221.

## MS35-P128 - LATE | INTERACTIONS IN COPPER(II), NICKEL(II) AND COBALT(II) COMPLEXES WITH N-METHYL-, N-ETHYL- AND N-PROPYLGLYCINE: MONOMERS, DIMERS AND POLYMERS

Matkovic-Calogovic, Dubravka (University of Zagreb, Faculty of Science, Department of Chemistry, Zagreb, HRV); Vušak, Darko (University of Zagreb, Faculty of Science, Department of Chemistry, Zagreb, HRV); Smrecki, Neven (University of Zagreb, Faculty of Science, Department of Chemistry, Zagreb, HRV); Prugovecki, Biserka (University of Zagreb, Faculty of Science, Department of Chemistry, Zagreb, HRV)

*N*-alkylated amino acids play an important role in the studies related to the structural properties and biological activity and are very interesting compounds in fields such as medicinal chemistry and crystal engineering. We are interested in structures and properties of essential metal complexes with amino acids and their derivatives [1] (grant of the Croatian Science Foundation IP-2014-09-4274).

In this research we have synthesized and structurally characterized twelve new copper(II), nickel(II) and cobalt(II)/cobalt(III) compounds with *N*-methyl-, *N*-ethyl- and *N*-propylglycine. In nine monomeric complexes,  $[M(\text{Rgly})_2(\text{H}_2\text{O})_2]$  ( $M = \text{Co}, \text{Ni}$ ;  $R = \text{Me}, \text{Et}, \text{or Pr}$ ), the metal ion is octahedrally coordinated with two *O,N*-donating *Rgly* ligands in the *trans*-fashion and two water molecules in the axial positions. In eight complexes the hydrogen bond donors ( $\text{N-H}$  and  $\text{O}_{\text{water}}\text{-H}$ ) interact with the neighboring carboxylic groups forming 2D networks. The alkyl groups point outward of the layers so there are only van der Waals interactions between them. Of the monomeric compounds only  $[\text{Cu}(\text{Megly})_2(\text{H}_2\text{O})_2]$  forms a 3D network. In  $[\{\text{Co}(\text{Etgly})_2\}_2(\mu\text{-OH})_2]\cdot 2\text{H}_2\text{O}$  oxidation occurred and it is a dimeric Co(III) complex with a 3D network.  $[\text{Cu}(\mu\text{-Rgly})_2]_n$  ( $R = \text{Me}$  or  $\text{Et}$ ) are coordination polymers with 2D layered structures. Influence of alkyl chain length, intermolecular interactions, isostructurality, polymorphs and other structural details and properties will be discussed.

[1] Vušak, D. *et al.* (2017). *Cryst. Growth Des.* **17**, 6049–6061.

# MS36: Amorphous Solids, Solid Solutions, Cocrystal Alloys and Cocrystals

---

## MS36-01 | IONIC CO-CRYSTALS

Braga, Dario (University of Bologna, Bologna, ITA)

In this talk the reasons for the widespread interest generated by ionic co-crystals, namely the co-crystals formed by a neutral molecule and a salt, are addressed. In particular, the class of compounds obtained by co-crystallization of neutral organic molecules and inorganic salts (e.g. alkali and alkaline earth halides, sulfates, phosphates etc.) is discussed with the focus on their applications in diverse areas, such as pharmaceuticals, food, fertilizers and enzyme activity inhibitors.

It is argued that, in terms of structure and intermolecular bonding features, these compounds do not differ from classical coordination compounds (complexes) and that their popularity arises from the effectiveness of the organic-inorganic assembly to enhance thermal stability, improve particle size and morphology and change significantly solubility and dissolution rate with respect to those of the pure active ingredients. Since most ionic co-crystals are prepared by solvent free mechanochemical methods, the importance of structure determination by powder diffraction is outlined. Furthermore, the preparation and characterization of solid solutions of isomorphous ionic co-crystals will be discussed.

[1] D. Braga, O. Shemchuk and F. Grepioni, *CrystEngComm*, 2018, 20, 2212-2220.

[2] D. Braga, F. Grepioni, L. Maini, S. Prospero, R. Gobetto, M. R. Chierotti, *Chem. Commun.*, 2010, 46, 7715-7717.

[3] D. Braga, F. Grepioni, L. Maini, D. Capucci, S. Nanna, J. Wouters, L. Aerts, L. Quéré, *Chem. Commun.*, 2012, 48, 8219-8221.

[4] L. Casali, L. Mazzei, O. Shemchuk, K. Honer, F. Grepioni, S. Ciurli, D. Braga, and J. Baltrusaitis, *Chem. Commun.*, 2018, 54, 7637-7640.

## MS36-02 | MANIPULATION OF THE CRYSTALLINE AND AMORPHOUS PHYSICAL STATES OF PHARMACEUTICAL MATERIALS: POSSIBILITIES, LIMITS AND CHALLENGES

ROCA PAIXAO, Luisa (University of Lille, Villeneuve-d'Ascq, FRA); Correia, Natalia (University of LILLE, VILLENEUVE D'ASCQ, FRA); Ngono Mebenga, Frederic (University of LILLE, VILLENEUVE D'ASCQ, FRA); Willart, Jean-Francois (University of Lille/CNRS, VILLENEUVE D'ASCQ, FRA); Cuello, Gabriel (Institut Laue-Langevin, Grenoble, FRA); Jimenez, Monica (Institut Laue-Langevin, Grenoble, FRA); Affouard, Frederic (University of LILLE, VILLENEUVE D'ASCQ, FRA)

The vast majority of drugs are generally prepared in the solid state (powder, tablets, and capsules) which can exist in multiple physical forms having fundamental different physical properties. Until now, pharmaceutical materials have been developed especially in the crystalline state for obvious reasons of stability. However, this state may often exhibit inadequate solubility or dissolution rate resulting in poor bioavailability, particularly for water-insoluble compounds. Different solutions have been proposed to overcome this major issue either based on chemical modifications of the drug molecules (salt formation) or physical manipulations of their physical states. For example, an interesting alternative is offered by the amorphous state which exhibits much greater dissolution rate. However, it is intrinsically unstable and capable of recrystallization which obviously negates its advantages. A “stabilization” is thus required and, for a few years, there has been a considerable interest on the so-called amorphous solid dispersions for which the strategy is to disperse pharmaceuticals in the amorphous state into a polymer matrix that hinders its recrystallization.

In this presentation, a review of the different possibilities, limits and challenges of the approaches based on the manipulation of the physical states and aiming to improve properties of pharmaceutical materials in terms of solubility, dissolution and stability will be presented.

This project has received funding from the Interreg 2 Seas programme 2014-2020 co-funded by the European Regional Development Fund under subsidy contract 2S01-059\_IMODE.

## MS36-03 | CHARACTERISATION OF “POLYAMORPHISM” AND THE MOLECULAR ORIGINS OF DISORDER USING COMPLEMENTARY METHODS

Skotnicki, Marcin (School of Pharmacy and Pharmaceutical Sciences, Dublin); Hodgkinson, Paul (Durham University, Durham, GBR)

Valsartan is a widely used antihypertensive drug marketed in an “amorphous” form. DSC studies show, however, that this form is distinct from a truly amorphous material produced by quench cooling from the melt. Powder diffraction and total scattering measurements show differences implying that the “as received” material has a greater degree of ordering, but neither material gives Bragg diffraction peaks. Counter-intuitively the more ordered material has a significantly higher solubility. Solid-state NMR is a powerful adjunct to diffraction-based techniques for the characterisation of pharmaceutical materials, particularly for characterising disorder. We used a combination of time-modulated DSC, PXRD and solid-state NMR to understand the molecular origin of this “polyamorphic” behaviour in terms of conformational “defects” [1]. Other examples are presented using co-crystals and solvates of pharmaceutical actives where quantum chemical calculations are invaluable in determining whether a disordered or an ordered structure is adopted [2,3]. Understanding why such disordered materials may be intrinsically stable is important in overcoming wariness about use of disordered materials as pharmaceutical forms.

[1] M. Skotnicki, D. C. Apperley, J. A. Aguilar, B. Milanowski, M. Pyda and P. Hodgkinson, *Mol. Pharmaceutics* **13** (2016) 13

[2] H. E. Kerr, H. E. Mason, H. A. Sparkes and P. Hodgkinson, *CrystEngComm* **18** (2016) 6700

[3] A. Bērziņš and P. Hodgkinson, *Solid State Nucl. Magn, Reson.* **65** (2015) 12

## MS36-04 | PHARMACEUTICAL SOLID SOLUTIONS FROM NON-SOLUBLE COMPONENTS

Lusi, Matteo (University of Limerick, Limerick)

Crystalline solid solutions of molecular species are a poorly understood class of material that allow the fine-tuning of structural and physicochemical properties, in continuum. Traditionally such phases are prepared according to simple guidelines as summarised by the Hume-Rotary and Kitaigorodskii set of rules. Similar size, isomorphism of the parent component and molecular isostructurality are often deemed as a requirement for solubility in the solid state.

Recent works show the limits of the above-mentioned rules and defines alternative supramolecular and synthetic strategies for the development of solid solutions from “non-soluble” components. Incidentally, the new strategy enable crystalline solid solutions of pharmaceuticals for more effective and simpler therapies.

## MS36-05 | CHARADE TRANSFER DONOR-ACCEPTOR COMPLEXES OF SEVERAL POLYCYCLIC AROMATIC MOLECULES

Rigin, Sergei (New Mexico Highlands University, LAS VEGAS, USA); Lesse, Daniel (Department of Chemistry, New Mexico Highlands University, Las Vegas, USA); Timofeeva, Tatiana (Department of Chemistry, New Mexico Highlands University, Las Vegas, USA)

For donor-acceptor pairs of 2,3-dichloro-5,6-dicyano-1,4-benzoquinone (DDQ, acceptor) and triphenylene, chrysene, dibenz[a,c]anthracene, and benzo[a]pyrene HOMO-LUMO energy levels have been calculated using DFT approach. Calculations demonstrated overlap of HOMO-LUMO gaps of acceptor and donors that suggested possibility of existence of charge transfer complexes for their adducts. Crystals of four adducts have been grown and their structures have been elucidated using X-ray diffraction analysis. It appears that all crystals are built of molecular stacks with alternating donor-acceptor positions (..D..A..D..A..). Degree of charge transfer was estimated using obtained molecular geometries. According to this approach, chrysene-DDQ complex has the highest charge-transfer degree among the other complexes with DDQ acceptor. The appearance of the chrysene-DDQ co-crystal is consistent with this result since a darker crystal usually indicates a stronger charge-transfer.

## MS36-P01 | FOUR-COMPONENT ISOMORPHISM IN THE CRYSTAL STRUCTURE OF [HL][Cd(HL)(NCS)<sub>2</sub>XY]·H<sub>2</sub>O, WHERE L = 2-ACETILPYRIDINE-AMINOGUANIDINE, X = Cl<sup>-</sup>/Br<sup>-</sup>, AND Y = Br<sup>-</sup>/SCN<sup>-</sup>

Rodic, Marko (Faculty of Sciences, University of Novi Sad, Novi Sad); Radanovic, Mirjana (Faculty of Sciences, University of Novi Sad, Novi Sad); Vojinovic-Ješić, Ljiljana (Faculty of Sciences, University of Novi Sad, Novi Sad); Leovac, Vukadin (Faculty of Sciences, University of Novi Sad, Novi Sad)

This study emerged from our ongoing research on transition metal complexes with Schiff base ligands, as this class of compounds has shown wide spectra of biological activities, catalytic behavior, magnetism, and optoelectronic properties, depending on the choice of the particular transition metal, and Schiff base ligand.

The title compound was obtained in the form of white rod-like single crystals, by reaction of warm aqueous solutions of CdBr<sub>2</sub> and the chloride salt of 2-acetylpyridine-aminoguanidine (L·2HCl), in molar ratio 1:1, in the presence of double excess of LiOAc and NH<sub>4</sub>NCS.

Single crystal X-ray analysis revealed that crystal structure consists of organic cation HL<sup>+</sup>, Cd(II)-containing complex anion of the formula [Cd(HL)(NCS)<sub>2</sub>XY]<sup>-</sup>, as well as one water molecule. Coordination environment of Cd(II) in the complex anion is distorted octahedral, with two axial sites occupied with NCS<sup>-</sup> ions, two equatorial sites occupied by bidentately coordinated organic ligand in monocationic form (HL<sup>+</sup>), while the remaining two equatorial sites (X, and Y) are occupied by Cl<sup>-</sup>/Br<sup>-</sup> and Br<sup>-</sup>/SCN<sup>-</sup> ions, respectively. This means that the crystal structure contains four different anions: [Cd(HL)(NCS)<sub>2</sub>Br<sub>2</sub>]<sup>-</sup> (ca. 3%), [Cd(HL)(NCS)<sub>2</sub>ClBr]<sup>-</sup> (ca. 35%), [Cd(HL)(NCS)<sub>2</sub>Br(SCN)]<sup>-</sup> (ca. 61%), and [Cd(HL)(NCS)<sub>2</sub>Cl(SCN)]<sup>-</sup> (ca. 1%).

The geometrical details of the crystal structure will be reported, as well as Hirshfeld surface analysis of the individual building-blocks with the aim of better understanding the nature of the isomorphism.

## MS36-P02 | DYNAMICAL DISORDER IN THE SOLID STATE: INSIGHTS FROM DIELECTRIC RELAXATION SPECTROSCOPIES

ROCA PAIXAO, Luisa (University of Lille, Villeneuve-d'Ascq, FRA); Viciosa, Maria Teresa (Univ of Lisbon, Lisboa); Correia, Natalia (University of Lille, Villeneuve d'Ascq, FRA); Affouard, Frederic (University of LILLE, VILLENEUVE D'ASCQ, FRA)

In order to obtain a thorough understanding of the behavior of simple or multiple-component crystalline and amorphous solids, various experimental techniques are conventionally used: X-ray diffraction, Infra-red & Raman spectroscopy, solid state nuclear magnetic resonance, calorimetric analysis... However, there are other less known techniques from the crystallographic community, namely Dielectric Relaxation Spectroscopy and Thermally Stimulated Currents, which can also be used to probe phase transformations and molecular mobility in a wide range of temperature and frequency (between  $10^{-3}$  Hz and 1 GHz). These are commonly used techniques for the characterization of amorphous and semi-crystalline disordered states.

In the present work, we will illustrate how these dielectric techniques can contribute significantly to the understanding of crystalline mesophases characterized by different levels of dynamic disorder, such as liquid crystals, plastic crystals and conformational disorder crystals.

This project has received funding from the Interreg 2 Seas programme 2014-2020 co-funded by the European Regional Development Fund under subsidy contract 2S01-059\_IMODE.

## MS36-P03 | MOLECULAR BASIS OF WATER SORPTION BEHAVIOR OF RIVAROXABAN-MALONIC ACID COCRYSTAL

Kale, Dnyaneshwar P. (National Institute of Pharmaceutical Education and Research (NIPER), S.A.S. Nagar, Mohali, IND); Ugale, Bharat (Indian Institute of Technology (IIT), Ropar, Rupnagar, IND); Nagaraja, C. M. (Indian Institute of Technology (IIT), Ropar, Rupnagar, IND); Dubey, Gurudutt (National Institute of Pharmaceutical Education and Research (NIPER), S.A.S. Nagar, Mohali, IND); Bharatam, Prasad V. (National Institute of Pharmaceutical Education and Research (NIPER), S.A.S. Nagar, Mohali, IND); Bansal, Arvind Kumar (National Institute of Pharmaceutical Education and Research (NIPER), S.A.S. Nagar, Mohali, IND)

We aim to investigate the molecular basis of water sorption behavior of rivaroxaban-malonic acid cocrystal (RIV-MAL). It was hypothesized that the amount of water sorbed by a crystalline solid is governed by surface molecular environment of different crystal facets, and their relative contributions to crystal surface. Water sorption behavior was measured using Dynamic Vapor Sorption Analyzer. Surface molecular environment of crystal facets and their relative contribution were determined using SC-XRD and face indexation, respectively. The surface area normalized water sorption for rivaroxaban (RIV), malonic acid (MAL), and RIV-MAL at 90% RH/25 °C was 0.28%, 92.6%, and 11.1% w/w, respectively. The crystal surface of MAL had larger contributions (58.7%) of hydrophilic (*Hphi*) chemical groups, showed the 'highest' water sorption (92.6% w/w). On the contrary, RIV had larger contribution (65.2%) of hydrophobic (*Hpho*) groups and smaller surface contributions (34.8%) of '*Hphi+Hpho*' groups, exhibited the 'lowest' water sorption (0.28% w/w). The 'intermediate' water sorption (11.1% w/w) by RIV-MAL as compared to RIV, was ascribed to the increased '*Hphi+Hpho*' contributions (from 34.8% to 42.1%) and reduced hydrophobic contributions (from 65.2% to 57.9%). However, the significantly higher water gained (~39 fold) by the cocrystal as compared to RIV, despite nominal change in the surface contributions, was further attributed to the relatively stronger hydrogen bonding interaction between the surface exposed carboxyl groups and water molecules. This study highlights that water sorption behavior of the cocrystal is governed by surface molecular environment, and additionally by the strength of hydrogen bonding interactions.

## MS36-P130 - LATE | COCRYSTALS OF CYCLOPENTYLAMINE WITH ALCOHOLS. SYNTHESIS AND STRUCTURAL STUDIES.

Sadocha, Anna (Uniwersytet Warszawski Wydział Chemii, Warszawa, POL); Nowosielska, Bernadeta (Uniwersytet Warszawski Wydział Chemii, Warszawa, POL); Rzepinski, Patryk (Uniwersytet Warszawski Wydział Chemii, Warszawa, POL); Cyranski, Michal (Uniwersytet Warszawski Wydział Chemii, Warszawa, POL); Boese, Roland (Uniwersytet Warszawski Wydział Chemii, Warszawa, POL); Dobrzycki, Lukasz (Uniwersytet Warszawski Wydział Chemii, Warszawa, POL)

Cyclopentylamine is a primary aliphatic amine, containing five carbon atoms ring. There has been known a number of structures containing cyclopentylamine mostly in cationic form as salts or as neutral ligand. However, up-to-now there has been reported only one hydrate with 1:1 water:amine stoichiometry [1]. The aim of the work was to crystallize and determine structures cocrystals containing cyclopentylamine with the following alcohols: methanol, ethanol, isopropanol, cyclopentanol and cyclohexanol. Because all these compounds, including also amine, are liquids at room temperature and ambient pressure, samples suitable for single crystal X-ray diffraction experiments were grown using IR laser assisted *in situ* method [2]. All of the obtained cocrystals crystallize in the *P* space group with the molecules arranged in ribbons with the same motif of hydrogen bonds present. Such reproducible behaviour towards alcohols makes cyclopentylamine very useful structural agent leading to similar and well defined 1D hydrogen-bonded networks.

Acknowledgements: The research was supported by the Polish National Science Center grant: SONATA BIS 6 NCN 2016/22/E/ST4/00461

[1] D. R. Allan, "Cyclopentylamine monohydrate", *Acta Cryst.*, 2006, E62, o1064-o1066.

[2] R. Boese, "Special issue on In Situ Crystallization", *Z. Kristallogr.*, 2014, 229, 595-601.

### CHARACTERIZATION

Marek, Paulina (Warsaw University of Technology, Warsaw, POL); Cichowicz, Grzegorz (University of Warsaw, Warsaw, POL); Madura, Izabela (Warsaw University of Technology, Warsaw, POL); Cyranski, Michal (University of Warsaw, Warsaw, POL); Ciesielski, Arkadiusz (University of Warsaw, Warsaw, POL)

Ionic co-crystals (ICC) are usually formed by organic molecule and inorganic salt. This class of compounds can combine properties of its components; e.g. bioactivity of organic molecule and good solubility of the salt, because of which it become of interest for crystal engineering and pharmaceutical applications. It was observed, that LiX-aminoacid ICCs can form structures of square grid topologies, build of 16-membered rings [1,2]. Whole networks are labile, and thus prone to polymorphs formation. Herein we present LiClO<sub>4</sub>·2βAla systems with both chiral and centrosymmetric basic motives, emerging from achiral components, crystallizing in *P2*<sub>1</sub> and *Pbca* space groups, respectively. What is more, ICCs were found to exhibit polymorphism with chiral – achiral solution – assisted phase transition analysed with PXRD and DSC experiments. Both polymorphic forms were structurally characterized using single-crystal X-ray diffraction showing topological similarity. Thermal tensor of kinetically and thermodynamically preferable forms was investigated, showing difference in thermal behaviour of both polymorphs. Periodic calculations allowed for confirmation of lattices energy differences in both structures.

This work was financed by a grant from the National Science Centre (DEC-2018/29/N/ST4/00451). This work was implemented as a part of Operational Project Knowledge Education Development 2014-2020 cofinanced by European Social Fund.

[1] Baran, J., et al., J. Mol. Struct. 927, 1-3 (2009) 43-53.

[2] Ong, T. T., et al., J. Am. Chem. Soc. 133, 24 (2011) 9224-9227.

## MS36-P141 | MULTICOMPONENT CRYSTALS OF 2,2'-BIPYRIDINE WITH ALIPHATIC DICARBOXYLIC ACIDS: STRUCTURE-PROPERTY CORRELATIONS

Batisai, Eustina (University of Venda, THOHOYANDOU, ZAF); Nethanani, Vhukhudo (University of Venda, THOHOYANDOU, ZAF)

Co-crystallization as a form of crystal engineering has been successfully employed in the preparation of pharmaceutical cocrystals with improved physical and chemical properties. Structure-property studies form a very important part of pharmaceutical co-crystal research. For example, the relationship between the supramolecular structure of a pharmaceutical co-crystal and some of its physical properties is not yet fully understood. The focus of this study is to investigate the relationship between melting point and the supramolecular structure of six model co-crystals of aliphatic dicarboxylic acids with 2,2'-bipyridine. The co-crystals were prepared by the solvent evaporation method and characterized using single crystal X-ray diffraction (SCXRD), powder X-ray diffraction (PXRD) and differential scanning calorimetry (DSC). The crystal structures were further analysed using Crystal Explorer and the results correlated with the melting points. The relationship between melting points and supramolecular structures is discussed.

## MS37: NMR Crystallography

---

### MS37-01 | NEW SENSITIVITY-ENHANCED NMR CRYSTALLOGRAPHY APPROACHES TO INVESTIGATE CRYSTALLIZATION AND POLYMORPHISM IN ORGANIC MATERIALS

Mollica, Giulia (CNRS, Marseille, FRA)

Polymorphism affects almost 50% of all the organic compounds referenced in the Cambridge Structural Database. It can have huge economic and practical consequences for industrial applications in pharmacy and energy because different polymorphs display different physicochemical properties. If, on the one hand, it offers great opportunities for tuning the performance of the organic material, on the other hand, manufacture or storage-induced, unexpected, polymorph transitions can compromise the end-use of the solid product. These transformations often imply the formation of metastable forms, which are receiving growing attention because they can offer new crystal forms with improved properties. Today, detection and accurate structural analysis of these – generally transient – forms remain challenging, essentially because of the present limitations in temporal and spatial resolution of the analysis, which prevents rationalization (and hence control) of crystallization processes.

We develop dynamic nuclear polarization (DNP) solid-state NMR approaches to overcome these limitations. In this contribution, I will present some of our latest results showing that cryogenic MAS NMR [1] combined with the sensitivity enhancement provided by DNP [2] can be an efficient way of monitoring the structural evolution of crystallizing solutions with atomic-scale resolution on a time scale of a few minutes.

This project has received funding from the European Research Council (ERC) under the European Union's Horizon 2020 research and innovation programme (grant agreement No 758498).

[1] P. Cerreia-Vioglio et al. *Angew. Chem. Int. Ed.* **2018**, *57*, 6619.

[2] P. Cerreia-Vioglio, et al. *J. Phys. Chem. Lett.* **2019**, *10*, 1505.

## MS37-02 | UNDERSTANDING SELF-ASSEMBLY OF MOLECULAR ORGANIC SOLIDS USING NMR CRYSTALLOGRAPHY: FROM MULTICOMPONENT SOLIDS TO SUPRAMOLECULAR HYDROGELS

Khimyak, Yaroslav (University of East Anglia, NORWICH, GBR)

Molecular level control of the self-assembly of organic molecules at different length scales is a significant challenge both in industrial and academic research. The strength of intermolecular interactions defines physical properties of such materials, which in turn may affect bioavailability. NMR crystallography has been successful in facilitating structural analysis of organic molecular solids. However, considerable challenges remain when applying structural and dynamic methods for multi-component molecular solids across different length and time scales.

Directing molecular aggregation of pharmaceuticals can be achieved by their encapsulation inside nanosize crystallisation chambers [1, 2]. Using advanced NMR methods, we have gained unique insight into self-assembly of multicomponent organic materials within the porous solids and identified different structural environments and mobility regimes from confined crystals to liquid-like species.

We have used single and multi-component hydrogels of *l*-phenylalanine and its derivatives to develop an NMR-based analytical approach to elucidate mechanisms of supramolecular gelation [3, 4]. Gelation of *l*-Phe results in formation of “crystalline” gel phases. The combination of rheology, XRD diffraction and NMR methods across different dynamic regimes (including high-field <sup>19</sup>F NMR) revealed a very detailed picture of self-assembly in the mixed gelator hydrogels both in the well-ordered fibres and at the solid-solution interphases. This enabled us to gain mechanistic understanding of the interplay of gelation, crystallisation and dynamics of self-assembly.

[1] Nartowski, *Khimiya Mol. Pharm*, **2018**, 4926

[2] Nartowski, *Khimiya, Angew. Chem. Int. Ed.* **2016**, 8904.

[3] Nartowski, *Khimiya, Cryst. Growth Des.* **2017**, 4100.

[4] Ramalhete, *Khimiya, Chem. Eur. J.* **2017**, 8014

## MS37-03 | <sup>1</sup>H, <sup>19</sup>F AND <sup>29</sup>Si MAS NMR INVESTIGATIONS OF SYNTHETIC LEPIDOLITE SAMPLES WITH VARIABLE OH/F RATIOS

Sulcek, Lara (Ruhr-Universität Bochum, Bochum, GER); Fechtelkord, Michael (Ruhr-Universität Bochum, Bochum, GER)

<sup>1</sup>H, <sup>29</sup>Si and <sup>19</sup>F solid state NMR spectroscopic, infrared spectroscopic and X-ray diffraction experiments were performed to investigate the cationic and anionic ordering in the octahedral and tetrahedral sheets in the system trilithionite - polyolithionite with composition  $K(Li_xAl_{3-x})[Al_{4-2x}Si_{2x}O_{10}](F_{2-y}OH_y)$  ( $1.5 \leq x \leq 2.0$ ;  $0.0 \leq y \leq 1.4$ ).

The influence of the different OH / F ratios on the composition of octahedral and tetrahedral layers and the resulting formation of secondary phases were considered. In addition, bonding preferences from F to Li-cations and OH to Al-cations should be elucidated. The changes in the tetrahedral and octahedral sheets and the relation to each other is another aspect of this work.

There are strong indications that signals from different polytypes can be separated in the <sup>19</sup>F MAS NMR spectra. Furthermore the X-ray diffraction experiments confirm the appearance of the polytypes 1M and 2M<sub>1</sub>. The percentage of both polytypes can be calculated by using the signal areas of the <sup>19</sup>F MAS NMR spectra. It can be shown, that the ratio of the polytypes is independent of the composition according to Heinrich (1967). Furthermore, the <sup>19</sup>F MAS NMR spectra show an F preference to Li-rich octahedral clusters and in contrast to this the <sup>1</sup>H MAS NMR spectra reveal the location of OH-groups in the Al-rich octahedral clusters.

[1] Heinrich, E.W. (1967) American Mineralogist, 52, 1110-1121.

## MS37-04 | DETERMINATION OF ELUSIVE CRYSTAL STRUCTURE OF SOLVATE-HYDRATE OF CATECHIN BY CRYSTAL STRUCTURE PREDICTION AND NMR CRYSTALLOGRAPHY

Dudek, Marta (Centre of Molecular and Macromolecular Studies, Polish Academy of Sciences, Lodz, POL); Paluch, Piotr (Center of Molecular and Macromolecular Studies, Polish Academy of Sciences, Lodz, POL); Sniechowska, Justyna (Center of Molecular and Macromolecular Studies, Polish Academy of Sciences, Lodz, POL); Nartowski, Karol (Wroclaw Medical University, Wroclaw, POL); Trebosc, Julien (CNRS, Universite Lille-Nord-de-France, Lille, FRA); Potrzebowski, Marek (Center of Molecular and Macromolecular Studies, Polish Academy of Sciences, Lodz, POL); Day, Graeme (Univeristy of Southampton, Southampton, GBR)

The idea standing behind crystal structure elucidation using NMR crystallography is based on the assumption, that a significant difference in the agreement between experimental NMR parameters and theoretical ones (obtained for the proposed structural models) for the correct and incorrect crystal structures will be observed. While in many cases this assumption is true, with a considerable number of examples found in the literature, for multi-component systems, such as solvates or hydrates, a different trend may be observed. In this work we present the limitations and applicability of a joint crystal structure prediction – NMR crystallography (CSP-NMR) approach to elucidate crystal structures of polyphenols epicatechin, catechin and procyanidin A-2, including a new, yet undescribed form, methanol solvate-hydrate of catechin. We demonstrate that when dealing with multi-component systems, the observed difference in terms of RMS values for predicted  $^1\text{H}$  solid-state NMR chemical shifts may not be as distinctive as this is the case of simpler crystal structures. Consequently, we try to answer the question how good agreement is good enough, when can we expect false-positive results to appear and can we learn from them about the molecule's crystallization preferences. Finally, we apply CSP-NMR protocol to determine crystal structure of a methanol hemisolvate – monohydrate of catechin, demonstrating a useful shortcut for the cases of crystal structure elucidation of multi-component flexible systems.

## MS37-05 | UNDERSTANDING THE ROLE OF MOLECULAR MOBILITY IN PHASE TRANSITIONS OF BULK AND CONFINED PHARMACEUTICALS

Nartowski, Karol (Wroclaw Medical University, Wroclaw, POL); Morrith, Alexander (University of East Anglia, Norwich, GBR); Fábíán, László (University of East Anglia, Norwich, GBR); Khimyak, Yaroslav (University of East Anglia, Norwich, GBR)

Understanding the phase transitions of pharmaceuticals is of increasing importance from both academic and industrial perspective. This is because different polymorphs of the same drug have different intrinsic properties such as compressibility or dissolution rate. The combined analysis of structure and dynamics of bulk and confined pharmaceuticals, as well as understanding the role of molecular mobility in polymorphic phase transitions present a considerable challenge. Solid-state NMR spectroscopy is well placed to probe both structure and dynamics of the molecules as bulk and confined nanocrystals due to its sensitivity to intermolecular interactions at different length scales from Å to mm and dynamic regimes from  $10^{-10}$  to 10 s.

This project aims at understanding the role of molecular mobility in phase transitions of bulk and confined pharmaceuticals using highly flexible, model drug with complex polymorphism (tolbutamide, TB) and variable temperature solid-state NMR analyses coupled with computational methods. TB form I as bulk and in the form of encapsulated nanocrystals inside the pores of MCM-41 mesoporous silica host were analyzed using solid-state NMR spectroscopy and relaxation measurements ( $^1\text{H } T_1$ ,  $^1\text{H } T_{1\rho}$  and  $^{13}\text{C } T_{1\rho}$ ) under MAS conditions. The mobility is compared between bulk and confined drugs displaying coexistence of crystalline and amorphous species within the pores. Furthermore, significant differences in the dynamics of TB forms I<sup>L</sup> and I<sup>H</sup>, which differ only in the conformation of aliphatic tail are explained using a combination of solid-state NMR and MD simulations.

## MS37-P01 | EXPANDING SOLID-STATE LANDSCAPE OF FLUCONAZOLE: COMBINED APPLICATION OF SOLID-STATE NMR, X-RAY DIFFRACTION AND COMPUTATIONAL METHODS TO UNCOVER POLYMORPHISM IN FLUCONAZOLE SOLVATES

Nowak, Maciej (Wroclaw Medical University, Wroclaw, POL); Nartowski, Karol (Wroclaw Medical University, Wroclaw, POL); Janczak, Jan (Institute of Low Temperature and Structure Research Polish Academy of Sciences, Wroclaw, POL); Morrill, Alexander (School of Pharmacy, Univeristy of East Anglia, Norwich, GBR); Fábián, László (School of Pharmacy, Univeristy of East Anglia, Norwich, AUT); Karolewicz, Bozena (Wroclaw Medical University, Department of Drug Form Technology, Wroclaw, POL); Khimyak, Yaroslav (School of Pharmacy, Univeristy of East Anglia, Norwich, AUT)

Fluconazole (FLU) is a drug widely used in treatment of fungal infections. Due to its activity against broad spectrum of fungi and its prescribing frequency, it was placed on the WHO Model List of Essential Medicines. The extensive polymorphism of fluconazole, which can be explained by conformational flexibility of the molecule and the presence of many hydrogen bond donor/acceptor groups, makes it an excellent model to investigate the effect of solvent properties and crystallization methods on the formation of new crystalline phases and solvates of the drug.

New solvates of fluconazole were prepared by slurring or cooling crystallization from the n-propanol, n-butanol, acetonitrile, toluene, DMSO and dichloromethane saturated solutions and analyzed using solid-state NMR and FTIR spectroscopy, single crystal and powder X-ray diffraction and thermal methods. The NMR parameters of solved structures were obtained using DFT calculations with CASTEP.

FLU forms isostructural solvates with known ethyl acetate solvate in acetonitrile, toluene, DMSO and n-butanol with a 4:1 FLU:solvent stoichiometry in cooling crystallisation experiments. This was confirmed using powder and single-crystal X-ray diffraction, solid-state NMR and FTIR spectroscopy and TGA analysis.

Second group of solvates with a 4:1 FLU:solvent stoichiometry was prepared by slurring crystallization from n-propanol, n-butanol, dichloromethane and acetonitrile. The structural similarity of the obtained solvates was confirmed by PXRD analysis. The PXRD patterns were indexed into tetragonal  $P-4_2c$  space group using Expo2014 software.

## MS37-P02 | TOWARDS UNDERSTANDING PHASE TRANSITIONS OF CONFINED

### PHARMACEUTICALS

Nartowski, Karol (Wroclaw Medical University, Wroclaw, POL); Morrirt, Alexander (School of Pharmacy, University of East Anglia, Norwich, GBR); Janczura, Natalia (Department of Drug Form Technology, Wroclaw Medical University, Wroclaw, POL); Fábíán, László (School of Pharmacy, University of East Anglia, Norwich, GBR); Khimyak, Yaroslav (School of Pharmacy, University of East Anglia, Norwich, AUT)

The change in the phases of matter has been extensively studied; from simplistic thermal changes of liquids, solids and gases to more the complex transitions of the different forms of the same material, namely polymorphism. This is important for pharmaceuticals as different crystalline forms of the same drug have different intrinsic properties such as solubility, which may in turn affect bioavailability.

Isolation of different phases of matter in early stages of crystallisation is difficult due to limited lifetime and possible interchange of these transitional phases. Therefore stopping/slowing microscale crystallisation in order to observe the early stages is the aim of this project. This is achieved by encapsulating the pharmaceutical into a host with confined nanoscale geometry, in this case a mesoporous silica host. This allows for an indirect route into understanding relationships between different phases and motilities of pharmaceutical materials.

The cocrystal of flufenamic acid and nicotinamide was encapsulated into the mesoporous silica pores using melt loading method. The loading of cocrystal at different ratios inside the pores was confirmed using DSC and nitrogen adsorption isotherms. Subsequent  $^1\text{H}$ ,  $^{13}\text{C}$  and  $^{19}\text{F}$  environments of encapsulated pharmaceuticals was completed by different correlation analyses using solid-state NMR methods under MAS conditions. Previous investigation of these materials enabled detection of separate phase peaks using  $^{19}\text{F}$  NMR; surface, crystalline and amorphous peaks. Using  $^{19}\text{F}$ - $^{19}\text{F}$  NOESY NMR, interactions between two out of three coexisting phases were observed giving insight into spatial distribution between the different phases of material.

## MS37-P03 | {<sup>1</sup>H/<sup>19</sup>F} -> <sup>29</sup>Si/<sup>27</sup>Al CPMAS AND HETCOR SPECTROSCOPY OF SYNTHETIC LEPIDOLITES: CONNECTIVITIES BETWEEN F/OH AND Si/Al IN THE OCTAHEDRAL AND TETRAHEDRAL SHEETS

Fechtelkord, Michael (Ruhr-Universität Bochum, Bochum, GER); Sulcek, Lara (Ruhr-Universität Bochum, Bochum, GER)

The lithian muscovite-lepidolite composition series involves the minerals muscovite (K(Al<sub>2</sub>)(AlSi<sub>3</sub>O<sub>10</sub>)(OH)<sub>2</sub>), trilithionite (K(Li<sub>1.5</sub>Al<sub>1.5</sub>)(AlSi<sub>3</sub>O<sub>10</sub>)(F,OH)<sub>2</sub>) and polyolithionite (K(Li<sub>2</sub>Al)(Si<sub>4</sub>O<sub>10</sub>F<sub>2</sub>)). The main interest of our work focuses on the spectroscopic investigation of the order / disorder of Si and Al in the tetrahedral sheets and of Al, Li, F, and OH in the octahedral sheets of lepidolites.

Direct neighbourhoods of F/OH- to Si/Al can be checked by application of cross polarization (CP) experiments. The polarisation transfer is strongly dependent on the spatial distance between fluorine/proton and Si/Al. By variation of contact time the distance between the two nuclei could be estimated (cross polarization time  $t_{CP}$ ) and additional information about the bonding behaviour of these nuclei is given by the longitudinal relaxation time of the <sup>19</sup>F or <sup>1</sup>H nucleus in the rotating frame ( $T_{1\rho}$ ).

HETCOR (heteronuclear correlation) experiments are also useful for determination of site connectivities between different nuclei. The two-dimensional correlation is achieved by cross-polarization. Similar as in previous studies[1], {<sup>1</sup>H/<sup>19</sup>F} → <sup>29</sup>Si HETCOR NMR- experiments should show that the tetrahedral sheets containing a high Al content are in direct neighbourhood of Al-rich clusters of the octahedral sheets. In addition, CPMAS-experiments could clarify if even OH and F are ordered in clusters.

[1] Langner, R., Fechtelkord, M., Garcia, A., Palin, E.J., Lopez-Solano, J. (2012) American Mineralogist, 97, 341–352.

## MS37-P04 | THE DRUG TARGET MONOACYLGLYCEROL LIPASE: STRUCTURE AND DYNAMICS, CONSERVATION AND DIVERGENCE

Aschauer, Philipp (University of Graz, Graz, AUT); Riegler-Berket, Lina (University of Graz, Graz, AUT); Grinninger, Christoph (University of Graz, Graz, AUT); Natmessnig, Helgit (University of Graz, Graz, AUT); Pavkov-Keller, Tea (University of Graz, Graz, AUT); Breinbauer, Rolf (Graz University of Technology, Graz, AUT); Birner-Grünberger, Ruth (Medical University of Graz, Graz, AUT); Zimmermann, Robert (University of Graz, Graz, AUT); Oberer, Monika (University of Graz, Graz, AUT)

Monoacylglycerol lipases (MGLs) are a class of enzymes that hydrolyze monoacylglycerol into a free fatty acid and glycerol. Fatty acids can be used for triacylglycerol synthesis, as energy source, as building blocks for energy storage, and as precursor for membrane phospholipids. In mammals, inhibitors for MGLs are sought after to act as modulators of endocannabinoid signalling, cancer, neurodegenerative and inflammatory diseases. In *Mycobacterium tuberculosis*, the generated fatty acids also serve as precursor for polyketide lipids and mycolic acids, major components of the cellular membrane associated to resistance for drug treatment of the deadly pathogen.

3D structural knowledge of MGLs has become available only within the last years. We will present the crystal structure of the MGL from *M. tuberculosis*, *S. cerevisiae* and *Bacillus* sp. H257. These structures reveals remarkable similarities with MGL from humans in the  $\alpha/\beta$  core as expected, yet unexpectedly also in the cap region despite the lack of significant sequence similarities. These cap modules provide the access path to the catalytic site and undergo conformational changes as observed in different crystals structures and using NMR dynamics and chemical shift perturbation studies.

Nevertheless, the available inhibitors appear to be rather specific for human MGL while not targeting MGL orthologs. This opens the possibility for specific inhibition of MGLs from pathogens without influencing human MGL. Therefore, these studies provide a structural basis for rational design of a novel generation of inhibitors for one of the oldest recognized pathogens.

## MS37-P05 | PHOTINITIATED SOLID-STATE REACTIONS OF KETONES WITH VINYL-ACETYLENE

### FRAGMENTS

Ushakov, Ivan (A.N.Nesmeyanov Institute of Organoelement Compounds, RAS, Moscow, RUS); Volodin, Alexander (INEOS, Moscow, RUS); Voronova, Evgenia (A. N. Nesmeyanov Institute of Organoelement Compounds, RAS, Moscow, RUS); Golovanov, Alexander (Togliatti State University, Togliatti, RUS); Odin, Ivan (Togliatti State University, Togliatti, RUS); Vologzhanina, Anna (A. N. Nesmeyanov Institute of Organoelement Compounds, RAS, Moscow, RUS)

Chalcones and cyclic ketones with vinyl fragments are known to undergo photoinitiated reactions both in solids and solution [1, 2]. Taking into account great potential of solid-state photoinitiated reactions for a single-step synthesis of cyclobutene derivatives a response of a series of cyclic and acyclic ketones with vinyl-acetylene fragments to UV irradiation was studied. Possibility of these compounds to take part in above reaction is evidenced by conversion of 5-phenyl-1-(pyrid-2-yl)pent-2-en-4-yn-1-one to rctt (3,4-bis(phenylethynyl)cyclobutane-1,2-diyl)bis(pyridin-2-ylmethanone) at recrystallization from MeCN on daylight. Irradiation of the title compounds with Xe laser (360 nm) for 16 – 20 h results in single crystal degradation, thus, reaction products were studied using  $^1\text{H}$ ,  $^{13}\text{C}$  NMR and FT-IR spectroscopies. Such solid-state reactions as degradation of cyclic ketones with ring opening, [2+2] cycloaddition of olefin bonds, and pedal motion were expected.

This study is supported by the Russian Science Foundation (project 17-13-01442).

[1] S. E. Hopkin, et al. J. Chem. Soc., Perkin Trans. 2 1991, 1131.

[2] S. Z. Vatsadze, et al. Russ. Chem. Bull. 2006, 55, 1184.

## MS37-P134 LATE | CONFIGURATION CONTROLLED CRYSTAL AND/OR GEL FORMATION OF FULLY PROTECTED D-GLUCOSAMINES

Harmat, Veronika (Eötvös Loránd University, Institute of Chemistry, Budapest, HUN); Kapros, Anita (Eötvös Loránd University, Institute of Chemistry, Budapest, HUN); Balázs, Attila (Eötvös Loránd University, Institute of Chemistry, Budapest, HUN); Háló, Adrienn (Eötvös Loránd University, Institute of Chemistry, Budapest, HUN); Budai, Livia (Semmelweis University, Budapest, HUN); Pintér, István (Eötvös Loránd University, Institute of Chemistry, Budapest, HUN); Menyhárd, Dóra K. (Eötvös Loránd University, Institute of Chemistry, Budapest, HUN); Perczel, András (Eötvös Loránd University, Institute of Chemistry, Budapest, HUN)

Gel formation is widely spread in nature, essential for living organisms. Gels of natural and synthetic sources are also used in various fields of industry (e.g. pharmaceuticals, food science, cosmetics, nano materials). Low molecular weight gelators (LMWGs) are of particular interest, having advantageous physico-chemical properties. For understanding and designing their characteristics, efforts are made to establish the molecular level criteria of gelation, including key interactions governing gel formation.

Carbohydrate derivatives having versatile configuration, molecular folds and self-assembly behaviours, are promising candidates of designing biocompatible LMWGs. Interactions stabilizing the gel structure were proposed for N-Fmoc-glucosamines, establishing a model for a group of free hydroxyl-containing hydrogels.

Here we present a comparative study of alpha and beta anomers of fully O-acetylated derivative of N-Fmoc-glucosamine. The beta anomer readily forms gels from different solvent mixtures, presenting solution-gel-crystalline transformation pathway. Interestingly the alpha anomer crystallizes from solution skipping the gel formation. This molecule pair makes a unique system to understand details of gelation, as they differ only in their anomeric configuration. We applied a combination of various methods for characterizing phase transformation processes of both anomers. Crystal structures along with results of NMR and ECD studies as well as in silico conformational analysis are presented. Key conformers as well as intra- and intermolecular interactions were identified proposing a possible explanation of the configuration dependent gelation ability of the protected D-glucosamines.

This study was supported by EU2020 grants VEKOP-2.3.2-16-2017-00014 and VEKOP-2.3.3-15-2017-00018, OTKA grant K116305 and the MedInProt program of the Hungarian Academy of Sciences.

## MS38: New Detectors for High Energy X-Ray Applications

---

### MS38-01 | RECENT ADVANCES IN HIGH-Z PIXEL DETECTORS

ruat, marie (ESRF, grenoble, FRA)

Future X-ray science at modern synchrotrons and X-ray Free Electron Lasers will bridge the gap between visible light and electron microscopy. The European Synchrotron Radiation Facility (ESRF) has launched an ambitious and innovative upgrade through the Extremely Brilliant Source (EBS) project to become the first high-energy fourth-generation synchrotron facility. Other facilities around the world will follow. If exploited with high-performance and tailored instrumentation, the highly brilliant and coherent beams produced by such photon sources will make possible new research opportunities in nano-science and nano-technologies, complex biological and soft-matter systems, time-resolved dynamical processes in complex materials, matter at extreme conditions, and in X-ray imaging techniques and applications. In this context, critically better X-ray detection is required, and a worldwide effort is put in pursuing or launching detector development programmes. Among these, the ESRF-EBS Detector Development Plan consists of a coherent combination of projects and activities including the prototyping of completely new advanced detector systems, in collaboration with other laboratories, as well as further developing detection related technologies that will be instrumental to maintaining the high overall level of quality and scientific productivity of the beamlines. The latest results obtained in the framework of this detector development plan will be presented, along with the outcomes of complementary developments at other facilities, laboratories or companies. The talk will be focused on pixelated X-ray detection solutions for high energy and high photon fluxes applications, using high-Z sensor technologies and new readout ASIC design.

## MS38-02 | SUBPIXEL SPATIAL RESOLUTION AT 122 KEV OF AN SPECTROSCOPIC IMAGER COMPOSED OF A PNCCD COUPLED TO A COLUMNAR CsI(TL) SCINTILLATOR

Schlosser, Dieter (PNSensor, Munich, GER); Hartmann, Robert (PNSensor, Munich, GER); Bechteler, Alois (PNSensor, Munich, GER); Abboud, Ali (University of Siegen, Siegen, GER); Shokr, Mohammad (University of Siegen, Siegen, GER); Pietsch, Ullrich (University of Siegen, Munich, GER); Strüder, Lothar (PNSensor, Munich, GER)

New generation beam lines offer energies up to 150 keV and above. With hard X-rays it is possible to investigate bulk properties of materials in Laue diffraction experiments with white X-ray beams. Therefore highly energy and spatially resolving detectors are required with high quantum efficiency up to 150 keV. We realized a detector consisting of a 450  $\mu\text{m}$  thick pnCCD with a pixel size of  $75\mu\text{m} \times 75\mu\text{m}$  coupled to a 700  $\mu\text{m}$  thick columnar CsI(Tl) scintillator with a high quantum efficiency in the energy range from 0.5 keV to 100 keV and above. The detector is front side illuminated, so that X-rays up to 15 keV are mainly absorbed “directly” inside the pnCCD and energies above are mainly stopped in the scintillator, where the deposited energy is converted into scintillation photons, which are also detected by the pnCCD. This mode is called “indirect detection”. In previous works we determined the energy resolution to be  $\text{FWHM}/E = 9\%$  at 122 keV for indirect detection and 0.7%. In this work we have investigated the spatial resolution of the imaging detector in a “knife edge” experiment at 122 keV. We will show that the spatial resolution reaches subpixel values of about  $30\mu\text{m}$ , which is mainly limited by the track length of the generated secondaries inside the scintillator. This is in agreement with Geant4 Monte Carlo Simulations, which have been performed.

## MS38-03 | PHOTON COUNTING WITH MIXED MODE DETECTION

Adam, Martin (Bruker AXS GmbH, Karlsruhe, GER); Durst, Roger (Bruker AXS GmbH, Karlsruhe, GER); Stuerzer, Tobias (Bruker AXS GmbH, Karlsruhe, GER); Kaercher, Joerg (Bruker AXS Inc., Madison, WI, USA); Becker, Bruce (Bruker AXS Inc., Madison, WI, USA)

Modern single-crystal X-ray diffraction relies entirely on two dimensional pixel array detectors (PADs). Their underlying CMOS technology allows shutterless data collection which has widely eliminated experimental overhead time. Today, two different techniques are competing in the home laboratory market. HPADs, now available for a number of years, count individual X-ray events, based on electron-electron hole pairs and apply an internal threshold to suppress the background noise including the noise originating from the sensor. These detectors produce clear images, which at a first glance are perfectly noise free. However, the need for a threshold introduces a new source of noise for HPADs: charge sharing between pixels resulting in signal loss. The limited count-rate capability, parallax and bind areas of HPADs are other sources of errors.

Mixed-mode detectors offer the advanced technical alternative to HPADs. This rather new technology is now implemented at large research facilities, such as free electron laser sites. For the home market Bruker has developed the PHOTON III series of detectors. Large monolithic sensors without gaps are standard in these detectors. Mixed-mode detectors do not suffer from charge sharing and can cope with higher count rates. X-ray photons are efficiently absorbed within thin high-Z absorber layers minimizing parallax and leading to a smaller signal point spread.

Technical details and users benefits of the large area mixed-mode detectors will be presented.

## MS38-04 | EIGER2 CdTe DETECTORS: TOOLS FOR HARD X-RAY STUDIES

Brandstetter, Stefan (DECTRIS Ltd, Baden-Daettwil, CH); Wagner, Lucas (DECTRIS Ltd, Baden-Dättwil, CH); Kaspar, Sebastian (DECTRIS Ltd, Baden-Dättwil, CH)

Hybrid Photon Counting (HPC) X-ray detectors have transformed synchrotron research in the last decade. They provide noise-free detection and permit new data acquisition modes such as continuous data collection and extremely high frame rates. The new HPC detector family EIGER2 enables even more ambitious X-ray science with different sensor materials suited for high-energy applications. These detectors combine the advantages of previous generations of detectors. They offer pixels sizes of  $75\ \mu\text{m} \times 75\ \mu\text{m}$ , frame rates in the kilohertz range, negligible dead time (100 ns), and count rates of up to  $10^7$  photons per pixel and second through DECTRIS retrigger technology. Moreover, EIGER2 technology is compatible with silicon and cadmium telluride (CdTe) sensor material, which offers high quantum efficiency up to around 80 keV. Two adjustable energy thresholds extend the usability of the EIGER2 detector family, allowing reduction of the cosmic background and higher harmonics. These properties not only empower new fields of X-ray photon research like X-ray diffraction computed tomography (XRD-CT) but will also advance established methods like X-ray crystallography in the high-energy range.

Here, we present results from first experiments and characterization methods. Detector properties like count rate capability, readout, and spatial resolution are demonstrated with dedicated key experiments. With an EIGER2 X 1M CdTe we collected excellent high-pressure data from crystals in a diamond anvil cell. Combined with characterization measurements at beamlines and in the laboratory, these results show how the latest HPC CdTe detectors empower advances in X-ray micro- and nanoanalysis.

## MS38-05 | COMBINING A NINE-CRYSTAL MULTIANALYSER STAGE WITH A HYBRID CdTe PHOTON COUNTING DETECTOR FOR HIGH-RESOLUTION X-RAY POWDER DIFFRACTION AT ESRF-ID22

Dejoie, Catherine (ESRF, Grenoble, FRA); Autran, Pierre-Olivier (ESRF, Grenoble, FRA); Covacci, Ezio (ESRF, Grenoble, FRA); Fitch, Andrew (ESRF, Grenoble, FRA)

The high-resolution powder diffraction beamline ID22 at ESRF combines a wide choice of photon energies with high brightness, allowing high-flux, high-resolution powder diffraction measurements at wavelengths down to 0.3 Å. In routine operation, a bank of nine scintillation detectors is scanned to record the diffracted intensity versus  $2\theta$ , each detector preceded by a Si 111 analyzer crystal. Although the current system has operated successfully for the past twenty years, recent developments in detector technology could be exploited to improve performance. To do so, a Pilatus3 X CdTe 300K-W was mounted on the arm of the diffractometer, replacing the nine scintillator detectors, and used for standard continuous-scanning acquisition. This arrangement offers major advantages in terms of data handling and processing. By varying the axial width of a region of interest as a function of  $2\theta$ , peak widths, peak shapes, and the statistical quality of the data, particularly at high angles, can be improved. In addition, an analyzer crystal maps a position in the sample directly onto a position on the detector, thus conferring spatial/depth resolution to the measurement. Even greater improvements are expected in the future by exploiting the smaller pixel size and the higher speed of the Eiger2 X CdTe 2M detector, leading to the possibility of 3-dimensional mapping of complex systems during in-situ and time-resolved experiments. Combining the high efficiency of a hybrid photon-counting area detector with the high angular resolution given by analyzer crystals is an innovative approach to improving the overall performance of high-resolution powder diffraction.

## MS38-P01 | CdTe BASED 2D DETECTORS FOR HARD RADIATION

de Vries, Roelof (Malvern Panalytical, Almelo); Prugovecki, Stjepan (Malvern Panalytical, Almelo); Bellazzini, Ronaldo (INFN - Istituto Nazionale di Fisica Nucleare, Pisa, ITA); Fransen, Martijn (Malvern Panalytical, Almelo)

There is a growing need for hard energy X-rays in diffraction and imaging applications, both for laboratory instruments and at synchrotron beam lines.

Hybrid pixel detectors, the new gold standard for two-dimensional X-ray detection, are generally equipped with Si sensors, severely limiting the detection efficiency when working with hard radiation. For example, for 22 keV photons (Ag K-Alpha) the efficiency of a detector equipped with a Si sensor of 300 micrometer thickness is only about 20%. Using thicker silicon sensors will increase the efficiency somewhat but to get efficiency close to 100%, or go to higher energies, other type of sensor materials are needed. With Cadmium Telluride (CdTe), a sensor 750 micrometer thickness has 100% efficiency up to 60 keV. Another advantage of CdTe is that it protects the sensitive readout circuitry below the sensor against potential radiation damage.

CdTe as a sensor material comes with its own challenges, however. Its crystalline quality is lower than a Si sensor. It needs to be cooled for optimal performance. We have been working with this material for many years, and optimized the detector design specifically for this sensor. In this contribution, the challenges of working with CdTe are being explained, and examples of the unique technology are shown.

## MS38-P02 | PUSHING DATA QUALITY FOR LABORATORY PAIR DISTRIBUTION FUNCTION

### EXPERIMENTS

Zobel, Mirijam (Universität Bayreuth, Bayreuth, GER); Thomä, Sabrina (University Bayreuth, Bayreuth, GER); Prinz, Nils (University Bayreuth, Bayreuth, GER)

Although the very first laboratory X-ray pair distribution function (PDF) measurement was carried out in the 1930s [1], laboratory PDF studies are rare. Only few studies emerged during the last decade [2], but limited  $Q_{\max}$  or insufficient instrumental resolution impeded a routine use for structural refinements. Based on a STOE STADI P powder diffractometer in transmission geometry, we designed a novel PDF diffractometer with monochromatic Ag  $K\alpha_1$  radiation covering a Q-range of 0.3 - 20.5  $\text{\AA}^{-1}$  ( $144^\circ 2\theta$ ). Four MYTHEN2 silicon strip detectors are arranged as a MYTHEN2 4K module on one detector arm, providing high instrumental resolution and low background. PDF data is collected in a moving mode within 6 hours for powders. For benchmarking, we measured and refined  $\text{LaB}_6$  standards with goodness-of-fits  $R_w = 0.14$  over 80  $\text{\AA}$ , and ca. 7 nm  $\text{TiO}_2$  nanoparticles over 30  $\text{\AA}$  with  $R_w = 0.18$ . While all previous lab PDF studies did not show or refine any data for distances  $> 30 \text{\AA}$  – due to a PDF peak overlap beyond ca. 25  $\text{\AA}$  due to a lack of monochromatization - we can readily refine our  $\text{TiO}_2$  PDF data with an  $R_w$  as low as 0.22 over 70  $\text{\AA}$ . [3] Further data on ionic liquids and metal organic frameworks will be presented.

[1] B.E. Warren, et a., *Physical Review* **46** (1934) 368

[2] J.T. Nijenhuis, et al., *Z. Kristallogr.* **2009** (2009) 163

[3] S.L.J. Thomä, et al., *Rev. Sci. Instr.* (2019), *accepted*

## MS38-P03 | THE POTENTIAL BENEFITS OF USING HIGHER X-RAY ENERGIES FOR MACROMOLECULAR CRYSTALLOGRAPHY

Dickerson, Joshua (University of Oxford, Oxford, GBR); Garman, Elspeth (University of Oxford, Oxford, GBR)

Using X-ray energies higher than those normally used for macromolecular X-ray crystallography (MX) at synchrotron sources can theoretically increase the achievable signal as a function of dose and reduce the rate of radiation damage [1]. In practice, a major stumbling block to the use of higher X-ray energy has been the reduced quantum efficiency of silicon detectors as the X-ray energy increases, but hybrid photon counting CdTe detectors are optimised for higher X-ray energies, and their performance has been steadily improving. The potential advantages of using higher incident beam energy together with a CdTe detector for MX are explored, with a particular focus on the advantages that higher beam energies may have for MX experiments with microbeams or microcrystals. Our Monte Carlo calculations [2] show a greater than a factor of 2 improvement in diffraction efficiency when using microbeams and microcrystals of 5  $\mu\text{m}$  or less. These take into account the escape of photoelectrons from the crystal as well as entry from the surrounding material [3], both of which have now been incorporated into RADDOSE-3D.

[1] Arndt, U. W. Optimum X-ray wavelength for protein crystallography. *J. Appl. Cryst.* **17**, 118–119 (1984).

[2] Dickerson, J.L. & Garman, E.F. (2019) *J. Synchrotron Rad.* in press

[3] Nave, C. & Hill, M. A. Will reduced radiation damage occur with very small crystals? *J. Synchrotron Radiat.* **12**, 299–303 (2005).

## MS38-P04 | MEASURING ACCURATE SINGLE CRYSTAL DIFFRACTION DATA USING A PILATUS3 CdTe DETECTOR

Krause, Lennard (Aarhus University, Aarhus, DNK); Tolborg, Kasper (Aarhus University, Aarhus, DNK); Brummerstedt Iversen, Bo (Aarhus University, Aarhus, DNK); Overgaard, Jacob (Aarhus University, Aarhus, DNK)

Pilatus3 detectors were released in 2012 and are widely established in macromolecular crystallography with over 4,000 PDB entries. The specifications of the Pilatus3 CdTe were quickly recognized as promising in charge density investigations, mainly due to the detection efficiency in the high-energy X-ray regime. Moreover, the dynamic range and low noise should overcome the perpetual problem of detecting strong and weak data simultaneously. However, to the best of our knowledge there is no publication available presenting high resolution data collected with a Pilatus3 CdTe detector.

Our experience with this detector family revealed two aspects that lead to systematically underestimated intensities at the two extremes of the detected intensity scale. Herein, Rubrene and FeSb<sub>2</sub> are representatives for the two cases. Additionally, a LaB<sub>6</sub> powder sample was consulted to validate the findings of the single crystal studies where counting statistics and reproducibility are more delicate.

The first aspect is indicated by systematically too low intensities for weak reflections, revealed by a variation of exposure time and beam attenuation. The origin was found in the data processing, specifically in the outlier rejection and data averaging.

The second case affects the most intense reflections and is connected to the maximum flux of the diffracted beam but not the total number of counts. We utilized a maximum flux estimation procedure to identify unproblematic flux ranges. Disregarding this issue leads to unreasonably large extinction parameters.

Our results conclude that only the combination of careful data collection and processing can result in high quality data.

## MS38-P05 | RESOLUTION FUNCTION FOR 2D PIXEL DETECTORS

Chernyshov, Dmitry (SNBL at the ESRF, Grenoble, FRA); Dyadkin, Vadim (Swiss-Norwegian BeamLines at the European Synchrotron Radiation Facility, Grenoble, FRA)

Advent of low-noise high-energy pixel detectors open doors for fast diffraction experiments covering large Q-range in one shot, this is of a particular importance for powder diffraction and PDF measurements. Qualitative analysis of the powder diffraction data assumes a model for instrumental line broadening, most of the time it is parameterized with Cagliotti or alike functions [1]. Here we show that such a parameterization is not sufficient for large area detectors and propose a new resolution model accounting for beam divergency, pixel size, thickness of the detector' sensitive layer and geometrical parameters of the experiment. The model is derived analytically and compared with the models reported previously [2, 3]; it can be easily implemented in the software for profile or PDF analysis. The analytical derivations are illustrated with calibration measurements at BM01 beamline (SNBL at the ESRF [4]) equipped with Pilatus2M detector.

[1] Gozzo, F., De Caro, L., Giannini, C., Guagliardi, A., Schmitt, B., & Prodi, A. *Journal of Applied Crystallography*, 39(3), 347–357, (2006)

[2] Norby, P. *Journal of Applied Crystallography*, 30(1), 21–30, (1997)

[3] Hinrichsen B., Dinnebier R. E. and Jansen M. in “Powder Diffraction: Theory and Practice”, edited by R. E. Dinnebier and S. J. L. Billinge, The Royal Society of Chemistry (2008)

[4] Dyadkin, V., Pattison, Ph., Dmitriev, V., Chernyshov, D. J. *Synchrotron Rad.*, 23, 3, (2016)

## MS39: Time-Resolved Diffraction and Scattering Techniques

---

### MS39-01 | ULTRAFAST DYNAMICS OF CHEMISTRY IN SOLUTION STUDIED BY TIME-RESOLVED X-RAY DIFFUSE SCATTERING AT LCLS

van Driel, Tim (LCLS / SLAC National Accelerator Laboratory, Menlo Park, USA)

Laser pump / X-ray probe experiments provide novel fundamental insight into ultrafast photo-induced processes. The arrival of X-ray Free Electron Lasers has pushed the time-resolution of such experiments to sub 100fs.

Here I will present the current capabilities of the XPP [1] and XCS [2] instruments at LCLS for the purpose of studying solution phase chemistry. This will include instrumentation, diagnostics and performance as well as some published and unpublished scientific/technical examples [3]. Furthermore I will describe and elaborate on the future upgrades of LCLS-II and LCLS-II-HE and the potential improvements we hope to achieve.

Recently improvements include implementing the setup at the XCS endstation, a new liquid sample chamber, new liquid delivery nozzles as well as a newly developed epix10k high dynamic range detector for scattering. These technical improvements in combination with improved analysis, diagnostics and real-time feedback have greatly improved the fidelity of such experiments in addition to decreasing the time spent on alignment and setup.

This makes it possible to accurately measure the time-resolved diffuse scattering to follow the photo-induced dynamics of molecules in solution. Combined with X-ray spectroscopic techniques, such measurements can provide a novel insight into excited state dynamics, solvent interactions as well as provide a direct measurement of the structure, spin and charge of many photo active molecules on the intrinsic timescale of such ultra-fast molecular processes.

[1] M.Chollet et al., J. Synchrotron Rad. **22**, 503-507. (2015)

[2] R.Alonso-Mori et al.,J. Synchrotron Rad. **22**, 508-513. (2015)

[3] van Driel et al., Nat. Comm. 7, 13678 (2016)

## MS39-02 | APPLICATION OF ULTRAFAST STRAIN FIELDS FOR X-RAY PULSE SHORTENING AND PULSE PICKING

Sander, Mathias (Paul Scherrer Institut, Villigen, CH)

We report a benchmark experiment that demonstrates shortening of hard x-ray pulses in a synchrotron-based optical pump - x-ray probe experiment. The pulse shortening device, a picosecond Bragg switch, reduces the temporal resolution of an incident x-ray pulse to 7.5 ps. We employ the Bragg switch to monitor propagating sound waves in nanometer-thin epitaxial films. With the experimental data we infer pulse duration, diffraction efficiency and switching contrast of the device. A detailed efficiency analysis shows, that the switch can deliver up to  $10^9 - 10^{10}$  photons/sec in high-repetition rate synchrotron experiments.

## MS39-03 | TIME-RESOLVED STRUCTURE ANALYSIS OF PIEZOELECTRIC CRYSTALS

### RESONANTLY VIBRATING UNDER ALTERNATING ELECTRIC FIELD

Aoyagi, Shinobu (Nagoya City University, Nagoya, JPN); Osawa, Hitoshi (Japan Synchrotron Radiation Research Institute, Hyogo, JPN); Sugimoto, Kunihisa (Japan Synchrotron Radiation Research Institute, Hyogo, JPN); Nakahira, Yuki (Hiroshima University, Hiroshima, JPN); Moriyoshi, Chikako (Hiroshima University, Hiroshima, JPN); Kuroiwa, Yoshihiro (Hiroshima University, Hiroshima, JPN); Takeda, Hiroaki (Tokyo Institute of Technology, Tokyo, JPN)

Piezoelectric crystals are widely used in many applications such as oscillators, sensors, and actuators. The mechanisms of piezoelectricity could be explained from atomic displacements under a static electric field. However, atomic displacements under a static electric field are usually too small to be detected by conventional X-ray diffraction (XRD) measurements. The small atomic displacements can be resonantly amplified by mechanical vibrations under an alternating electric field with the resonant frequency. We have recently succeeded in detecting the small atomic displacements of resonantly vibrating quartz ( $\text{SiO}_2$ ) and langasite-type ( $\text{La}_3\text{Ga}_5\text{SiO}_{14}$  and  $\text{Nd}_3\text{Ga}_5\text{SiO}_{14}$ ) piezoelectric crystals by the time-resolved synchrotron radiation XRD measurements under an alternating electric field [1-3].

The time-resolved crystal structure analyses of the quartz and langasite-type crystals revealed that bridging angles of oxygen tetrahedra are deformed with displacements of specific oxygen atoms along the applied electric field during the resonant vibrations. Deformations of specific oxygen tetrahedra were also observed in the langasite-type crystals.  $\text{GaO}_4$  and  $\text{Ga}_{0.5}\text{Si}_{0.5}\text{O}_4$  tetrahedra in the langasite-type crystals are more deformable than  $\text{SiO}_4$  tetrahedra in the quartz crystal. This seems the reason why the piezoelectric constants  $d_{11}$  of the langasite-type crystals are larger than that of the quartz crystal.

[1] Aoyagi, S. et al. (2015). Appl Phys. Lett. 107, 201905

[2] Aoyagi, S. et al. (2016). Jpn. J. Appl. Phys. 55, 10TC05

[3] Aoyagi, S. et al. (2018). Jpn. J. Appl. Phys. 57, 11UB06

## MS39-04 | LIQUID-METAL-JET X-RAY SOURCE FOR TIME-RESOLVED SAXS STUDIES IN THE HOME LABORATORY

Hållstedt, Julius (Excillum AB, Kista, SWE); Espes, Emil (Excillum AB, KISTA, SWE)

High-end x-ray scattering techniques rely heavily on the x-ray source brightness for resolution and exposure time. Traditional x-ray tubes are typically limited in brightness by when the e-beam power density melts the anode. The liquid-metal-jet technology has overcome this limitation by using an anode that is already in the molten state.

Since the liquid-metal-jet technology was introduced over 10 years ago, it has moved from prototypes into fully operational and stable X-ray tubes running in labs all over the world. Multiple users and system manufacturers have since installed the metal-jet anode x-ray source into their high-end SAXS set-ups demonstrating unprecedented home-lab results.

A specifically challenging SAXS application is to monitor dynamic systems, requiring time-resolved data. In this communication we will focus on few recent time-resolved SAXS results from both materials science and biological applications.

One example is from researchers at the Slovak Academy of Science and STU Centre for Nano-diagnostics performed in-situ tests on a strain gauge, based on a monolayer of colloidal gold nanoparticles deposited on a flexible Mylar foil where the MetalJet allowed a very fast data collection, with 10 seconds temporal resolution.

Another SAXS application that is attracting significant interest at synchrotrons is BIO-SAXS using SEC-SAXS technique. Researchers at University of Copenhagen together with scientists from Xenocs SAS has successfully demonstrated home lab SEC-SAXS of protein solutions with concentrations as low as 1 mg/ml.

## MS39-05 | AT THE INTERSECTION OF CRYSTALLOGRAPHY AND SPECTROSCOPY - STUDIES OF SELECTED PHOTOACTIVE COINAGE METAL COMPLEXES

Jarzemska, Katarzyna (Department of Chemistry, University of Warsaw, Warsaw, POL); Kaminski, Radoslaw (Department of Chemistry, University of Warsaw, Warsaw, POL); Laski, Piotr (Department of Chemistry, University of Warsaw, Warsaw, POL); Szarejko, Dariusz (Department of Chemistry, University of Warsaw, Warsaw, POL); Drapala, Jakub (Department of Chemistry, Warsaw University of Technology, Warsaw, POL); Durka, Krzysztof (Department of Chemistry, Warsaw University of Technology, Warsaw, POL)

Polynuclear transition-metal complexes frequently constitute the active sites of both biological and chemical catalysts, provide access to unique chemical transformations derived from specific metal-metal interactions and cooperation. Among this group, the  $d^8$  or  $d^{10}$  transition-metal coordination compounds are worth mentioning due to their interesting optoelectronic properties. Nevertheless, conscious design of functional materials of specific and controllable properties, requires a deep understanding of the nature of physical phenomena behind them.

Hence, the current project was dedicated to investigations of light-induced processes in selected coinage metal complexes. Emphasis was put on the direct determination of structural changes via advanced experimental methods supplemented by theoretical computations. The studied systems include both the literature-reported complexes as well as newly designed and synthesised ones. All of them exhibit luminescent properties which were carefully examined. The determined Stokes shifts and emission decay times were used to plan the time-resolved photocrystallographic experiments. The laser-induced excited states were probed with both 100 ps and 250 ns delay times at the 14-ID-B BioCARS APS beamline using the pink-Laue X-ray radiation. The results of such investigations are presented.

Overall, the project constitutes continuation of our studies on silver-copper complexes, in which we attempted to deepen the nature of the excited state, relate structural and spectroscopic properties of the system and analyse the effects of high pressure.

The authors thank NSC (2014/15/D/ST4/02856) and WCSS (grant No. 285) in Poland, EU programme (POIG.02.01.00-14-122/09) and APS, USA (DOE: DE-AC02-06CH11357, NIH: R24GM111072) for financial support and access to facilities.

## MS39-P01 | DEVELOPMENT OF DATA PROCESSING METHODS IN TIME-RESOLVED LAUE PHOTOCRYSTALLOGRAPHY

Kaminski, Radoslaw (Department of Chemistry, University of Warsaw, Warsaw, POL); Szarejko, Dariusz (Department of Chemistry, University of Warsaw, Warsaw, POL); Laski, Piotr (Department of Chemistry, University of Warsaw, Warsaw, POL); Jarzemska, Katarzyna (Department of Chemistry, University of Warsaw, Warsaw, POL)

Time-resolved X-ray Laue photocrystallography have recently become a promising experimental method for elucidation of short-lived species' structures in molecular crystals. Recent successful examples include determination of excited state structures in rhodium,[1] copper [2] or bimetallic [3] coordination complexes. In all of these cases the required data quality was achieved via application of very short (down to 80 ps) and intense X-ray pulses, available only at synchrotron beamlines using 'pink' X-ray beam. However, the use of polychromatic radiation imposes some difficulties in further data processing. Some of these problems have recently been actively studied and to some extent overcome, especially in the case of data indexing.[4] Nevertheless, some aspects of data processing methods are still in their infancy and further progress is needed. Hence, here we present our most recent developments in data processing concerning the integration methods Our approach is tested on several real-life examples of data collected at APS (USA) or ESRF (France) synchrotron sources.

The authors thank NSC (2014/15/D/ST4/02856, 2016/21/D/ST4/03753) and WCSS (grant No. 285) in Poland, and APS (DOE: DE-AC02-06CH11357, NIH: R24GM111072) and ESRF, for financial support and access to facilities.

[1] J. B. Benedict *et al.*, *Chem. Commun.* **2011**, 47, 1704.

[2] (a) A. Makal *et al.* *J. Phys. Chem. A* 2012, 116, 3359; (b) P. Coppens *et al.*, *Phys. Scr.* **2016**, 91, 023003;

[3] K. N. Jarzemska, R. Kamiński *et al.*, *Inorg. Chem.* **2014**, 53, 10594.

[4] J. A. Kalinowski *et al.*, *J. Appl. Cryst.* **2011**, 44, 1182.

## MS39-P02 | A NOVEL X-RAY DIFFRACTION TECHNIQUE FOR IN-SITU OBSERVATIONS OF CATHODE/ANODE REACTION IN ELECTROLYTES

Kubicek, Sabine (KAI GmbH, Villach, AUT)

Surface sensitive *in-situ* techniques are helpful to get a deeper understanding of electrochemical reactions because they can give information about electrode reaction products during the reaction process. Structural and phase properties of thin solid films are commonly measured by grazing incident X-ray diffraction. *Ex-situ* measurements are sometimes not feasible because of alteration of deposits in contact with air, moisture or aging within the time gap between formation and measurement. Therefore *in-situ* X-ray diffraction cells for electrochemical experiments were developed. Such cell designs are limited due to geometry restrictions and, more importantly, due to radiation intensity loss because of the interaction of the beam with thick window materials or the electrolyte. Therefore, existing cells are frequently used in combination with synchrotron radiation.

We present a novel grazing incident X-ray diffraction setup for *in-situ* observations of cathode/anode reaction in electrolytes, which uses a backside-illuminated working electrode. The cell uses a polyimide foil with a thin sputtered metal layer as working electrode. The X-ray penetrates the foil with the thin metal layer from the backside and interacts with the metal layer and reaction products formed at the interface between working electrode and electrolyte solution. Because of the relatively small intensity losses, lab-scale equipment with a copper radiation source is appropriate. The cell can be operated in a three-electrode setup without any restrictions in current density distribution or electrolyte flow and can be used for any electrochemical method like voltammetry, deposition in galvanostatic and potentiostatic mode and electrochemical impedance spectroscopy (EIS).

## MS39-P03 | DEVELOPMENT OF CHANNEL-CUT X-RAY OPTICS FOR LABORATORY SMALL-ANGLE X-RAY SCATTERING SETUPS

Nádaždy, Peter (Institute of Physics SAS, Bratislava, SVK); Hagara, Jakub (Institute of Physics SAS, Bratislava, SVK); Jergel, Matej (Institute of Physics SAS, Bratislava, SVK); Majková, Eva (Institute of Physics SAS, Bratislava, SVK); Mikulík, Petr (Department of Condensed Matter Physics, Faculty of Science, Masaryk University, CEITEC, Brno, CZE); Zápražný, Zdenko (Institute of Electrical Engineering SAS, Bratislava, SVK); Korytár, Dušan (Institute of Electrical Engineering SAS, Bratislava, SVK); Šiffalovic, Peter (Institute of Physics SAS, Bratislava, SVK)

A modern small-angle X-ray scattering (SAXS) laboratory setup equipped with a micro-focus X-ray source coupled to 2D collimating Montel optics provides a beam with relatively low divergence of hundreds of  $\mu\text{rad}$ . Nevertheless, resolution of such a setup in small angle region is still limited by the divergence of X-ray beam. To increase resolution, it is often necessary to sacrifice big portion of beam intensity. Supposing 500 mrad divergence of the primary beam, comprehensive ray-tracing simulations of Ge(111) and Ge(220) channel-cut monochromators and their combinations were used to map the distribution of the output beam parameters over the entire space of the asymmetry angles of the respective diffractions. This allowed us to design a channel-cut based X-ray optics with theoretical loss in intensity of just one order of magnitude and the output divergence reduced by a factor of 5. The numerical simulations were validated by the experiments performed on a commercial SAXS setup (Bruker AXS, Nanostar) equipped with a liquid-metal jet anode X-ray source (Excillum, MetalJet D2+) and 2D collimating Montel optics, demonstrating thus potential of the combined reflective-diffractive X-ray optics for microfocus laboratory X-ray sources.

## MS39-P04 | SILICA NANOPARTICLE AGGLOMERATION STUDIES UNDER PHYSIOLOGICAL CONDITIONS USING DYNAMICAL SAXS METHODS

Iranpour, Neda (Empa, 8600, CH); Sadeghpour, Amin (Empa, Dübendorf, CH); Tonceli, Claudio (Empa, St. Gallen, CH); Dommann, Alex (Empa, Dübendorf, CH); Wick, Peter (Empa, St. Gallen, CH); Neels, Antonia (Empa, Dübendorf, CH)

Nanoparticles (NPs) colloidal stability in biological environments is one of the main issues in their biological and medical applications [1,2]. Minor changes in stability and / or the agglomeration state can influence NPs uptake, accumulation, and fate in living systems and accordingly cause some undesired consequences. Although many investigations have been conducted on NPs agglomeration behavior in aqueous biological systems, a systematic and quantitative description of the early stage of NPs agglomeration kinetics has not yet been established. We have developed an in-situ approach based on a combination of small angle X-ray scattering (SAXS) and microfluidics to study these early changes in the nanoparticles size distribution. The generalized indirect Fourier transformation (GIFT) data analysis method has been followed to understand the influence of effective parameters namely ionic strength, pH, and temperature. Using our new method, we can determine the mean agglomeration number for nanoparticles at the very early stages, enabling us to resolve time-dependently the effect of the mentioned various parameters on colloidal stability. To support our results, we have also investigated dynamic light scattering (DLS) and liquid phase transmission electron microscopy (TEM) as two complementary methods and have obtained similar results.

In this contribution, we will present our recent results which identify an appropriate range of different parameters such as ion strength and pH influencing NPs stability. This supports in designing new and safe particle systems for therapeutic and/or theranostics purposes.

## MS39-P05 | STRUCTURAL MECHANISMS GOVERNING REDOX-LINKED PROTON PUMP IN CYTOCHROME C OXIDASE STUDIED BY TIME-RESOLVED X-RAY METHODS

Ghosh, Swagatha (University of Gothenburg, Göteborg, SWE)

Cytochrome c oxidase (CcO) is an integral membrane protein that catalyzes the four-electron reduction of oxygen to water and pumps protons across the inner mitochondrial membrane to establish an electrochemical proton gradient that is used for ATP synthesis. As CcO plays an inevitable role during respiration and defects in CcO functionality are associated with many mitochondrial diseases, the enzyme has been under intense investigation. Crystal structures of CcO have been known for a few decades and these enzymes have been studied with virtually all biophysical and biochemical methods. However, the mechanism and structures of catalytic intermediates during this redox-linked proton translocation still remains elusive. This project aims to elucidate structural mechanisms that couple oxygen-reduction to proton-pumping and gating of proton channel in CcO using time-resolved X-ray methods like wide-angle X-ray scattering (Tr-WAXS) and serial crystallography (Tr-SX). We attempted to study structural changes in *ba<sub>3</sub>-type* CcO from *Thermus thermophilus* on binding and photo-dissociation of CO (a mimic of oxygen) and controlled photolysis of a caged-oxygen compound using Tr-WAXS. Moreover, our group has recently determined room temperature structures of oxidized and CO-bound forms of *ba<sub>3</sub>-type* CcO from *Thermus thermophilus* using SX. We aim to determine structures of transient intermediates during CcO catalytic cycle with Tr-SX and using CO and caged-oxygen as substrates. These experiments will have major scientific impact on addressing fundamental questions in bioenergetics of cells and possibly provide a guide to develop novel therapeutic agents targeting numerous human mitochondrial diseases.

## MS39-P06 | RECENT DEVELOPMENTS TOWARDS HIGH-FLUX TIME-RESOLVED AND THz - SAXS-EXPERIMENTS AT THE EMBL P12 BioSAXS BEAMLINE

Schroer, Martin A. (EMBL Hamburg, Hamburg, GER); Schewa, Siawosch (TH Lübeck, Lübeck, GER); Blanchet, Clement E. (EMBL Hamburg, Hamburg, GER); Gruzinov, Andrey Yu. (EMBL Hamburg, Hamburg, GER); Zickmantel, Till (TH Lübeck, Lübeck, GER); Fiedler, Stefan (EMBL Hamburg, Hamburg, GER); Katona, Gergely (University of Gothenborg, Gothenborg, SWE); Roessle, Manfred (TH Lübeck, Lübeck, GER); Svergun, Dmitri I. (EMBL Hamburg, Hamburg, GER)

The high-brilliance beamline P12 of the EMBL at PETRA III (DESY) is dedicated to biological small-angle X-ray scattering (SAXS) and is optimized for scattering experiments on macromolecular solutions. P12 offers automated sample delivery with on-line data processing capabilities but also tailored sample environments. In addition, the recent developments aim at exploiting the high flux for time-resolved SAXS experiments to study kinetics of proteins.

In the standard mode SAXS data are collected within 30-50 ms allowing one to study kinetics using e.g. a stopped flow device. For faster kinetics, a double multilayer monochromator (MLM) provides a flux of  $5 \cdot 10^{14}$  photons/second. With the MLM, the exposure times of about 1 ms on standard protein samples yield data of sufficient quality for further analysis and subsequent structural modelling. A fast rotating beam chopper was built to provide X-ray pulses for stroboscopic or pump-probe experiments with a tunable pulse length. A nanosecond laser was installed covering a spectral range from 335 to 2300 nm to trigger reactions through temperature-jump, release of caged compound or by perturbing photo-sensitive protein.

An additional setup utilizes terahertz (THz) radiation, which is expected to excite collective motions of protein domains, detectable by SAXS. As this non-equilibrium effect is assumed to be extremely weak and highly dynamic, a number of new developments in hardware, sample handling and software are necessary for such experiments. We present developments on the THz setup employing newly-developed microfluidic cells dedicated for combined SAXS-THz measurements.

We acknowledge support from the RAC-grant "TT-SAS" (BMBF-no 05K16YEA).

## MS40: The Use of X-Rays and Neutrons for Experiments in Nanoscience

---

### MS40-01 | NANOSCALE IN-SITU 3D IMAGING OF DEFECT DYNAMICS IN OXIDE

#### FERROELECTRICS

Simons, Hugh (Technical University of Denmark, Kgs. Lyngby, DNK); Ormstrup, Jeppe (Technical University of Denmark, Kgs. Lyngby, DNK)

Lattice defects create long-ranging strain fields that lower local crystal symmetry. For systems with strong lattice coupling, such as functional oxides, this results in unpredictable and potentially debilitating functionality and device performance. Here, we used dark-field X-ray microscopy to nondestructively map lattice distortions around deeply embedded lattice defects in a range of ferroelectric and multiferroic materials. We show that individual dislocations, domain walls, and grain boundaries create weak, long-ranging strain fields that extend up to several  $\mu\text{m}$  – orders of magnitude more than generally assumed. Capturing real-time movies of these defects during phase transformations and electrical poling then reveals how heterogeneous structural distortions affect functionality over multiple length and time scales. Such extrinsic strains are pivotal in defining the local properties and self-organization of defects, and must be accounted for in the design of new materials and devices.

## MS40-02 | OPPORTUNITIES WITH COHERENT X-RAY NANOBEAMS: A SHORT PERSPECTIVE FROM A BEAMLINE

Carbone, Dina (Max IV Laboratory, Lund, SWE)

Coherence has become the crucial property of X-ray beams at new generation sources. The main drive for the science developed at diffraction limited storage rings sources is the exploitation of the coherence of X-rays for imaging smaller and smaller structures and accessing dynamics of materials at small time-scales [1]. The interference patterns created by the scattering of coherent waves from a material, both in the near and far field, contain a wealth of information that can be exploited for a wide range of applications, ranging from the disclosure of subtle details of complex materials [2,3] to the investigation of the dynamics of complex systems [4].

Nanobeams of coherent X-rays are used as local probe as well as for scanning microscopy approaches when access to laterally resolved structural and chemical information is demanded, as in complex or inhomogeneous systems (e.g. heterostructures, device-like structures, etc.) [5].

In this talk I will show a selection of different uses of coherent X-ray nanobeams, with a special focus on the possibilities for coherent x-rays approaches at new generation synchrotron sources.

[1] M. Eriksson et al. (2014) *J. Synchrotron Rad* **21**837

[2] F. Mastropietro et al. (2017) *Nature Materials* **16**946

[3] V. L. R. Jacques et al. (2013). *Phys. Rev. Lett.* **111**, 065503.

[4] A. Madsen et al (2015). "Structural Dynamics of Materials Probed by X-Ray Photon Correlation Spectroscopy". Springer International Publishing. DOI: 10.1007/978-3-319-04507-8\_29-1.

[5] J. Stangl *et al.* (2013). "Nanobeam X-Ray Scattering: Probing Matter at the Nanoscale" Wiley-VCH Verlag GmbH & Co ISBN: 978-3-527-41077-4.

## MS40-03 | NANO-SCALE STRAIN MAPPING IN COMPLETE NANOWIRE BASED ELECTRONIC DEVICES BY BRAGG COHERENT X-RAY DIFFRACTION

Dzhigaev, Dmitry (Lund University, Lund, SWE)

The progress achieved in a growth of heterostructured nanowires led to design of nano-electronic devices with record-breaking parameters in transistors, quantum computations, solar cells and light emitting technologies. The strain plays significant role in the performance of these nano-electronic devices. In multi-segment nanowires the strain induced at the interfaces significantly change a charge carrier mobility, thus alternating the speed and power consumption during operation. The only way to image the strain in real functional device with many functional layers and over extended field of view is to employ scanning techniques with the use of nano-focused X-ray beams.

We made a deeper look at nanoscale features within single heterostructured nanowires, which are embedded in realistic devices. These are InAs/GaSb segments of TFETs, lateral nanowires of InGaAs MOSFETs and GaAs/InGaAs/InAs nanowires for quantum computation applications. Exploiting extraordinary brilliance of 4<sup>th</sup> generation synchrotron MAX IV (Lund, Sweden) and dedicated nano-focusing end-station NanoMax we could obtain the information which was not accessible before at resolution of 60 nm and below. Development of Bragg diffraction mapping and Bragg ptychography techniques in recent years opened exciting possibilities for 3D imaging of strain and tilt in various structures. These techniques were employed during our studies. The experimental challenges will be discussed in more detail. Interpreting of the results plays a significant role in obtaining quantitative information, which includes developing of proper models for strain engineering in nano-electronics.

## MS40-04 | IN SITU X-RAY SCATTERING STUDY OF HYDROTHERMAL SYNTHESIS OF ANATASE TiO<sub>2</sub> NANOPARTICLES FROM COMMERCIAL PRECURSOR TiOSO<sub>4</sub>

Søndergaard-Pedersen, Frederik (Aarhus University, Aarhus C, DNK); Broge, Nils Lau Nyborg (Aarhus University, Aarhus C, DNK); Yu, Jinlong (Aarhus University, Aarhus C, DNK); Mamakhel, Aref (Aarhus University, Aarhus C, DNK); Beyer, Jonas (Aarhus University, Aarhus C, DNK); Brummerstedt Iversen, Bo (Aarhus University, Aarhus, DNK)

TiO<sub>2</sub> is one of the most important metal oxides in modern materials science. Due to its low cost and non-toxicity it is very attractive in applications such as water splitting, photocatalysis and as a support material for catalytically active species e.g. in selective catalytic reduction of NO<sub>x</sub> gases.

Hydrothermal synthesis is an environmentally benign method for obtaining nanoparticles of TiO<sub>2</sub>, which allows easy upscaling and tailoring of the products. Rutile (P4<sub>2</sub>/mnm) is the thermodynamically stable bulk TiO<sub>2</sub> phase, but anatase (I4<sub>1</sub>/amd) is usually observed as the initial phase in hydrothermal synthesis of TiO<sub>2</sub>, which has been explained in terms of anatase having a lower surface energy than rutile. This causes anatase to have a lower overall free energy at small particle sizes until a certain critical size is reached at which rutile becomes the most stable phase.

Most academic TiO<sub>2</sub> studies start from precursors that are very expensive and/or highly reactive (e.g. titanium alkoxides, TiCl<sub>4</sub> and titanium metal). This makes the procedures unsuitable for upscaling to industrial production thus preventing their use in real world applications. TiOSO<sub>4</sub> is an alternative precursor, which is cheap, easy to handle and relatively safe. Hydrothermal treatment of TiOSO<sub>4</sub> is observed to yield anatase nanoparticles that are larger than the critical size. To understand why, *in situ* observations of the nucleation and growth processes are necessary. Findings using a capillary setup which allows measurement of X-ray powder diffraction and total scattering during hydrothermal synthesis will be presented.

## MS40-05 | ATOMIC INSIGHT INTO HYDRATION SHELLS AROUND FACETTED IRON OXIDE NANOPARTICLES

Thomä, Sabrina (Universität Bayreuth, Bayreuth, GER); Krauss, Sebastian (Universität Bayreuth, 95440, GER); Eckardt, Mirco (Universität Bayreuth, 95440, GER); Chater, Phil (Diamond Light Source, Didcot, GBR); Zobel, Mirijam (University of Bayreuth, Bayreuth, GER)

Whilst the strength of hydrogen bond networks within solvation shells around colloidal nanoparticles can be accessed with various spectroscopic techniques, the structure of those shells had hitherto remained inaccessible. Thanks to the increase of detection efficiencies and flux at high X-ray energies > 60 keV, we could recently access the solvent layering of alcohols with a robust data processing routine over 3 to 5 molecular layers for the first time via pair distribution function (PDF) analysis [1]. Detection of water remained challenging due to the small molecule size and the weak scattering contribution of hydrogen.

Now we have pushed the boundaries and even gained atomic insight into hydration shells around faceted iron oxide nanoparticles (IONPs). For this, we synthesized variably functionalized IONPs of two diameters – 7 and 15 nm – via coprecipitation in basic solution. TEM proved the faceting, TGA the partial ligand coverage and PDF analysis the hydration shell structure. Via double difference PDFs of the dispersions, nanopowders and bulk water, we identified three distinct interatomic distances within 2.5 Å from the IONP surface, irrespective of the capping agent. These distances correspond to molecularly and dissociatively adsorbed water molecules in accordance with theoretical predictions [2]. Despite the small IONP diameters, the interfacial fingerprint of the water structure is just like for large 2D interfaces.

[1] Zobel, M. *et al.*, *Science* 2015, 347 (6219), 292

[2] Thomä, S. L. J. *et al.*, *Nat. Commun.* 2019, 10 (1), 995

## MS40-P01 | STRUCTURAL CHARACTERIZATION OF EXCHANGE BIASED Au-Fe<sub>3</sub>O<sub>4</sub> DUMBBELL NANOPARTICLES

Feygenson, Mikhail (Juelich Centre for Neutron Science (JCNS-1), Juelich, GER)

We have studied the origin of the exchange bias effect in the Au-Fe<sub>3</sub>O<sub>4</sub> dumbbell nanoparticles in two samples with different sizes of the Au seed nanoparticles (4.1 and 2.7 nm) and same size of Fe<sub>3</sub>O<sub>4</sub> nanoparticles (9.8 nm). The synchrotron x-ray pair-distribution function measurements, small-angle x-ray/neutron-scattering and scanning transmission electron microscope measurements determined the antiferromagnetic FeO wüstite phase within Fe<sub>3</sub>O<sub>4</sub> nanoparticles, originating at the interface with the Au nanoparticles. The interface between antiferromagnetic FeO and ferrimagnetic Fe<sub>3</sub>O<sub>4</sub> is giving rise to the exchange bias effect. The strength of the exchange bias fields depends on the interfacial area and lattice mismatch between both phases. We propose that the charge transfer from the Au nanoparticles is responsible for a partial reduction of the Fe<sub>3</sub>O<sub>4</sub> into the FeO phase at the interface with Au nanoparticles. The Au-O bonds are formed, presumably across the interface to accommodate an excess of oxygen released during the reduction of magnetite.

## MS40-P02 | STRUCTURAL AND OPTICAL PROPERTIES OF CuS NANOPARTICLES

SOUICI, Abdelhafid (University, Bejaia, DZA); CHIBANI, Sarra (University, Bejaia, DZA)

Materials in the nanometre scale possess important physical and chemical properties which are very different to those of the bulk. Among these nanomaterials, semiconductor nanoparticles have attracted particular attention due to their varied technological applications mainly in nanotechnology, biology and medicine. This work investigate the effect of the polyethylene glycol molecule on the structural, morphology and optical properties of copper sulfide nanoparticles (CuS). CuS nanoparticles are synthesized in solution by chemical precipitation of dissolved precursors, copper sulfate ( $\text{CuSO}_4$ ) and thioacetamide ( $\text{CH}_3\text{CSNH}_2$ ). The determination of size, morphology and lattice parameters was performed by the Rietveld analysis of the X-ray diffraction patterns and the optical properties by UV-visible spectrophotometer. The results show that the presence of polyethylene glycol (PEG) as a stabiliser molecule has a crucial role on structural and optical properties of CuS nanoparticles.

## MS40-P03 | MULTISCALE STRUCTURAL DECODING OF ELECTROSPUN NANOFIBERS: FROM PROCESSING TO POSSIBILITIES FOR STEERING FUNCTIONALITY

Maurya, Anjani K. (Empa, Swiss Federal Laboratories for Materials Science and Technology, Center for X-Ray Analytics, St. Gallen, CH); Weidenbacher, Lukas (Empa, Swiss Federal Laboratories for Materials Science and Technology, Laboratory for Biomimetic membranes and Textiles, St. Gallen, CH); Spano, Fabrizio (Empa, Swiss Federal Laboratories for Materials Science and Technology, Laboratory for Biomimetic membranes and Textiles, St. Gallen, CH); Fortunato, Giuseppino (Empa, Swiss Federal Laboratories for Materials Science and Technology, Laboratory for Biomimetic membranes and Textiles, St. Gallen, CH); Rossi, René M. (Empa, Swiss Federal Laboratories for Materials Science and Technology, Laboratory for Biomimetic membranes and Textiles, St. Gallen, CH); Frenz, Martin (Institute of Applied Physics, University of Bern, Bern, CH); Dommann, Alex (Empa, Swiss Federal Laboratories for Materials Science and Technology, Center for X-Ray Analytics, St. Gallen, CH); Sadeghpour, Amin (Empa, Swiss Federal Laboratories for Materials Science and Technology, Center for X-Ray Analytics, St. Gallen, CH); Neels, Antonia (Empa, Swiss Federal Laboratories for Materials Science and Technology, Center for X-Ray Analytics, St. Gallen, CH)

Over the years, electrospinning has been developed as a technique to produce nano- to micron-sized fibers for filtration and biomedical applications [1]. It is well understood that the internal structure of these fibers highly depends on the polymer type, the spinning solution properties and the spinning parameters. In this contribution we present our recent advances in structural insights into electrospun poly(vinylidene fluoride-co-hexafluoropropylene), PVDFhfp, based fiber membranes for non-aligned and aligned (by using a high speed rotating drum) samples using X-ray scattering and diffraction techniques [2]. The densely packed lamellar structures in nanoscale with respect to fiber orientation axis have been analyzed by small angle X-ray scattering (SAXS) while molecular arrangement in orthorhombic structure are visualized by wide angle X-ray diffractions (WAXD). The nanofibrillar surface structures have also been seen by AFM performed on single fibers.

Furthermore, we will discuss our vision for nanoscale structural modification of the fibers by applying extreme drawing achieved using a high speed rotating drum electrospinning collector. The possibilities for significant variation in the ratio of crystalline  $\alpha$  and  $\beta$  phases will also be discussed. These studies and our further investigation shall establish new strategies for designing and processing novel functional electrospun membranes.

[1] A. G. Guex, L. Weidenbacher, K. Maniura-Weber, R. M. Rossi and G. Fortunato, *Macromol. Mater. Eng.*, 2017, **302**, 8.

[2] A. K. Maurya, L. Weidenbacher, F. Spano, G. Fortunato, R. M. Rossi, M. Frenz, A. Dommann, A. Neels and A. Sadeghpour, *Nanoscale*, 2019, **11**, 7176-7187.

## MS40-P04 | A LABORATORY RHEO-SAXS SETUP - RELATING NANOSTRUCTURE TO MACROSCOPIC PROPERTIES IN ONE GO

Pirolt, Franz (Anton Paar GmbH, Graz, AUT); Ehmann, Heike M. A. (Anton Paar GmbH, Graz, AUT); Jones, Andrew O. F. (Anton Paar GmbH, Graz, AUT); Pühr, Barbara (Anton Paar GmbH, Graz, AUT); Kotnik, Petra (Anton Paar GmbH, Graz, AUT)

Material research in all its complexity continuously calls for new analysis solutions to solve sophisticated issues in one go.

Relating the nanostructure of a material to its macroscopic mechanical properties requires *in-situ* characterization techniques such as rheology combined with SAXS. Rheo-SAXS experiments have so far been conducted only at synchrotron beam lines, mainly due to insufficient X-ray flux of laboratory X-ray sources and the lack of dedicated Rheo-SAXS laboratory instrumentation.

Anton Paar presents a novel experimental set-up for performing simultaneous Rheo-SAXS studies with the SAXSpoint 2.0 laboratory SAXS system in one go.

The integrated Rheo-SAXS sample stage enables temperature-controlled rheological experiments with in-situ determination of shear-induced structural changes of nanostructured materials on a nanoscopic length scale (from approx. 1 nm to 200 nm) by small-angle X-ray scattering.

The Rheo-SAXS unit includes a rheological sample compartment which is integrated in the evacuated SAXS measurement chamber. The rheometer measuring head comprises a high-precision air-bearing motor which holds and controls the rheological scattering measuring system in the SAXS instrument chamber.

We present combined rheology-SAXS studies of colloidal systems for investigating shear-induced structural changes at the nanometer level which were performed with this novel and optimized Rheo-SAXS laboratory set-up.

## MS40-P05 | POSSIBILITIES OF THE X-RAY DIFFRACTION METHOD FOR THE STUDY OF ULTRADISPERSED SYSTEMS AND NANOPOWDERS

Yatsenko, Dmitriy (Novosibirsk State University, Federal Research Center Boreskov Institute of Catalysis, Novosibirsk, RUS)

It is known that the physical and chemical properties of ultradispersed systems and nanomaterials are defined by features of the atomic structure. For structural investigations X-ray diffraction analysis is one of the main methods. Diffraction patterns contain information on the structure and morphology of nanoparticles: the shape and size of crystallites, the presence of defects and microstresses of atomic order, the mutual orientation of the blocks and the inter-grain boundaries of structured systems.

This information can be obtained from diffraction data, but studying of atomic structure of such small objects is an actual problem. Often, the diffraction patterns of such samples cannot be fully analyzed by standard approaches (for example, the Rietveld method) that are related to the measurement of positions, intensities and widths of diffraction reflections without diffuse scattering consideration.

A more general method Debye Function Analysis (DFA) method based on Debye scattering equation (DSE) can be used. It is full-profile method which is applicable for any an arbitrary atoms collection, and therefore can be used for crystalline objects, non-crystalline materials or nanostructures. The method is the most general and does not require artificial corrections (in contrast to the method Rietveld).

Possibilities of modelling diffraction patterns by the DFA will be shown for examples of various nanocrystalline materials: hydroxides of magnesium and tungsten, layered structures, metastable forms of aluminum oxide, ultradispersed iron oxides et al.

## MS40-P06 | STUDY OF STRUCTURAL POLYMORPHISM IN MOLECULAR COMPOSITES:APPLICATION TO ENERGY STORAGE

Ouaaka, Elmustafa (Laboratory of Physics of Materials and Modeling of Systems, Faculty of Sciences, Moulay Ismail University, Meknes, MAR); Haiki, F.Z (Laboratory of Physics of Materials and Modeling of Systems, Faculty of Sciences, Moulay Ismail University, Meknes, MAR); Ettakni, Mahmoud (Laboratory of Physics of Materials and Modeling of Systems, Faculty of Sciences, Moulay Ismail University, Meknes, MAR); Khechoubi, El Mostafa (Laboratory of Physics of Materials and Modeling of Systems, Faculty of Sciences, Moulay Ismail University, Meknes, MAR); Khmou, Ahmed (Laboratory of Physics of Materials and Modeling of Systems, Faculty of Sciences, Moulay Ismail University, Meknes, MAR); Kassou, Said (Laboratory of Physics of Materials and Modeling of Systems, Faculty of Sciences, Moulay Ismail University, Meknes, MAR)

The solid-solid phase transitions in the molecular composites of pérovskite-type layer (C10Zn, C12Zn and C10Cu) are studied by differential enthalpy analysis and X rays diffraction. These studies show that these composites possess a rich and complex structural poly morphing. The parameters of the crystalline cell in the different phases put in evidence are determined. The enthalpy differences ( $\Delta H$ ) are of 39.4 kJ/mol for the composite C10Cu, 49.2 kJ/mol for C10Zn and 62.0 kJ/mol in the case of the C12Zn. The crystallographic and thermodynamic studies show that the values of the temperatures and the enthalpy variations of the different transition increase with the chain length. The mechanisms of the phase transitions observed can be described by ordre-desordre process as well as by changes of conformation of the organic chains.

Keywords: Phase transition, Storage of energy, DSC, X-ray diffraction, Molecular composite, perovskite. Organic-inorganic hybrid.

## MS40-P07 | DIFFRACTION EXPERIMENTS UNDER EXTREME CONDITIONS ON SINGLE CRYSTALS WITH HOT NEUTRONS ON HEiDi

Meven, Martin (RWTH Aachen University, Garching bei München, GER); Grzechnik, Andrzej (RWTH Aachen University, Aachen, GER); Friese, Karen (Forschungszentrum Jülich GmbH, Jülich, GER)

Single crystal diffraction is one of the most versatile tools for detailed structure analysis. Due to their specific peculiarities neutrons are a very useful probe for structural studies on various hot topics related to physics, chemistry and mineralogy. The single crystal diffractometer HEiDi at the research neutron source at the Heinz Maier-Leibnitz Zentrum (MLZ) offers high flux, high resolution and large  $q$  range, low absorption and high sensitivity for light elements.

At very high temperatures studies on  $\text{Nd}_2\text{NiO}_{4+\delta}$  and  $\text{Pr}_2\text{NiO}_{4+\delta}$  brownmillerites concerning their oxygen diffusion pathways reveal anharmonic displacements of the apical oxygens pointing towards the interstitial vacancy sites which create a quasicontinuous shallow energy diffusion pathway between apical and interstitial oxygen sites [1]. A special mirror furnace which allows not only temperatures  $> 1300$  K but also atmospheres with various oxygen contents and different pressures around the sample allows to study their influence to the evolution of the occupation of the interstitial sites.

A BMBF (German ministry for education and research) funded project was launched in 2016 in order to allow studies on tiny samples  $< 1 \text{ mm}^3$  and to develop new high pressure cells for HEiDi which can be combined with its existing low temperature equipment for studies on structural properties down to temperatures below 10 K, e.g.  $\text{MgFe}_4\text{Si}_3$  compounds and their magnetic features [2].

[1] M. Ceretti et al.; J. Mater. Chem. A 3, 21140-21148 (2015).

[2] A. Grzechnik et al.; J. Appl. Cryst. 51, 351-356 (2018).

## MS40-P08 | MORPHOLOGY CHARACTERIZATION OF ANATASE $\text{TiO}_2$ NANOCRYSTALS BY ADVANCED RIETVELD REFINEMENT OF POWDER X-RAY DIFFRACTION DATA INCLUDING ANISOTROPIC SIZE BROADENING MODELS

Yu, Jinlong (Center for Materials Crystallography (CMC), Chemistry Department, Aarhus University, Aarhus, DNK)

Control of the crystalline nanocrystal morphology is important since it is known that certain facets substantially promote catalytic activity. It is, however, in itself challenging to determine nanocrystal morphology to provide a rational basis for the synthesis control. One widely used technique to characterize morphology of crystalline nanocrystal is Transmission Electron Microscopy (TEM) and High Resolution Transmission Electron Microscopy (HRTEM). While the main challenge of TEM and HRTEM is the so-called 3D-to-2D dilemma: the TEM and HRTEM images are the two-dimensional (2D) projections of the real three-dimensional (3D) nanocrystal along the direction of the incident electron beam (EB), and accurate reconstruction of the 3D morphology requires additional crystallographic knowledge and insight to the material under study.

Here, an alternative method, namely incorporation of an anisotropic size broadening model based on a linear combination of symmetrized spherical harmonic functions into the Rietveld refinement of synchrotron PXRD data is utilized to establish the sample averaged 3D morphology of anatase  $\text{TiO}_2$  nanocrystals obtained from supercritical flow synthesis. This procedure can not only overcome the intrinsic limitation of utilizing Scherrer equation on a non-refined diffraction pattern, but also intuitively display the average 3D morphology of nanocrystals by using the refined parameters. The robustness of this strategy is verified by comparing the anisotropic peak broadening models with results obtained from HRTEM and Raman spectra. In addition, it is shown that 3D morphologies determined from laboratory PXRD data give nearly identical results to reconstruction from synchrotron PXRD, demonstrating the broad applicability of the approach.

## MS40-P09 | QUANTIFICATION OF THE STRAIN RELAXATION PROCESSES IN SILICON NANOWIRES ARRAYS USING COMBINED X-RAY DIFFRACTION ANALYSES

Romanitan, Cosmin ([1] National Institute of Microtechnologies, Bucharest [2] Faculty of Physics, University of Bucharest, 405 Atomistilor Street, RO-077125, Magurele, Bucharest, ROU); Kusko, Mihaela ([1] National Institute of Microtechnologies, Bucharest, Bucharest, ROU); Popescu, Marian ([1] National Institute of Microtechnologies, Bucharest, Bucharest, ROU); Varasteanu, Pericle ([1] National Institute of Microtechnologies, Bucharest [2] Faculty of Physics, University of Bucharest, 405 Atomistilor Street, RO-077125, Magurele, Bucharest, ROU); Radoi, Antonio ([1] National Institute of Microtechnologies, Bucharest, Bucharest, ROU); Pachiu, Cristina ([1] National Institute of Microtechnologies, Bucharest, Bucharest, ROU)

Semiconductor nanowires (NWs) gained an increased attention in the last years due to their improved physical properties, favourable for opto- and upwards bio-electronic applications. In particular, silicon based low dimensional systems stand out among the other systems since silicon represented the material for the solid state electronics that drove to novel ideas concerning both fundamental phenomena and application developments. In this paper, we investigate the strain evolution and emerged relaxation processes in highly dense arrays of silicon nanowires obtained through metal assisted chemical etching, focusing mainly on the morphology induced effects. To circumvent the issues related to the anisotropic distribution of the strain and structural defects along the nanowires, we proposed a non-destructive X-ray method that exploits the finite penetration depth nature of X-rays and also their ability to imagine the arrays morphology in terms of tilt and twist. Thus, if in most cases, the X-rays diffraction studies concerning the strain in nanowires systems employ synchrotron X-ray sources, our formalism enables us to build unambiguously the bending and torsion profiles and to gain a quantitative description of the relaxation processes in connection with their morphological features using laboratory X-ray diffraction experiments.

## MS40-P10 | THE DYNAMIC STRUCTURE OF $\text{Au}_{38}(\text{SR})_{24}$ NANOCCLUSERS SUPPORTED ON $\text{CeO}_2$ UNDER CO OXIDATION

Pollitt, Stephan (TU Wien - Institute of Materials Chemistry, Vienna, AUT); Barrabés, Noelia (TU Wien - Institute of Materials Chemistry, Vienna, AUT); Rupprechter, Günther (TU Wien - Institute of Materials Chemistry, Vienna, AUT)

Thiolate protected gold nanoclusters ( $\text{M}_n(\text{SR})_m$ ) with sizes around one nanometer have become an extensively studied field. This is due to their unique properties resulting from quantum size effects and molecule-like structures. In nanocatalysis, it is a challenge to study structure reactivity relations under real life conditions because of the variety in active sites due to the size distribution in nanoparticles. With UHV (Ultra High Vacuum) techniques, well defined model systems can be perfectly understood, but the pressure gap impedes the transfer of information to real life conditions.

Thiolate protected Au nanoclusters offer the possibility to synthesize a homogenous and monodisperse active site. Thus, they allow for new pathways in catalyst design and fundamental research. Supported on oxides, these clusters have been proven to be highly active catalysts in several reactions. The amount of clusters on a support is about 1%wt in common cases, therefore structural investigations are impeded. However, XAFS (X-ray Absorption Fine Structure Spectroscopy) is well suited due to its low detection limit and elemental selectivity, that allows the investigation of the sample from different elemental points of view.

In our study,  $\text{Au}_{38}(\text{SC}_2\text{H}_4\text{Ph})_{24}$  clusters supported on  $\text{CeO}_2$  were investigated during an oxidative pre-treatment and in heterogenous CO oxidation under reaction conditions to understand structure reactivity relations. *In-situ* XAFS measurements were performed at Au-L<sub>3</sub> edge and static measurements at liquid N<sub>2</sub> temperature at S K-edge and Au-L<sub>3</sub> edge. Thereby, we clearly evidenced structural changes related to different behavior in reactivity, including distinct changes in the cluster's protecting ligand sphere.

## MS40-P11 | BEAM DAMAGE OF SINGLE SEMICONDUCTOR NANOWIRES DURING X-RAY NANO BEAM DIFFRACTION EXPERIMENTS

Pietsch, Ullrich (University of Siegen, Siegen, GER); AlHassan, Ali (University of Siegen, Siegen, GER); Davtyan, Arman (University of Siegen, Siegen, GER); Bahrami, Danial (University of Siegen, Siegen, GER); Bertram, Florian (DESY - Photon Science, Hamburg, GER)

Nano X-ray diffraction (nXRD) using focused synchrotron radiation is a powerful technique to study the structural properties of individual semiconductor nanowires (NWs). However, due to focusing the highly intense radiation down to a footprint of less than  $100 \times 100 \text{ nm}^2$  high radiation dose is deposited into a small sample volume which may cause radiation damage during measurements requesting long exposure time. Here, we report on nXRD experiments carried out at semiconductor NWs which are supposed to be resistant against radiation damage. The experiment has been performed under ambient conditions at the microfocus station of the P08 beamline at 3<sup>rd</sup> generation source PETRA III. Individual NWs were monitored continuously over a time interval up to 5 hours recording reciprocal space maps (RSM) of the 111 Bragg reflection at the same spatial position. For exposure time of about 1h we observe a reduce in integral intensity accompanied by minor axial lattice expansion and small tilts of the NW axis with respect to the substrate normal. NWs exposed for more than 2 hours show an increase of lattice expansion and after 3 and more hours of exposure we see NW melting. SEM after nXRD displays formation of amorphous shell around the NW which is maximum at the position of exposure. Our findings are explained by the huge energy impact into a small NW volume due to massive generation of electrons and subsequent electron-phonon interaction.

## MS40-P12 | NANOCRYSTALLINE CdS AND (Cd,Mn)S PARTICLES: STRUCTURE AND MORPHOLOGY

Evtushok, Boyan (Novosibirsk State University, Novosibirsk, RUS); Cherepanova, Svetlana (Novosibirsk State University, Novosibirsk, RUS)

Defect structure and morphology of CdS and (Cd,Mn)S nanocrystalline samples synthesized by hydrothermal synthesis at temperatures of 80, 100, 120, and 140° C were investigated. The full-profile analysis by the Rietveld method showed that the experimental X-ray diffraction patterns do not correspond to either the cubic structure of the sphalerite or the hexagonal structure of wurtzite, which are characteristic of well-crystalline CdS. In addition, X-ray diffraction patterns are not fitted by scattering on a mixture of these two modifications. Simulation of X-ray diffraction patterns with use of Debye scattering equation [1] showed that CdS and (Cd,Mn)S nanoparticles contain high concentration of stacking faults (SFs). Optimization of the structural models using the genetic algorithm showed that the probability of SFs (relative to the wurtzite structure) decreases for CdS from 0.55 to 0.46, and for (Cd,Mn)S from 0.47 to 0.36. Therefore, the structure of nanoparticles in both series gradually approaches the structure of wurtzite. It was also shown that at all synthesis temperatures the CdS and (Cd,Mn)S particles have an ellipsoidal shape, with the ellipsoids stretched along the direction perpendicular to the SFs. With an increase in the synthesis temperature, the average particle size increases. Ellipsoidal shape of particles was confirmed by TEM data.

[1] Proffen, Th., Neder, R.B. DISCUS: A program for diffuse scattering and defect-structure simulation (1997) *Journal of Applied Crystallography*, 30 (2), pp. 171-175

## MS40-P13 | INTERPLAY BETWEEN CRYSTAL STRUCTURE, SHAPE AND FUNCTIONALITY OF COLLOIDAL NANOCRYSTALS AND SUPERCRYSTALS

Lechner, Rainer T. (Montanuniversitaet Leoben, Leoben, AUT); Ludescher, Lukas (Montanuniversitaet Leoben, Leoben, AUT); Burian, Max (TU Graz, Graz, AUT); Karner, Carina (University of Vienna, Wien, AUT); Amenitsch, Heinz (TU Graz, Graz, AUT); Yarema, Maksym (ETH Zurich, Zürich, CH); Dirin, Dmitry N. (ETH Zurich, Zürich, CH); Kovalenko, Maksym V. (ETH Zurich, Zürich, CH); Heiss, Wolfgang (FAU Nürnberg Erlangen, Nürnberg, GER); Dellago, Christoph (University of Vienna, Wien, AUT)

Chemical synthesised colloidal nanocrystals (NCs) offer the opportunity for realising novel materials with tailored functionalities. A large variety of semiconducting and metallic NCs can be realised [1]. Especially an inner core/shell structure of the semiconducting NCs leads to an increased photoluminescence (PL) output. But also the NCs' shape determines their optical performance. We have revealed a relation between structure and functionality by combining different scattering techniques at lab and synchrotron sources with microscopy techniques [2]. In a recent study at the synchrotron ESRF, we have investigated hexagonal CdSe/CdS core/shell NCs with different dimensions by recording ASAXS and WAXS spectra. By means of a shape retrieval method for SAXS data [3, 4], we could reveal an elliptical particle shape with pronounced surface facets for the largest core/shell NCs and related this shape to specific crystallographic directions. The increased anisotropy is directly connected to a decreased PL.

The NC's shape can also significantly influence the super-crystal structure of colloidal supercrystals [1], where NCs act as building blocks to form 3D nanocrystal solids with designed properties. We were able to link their supercrystal structure to the atomic Bi NC structure [4].

[1] M. V. Kovalenko, et al., & W. Heiss, *ACS Nano* 9, 1012–1057 (2015)

[2] L. Ludescher, et al., & R.T. Lechner, *Front. Chem.* 6, 672 (2019)

[3] M. Burian, G. Fritz-Popovski, et al., & R.T. Lechner, *J. Appl. Cryst.* 48, 857-868 (2015)

[4] M. Burian, C. Karner, et al., & R.T. Lechner, *Adv. Mater.* 30, 1802078 (2018)

## MS41: Crystallisation for Small and Large Molecules

---

### MS41-01 | CRYSTALLISATION FOR SERIAL CRYSTALLOGRAPHY IN LIPIDIC CUBIC PHASE (LCP)

#### MADE SIMPLE

Moraes, Isabel (National Physical Laboratory, Teddington, GBR)

In recent years, serial millisecond and femtosecond crystallography has emerged as promising tool for structural studies of membrane proteins. The possibility of collecting data from very small crystals at room temperature with reduced radiation damage has opened new opportunities to the membrane protein scientific community, in particular in the field of time-resolved studies. However, one of the technical bottlenecks of the method is the production of large amounts of tiny optimized crystals in mesophases (LCP). Here, we present a simple and fast method to prepare hundreds of microliters of high-density microcrystals in lipidic cubic phase for serial crystallography. This approach does not only eliminates the need of using large quantities of gas-tight syringes as also may be used as a high-throughput tool when screening conditions for the growth of high density well-diffraction crystals. The crystals grown by this technique are compatible with the current LCP extruders existent in the free electron lasers and synchrotron sources. This semi-automated method is also easily implemented in any standard crystallisation laboratory.

## MS41-02 | FOUR FOR THE PRICE OF ONE: CROSS-SEEDING TO OBTAIN CRYSTALS OF ANCESTRAL ELONGATION FACTOR TUS

Majumdar, Soneya (Department of Cell and Molecular Biology, Uppsala University, Uppsala, SWE); Bergfors, Terese (Department of Cell and Molecular Biology, Uppsala University, Uppsala, SWE); Sanyal, Suparna (Department of Cell and Molecular Biology, Uppsala University, Uppsala, SWE)

Elongation factor Tu (EF-Tu) is an essential translation factor which brings aminoacyl tRNAs to the ribosome. The strong correlation between the thermal stability of EF-Tu and the optimal growth temperature of the host makes EF-Tu an attractive candidate for studying protein evolution. Gaucher et al. [1] have reconstructed several sequences of EF-Tu, which represent the ancient nodes of the bacterial evolutionary tree.

In this study we crystallised, and subsequently determined, high-resolution structures of four of these nodal EF-Tus—EF-Tu 170, 184, 262, and 317. They have high sequence identity with each other (84-92%), and  $T_m$  values ranging from 39.1 to 66.7°C. Crystals of EF-Tu 262 which were obtained first, diffracted to 2Å and were used to cross-seed the other three homologs by matrix microseeding [2]. Hits generated in this round of matrix microseeding were then used for further cross-seeding experiments of the proteins with each other in various permutations. Intriguingly, the best crystals were obtained by cross-seeding the nodes that had more similar biophysical characteristics, rather than the highest sequence identity.

Despite the many successes reported with cross-seeding [2], it is still unclear why it works for some homologs and not others. We suggest that the biophysical properties of the homologs may be a more important consideration than their sequence identity when selecting an appropriate cross-seed.

[1] Gaucher EA, Govindarajan S & Ganesh OK (2003) *Nature* 451, 704–707.

[2] D'Arcy A, Bergfors T, Cowan-Jacob SW & Marsh M (2014) *Acta Crystallogr. F Struct. Biol. Commun.* 70(Pt 9): 1117–1126.

## MS41-03 | NANO-CRYSTALLIZATION: APPLYING THE METHODS OF MACROMOLECULAR CRYSTALLOGRAPHY FOR SMALL MOLECULES

Babor, Martin (University of Chemistry and Technology, Prague, Prague, CZE); Nievergelt, Philipp P. (University of Zurich, Zürich, CH); Čejka, Jan (University of Chemistry and Technology, Prague, Prague, CZE); Spingler, Bernhard (University of Zurich, Zürich, CH)

We have recently developed a method for the crystallization of cationic moieties with the help of novel anion screen [2]. Salts that are at least water soluble at a concentration of 2 mg / ml water can be crystallized to directly yield single crystals. So far, we have shown that the new method works for organic cations by either vapour diffusion at the nanoliter scale (Nievergelt *et al.*, 2018) or the under-oil technique [1]. In the presentation, we will show that we could successfully extend our method for the determination of protein and coordination complexes.

We thank the University of Zurich, the Czech Science Foundation (grant No. 16-10035S) and the Specific University Research (MSMT No. 21-SVV/2018) for financial support.

[1] Babor, M., Nievergelt, P. P., Čejka, J., Zvoníček, V. & Spingler, B. (2019). *IUCrJ* **6**, 145-151.

[2] Nievergelt, P. P., Babor, M., Čejka, J. & Spingler, B. (2018). *Chem. Sci.* **9**, 3716-3722.

## MS41-04 | SUBSTRATE INDUCED POLYMORPHISM OF ORGANIC ELECTRONIC MOLECULES

Resel, Roland (Graz University of Technology, Graz, AUT); Demitri, Nicola (Elettra – Sincrotrone, 34149 Basovizza, ITA); Werzer, Oliver (University Graz, Graz, AUT); Geerts, Yves (Université libre de Bruxelles, Brussels, BEL)

Crystallisation of molecular crystals at defined substrate surfaces can lead to unknown polymorph phases. Several examples are known for organic electronic molecules, but also for pharmaceutical molecules. These polymorphs can have considerably different optical, electronic, mechanical and dissolution properties which influences their potential applications. A first step of understanding the origin of substrate induced phases is the determination of the molecular packing. A combination of grazing incidence x-ray diffraction with molecular dynamics simulation is used for crystal structure solution. Recently, also single crystal diffraction is used for crystal structure solution of substrate induced phases. We selected a number of different molecules and demonstrate fundamental properties of the crystalline structure in relation to the bulk crystal structure. It is shown that confirmation of the molecular packing with the substrate surface is an important parameter, additionally the different polymorphs can show fundamental different packing motifs like herringbone packing and stacking of aromatic rings. In a subsequent step the importance of the crystal growth kinetics is presented which causes the substrate induced polymorph and finally the thermodynamic stability of these phases. The selected examples are molecules which forms van der Waals crystals like pentacene, oligothiophenes, benzo-thieno-benzthiophene based molecules but also examples from molecules with hydrogen bonds are discussed like dibromo-indigo and phenytoin.

## MS41-05 | SHAPING DRUG PROCESS DEVELOPMENT WITH CRYSTAL STRUCTURE DATABASES

Janbon, Sophie (AstraZeneca, Macclesfield, GBR)

Crystal structures are invaluable to the pharmaceutical industry. During early stages in the development of an active pharmaceutical ingredient (API), they are used to determine what molecular features are required for efficient protein binding. In late stage development, they are used to de-risk issues; often seen with API stability and processability. Applying predictive approaches to API crystal structures can reduce the time to market by guiding experimental work. Approaches based on energy calculation, are complex in contrast to empirical approaches via crystal structures data mining.

Data-mining requires a large set of data and this has been compiled and curated for more than 50 years by the Cambridge Crystallography Data Centre. The Cambridge Structural Database can then be probed to drive discovery and research. The empirical approaches become even more powerful when coupled with internal company databases, which contain chemical moieties which are more pharmaceutically relevant. This has been used with great success within our business in terms of rapid data generation and user-friendly methods, and as a result easy implementation for non-expert users.

This presentation will describe how we use data mining methods into our scientific decision-making processes. Examples will be provided with an emphasis on API crystallisation process development; and will showcase the power and ease of data-mining.

## MS41-P01 | WATCHING NANODEFECTS GROW IN SI CRYSTALS

Magerl, Andreas (University Erlangen-Nürnberg, Erlangen, GER)

Thickness-dependent Pendellösung oscillations as described by the dynamical theory of X-ray diffraction are extremely sensitive to strain fields from defects in a host crystal. Based on this, we initiated a novel approach to study nucleation and growth of oxygen precipitates in moderately ( $\approx 10^{15}$  1/cm<sup>3</sup>) and highly ( $\approx 10^{18}$  1/cm<sup>3</sup>) boron doped Czochralski Si crystals in-situ up to 1000°C. This provides a unique access to monitor continuously the evolution of defects from their very early stages to the long time behavior. The data is interpreted within a diffusion-limited model of growing spherical precipitates with two growth regimes, where an initial diffusion driven mode is followed by a long time precipitation behavior, interpreted as Ostwald ripening.

## MS41-P02 | MULTIFERROIC $\text{Bi}_2\text{Fe}_4\text{O}_9$ : TUNING OF CRYSTALLIZATION PATHWAYS AND KINETICS

Kirsch, Andrea (University of Bremen, Bremen, GER); Gesing, Thorsten (University of Bremen, Bremen, GER)

The Physical properties of many functional materials show a strong size-dependence if the material is decreased to the nanosize-regime.  $\text{Bi}_2\text{Fe}_4\text{O}_9$  shows huge distortions of the Fe-polyhedra below 122(2) nm leading the magnetic spins to rotate [1]. Its frustrated pentagonal magnetic lattice is very complex exhibiting 5 different exchange interactions and concomitant ferromagnetic and antiferromagnetic coupling in the *c*-axis and *ab* – plane, respectively [2]. A high controllability of the materials characteristics such as particle/crystallite dimensionality, crystallinity and morphology is therefore of crucial importance. The  $\text{Bi}_2\text{O}_3$  –  $\text{Fe}_2\text{O}_3$  phase system is very rich and complex since many different binary and ternary oxides tend to crystallize. In this study, we investigated how the type of complexing agent and pH change the crystallization pathways and kinetics for the  $\text{Bi}_2\text{Fe}_4\text{O}_9$  stoichiometry. In total, 25 Precursor were synthesized by a sol-gel method using the corresponding metal nitrates. Each precursor was heat treated at 873 K for 1 h and 973 K for 2 h to follow the crystallization of the  $\text{Bi}_2\text{Fe}_4\text{O}_9$  structure. The samples were analyzed by SEM, TGA/DSC, FTIR spectroscopy and in-house X-ray powder diffraction at ambient temperature and *in-situ* at high temperatures followed by Rietveld refinements. The crystallization pathways and kinetics are strongly directed by the synthesis parameters.

[1] Kirsch, A. et al. J. Phys. Chem. C, 2019, 123, 3161.

[2] Ressouche, E. et al. Phys. Rev. Lett., 2009, 103, 267204.

## MS41-P03 | AMINE-IMINE PROTON TAUTOMERISM IN ISOMERIC 2-PHENYLAMINO-1,3-THIAZOL-4(5H)- AND 4-PHENYLAMINO-1,3-THIAZOL-2(5H)-ONE DERIVATIVES

Pyrih, Andrii (Adam Mickiewicz University in Poznan, Poznan, POL); Gzella, Andrzej (Poznan University of Medical Sciences, Poznan, POL); Lesyk, Roman (Danylo Halytsky Lviv National Medical University, Lviv, UKR); Jaskólski, Mariusz (Institute of Bioorganic Chemistry, Polish Academy of Sciences, Poznan, POL)

Newly synthesized derivatives of 2-phenylamino-5-dimethylaminomethylidene-1,3-thiazole-4(5H)-one and 4-phenylamino-5-dimethylaminomethylidene-1,3-thiazolin-2(5H)-one, with the potential to form tautomeric equilibria, have been studied by single-crystal X-ray diffraction, in order to determine the tautomeric form induced by -CF<sub>3</sub> substitution at the *para* position of the phenyl ring.

Location of the amidine hydrogen atom, carried out using difference electron density maps, unambiguously revealed the prevalence of the amino tautomeric form, with the H atom placed outside the thiazolinone cycle. This observation is corroborated by the presence of an intermolecular N-H...O hydrogen bond, with the exocyclic nitrogen atom as the donor and the carbonyl O atom as the acceptor. The thiazolinone and phenyl rings are nearly coplanar, facilitating a non-classical intramolecular C-H...N hydrogen bond between the phenyl ring H atom at the *ortho* position and the thiazolinone N atom, which further stabilizes the amino tautomeric form.

In addition, the conformational isomerism of the title molecules will be discussed in the context of biological activity of heterocyclic compounds and as an important factor influencing intermolecular interactions and crystal packing.

The work was supported by grant no. POWR.03.02.00-00-I020/17 co-financed by the European Union through the European Social Fund under the Operational Program Knowledge Education Development.

## MS41-P04 | TWO NEW POLYMORPHS OF $\text{CuCl}_2 \cdot 2\text{DMF}$ OBTAINED VIA HIGH-TEMPERATURE CRYSTALLIZATION

Goreshnik, Evgeny (Jožef Stefan Institute, Ljubljana, SVN)

Crystal structure of  $\alpha\text{-CuCl}_2 \cdot 2\text{DMF}$  was published first time on late 1970-th [1, 2]. Crystallization of titled compound from dimethylformamide at 60-65 °C results in a formation of two another polymorph modifications. Contrary to monoclinic (sp. gr.  $P2_1/n$ ) structure of earlier discovered polymorph new **b**- and **g**-modifications are triclinic, sp. gr.  $P\bar{1}$ ). All three polymorphs are built up from  $\text{Cu}_2\text{Cl}_4 \cdot 4\text{DMF}$  dimers with slightly different mutual orientations of DMF molecules attached to the same metal ion. The presence of inter- and intra-molecular hydrogen bonds results also in a formation of different crystal structures. Surprisingly the DSC measurements do not show any noticeable effects.

	<b>a</b>	<b>b</b>	<b>c</b>	<b><math>\alpha</math></b>	<b>b</b>	<b>g</b>	<b>V/Z</b>
<b><math>\alpha</math></b>	11.568(5)	11.617(7)	8.992(4)		111.87(5)		1195.71/4
<b>b</b>	8.1549(4)	10.2410(5)	13.5866(7)	91.855(4)	90.777(4)	90.850(4)	1133.85/4
<b>g</b>	7.389(1)	8.281(1)	10.484(1)	99.58(1)	102.45(1)	110.36(1)	566.48/2

[1] I.P. Lavrent'ev, L.G. Korableva, E.A. Lavrent'eva, G.A. Nifontova, M.L. Khidekel, I.G. Gusakovskaya, T.I. Larkina, L.D. Arutyunyan, O.S. Filipenko, V.I. Ponomarev, L.O. Atovmyan. *Koord. Khim. (Russ.) (Coord. Chem.)*, 5, 1484 (1979)

[2] H. Suzuki, N. Fukushima, Shin-ichi Ishiguro, H. Masuda, H. Ohtaki. *Acta Crystallogr., Sect. C: Cryst. Struct. Commun.*, 47, 1838 (1991)

## MS41-P05 | PHYTOCHEMICAL AND BIOLOGICAL STUDIES OF *ANACYCLUS PYRETHRUM* L. FROM IFRANE-MOROCCO

Remok, Firdaous (Moulay Ismail University, Faculty of Sciences, Meknes, MAR); ZAIR, Touriya (Moulay Ismail University, Faculty of Sciences, Meknes, MAR)

As part of the Moroccan aromatic and medicinal plants valorization, we were interested in the study of a Moroccan endemic specie, commonly called Tigendest. In this context, we used male and female roots of the *A. pyrethrum* from Ifrane-Morocco to determinate the chemical composition of their extracts and essential oil. We also carried out antioxidant, antimicrobial and insecticidal activities of their hydromethnolic extracts.

The phytochemical screening revealed the presence of alkaloids, polyphenols, flavonoids, sterols and triterpenes. Total phenolic and total flavonoid contents of the extracts were determined respectively by Folin–Ciocalteu method and aluminium chloride colorimetric method.

The antioxidant effect of the extracts was evaluated by the DPPH method. Their antimicrobial activity was carried out on specific microbiological strains. The insecticidal power of *A. Pyrethrum* extract used in different doses showed a significant insecticidal effect on *C. maculatus*; main pest of the stored food of legumes. This indicates that long-lasting, low-cost protection against this pest is possible by using *A. pyrethrum* root extracts, which may represent an interesting alternative to chemical insecticides.

The study of its EO chemical composition by GC-MS showed a quantitative and qualitative variation of its chemical profile: Spathulenol (16.9%), Germacra-4 (15%), 5.10 (14) -trien-1-a-ol (12.28%), Selina-3,11-dien- 6-a-ol (9.24%), Caryophyllene oxide (7.11%).

In perspective, the molecules responsible for the antioxidant and / or insecticidal activity must be separated, purified and identified using spectroscopic methods (UV, FT-IR, NMR and diffraction X-ray) for possible obtaining of a pure and natural active ingredient.

## MS41-P06 | DYNAMIC THEORY OF PROTEIN CRYSTALLIZATION

Hasek, Jindrich (Institute of Biotechnology, Academy of Sciences, Vestec, CZE); Skálová, Tereza (Institute of Biotechnology, Academy of Sciences, Vestec, CZE); Dušková, Jarmila (Institute of Biotechnology, Academy of Sciences, Vestec, CZE); Koval, Tomáš (Institute of Biotechnology of the Czech Academy of Sciences, Vestec, CZE); Dohnálek, Jan (Institute of Biotechnology of the Czech Academy of Sciences, Vestec, CZE)

Classical crystallization theories use model of ideally dissolved molecules in homogeneous crystallization solution. However, components of crystallization solution often form temporary adducts leading to preorganization of target molecules. Adhesion of all components of crystallization solution, competition of different adhesion modes and formation of temporary protein clusters is of principal importance namely in protein crystallization.

The new dynamic theory of protein crystallization is based on analysis of intermolecular interactions responsible for regular deposition of protein molecules in crystal. It introduces a general term “adhesion mode” describing the tendency of molecules to realize a specific configuration during interaction of two molecules in a given environment. The new concept describing crystallization as a competition between possible adhesion modes mutually incompatible within a given crystal form gives us a rational tool to see why “crystallization attempt” leads to amorphous precipitate or for to regular crystalline form. Crystallographer equipped with knowledge of basic principles of intermolecular adhesion can rationalize any crystallization method respecting the „principle of a single adhesion mode“.

Recognition of intermolecular adhesion as a principle driving force of protein crystallization explains many formerly mysterious effects observed in practice in many crystallization techniques. It

- explains excellent performance of PEG,  $(\text{NH}_3)_2\text{SO}_4$ , etc. in crystallization experiments,
- shows how the composition of mother liqueur influences the crystal form (space group),
- explains initiation of crystallization in under-saturated solution in the confined space of cavities in some nanoporous materials,
- allows preparation of better crystals and different polymorphs of the same protein.

## MS42: In Situ and In Operando Analysis of Functional Materials

---

### MS42-01 | HIGH ENERGY SURFACE X-RAY DIFFRACTION FROM SURFACES AND NANOPARTICLES IN OPERANDO CATALYSIS

Hejral, Uta (Lund University, Lund, SWE)

Catalysts are complex material systems consisting of metal nanoparticles dispersed on highly branched oxide supports. They accelerate desired chemical reactions with applications ranging from exhaust gas treatment to chemical industry. To improve catalyst performance, an atomic-scale understanding of the catalyst structure and its correlation to the catalytic activity under realistic reaction conditions is inevitable.

In my presentation I will discuss how High-Energy Surface X-Ray Diffraction (HESXRD: photon energy  $E=70-80$  keV) allows for studying under operando conditions the structure of different model catalyst systems, including epitaxial metal nanoparticles and single crystal surfaces. Hence, our CO oxidation study performed at beamline ID15 (ESRF) revealed the composition- and shape-dependent sintering of  $\text{Al}_2\text{O}_3(0001)$ -supported alloy nanoparticles of varying Pt-Rh composition: while the flat-shaped Pt-rich particles underwent tremendous sintering, the compact-shaped Rh-rich particles featured a high stability suppressing the sinter-induced catalyst deactivation.

In a recent experiment at beamline P07 (DESY) we combined for the first time HESXRD with Planar Laser Induced Fluorescence (PLIF), optical LED Surface Optical Reflectance (SOR) and in-situ Mass Spectrometry (MS) to study self-sustained reaction oscillations during CO oxidation over Pd(001). This allowed, with sub-second time resolution, for correlating the structure (HESXRD, SOR) to the sample's  $\text{CO}_2$  production (PLIF, MS). Our data show that the oxidation and reduction of (111)-oriented Pd islands on top of an epitaxial PdO(101) oxide layer, previously reported under reducing conditions close to UHV, play a crucial role in the underlying oscillation mechanism.

## MS42-02 | NEUTRON DIFFRACTION STUDIES OF ENERGY MATERIALS

Hull, Stephen (The ISIS Facility, Didcot, GBR)

The increasing demand for new, cheap and environmentally benign technologies for energy production and storage provides many challenges for the field of materials science. Examples include the development of new electrode materials for lightweight rechargeable batteries, proton and oxide-ion conducting ceramics for high temperature fuel cells and novel thermoelectric compounds to convert waste heat into usable electrical power. Its sensitivity to locating light atoms in the presence of heavier ones makes neutron powder diffraction a powerful tool for structural studies of many of these 'energy materials' which, for example, rely on rapid diffusion of ions such as H<sup>+</sup>, Li<sup>+</sup> and O<sup>2-</sup> through the solid. Furthermore, the penetrating power of neutrons allows diffraction studies to be performed on the materials within complex sample environment devices. This presentation will show examples of the use of neutron powder diffraction to characterise the structural properties of materials of relevance to battery, fuel cell and thermoelectric technologies, using in-situ electrochemical devices, high temperature studies performed under controlled reducing and oxidizing conditions and the development of cells which allow simultaneous measurements of relevant bulk properties (e.g. conductivity, Seebeck coefficient) whilst structural studies are performed on the neutron diffractometer.

## MS42-03 | MORPHOLOGY AND STRUCTURE OF METAL-ORGANIC FRAMEWORK ZIF-8 DURING CRYSTALLISATION MEASURED BY A NEW TECHNIQUE: DYNAMIC ANGLE RESOLVED SECOND-HARMONIC SCATTERING (AD-SHS)

Van Cleuvenbergen, Stijn (University of Leuven - KULAK, Kortrijk, BEL); Smith, Zachary J. (University of Science and Technology of China, Hefei, AUT); Deschaume, Olivier (University of Leuven, 3001, BEL); Bartic, Carmen (University of Leuven, Heverlee, BEL); Wachsmann Hogiu, Sebastian (McGill University, Montreal, CAN); Verbiest, Thierry (University of Leuven, Heverlee, BEL); van der Veen, Monique (Delft University of Technology, Delft)

Morphology and structure of a metal-organic framework measured during crystallization measured by a new technique: Dynamic Angle Resolved Second-Harmonic Scattering (AD-SHS).

Crystallization is often much more complex than a classical nucleation and growth process, involving intermediates, metastable phases, etc. Second-order nonlinear optical techniques might be particularly interesting in investigating these early stages as they are inherently sensitive to the way matter is organized. Indeed, recent developments in these techniques have opened a window into morphological and structural characteristics for a variety of supramolecular systems [1]. To interrogate the structure of a species in solution, second-harmonic scattering (SHS) can be used, yet to study the dynamics of the early stages of crystallization, the measurement technique is too slow. We developed a new measurement scheme where the dependence of SHS on the polarization of light and on the scattering angle is measured in a time resolved manner. Fast acquisition times are achieved through Fourier imaging. The angular dependence provides morphological insight including shape and size, while the polarization provides structural insight related to point group symmetry. We applied the technique to the crystallization of the metal-organic framework ZIF-8 [2]. Our findings highlight the potential of dynamic angle-resolved harmonic light scattering to probe crystal growth processes, assembly–disassembly of biological systems, adsorption, transport through membranes and myriad other applications.

[1] S. Van Cleuvenbergen et al. *Angew. Chem. Int. Ed.* 56, 9546–9550 (2017); P. D. Schmitt et al. *Anal. Chem.* 88, 5760–5768 (2016); A. Ferguson et al. *Nat. Chem.* 8, 250–257 (2016).

[2] S. Van Cleuvenbergen et al. *Nat. Commun.* 9, 3418 (2018).

## MS42-04 | IN SITU MECHANOCHEMISTRY OF HYBRID MATERIALS

Wilke, Manuel (PSI, Villigen PSI, CH); Casati, Nicola (PSI, Villigen PSI, CH)

Mechanochemistry is increasingly used for solid state reactions because of its advantages like high yields, high conversion rates, the small produce of waste and the good energy consumption, for which it belongs to green chemistry.[1] Nevertheless, the mechanisms behind mechanochemical reactions are still under investigation which is why *in situ* setups are needed.[2]

Here we present the *in situ* investigation of the formation of a series of organic-inorganic hybrid materials from mechanochemical synthesis. The compounds are constructed by guanidinium-, lead(II)- and iodide-ions, with the formula  $(\text{C}(\text{NH}_2)_3)_n\text{PbI}_{2+n}$  ( $n = 1, 2, 3, 4$ ).[3] For the *in situ* investigations a new setup, developed at the MS beamline (PSI, Switzerland) is used.[4] Due to the gained high quality data an automatic quantitative analyses of the time-resolved powder X-ray diffraction patterns was possible and revealed intermediate formations, solid-solid phase transitions and reactions between the guanidinium lead(II) iodides during the syntheses. We consider these discovered pathways to be linked to the respective structural features of the different compounds. Recent results suggest that **3** is a necessary intermediate for the formation of **4** and that both steps have very different energy dependencies.[5]

[1] James et al., Chem. Soc. Rev. **2012**, 41, 413-447.

[2] Užarević et al., J. Phys. Chem. Lett. **2015**, 4129-4140.

[3] Wilke et al., Chem. - Eur. J. **2018**, 24, 17701-17711.

[4] Ban et al., Anal. Chem. **2017**, 89, 13176-13181.

[5] Wilke et al., in preparation.

## MS42-05 | INSPECTING PIEZOELECTRICITY IN $\text{PbZr}_{1-x}\text{Ti}_x\text{O}_3$ SINGLE CRYSTALS WITH FERROELASTIC DOMAINS

Gorfman, Semën (Tel Aviv University, Tel Aviv, ISR); Choe, Hyeokmin (Tel Aviv University, Tel Aviv, ISR); Nan, Zhang (Electronic Materials Research Laboratory, Xi'an, CHN); Chernyshov, Dmitry (SNBL at the ESRF, Grenoble, FRA); Ye, Zuo-Guang (Department of Chemistry and 4D Lab, Simon Fraser University, Vancouver, CAN)

Piezoelectricity is the ability of some materials to get electrically polarized under mechanical stress and mechanically deformed under electric field. Despite increasingly high demand and expanding realm of application, the choice of practically explored piezoelectrics is limited to quartz ( $\text{a-SiO}_2$ ) crystals,  $\text{PbZr}_{1-x}\text{Ti}_x\text{O}_3$  (PZT) ferroelectric ceramics and  $\text{PbMg}_{2/3}\text{Nb}_{1/3}\text{O}_3$  -  $\text{PbTiO}_3$  (PMN-PT) relaxor-ferroelectric crystals. Piezoelectricity is well studied phenomena, however, some aspects like the role of ferroelectric / ferroelastic domains) remains poorly understood. Therefore, the design of new functional piezoelectrics – e.g. lead-free alternatives to PZT remains complicated.

Here we develop X-ray diffraction-based technique and data-analysis algorithm for separation of "domain-related" and "intrinsic" response of ferroelectric / ferroelastic domains in PZT single crystals to external electric field. We measured three-dimensional high-resolution reciprocal space maps around selected families of split Bragg peak, representing diffraction from differently oriented ferroelastic twin domains. The crystal was loaded into specially designed sample environment cell [1], while external electric field was synchronized with PILATUS2M detector using microcontroller-based data-acquisition system [2]. We developed the algorithm for assignment of different components of each family to individual domain variants with known direction of spontaneous polarization relative to applied electric field. Using this algorithm, we are able to track the change of lattice constants and domain volume fraction of each domains.

[1] T. Vergentev et al. *J. Appl. Crystallogr.* **49**, 1501 (2016).

[2] H. Choe et al. *J. Appl. Crystallogr.* **50**, 975 (2017).

## MS42-P01 | PHASE DIAGRAM AND REDOX BEHAVIOR OF (Nd/Pr)<sub>2</sub>NiO<sub>4+δ</sub> ELECTRODES EXPLORED BY IN SITU NEUTRON POWDER DIFFRACTION DURING ELECTROCHEMICAL OXYGEN INTERCALATION

Ceretti, Monica (ICGM CNRS, Montpellier, FRA); Wahyudi, Olivia (ICMCB, Pessac, FRA); Meven, Martin (RWTH Aachen University and Jülich Centre for Neutron Science, Garching bei München, GER); Paulus, Werner (ICGM Université de Montpellier, Montpellier, FRA)

Oxygen intercalation/deintercalation in Pr<sub>2</sub>NiO<sub>4+δ</sub> and Nd<sub>2</sub>NiO<sub>4+δ</sub> was followed by *in situ* neutron powder diffraction during electrochemical oxidation/reduction, in a dedicated reaction cell at room temperature [1]. For both systems three phases, all showing the same line-width, were identified. The starting phases, Pr<sub>2</sub>NiO<sub>4.23</sub> and Nd<sub>2</sub>NiO<sub>4.24</sub>, considered with an average orthorhombic *Fmmm* symmetry, although both show a slight monoclinic distortion, get reduced in a 2-phase reaction step to tetragonal intermediate phases with  $0.07 \leq \delta \leq 0.10$  and *P4<sub>2</sub>/ncm* space group, which on further reduction transform, again in a 2-phase reaction step, towards the respective stoichiometric (Pr/Nd)<sub>2</sub>NiO<sub>4.0</sub> phases, with *Bmab* space group. Electrochemical oxidation does, however, not proceed fully reversibly for both cases: while the re-oxidation of Nd<sub>2</sub>NiO<sub>4+δ</sub> is limited to the tetragonal intermediate phase with  $\delta = 0.10$ , the homologous Pr<sub>2</sub>NiO<sub>4+δ</sub> can be re-oxidized up to  $\delta = 0.17$ , showing orthorhombic symmetry. For the intermediate tetragonal phase, we were able to establish for Pr<sub>2</sub>NiO<sub>4.09</sub> complex anharmonic displacement behaviour of the apical oxygen atoms, as analysed by single crystal neutron diffraction and Maximum Entropy Analysis, in agreement with a low-T diffusion pathway for oxygen ions, activated by lattice [2-3].

[1] M. Ceretti *et al.*, *Inorg. Chem.*, (2018), 57, 8, 4657-4666

[2] M. Ceretti *et al.*, *J. Mat. Chem. A*, (2015), 21140-21148.

[3] A. Piovano *et al.*, *Phys. Chem. Chem. Phys.*, (2016), 17398-17403

## MS42-P02 | EXTRACTING COHERENT INFORMATION ABOUT PHASE TRANSFORMATIONS IN A FUNCTIONAL MATERIAL STUDIED BY X-RAY POWDER DIFFRACTION

Gertenbach, Jan (Malvern Panalytical BV, Almelo); Herbert, Simon A. (Stellenbosch University, Stellenbosch, ZAF); Jacobs, Tia (Stellenbosch University, Stellenbosch, ZAF); Janiak, Agnieszka (Stellenbosch University, Stellenbosch, ZAF); Degen, Thomas (Malvern Panalytical BV, Almelo); Barbour, Len (Stellenbosch University, Stellenbosch, ZAF)

Structural phase transformations of polymorphic materials are mostly studied using an X-ray diffraction method. Numerous reports exist where the polymorphic products of a phase transformation have been identified using this technique. What is somewhat more challenging is collecting structural snapshots of a polymorphic transformation as it progresses and extracting coherent information from data that has not benefitted from a lengthy data collection. This type of analysis relies on rapid data collection and the ability to easily process numerous datasets.

In this work we describe a system where temperature- and pressure-induced phase transformations are studied by powder diffraction data collected on a laboratory diffractometer. The phase transformations influence the ability of the material's gas storage ability. The rapid and automated processing of data to extract salient features is demonstrated. In particular, relative phase abundances and structural information from each polymorph is determined. The structural characterization technique and data processing tools described here is of general relevance to crystalline functional materials.

## MS42-P03 | FORMATION MECHANISM OF EPITAXIAL PALLADIUM-PLATINUM CORE-SHELL NANOCATALYSTS IN A ONE-STEP SUPERCRITICAL SYNTHESIS

Broge, Nils Lau Nyborg (Aarhus University, Aarhus N, DNK)

Platinum-based nanomaterials are efficient catalysts for important processes such as NO<sub>x</sub> reduction, carbon monoxide oxidation, and hydrogen evolution. The catalytic properties makes the materials relevant in a large number of applications but the scarcity and high cost of platinum group metals provide an incentive for optimization of performance. In this study we demonstrate how core-shell Pd-Pt nanoparticles can be synthesized in a one-step hydrothermal method. Using in situ X-ray scattering analyzed through sequential fitting of the pair distribution function, it is found that primary particles are initially formed and that these agglomerate and crystallize into core-shell particles. Transmission electron microscopy (TEM) is utilized to show the elemental distribution, an epitaxial relationship between core and shell, and to confirm the results from X-ray scattering. Finally, the synthesis is performed on a flow reactor as a strategy for large-scale production. Here, small particles of pure Pt are observed in addition to the core-shell particles. The study points out the relevant parameters space for obtaining particles with desirable characteristics, and presents a strategy for large scale production with accurate parameter control.

## MS42-P04 | SNBL's BM31 AT ESRF BEYOND 2020 - COMBINED XRD-PDF-XAS

van Beek, Wouter (SNBL at ESRF, Grenoble, FRA); Emerich, Hermann (SNBL at ESRF, Grenoble, FRA); Chernyshov, Dmitry (SNBL at the ESRF, Grenoble, FRA); Dyadkin, Vadim (SNBL at ESRF, Grenoble, FRA); Wiker, Geir (SNBL at ESRF, Grenoble, FRA); Dmitriev, Vladimir (SNBL at ESRF, Grenoble, FRA)

The availability of experimental methods that probe a material's structure, complex and dynamic, at different length and time scales is key to obtain fundamental insight in technologically relevant materials. Progress relies on the development of innovative materials utilizing an in-depth understanding of the interplay between a material's structure and its macroscopic properties.

BM31 of the Swiss Norwegian Beam Lines, offers the possibility to combine X-ray absorption spectroscopy (XAS) and X-ray powder diffraction (XRD) in an alternating fashion in the same experimental setup. SNBL aims at extending these capabilities, by upgrading the current setup with a new CdTe area detector and focusing options. This will allow to i) implement pair distribution function analysis (PDF) of total scattering data, enabling combined XRD-PDF-XAS experiments and ii) enhance appreciably both the temporal ( $\sim 1$  s for XAS,  $\sim 100$  ms for XRD-PDF) and spatial resolution ( $\sim 100 \times 100 \mu\text{m}^2$ ) of the experiments.

The combined XRD-PDF-XAS measurements will allow the acquisition of complementary information of a material under the relevant working conditions: covering the length-scale from short to mid-range atomic arrangements viz.  $\sim 1 \text{ \AA}$  to several nm by PDF, the average structure by XRD, as well as the electronic state, and geometry around the element of interest by XAS. All data can be acquired in a temporal and spatially resolved manner in a single experiment. This will constitute a unique tool allowing the detailed study of materials for a wide range of applications, for instance: heterogeneous and electro-catalysis,  $\text{CO}_2$  capture, gas separation and batteries.

## MS42-P05 | SEQUENTIAL SHELXL REFINEMENT OF CONSECUTIVE DATASETS: A TOOL TO PROBE DYNAMICALLY EVOLVING SINGLE CRYSTAL STRUCTURES

Chernyshov, Dmitry (SNBL at the ESRF, Grenoble, FRA); Dyadkin, Vadim (Swiss-Norwegian Beam Lines, Grenoble, FRA); Törnroos, Karl Wilhelm (Department of Chemistry, University of Bergen, Bergen, NOR)

Modern area detectors combined with bright synchrotron radiation allow for collection of powder or even single crystal data with high time resolution, while external conditions (e.g. P or T) are changing at a certain rate. Such experiments are quite common for powder diffraction where crystal structure analysis for many datasets is conveniently done with sequential or parametric refinement [FullProf & TOPAS]. As far as we are aware, a similar generic option for single crystals experiments is still absent.

If the temperature change or any other external stimuli step is small, and there is no rapid phase transition, one may consequently expect that the inherited parameters, e.g. atomic positions and ADPs, would serve as a good starting model for the succeeding data point. Starting from this idea, we have developed a tool for a sequential SHELXL refinement of the evolution of a crystal structure documented in a set of closely time spaced temperature steps as well as the automated extraction of any parameter from the resulting output.

The software was tested against a series of data collected upon slow cooling for a spin crossover compound. The analysis uncovered that in the temperature range 300-80 K the compound possesses a crossover from high spin (HS) to a mixed HS-LS state. The later state is intrinsically disordered and the gain in entropy seems to be enough to overcome the thermal contraction upon cooling: we observe an increase of the unit cell volume at low temperatures.

## MS42-P06 | TESTING A HOME-MADE SAMPLE HOLDER WITH FLOW-THROUGH CAPILLARY TO STUDY IN-SITU RE-SOLVATION PROCESS

Rohlicek, Jan (Institute of Physics of the CAS, Prague 8, CZE); Zvoníček, Vít (Institute of Physics of the CAS, Prague 8, CZE); Skořepova, Eliska (Institute of Physics of the CAS, Prague 8, CZE)

In our powder diffraction laboratory, we studied the desolvation and resolution of solvates of a pharmaceutical substance called ibrutinib [1,2]. We have chosen its known structures of methanol, fluorobenzene and anisole solvates as suitable compounds for testing because of several reasons. First of all, their crystal structures are known and they form both the channel-making and cavity-making arrangement of the ibrutinib molecules, where particular solvents are occupying channels or cavities, respectively. The second reason was much more practice – we had enough amount of different ibrutinib solvates in our laboratory.

For in-situ study of the desolvation processes we have used a simple setup of an open capillary in Debye-Scherrer configuration. However, for the in-situ study of the resolution processes a completely new holder was constructed. This holder can be precisely aligned to the center of the powder diffractometer by using two perpendicular micrometer position stages in z and y directions. The borosilicate-glass flow-through capillary is connected to the holder by both ends allowing liquid or gas to pass. Both connectors allows connection of e.g. PTFE tubes for liquid or gas supply to the capillary.

[1] Zvoníček, V.; Skořepová, E.; Dušek, M.; Žvátora, P.; Šoóš, M. Ibrutinib Polymorphs: Crystallographic Study. *Cryst. Growth Des.* **2018**, *18*, 1315–1326.

[2] Zvoníček, V.; Skořepová, E.; Dušek, M.; Babor, M.; Žvátora, P.; Šoóš, M. First Crystal Structures of Pharmaceutical Ibrutinib: Systematic Solvate Screening and Characterization. *Cryst. Growth Des.* **2017**, *17*, 3116–3127.

Acknowledgement: *This work was supported by the GACR no. 17-23196S.*

## MS42-P07 | A NEW CONCEPT FOR SAPPHIRE SINGLE-CRYSTAL CELLS TO STUDY SOLID-GAS REACTIONS VIA REAL-TIME IN SITU NEUTRON SCATTERING

Finger, Raphael (Leipzig University, Leipzig, GER); Kohlmann, Holger (Leipzig University, Leipzig, GER)

Solid-gas reactions get high attention due to far reaching applications, e.g. hydrogen storage, catalysis or the synthesis of functional materials. Revealing reaction pathways and intermediate products by *in situ* neutron diffraction in real-time can help to understand and control such reactions.

Elevated temperature and reactive gases at high pressure require specially designed sample environments. In order to avoid parasitic reflections from the sample holder, sapphire single-crystals are being used. The detection of Bragg reflections of the single crystals can be avoided by proper orientation, resulting in a very low background. Nevertheless, small contributions of the sample holder may still occur due to inelastic scattering from the large crystals, leading usually to the exclusion of about 5° in 2θ from neutron powder data. Heating is performed contactless by two 100W diode lasers and measured by a pyrometer.

Recent developments are aiming for a reduced mechanical tension between the sample holder and the corpus of the gas pressure cell as well as higher sample temperatures. Therefore, single crystals with reduced wall thickness are used for a better heating efficiency. Further, a newly designed corpus has been developed and tested.

The setup allows to acquire real-time neutron powder diffraction data on solid-gas reactions up to 700 K and 100 bar at the D20 diffractometer (Institute Laue-Langevin, Grenoble). In general, detailed structural information can be extracted by Rietveld analysis with a time resolution in the order of one minute.

## MS42-P08 | LATEST DEVELOPMENTS IN NON-AMBIENT XRD ATTACHMENTS FROM ANTON

### PAAR

Puhr, Barbara (Anton Paar GmbH, Graz, AUT); Jones, Andrew O.F. (Anton Paar GmbH, Graz, AUT); Kotnik, Petra (Anton Paar GmbH, Graz, AUT)

Non-ambient XRD has developed into a vital tool for a complete understanding of a materials behavior under different environmental conditions. Parameters such as temperature, pressure, relative humidity, gas environments (including reactive or explosive gases), mechanical load, and electric fields, can be altered allowing samples to be measured in-situ.

This contribution will present the latest developments in non-ambient XRD equipment from Anton Paar which further extend the capabilities of in-house XRD measurements.

These improvements include methods to maximize the temperature accuracy and stability of the non-ambient attachment while minimizing the deviation between the actual sample temperature and that displayed on the non-ambient control unit. In addition, new specialized sample holders have been developed for the measurement of battery samples in-operando while changing the sample temperature. Dedicated equipment offers a solution for highly air sensitive samples by means of a sealed transfer to the non-ambient chamber. Furthermore pair distribution function (PDF) measurements are now possible under non-ambient conditions using special PDF parts. Finally, an extended temperature range of the cooling stage for four-circle goniometers could be achieved by improvements of the cooling and heating system.

Presented measurement data prove the functionality of the equipment and point to potential applications.

## MS42-P09 | SPACE- AND TIME-RESOLVED ANALYSIS OF THE DECOMPOSITION OF THERMOELECTRIC MATERIALS WITH MOBILE ATOMS UNDER WORKING CONDITIONS

Oeckler, Oliver (Leipzig University, Leipzig, GER); Jakob, Matthias (Leipzig University, Leipzig, GER); Grauer, Maxim (Leipzig University, Leipzig, GER); Vaughan, Gavin B. M. (European Synchrotron Radiation Facility, Grenoble, FRA)

Mixed ionic and electronic conductors such as  $\text{Cu}_{2-x}\text{Se}$  [1] or  $\text{Zn}_4\text{Sb}_3$  [2] have attracted much interest as thermoelectric materials, but tend to decompose under electrical currents due to electromigration of Cu or Zn. This is complicated by transitions to superionic HT phases, whose stability interval depends on the (changing) composition. This decay can be simulated in stress tests applying external currents, which were done for several materials. In addition to *ex situ* measurements, X-ray computed diffraction tomography (XRCT) with microfocused high-energy synchrotron beams at beamline ID15A (ESRF) yields time and space resolved information under *operando* conditions. It yields 3D resolved powder diffraction data with ca. 25  $\mu\text{m}$  spatial resolution, which, in principle, allow the mapping of all information that is present in diffraction patterns. Samples of  $\text{Cu}_{2-x}\text{Se}$  were investigated *in situ*, applying various currents and temperature gradients. 3D-XRCT reconstructions reveal the Cu migration in  $\text{Cu}_2\text{Se}$  even at low temperatures even though it had only been described for the superionic phase.[1] Mapping the content of the cubic HT phase shows how it may form at both electrodes and how the boundary between ordered and disordered phases moves as a function of time. This unique access to *in situ* data of MIECs can explain the changing transport properties of a broad range of thermoelectric materials.

[1] D. R. Brown, T. Day, T. Caillat, G. J. Snyder, *Mater.* **42**, 2014 (2013).

[2] G. J. Snyder, M. Christensen, E. Nishibori, T. Caillat, B. B. Iversen, **3**, 458 (2004)

## MS42-P10 | IN-SITU WIDE-ANGLE X-RAY SCATTERING ON LIQUID CRYSTALLINE ELASTOMERS FOR ORTHOPEDIC APPLICATIONS

Dadivanyan, Natalia (Malvern Panalytical GmbH, Kassel, GER); Gateshki, Milen (Malvern Panalytical B.V., Almelo); Gotz, Detlev J. (Malvern Panalytical B.V., Almelo); Yakacki, Christopher M. (The University of Colorado Denver, Denver, USA)

Liquid-crystal elastomers (LCEs) are a class of stimuli-responsive and mechanically-active polymers that combine the properties of anisotropic liquid crystals and rubber elasticity, making them capable of exceptional mechanical and optical properties. The stimuli-induced actuation and shape-memory properties of LCEs have shown significant potential in use as actuators, artificial muscles, and soft robotics [1-5].

In this contribution, we report in-situ tensile investigation using fast wide-angle X-ray scattering experiments on main-chain liquid crystalline elastomers for orthopedic applications. Our results show that stretching of the sample to different degrees of orientation is possible due to elasticity of the polymer chains between adjacent liquid crystal units. Yet, liquid crystal units do not orient instantly along mechanical field but follow the behavior of polymer chains with some delay.

These results allow us to gain better understanding of mechanical properties of this important group of materials.

- [1] R. S. Kularatne, H. Kim, J. M. Boothby and T. H. Ware, *J. Polym. Sci., Part B: Polym. Phys.*, 2017, 55, 395–411.
- [2] D. L. Thomsen, P. Keller, J. Naciri, R. Pink, H. Jeon, D. Shenoy and B. R. Ratna, *Macromolecules*, 2001, 34, 5868–5875.
- [3] C. Ohm, M. Brehmer and R. Zentel, *Adv. Mater.*, 2010, 22, 3366–3387.
- [4] J. D. W. Madden, N. A. Vandesteeg, P. A. Anquetil, P. G. A. Madden, A. Takshi, R. Z. Pytel, S. R. Lafontaine, P. A. Wieringa and I. W. Hunter, *IEEE J. Oceanic Eng.*, 2004, 29, 706–728.
- [5] H. Wermter and H. Finkelmann, *e-Polymers*, 2001, 1, 111–123.

## MS42-P11 | CRYSTALLIZATION OF TIN OXIDE QUANTUM DOTS PROBED BY COUPLED IN SITU HIGH TEMPERATURE SAXS AND WAXS EXPERIMENTS ON THE BM02 BEAMLINE AT THE ESRF

Costille, Benjamin (IRCER, Limoges, FRA); Bacouel, Alexandre (IRCER, Limoges, FRA); Thune, Elsa (IRCER, Limoges, FRA); Guinebretiere, Rene (IRCER, Limoges, FRA)

The crystallization of nanosized crystals in amorphous matrix result of two interconnected phenomena. Starting from an amorphous material homogeneous at the molecular scale, incongruent crystallization occurs in fact after amorphous-amorphous phases separation processes. Such fluctuations can be evidenced through Small Angle X-ray Scattering (SAXS). Because crystallization of the phase separated areas is a stochastic phenomenon, related in particular to the nuclei size, at the global scale of the material crystallization and phases separation processes are very often observed simultaneous. As a consequence, the determination of their both kinetics require in principle coupled SAXS and Wide Angle X-ray Scattering (WAXS) in situ measurements. We synthesized through the sol-gel process amorphous silica-based material containing various amount of tin. Dense bulk samples are obtained without any high temperature and cooling process and the obtained materials are in a far from the thermodynamic equilibrium state. Tin oxide crystallization occurs during isothermal treatment realized at few hundred of degrees [1] through mechanisms that are far from the classical nucleation theory (CNT). The BM02 beamline at the ESRF is equipped with an experimental bench allowing simultaneous measurements of the WAXS and SAXS signals [2]. We will show how such set-up allows to determine at the second time-scale the kinetics of phases separation and SnO<sub>2</sub> crystallization processes.

[1] B. Costille, M. Dumoulin, A.M. Ntsame Abagha, E. Thune, R. Guinebretière, J. Phys. D Appl. Phys. 51 (2018) 255303.

[2] G.A. Chahine, N. Blanc, S. Arnaud, F. de Geuser, R. Guinebretière, N. Boudet, Metals 9 (2019) 352.

## MS42-P12 | OPERATIONAL NON-UNIFORMITIES OF LITHIUM DISTRIBUTION IN LI-ION BATTERIES PROBED BY DIFFRACTION TECHNIQUES

Senyshyn, Anatoliy (Technische Universität München, Garching bei München, GER)

Energy storage devices based on different technologies have gained in relevance for a wide range of applications from supplying portable devices to large electric vehicles. The lithium-based energy storage technology dominates to the market due to the best compromise between energy and power densities, low self-discharge when not in use, tiny memory effect *etc.*

Modern Li-ion batteries are sophisticated electrochemical devices, where numerous degrees of freedom (either chemical, morphological or transport) are combined with complicated geometries of the electrode integration. The understanding of processes supplementing the cell operation, fatigue and abuse requires new dedicated experimental techniques capable to reveal “live” information. In this instance the use of diffraction techniques in combination with electrochemical studies has been found well-suited for *in situ* and *in operando* characterization of electrochemical energy storage systems.

Operation of typical Li-ion cell is supplemented by the development of spatial inhomogeneities of current, lithium and/or electrolyte distribution (often difficult to quantify), but surely affecting performance, cycling stability and safety. The problem of cell non-uniformity (indirectly pointed by electrochemical measurements) and its effect is quite poorly accounted in literature. In the current contribution a combination of spatially-resolved neutron powder diffraction [1] and powder diffraction using high-energy photon beams (X-ray diffraction radiography [2] and tomography) applied *in situ* for studies on commercial Li-ion cells of prismatic- and 18650-type will be presented.

[1] M.J.Mühlbauer, O. Dolotko, M.Hofmann et al., J. Power Sources 348 (2017) 145-149

[2] M.J. Mühlbauer, A. Schökel, M. Etter et al., J. Power Sources 403 (2018) 49-55

## MS42-P13 | STUDYING MOLECULAR CRYSTALS AT HIGH PRESSURES: EXPERIMENTAL STRATEGY AND HARDWARE MATTERS

Zakharov, Boris (Boreskov Institute of Catalysis SB RAS & Novosibirsk State University, Russia, Novosibirsk, RUS); Boldyreva, Elena (Boreskov Institute of Catalysis SB RAS, Novosibirsk State University, Novosibirsk, RUS)

The studies under extreme conditions offer insight into the fine structural changes that occur as a function of temperature or pressure variations. Molecular crystals are of special interest both from fundamental and applied point of view. Many of them are promising as pharmaceuticals, materials for electronics, optics and soft robotics. Despite new developments in high-pressure instrumentation and diffraction techniques, the quality of diffraction data and a way of performing diffraction experiment still remain critically important for obtaining reliable information on crystal structure behavior at high pressures.

In this contribution several examples of single-crystal studies at high pressures on laboratory and synchrotron facilities will be discussed. In each of the examples pressure variation protocol, data collection time, hardware and facility type influenced strongly not only the quality and completeness of experimental data, but even the crystal structures of resulting high pressure phases. Advantages and disadvantages of different instrumentation will also be discussed along with information which high-pressure single-crystal X-ray diffraction can provide for studying solid state processes.

This work was supported by Ministry of Science and Higher Education of the Russian Federation (project AAAA-A19-119020890025-3).

Keywords: high pressures, crystallography instrumentation, structural transformations

## MS42-P14 | DIFFUSION MECHANISMS OF GAS ADSORPTION BY POROUS FRAMEWORKS FROM SUB-SECOND SYNCHROTRON POWDER X-RAY DIFFRACTION

Dovgaliuk, Iurii (Swiss–Norwegian Beamlines at ESRF, Grenoble, FRA); Li, Xiao (Université Catholique de Louvain, Louvain-la-Neuve, BEL); Dyadkin, Vadim (Swiss–Norwegian Beamlines at ESRF, Grenoble, FRA); Filinchuk, Yaroslav (Université Catholique de Louvain, Louvain-la-Neuve, BEL); Chernyshov, Dmitry (SNBL at the ESRF, Grenoble, FRA)

Nanoporous frameworks attract much attention as the potential materials for technological applications in diffusion-controlled processes such as selective guest adsorption and separation. Particular interest is paid for selective capture and separation of chemically inert Kr and Xe generated by nuclear fission [1]. Using advanced sub-second *in situ* powder X-ray diffraction (PXR), three diffusion scenarios have been evaluated from the isothermal kinetics adsorption by nanoporous  $\gamma$ -Mg(BH<sub>4</sub>)<sub>2</sub> for a series of gases: Ar, Kr and Xe [2]. The microscopic diffusion pathways and the activation barriers were rationalized from the macroscopic kinetic models and the crystal structure analysis. The lowest activation barrier has been estimated for the Ar atoms, which are smallest in the series. Consequently, these atoms easily diffuse through the intra- and interchannel apertures of  $\gamma$ -Mg(BH<sub>4</sub>)<sub>2</sub> crystal structure. The diffusion of larger Kr atoms involves two activation energies: both intra- and interchannel barriers, which are higher than ones for Ar. Finally, the largest from the series Xe atoms diffuse only along 1-D channels with the highest activation barrier. The obtained kinetic characteristics are essential for the estimation of gas selectivity.

Therefore, sub-second PXR offers unique information on the energetics and microscopic mechanisms of diffusion not accessible in macroscopic gravimetric and volumetric methods. This information relates solely to the crystalline fraction of material and can be compared with the atomistic models of diffusion.

[1] L. Chen et al. *Nat. Mater.* **2014**, *13*, 954–960;

[2] Y. Filinchuk et al. *Angew. Chemie - Int. Ed.* **2011**, *50*, 11162–11166.

## MS42-P15 | IN SITU X-RAY STUDIES OF ELECTRODEPOSITION OF LEAD-HALIDE COMPOUNDS ON THE ELECTROLYTE-LIQUID MERCURY INTERFACE

Sartori, Andrea (Kiel University, Kiel, GER); Festersen, Sven (Kiel University, Kiel, GER); Fujii, Hiromasa (Osaka University, Osaka, JPN); Warias, Jonas (Kiel University, Kiel, GER); Giri, Rajendra (Kiel University, Kiel, GER); Bertram, Florian (DESY, PETRA III, Hamburg, GER); Magnussen, Olaf (Kiel University, Kiel, GER); Murphy, Bridget (Kiel University, Kiel, GER)

We investigate nucleation and growth by in situ x-ray reflectivity and diffraction at liquid-liquid interfaces. Here we focus Hg as liquid metal substrate in an electrochemical environment. By changing the concentration, species and potential we can control the deposition mechanism. Liquid electrodes provide a stresses and defects-free template for nucleation and growth and ensure high mobility of reagent and products leading to high quality crystals.

In previous studies of electrolyte containing NaF+NaBr+PbBr<sub>2</sub> the growth of a monolayer followed by 3D nanocrystal formation of PbBrF was observed [1][2]. In the current experiments a fluoride free electrolyte with the halogens NaBr+PbBr<sub>2</sub> and NaCl+PbCl<sub>2</sub> is employed. By changing the potential from negative values < 0.8 V, where the Pb<sup>2+</sup> ions are amalgamated in the Hg, to a potential > 0.7 V, the lead ions are deamalgamated and we see clear evidence of growth of a layer due to the formation of PbBr<sub>2</sub>, PbCl<sub>2</sub> in the respectively experiments. The composition was confirmed by X-ray diffraction and grazing incident diffraction. The similar behaviour indicates that this growth behaviour is a general phenomena.

The layer growth may be explained by considering that for a potential greater than the amalgamation potential, the halide ions specifically adsorb onto the Hg surface. When the Pb<sup>2+</sup> is released from the Hg bulk, they accumulate on top of the halide and form the detected layer.

[1] A. Elsen et al., PNAS., 110:6663 (2013)

[2] B. M. Murphy et al., Nanoscale, 29:13859 (2016)

## MS42-P136 - LATE | IN SITU CRYSTALLIZATION OF THE VISCOUS ORGANOSILICON LIQUIDS

Volodin, Alexander (INEOS, Moscow, RUS); Korlyukov, Alexander (INEOS, Moscow, RUS); Smo'yakov, Alexander (INEOS, Moscow, RUS)

This work presents the results of a study on the structure of various organosilanes and siloxanes. These substances are widely used in synthetic organometallic chemistry and in industry. Unfortunately, at room temperature, they are viscous liquids, that makes impossible to establish their structure using conventional X-ray diffraction studies. Such viscous compounds do not crystallize with slow cooling. For their crystallization, only shock freezing is appropriate. To establish the crystal structure of such compounds, we assembled the device of the zone melting of a crystal in a capillary with nichrome wire as heater. The features of this device are its simplicity and low cost, if we draw an analogy with commercially available OHCD (Optical Heating and Crystallization Device). In addition, being the authors of the device, we can freely complement and modify it.

Using this device, we were able to obtain previously unknown structures of more than a dozen of organosilicon compounds, which are liquids at room temperature. For some of the compounds studied, several crystalline phases were established. For example, the structure of octamethylcyclotetrasiloxane (D4) crystals at 12 different temperatures. A subsequent study of these structures by quantum chemistry methods made it possible to establish the most probable path of the solid-phase phase transition in the D4 crystal.

## MS43: Total Scattering Studies and Disorder

---

### MS43-01 | HIDDEN VACANCY-NETWORK POLYMORPHISM OF PRUSSIAN BLUE ANALOGUES

Goodwin, Andrew (University of Oxford, Oxford, GBR)

Prussian Blue analogues (PBAs) are an important and broad family of materials, with applications in e.g. catalysis, energy, proton conduction, and gas storage. The vast majority of PBAs are defective materials that contain a very large fraction of transition-metal vacancies; these vacancies in turn connect to form extended micropore networks. We have used 3D total scattering measurements to characterise the nature of these disordered pore networks in a variety of PBAs. This talk will present our results, and demonstrate how PBA composition and synthesis approach allow for correlated defect engineering in PBAs as a means of controlling storage capacity, anisotropy, and transport efficiency.

## MS43-02 | CHARACTERIZING STRUCTURE, MICROSTRUCTURE AND MORPHOLOGY OF NANOMATERIALS THROUGH RECIPROCAL SPACE TOTAL SCATTERING METHODS

Bertolotti, Federica (University of Insubria and To.Sca.Lab, Como, ITA); Moscheni, Daniele (University of Insubria and To.Sca.Lab, Como, ITA); Cervellino, Antonio (SLS, Laboratory for Synchrotron Radiation-Condensed Matter, Paul Scherrer Institut, Villigen, CH); Masciocchi, Norberto (University of Insubria and To.Sca.Lab, Como, ITA); Guagliardi, Antonietta (Istituto di Cristallografia (CNR) and To.Sca.Lab, Como, ITA)

Among total scattering (TS) techniques, the Debye Scattering Equation (DSE) based approach has become a valuable tool for characterizing nanomaterials with different structure, size and morphology, with all the well-known advantages associated to the use of reciprocal space methods [1]. Since the computation operates starting from real space atomistic models, structural and microstructural information can be simultaneously derived within a unified approach. Moreover, the possibility of modeling both the small- and wide-angle regions of the X-ray TS pattern, with the DSE method, taking advantage of their complementarity in terms of length scales (from the atomic to the nanometer one), offers the opportunity of detecting sophisticated nanocrystals morphologies and disentangling defects-induced peak broadening in the TS pattern, from size-induced effects [2,3].

Here, experimental and modeling aspects related to the DSE approach, along with an overview of applications, from nanosized colloidal quantum dots and perovskites up to innovative engineered nanoapatites, will be presented.

Acknowledgement: Partial support by Fondazione Cariplo, HYPATIA Project: 2016-0248 is acknowledged.

[1] Bertolotti, F.; Moscheni, D.; Guagliardi, A.; Masciocchi, N. *Eur. J. Inorg. Chem.* 2018, 3789-3803.

[2] Bertolotti, F.; Dirin, D. N.; Ibanez, M.; Krumeich, F.; Cervellino, A.; Frison, R.; Voznyy, O.; Sargent, E. H.; Kovalenko, M. V.; Guagliardi, A.; Masciocchi, N. *Nat. Mater.* 2016, 15, 987-994.

[3] Moscheni, D.; Bertolotti, F.; Piveteau, L.; Protesescu, L.; Dirin, D. N.; Kovalenko, M. V.; Cervellino, A.; Pedersen, J. S.; Masciocchi, N.; Guagliardi, A. *ACS Nano* 2018, 12, 12558-12570.

## MS43-03 | STUDY OF THE CONFINEMENT EFFECT OF WATER IN BIOACTIVE GLASSES USING ATOMIC PAIR

Khoder, Hassan (Université de Lorraine, Vandoeuvre Les Nancy CEDEX, FRA); Bendeif, El-Eulmi (Université de Lorraine, Vandoeuvre Les Nancy CEDEX, FRA); Schaniel, Dominik (Université de Lorraine, Vandoeuvre Les Nancy CEDEX, FRA); Dorbez-Sridi, Rachida (Université de Monastir, Monastir, TUN); Pillet, Sébastien (Université de Lorraine, Vandoeuvre Les Nancy CEDEX, FRA)

Significant therapeutical progress has been achieved in recent years by using bioactive glasses for bone reparation and replacement [1-4]. The biomedical applications of these biomaterials are mainly due to their high biocompatibility and high reactivity with the human physiological environment, since the reaction products obtained from these bioglasses and the physiological fluids lead to the deposition of a layer of crystalline bone-like carbonate calcium phosphate (*Hydroxy-Carbonate Apatite, HCA*) on their surface shortly after interaction. The internal porosity of these biomaterials further allows for progressive colonization of the tissues, ensures the vascularization and free circulation of cells, body fluids and nutriments.

The understanding of the impact of the confinement on the organization and diffusion of the physiological liquids encapsulated in these bio-nanomaterials is thus crucial for improving the bioglasses properties. We will present in this contribution, the detailed structural analysis of confined physiological liquids inside new mesoporous bioactive glasses. The structural investigations were performed using a complementary approach based on total X-ray scattering data coupled with the PDF analysis and appropriate calorimetric (DSC) measurements. Furthermore, we will discuss the comparison of the experimental and the simulated PDFs parameters.

[1] Hench, L. L. *Science*. 1984, 226, 630.

[2] Hench, L. L.; Polak, J. M. *Science* 2002, 295, 1014.

[3] Hench, L. L. *J. Am. Ceram. Soc.* 1998, 81, 1705.

[4] Izquierdo-Barba, I.; Arcos, D.; Sakamoto, Y.; Terasaki, O.; López-Noriega, A.; Vallet-Regí, M. *Chemistry of Materials* 2008, 20 (9), 3191–3198

## MS43-04 | USING NUCLEAR MAGNETIC RESONANCE SPECTROSCOPY, NEUTRON AND X-RAY PAIR

Hansen, Anna-Lena (Karlsruhe Institute of Technology, Eggenstein-Leopoldshafen, GER)

To develop all-solid-state batteries it is crucial to understand the structure property relationship in solid-state electrolytes (SE). However, freely after the quote of Wolfgang Pauli: *“The best that most of us can hope to achieve in physics is simply to misunderstand at a deeper level”*, our knowledge of the real structure of SEs remains oversimplified. Nonetheless, it is crucial to understand the role of defects and distortions in these materials in detail, since such structural peculiarities highly correlate with ion migration. Like many promising SE candidates, the argyrodites  $\text{Li}_6\text{PS}_5\text{X}$  ( $X = \text{Cl}, \text{Br}, \text{I}$ ) are built up by isolated polyhedral species, in this case  $[\text{PS}_4]^{3-}$  tetrahedra. A review of the effect of lattice distortions and ion migration barriers revealed a discrepancy between proposed mechanisms for argyrodites and other solid state electrolytes, indicating that the defect structure is not well understood yet. Our Neutron and X-Ray PDF study of  $\text{Li}_6\text{PS}_5\text{Cl}$ , revealed that the low  $r$  region ( $< 5 \text{ \AA}$ ) of the PDF could not be satisfactorily fitted using a cubic model, mainly due to the strongly increased peak corresponding to S – S distances within  $[\text{PS}_4]^{3-}$  tetrahedra and a missing peak corresponding to inter-tetrahedra  $S_{\text{tet}} - S_{\text{tet}}$  distances. Although it is possible to use models with reduced symmetry to fit the low  $r$  region better, we have strong indications that this is still an oversimplified model to the real structure.

## MS43-05 | TEXTURE CORRECTION FOR TOTAL SCATTERING FUNCTIONS

cervellino, antonio (Paul Scherrer Institut - Photon Science Division, Villigen, CH); Frison, Ruggero (EMPA - Swiss Federal Laboratories for Materials Science and Technology, Center for X-ray Analytics, Dübendorf, CH)

Preferred orientation (texture) is a complex effect that bridges powder diffraction to single crystal diffraction. Corrections for Bragg intensities are known [1-3]. However, within the Total Scattering approach, that prescind from periodicity and therefore avoids ragg formalism, the problem of evaluating the  $S(Q)$  and  $G(r)$  scattering functions in the presence of texture has never been quantitatively tackled. A complete treatment in the framework of spherical harmonics for the most common powder diffraction experimental geometries is presented. The  $S(Q)$  can be computed by an extended version of the commonly used Debye scattering equation (DSE) [4] comprising now sums over spherical Bessel functions of all (even) orders. Selection rules arising from sample and experimental symmetries are given. Concerning the  $G(r)$ , the effects of texture result in a fundamental indetermination that has important consequences. Example calculations for various interesting cases will be shown. As an aside, a second DSE-like formula for computing the antisymmetric intensity change in 3-D reciprocal space due to anomalous/resonant scattering is given. This is meant for single crystal or single particle studies. As with the DSE, this equation prescind from spatial periodicity and can be used for non-crystalline matter.

[1] *J. Appl. Phys.* **36** (1965) 2024

[2] H.J. Bunge, *Texture Analysis in Materials Science*. Butterworth:London (1982) ISBN:**0408104625**

[3] *J. Appl. Cryst.* **25** (1992) 611

[4] *Annalen der Physik* **46** (1915) 809

## MS43-P01 | COOKING CRYSTALS: RADIATION DAMAGE IN MOLECULAR MODULATED MATERIALS

Scurfield, Georgia (Chemical Crystallography, University of Oxford, Oxford, GBR); Morgan, Lewis (Chemical Crystallography, University of Oxford, Oxford, GBR); Christensen, Kirsten E. (Chemical Crystallography, University of Oxford, Oxford, GBR); Thompson, Amber L. (Chemical Crystallography, University of Oxford, Oxford, GBR)

Single-crystal X-ray diffraction is a maturing technique; with structure determination becoming more routine, there are an increasing number of non-expert users collecting data, solving and refining structures. As the technique improves, easier access to synchrotron radiation and more sensitive detectors means that more data collections are showing features beyond the realms of conventional crystallography. The concept of non-Bragg diffraction is well understood in solid state chemistry, however, the phenomena of diffuse scattering and modulation have been studied less in molecular materials.

Barluenga's reagent,  $\text{IPy}_2\text{BF}_4$ , has been shown to exhibit a transient modulated phase on cooling from a dynamic room temperature phase to an ordered low temperature structure. Systematic studies on the derivatives of Barluenga's reagent have been carried out in which iodine with bromine, the  $\text{BF}_4$  anion is replaced with other small anions including  $\text{ClO}_4$  and  $\text{PF}_6$  and the pyridine is replaced with 2,4,6-trimethyl pyridine (collidine). While attempting to map the phase behaviour of these materials we discovered that the intense radiation at synchrotron facilities can interact with the satellite reflections indicative of the modulated phase. Understanding these effects could, not only improve our knowledge of the causes of modulation in molecular materials, but also further our understanding of the causes of radiation damage.

## MS43-P02 | INSTRUMENTAL EFFECTS IN LABORATORY PAIR DISTRIBUTION FUNCTION (PDF) ANALYSIS.

Gateshki, Milen (Malvern Panalytical B.V., Almelo); Beckers, Detlef (Malvern Panalytical B.V., Almelo); Kogan, Vladimir (Dannalab B.V., Enschede)

The PDF technique utilizes a Fourier transformation of the X-ray powder diffraction (XRPD) data and gives information about the inter-atomic distances of the material. The accuracy of this determination of inter-atomic distances depends strongly on the energy of the utilized radiation source and the ability to correct for sample-related effects and for aberrations from the instrumental set-up that is used. Recent advances in laboratory X-ray diffractometer technology e.g. new generation detectors optimized for hard radiation (e.g. Mo and Ag radiation) allow to minimize artifacts or fluctuations in the PDF arising from statistical noise, resulting in more reliable data. Nevertheless, effects of instrumental aberrations such as axial divergence or spectral features of the X-ray source may still influence the accuracy of the final result.

In this contribution we evaluate the effect of different instrumental parameters on the calculated PDF and discuss possible ways to minimize the influence of instrumental aberrations. In the specific case of axial divergence this can be done by using narrow Soller slits, which necessarily reduce the intensity of the measured scattering signal or by applying a data correction procedure before the PDF is calculated. This procedure [1, 2] can correct for systematic instrumental aberrations while considering multiple overlapping peaks as a single continuum. It is based on an integral transformation algorithm and converts the measured pattern into the corrected one without influencing the angular resolution of the measurement.

[1] Kogan V.A., Kupriyanov M.F., J.Appl.Cryst, 1992, 25,16-2

[2] Kogan V.A. US7516031B2 "Apparatus and method for correcting for aberrations"

## MS43-P03 | STRUCTURES OF THE GROUP 13 PRENUCLEATION CLUSTERS

Gjerlevsen Nielsen, Ida (Center for Materials Crystallography, Aarhus University, Aarhus C, DNK); Sommer, Sanna (Center for Materials Crystallography, Aarhus University, Aarhus C, DNK); Brummerstedt Iversen, Bo (Aarhus University, Aarhus, DNK)

Commonly classical nucleation theory have been used to explain nucleation, but this is now being challenged as atomic scale techniques has been developed to study solutions showing larger clusters before nucleation. Thus, a new theory including prenucleation clusters (PNCs) with predictive value is needed. To achieve this, it is essential to settle the atomic structure of PNCs across numerous elements as well as chemical environment.

The group 13 metal oxides have been chosen as a starting system. Al, In and Ga form similar oxides and hydroxides such as  $M(OH)_3$ ,  $MOOH$  and  $M_2O_3$  in solvothermal synthesis. The individual systems exhibit complex polymorphism, which can be controlled with different synthesis parameters such as solvent and temperature, however, the actual mechanisms are unknown.

The PNCs structures of the group 13 metal oxides have been determined by combining PDF and EXAFS analysis of the three metal nitrates in various solvents. Based on this, a synthesis pathway have been suggested which facilitate  $\gamma\text{-Al}_2\text{O}_3$  formation without intermediate  $AlOOH$ , a material currently used in industry in large scale.

## MS43-P04 | MAPPING NON-CRYSTALLINE NANOSTRUCTURE WITH LOW-DOSE SCANNING ELECTRON PAIR DISTRIBUTION FUNCTION ANALYSIS

Laulainen, Joonatan E. M. (Department of Materials Science and Metallurgy, University of Cambridge, Cambridge, GBR); Johnstone, Duncan N. (Department of Materials Science and Metallurgy, University of Cambridge, Cambridge, GBR); Bogachev, Ivan (Department of Materials Science and Metallurgy, University of Cambridge, Cambridge, GBR); Collins, Sean M. (Department of Materials Science and Metallurgy, University of Cambridge, Cambridge, GBR); Longley, Louis (Department of Materials Science and Metallurgy, University of Cambridge, Cambridge, GBR); Bennett, Thomas D. (Department of Materials Science and Metallurgy, University of Cambridge, Cambridge, GBR); Midgley, Paul A. (Department of Materials Science and Metallurgy, University of Cambridge, Cambridge, GBR)

Determining the structure and distribution of non-crystalline phases in complex multi-phase materials is important for understanding novel nanostructured materials such as recently developed glassy MOF composites [1]. Spatially resolved pair distribution function (PDF) analysis, based on scanning electron diffraction (SED) data, provides a route to meet this need [2] as we demonstrate here in application to a glassy ZIF-62: glassy-60NaPO<sub>3</sub>-40AlF<sub>3</sub> composite. Both materials are highly sensitive to electron radiation and it was therefore necessary to perform low-dose ( $\sim 10 \text{ e}/\text{\AA}^2$ ) SED experiments, which were enabled using a counting type direct electron detector. The low-dose SED data has an expected low signal-to-noise ratio and we show that independent component analysis (ICA) can be applied to such data to learn physically interpretable PDFs corresponding to the two phases, without the use of prior knowledge. The learnt PDFs are compared with PDFs determined after binning data within phase pure regions to confirm their validity and the spatial localisation determined by ICA is correlated with compositional maps obtained using X-ray energy dispersive spectroscopy (EDS). This analysis shows that ICA combined with low-dose SED can achieve reliable spatially resolved PDF analysis on the nanoscale in beam sensitive materials.

[1] J. M. Tuffnell et al. "Novel Metal—Organic Framework Materials: Blends, Liquids, Glasses and Crystal-Glass Composites." *Chemical Communications* (2019).

[2] X Mu et al. "Mapping structure and morphology of amorphous organic thin films by 4D-STEM pair distribution function analysis." *Microscopy* (2019).

## MS43-P05 | INVESTIGATION OF THE NANOSTRUCTURED MATERIALS BY XRD METHOD WITH USE OF SIMULATION

Cherepanova, Svetlana (Novosibirsk State University, Novosibirsk, RUS)

Nanostructured materials are specific objects of the structural analysis. Peculiarities of their X-ray diffraction (XRD) patterns arise from the presence of planar defects and/or coherently connected domains, which are elements of nanostructure. Such disordering of 3D periodic crystal structure gives rise to the diffuse scattering both in the vicinity of Bragg maxima (broadening of peaks, their shift and splitting) and/or in background region (appearance of diffuse peaks or halo). This complicates or even makes impossible the application of the traditional techniques of structural and microstructural analysis. Simulation of the XRD patterns on the base of the models of partially disordered crystals allows us to analyse all diffraction effects. It will be shown what peculiarities arise on the XRD patterns due to twinning as well due to formation of coherently connected domains having 1) the same structure, 2) the same composition but different structure, 3) different structure. Various structural types will be considered.

## MS43-P05 | THE INVERSION MODEL AND ITS LIMITATIONS FOR SPINEL $\text{ZnAl}_2\text{O}_4$ : A MULTI-TECHNIQUE STUDY.

Sommer, Sanna (Center for Materials Chemistry, Aarhus University, Aarhus C, DNK); Drath Bøjesen, Espen (Monash University, Monash Centre for Electron Microscopy, Melbourne, AUT); Lock, Nina (Aarhus University, Department of Engineering and iNANO, Aarhus C, DNK); Kasai, Hidetaka (University of Tsukuba, Faculty of Pure and Applied Sciences, Tsukuba, JPN); Skibsted, Jørgen (Aarhus University, Department of Chemistry and iNANO, Aarhus C, DNK); Brummerstedt Iversen, Bo (Aarhus University, Aarhus, DNK)

Point defects in spinel compounds have a significant influence on the physical properties, and they are therefore highly useful for modifying the properties of the materials. While simplified models may reasonably describe experimental data, the inability to model the full complexity of the defects can lead to erroneous structural trends. With a commonplace assumption that inversion of the cations are the only contributing defect, most research in this area relies on a single characterization technique. Taking a multi-technique approach shows why a single technique approach is insufficient for accurately modeling the contribution from point defects in spinel compounds. By using  $\text{ZnAl}_2\text{O}_4$  as a benchmark material, our multi-technique structural investigation clearly shows that the current cation inversion model is inaccurate, and instead the nature of the  $\text{ZnAl}_2\text{O}_4$  spinel structure include several synthesis dependent point defects. Based on a comprehensive parameter-study of  $\text{ZnAl}_2\text{O}_4$ , which was synthesized using four different techniques, and combined with various post treatments, we suggest a way forward for systematically incorporating defects in the spinel structure.

## MS44: Solving structures through combination of reciprocal and direct space methods

---

### MS44-01 | CRYSTAL STRUCTURE OF NEW AND HIGHLY COMPLEX ORGANIC MOLECULES

#### SOLVED BY 3D ELECTRON DIFFRACTION

Gemmi, Mauro (Istituto Italiano di Tecnologia, Pisa, ITA); Andrusenko, Iryna (Istituto Italiano di Tecnologia, Pisa, ITA); Lanza, Arianna (Istituto Italiano di Tecnologia, Pisa, ITA); Mugnaioli, Enrico (Istituto Italiano di Tecnologia, Pisa, ITA)

3D electron diffraction allows data collection on nanocrystalline domains, which can be used as kinematical intensities in ab-initio structure solution methods. The development of single electron detectors for diffraction and of fast recording protocols based on continuous rotation of the sample have dramatically reduced the electron dose necessary for collecting a data set with a large coverage. With total doses of less than  $1 \text{ e}/\text{\AA}^2$  very beam sensitive samples like organic and macromolecular crystals can now be studied by electron diffraction in nanocrystalline form. Examples of structure solution on known pharmaceutical compounds based on simulated annealing will be presented, as the structure solution attempted in case of low quality 3DED data. Combining STEM imaging with weak beams and the sensitivity of direct electron detectors we will show how it is possible to record high quality 3DED data on organic crystals without the need to work under cryo condition. Standard precession assisted step-wise 3DED data collection allowed the structure solution of metaxalone and of the unknown crystal structure of orthocetamol.

## MS44-02 | PROSPECTS OF SINGLE MOLECULE ELECTRON DIFFRACTION FOR STRUCTURAL BIOLOGY

Latychevskaia, Tatiana (Paul Scherrer Institute, Villigen, CH); Abrahams, Jan Pieter (PSI, Villigen, CH)

Diffraction data have a higher contrast, are less susceptible to sample movement and are electron-optically more robust. Diffraction patterns are insensitive to the sample movement and therefore allow obtaining highest possible resolution. We will discuss the possibilities of electron diffraction data of single protein complexes. The contrast of diffraction patterns can be enhanced by averaging data of similarly oriented molecules, which for well-defined molecular complexes could yield three-dimensional distribution of the scattering potentials with enough resolution for atomic interpretation. In diffraction mode, the phase of the scattered wave is not acquired by the detector and need to be retrieved for the sample structure retrieval. There are several strategies that would allow phasing data collected in diffraction mode and we discuss progress in this area.

## MS44-03 | THE NEED FOR CORRELATION COEFFICIENTS IN THE MODELING OF STACKING FAULTED CRYSTAL STRUCTURES

Rae, Alan David (the Australian National University, Canberra, AUS)

Standard refinement programs restrict the user to a model that allows twinning of a partially disordered average structure. However, there are structures where there are alternative relationships between adjacent ordered layers and this allows regions of commensurately related ordered structure with different origins, different orientations and different space groups. Each region can be described as a different occupancy modulation of an equally disordered structure of higher symmetry with subsequent atom displacements consistent with the local space group defined by the relative positions of immediately adjacent layers. Specific reflections can have contributions from different numbers of the component structures. The diffraction pattern identifies unit cells consistent with the options to be considered.

Locally the structure factor is  $F(\mathbf{h}) = \sum_n P_n F_n(\mathbf{h})$  so that averaging over the crystal

$$|F(\mathbf{h})|^2 = \sum_n \langle P_n^2 \rangle |F_n(\mathbf{h})|^2 + \sum_{m>n} \langle P_m P_n \rangle [F_m(\mathbf{h})^* F_n(\mathbf{h}) + F_m(\mathbf{h}) F_n(\mathbf{h})^*]$$

$$\text{where } \langle P_m P_n \rangle = X_{mn} [\langle P_n^2 \rangle \langle P_n^2 \rangle]^{1/2}$$

Twinning and allo twinning imply a correlation coefficient  $X_{mn}$  of 0, ie sample regions see only a single structure in a single orientation and intensities are a sum of component intensities. Correlation coefficients of 1.0 imply sample regions all see the same average disordered structure. Reality is often somewhere in between and this can be seen by using separate scales for data with different index conditions and for differences in pseudo equivalent reflections using a prototype structure that is a mixture of the space group options described using a space group that only includes the symmetry elements the options have in common. Worked examples will be given.

## MS44-04 | STRUCTURE STUDY OF A DISORDERED ZEOLITE BY cRED AND HRTEM

Zhao, Jingjing (Stockholm University, Stockholm, SWE)

### Structure study of a disordered zeolite by electron crystallography

Intergrowth and stacking disorders occur very often in synthetic zeolites, making their structural determination very challenging. Electron crystallography is a powerful method, which enables us to solve disordered structures by combining reciprocal (3D electron diffraction) and direct space (high-resolution transmission electron microscopy, HRTEM) methods. Continuous rotation electron diffraction (cRED) is an effective and high-throughput method for structure determination of micron- to nano-sized single crystals [1–3]. HRTEM images can give us local information in direct space, which is crucial to study disordered materials [4,5]. In this work, a new and disordered aluminosilicate zeolite was studied by the combination of cRED and HRTEM. cRED data were used to determine the average structure of this zeolite, whereas HRTEM images were used to study the disorder types.

[1] Nannenga, B. L. *et al. Nature Methods* **11**, 927 (2014).

[2] Wang, Y. *et al. Journal of Applied Crystallography* **51**, 1094–1101 (2018).

[3] Cichocka, M. O. *et al. Journal of Applied Crystallography* **51**, 1652–1661 (2018).

[4] Willhammar, T. *et al. Nature Chemistry* **4**, 188–194 (2012).

[5] Cichocka, M. O. *et al. Crystal Growth & Design* **18**, 2441–2451 (2018).

## MS44-05 | DIRECT AND FOURIER SPACE TRAVELING: MULTI-DIMENSIONAL MAPPING OF LATTICE STRAIN AND TILT OF A SUSPENDED SILICON NANOWIRE IN A MONOLITHIC SYSTEM

Dolabella, Simone (Empa- Swiss Federal Laboratories for Material Sciences and Technology, Dübendorf, CH)

Silicon nanowire based sensors such as micro and nano electrical mechanical systems (MEMS and NEMS) are well known in many fields of application due to their unique characteristics of flexibility and strength that emerge at the nano scale. In this work, we show a first study on this class of micro- and nano-fabricated silicon structures adopting the Scanning X-ray Diffraction Microscopy (SXDM) technique [1] by mapping the in-plane strain and tilt of a monolithic device structure comprised of suspended nanowires (NWs) and their monolithic pillars [2]. As a first step, we studied how the atomic structure of these new type of NWs is affected by the designed sample geometry including size and shape and critical steps of the fabrication process such as e-beam and DRIE. The combination of three-dimensional reciprocal space maps (3D-RSMs) with the distributions of in-plane strain and tilt plotted in two-dimensional real space images, allowed us to make a full analysis of the device structure. X-ray analysis performed on the (022) and (044) reflections show a very low level of lattice in-plane strain but a significant degree of lattice tilt.

[1] Chahine, G. A., Richard, M.-I., Homs-Regojo, R. A., Tran-Caliste, T. N., Carbone, D., Jacques, V. L. R., Grifone, R., Boesecke, P., Katzer, J., Costina, I., Djazouli, H., Schroeder, T. & Schulli, T. U. (2014). *Journal of Applied Crystallography* 47, 762-769.

[2] Tasdemir, Z., Peric, O., Sacchetto, D., Fantner, E. G., Leblebici, Y., & Alaca, B. E. (2018). *IEEE Transactions on Nanotechnology* 17, 6.

## MS44-P01 | SYNTHESIS AND STUDY OF HIGHLY SENSITIVE SERS SUBSTRATE BY FERROMAGNETIC HOLLOW MICRO-SPHERES

Huang, Yu-Fang (Department of Materials Science and Engineering, National Taiwan University of Science and Technology, Taipei, TWN); Huang, Wen-Chi (Department of Materials Science and Engineering, National Taiwan University of Science and Technology, Taipei, TWN); Hsu, Pei-Kai (Department of Materials Science and Engineering, National Taiwan University of Science and Technology, Taipei, TWN); Chen, ShihYun (National Taiwan University of Science and Technology, Taipei, TWN); Song, Jenn-Ming (National Chung Hsing University, Taichung, TWN)

In this study, a composite with the integration of magnetic, plasmonic and buoyant properties was designed and synthesized for facilitating sensitive detection of surface-enhanced Raman scattering (SERS). At first, iron oxide hollow spheres were synthesized by spray pyrolysis method at first, which is a simple and mass-produced process. Various reducing treatment were performed to maximize ferromagnetic strength and then Ag nanoparticles were deposited on the surface of the magnetic hollow spheres to provide the hotspots in the SERS measurements. Electron microscopy and electron energy loss spectroscopy were utilized to study the microstructure and identify the phase of the samples obtained in each stage. The experimental results show that the as-prepared iron oxide hollow spheres are  $\alpha$ -Fe<sub>2</sub>O<sub>3</sub>. The spheres have a size of 0.5  $\mu$ m to 3  $\mu$ m and an average shell thickness of about 20 nm. After annealing in a reducing atmosphere,  $\alpha$ -Fe<sub>2</sub>O<sub>3</sub> transformed to Fe<sub>3</sub>O<sub>4</sub> successfully. The maximum saturation magnetization up to 120 emu/g at 300 K was observed of samples annealing in Ar/H<sub>2</sub> at 400°C for 3 hours, which was 50% higher than that of the reported Fe<sub>3</sub>O<sub>4</sub> nanoparticle. With the optimized synthesis protocol of Ag deposition, the size as well as the inter particle spacing between Ag nanoparticles reached 5 nm and 10 nm, respectively. At last, with applying magnetic field, the intensity of the SERS signal from the composite was strong enough to provide single particle-level detection.

## MS44-P02 | HYDRAULIC, STRUCTURAL AND PHOTOCATALYTIC BEHAVIOR OF CEMENTITIOUS PHASES INCORPORATING NANOCOMPOSITE MIXED Zn-Al-Ti OXYDES

Amor, Fouad (Faculty of Sciences Rabat, Temara, MAR)

The development of new modified cement-based materials has become a necessity for improving durability performance and removing pollutants from building surfaces. This research is focused on the synthesis, by co-precipitation method, of photocatalyst based on Zn-Al layered double hydroxides (LDH) impregnated by  $\text{TiO}_2$  diluted in a basic solution of  $\text{Na}_2\text{CO}_3$ , to form, after calcinations, nanocomposite mixed Zn-Al-Ti oxides denoted C<sub>Zn-Al-Ti</sub>, added to clinker pastes in proportion ranged from 0 to 5 wt %. The photocatalytic activity of C<sub>Zn-Al-Ti</sub> nanoparticles as well as the mineralogical behavior of clinker pastes was evaluated. The memory effect of LDHs is evaluated by monitoring the hydration of the nanocomposite using X-ray diffraction. Characterizations of samples are following by X-ray diffraction, Fourier transform infrared spectroscopy and scanning electron microscopy. Degradation of Rhodamine B under UV light was selected as photocatalytic test reaction. The structures of the formed C-S-H show that the hydrates with the highest Ca/Si ratios having the shortest chains, and consequently the interlaminar spaces are smaller. The studied pastes showed that the synergistic effect between  $\text{TiO}_2$  and Zn-Al-LDH contributes to overall photocatalytic performance due to the presence of C<sub>Zn-Al-Ti</sub> in the matrix.

## MS44-P03 | STRUCTURAL CHARACTERIZATION OF ZnO/GRAPHENE NANOCOMPOSITE

Sbarcea, Beatrice Gabriela (INCDIE ICPE-CA, Bucharest, ROU); Banciu, Cristina (INCDIE ICPE-CA, Bucharest, ROU); Marinescu, Virgil (INCDIE ICPE-CA, Bucharest, ROU); Patroi, Delia (INCDIE ICPE-CA, Bucharest, ROU); Lungulescu, Marius (INCDIE ICPE-CA, Bucharest, ROU)

Zinc Oxide (ZnO) is a multifunctional semiconductor material and its used in applications involving sensors, light-emitting diodes (LEDs), piezoelectric devices, solar cells. Graphene, exhibits properties such as ultrahigh electron mobility, large surface area, high chemical and thermal stability, excellent electrical and optical properties.

The goal of this study is to obtain the porous 3D graphene network on nickel foam template by chemical vapor deposition (CVD) at high temperatures using methane as carbon source. ZnO-graphene (ZG) composite was developed using hydrothermal method to deposit zinc oxide directly on the 3D graphene network.

The prepared ZG were structurally characterized by X-ray diffraction, Raman technique and Scanning Electron Microscopy. The analysis of X-ray diffraction showed that the samples had hexagonal wurtzite structure. From SEM imagine we obtain hexagonal ZnO nanorods structures.

ZnO-graphene nanocomposites were synthesized in order to develop a good material for energy applications.

## MS44-P04 | EFFECTS OF X-RAY IRRADIATION AND THERMAL ANNEALING ON THE CO DOPANT LOCATION IN CO-DOPED TiO<sub>2</sub> NANOCRYSTALS

Soo, Yun-Liang (National Tsing Hua University, Hsinchu, TWN); Wu, Tai-Sing (National Tsing Hua University, Hsinchu, TWN); Jeng, Horng-Tay (National Tsing Hua University, Hsinchu, TWN); Chang, Shih-Lin (National Tsing Hua University, Hsinchu, TWN)

Extended x-ray absorption fine structure (EXAFS) and x-ray absorption near-edge structure (XANES) techniques have been employed to investigate the variations of dopant local structures due to x-ray irradiation and thermal annealing in Co-doped TiO<sub>2</sub> nanocrystals. The Co dopant atoms were found to occupy Ti sites in the as-made nanocrystal sample. After thermal annealing at elevated temperatures, Co atoms were relocated to an interstitial site and the oxygen coordination around Co atoms changed from an octahedral coordination to a square-planar coordination. The UV-vis diffuse reflectance spectra also indicate a substantial band-gap change from 3.1eV to 2.3eV as a result of the local structural change. The variation of Co dopant location due to thermal annealing was then found to be reversed by x-ray irradiation. First-principle density functional theory (DFT) calculations were carried out to determine the formation energies and to verify the structural stability of the supercells associated with the two distinct Co local structures. Control of dopant locations and band-gap width using x-ray irradiation and thermal annealing may provide unprecedented opportunities for technological applications of the Co-doped TiO<sub>2</sub> nanocrystal system.

## MS44-P05 | EVALUATION OF CRYSTAL STRUCTURES WITH PARTIAL OCCUPANCIES USING BOOLEAN SATISFIABILITY TECHNIQUES IN STRUPLOX

Fischer, Reinhard (Universität Bremen, Bremen, GER); Soeken, Mathias (EPFL, Lausanne, CH); Drechsler, Rolf (Universität Bremen, Bremen, GER)

The crystal-chemical evaluation of crystal structures is usually based on the interpretation of interatomic distances and angles, as, e.g., done just recently [1] evaluating more than 7000 crystal structures of zeolites in terms of the values of their bondlengths T–O (T = Si, Al, P, Zn, Be, Ge, B, As, Ga, Co) and their variability. This approach works well for ordered structures with well-defined distances. If atom positions are partially occupied, the interpretation of crystal structures becomes difficult or nearly impossible if there are multiple positions with partial occupancies. In order to find a solution for possible atom distributions where the simultaneous occupancy does not yield conflicting distances to nearest neighbors, we have employed Boolean satisfiability (SAT) techniques [2] assigning Boolean variables to each atom position in the unit cell being true if it is occupied and false if it is vacant. Restrictions due to site occupancies calculated in crystal-structure refinements are encoded as Boolean expressions which are then combined and passed to the SAT algorithm. Here we present the program STRUPLOX providing an automated procedure for the interpretation of the crystal structure starting with the input of atom parameters until the presentation of possible solutions for the atom distribution. Restrictions for interatomic distances are derived from the sum of ionic radii of adjacent atoms. Interatomic distances are calculated and coordination numbers are determined from bond-valence sum calculations.

[1] Baur, Fischer. *Chem. Mater.* 31 (2019) 2401-2420

[2] Soeken, Drechsler, Fischer. *Z. Kristallogr.* 231 (2016) 107-111

## MS44-P06 | AUTOMATED SERIAL ROTATION ELECTRON DIFFRACTION COMBINED WITH CLUSTER ANALYSIS AS A TOOL FOR STRUCTURE DETERMINATION

Wang, Bin (Stockholm University, Stockholm, SWE); Zou, Xiaodong (Stockholm University, Stockholm, SWE); Smeets, Stef (Delft University of Technology, Delft)

Electron diffraction techniques have reached a level where crystal structures can be determined quickly and routinely, but data collection is still very time-consuming and laborious. Therefore, we have developed a strategy to automatically screen for crystals and collect electron diffraction data. In a Serial Rotation Electron Diffraction (SerialRED) experiment, submicron-sized crystals are detected at a low magnification using image processing algorithms, and continuous rotation electron diffraction (cRED) data are collected on each crystal while dynamically tracking the crystal movement during rotation using defocused diffraction patterns. On our JEOL 2100-LaB<sub>6</sub> microscope with a TimePix direct electron detector, data acquisition has been automated entirely, and can run unsupervised for hours after initial setup. In a typical experiment, data are collected on 50-100 crystals per hour. To deal with the large number of data collected, we employed hierarchical cluster analyses to select the optimal data sets for merging. Our tests on several zeolite and metal-organic framework samples show that the structures are determined and refined effectively against these data using standard crystallographic software and that the results are indistinguishable from data collected manually. The large number of crystals also enables phase analysis of materials with known and unknown phases. Data collected on two multi-phase samples show that hierarchical cluster analysis enables the individual phases to be grouped and their structures determined. SerialRED has lower requirements of expertise in TEM and is less labor intensive, and, in combination with cluster analysis, this makes it a promising high-throughput crystal screening and structure analysis tool.

### TILING

ABOUFADIL, Youssef (Multidisciplinary Faculty Safi, Cadi Ayyad University, Safi, MAR); Thalal, Abdelmalek (Faculty of Sciences Semlalia, Cadi Ayyad University, Marrakech, MAR); El Idrissi Raghni, My Ahmed (Faculty of Sciences Semlalia, Cadi Ayyad University, Marrakech, MAR); Jali, Abdelaziz (Faculty of Sciences Semlalia, Cadi Ayyad University, Marrakech, MAR); Oueriagli, Amane (Faculty of Sciences Semlalia, Cadi Ayyad University, Marrakech, MAR)

Moroccan geometric ornamental art encompasses great achievements in two-dimensional ornaments such as rosettes, friezes and wallpaper patterns, as well as in the three-dimensional ornament called Muqarnas (Stalactites). The Muqarnas, characteristic of Arab-Islamic art, were used by Muslim architects as decorative elements before the 10th century. The Muqarnas are made of wood, stone, stucco, marble or ceramic. The techniques of their construction and the resulting variants differ according to the regions of the Islamic world. Muqarnas art flourished in Morocco during the reign of the Almohad dynasty (between the twelfth and thirteenth century), it was among the most used architectural elements in the construction of private or religious buildings. The method of construction of the Muqarnas uses the principles of three-dimensional geometry. This is a tiling of space by a repetition of concave surface units whose, the perpendicular projection on a plane defines a tiling that can have axial symmetry (Figure 1). In this presentation, we describe the method of building Muqarnas from two-dimensional tiling. We then show how Muqarnas evolve, according to the shape and symmetry of their units, from simple to complex. Finally, we present an example of Muqarnas obtained from a two-dimensional quasi-periodic tiling.

Keywords: Symmetry, Muqarnas, Moroccan geometric art, tiling

[1] Castera JM. Arabesques, ACR Edition; 1996.

[2] Thalal. A & al. "Symmetry in art and architecture of the Western Islamic world" Crystallography Reviews, 2017.

[3] Roxana RECIO, Antonio CORTIJO OCAÑA (orgs.). Mirabilia 22 (2016/1)

[4] Yvonne Dold-Samplonius, Practical Arabic Mathematics : Measuring the Muqarnas by al-Kashi. Centaurus 1992 : Vol. 35 : pp. 193-242.

## MS44-P08 | UTILISING MAXRD IN THE STUDY OF INCLUSION COMPOUNDS

Ramsnes, Stian (University of Stavanger, Stavanger, NOR); Larsen, Helge Bøvik (University of Stavanger, Stavanger, NOR); Thorkildsen, Gunnar (University of Stavanger, Stavanger, NOR); Nicholson, David Graham (Norwegian University of Science and Technology, Trondheim, NOR)

The *Mathematica* X-ray diffraction package *MaXrd* has now been expanded with the capability to compose custom crystal structures, particularly aimed at facilitating the embedment of a guest phase into a host lattice. After importing the required crystallographic information from a cif file, one can extend the asymmetric unit to a desired number of unit cells while inserting atoms, molecules or other structures in the process. The embedded phase can also be distorted and/or rotated by a specified or random amount when placed into the host. The resulting structure can be visualised in three dimensions in direct space and the information may be utilised automatically by *DISCUS* to obtain a simulated diffraction pattern. A consequence of this technique is that the space group of the guest phase becomes independent of that of the host (essentially having *P1* symmetry). This gives the means to test hypotheses on the crystal structure and simultaneously investigate reciprocal space for any implied characteristics in a relatively swift and easy manner. This functionality is used in our ongoing study of a thiourea-ferrocene clathrate, which has proven challenging with regard to its phase transitions and the five-fold symmetry of the cyclopentadienyl rings.

## MS44-P09 | EVIDENCE OF CHARGE DENSITY WAVE TRANSVERSE PINNING BY X-RAY MICRO-DIFFRACTION

Bellec, Ewen (University Paris-Sud, Orsay, FRA); Le Bolloc'h, David (CNRS, Orsay, FRA); Jacques, Vincent (CNRS, Orsay, FRA); Gonzalez-Vallejo, Isabel (University Paris-Sud, Palaiseau, FRA)

In low-dimensional material (quasi-1D in NbSe<sub>3</sub> or quasi-2D in TbTe<sub>3</sub>), a phase transition can occur in which the charge density becomes periodic and a gap opens in the electronic band. This is called the Charge Density Wave (CDW) transition.

Under applied electric field, the CDW will act as an elastic object and deform. Plus, above a threshold field, a collective current appears due to a periodic nucleation of charged topological solitons. In order to fully describe this process, one has to understand the CDW's deformation first.

Several resistivity measurements suggested that sample's surfaces had a strong influence on the CDW behavior, but none could clearly show the origin of this effect.

Here, we present results of x-ray diffraction using a nanometer size beam on a CDW material NbSe<sub>3</sub> pre-patterned by a focused ion beam (FIB). This technique enabled us to reconstruct the CDW spatial deformation by simple integration. Surprisingly, the results show a pinning of the CDW at the sample borders, explaining the surface influence on electronic conduction.

Beyond CDW materials, the analytical procedure presented here to reconstruct the CDW phase from a weakly coherent x-ray beam can be applied to recover the phase of any modulation, weakly deformed, with a resolution in the order of the beam size, without the need to use fully coherent x-ray beams.

Finally, using a description at low energy of the CDW deformation, we theoretically showed that surface pinning and nucleation of topological soliton at the contact can fit the resistivity measurements mentioned above.

## MS44-P10 | INDEXING GRAZING INCIDENCE X-RAY DIFFRACTION PATTERNS OF THIN FILMS

Simbrunner, Josef (Dept. of Neuroradiology, Vascular and Interventional Radiology; Medical University Graz, Graz, AUT); Hofer, Sebastian (Institute of Solid State Physics, Technical University Graz, Graz, AUT); Schrode, Benedikt (Institute of Solid State Physics, Technical University Graz, Graz, AUT); Salzmann, Ingo (3Department of Physics, Department of Chemistry & Biochemistry, Centre for NanoScience Research (CeNSR), Concordia University Montreal, Montreal, CAN); Resel, Roland (Institute of Solid State Physics, Technical University Graz, Graz, AUT)

Grazing incidence X-ray diffraction (GIXD) studies on organic thin films are often performed on systems showing fibre-textured growth. However, indexing their experimental diffraction patterns is generally challenging, especially if low-symmetry lattices are involved. Recently, analytical mathematical expressions for indexing experimental diffraction patterns of triclinic lattices were provided. In the present work, we provide a unifying framework for the indexing reciprocal-space maps obtained by GIXD for monoclinic lattices and lattices of higher symmetry. Our approach of including the Bragg peak from a specular X-ray diffraction experiment into the mathematical formalism is of considerable help for indexing of GIXD pattern, where the spatial orientation of the unit cell must be considered. Mathematical expressions with a significantly reduced number of unit cell parameters are derived, which facilitates the computational efforts. For crystallographic lattices of higher symmetry, where the set of unit cell parameters is reduced, the specular diffraction peak is still important for determining the orientation of the crystallographic unit cell relative to the sample surface. Procedures are described in detail for how to use the derived mathematical expressions. Two examples are presented to demonstrate the feasibility of our indexing method. For layered crystals of the prototypical organic semiconductors diindenoperylene and (*ortho*-difluoro) sexiphenyl, as grown on highly oriented pyrolytic graphite, their yet unknown unit-cell parameters are determined and their crystallographic lattices are identified as monoclinic and orthorhombic, respectively.

## MS44-P138 LATE | ON PHASING OF OVERSAMPLED DIFFRACTION DATA

Misnovs, Anatolijs (Latvian Institute of Organic Synthesis, Riga, LVA); Mishnev, Anatoly (Latvian Institute of Organic Synthesis, Riga, LVA)

The latest progress in X-ray free-electron lasers demonstrated an ability to acquire continuous diffraction data for nanocrystals and non-periodic objects [1-2]. Most of the oversampling phasing algorithms are iterative and may require knowledge of a support to avoid stagnation. Therefore new approaches which benefit directly from intensity oversampling particularly for *de novo* phasing may be of interest. Thus, Elser [3] has developed phase recovery algorithm which employs intensity gradient extracted from the continuous intensity distribution around a Bragg peak.

We investigate a new approach to phase retrieval when continuous intensity is available. The method employs Whittaker-Shannon sampling theorem (ST) [4] for the structure factor (SF). The phases of reflections (for non-periodic objects reflections refer to an artificial unit cell constructed to embrace a particle) are permuted to give the best agreement between moduli of measured structure factors and calculated by means of the ST at non-integral points in the reciprocal space. Application of the ST to the points with close to zero intensity gives rise to approximate linear equations for SFs in the neighbourhood of these points. Preliminary results for simulated data will be presented.

[1] Chapman H.N. et al. (2011). Nature (London), 470, 73-77.

[2] Sun Z., Fan J., Li H., Jiang H. (2018). Appl. Sci., 8(1), 132.

[3] [Elser V.](#) (2013). Acta Cryst. A69, 559-569.

[4] Shannon C.E. (1949). Proc.IRE, 37, 10-21.

## GI-MS45: How to... Successfully Collaborate as a Crystallographer

---

### GI-MS45-01 | FIGHTING THE WIND MILLS: ARE CRYSTALLOGRAPHERS THE SUCCESSORS OF DON QUIXOTE?

Nespolo, Massimo (Université de Lorraine, Vandoeuvre-lès-Nancy, FRA)

Crystallography is a perfect candidate to represent the popular adagio “victim of its success”. Everybody agrees that the contribution of crystallographers to a wide range of disciplines is of paramount importance, yet lectures specifically devoted to crystallography are becoming an endangered species, and open positions for crystallography as rare as unicorns. The consequences of this pernicious choice are multiple, including the frequent occurrence of sloppy, if not fundamentally incorrect, statements in the literature, and the huge difficulties experimentalists meet to find answers to practical problems which would not be an obstacle had they received a solid crystallographic education. An increasing demand for intensive lectures and short courses has arisen in the last twenty years, to which the IUCr commissions have responded with tireless efforts. In this talk I will report about my personal experience as lecturer in tens of international schools around the world, which have been occasion to meet colleagues working in different fields and start collaborations which have taken advantage of the respective knowledge and expertise. In particular, I will emphasize the striking contrast between the reluctance of crystallographers to identify themselves as such and the request for crystallographers as lecturers in research facilities and Universities.

## GI-MS45-02 | SECRETS TO A SUCCESSFUL COLLABORATION

Moraes, Isabel (National Physical Laboratory, Teddington, GBR)

In the world where multidisciplinary approaches are crucial to achieve a high impact scientific success, effective collaborations are a must!

Collaborative effectiveness is always a complex process that depends of many variables such as interpersonal skills, trust, culture, and occasionally of the physical distance between collaborators. In this interactive talk, approaches to a successful collaboration will be discussed. We must always remember that scientific collaborations are based on passion for a relevant scientific subject!

## **GI-MS45-03 | EDUCATION FOR NEW SYNCHROTRON SOURCES: AN INTERDISCIPLINARY MASTER PROGRAM OF THE NOVOSIBIRSK STATE UNIVERSITY**

Boldyreva, Elena (Novosibirsk State University, Novosibirsk, RUS)

Synchrotron radiation facilities are no longer “exotic” experimental tools for many researchers. A network of synchrotrons already covers Europe, North and South Americas, Asian countries and is widely used by a highly international scientific community. Construction of new synchrotrons in other geographical regions is planned. In particular, three new synchrotrons are planned to be constructed and subsequently used in Russia, including the one of the three (SKIF) to be located in Novosibirsk region.

One of the problems related to constructing the synchrotrons in new regions is to educate a broad enough research community, so that sufficient number of efficient users of these facilities appears, who can submit high-level proposals which are adequate to the level of the unique instruments, perform experiments, process and interpret data. Not only technical support engineers, but also beamline scientists and educated users are needed. Here I share the first experience of launching an interdisciplinary Master program at the Novosibirsk State University aimed at preparing a new generation of researchers who can deal with problems at the borderlines between Physics, Chemistry, Biology, Planetary Sciences, Cultural Heritage and other research field.

This work was supported by Ministry of Science and Higher Education of the Russian Federation (project 5-100 of the Novosibirsk State University and AAAA-A19-119020890025-3 of Boreskov Institute of Catalysis).

## GI-MS45-04 | HOW, AND WHEN, TO EFFECT COLLABORATIONS

Helliwell, John (University of Manchester, Manchester, GBR)

It is a major possibility that at some stage of your scientific career you will wish to take on a project of such wide scope, or respond to an invitation to join such a project as a partner, that collaboration is the way forward. Funding agencies also have recognised this, and there are many schemes and variants of scale of collaboration for you to choose from. One overriding principle to keep in sight of is the compatibility of your potential collaborator. An aspect that will perhaps cause the most diverse of behaviours from your collaborators will be the publications that result from your collaborations. I will draw on examples from my recent book [1] and from my research career.

[1] John R Helliwell (2017) "Skills for a Scientific Life" published by CRC Press, Taylor and Francis Group

## GI-MS45-05 | USING CRYSTAL STRUCTURES TO GUIDE PHARMACEUTICAL DRUG SUBSTANCE DEVELOPMENT

Agnew, Lauren (AstraZeneca, Macclesfield, GBR)

The use of crystal structures to understand the behaviour of compounds in the development of drug substance and drug product processes is becoming commonplace in industry. This talk will look at how the use of crystal structures and the learning from the interrogation of their structural features has laid the foundation blocks for developing compounds and launching drugs to the market.

An outline will be given to show how industrial scientists use a variety of tools to build up an understanding of the solid form. It will then show how this knowledge is communicated to wider project teams of non-specialists to impact manufacturing processes and crystallisation development, formulation design, particle sizing, setting of storage conditions, supporting regulatory submissions and manufacturability of the drug substance.

A number of case studies will be shown throughout the development of drug products to show how the findings from crystal structure analysis have been successfully communicated to project teams to help solve and explain problems in the manufacture of a number of pharmaceutical compounds.

## GI-MS45-P01 | CRYSTALLOCHEMICAL COMPUTATIONAL TOOLS, WEB SERVICES, DATABASES, AND APPROACHES FOR JOINING RESEARCHERS OVER THE WORLD

Alexandrov, Eugeny V. (Samara Center for Theoretical Materials Science (SCTMS), Samara University, Samara, RUS); Proserpio, Davide M. (Dipartimento di Chimica, Università degli Studi di Milano, Samara, RUS); Blatov, Vladislav A. (Samara Center for Theoretical Materials Science (SCTMS), Samara State Technical University, Samara, RUS); Addicoat, Matthew (Nottingham Trent University, School of Science and Technology, Nottingham, AUT)

The Samara Center for Theoretical Materials Science (SCTMS) started in 2013 from one successful collaboration (<http://english.sctms.ru/about/>) and then the collaboration network was enlarged to more than 15 countries, 30 groups, and 100 researchers. The approaches for geometrical-topological analysis (<https://topospro.com/>; <https://topocryst.com/>) developed in SCTMS cover crystal chemistry of almost all classes of crystalline materials [1-3]. Use of them in couple with knowledge-based approach results in establishing structures taxonomy, finding correlations between structural descriptors, and predicting structures and properties on a qualitative level [4,5]. We see three conditions to be crucial for a long, stable and fruitful collaboration: (i) a rigorously defined scientific task, (ii) flexibility and diversity of research interests, and (iii) development in line with modern trends in science.

The work was supported by RSF (18-73-10116, 16-13-10158), the Russian Government (1.6101.2017/9.10, MK-415.2019.3) and RFBR (17-57-10001).

- [1] V.A. Blatov, A.P. Shevchenko, D.M. Proserpio *Cryst. Growth Des.* 14, 3576-3586 (2014)
- [2] V.A. Blatov, E.V. Alexandrov, A.P. Shevchenko *Topology: ToposPro*, In: *Comprehensive Coordination Chemistry III*, Elsevier. To be published, doi: 10.1016/B978-0-12-409547-2.14576-7 (2019).
- [3] E.V. Alexandrov, A.P. Shevchenko, V.A. Blatov *Cryst. Growth Des.* doi: 10.1021/acs.cgd.8b01721 (2019)
- [4] H. Wang, X. Dong, J. Lin, S.J. Teat, S. Jensen, J. Cure, E.V. Alexandrov, Q. Xia, K. Tan, Q. Wang, D.H. Olson, D.M. Proserpio, Y.J. Chabal, T. Thonhauser, J. Sun, Y. Han, J. Li *Nature Comm.*, 9, 1745 (2018).
- [5] Y. Sun, X. Chen, F. Wang, R. Ma, X. Guo, S. Sun, H. Guo, E.V. Alexandrov *Dalton Trans.* 48, 5450–5458 (2019)

## GI-MS45-P02 | STRUCTUREFINDER

Kratzert, Daniel (Albert-Ludwigs-Universität Freiburg, Freiburg, GER)

Presented is a new computer program called StructureFinder. It creates a database of crystallographic structures on a computer and makes them searchable. The program can search for various properties: Unit cell, free text, creation date, included atom types and space group. To build the database, StructureFinder collects all computer information files (cif file format) below certain directories on a hard disk. The containing information is stored into a SQLite database. The database can be accessed by two different interfaces. Either, a stand-alone Qt program to install on a single computer or a web interface to be accessed by a whole work group.

StructureFinder greatly enhances the ability to find old structures in huge collections of crystallographic datasets. The program can easily handle more than 10.000 structures. It can be downloaded at [1].

[1] <https://www.xs3.uni-freiburg.de/research/structurefinder>

## GI-MS45-P03 | EXTENDING NXMX METADATA TO FACILITATE DATA SHARING

Bernstein, Herbert J. (Ronin Institute for Independent Scholarship, Upton, NY, USA)

It is increasingly important to be able to combine data from multiple experiments by multiple experimenters at multiple facilities. For synchrotron MX data there are two major standards for diffraction images: the Crystallographic Binary Format (CBF/imgCIF) [1] adopted for the Dectris Pilatus in 2007 and the NeXus/HDF5 NXmx applications definitions [2]. The High Data Rate Crystallography (HDRMX) group has been working to extend and harmonize the necessary additions to NXmx and CBF to facilitate data sharing.

[1] H. J. Bernstein, A. P. Hammersley. "Specification of the Crystallographic Binary File (CBF/imgCIF)." International Tables for Crystallography (2006).

[2] H. J. Bernstein. "Software for processing high-data-rate MX in CIF and NeXus/HDF5." Foundations of Crystallography 70 (2017): C1363.

## GI-MS46: Status and New Activities @ Large Scale Facilities

---

### GI-MS46-01 | THE ESRF-EBS AND THE NEXT CHAPTER IN X-RAY SCIENCE

Reichert, Harald (ESRF, Grenoble, FRA)

The European Synchrotron Radiation Facility (ESRF) is currently installing the first 4th generation high energy synchrotron radiation source. The start of the user operation of the ESRF-EBS in 2020 will mark the opening of the next chapter in X-ray science. After an introduction into the concepts behind this new revolutionary source, the so-called hybrid multiple bend achromat lattice (HMBA), the status of the project will be briefly reviewed.

The recently upgraded beamline portfolio (Phase I of the Upgrade Programme) is complemented by the construction of four new flagship beamlines and a full refurbishment of the remaining beamlines. In conjunction with the vastly enhanced source performance new opportunities will be opened to explore matter and materials in unprecedented detail.

Opportunities for new science will be presented and the challenges that come with it, including the challenge of handling very large data sets. New approaches for data analysis and curation must be developed in collaboration with the user community for the optimum use of resources.

## GI-MS46-02 | MEGAHERTZ RATE SERIAL CRYSTALLOGRAPHY AT THE EUROPEAN XFEL

Letrun, Romain (European XFEL, Schenefeld, GER)

Serial Femtosecond Crystallography (SFX) [1] is relatively novel variant of crystallography developed for X-ray Free Electron Lasers which is exceptionally useful for radiation damage sensitive samples, irreversible time-resolved systems and more [2]. Since its inception, SFX has also been realized at high brightness synchrotron sources [3].

The European X-ray Free Electron Laser (EuXFEL) is the only operating high repetition rate XFEL in the world [4]. It can produce up to 27000 pulses of highly intense, hard X-ray wavelength pulses of tens of femtoseconds duration every second. High repetition rate XFELs offer an unprecedented ability to generate large quantities of serial crystallography data. Specifically, this is particularly useful for time-resolved studies where a given quantity of data frames need to be collected for each time point investigated.

This presentation will give an overview of the capabilities of the SPB/SFX instrument at the EuXFEL [5], as well as show some of the science performed to date including megahertz repetition rate serial crystallography [6,7] as well as time-resolved work. An outlook to future capabilities will also be shown.

[1] Chapman *et al.*, *Nature* **470**, 73–77 (2011).

[2] Spence, *IUCrJ* **4**, 322–339 (2017).

[3] Gati *et al.*, *IUCrJ* **1**, 87–94 (2014).

[4] Tschentscher *et al.*, *Appl. Sci.* **7**, 592 (2017).

[5] Mancuso *et al.*, *J. Synchrotron Radiat.* **26**, 660–676 (2019).

[6] Grünbein *et al.*, *Nat. Commun.* **9**, 3487 (2018).

[7] Wiedorn *et al.*, *Nat. Commun.* **9**, 4025 (2018).

## GI-MS46-03 | EMBL BEAMLINES FOR MACROMOLECULAR CRYSTALLOGRAPHY AT PETRA

### III

Bourenkov, Gleb (EMBL Hamburg, Hamburg, GER); Pompidor, Guillaume (EMBL Hamburg, Hamburg, GER); Bento, Isabel (EMBL Hamburg, Hamburg, GER); Hakanpää, Johanna (EMBL Hamburg, Hamburg, GER); Panneerselvam, Saravanan (EMBL Hamburg, Hamburg, GER); von Stetten, David (EMBL Hamburg, Hamburg, GER); Schneider, Thomas R. (EMBL Hamburg, Hamburg, GER)

EMBL-Hamburg operates two MX beamlines, P13 and P14, at PETRA III (DESY, Hamburg).

On P13, combining X-rays in the 4-6 keV energy range with beam sizes down to 15  $\mu\text{m}$  diameter while maintaining high photon flux allows to perform full anomalous data collections in less than 5 minutes. S-SAD phasing is achieved routinely. Diffraction measurements at low energies on P13 do not require any special preparation of the sample, i.e. a crystal attached to a standard SPINE-pin can be automatically mounted onto the goniostat.

P14 can be run in two modes, one providing a collimated homogeneous beam that can be shaped to any size between 10 and 200  $\mu\text{m}$ , the second mode producing micro-focus conditions with a beam size on the 5  $\mu\text{m}$  scale. The collimated beam can be used to illuminate large (50-200  $\mu\text{m}$ ) and small crystals homogeneously and/or to resolve diffraction from large (>1000 Å) unit cells. The micro-focus beam can be used conveniently for serial data collections both on cryogenically cooled crystalline suspensions and *in situ* on crystals as grown in CrystalDirect™ crystallization plates. *In situ* structure determinations have been successfully performed from crystals in crystallization drops, in lipidic cubic phase, or as grown in living cells.

In 2018, a second endstation 'T-REXX' has been added to P14 providing an environment optimized for pump-probe time-resolved experiments.

The beamlines are part of the Integrated Facility for Structural Biology that offers access to services such as characterization of samples prior to crystallization, HT-crystallization, and crystal harvesting with a CrystalDirect™ Harvester.

## GI-MS46-04 | MACROMOLECULAR CRYSTALLOGRAPHY AT MAX IV

Gonzalez, Ana (MAX IV, Lund, SWE)

BioMAX is one of the first operational beamlines at the MAX IV facility. It is a multipurpose beamline for macromolecular crystallography, capable of conventional data collection, high throughput and microcrystal applications. The beamline equipment includes a double crystal LN2 cooled monochromator, KB mirrors, a Beam Conditioning Unit, a MD3 diffractometer and a 16M Dectris Eiger detector. Samples are automatically mounted with a ISARA sample exchanger. The beamline uses MXCuBE3 [1] as the data collection interface. Data are processed automatically and the results are displayed to the users with ISPyB [2].

BioMAX has been open to general users since 2017. It has been used by hundreds of users from different countries and it also supports in-house projects to develop serial crystallography and a fragment-based drug discovery facility (FRAGMAX). A second beamline, MicroMAX, with a beam size between 1 and 10 microns, will be dedicated to micron-size beam and crystal sizes, and include serial crystallography and time-resolved applications. MicroMAX has secured funding and first user experiments are planned for 2022.

[1] Delagenière, S. *et al* (2011) *Bioinformatics*, **27**, 3186-3192.

[2] Mueller, U. *et al* (2017) *Synchrotron Radiation News*, **30**, 22-27.

## GI-MS46-05 | FACILITY UPGRADES AT THE AUSTRALIAN SYNCHROTRON: EXTENDING THE POWDER DIFFRACTION CAPABILITIES

D'Angelo, Anita (Australian Synchrotron (ANSTO), Clayton, AUS); Kimpton, Justin (Australian Synchrotron (ANSTO), Clayton, AUS); Gu, Qinfen (Australian Synchrotron (ANSTO), Clayton, AUS); Brand, Helen (Australian Synchrotron (ANSTO), Clayton, AUS)

Here we report on the recent upgrades to the existing Powder Diffraction (PD) beamline, and planned Advanced Diffraction and Scattering (ADS) beamline at the Australian Synchrotron. The PD beamline has been operational since 2007 and is optimised for in situ measurements carried out between 8-22 keV. In late 2018, the vertical collimating mirror (VCM) and double crystal monochromator (DCM) were upgraded to increase the flux and stability, and address end-of-life issues. The VCM was replaced with a substrate with both flat and toroid Rh-coated mirror stripes to increase flux following coating degradation and permit horizontal focussing using the toroid. The existing DCM Si(111) pair was replaced and the Si(311) crystal pair was removed to increase stiffness in the crystal cage. Replacement of the vertically focusing mirror will occur in late 2019. A new ADS beamline is currently being built to complement the PD beamline and extend Australia's research infrastructure in high energy X-ray diffraction and imaging. ADS will have a superconducting multipole wiggler (30-150 keV) and two simultaneously operating end stations. A wide range of techniques will be possible including: 2D powder diffraction, energy dispersive diffraction, tomography, total scattering, and white/pink beam Laue diffraction.

## GI-MS46-P01 | ESTABLISHMENT OF A HIGH CAPACITY X-RAY SOURCE IN AUSTRIA FOR THE USE IN MATERIALS SCIENCE

Prost, Josef (AC2T research GmbH, Wiener Neustadt, AUT); Brenner, Josef (AC2T research GmbH, Wiener Neustadt, AUT); Hradil, Klaudia (X-Ray Center, TU Wien, Wien, AUT); Budnik, Serhiy (AC2T research GmbH, Wiener Neustadt, AUT)

Constantly increasing demand on modern solutions for development of industrial technologies and high-performance analytical methods accelerates the competition between interdisciplinary research groups targeting new insights into the nature of materials. An innovative development combines laser and electron-beam interaction (inverse Compton scattering) to design a specific laboratory-sized X-ray source (Compact Light Source, CLS). Despite its small size, the CLS offers the favourable features of synchrotron radiation, such as a continuously tuneable energy spectrum and high spatial resolution due to small beam size and angular divergence at high brilliance. Focusing the beam enables the operation with uniform area section within a distance of several meters from the input area. These properties make the CLS a promising solution for a wide range of X-ray applications related to tomography, diffraction, scattering and elemental analyses experiments. An installation of such a CLS facility in Austria opens new perspectives for a wide range of applications for multiple users in Austria including universities, scientific companies and research divisions of local high-tech industry. In-situ, non-destructive analysis of materials and related phenomena, such as (re-)crystallization, films and coatings as well as corrosion and wear processes, will be possible. Additionally, the assignment of the CLS for education purposes in combination with pre-characterization and evaluation of samples and experimental setups in preparation for a measurement at a large scale European synchrotron facility cannot be underestimated. The installation of a CLS system will enable the flexible and tailored training for young scientists and professionals in research and industry.

## GI-MS46-P02 | A NON-AMBIENT SINGLE CRYSTAL X-RAY DIFFRACTION BEAMLINE AT TAIWAN PHOTON SOURCE

Lee, Jey-Jau (National Synchrotron Radiation Research Center, Hsinchu, TWN); Wu, Lai-Chin (National Synchrotron Radiation Research Center, Hsinchu, TWN); Chang, Shih-Hung (National Synchrotron Radiation Research Center, Hsinchu, TWN)

Structural information are elementary knowledge of molecule but always be the key to understand physical and chemical properties. However, the in-house X-ray diffractometer is not sufficient for many new materials that only can get tiny crystal, and also are inconvenient for non-ambient research requests from Taiwan's scientists.

A dedicated small-molecule single-crystal X-ray diffraction beamline is phase-II beamline at TPS (Taiwan Photon Source). A Cryogenic Tapered Undulator with period length 18 mm (CTU18) will be used as X-ray source to generate high brilliance X-ray. The energy of this beam line is tunable which is depend on different experiments within 8-35 KeV range. Monochromatic mode and pink beam mode both will be available at this beamline. The monochromatic beam mode will be selected by a "Double Crystal Monochromator" (DCM) and the pink beam mode (with bandwidth  $\sim 3-5\%$ ) can be selected. A Kirkpatrick-Baez (KB) mirror will be used to focus the beam size to few microns in diameter at sample position. The end-station will be installed with a ARINAX MD3-up four-circle Kappa diffractometer for data collection.

This beamline is designed for advanced crystallographic purposes, which are not only dedicated to hard structure determination, but also for structure at non-ambient conditions . Those techniques will include (1) Micro-crystal and large porous structure determination (2) Extreme condition structural studies (3) Photo-induced excited state (4) Time-resolved dynamic structural studies via Laue diffraction technique. (5) charge density analysis (6) Resonance diffraction. These technic details of this beamline will be shown in this presentation .

## GI-MS46-P03 | AN EFFECTIVE NEUTRON CROSS SECTION FOR HYDROGEN IN ORGANIC COMPOUNDS

Capelli, Silvia (UKRI-Science and Technology Facilities Council, Didcot, GBR)

The wavelength dependence of the effective neutron cross section for hydrogen has been investigated by measuring the transmitted total scattering cross section in urea, beta-alanine, tartaric acid and polyethylene, over the energy range 3 meV to 10 eV. Data show a linear dependence on wavelength between 0.55 and 2.0 Å, i.e. a small bandwidth compared to that used in Laue neutron diffraction experiments, for example at pulsed sources. Under the assumption that carbon, nitrogen and oxygen atoms contribute a small and invariant amount to the measured total cross section, these data represent a direct measure of the wavelength dependence of the overall scattering contribution of the hydrogen atoms to the total cross section and can be used to apply effective wavelength-dependent corrections to neutron scattering data on hydrogen-rich simple organic compounds.

## **GI-MS46-P04 | THE HIGH ENERGY X-RAY DIFFRACTION BEAMLINE AT THE PETRA III SYNCHROTRON LIGHT SOURCE AT DESY.**

Tolkiehn, Martin (DESY, Hamburg, GER); Noohinejad, Leila (DESY, Hamburg, GER); Paulmann, Carsten (DESY, Hamburg, GER)

In recent years, high-energy diffraction beamlines have become standard at new synchrotron facilities. High-energy beamlines add powerful tools for materials characterization: in situ X-ray diffraction, high resolution measurements for charge density studies, tracing phase transitions, and modulated structures at ambient and non-ambient conditions. The P24, new beamline for chemical crystallography, provides a powerful instrument for new applications, which will make use of the superior properties of PETRA III. We would like to present the development of the P24 beamline for advanced chemical and physical measurements.

## GI-MS46-P05 | AZIMUTHAL INTEGRATION AND CRYSTALLOGRAPHIC ALGORITHMS ON MALLEABLE HARDWARE

Skovhede, Kenneth (MAX IV Laboratory, Lund University, Lund, SWE); Barczyk, Artur (MAX IV Laboratory, Lund University, Lund, SWE); Johnsen, Carl (Niels Bohr Institute, University of Copenhagen, Copenhagen, DNK); Kristensen, Mads R.B. (Niels Bohr Institute, University of Copenhagen, Copenhagen, DNK); Vinter, Brian (Niels Bohr Institute, University of Copenhagen, Copenhagen, DNK); Matej, Zdenek (MAX IV Laboratory, Lund University, Lund, SWE)

Field-programmable gate arrays (FPGAs) present a sort of malleable computer hardware that is nowadays extensively used for readout of fast X-ray cameras or real-time applications controlling experiments. Contrary crystallographic analysis and data reduction codes on FPGAs are not common. Within this work the azimuthal integration (AZINT) of 2D-detector data for powder diffraction and small angle scattering is implemented on FPGAs. The project demonstrates possibilities of this type of compute accelerators for data analysis in crystallography and other photon or neutron sciences. Possible future applications include frame filtering, spot finding or diffraction features classification with machine learning. Contrary to existing solutions the FPGA implementation allows all the tasks of receiving and decoding the image stream and the AZINT computation itself to be handled on a single chip with fixed and low latency. The integrated patterns can be fitted in other parts of the configurable pipeline and provide a real-time feedback to the experiment. The solution can be integrated with compute infrastructures at large scale facilities or as a compact embedded device it can increase handling data capabilities from high throughput detectors in any lab. Azimuthal integration represents the first demonstration case of a project which aims for making FPGAs easily available for scientists with use of industrial standards as OpenCL as well as with free and open-source numeric algebra toolbox based on synchronous message exchange (SME). Initial benchmarks show that SME based implementation of a histogram computation, which is a basis for AZINT, can process 600 Gb/s of uncompressed data stream.

## GI-MS46-P06 | DEVELOPMENT OF MICROSPECTROPHOTOMETER FOR THE

### MACROMOLECULAR CRYSTALLOGRAPHY BEAMLINE AT THE PHOTON FACTORY, JAPAN

Hikita, Masahide (Structural Biology Research Center, KEK, Tsukuba, JPN); Yamada, Yusuke (Structural Biology Research Center, KEK, Tsukuba, JPN); Matsugaki, Naohiro (Structural Biology Research Center, KEK, Tsukuba, JPN); Hiraki, Masahiko (Mechanical Engineering Center, KEK, Tsukuba, JPN); Senda, Toshiya (Structural Biology Research Center, KEK, Tsukuba, JPN)

In the functional analysis of proteins, it is essential to know the crystal structure at the atomic level and its electronic and chemical changes. Spectroscopy is the effective technique for detecting the structural states of proteins, even within protein crystals. Therefore, the spectroscopic methods such as Raman and UV-Visible absorption have been complementarily combined with X-ray diffraction studies to evaluate the protein status. In order to utilize the spectroscopic study at macromolecular crystallography beamline at the Photon Factory, the development of spectroscopic instrumentation for both offline and online has been started at beamline AR-NW12A. For development of offline spectroscopic instrumentation, the laser booth has been built beside of control cabin of AR-NW12A. After the end of the construction of the laser booth, we have started to develop the offline UV-Visible absorption spectroscopic instrumentation and it has now been in general user operation. Herein, we describe the outline of the offline UV-Visible and Raman spectroscopic instrumentations. The continuing development of the online spectroscopic instrumentation is also outlined. In the future, macromolecular crystallographic beamline users will be able to not only determine the atomic structure of their samples but also to explore the electronic and vibrational characteristics of their sample, before, during and after data collection.

## GI-MS46-P07 | FACILITIES FOR MACROMOLECULAR CRYSTALLOGRAPHY AT THE HZB

Gerlach, Martin (Helmholtz-Zentrum Berlin, Berlin, GER); Feiler, Christian (Helmholtz-Zentrum Berlin, Berlin, GER); Förster, Ronald (Helmholtz-Zentrum Berlin, Berlin, GER); Gless, Christine (Helmholtz-Zentrum Berlin, Berlin, GER); Hauß, Thomas (Helmholtz-Zentrum Berlin, Berlin, GER); He, Huiling (Helmholtz-Zentrum Berlin, Berlin, GER); Hellmig, Michael (Helmholtz-Zentrum Berlin, Berlin, GER); Kastner, Alexandra (Helmholtz-Zentrum Berlin, Berlin, GER); Steffien, Michael (Helmholtz-Zentrum Berlin, Berlin, GER); Taberman, Helena (Helmholtz-Zentrum Berlin, Berlin, GER); Wollenhaupt, Jan (Helmholtz-Zentrum Berlin, Berlin, GER); Weiss, Manfred S. (Helmholtz-Zentrum Berlin, Berlin, GER)

The Helmholtz-Zentrum Berlin (HZB) operates three beamlines for macromolecular crystallography (MX) at the electron storage ring BESSY II [1,2,3]. BL14.1 and BL14.2 are tunable in the photon energy range from 5 to 16 keV, while BL14.3 is a fixed-energy side station (13.8 keV). They feature state-of-the-art experimental stations and ancillary facilities, serving more than 100 research groups across Europe. With almost 3000 protein structures measured at BESSY II that have resulted in protein data base (PDB) depositions so far, they are the most productive MX-stations in Germany.

The experimental endstation of BL14.1 provides high degree of automation and is equipped with a PILATUS 6M detector, a CATS sample changer robot and an MD2 multi-axis goniometer. BL14.2 features a PILATUS3 S 2M detector, a G-Rob sample changer and a piezo-controlled nanodiffractometer. Its sample dewar can accommodate up to 294 samples, supporting both, SPINE- and UNIPUCK standards, allowing for high sample-throughput data collection. BL14.3 is equipped with a fast MD2-S microdiffractometer, including a mini-kappa axis and a plate manipulator option for *in situ*-crystal screening, supporting several types of 96-well plates. Furthermore, an HCLab dehydration device is available that can be used in combination with a REX rapid nozzle exchanger to freeze samples in a defined hydration state within less than a second.

[1] U. Mueller et al., *J. Synch. Rad.* **19**, (2012), 442

[2] U. Mueller et al., *Eur. Phys. J. Plus* **130**, (2015), 141

[3] M. Gerlach et al., *Journal of large-scale research facilities* **2**, (2016), A47

## GI-MS46-P08 | NEW TRICKS FOR AN OLD DOG: THE POWDER DIFFRACTION AND TOTAL SCATTERING BEAMLINE P02.1 AT PETRA III, DESY

Wharmby, Michael (Deutsches Elektronen Synchrotron (DESY), Hamburg, GER); Etter, Martin (Deutsches Elektronen-Synchrotron (DESY), Hamburg, GER); Schoekel, Alexander (Deutsches Elektronen-Synchrotron (DESY), Hamburg, GER); Tseng, Jo-Chi (Deutsches Elektronen-Synchrotron (DESY), Hamburg, GER); Wendt, Mario (Deutsches Elektronen-Synchrotron (DESY), Hamburg, GER); Wenz, Sergej (Deutsches Elektronen-Synchrotron (DESY), Hamburg, GER)

Powder X-ray diffraction (PXRD) is widely used as an initial characterisation method or to study bulk behaviour of periodic solids under application of external stimuli. In many cases, local structural changes which occur are as interesting as the periodic behaviour; moreover, being able to probe partially or fully amorphous compounds, by Pair Distribution Function (PDF) analysis, allows the researcher to investigate a wider range of samples. Following a recent upgrade of the Powder Diffraction and Total Scattering Beamline (PETRA III, DESY, Hamburg), it is now possible to simultaneously collect PXRD and total scattering data (which can be processed into PDFs). With a fixed energy of 60keV the beamline provides total scattering data at  $Q_{\text{Max}}$  up to  $30\text{\AA}^{-1}$ . PXRD data suitable for Rietveld refinement can be collected with a resolution of  $0.005^\circ$  ( $\Delta Q \sim 2.65 \times 10^{-3} \text{\AA}^{-1}$ ) over an angular range of  $0-12^\circ 2\theta$ . New software to automatically process 2d diffraction data and a sample changing robot have recently been incorporated to automate beamline operation. Furthermore, a wide range of non-ambient sample environments are available for beamline users to investigate *in situ* or *operando* behaviour of their samples, including variable temperatures (hot-air blower: RT-1100K; cryostream: 90-500K; cryostat: 10-300K), gas sorption (up to 1bar pressure) and electrochemistry.

This poster provides an opportunity for current and future users to find out about the recent developments at P02.1, as well as future plans for automation. It is also a chance to discuss these and other user requirements for upcoming beamtime applications.

## GI-MS46-P09 | NMX MACROMOLECULAR DIFFRACTOMETER AT ESS

Aprigliano, Giuseppe (European Spallation Source ESS ERIC, Lund, SWE); Nagy, Gergely (Wigner Research Centre for Physics, Budapest, HUN); Markó, Márton (Wigner Research Centre for Physics, Budapest, HUN); Ferrer, Jean-Luc (Institut de Biologie Structurale, Grenoble, FRA); Pfeiffer, Dorothea (European Spallation Source ESS ERIC, Lund, SWE); Andersen, Ken (European Spallation Source ESS ERIC, Lund, SWE); Oksanen, Esko (European Spallation Source ESS ERIC, Lund, SWE)

The European Spallation Source (ESS) to be built in Lund, Sweden will be the most powerful source of neutrons in the world and will be available to users from 2023. The ESS long pulse source is well suited for structural biology techniques such as macromolecular crystallography or small-angle neutron scattering (SANS). A time-of-flight (TOF) quasi-Laue macromolecular diffractometer NMX is optimised for small samples and large unit cells in order to locate the hydrogen atoms relevant for the function of biological macromolecules. We estimate that NMX at the ESS could be used to collect data from crystals of ~200  $\mu\text{m}$  dimension in a few days, which represent an order of magnitude improvement in both crystal size and data collection time over currently available sources. The robotic detector positioning system also overcomes present limitations in unit cell size can resolve cell edges up to 300 Å. This would broaden the range of systems that can be investigated by neutrons to many biologically very interesting molecules, including membrane proteins such as proton pumps and would transform neutron crystallography into a technique that could answer a significantly larger number of hydrogen related questions in biomolecular science than before.

## GI-MS46-P10 | EXPLORING NEW DATA COLLECTION PROTOCOLS WITH THE EIGER2 DETECTOR AND SMARGON ON THE VARIABLE AND MICROFOCUS BEAMLINE I04 AT DIAMOND LIGHT SOURCE

Flaig, Ralf (Diamond Light Source, Didcot, GBR)

The variable and microfocus beamline I04 at Diamond [1] has recently installed the first second generation Eiger2 X 16M detector. The combination with the SmarGon multi-axis goniometer, which is now in use routinely, and fast variable beam focus is enabling new scientific capability and easy optimisation of the experiment based on sample property. This can be addressed by applying improved data collection protocols. The hardware combination on the beamline has not only enabled significantly faster data collection, which is benefitting from the improved detector performance and specifications, but also very fast grid scans which is enabling automated data collection based on sample detection using X-ray centring. In addition, the multi-axis SmarGon goniometer is enabling an easy setup of multi-sweep, multi-orientation data collection protocols that are particularly useful for SAD experiments or stepped transmission data collections [2]. The beamline is now starting to explore non-standard experiments and developments (e.g. serial crystallography or drop on-demand experiments) with a new sample delivery experiments platform that allows fast positioning and scanning. Further work is ongoing with the aim of streamlining the experiments and user experience and an outlook will be given.

[1] <https://www.diamond.ac.uk/Instruments/Mx/I04.html>

[2] How best to use photons, Winter, G. *et al.*, *Acta Cryst.* (2019). **D75**, 242-261

## GI-MS46-P11 | CURRENT STATUS OF SAMPLE EXCHANGE ROBOTS AT THE PHOTON FACTORY MACROMOLECULAR CRYSTALLOGRAPHY BEAMLINES

Hiraki, Masahiko (Mechanical Engineering Center, Applied Research Laboratory, KEK, Tsukuba, JPN); Matsugaki, Naohiro (Structural Biology Research Center, Institute of Materials Structure Science, KEK, Tsukuba, JPN); Yamada, Yusuke (Structural Biology Research Center, Institute of Materials Structure Science, KEK, Tsukuba, JPN); Hikita, Masahide (Structural Biology Research Center, Institute of Materials Structure Science, KEK, Tsukuba, JPN); Senda, Toshiya (Structural Biology Research Center, Institute of Materials Structure Science, KEK, Tsukuba, JPN)

Structural Biology Research Center of Institute of Materials Structure Science operates five macromolecular crystallography beamlines at Photon Factory. We have developed sample exchange robots to achieve high-throughput, remote-controlled and/or fully-automated experiments. We developed and installed double tongs system that can grasp two cryo-pins simultaneously for rapid sample exchange on the robot PAM at beamlines BL-5A, BL-17A, AR-NW12A and AR-NE3A. A beamline BL-1A was built for low energy SAD experiments and PAM was also installed. Because we covered a diffractometer with a helium chamber for effective low energy experiments, we developed another sample exchange robot PAM-HC. Only the Uni-Puck can be used for PAM-HC. We are developing a lid of PAM and PAM-HC. The lid consists of several doughnut shape plates and moves according to the movement of the robot arm. PAM can exchange cryo-pins for 10 seconds, but it takes 80 seconds for taking cryo-pin in and out a cassette under liquid nitrogen. This behavior is carried out in parallel with sample centering and diffraction experiment. Because fast detectors were installed in our all beamlines, a faster sample exchange robot is desired. Then with a cooperation of RIKEN and JASRI, we are developing a new sample exchange robot PAM3 having both features of double tongs of PAM and simple movement of PAM-HC.

## GI-MS46-P12 | FXE STATUS: FEMTOSECOND X-RAY EXPERIMENTS FOR CHEMICAL DYNAMICS RESEARCH AT THE EUROPEAN XFEL

Rodriguez Fernandez, Angel (European XFEL, Schenefeld, GER); Bressler, Christian (European XFEL, Schenefeld, GER); Gawelda, Wojciech (European XFEL, Schenefeld, GER); Galler, Andreas (European XFEL, Schenefeld, GER); Khakhulin, Dmitry (European XFEL, Schenefeld, GER); Zalden, Peter (European XFEL, Schenefeld, GER); Alves Lima, Federico (European XFEL, Schenefeld, GER); Kubicek, Katharina (European XFEL, Schenefeld 4, GER)

The instrument for Femtosecond X-ray Experiments (FXE) at the European X-ray Free Electron Laser (Eu XFEL) is a instrument desing for measuring the electronic and geometric sturcture changes on matter. Different techniques are available at the FXE instrument for both X-ray scattering (XRD) and X-ray emission spectroscopy (XES). XES is sensitive to electronic changes, such as oxidation and spin states, while x-ray absorption fine structure tools deliver information about the local geometric structure around the selected absorbing atom. Combining these tools with forward scattering in one single setup allows extracting simultaneous information about the local to rather global structural changes occurring in the reacting system.

We will present some case examples, for which pico- and femtosecond x-ray experiments deliver new insight into evolving dynamic processes, including reactive high-valent iron compounds and a class of spin transition systems. This will be preceded by an introduction about the information content of x-ray tools.

Finally, we will present the current status of this new instrument at European XFEL together with some results.

## GI-MS46-P13 | CALIPSOPLUS - OVERVIEW AND TARGETED RESEARCH POSSIBILITIES

Seidlhofer, Beatrix-Kamelia (Helmholtz-Zentrum Berlin, Berlin, GER)

The Trans-national Access programme of the project CALIPSOplus (Convenient Access to Light Sources Open to Innovation, Science and to the World), funded by the European Commission within the EU Framework Programme for Research and Innovation Horizon 2020, supports access of European researchers to European and Middle Eastern light sources. The consortium consists of 19 partner organisations from 12 countries, involving a total of 14 synchrotrons and 8 free electron lasers totalling up to 82 500 hours of available experimental time.

Free access to the infrastructures is complemented by CALIPSOplus, which offers financial support to users coming from EU Member States or Associated States in the form of travel funding. CALIPSOplus also runs a special programme focused on leveraging scientific excellence across the EU and widening the use of light sources throughout the region. With the Twinning programme, researchers not yet active in synchrotron-based research are partnered with an experienced group for a hands-on introduction to the facilities. The short stay is fully financed. This programme aims at establishing and further developing new scientific communities, particularly from countries without own light source.

In this contribution, a short overview of the project, the scientific infrastructures available and a variety of research opportunities as well as first achievements will be presented.

## GI-MS46-P14 | A NEW SINGLE CRYSTAL DIFFRACTOMETER AT BM20/ESRF

Hennig, Christoph (Helmholtz-Zentrum Dresden-Rossendorf e. V., Dresden, GER); Ikeda-Ohno, Atsushi (Helmholtz-Zentrum Dresden-Rossendorf, Dresden, GER); Radoske, Thomas (Helmholtz-Zentrum Dresden-Rossendorf, Dresden, GER); Scheinost, Andreas C. (Helmholtz-Zentrum Dresden-Rossendorf, Dresden, GER)

The Institute of Resource Ecology / Helmholtz-Zentrum Dresden-Rossendorf operates since 20 years the Rossendorf Beamline (ROBL/BM20) at the European Synchrotron Radiation Facility (ESRF) [1]. A new diffractometer for single crystal diffraction will be installed at the beamline until July 2020.

This diffractometer intends to fill the gap between small and large molecule crystallography. The photon flux of up to  $10^{12}$  photons/sec allow the structure determination of small single crystals. The analysis of complex intergrown crystals and electron density studies is possible. The energy range of 5-35 keV allows the use of anomalous dispersion. In-situ experiments will be supported.

This objective requires the combination of a large detector, precise sample position and sufficient space for additional equipment. The diffractometer consists of an adjustable granite table with a metal frame which carry a Pilatus3 X 2M detector. The detector can be tilted and the distance between sample and detector can be varied from 140 to 600 mm. Samples will be mounted on a kappa goniometer. A microscope will be placed in a distance 170 mm from the crystal, which allows to install a cryo cooler (80-400 K), a heater (up to 1200 K), and a Vortex X90 CUBE silicon drift detector with a FalconX1 processor to align small crystals. The fluorescence detector serves also to determine simultaneously oxidation states of metals with XANES spectroscopy. The data extraction will be performed with CRYVALIS.

[1] <http://www.esrf.eu/UsersAndScience/Experiments/CRG/BM20>

## GI-MS46-P15 | BIOLOGICAL USER SUPPORT AT THE EUROPEAN XFEL

Schubert, Robin (European XFEL, Schenefeld, GER); Han, Huijong (European XFEL, Schenefeld, GER); Meza, Domingo (European XFEL, Schenefeld, GER); Round, Ekaterina (EMBL Hamburg Outstation, Hamburg, GER); Schulz, Joachim (European XFEL, Schenefeld, GER); Lorenzen, Kristina (European XFEL, Schenefeld, GER)

The **European XFEL Sample Environment and Characterization** group provides in-house expertise in sample preparation, delivery and diagnostics methods for the six scientific instruments at European XFEL. The group operates the user sample preparation laboratories and aims to provide excellent support for users coming for beam-time. This includes supporting them with state-of-the-art sample preparation and characterization methods as well as the support and development of novel sample delivery techniques.

The Sample Environment and Characterization group provides large scale instrumentation like X-ray generators, electron microscopes and vacuum test chambers and is involved in the fields of surface science, fluidic systems, cryogenics, magnetism, chemistry, and biology to provide assistance for users preparing their samples and bringing their samples into the beam.

The XBI User Consortium operates sample preparation and characterization facilities for biological samples at the European XFEL. This purpose built laboratory offers a wide range of biochemical and biophysical characterization techniques. The Sample Environment and Characterization and XBI staff can support users in all steps from gene expression through protein purification, biophysical characterization, and crystallization up to sample delivery of both crystalline and non-crystalline samples of a wide range of biological systems at the instruments of the European XFEL.

The poster will present an overview about available equipment in the labs. In addition, possible workflows for sample preparation and characterization are combined and visualized. It serves as a roadmap to optimize samples step by step in order to ensure the best sample quality for experiments at European XFEL.

## GI-MS46-P16 | LONG-WAVELENGTH PROTEIN CRYSTALLOGRAPHY AT DIAMOND LIGHT

### SOURCE

Mykhaylyk, Vitaliy (DLS, Didcot, GBR); Duman, Ramona (DLS, Didcot, GBR); El-Omari, Kamel (DLS, Didcot, GBR); Wagner, Armin (DLS, Didcot, GBR)

The long wavelength I23 beamline at Diamond Light Source is a unique facility dedicated to streamline solving the crystallographic phase problem by conducting anomalous dispersion experiments close to the atomic absorption edges of light atoms naturally occurring in proteins. The beamline operates in a core wavelength range from 1.5 to 4 Å, offering an experimental setup complementing a suite of five MX beamlines at Diamond Light Source. To minimize absorption effects, the entire beamline including end station with goniometer and detector operate in vacuum environment ( $<10^{-7}$  mbar). Cooling the samples during storage, transfer and data collection is realized through the manifold of conductive links connecting pulse tube cryocoolers with sample storage and kappa goniometer. A large cylindrical Pilatus 12M detector allows access to diffraction data up to  $2\theta = \pm 90^\circ$  that in combination with the absence of X-ray scattering results in superior quality of diffraction data.

The unique wavelength range towards the sulfur and phosphorous K-absorption edges opens new opportunities for macromolecular crystallography. A multitude of native phasing experiments can be performed, including sulphur/phosphorus single wavelength anomalous dispersion (S/P-SAD). Additionally, access to the absorption edges of calcium, potassium and chlorine allows an unambiguous determination of ions from these biologically vital elements. Recent results from the beamline and the emerging novel applications from extending the wavelength range will be discussed. Examples will be shown on identification of using anomalous contrast as well as structures solved on the beamline based on the anomalous signal from S, Cl, I, K, Ca, V.

## GI-MS46-P17 | ADVANCED PROTEIN CRYSTALLISATION FOR NEUTRON MACROMOLECULAR CRYSTALLOGRAPHY

Brockhauser, Sandor (European XFEL GmbH, Schenefeld, GER); Brockhauser, Sandor (Biological Research Center, Hungarian Academy of Sciences, Szeged, HUN); Oksanen, Esko (European Spallation Source ESS ERIC, Lund, SWE); Csankó, Krisztián (Biological Research Center, Hungarian Academy of Sciences, Szeged, HUN); Szegletes, Zita (Biological Research Center, Hungarian Academy of Sciences, Szeged, HUN); Harmat, Veronika (Eötvös Loránd University, Institute of Chemistry, Budapest, HUN); Bugris, Valéria (Biological Research Center, Hungarian Academy of Sciences, Szeged, HUN)

The major tool to determine the 3D structure with atomic resolution of large molecules is X-ray crystallography. With X-ray data collection heavy atoms could be seen for 3D structure calculation, but the position of hydrogen atoms, which are biologically important could only be estimated due to the fact that such small atoms couldn't diffract high energy radiation and particle radiation. To locate these hydrogens the frequently used methods are 2D-NMR and Neutron Crystallography where the hydrogens are replaced with a heavier isotope → deuterium atoms that can produce cleaner neutron diffraction. With the combination of the listed methods, the complete biologically active macromolecular structure and function could be determined. In collaboration with European Spallation Source, we have developed a method to produce standard deuterated test crystals for instrument characterisation. The method can be extended to support hanging and sitting drop crystallisation experiments in deuterated environment.

## GI-MS46-P17 | USER INFRASTRUCTURES AT THE HELMHOLTZ-ZENTRUM BERLIN FÜR MATERIALIEN UND ENERGIE HZB

Wolter, Bettina (Helmholtz-Zentrum Berlin für Materialien und Energie GmbH, Berlin, GER)

Helmholtz-Zentrum Berlin für Materialien und Energie is a world-class research centre for energy materials research, contributing to knowledge-based solutions to great societal challenges. HZB explores synergies by integrating excellent research with the operation of dedicated infrastructures to create a unique research environment. We provide BESSY II a third-generation synchrotron radiation source for the national as well as international scientific community and industry. BESSY II delivers brilliant X-ray light from Terahertz to hard X-rays with an emphasis on soft X-rays which allows the investigation of a wide range of materials from semiconductors and nanomaterials to polymers and proteins towards meteorites and archaeological artefacts. EMIL, our Energy Materials In-Situ Laboratory, directly adjoins BESSY II and enables insights into thin-film materials to be obtained during their actual fabrication processes. Our multi-user platform CoreLabs at HZB complements the synchrotron infrastructures. CoreLabs are dedicated to research and development of new and improved materials for energy conversion and storage applications as well as energy-efficient future IT. They provide state-of-the-art laboratories and unique equipment and will serve the wider scientific community by offering services and access to external academic and industrial partners. Modern X-ray diffractometers are available in the X-Ray CoreLab for crystallography analyses. The Correlative Microscopy and Spectroscopy CoreLab is being operated in collaboration with ZEISS labs@location. Researchers are able to fabricate and image nanomaterials using the very latest electron and ion microscopes. The development of hybrid materials and components based on silicon and perovskite used for energy conversion is the task of the HySPRINT CoreLab.

## MS46-P140 LATE | XALOC, THE MX BEAMLINE AT ALBA SYNCHROTRON: CURRENT STATUS AND PERSPECTIVES

Gil-Ortiz, Fernando (ALBA Synchrotron, Cerdanyola del Valles, ESP); Carpena, Xavier (ALBA Synchrotron, Cerdanyola del Valles, ESP); Calisto, Barbara (ALBA Synchrotron, Cerdanyola del Valles, ESP); Gonzalez, Nahikari (ALBA Synchrotron, Cerdanyola del Valles, ESP); Alvarez, Jose Maria (ALBA Synchrotron, Cerdanyola del Valles, ESP); Andreu, Jordi (ALBA Synchrotron, Cerdanyola del Valles, ESP); Valcarcel, Ricardo (ALBA Synchrotron, Cerdanyola del Valles, ESP); Avila, Jose (ALBA Synchrotron, Cerdanyola del Valles, ESP); Villanueva, Jorge (ALBA Synchrotron, Cerdanyola del Valles, ESP); Juanhuix, Judith (ALBA Synchrotron, Cerdanyola del Valles, ESP); Boer, Roeland (ALBA Synchrotron, Cerdanyola del Valles, ESP)

XALOC is a tunable MX beamline, in user operation since 2012, located at the 3<sup>rd</sup> generation synchrotron ALBA (Barcelona). XALOC has been designed to deal with automatable X-ray diffraction experiments of micrometer-sized crystals, including a variety of crystal sizes, unit-cell dimensions and crystals with high mosaic spread and/or poor diffraction. The aim for a reliable all-in-one beamline is equaled by the aim to maximize ease-of-use and automatization. Mail-in data collection is now in routine operation and dewar transport expenses are covered for users from Spain and abroad. To achieve a high-throughput MX beamline, we have implemented a new double gripper at the CATS sample changer that allows sample interchange in less than 20 seconds. Besides, an improvement in the CATS dewar allows to allocate up to 6 Unipucks (96 samples). EMBL/ESRF pucks are also acceptable with a capacity of 30 samples. In addition, MXCube and ISPyB software platforms for data collection and sample tracking/experiment reporting are routinely used at the beamline, allowing automated centering and the possibility to download the results obtained with the EDNA automated data processing pipeline through a web browser (<https://ispyb.cells.es/>). Native data collection has been facilitated by a Helium chamber developed “in-house” providing initial promising results. The beamline allows “in-situ” diffraction and serial crystallography experiments have been carried out successfully. XALOC is continuously open to new proposals providing beamtime within a few weeks. Current possibilities and upgrades that will become available in the near future will be discussed.

## GI-MS47: Women in Crystallography

---

### GI-MS47-01 | 32 YEARS OF TRAVELS IN CRYSTALLOGRAPHY

Garman, Elspeth (University of Oxford, Oxford, GBR)

Crystallography has a proud historical record and current practice of outstanding researchers who were/are women. It is interesting to reflect on why this aspect of our field is a positive outlier in the STEM arena, and also how this can not only be maintained but also improved upon. The Braggs, father and son, contrary to the norm for the times during which they worked, had many women in their research groups (WH Bragg: 10/17 and WL Bragg 4/6 [1]), establishing crystallography as a subject in which women don't just survive, but in which they can excel. Crystallographers trained by the Braggs then became inspiring role models for several more generations of highly successful female researchers.

I have been privileged to know and work with some of these scientists, and in this highly personal account, I will comment on the general attitude and climate towards women in STEM and how it is changing and still needs to improve. I will draw on my experiences as a scientist who happens to be a woman, as well as tracking research on developing new methods in structural biology with which I have been involved during the last 32 years.

[1] Maureen M. Julian, "Women in Crystallography," in *Women of Science: Righting the Record*, ed. G. Kass-Simon and Patricia Farnes (Bloomington: Indiana University Press, 1990), pp. 342

## GI-MS47-02 | WOMEN IN SCIENCE – AN AFRICAN PERSPECTIVE

Haynes, Delia (Stellenbosch University, Stellenbosch, ZAF)

This presentation will consider the issues faced by women in science from the African perspective. Many of the problems faced by women in Africa are the same as those faced by our colleagues around the world, but some challenges are unique to the African continent. The perspectives of women from across Africa, particularly those involved in crystallography, a growing field on the continent, will be shared. Suggestions for effecting change from the scientists themselves will also be discussed.

## GI-MS47-03 | MODEST RECOGNITION FOR HIGH ACHIEVEMENTS

Kojic-Prodic, Biserka (Rudjer Boškovic Institute, Zagreb, HRV)

There are women at the highest political and business positions, obviously they are getting closer to the gender equality. In science such relations are exceptions. One should expect that the progress in technology will change these relations. Crystallography has immensely influenced technology over a century. Numerous Nobel Prizes for crystallography convincingly illustrate an impact of the field on other branches of science and technology. Among them two were awarded to ladies D. C. Hodgkin (1964) and A. Yonath (2009). In spite of unexpectedly high number of women in crystallography and their significant contributions, they have not been adequately recognised.

During 72 years of IUCr there were 3 lady-presidents, only. A. Bacchi, the first lady-president of ECA was elected after three decades of male domination. The list of extraordinary women in crystallography who were deprived from recognition would surprise many of us. In order to be realistic, one should admit that male scientists are also not saved from such life disappointments. There are strong demands for positive changes and IUCr is working permanently to reach gender equity.

An impact of women on crystallography in Croatia and former Yugoslavia will be presented; the most influential persons and their achievements will be briefly illustrated. Yugoslav Crystallographic Association was established 1966 and in 1991 Croatian Association was formed. In both associations about 50% members have been women. D. Matković Čalogović is the only lady-president of the national association (2018) and M. Đaković is vice-president of ECA (2018).

## GI-MS47-04 | “It’s JUST LIKE PLANNING A DINNER...” - WOMEN IN CRYSTALLOGRAPHIC COMPUTING

Thorn, Andrea (University of Würzburg, Würzburg, GER)

In the early days of crystallography, every structure solution involved performing many laborious and repetitive calculations. Up until the 1960s, this kind of manually performed computation as well as coding were considered predominantly women’s work [1] - and advertised as such in magazines like Cosmopolitan.

The women who played a pivotal role in early crystallography contributed almost all also to crystallographic computation [2]: Kathleen Lonsdale, Helen Dick Megaw, Dorothy Hodgkin, and Isabella Karle, just to name a few; and their work inspired later generations. However, today, the number of women developing new computational techniques seems to be declining.

This talk will search for reasons, give a historical perspective for the future of female methods developers and highlight how crystallographers of all genders can start to develop their own software, methods and algorithms.

[1] Thompson, C. (2019) "The Secret History of Women in Coding", New York Times

[2] Neumann, W., Benz, K.-W. (2018) "Kristalle verändern unsere Welt: Struktur – Eigenschaften – Anwendungen", De Gruyter, Berlin/Boston, 2018

## GI-MS47-05 | WOMEN IN A HISTORICAL FRENCH LABORATORY OF CRYSTALLOGRAPHY

Cabaret, Delphine (Sorbonne Université, Paris, FRA); Brouder, Christian (Sorbonne Université, CNRS, Paris, FRA)

The Chair of Mineralogy of The Sorbonne, created in 1809 for René-Just Haüy, evolved to the present Institute of Mineralogy, Materials Physics and Cosmochemistry (IMPMC) of Sorbonne Université. Brilliant women crystallographers have been working or still work in this laboratory, which also is the headquarter of the two French societies of crystallography (AFC and SFMC). The research activities of these women scientists range from experimental to theoretical diffraction, and concern the exploration of extraterrestrial samples as well as the development of synchrotron beamlines.

In this talk, we will examine the careers of some women researchers of our laboratory, who had striking contributions in the French crystallography from the 60s to nowadays. This presentation will be set in a more general context of women crystallographers in Paris in the twentieth century.

## GI-MS48: Teaching New Dogs Old Tricks

---

### GI-MS48-01 | SOME REFLECTIONS ON SYMMETRY

Clegg, William (Newcastle University, Prudhoe, GBR)

Surely nobody needs to learn any details of symmetry these days - point groups, space groups, Laue classes... After all, the decisions we once had to make are looked after now by automatic software. Diffractometer control programs choose the unit cell and probable space group, and set up an appropriate data collection strategy. The space group is more clearly decided by post-collection data processing and analysis with virtually no user intervention. Modern structure solution methods don't assume a particular space group anyway; they find it as part of solving the structure. And symmetry-imposed constraints on atom positions and displacements are worked out automatically, along with the correct asymmetric unit for Fourier map calculations. This may be true for lots of routine well-behaved structures, but major developments in radiation sources and detectors, together with research interest in more challenging materials, are increasingly presenting us with problems that are anything but routine, and a knowledge of basic symmetry concepts and their consequences is vital if we are to avoid mistakes. Particular aspects include pseudosymmetry (especially structures in which homochiral molecules are related by approximate inversion centres), structures with several chemically identical molecules in the asymmetric unit, and twinning, where the distinction between apparent and real symmetry of reciprocal and direct spaces is important. The talk will cover both principles and specific examples.

## GI-MS48-02 | SEEING IS BELIEVING: MODEL FINALISATION AND INTERPRETATION OF RESULTS

Linden, Anthony (University of Zurich, Zürich, CH)

User-friendly software and tools for solving, model-building and refining structures have advanced tremendously over the last 15 years or so. Even fully-automated routines are available, which, in many cases, do a handsome job of producing an almost finished structure. This talk will look at some of the ways of going beyond the automatic and push-button procedures to ensure that the final structure model is truly correct and the best possible outcome from the data at hand. Aside from validation with *checkCIF*, simply looking at and rotating the structure model on-screen can give a good impression of the quality of the results; if it looks weird, it probably is. Unusual geometry, strange-looking atomic displacement ellipsoids or inexplicable residual electron density peaks can all be indicators that the structure model (or the reflection data) is deficient in some way and might be in need of additional thought. After the refinement has been completed and validated, the real objective of the study, to answer a scientific question that lead to the need for a structure determination in the first place, can hopefully be addressed. This involves interpretation of the results. The presentation will discuss how to derive, compare and correctly evaluate useful information from the structure determination, while keeping in mind the statistical significance of any numerical differences.

## GI-MS48-03 | THE DIFFERENCE ELECTRON DENSITY MAP AS A CRYSTAL STRUCTURE

### VALIDATION TOOL

Spek, Ton (Utrecht University, Utrecht)

Structure validation as implemented by the IUCr aims at providing authors, referees, readers and users a tool to evaluate the results of a crystal structure report. The WEB based checkCIF tool offers a list of alerted for issues, ALERTS, to be inspected, acted or commented upon. ALERTS may report issues ranging from potentially serious (i.e. A-level ALERTS) to interesting info but not necessarily erroneous (i.e. G-level ALERTS). The messages are short assuming sufficient crystallographic knowledge of their meaning. For each ALERT there is also some explanatory WEB-based text available. Most ALERTS have their origin with issues encountered in the past with papers submitted to Acta Crystallographica journals. The set of ALERTS is frequently extended and finetuned on the basis reported new issues. Several ALERTS are based on information that can be derived from a difference electron density map. Alternatively, a significantly number of ALERTS are based on the analysis of the FCF file. Details with examples of this tool along with those of some other tools will be discussed in this talk.

## GI-MS48-04 | CRYSTAL STRUCTURE EXPLORATION – I DIDN'T KNOW MERCURY COULD DO THAT!

Stevens, Joanna (The Cambridge Crystallographic Data Centre, Cambridge, GBR); Maloney, Andrew (The Cambridge Crystallographic Data Centre, Cambridge, GBR)

It's been an 18-year journey from leaving Pluto for Mercury, the original to current version (4.0) of the CCDC's visualisation software – and it's come a long way, having boldly gone beyond its original mission as a simple package for the display of crystal structures.

Mercury has developed into a powerful platform, encompassing a wide range of structural analysis and visualisation capabilities, delivering analysis, design and prediction functionality. This includes the ability to easily examine interactions and symmetry elements, structure editing and overlaying of structures, through to tools for assessing and ultimately gaining insights in different aspects such as hydrogen bonding, conformation and packing. This is not to mention the interactive data analysis functionality and interfacing with results from searching the Cambridge Structural Database, the collective repository for small-molecule organic and metal-organic crystal structures.

This presentation will highlight some of the less well known, underutilised or simply overlooked features within Mercury, in order to more effectively explore your crystal structures and the universe of crystallography.

[1] Mercury CSD 2.0 – new features for the visualization and investigation of crystal structures, C. F. Macrae, I. J. Bruno, J. A. Chisholm, P. R. Edgington, P. McCabe, E. Pidcock, L. Rodriguez-Monge, R. Taylor, J. van de Streek and P. A. Wood, *J. Appl. Cryst.*, 2008, 41, 466–470, DOI: 10.1107/S0021889807067908

[2] The Cambridge Structural Database, C. R. Groom, I. J. Bruno, M. P. Lightfoot and S. C. Ward, *Acta Cryst.*, 2016, B72, 171-179, DOI: 10.1107/S2052520616003954

## GI-MS48-05 | RESOLUTION OF CRYSTALLOGRAPHIC PROBLEMS USING THE BILBAO

### CRYSTALLOGRAPHIC SERVER

de la Flor, Gemma (Institute of Applied Geosciences, Karlsruhe Institute of Technology, Karlsruhe, GER); Tasci, Emre (Department of Physics Engineering, Hacettepe University, Ankara, TUR); Elcoro, Luis (Departamento Física de la Materia Condensada, Universidad del País Vasco UPV/EHU, Leioa, ESP); Madariaga, Gotzon (Departamento Física de la Materia Condensada, Universidad del País Vasco UPV/EHU, Leioa, ESP); Perez-Mato, Juan Manuel (Departamento Física de la Materia Condensada, Universidad del País Vasco UPV/EHU, Leioa, ESP); Aroyo, Mois I. (Departamento Física de la Materia Condensada, Universidad del País Vasco UPV/EHU, Leioa, ESP)

Operating since 1997, the *Bilbao Crystallographic Server* ([www.cryst.ehu.es](http://www.cryst.ehu.es)) is a free web site that grants access to specialized databases and tools for the resolution of different types of problems related to crystallography, solid-state physics and structural chemistry. The server is built on a core of databases that contain crystallographic data of space, magnetic, subperiodic, double, plane and point groups, their representations and group-subgroup relations [1-2]. The programs available on the Bilbao Crystallographic Server aim to bring the potential of symmetry and group theory to those users who are not necessarily experts in this matter but want to benefit from them in their studies. Therefore, the purpose of this contribution is to show by illustrative examples the utility of the server in the resolution of different common problems that many theoretical and experimental crystallographers face everyday. Different systems such as layered materials, magnetic structures, ferroelectric materials, topological insulators and modulated structures can be analyzed by our software. A wide range of topics are covered by our programs, from fundamentals of crystallography to more advanced problems such as the prediction of phase transitions, identification of ferroic materials, detection of false symmetry assignments, planification of Raman scattering experiments or to cross-check different experimental and/or theoretical structural models of the same phase coming from different sources. Some of these topics will be discussed in this contribution.

[1] M. I. Aroyo et al. (2006) *Z. Kristallog.*, 221, 15-27

[2] M. I. Aroyo et al. (2011) *Bulgarian Chemical Communication*, 43(2), 183-197

## GI-MS48-P01 | HOW BEST TO SEARCH AND LOOK FOR CHAOS IN CRYSTALS BY DIFFRACTOMETRIC METHODS

Kodess, Boris (FSUE "VNIIMS", ICSE, Moscow, RUS)

In a crystals there are structural defects or the local disorder due to impurity atoms. The existing and developed models of the crystal structure describe the accumulation of defects and originate of a web of defects, which condition the transition to a quasi-crystalline or amorphous state of substance. How accurately find these defects and determine a signs of transition from strong order to weak turbulent state or strong and transformative, and sometimes destructive chaotic behavior of some characteristics of crystals?

The defects classification and diffractometric methods is related to the length scales of the phenomena in crystals. An increase in the number of disturbances in the arrangement of atoms may leads to the static displacements of atoms. The displacements are fixed by precision measurements of the single crystals diffraction pattern and/or by the results of low-temperature measurements. With have an increase in scale and the number of defects, a microstructure arises in the samples. Microstructural defects are analyzed by measuring the integral width of Bragg reflections. The next type of defects is associated with reaction or adaptation to high surface tension and/or to chemical exposures. These defects are determined by the changes angular positions results and/or the time series of these angular positions observation. For example, we has been observed oscillatory changes of the angular positions during the long-time series (from 250 to 950 hours) for YBCO breathing-crystal [1]. Another examples is the chaotic behavior in the vicinity of phase transitions in the KDP, others ferroelectrics, Pd(H:Me) and some bio-crystal.

## GI-MS48-P02 | THE HyPIX-ARC 150°

White, Fraser (Rigaku Europe, Neu-Isenberg, GER); Kucharczyk, Damian (Rigaku Polska, Wroclaw, POL); Meyer, Mathias (Rigaku Polska, Wroclaw, POL); Wojciechowski, Jakub (Rigaku Europe, Neu-Isenberg, GER)

The HyPix Arc 150° detector takes the latest, direct X-ray detection, hybrid photon counting technology and forms it into a curved detector for unparalleled data collection efficiency and quality.

As the geometry of a single crystal experiment involves diffraction from a point source, the crystal, the ideal detector would be spherical, encapsulating the sample. Through this simple fact, the advantages of a curved detector, an approximation of the ideal spherical detector have been widely accepted since X-ray crystallography was conducted with photographic film.

The HyPix-Arc 150° applies this approach to the highest performing, currently available detector technology, direct X-ray hybrid photon counting (HPC), for an ultra-high performance detector which provides high data quality, the most consistent measurement conditions for every peak in a dataset and counting of X-ray photons without readout noise or dark noise.

With the recent advances in instrumentation, and now with the HyPix-Arc 150°, a new modern era of interactive crystallography is now possible with ultra short experiments allowing on the fly results and decision making.

The merits of both HPC technology, curved architecture and ultra-fast experiments are discussed, and some results from the HyPix-Arc 150° presented herein.

## GI-MS48-P03 | MICAPENROSE: A WORK OF ART AS A TOOL TO TEACH ANBD POPULARIZE CRYSTALLOGRAPHY

Ravy, Sylvain (Laboratoire de Physique des Solides, Orsay, FRA)

We present a recently created work of art, a Penrose tiling made of mica tiles sandwiched between two sheets of polarizers, and placed on a LED panel of 60 cm x 60 cm. Due to the birefringence of mica, the piece exhibits beautiful and shimmering interference colors, which changes as the viewer moves around. The irregularity of the muscovite mica gives different colors to the tiles themselves, enhancing the shimmering aspect of the piece. The frame is made in aluminium, reminiscent of quasi-crystals. The striking beauty of this artwork encourages the viewer to ask questions about the physical principles involved, the material it is made of, and the tiling it represents.

In this way, we can discuss: the nature of light and its polarization; the interference colors versus the rainbow colors; the birefringence of mica and its relation to its anisotropic, lamellar, atomic, crystalline structure; the chemical binding involved; the short-range ordered polymeric structure of the polarizer; the application of birefringence to mineralogy; the aperiodic long-range ordered crystalline structure represented by the Penrose tiling; the aluminium frame and the quasi-crystalline aluminium alloys. A future version of the piece will include a dislocation of the tiling, broadening the discussion to include the role of defects in solid state physics.

The poster, on which the piece will be installed, will detail all the pedagogical aspects which can be discussed from this very rich artwork.

[1] [https://www.lps.u-psud.fr/IMG/jpg/micapenrose\\_1.jpg?5065/2587a1feab58a0583b0e0a0bc5ddc818372b1f45](https://www.lps.u-psud.fr/IMG/jpg/micapenrose_1.jpg?5065/2587a1feab58a0583b0e0a0bc5ddc818372b1f45)

## GI-MS48-P04 | CRYALISPRO 40: 64-BIT, SYNERGY, HYPIX-ARC 150°, AUTOCHEM4.0, EWALD 3D

Meyer, Mathias (Rigaku Oxford Diffraction, Wroclaw, POL)

The new version of CrysAlis<sup>Pro</sup> (CAP<sup>40</sup>) was released to the general public in May 2019. For the first time it is available in a 32/64-bit version.

CAP<sup>40</sup> also supports all variants of Synergy instrument platforms alongside with a large set of attachments and their proper handling in collision and operation. XtalCheck-S is an in-situ plate checker, which allows automated sample screening using crystallization plates.

The HyPixArc 150 is a new generation of Hybrid Pixel Counters that surrounds the sample in a curve-like fashion giving a massive >150° opening angle. This allows a much more rapid acquisition of complete and redundant data for excellent data quality over much large flat detector arrangements.

CAP<sup>40</sup> also features the new version AutoChem<sup>4.0</sup>. All instrument users can perform standard crystal reference experiments with it to bench mark their systems easily.

The Ewald<sup>3D</sup> tool is further expanded. Users can now use various modes of symmetry expansion to produce more intuitive and meaningful views. During the experiments the patented Ewald<sup>3D</sup> 'live view' allows instant undistorted visualization of the measured data, which is useful for rapid detection of experimental artifacts.

The new 64-bit version features multi-core support of up to 32 cores. The data reduction output now also covers the popular CC<sup>1/2</sup> and other statistic indicators.

The external format compatibility was further expanded and with the 64bit can now handle very demanding synchrotron cases.

The poster will highlight these and other aspects of the new CAP<sup>40</sup>

## GI-MS48-P05 | WANTED -- K-BETA!

Bodensteiner, Michael (University of Regensburg, Regensburg, GER); Mayer, Tobias (University of Regensburg, Regensburg, GER)

The Cu-K $\beta$  wavelength ( $\lambda = 1.39 \text{ \AA}$ ) has been known for a very long time, mostly as result of an unsuccessful alignment of the diffractometer optics. However, there are benefits and powerful features of this radiation that many crystallographers are not aware of. Compared to Cu-K $\alpha$  ( $\lambda = 1.54 \text{ \AA}$ ) the amount of available data is increased by more than 35 per cent and the absorption significantly lowered. The latter is also true for a number of elements (Cu to Y) in comparison to Mo-K $\alpha$  radiation ( $\lambda = 0.71 \text{ \AA}$ ). In addition, the diffraction power as well as the detective quantum efficiency is much higher for Cu-K $\beta$  relative to Mo-K $\alpha$ . Another general advantage of K $\beta$  radiation compared to K $\alpha$  is the absence of  $\alpha_1/\alpha_2$  splitting at higher diffraction angles. This leads to a relative improvement of the  $I/\sigma(I)$  at higher resolution. Our investigations have shown that in many cases almost identical or even better quality structures could be obtained by using Cu-K $\beta$  compared to either Mo or Cu standard K $\alpha$  wavelengths. The presentation will show this at a number of examples and provide insight into the technical and refinement procedures within Cu-K $\beta$  experiments.

## GI-MS48-P06 | A LIFE WITH CRYSTALLOGRAPHY...

Đakovic, Marijana (University of Zagreb, Zagreb, HRV)

To stay living with crystallography or to go...? is a question that probably (earlier or later) crossed minds many of big names in crystallography. Finishing one stage in a career, and needing to decide which direction to go, is a crossing that all need(ed) to pass. Which is the right path to hit?

In this presentation some examples from a real life of a crystallographer, which will provide you with convincing evidences why to stay in the field and share your life with crystallography, will be addressed. Potential answers to questions such as what crystallography can give you, what you can give to crystallography, or pros and cons in dealing with dilemmas to stay at home or to move to the places perceived as places with vivid crystallographic life will be underpin. Or, ...

## GI-MS48-P07 | BENEFITS OF TRANSMISSION MODE IN XRD

Berthier, Eric (Thermo Fisher Scientific, Ardenay, FRA); Pillière, Henry (Thermo Fisher Scientific, Ardenay, FRA)

Powder X-ray diffraction (XRD) is an analytical technique which offer a wide range of instrumental configuration, in order to respond to specific structural characterization. The most frequent setup is based on the irradiation of the sample surface by an incident beam, to allow sample the surface emission of the diffracted signal (Bragg-Brentano or asymmetric geometry). However, diffraction signal can also be obtained by transmission, as described by the Debye-Scherrer geometry. Because of its original instrumental configuration, ARL EQUINOX X-Ray diffractometers allow to perform both setups, and allow to get complementary information on the sample itself. This is the case for bi-dimensional structures like clays, graphite family, etc. For any crystallized material, transmission mode always offers a higher resolution signal, because there is a low impact of the incident angle. Preferred orientation is also minimized, and quantitative analysis is often better accuracy. From a reactional point of view, transmission allow to record sample under a certain conditioning (atmosphere, in a liquid, to avoid reactivity), at room conditions or by applying temperature or pressure. We proposed to show some examples explaining the benefit of transmission mode in XRD.

## GI-MS48-P08 | OLEX2: TEACHING NEW SOFTWARE OLD AND NEW TRICKS

Puschmann, Horst (OlexSys Ltd, Durham, GBR); Dolomanov, Oleg (OlexSys Ltd, Durham, GBR)

Olex2 [1] is now firmly established as a major software package in the field of small-molecule crystallography: new and some (open-minded) old dogs find it a very useful and user-friendly platform from which to perform all sorts of tricks.

This contribution will be in two parts. In the first part, I will present some of the new tricks we have included in Olex2 over the last few years, including the streamlined management of solvent masking, fast refinement using our very own refinement engine olex2.refine [2] and the refinement of standard X-ray structures using non-spherical form factors.

In the second part, I will convince you that Olex2 is the perfect open-source and free platform that YOU can use to teach New Dogs Old Tricks: Programming Olex2 is quite easy and accessible to all, and if you've got an Old Trick, why not consider using Olex2 as a platform to implement it rapidly and then make these available to all of our users?

[1] OLEX2: a complete structure solution, refinement and analysis program

OV Dolomanov, LJ Bourhis, RJ Gildea, JAK Howard, H Puschmann

Journal of Applied Crystallography 42 (2), 339-341

[2] The anatomy of a comprehensive constrained, restrained refinement program for the modern computing environment—Olex2 dissected

LJ Bourhis, OV Dolomanov, RJ Gildea, JAK Howard, H Puschmann

Acta Crystallographica Section A: Foundations and Advances 71 (1), 59-7

## GI-MS48-P09 | CRENEL OR NOT CRENEL, WHAT IS THE FUNCTION?

Duverger-Nédellec, Elen (Charles University, Faculty of Math. & Phys., DCMP, Praha 2, CZE); Bretosh, Kateryna (Laboratoire de Chimie de Coordination du CNRS, Toulouse, FRA); Béreau, Virginie (Laboratoire de Chimie de Coordination du CNRS, Toulouse, FRA); Duhayon, Carine (Laboratoire de Chimie de Coordination du CNRS, Toulouse, FRA); Sutter, Jean-Pascal (Laboratoire de Chimie de Coordination du CNRS, Toulouse, FRA); Petříček, Václav (Institute of Physics CAS, Department of Structure Analysis, Prague 8, CZE)

Modulated structures are not a piece of cake to solve but some of them can be trickier than the others. The most obvious solution is not always the proper one and conscientious verifications of the model have to be done in order to obtain the best structural model. We will focus here on the example of the (3+1)D structure of the FeLN5PhenMeCl<sub>2</sub> complex presenting a typical misleading modulation. The resolution and refinement of the structure were performed using the software Jana2006 [1]. The average structure of FeLN5PhenMeCl<sub>2</sub> was determined using Superflip program. The structure is composed of two superimposed inversed configurations of the complex, indicating the presence of disorder. This disorder is the tricky point of the structural resolution! To model it, two options can be considered: the use of a crenel-type occupational modulation or the use of a sinusoidal occupation-function coupled with a positional modulation function. In the first case, the disorder observed in the average structure is, in fact, a hidden-order: both configurations would exist independently, appearing alternately along the periodicity axis of the modulation. In the second case, the disorder can reflect an ordered-disorder along the fourth dimension: each configuration presents a positional modulation (the order) and a probability of presence given by the occupational modulation (the disorder). Both possibilities will be investigated. Final structures will be observed via the new graphic tool developed in Jana2020 enabling the direct observation of mixed modulations on the structure.

[1] V. Petříček *et al* (2014), Z. Kristallogr. 229(5), 345-352.

## GI-MS48-P10 | MATHEMATICAL JUSTIFICATIONS FOR CRYSTAL SYSTEMS, BRAVAIS LATTICES AND A NEW CONTINUOUS CLASSIFICATION

Kurlin, Vitaliy (University of Liverpool, Liverpool, GBR)

A crystal structure is a periodic arrangement of atoms or molecules in an infinite lattice defined by a linear basis. Crystallography distinguishes crystal systems and Bravais types of lattices. These discrete classes are justified by types of transformations that keep a given lattice stable. The groups of orthogonal transformations define crystal systems (7 in dimension 3). Any lattice has the corresponding quadratic form (a symmetric positive definite matrix) that remains invariant under orthogonal transformations. The general linear group (with integer elements) acts on the space of quadratic forms. Different strata (subgroups of various sizes) that keep a given quadratic form invariant define the Bravais class of the corresponding lattice (14 in dimension 3). Since geometric positions of atoms are continuous, crystals are more naturally classified by continuous invariants stable under atomic vibrations. The talk will outline a new continuous approach that rigorously quantifies a similarity between crystals by a proper metric (a distance function) based on geometric invariants. Then different crystals with the same chemical compositions can be connected by continuous transition paths through lowest energy barriers. Such a continuous map on the space of all crystals will show which shallow minima should be merged with closely located deeper minima that represent realistic crystals.

The ultimate aim is to resolve the "embarrassment of over-prediction" when computers only generate more hypothetical crystals without accurately predicting most promising materials. Parts of this work are done in collaboration with the groups of Andrew Cooper and Matthew Rosseinsky at the Materials Innovation Factory, Liverpool.

## GI-MS48-P11 | PERVASIVE APPROXIMATE SYMMETRY IN P1 AND HIGH-Z' ORGANIC CRYSTALS

Brock, Carolyn P. (University of Kentucky, Lexington, USA)

Ca. half (*i.e.*, 750) of the organic crystal structures in space group  $P1$  with  $Z > 1$ , and ca. 300 more with  $Z' > 4$  (Brock, 2016; *Acta Cryst.* B72, 807), have been investigated in detail. Obvious approximate symmetry has been found in well over 50% of them, while overlooked symmetry was identified in only ca. 10% of the  $P1$  structures and 5% of the  $Z' > 4$  structures. Approximate  $2_1$  screw axes, pseudoinversion centers and pseudotranslations all occur frequently; pseudoglide are less common. A program to find and characterize pseudotranslations (*i.e.*, modulations) has been written (Taylor & Brock, in preparation) and used to find relationships between phases.

The  $P1$  structures examined were not chosen randomly; ca. 60% of them have a cell angle in the range 88.5 – 91.5° because such structures are especially likely to have been described in a cell of too-low symmetry. Ca. 10% more are kryptoracemates, quasiracemates, and compounds of diastereomers. Another ca. 10% were found using the new program that identifies pseudotranslations.

About a quarter of the  $P1$ ,  $Z > 1$  structures examined have obvious layers with approximate 2-D symmetry higher than the 3-D symmetry of the crystal. Offsets between adjacent layers account for the symmetry lowering. If interlayer forces are weaker than intralayer forces then deformations during the early stages of crystal growth are more likely between layers than within them. Perhaps the crystal nucleus is often more symmetric than the macroscopic crystal.

## GI-MS48-P12 | OVERCOMING AMBIGUOUS TAUTOMER ASSIGNMENT IN 1,2,4-TRIAZOLE

### CRYSTAL STRUCTURES

Schwalbe, Carl (Aston University, Birmingham, GBR)

Formerly we located hydrogen atoms in difference maps. Modern software conveniently calculates positions, but 1,2,4-triazole tautomers should provide warning. A hydrogen atom on one of two adjacent N atoms gives *1H* with C-NH and C=N bonds. Placing that H atom on the isolated N atom; *4H*, leaves C=N bonds and approximate  $C_{2v}$  symmetry. The parent *1H* tautomer, TRAZOL02 (neutron data, 15 K, R = 2.9 %) has misleadingly similar C-NH and C=N distances of 1.334 and 1.325 Å but distinctive annular bond angles: 110.20° at NH, 102.67° and 102.89° at “bare” N. Chatar Singh (1965) guided the placement of H atoms by such angles.

High-level *ab initio* calculations (Balabin, 2009) show greater stability of the *tH* tautomer by 6.25 kcal mol<sup>-1</sup>. Searching the November 2018 CSD for neutral 1,2,4-triazoles yielded 198 hits in the *1H* form, just 7 in *4H*. Are these 7 legitimate? CLTRZL and JUGYOB were redetermined as *1H*. DAMTRZ21 with similar cell dimensions to earlier *1H* structures should be *1H*. Endocyclic angles in MAJSOH and both independent triazole moieties of FALDAZ imply *1H*. FUZPOH lacks possible N-H...N interactions, but changing tautomer to *1H* facilitates C-H...N. DEGNIM is credible as *4H*: its triazole ring, incorporated in a crown ether, donates N4-H...O to an enveloped water molecule.

Keywords: 1,2,4-triazoles, tautomers, geometrical criteria

[1] Balabin, R. M. (2009) J. Chem. Phys., 131, 154307.

[2] Chatar Singh (1965) Acta Cryst., 19, 861.

## GI-MS48-P13 | OPTICAL SIMULATION OF CRYSTAL DIFFRACTION USING MODIFIED VIDEO PROJECTORS - A TEACHING PROPOSAL

Lehmann, Jannis (ETH Zurich, Zürich, CH); Tzschaschel, Christian (ETH Zurich, Zürich, CH); Fiebig, Manfred (ETH Zurich, Zürich, CH); Weber, Thomas (ETH Zurich, Zürich, CH)

In this presentation, we will demonstrate an advanced method for teaching the principles of diffraction in the classroom. Using low-cost microdisplays extracted from commercial video projectors, we generate, in real time, optical diffraction patterns of any structure that can be displayed on a computer screen. By upscaling to the optical regime, this interactive framework provides hands-on experience of scattering phenomena that can go beyond simplest-case examples. Hence, it can be applied to perform diffraction studies from incommensurate structures or other systems with great complexity. Furthermore, an evolution of diffraction patterns from dynamic processes such as structural changes or phase transitions can be demonstrated. As a result, students will get a realistic impression of fundamental concepts of diffraction such as reciprocal space, structure factors, selection rules, symmetry and symmetry violation as well as diffuse and satellite scattering. In comparison to traditional experimental (illuminating slides of ink patterns) or computational (calculating the fourier transform) teaching approaches, our method has the advantage of being interactive and intuitive. In particular, the physical equivalence of the diffraction process as well as the flexible and immediate control over displayed structures overcomes static limitations of printed ink patterns and avoids numerical artefacts of calculated transforms. Our novel approach has proven very helpful in teaching crystal diffraction to undergraduate students in materials science.

## GI-MS48-P14 | TEACHING OLD TRICKS: ROTATION CONVENTIONS IN CRYSTALLOGRAPHY AND CRYOEM

Urzhumtsev, Alexandre (IGBMC, Illkirch, FRA); Urzhumtseva, Ludmila (IBMC, Strasbourg, FRA)

An unambiguous descriptor of rotations is the matrix that links two sets of Cartesian coordinates of each point of a rotated object, those before and after rotation. However, the matrix elements are mutually dependent and hardly interpretable in a straightforward way. To overcome these difficulties, crystallographic and cryo-EM software usually refers to polar (a single rotation about an axis in a general orientation) or to Euler angles (three consecutive rotations about the chosen coordinate axes). Different software uses different sets of parameters as: both polar and Euler angles may be defined with respect to different coordinate axes; Euler angles may be defined with respect to both fixed and rotating axes; positive rotation direction may be chosen in opposite ways; one can consider the object rotating with respect to a fixed coordinate system or *vice versa*.

All these possible parametrizations of rigid-body rotations can be interactively illustrated with the program *py\_convrot*. It deals with all kinds of Euler angles, including all choices of rotation axes and rotation directions, and with all possible choices of polar angles. Using a kind of 'lego', a user can build their own rotation convention and view its action using an interactive *Demo*. An extended *Help* describes details of these parameterizations. Available *Tables* explain all possible interpretations of the rotation matrices in terms of various parameters and *vice versa*. The program can be used both as a teaching and as a practical tool converting one set of rotation parameters to another.

## GI-MS48-P15 | WHEN ARE “BAD DATA” “GOOD” DATA?

Thompson, Amber L. (Chemical Crystallography, University of Oxford, Oxford, GBR)

Over ten years of running the Chemical Crystallography Service in Oxford there have been a lot of apparently simple questions like, "What is the R-factor for this structure?" and "Is it publishable?". For some structures, the answer will be, "2%" and "Yes!", but it is often not as simple as that and there are usually follow up questions. More importantly, despite the best efforts of IUCr and checkCIF, crystallography is still an experimental science with real data which are never perfect: data quality can range from good to truly dreadful. Indeed, Murphy's Law [1] suggests that problems will be particularly complex when the science is most interesting, and in such cases, the answers to the Chemists' questions are rarely straight forward.

A selection of problem structures will be presented highlighting some of the challenges of working with "difficult data". The discussion will attempt to justify the premise that there is no such thing as unpublishable data, just data that are not fit for purpose.

[1] Roe, A., *Genet. Psychol. Monogr.*, 1951, 43(2), 121-235.

## GI-MS48-P16 | ABSOLUTE STRUCTURE OF (E)-2,2'-[3-(4-FLUOROPHENYL)PROP-2-ENE-1,1-DIYL]BIS(3-HYDROXY-5,5-DIMETHYLCYCLOHEX-2-EN-1-ONE)

Cha, Joo Hwan (Korea Institute of Science & Technology, Seoul, KOR); Lee, Jae Kyun (Korea Institute of Science & Technology, Seoul, KOR); Jeon, Se Yeon (Korea Institute of Science & Technology, Seoul, KOR)

Herewith we present the crystal structure of (E)-2,20-[3-(4-Fluorophenyl)prop-2-ene-1,1-diy]bis(3-hydroxy-5,5-dimethylcyclohex-2-en-1-one) (**A**)[1], (E)-9-(4-Fluorostyryl)-3,3,6,6-tetramethyl-3,4,5,6,7,9-hexahydro-2Hxanthene-1,8-dione (**B**)[2]. In the compound (**A**),  $C_{25}H_{29}FO_4$ , each cyclohexenone ring has an envelope conformation with the dimethyl-substituted atom as the flap. The hydroxy and carbonyl groups form two intramolecular O—H---O hydrogen bonds, as is typical for xanthene derivatives. In the crystal, very weak C—H---O hydrogen bonds link molecules into dimers. The compound (**B**),  $C_{25}H_{27}FO_3$ , each of the cyclohexanone rings adopts a half-chair conformation, whereas the sixmembered pyran ring adopts a flattened boat conformation, with the O and methine C atoms deviating by 0.0769 (15) and 0.196 (2) Å, respectively, from the plane of the other four atoms (r.m.s. deviation = 0.004 Å). The C=C double bond adopts an *E* conformation. The dihedral angle between the benzene and pyran (all atoms) rings is 89.94 (10)°. In the crystal, weak C—H---O hydrogen bonds link the molecules into chains running parallel to the *b* axis.

[1] Cha, J. H., Min, S. J., Cho, Y. S., Lee, J. K. & Park, J. H. (2013). *Acta Cryst.* **E69**, o397. [2] Lee, J. K., Min, S. J., Cho, Y. S., Cha, J. H. & Won, S. O. (2013). *Acta Cryst.* **E69**, o985.

## Autoren-Index

### A

A.E.Arbuzov .....	488
Aav, Riina .....	520
Abakumov, Artem .....	293
Abbasi Tyula, Yunes .....	364
Abboud, Ali .....	608
Abdelbaky, Mohammed S. M. ....	549
Abdelhak, Ferroudj .....	272
Abela, Rafael .....	4
ABOUFADIL, Youssef .....	700
Abrahams, Jan Pieter .....	690
Actinš, Andris .....	531
Adam, Jonathan .....	333
Adam, Martin .....	45, 205, 344, 609
Adams, Paul D. ....	69
Addicoat, Matthew .....	710
Adjiman, Claire .....	535, 536
Affouard, Frederic .....	538, 586, 591
Afonine, Pavel V. ....	69
AGBAHOUNGBATA, Marielle Yasmine .....	274
Agnew, Lauren .....	709
Agthe, Michael .....	8, 16, 17
Aguirrechu-Cameron, Amagoia .....	290
Ahmed Osman, Doaa .....	550
Ait Haddouch, Mohammed .....	249
Akimoto, Junji .....	294
Aksenov, Sergey .....	188
Alabarse, Frederico .....	242
ALAMI, Jones .....	266
Aleshin, Dmitry .....	452
Alexander, Orbett T .....	474
Alexandrov, Eugeny .....	500, 710
AlHassan, Ali .....	643
Allan, Dave .....	255
Allieta, Mattia .....	261
Almeida, Carolane .....	200
Álvarez, José María .....	29, 736
Alvaro, Matteo .....	238, 245
Alves Lima, Federico .....	729
Amenitsch, Heinz .....	645
Amo-Ochoa, Pilar .....	290
Amor, Fouad .....	695
Andersen, Ken .....	726
Andi, Babak .....	5
Ando, Nozomi .....	424
André, Ingemar .....	52
Andreasen Klahn, Emil .....	347
Andreev, Alexander .....	384
Andreu, Jordi .....	736
Andronikova, Daria .....	415
Andrulionis, Natalia .....	186
Andrusenko, Iryna .....	689
Angel, Ross J. ....	238, 245
Antonyuk, Svetlana .....	53
Antson, Fred .....	87
Aoyagi, Shinobu .....	619
Aprigliano, Giuseppe .....	726
Aquilano, Dino .....	185
Arita, Kyohei .....	132, 135

Arkipov, Dmitry .....	359
Arkipov, Sergey .....	287
Armakovic, Sanja .....	554
Armakovic, Stevan .....	554
Armentano, Donatella .....	9
Armstrong, David .....	151
Arnese, Renato .....	59
Arnling Bååth, Jenny .....	107
Arolas, Joan .....	128
Arold, Stefan .....	58
Aroyo, Mois I. ....	746
Arruda Bezerra, Gustavo .....	23
Arumughan, Anup .....	127
Aschauer, Philipp .....	56, 604
Asgari, Mehrdad .....	498
Ashcroft, N. W. ....	338
Atanasov, Michael .....	356
Attfeld, J. Paul .....	318
Autran, Pierre-Olivier .....	611
Avila, Jose .....	29, 736

### B

Baba, Seiki .....	27
Babor, Martin .....	444, 648
Babu, Ramesh .....	565
Bacchi, Alessia .....	508, 574
Bacouel, Alexandre .....	672
Bae, Euiyoung .....	133
Bærentsen, René .....	134
Bahrami, Danial .....	643
Bailey, Henry .....	23
Balázs, Attila .....	606
Balázs, Gábor .....	342
Baldelli Bombelli, Francesca .....	573
Balestri, Davide .....	508
Ballard, Charles .....	154, 160
Banchenko, Sofia .....	127
Banciu, Cristina .....	696
Bansal, Arvind Kumar .....	592
Barbour, Len .....	663
Barczyk, Artur .....	722
Bärland, Natalie .....	102
Baron, Geoffrey .....	207
Barrabés, Noelia .....	642
Barrier, Nicolas .....	187
Bartic, Carmen .....	659
Baschieri, Selene .....	131
Basle, Arnaud .....	157
Basle, Arnaud .....	90
Bassani, Dario .....	504
Bathori, Nikoletta .....	490, 542, 579
Batai, Eustina .....	595
Bauer, Jacob .....	116
Bauer, Jacob .....	171
Bauerova, Vladena .....	116, 171
Bechteler, Alois .....	608
Becker, Bruce .....	609

Becker, Petra.....	320	Blanchet, Clement E. ....	627
Beckers, Detlef.....	684	Blasco, Javier.....	377
Beddard, Godfrey S.....	8	Blatov, Vladislav A.....	500, 710
Bedekovic, Nikola.....	482	Blockhuys, Frank.....	543
Bednarchuk, Tamara.....	277	Blondieau, Michel.....	227
Beekman, Christianne.....	319	Boanini, Elisa.....	176
Beg, Marijan.....	7	Bodensteiner, Michael.....	342, 421, 751
Belabbas, Imad.....	183	Boer, Roeland.....	29, 736
Belik, Alexei A.....	323	Boese, Roland.....	423, 453, 497, 593
Bellazzini, Ronaldo.....	612	Boev, Andrey.....	186
Bellec, Ewen.....	702	Bogachev, Ivan.....	686
Belli, Stuart.....	350	Boinski, Tomasz.....	557
Belokoneva, Elena.....	219	Bojarska, Joanna.....	576
Beloševic, Svetlana.....	209	Bold, Victor.....	560
Belyakov, Sergey.....	522	Boldyreva, Elena.....	287, 674, 707
Bemmerad, Belkacem.....	553	Bolton, Rachel.....	6
Ben-Abraham, Shelomo.....	362	Bombicz, Petra.....	445, 572, 578
Benali-Cherif, Nourredine.....	459, 563	Bondar, Valerii.....	7
Benali-Cherif, Rim.....	459, 563	Booth, Simon.....	90
Bendeif, El-Eulmi.....	459, 467, 563, 680	Bordet, Pierre.....	396
Benko, Mário.....	75	Bordignon, Simone.....	513
Benndorf, Christopher.....	217	Borges, Rafael.....	140, 144, 390
Bennett, Thomas D.....	686	Borišek, Jure.....	108
Bentata, Samir.....	325	Boros, Eszter.....	103
Bentien, Anders.....	297	Borovina, Mladen.....	477
Bento, Isabel.....	715	Borowski, Patryk.....	461, 463
Bényei, Attila.....	490	Borowski, Tomasz.....	42
Béreau, Virginie.....	755	Borrmann, Horst.....	448
Bereciartua, Pablo J.....	382	Borsa, Christopher.....	70
Bereczki, Laura.....	445	Bosak, Alexei.....	411, 414, 415, 380
Bergemann, Martin.....	7	Boström, Hanna.....	418
Berger, Tamara.....	129	Bouadjemi, Bouabdellah.....	325
Bergfors, Terese.....	647	Bouanga Boudiombo, Jacky Sorrel.....	451
Berinato, Molly.....	350	Boudet, N.....	407
Berni, Francesca.....	179	Boufala, Khaled.....	183
Bernstein, Herbert J.....	5, 12, 712	Boullay, Philippe.....	328
Berrin, Jean-Guy.....	107	Bourenkov, Gleb.....	8, 16, 17, 715
Berrisford, John.....	154	Bourne, Susan.....	451
Berry, Richard.....	74	Bowler, Matthew.....	24
Berthier, Eric.....	753	Bowskill, David.....	536
Bertolotti, Federica.....	679	Bozikova, Paulina.....	85
Bertram, Florian.....	643, 676	Braga, Dario.....	585
Berzinš, Agris.....	531, 532	Brammer, Lee.....	502
Betrancourt, Damien.....	183	Brand, Helen.....	717
Betti, Camilla.....	131	Brandenburg, Gerit.....	525
Betzel, Christian.....	41, 50	Brandstetter, Stefan.....	610
Beutier, G.....	407	Braun, Doris.....	535
Beyer, Jonas.....	631	Brázda, Petr.....	392, 444
Bharatam, Prasad V.....	592	Breinbauer, Rolf.....	604
Bhattacharya, Biswajit.....	568	Brenner, Josef.....	718
Bianchi, Federica.....	508	Bressler, Christian.....	729
Bielecki, Johan.....	7	Bretosh, Kateryna.....	755
Biernacka, Marta.....	485	Brink, AliceC.....	474
Bindi, Luca.....	8	Brock, Carolyn P.....	757
Bini, Roberto.....	247	Brockhauser, Sandor.....	7, 734
Birner-Grünberger, Ruth.....	604	Broge, Nils Lau Nyborg.....	631, 664
Biryukov, Yaroslav.....	251	Brognao, Hevila.....	50
Bjerregaard-Andersen, Kaare.....	38	Bronisz, Robert.....	545
Blaha, Jan.....	44	Bronwald, Iurii.....	415
Blake, Graeme.....	206	Brouder, Christian.....	741
Blanc, N.....	407	Brown, Craig.....	498
Blanchard, Marc.....	236		

Brummerstedt Iversen, Bo .....	5, 297, 339, 343, 430, 457, 615, 631, 685, 688
Bruni, Yannick .....	226, 227
Bruno, Marco .....	185
Brzezinski, Dariusz .....	147
Bubnova, Rimma .....	233, 251, 258
Bucar, Dejan-Kresimir .....	539
Bücker, Robert .....	394
Bücker, Robert .....	389
Budai, Livia .....	606
Budniak, Urszula .....	349
Budnik, Serhiy .....	718
Buffière, Sonia .....	235
Buganski, Ireneusz .....	366
Bugris, Valéria .....	734
Buixaderas, Elena .....	428
Bull, Craig .....	256
Bunk, Oliver .....	4
Bunting, Philip C. ....	356
Buntschu, Dominik .....	4
Bureau, Helene .....	236
Burghammer, Manfred .....	177
Bürgi, Hans-Beat .....	425, 427
Burian, Max .....	645
Burkhardt, Anja .....	15
Burkhardt, Ulrich .....	448
Burnley, Tom .....	67
Burschowsky, Daniel .....	78
Butkiewicz, Helena .....	547, 557
Buyuklyan, Julia .....	92
Bykov, Maxim .....	237, 285
Bykova, Elena .....	12, 237, 285

## C

Cabaj, Malgorzata .....	495
Caballero, Iracema .....	180
Cabaret, Delphine .....	741
Cabassi, Riccardo .....	261
Cabra, Daniel .....	375
Cadot, Emmanuel .....	514
Caffrey, Martin .....	18
Caldararu, Octav .....	97, 150
Calisto, Barbara .....	29, 736
Cametti, Georgia .....	270
Cammi, Roberto .....	338
Campanale, Fabrizio .....	194
Campany, Josep .....	13
Canadillas-Delgado, Laura .....	438
Canossa, Stefano .....	427
Capelli, Silvia .....	720
Capone, Mara .....	256
Carbone, Dina .....	629
Careri, Maria .....	508
Cariati, Elena .....	560
Cariati, Elena .....	489
Carinan, Cammille .....	7
Carmalt, Claire .....	524
Carpena, Xavier .....	29, 736
Carraro, Claudia .....	508, 574
Carroni, Marta .....	64

Caruso, Francesco .....	350
Casaretto, Nicolas .....	467
Casati, Nicola .....	283, 600
Case, David .....	424
Cassidy, Cathal .....	401
Cavallo, Luigi .....	93
Cejka, Jan .....	648
Cejpek, Petr .....	371
Celic, Andjelka .....	168
Cerantola, Valerio .....	237
Ceretti, Monica .....	379, 380, 414, 662
Cerný, Jiri .....	85, 152
Cervellino, Anonio .....	322, 379, 679, 682
Cha, Joo Hwan .....	762
CHAI, Ziwei .....	422
Chaloupkova, Radka .....	109
Chang, Shih-Hung .....	719
Chang, Shih-Lin .....	697
Chaouch, Souad .....	224, 302
Chapman, Henry .....	48
Charkin, Dmitri .....	233
Charnavets, Tatsiana .....	39
Chastanet, Guillaume .....	458
Chater, Phil .....	632
Chavez, Haydee .....	350
Chayen, Naomi .....	16
Checchia, Stefano .....	261
Chechik, Maria .....	87
Checinska, Lilianna .....	178, 485
Chen, Bin .....	570
Chen, Bochao .....	313
Chen, Bo-Hao .....	416
Chen, Hong-Jie .....	383
Chen, Jie .....	323
Chen, Pei-Lin .....	559
Chen, ShihYun .....	383, 694
Chen, Yan-An .....	416
Cheng, Qing-di .....	50
Cherepanova, Svetlana .....	644, 687
Chernyshov, Dmitry .....	415, 616, 661, 665, 666, 675
Chibani, Sarra .....	634
Chicot, Didier .....	183
Chierotti, Michele Remo .....	513
Chisca, Diana .....	560
Chistyakov, Alexandr S. ....	376, 468
Chodkiewicz, Michal .....	398, 440
Choe, Hyeokmin .....	661
Chojnowski, Grzegorz .....	158
Christensen, Kirsten E. ....	683
Chuang, .....	416
Chumakov, Aleksandr .....	237, 246
Churakov, Sergey .....	270
Chuvashova, Irina .....	237
Cichowicz, Grzegorz .....	582, 594
Ciesielski, Arkadiusz .....	594
Cincic, Dominik .....	480, 482
Citroni, Margherita .....	247
Clabbers, Max .....	399
Claiser, Nicolas .....	337
Clark, Stewart J. ....	281
Clausen, Tim .....	59, 60, 80
Clegg, Jack K. ....	457

Clegg, William.....	742
Clever, Guido .....	570
Coates, Chloe.....	255
Cockcroft, Jeremy.....	484
Codee, Jeroen.....	179
Coduri, Mauro.....	261
Colin, Claire V.....	396
Colldelram, Carles.....	13
Collings, Ines.....	281, 285
Collins, Sean M.....	686
Conesa-Egea, Javier.....	290
Conrad, Matthias.....	369
Cool, Pegie.....	509
Cormier, Laurent.....	236
Cornaciu, Irina.....	21
Correia, Natalia.....	538, 586, 591
Cortona, Pietro.....	337
Costa Junior, Raul.....	7
Costille, Benjamin.....	672
Cott-Garcia, Joelson.....	243
Covacci, Ezio.....	611
Crawshaw, Adam.....	6
Crepisson, Celine.....	236
Croll, Tristan I.....	148, 165
Crosas, Eva.....	15
Csankó, Krisztián.....	734
Cuello, Gabriel.....	118
Curetti, Nadia.....	231
Cyranski, Michal.....	423, 453, 497, 582, 593, 594

## Đ

Đakovic, Marijana.....	540, 471, 477, 752
Đilovic, Ivica (University of Zagreb, AUT).....	336

## D

Dadivanyan, Natalia.....	671
Dal Bo, Fabrice.....	226
Dal Canale, Enrico.....	512
Dall'Antonia, Fabio.....	7
Damay, Françoise.....	21
Damborsky, Jiri.....	109
Damgaard-Møller, Emil.....	347
Damisch, Elisabeth.....	54, 179
DANEDE, Florence.....	538
D'Angelo, Anita.....	220, 717
Danilevski, Cyril.....	7
Danylyuk, Oksana.....	557, 547
Dara, Olga.....	186
Darie, Céline.....	396
Das, Chandrima.....	55
Das, Susobhan.....	569
Daszkiewicz, Marek.....	548
Daumke, Oliver.....	22
Dauter, Zbigniew.....	372
Davtyan, Arman.....	643
Day, Graeme.....	599
de Almeida Ribeiro, Euripedes.....	126

de Boissieu, Marc.....	407
de Bruyne, Benjamin.....	337
de Gelder, Rene.....	501
de la Flor, Gemma.....	746
de Poel, Wester.....	501
de Riccardis, Francesco.....	456
de Sanctis, Daniele.....	11
de Vries, Roelof.....	612
De Zitter, Elke.....	514
Defossez, Pierre-Antoine.....	132, 135
Degen, Thomas (Malvern Panalytical BV, Almelo).....	663
DeGrado, William.....	123
Dehio, Christoph.....	79
Dejoie, Catherine.....	611
Delimitis, Andreas.....	305
Dellago, Christoph.....	645
Demitri, Nicola.....	649
Denux, Dominique.....	235
Dera, Przemyslaw.....	250
Deschaume, Olivier.....	659
Deslandes, Jean-Pierre.....	253
Destefanis, Enrico.....	231
Deuss, Felix.....	74
Devenish, Nicholas.....	6
Dey, Somnath.....	569
di Gregoria, Maria Chiara.....	446
di Marco, Valerio B.rino, Camerino, ITA).....	513
di Stefano, Davide.....	192
Dickerson, Joshua.....	614
Diebold, Ulrike.....	314
Diederichs, Kay.....	58
Dietz, Nikolaus.....	79
Dimitrova, Olga.....	219
Ding, Lei.....	396
Dinnebier, Robert E.....	480
Direm, Amani.....	549
Dirin, Dmitry N.....	645
Diskin-Posner, Yael.....	469
Dittrich, Birger.....	348, 434
Djinovic, Kristina.....	37, 116
Djinovic-Carugo, Kristina.....	34, 125, 126, 128
Dmitrienko, Vladimir.....	269, 376
Dmitriev, Vladimir.....	665
Dmytriv, Grygoriy.....	408
Dobó, József.....	103
Dobrynin, Alexey.....	562
Dobrzycki, Lukasz.....	10, 423, 453, 497, 582
Dodson, Eleanor.....	10
Doert, Thomas.....	373
Dohnálek, Jan.....	39, 44, 104, 656
Dolabella, Simone.....	693
Doležal, Petr.....	371
Dolomanov, Oleg.....	754
Dominiak, Paulina.....	349, 398, 440, 495
Dommann, Alex.....	264, 420, 575, 625, 635
Donnard, Morgan.....	558
Dorbez-Sridi, Rachida.....	680
Dordic, Andela.....	54, 179
Dorofeeva, Yulia.....	56
Dovgaliuk, Iurii.....	675
Drapala, Jakub.....	621
Drath Bøjesen, Espen.....	688

Drechsler, Rolf.....	126, 128, 698
Dronskowski, Richard.....	249
Dsouza, Raison.....	96
Dubey, Gurudutt.....	592
Dubrovinskaia, Natalia.....	285
Dubrovinsky, Leonid.....	237, 246, 285
Duchateau, Alexander L.L.....	501
Dudek, Marta.....	599
Duetsch, Luis.....	421
Duhayon, Carine.....	208, 210, 229, 755
Duman, Ramona.....	733
Durka, Krzysztof.....	621
Durst, Roger.....	609
Dürvanger, Zsolt.....	103
Dušek, Michal.....	364
Dušková, Jarmila.....	44, 104, 656
Dutkiewicz, Zbigniew.....	355
Dutta, Rajesh.....	380, 414
Duttine, Mathieu.....	235
Duverger-Nédellec, Elen.....	361, 755
Dyadkin, Vadim.....	616, 665, 666, 675
Dzhigaev, Dmitry.....	630
Dziubek, Kamil.....	247, 281
Džolic, Zoran.....	494

## E

Echols, Nathaniel.....	148
Eckardt, Mirco.....	632
Eder, Markus.....	54, 179
Edwards, Alison.....	437
Effenberger, Herta.....	239
Efthimiopoulos, Ilias.....	243
Egelman, Edward.....	128
Ehmann, Heike M. A.....	636
Ehrenberg, Helmut.....	291, 309, 408
Ehsan, Wajid.....	7
Eich, Andreas.....	249
Eikeland, Espen Zink.....	457
Eisele, Claudio.....	322
Eisenburger, Lucien.....	191
Eisenhaber, Birgit.....	164
Eisenhaber, Frank.....	164
EL Amane, Mohamed.....	208, 229
EL Bachraoui, Fatima.....	266
EL Bali, Brahim.....	224, 304
El Hamdani, Hicham.....	208, 210, 229
El Idrissi Raghni, My Ahmed.....	700
Elcoro, Luis.....	746
Elliott, Jenna.....	157
El-Omari, Kamel.....	733
Elsegood, Mark.....	555
Emerich, Hermann.....	665
Emmerling, Franziska.....	568
Emsley, Paul.....	137
Ende, Martin.....	248, 282, 284
Engilberge, Sylvain.....	40
Englert, Ulli.....	515
Eremenko, Igor L.....	468
Eremina, Tatiana.....	219

Ernst, Michelle.....	283
Esenov, Sergey.....	7
Espes, Emil.....	10, 620
Eszenyi, Tibor.....	490
Ettakni, Mahmoud.....	638
Etter, Martin.....	216, 480, 725
Evans, Gwyndaf.....	6, 143, 157, 174
Evstigneeva, Tatiyana.....	197
Evtushok, Boyan.....	644

## F

Fabbri, Riccardo.....	7
Fabelo, Oscar.....	377, 438
Faber, Kurt.....	102
Fábián, László.....	600, 601, 602
Fahrenkamp, Dirk.....	118
Falke, Sven.....	41, 48, 50
Fando, Maria.....	92
Fanetti, Samuele.....	247, 281
Fangohr, Hans.....	7
Farhan, Rida.....	310
Favretto, Filippo.....	83
Fayzullin, Robert R.....	353, 450, 486
Fechtelkord, Michael.....	598, 603
Feiler, Christian.....	46, 724
Fejfarová, Karla.....	104
Felici, Roberto.....	225
Feliciotti, Irene.....	119
Feng, Hai L.....	323
Fermani, Simona.....	98
Fernandez-Diaz, Lurdes.....	181
Ferrer, Jean-Luc.....	726
Ferry, Laure.....	132
Fertey, Pierre.....	244
Festersen, Sven.....	676
Feygenson, Mikhail.....	633
Ficner, Ralf.....	83, 146
Fiebig, Manfred.....	759
Fiedler, Stefan.....	8, 17, 627
Filatov, Stanislav.....	251, 257, 258
Filimonov, Alexey.....	415
Filinichuk, Yaroslav.....	675
Filipovic, Nenad.....	554, 558
Finger, Raphael.....	668
Fink, Lothar.....	232
Fischer, Pontus.....	15
Fischer, Reinhard.....	234, 698
Fitch, Andrew.....	611
Flaig, Ralf.....	727
Flucke, Gero.....	7
Focke-Tejkl, Margarete.....	56
Fodor, Krisztián.....	103
Folco, Luigi.....	194
Folkers, Laura.....	368
Fonari, Marina.....	489, 560
Foran, Ross.....	499
Forment Aliaga, Alicia.....	278
Fornari, Fabio.....	508
Forni, Alessandra.....	489, 560

Förster, Ronald.....	724
Förster, Stefan.....	225
Fortes, Dominic.....	207
Fortunato, Giuseppino.....	575, 635
Foster, William.....	23
Franceschi, Giada.....	314
Francoval, Sonia.....	382
Frandsen, Kristian E.H.....	107
Fransen, Martijn.....	612
Frenz, Martin.....	635
Friedrich,.....	243, 281
Friese, Karen.....	249, 639
Frisic, Tomislav Frison, Rugge.....	264, 565, 682
Fritsch, Charlotte.....	309
Fritsch, Katharina.....	304
Fromm, Katharina.....	504
Fromme, Raimund.....	57
Fu, Zhihui.....	74
Fucci, Rosa.....	509
Fuchs, Martin R.....	5
Fujii, Hiromasa.....	676
Fullà-Marsà, Daniel.....	7
Funnell, Nicholas.....	256
Furukawa, Yukito.....	27

## G

G. Vertessy, Beata.....	100
Gácsai, Zoltán.....	201
Gaimster, Hannah.....	90
Gajda, Roman.....	244
Gál, G. Tamás.....	572
Gál, Gyula Tamás.....	578
Gál, Péter.....	103
Galica, Tomasz.....	254
Galimova, Milyausha.....	562
Gallagher, John F.....	571
Galler, Andreas.....	729
Galli, Simona.....	513
Galuskin, Evgeny V.....	189
Galuskina, Irina O.....	189
Ganasen, Menega.....	130
Gao, Feng.....	311
Gao, Shang.....	375
Gao, Yuan.....	5
García Granda, Santiago.....	549, 550
Garcia, Maria.....	31
Garcia-Muñoz, Jose Luis.....	377
Garcia-Santamarina, Sarela.....	107
Garipov, Marsel.....	541
Garman, Elspeth.....	3, 614, 737
Garratt, Richard.....	52, 53
Garriga, Damià.....	13
Gateshki, Milen.....	671, 684
Gatti, Carlo.....	339
Gatto, Claudia.....	200, 203
Gaulin, Bruce.....	6
Gautel, Mathias.....	125
Gavezzotti, Angelo.....	527
Gawelda, Wojciech.....	729
Gawryluk, Dariusz.....	378
Gaydamaka, Anna.....	287
Ge, Meng.....	395
Ge, Mengyu.....	87
Geerts, Yves.....	289, 510, 649
Gegenwart, Philipp.....	285
Gehrmann, Thomas.....	8
Geist, Leonhard.....	126
Gemmi, Mauro.....	194, 512, 689
Genoni, Alessandro.....	340
Genoni, Alessandro.....	356
George, Janine.....	192
Georgii, Robert.....	322
Gerasimova, Daria.....	450
Gerlach, Martin.....	724
Germann, Luzia S.....	480
Gertenbach, Jan.....	663
Gesing, Thorsten.....	204, 248, 652
Ghaithan, Hamid.....	193
Ghosh, Swagatha.....	626
Giacobbe, Carlotta.....	261
Giambastiani, Giuliano.....	513
Gibbs, Alexandra.....	321
Giester, Gerald.....	196, 284
Gille, P.....	407
Gillet, Jean-Michel.....	337
Gillon, Beatrice.....	337
Gil-Ortiz, Fernando.....	29, 736
Gilski, Mirosław.....	147, 372
Giménez Marqués, Mónica.....	278
Ginn, Helen.....	139
Giovanetti, Gabriele.....	7
Girani, Alice.....	245
Girard, Eric.....	40
Giri, Rajendra.....	676
Gjerlevsen Nielsen, Ida.....	685
Glazyrin, Konstantin.....	237, 249
Gless, Christine.....	4
Gloter, Alexandre.....	383
Glowka, Marek.....	276
Glueck, Silvia M.....	102
Gobbo, Alexandre.....	4
Gobetto, Roberto.....	513
Gogolin, Mathias.....	248
Golovanov, Alexander.....	452, 605
Goloveshkin, Alexander.....	335
Golub, Alexandre.....	335
Gómez Muñoz, Iván.....	278
Go'omez, Flavia.....	375
Gomis-Rüth, F. Xavier.....	118
González Chávez, Fernando.....	506
Gonzalez Nelson, Adrian.....	427
Gonzalez, Ana.....	716
González, Nahikari.....	13, 29, 736
Gonzalez-Nelson, Adrian.....	503
Gonzalez-Platas, Javier.....	290, 702
Goodwin, Andrew.....	385, 418, 431, 678
Gorbunov, Denis.....	384
Goreshnik, Evgeny.....	654
Gorfman, Semën.....	334, 661
Görries, Dennis.....	7
Gorrec, Fabrice.....	32, 36

Gottstein, Nina Alice .....	47
Gotz, Detlev J. ....	671
Goujon, Céline .....	396
Grabowski, Slawomir.....	476
Grabowsky, Simon.....	340
Graf, Jürgen .....	250
Grape, Erik .....	465
Grauer, Maxim.....	670
Gravogl, Georg.....	308
Gražulis, Saulius.....	173
Greiner, Martina.....	182
Greive, Sandra .....	87
Grepioni, Fabrizia .....	442
Grguric, Toni.....	494
Griese, Julia .....	399
Griesshaber, Erika.....	181
Grin, Yuri .....	409
Grinninger, Christoph.....	604
Grinzato, Alessandro.....	131
Grohmann, Elisabeth.....	129
Grosjean, Arnaud .....	457
Gruber, Karl.....	102
Grudin, Sergei.....	170
Gruene, Tim .....	387
Grünewald, Tilman .....	177
Grupe, Gisela .....	182
Gruza, Barbara .....	398, 440
Gruzinov, Andrey Yu.....	627
Grybauskas, Algirdas.....	173
Gryl, Marlena.....	354, 358
Grzechnik, Andrzej .....	249, 639
Gu, Qinfen .....	717
Gu, Wenlong .....	312
Guagliardi, Antonietta .....	679
Guagnini, Francesca.....	512
Gubaidullin, Aidar .....	447, 479, 541
Gudim, Ingvild.....	106, 111
Gudino, Ricardo.....	59
Gueddida, Saber .....	337
Guignot, Nicolas .....	253
Guinebretiere, Rene .....	672
Guionneau, Philippe .....	458
Gulea, Michaela.....	558
Gunjan, Sarika.....	55
Günther, Daniel .....	191
Günther, Sebastian .....	15
GUO, Wenbin .....	458
Gurieva, Galina.....	263
Guskov, Albert.....	73
Guthrie, Malcolm .....	256
Gutmann, Matthias .....	228
Gzella, Andrzej .....	653

## H

Habermehl, Stefan.....	526
Habib, Faiza .....	523
Habicht, Klaus .....	304
Hadda, Krarcha .....	271
Hagara, Jakub .....	624

Haid, Slimane.....	325
Haiki, F.Z .....	638
Haines, Julien .....	252
Hajdusits, Bence .....	60
Hakanpää, Johanna .....	15, 715
Halasyamani, Shiv .....	265
Hållstedt, Julius.....	10, 620
Háló, Adrienn .....	606
Hamann, Florian .....	83
Hamdi, Najlaa .....	224, 302
Hammer, Karin.....	88
Hammer, Sonja M. ....	329
Hammerstad, Marta .....	106, 111
Han, Huijong .....	732
Han, Seungsu .....	76
Hanfland, Michael .....	246, 247, 281, 285
Hanopolskyi, Anton .....	469
Hansen, Anna-Lena .....	309, 681
Hansen, Thomas.....	252
Hansen, Vidar .....	305
Happonen, Lauri .....	483
Harmat, Veronika .....	103, 606, 734
Harris, Kenneth .....	7
Hartmann, Robert.....	608
Hasegawa, Kazuya .....	27
Hašek, Jindrich .....	104, 656
Haselbach, David.....	80
Hashizume, Daisuke .....	511
Hasnain, S. Samar .....	53
Hatert, Frederic .....	226, 227
Hatti, Kaushik .....	148, 165
Hauß, Thomas .....	724
Hautier, Geoffroy.....	192
Hayashi, K. ....	407
Haynes, Delia.....	346, 738
He, Huiling .....	724
Hearshaw, Meredith .....	542
Hegedus, Rózsa .....	103
Heggelund, Julie .....	38
Heine, Andreas .....	26
Heine, Miriam.....	232
Heinemann, Udo .....	127
Heiss, Wolfgang .....	645
Hejny, Clivia.....	212
Hejral, Uta .....	657
Helliwell, John.....	708
Hellmig, Michael.....	724
Hennig, Christoph .....	731
Henriques, Margarida .....	384
Herbert, Simon A.....	663
Herbst-Irmer, Regine.....	436, 439
Hergert, Wolfram.....	225
Hermet, Patrick .....	252
Herrmann, Markus .....	249
Hersleth, Hans-Petter .....	
Hervé, Laurence .....	361
Heuser, Philipp .....	158
Hewitt, Lorraine.....	90
Hickin, David .....	7
Hikima, Takaaki .....	51
Hikita, Masahide .....	723, 728
Hiller, Wolf .....	570

Himo, Fahmi .....	102
Hinterstein, Manuel.....	252
Hiraki, Masahiko .....	723, 728
Hirata, Kunio.....	27
Hlinka, Jiri.....	428
Hodgkinson, Paul .....	587
Hofer, Gerhard.....	47, 56, 102
Hofer, Gregor .....	413
Hofer, Sebastian.....	703
Hoffmann, Christina.....	436, 439
Hoffmann, Jan-Ekkehard .....	304
Hoffmann, Roald.....	338
Hogan-Lamarre, Pascal .....	389, 394
Högbom, Martin	
Holczbauer, Tamás.....	445
Holíková, Viera .....	75
Höllerl, Eneida.....	128
Holm, Kristoffer.....	430
Holstein, Julian .....	570
Honing, Maarten .....	501
Hora, Jan.....	4
Horiuchi, Shinnosuke.....	570
Hornfeck, Wolfgang.....	405
Horrell, Sam .....	8, 16, 17
Hoshino, Manabu .....	511
HOUARI, Mohamed.....	325
Houben, Lothar.....	446
Hovestreydt, Eric .....	402
Howard, Christopher.....	207
Hradil, Klaudia .....	718
Hsaio, Yu-Yuan .....	84
Hsiao, Chwan-Deng.....	124
Hsiao, Yu-Yuan .....	84
Hsu, Chun-Hua .....	43
Hsu, I-Jui .....	416
Hsu, Pei-Kai .....	383, 694
Hu, Hongyi.....	393
Hua, Xiao.....	299
Huang, Chia-Ying .....	4
Huang, Kuan-Wei .....	84
Huang, Qian .....	107
Huang, Wen-Chi.....	694
Huang, Yu-Fang .....	694
Huang, Zhehao.....	395
Huber, Markus.....	79
Huber, Stefan .....	136
Hübschle, Christian.....	351
Hudson, Matthew .....	498
Hull, Stephen.....	658
Hundt, Nikolas .....	60
Hung, Ling-I.....	559
Hungler, Arnaud .....	58
Huse, Nils .....	8, 17
Huse, Nils .....	8

## I

Idboumlik, Meryem .....	224
Ienco, Andrea .....	528
Ikeda, Fumiyo.....	80

Ikeda-Ohno, Atsushi.....	731
Inaba-Inoue, Satomi.....	51
Indris, Sylvio.....	309
Inge, Andrew Ken.....	465
Ingmer, Hanne .....	88
Inoue, Katsuaki .....	51
Iranpour, Neda .....	625
Ishii, Yasushi.....	406
Ishiyama, Satoshi .....	135
Itié, Jean-Paul.....	253
Ivlev, Sergei.....	369
Izhitskiy, Alexander .....	186
Izzo, Irene .....	456

## J

J. Borges, Rafael.....	167
Jacobs, Tia .....	663
Jacques, Vincent.....	702
Jahnen-Dechent, Willi .....	118
Jakob, Matthias.....	670
Jakoncic, Jean .....	5
Jali, Abdelaziz.....	700
Janbon, Sophie .....	650
Janczak, Jan .....	601
Janczura, Natalia .....	602
Jang, Soonmin .....	537
Janiak, Agnieszka .....	663
Janssen, Bert .....	71
Janssens, Koen .....	2
Jaques, Dominic .....	157
Jarosiewicz, Tobiasz.....	7
Jarzemska, Katarzyna.....	461, 463, 621, 622
Jaskolski, Mariusz.....	147, 372, 653
Jeangerard, Damien.....	514
Jelsch, Christian.....	357
Jeng, Horng-Tay .....	697
Jenkins, Huw .....	87
Jeon, Se Yeon .....	762
Jeong, Hyunah.....	537
Jergel, Matej.....	624
Jha, Kunal.....	440
Jian, Jie.....	328
Jie, Liu .....	472
Jimenez, Monica .....	586
Jiménez-Mellado, Elisabet .....	161
Jin, Yi.....	87
Johannesen, Hedda.....	38
Johansen, Katja S.....	107
Johansson, Erik .....	81
Johnsen, Carl.....	722
Johnson, Natalie .....	156
Johnstone, Duncan N.....	686
Jones, Andrew O. F. ....	636, 669
Joo, EunSook.....	537
Joosten, Robbie .....	153
Joseph, Agnel .....	67
Joseph, Boby .....	242
Jovine, Luca.....	14, 118
Juanhuix, Judith .....	13, 29, 736

Jung, Seungyong.....	133
Jüttner, Philipp.....	117

## K

Ka, Donghyun.....	133
Kaabel, Sandra.....	520
Kaczmarek, Krzysztof.....	576
Kaelin, Robert.....	4
Kaercher, Joerg.....	344, 609
Kahlenberg, Volker.....	212
Kale, Dnyaneshwar P.....	592
Kalienko, Maksim.....	268
Kalinina, Olga.....	186
Kalousková, Barbora.....	44
Kaltenegger, Martin.....	510
Kama, Dumisani V.....	474
Kamecka, Anna.....	546
Kamerlin, Lynn.....	97
Kamil, Ebad.....	7
Kaminski, Radoslaw.....	461, 463, 621, 622
Kandiah, Eaashisai.....	131
Kantamneni, Sravya.....	142, 158
Kantor, Innokenty.....	606
Kapturkiewicz, Andrzej.....	546
Karancsiné Menyhárd, Dóra.....	103
Karimova, Oxana.....	197
Karner, Carina.....	645
Karolewicz, Bozena.....	601
Karpics, Ivars.....	8, 17
Karttunen, Antti.....	369
Kasai, Hidetaka.....	688
Kaspar, Sebastian.....	610
Kassier, Günther.....	389, 394
Kassou, Said.....	638
Kastner, Alexandra.....	724
Kataoka, Kunimits.....	294
Katona, Gergely.....	627
Katrusiak, Andrzej.....	286, 487
Katsura, Tomoo.....	246
Katsuya, Yoshio.....	323
Kaur, Guratinder.....	375
Kaur, Kirandish.....	33
Kavanagh, Oisin.....	577
Kawano, Yoshiaki.....	27
Kazmierczak, Michal.....	286, 487
Keates, Adam.....	524
Keegan, Ronan.....	141, 154, 160, 166, 174
Keller, Lukas.....	378, 379
Keller, Walter.....	47, 56, 102, 129
Kelpsas, Vinardas.....	97
Kerkhoff, Linda.....	320
Khakhulin, Dmitry.....	729
Khazai, Nariman.....	394
Khechoubi, El Mostafa.....	638
Khimyak, Yaroslav.....	597, 600, 601, 602
Khmou, Ahmed.....	638
Khoder, Hassan.....	680
Kibalin, Iuri.....	337
Kikuchi, Takashi.....	519

Kilstrup, Mogens.....	88
Kim, KI-BOK.....	307
Kim, Tae-Houn.....	76
Kim, YONG-IL.....	307
Kimpton, Justin.....	717
Kimura, K.....	407
King, Andrew.....	253
Kirienko, Yury.....	7
Kiriukhina, Galina.....	222
Kirkwood, Henry.....	7
Kirsch, Andrea.....	652
Kiss-Szemán, Anna.....	112
Kjeldgaard, Solveig.....	297
Kjendseth Røhr, Åsmund.....	111
Klajn, Rafal.....	469
Klebe, Gerhard.....	22, 26
Klein, Holger.....	396, 397
Kleist, Wolfgang.....	295
Klimovskaia, Anna.....	7
Klisuric, Olivera.....	554, 558
Kloß, Simon D.....	191
Klusch, Niklas.....	62
Kluyver, Thomas.....	7
Knapp, Michael.....	309
Knecht, Wolfgang.....	20
Knoll, Christian.....	308
Kochetygov, Ilia.....	498
Koch-Müller, Monika.....	243
Kocsis, Andrea.....	103
Kocsis, Balazs.....	182
Kodera, Noriyuki.....	132
Kodess, Boris.....	195, 747
Kodjikian, Stéphanie.....	396, 397
Kodrin, Ivan.....	477
Koemets, Egor.....	246
Koemets, Iuliia.....	246
Kogan, Vladimir.....	684
Köhler, Christian.....	436, 439
Köhler, Katharina.....	410
Köhler, Thomas.....	273
Kohler, Verena.....	129
Kohlmann, Holger.....	215, 668
Kojic-Prodic, Biserka.....	739
Kolenko, Petr.....	104
Kolida, Sofia.....	119
Kolincio, Kamil.....	361
Komadina, Dana.....	48
Komerist, Yevgeniy.....	178
Konrat, Robert.....	126, 128
Kons, Artis.....	532
Konstan, Julius.....	37
Koo, Jasung.....	114
Kopecky, Milos.....	428
Koppány, Gergely.....	100
Kori, Satomi.....	132
Korlyukov, Alexander.....	335, 359, 677
Körösi, Márton.....	445
Körschgen, Hagen.....	118
Korsunsky, Alexander.....	326
Korytár, Dušan.....	624
Korzanski, Artur.....	355
Korzun, Barys.....	333

Kosiorek, Sandra	547, 557
Kostan, Julius	34, 116
Kot, Ewa	42
Kotnik, Petra	636, 669
Kotov, Vadim	34
Koval, Tomáš	44, 104, 656
Kovalenko, Maksym V.	645
Kovalevskiy, Oleg	137, 154
Kowiel, Marcin	147
Kozina, Nina	186
Kozlovskaya, Ksenia	269
Kr. Srivastava, Dushyant	55
Kralj, Marijeta	544
Kratzert, Daniel	711
Kraus, Florian	369
Krause, Lennard	436, 439, 615
Krauss, Sebastian	632
Kravtsov, Victor	489, 560
Krawczuk, Anna	358, 433
Kremer, Marius	515
Kremlicka, Thomas	248
Krengel, Ute	38
Krikunova, Polina	221
Krissinel, Eugene	10, 154
Kristály, Ferenc	201
Kristensen, Mads R.B.	722
Kröger, Martin	413
Krogstad, Matthew	412
Krüger, Biljana	189
Krüger, Hannes	189, 212
Krukle-Berzina, Kristine	522
Krzyszczakowska, Joanna	398
Krzhizhanovskaya, Maria	233, 258
Ksiazek, Maria	545
Kub, Jiri	428
Kubicek, Katharina	729
Kubicek, Sabine	623
Kubicki, Maciej	355
Kubo, Minoru	2
Kuchár, Juraj	552
Kucharczyk, Damian	748
Kuepers, Michael	249
Kühlbrandt, Werner	62
Kukura, Philipp	60
Kulda, Jiri	428
Kulkarni, Yashraj	97
Kumasaka, Takashi	27
Kuo, Wan-Ching	77
Kupcewicz, Bogumila	485
Kupenko, Ilya	237
Kurbangalieva, Almira	450
Kurlin, Vitaliy	534, 756
Kurnosov, Alexander	237
Kuroiwa, Yoshihiro	619
Kurpiewska, Katarzyna	42
Kurz, Maditha	284
Kusko, Mihaela	641
Kusz, Joachim	545
Kuta Smatanova, Ivana	109
Kutejová, Eva	171
Kutniewska, Sylwia	461, 463
Kuty, Michal	109

Kwon, Ae-Ran	91
Kyratsi, Theodora	305

## L

Laatsch, Bernhard	117
Labourel, Aurore	107
Labrugère, Christine	235
Lachkar, Mohammed	224, 302
Lahav, Michal	446
Lammer, Anna	129
Lamzin, Victor	142, 158
Langenmaier, Michael	213
Langer, Julian	62
Lantri, Tayeb	325
Lanza, Arianna	512, 689
Lapi, Michela	49
Larsbrink, Johan	107
Larsen, Helge Bøvik	701
Laski, Piotr	621, 622
Latychevskaia, Tatiana	401, 690
Laufek, Frantisek	214
Laulainen, Joonatan E. M.	686
Launois, Pascale	422
Lausi, Andrea	242
Lavin della Ventura, Victor	290
Lazo, Edwin O.	5
Lazor, Peter	266
Le Bolloc'h, David	702
Lebedev, Andrey	154, 160
Lebedev, Andrey	141
Lebrette, Hugo	64, 399
Lechner, Rainer T.	645
Lecomte, Claude	337, 341
Lee, Hyung Ho	537
Lee, Jae Kyun	762
Lee, Jey-Jau	416, 719
Lee, Ji-Young	76
Lee, Ming Ying	43
Lee, Sangho	76
Lee, Yongmok	76
Legendre, Murielle	396
Lehmann, Frederike	301
Lehmann, Jannis	759
Leimkohl, Jan-Philipp	16
Leineweber, Andreas	288
Leithner, Andreas	177
Lekontseva, Natalia	92
Lemke, Henrik	4
Lemmerer, Andreas	581
Lenenko, Natalia	335
Lengauer, Christian	196, 308
Lenhartová, Simona	75
Lenz, Stephan	234
Lenzen, Dirk	505
Leonardo, Diego	52
Leonarski, Filip	4
Leovac, Vukadin	209, 590
Leroy, Clemence	236
Lesse, Daniel	589

Lesyk, Roman.....	653
Letrun, Romain.....	714
Leveles, Ibolya.....	100
Levendis, Demetrius.....	493
Lewis, Richard J.....	90
Leys, David.....	102
Leyva–Pérez, Antonio.....	9
Ležaic, Katarina.....	517
Li, Fei.....	381
Li, Jian.....	331
Li, Leigang.....	328
Li, Man-Rong.....	323
Li, Tai-De.....	333
Li, Xiao.....	675
Lian, Hong.....	206
Liang, Hongbin.....	323
Liao, Libing.....	312, 313
Lichtenegger, Helga.....	177
Lico, Chiara.....	131
Lidin, Sven.....	368
Liebschner, Dorothee.....	19
Liegl-Atzwanger, Bernardette.....	177
Lifshitz, Ron.....	404
Lightowler, Molly.....	435
Lima, Francielle.....	203
Lima, Gustavo.....	20, 28
Lin, John Han-You.....	77
Lin, Meng Hsuan.....	43
Lin, Shih-Ming.....	77
Lin, Tsang-Lang.....	184
Lindeman, Sergey.....	466, 492
Lindemann, Tobias.....	217
Linden, Anthony.....	274, 516, 743
Lindenthal, Lorenz.....	298
Lindley, Peter.....	120, 175
Lisac, Katarina.....	480
Liu, Fupin.....	419
Liu, Guangfeng.....	289, 472
Liu, Hao.....	312, 313
Liu, Jie.....	289
Liu, Lijun.....	123
Liu, Li-Min.....	422
Liu, Qun.....	5
Liu, Tung-Chang.....	84
Liu, Xiaojiao.....	240
Lo Leggio, Leila.....	88, 107
Lo Presti, Leonardo.....	527
Loboda, Jure.....	113
Lock, Nina.....	688
Lodochnikova, Olga.....	353, 447, 450, 541
Lofstad, Marie.....	106, 111
Logan, Derek.....	20
Loitzenbauer, Michael.....	282
Long, Fei.....	137
Long, Jeffrey R.....	356, 498
Longley, Louis.....	686
Lopez Arolas, Joan.....	125, 126
Lorenzen, Kristina.....	732
Løset, Geir Åge.....	38
Lotti, Paolo.....	242
Louhi, Said.....	266
Louis, Ghislain.....	183

Loveday, John.....	256
Löwe, Jan.....	4
Lu, Ping.....	328
Lübben, Jens.....	436, 439
Lucenti, Elena.....	489, 560
Ludescher, Lukas.....	645
Luger, Peter.....	348
Lungulescu, Marius.....	696
Lunin, Vladimir.....	138
Lunn, Richard.....	524
Luo, Yi.....	332
Lusi, Matteo.....	577, 588
Lv, Guocheng.....	312, 313

## M

Ma, Yanhang.....	443
Macchi, Piero.....	283
Macedi, Eleonora.....	456
Macron, Pedro.....	200
Madariaga, Gotzon.....	746
Madsen, Anders Østergaard.....	432
Madura, Izabela.....	594
Magdysyuk, Oxana.....	507
Magerl, Andreas.....	651
Magnussen, Olaf.....	676
Maity, Avishek.....	380, 414
Maity, Sumit Ranjan.....	379
Majková, Eva.....	624
Majumdar, Soneya.....	647
Makal, Anna.....	244, 460, 491, 564
Makoshi, Kenji.....	406
Malagurski, Ivana.....	565
Malapile, Ramokone.....	579
Malaspina, Lorraine.....	340
Malecka, Magdalena.....	485
Malinska, Maura.....	438
Maloney, Andrew.....	745
Mamakhel, Aref.....	631
Mamchyk, Denys.....	7
Mancuso, Adrian P.....	7
Mangin, Thomas.....	396
Manna, Rudra.....	237, 285
Manoun, Bouchaib.....	266
Marchetti, Danilo.....	512
Marchivie, Mathieu.....	458
Marcos, Jordi.....	13
Mardegan, Jose R. L.....	382
Marder, Todd B.....	281
Marek, Paulina.....	594
Marinescu, Virgil.....	696
Marjanovic, Ivana.....	558
Markó, Márton.....	726
Markovic, Sanja.....	554
Markovski, Mishel.....	230
Marlovits, Thomas C.....	34
Marot, Jerome.....	514
Marquardt, Hauke.....	279
Marquez, Jose A.....	21, 159
Marschall, Stephen A.....	102

Marsh, May.....	4	Michalchuk, Adam A. L.....	568
Marshall, Jessica.....	267	Michelat, Thomas.....	7
Marsicano, Anna.....	414	Midgley, Laura.....	345
Martiel, Isabelle.....	4	Midgley, Paul A.....	686
Masciocchi, Norberto.....	679	Mihailova, Boriana.....	238
Masicano, Anna.....	380	Mihalkovic, M.....	407
Masmaliyeva, Rafiga.....	149	Mikkelsen, Anders.....	11
Massera, Chiara.....	512	Mikó, Tamás.....	201
Masunaga, Takuya.....	27	Mikulík, Petr.....	624
Matano, Shohei.....	132	Milas, Mirko.....	9
Matej, Zdenek.....	722	Miletich, Ronald.....	239, 248, 282, 284
Matkovic-Calogovic, Dubravka.....	336, 517, 544, 584	Millán Nebot, Claudia Lucía.....	54, 140, 144, 161, 167, 390
Matougui, Mohamed.....	325	Miller, R. J. Dwayne.....	8, 16, 17, 96, 389, 394
Matsugaki, Naohiro.....	723, 728	Mills, Deryck.....	62
Matsushita, Yoshitaka.....	323	Minde, Mona Wetthus.....	305
Matzinger, Philipp.....	282	Minguez Espallargas, Guillermo.....	455
Mauk, Grant.....	130	Minns, Jake.....	417
Maurin, Guillaume.....	505	Minor, Wladek.....	441
Mauro, Prencipe.....	238	Mirecka, Jola.....	67
Maury, Olivier.....	40	Mirzaei, Saber.....	466
Maurya, Anjani.....	565, 575, 635	Mishnev, Anatolijs.....	522, 704
May, Nóra V.....	572, 578	Misini Ignjatovic, Majda.....	150
Mayer, Katrin.....	182	Miškov-Pajic, Vukoslava.....	209
Mayer, Tobias.....	751	Misnovs, Anatolijs.....	704
Mazurkewich, Scott.....	107	Mizuno, Nobuhiro.....	27
Mazzeo, Paolo Pio.....	508, 574	Mlynek, Georg.....	34, 126
McCabe, Patrick.....	529	Moeini, Keyvan.....	549, 550
McCammon, Catherine.....	237, 246	Mohacsi, Istvan.....	7
McCoy, Airlie J.....	148, 165, 180	Mohseni, Katayoon.....	225
McGrath, Ronan.....	403	Mokolokolo, Pennie P.....	474
McMillan, Paul.....	247	Molcanov, Krešimir.....	357
McMonagle, Charlie.....	241	Mollica, Giulia.....	596
McMurtrie, John C.....	457	Momin, Afaque.....	58
McNicholas, Stuart.....	141	Momma, Koichi.....	239
McSweeney, Sean.....	5	Moncol, Jan.....	580
Mechtler, Karl.....	80	Monet, Geoffrey.....	422
Medarde, Marisa.....	322	Monkenbusch, Michael.....	117
Medina, Ana.....	140, 161, 167	Monteiro, Diana C.F.....	8
Meents, Alke.....	15	Montgomery, Mark.....	524
Mehner, Erik.....	262, 273, 275	Moraes, Isabel.....	646, 706
Mehrabani, Pedram.....	8, 16, 17, 96, 389	Morana, Marta.....	245
Mei, Lefu.....	312, 313	Morant Giner, Marc.....	278
Meinhart, Anton.....	60	Morgan, Lewis.....	683
Meisburger, Steve.....	424	Morgenroth, Wolfgang.....	243
Melnic, Elena.....	489	Moriyoshi, Chikako.....	619
Menyhárd, Dóra K.....	606	Morkhova, Yelizaveta.....	316
Merlini, Marco.....	242	Morritt, Alexander.....	600, 601, 602
Meshi, Louisa.....	386	Mortensen, Simon A.....	679
Mess, Pamela.....	545	Mostosi, Philipp.....	65
Metrangolo, Pierangelo.....	573	Mozzanica, Aldo.....	4
Metz, Alexander.....	22	Mrosek, Michael.....	45
Meusburger, Johannes.....	282	Mudogo, Celestin Nzanu.....	41, 50
Meven, Martin.....	379, 639, 662	Mueller, Uwe.....	9, 14, 20
Meyer, Dirk C.....	273, 275	Mugnaoli, Enrico.....	194, 689
Meyer, Jan.....	15	Müller, Danny.....	308
Meyer, Jochen.....	8	Müller, Peter.....	434
Meyer, Mathias.....	748, 750	Müller-Werkmeister, Henrike M.....	96
Meyerheim, Holger.....	225	Münchhafen, Marie.....	262
Meza, Domingo.....	57, 732	Murakami, Hironori.....	27
Mezo, Gábor.....	103	Murphy, Bonnie.....	62
Miao, Jennifer.....	390	Murphy, Bridget.....	676
Michaelsen, Carsten.....	250	Murray, Heath.....	90

Murri, Mara .....	245
Murshed, M. Mangir .....	204, 248
Murshudov, Garib .....	68, 137, 149, 157
Musina, Elvira .....	562
Musselle-Sexton, Jake .....	462
Myers, Stuart F. ....	5
Mykhaylyk, Vitaliy .....	733

## N

Nádaždy, Peter .....	624
Naemi, Waeselmann .....	238
Nagaraja, C. M. ....	592
Nagy, Gergely .....	726
Nagy, Michael .....	34
Najbjerg Skov, Lasse .....	297
Nakahira, Yuki .....	619
Nakamura, Yuki .....	27
Nakanishi, Makoto .....	135
Nakanishi-Ohno, Yoshinori .....	511
Nan, Jie .....	14
Nan, Zhang .....	661
Nartowski, Karol .....	599, 600, 601, 602
Nascimento, André .....	52
Nass, Karol .....	4
Nassimbeni, Luigi .....	451, 473, 579
Natmessnig, Helgit .....	604
Naumov, Pance .....	454
Nazarchuk, Evgeny .....	211
Nazarenko, Alexander .....	352
Nazaretski, Evgeny .....	5
Neder, Reinhard B. ....	426
Neels, Antonia .....	264, 420, 565, 575, 625, 635
Neese, Frank .....	356
Nemcovic, Marek .....	75
Nemec, Ivan .....	324
Nenert, Gwilherm .....	206, 265
Nenning, Andreas .....	298, 306
Nentwich, Melanie .....	273, 275
Nentwig, Markus .....	191
Nespolo, Massimo .....	190, 705
Nethanani, Vhukhudo .....	595
Neudert, Lukas .....	191
Neumann, Piotr .....	146
Ngono Mebenga, Frederic .....	586
Nguyen, Hong Hai .....	304
Nicholls, Robert .....	137, 154
Nicholson, David Graham .....	701
Nicolas, Josep .....	13
Niedenzu, Sara .....	263
Nievergelt, Philipp P. ....	648
Nikodinovic-Runic, Jasmina .....	565
Nikolova, Marina .....	8, 17
Nikulin, Alexey .....	92
Ning, Weihua .....	311
Nishiyama, Atsuya .....	135
Noble, Martin .....	10
Nobrega, Marcelo .....	247
Nomura, Takashi .....	2
Noohinejad, Leila .....	360, 721

Norton, Lois .....	90
Novikov, Dmitri .....	273
Nowak, Maciej .....	601
Nowosielska, Bernadeta .....	423, 593
Nozawa, Kazuki .....	300, 303, 406
Nyamayaro, Kudzanai .....	542
Nyiri, Kinga .....	100
Nyvang, Andreas .....	356

## O

O'Connor, Kevin .....	565
Oberer, Monika .....	179, 604
Ochocki, Justyn .....	178
Oda, Takashi .....	132
Odin, Ivan .....	605
Oeckler, Oliver .....	191, 670
Oeffner, Robert .....	148, 165
Oezugurel, Umut .....	158
Ohashi, Haruhiko .....	27
Oksanen, Esko .....	97, 150, 726, 734
Olejniczak, Anna .....	280
Oleynikov, Peter .....	443
Olieric, Vincent .....	4
Oliva, Romina .....	93
Oliver, Christopher .....	154
Oliver, Clive L. ....	470
Ondrejko, Petr .....	428
Opitz, Alexander .....	298, 306
Opletal, Petr .....	371
Orban-Nemeth, Zsuzsanna .....	80
Oreshko, Alexey .....	269
Ormstrup, Jeppe .....	628
Ortenzi, Marco Aldo .....	231
Osawa, Hitoshi .....	619
Osborn, Raymond .....	412
Osman, Islam Ali .....	571
Osokawa, S. ....	407
Öster, Linda .....	33
Østergaard, Lars .....	104
Ostermann, Andreas .....	117
Otani, Yusuke .....	300
Otgonbayar, Chimednorov .....	202
Ott, Holger .....	205, 250, 344
Ouaaka, Elmustafa .....	638
Oueriagli, Amane .....	700
OUIS, Sakina .....	521
Ouladdiaf, Bachir .....	384
Oursal, Rachid .....	302
Ovchinnikova, Elena .....	269
Overgaard, Jacob .....	347, 356, 615
Ovsyannikov, Sergey .....	237
Owen, Robin .....	3

## P

Pachiu, Cristina .....	641
Page, Katharine .....	19
Pages, Guillaume .....	170

Pai, Emil F.	96
Paineau, Erwan	422
Pakendorf, Tim	15
Pakhomova, Anna	237
Pál, Gábor	103
Palatinus, Lukas	392, 444
Palmer, Colin	67
Paluch, Piotr	599
Palva, Airi	179
Panchenko, Anna	163
Panepucci, Ezequiel	4
Panne, Daniel	715
Pannu, Navraj	536
Pantelides, Costas	535
Paoli, Paola	528
Pardo, Emilio	9
Parenti, Andrea	7
Parkhurst, James	157
Pasciak, Marek	428
Pastero, Linda	185, 231
Patroi, Delia	696
Patyk-Kazmierczak, Ewa	286
Paulmann, Carsten	721
Paulus, Werner	379, 380, 414, 662
Pautrat, Alain	361
Pavese, Alessandro	231
Pavkov-Keller, Tea	54, 56, 102, 179, 604
Pavlíček, Jirí	39
Pavlovic, Jelena	116, 171
Pavlyuk, Volodymyr	408
Pawinski, Tomasz	441
Pawledzio, Sylwia	491
Payer, Stefan E.	102
Pazicky, Samuel	44
Pearce, Nick	25
Pearson, Arwen R.	8, 16, 17
Péchev, Stanislav	235
Pedersen, Björn	322
Pedrini, Bill	4
Pei, Xiaokun	427
Pelagatti, Paolo	508, 574
Pellicer-Porres, Julio	281
Penic, Nikolina	567
Perbandt, Markus	41
Perczel, András	606
Perdih, Andrej	108
Peresypkina, Eugenia	478, 518
Pérez, Olivier	328, 361
Perez-Mato, Juan Manuel	746
Perrakis, Anastassis	153
Perrone, Roberto	508
Peterbauer, Thomas	126
Petri, Edward	168
Petríček, Václav	364, 369, 755
Petrovic, Sasa	127
Petry, Winfried	117
Pettinari, Claudio	513
Pfeiffer, Dorothea	726
Philip, Kollmannsberge	65
Picca, Frédéric-Emmanuel	382
Pierrí, Giovanni	456
Pietsch, Ullrich	608, 643

Pigliacelli, Claudia	573
Pillet, Sébastien	680
Piltz, Ross	437
Pintar, Sara	108
Pintér, István	606
Pirolt, Franz	636
Pisacic, Mateja	471
Pisk, Jana	583
Pizzi, Andrea	573
Plasch, Katharina	102
Plitzko, Juergen	63
Poddig, Hagen	373
Poellmann, Herbert	202
Pogácsás, Ákos	490
Polikarpov, Maxim	8
Pollitt, Stephan	642
Pomjakushin, Vladimir	378, 381
Pomjakushina, Ekaterina	378, 379, 381
Pompach, Petr	39
Pompidor, Guillaume	715
Poon, Billy K.	69
Popescu, Marian	641
Popov, Alexey A.	419
Popovic, Janko	298
Poreba, Tomasz	283, 464
Portalone, Gustavo	554
Potrzebowski, Marek	599
Poulsen, Jens-Christian N.	107
Poupon, Morgane	364
Povolotskiy, Alexey	233
Pradervand, Claude	4
Pravda, Luká	169
Prill, Dragica	526
Prinz, Nils	295, 613
Probert, Michael	241, 462
Probst, Ines	129
Proserpio, Davide	500
Proserpio, Davide M.	710
Prost, Josef	718
Prudnikova, Tatyana	109
Prugovecki, Biserka	517, 544, 584
Prugovecki, Stjepan	206, 265, 612
Pruszkowska, Kamila	561
Puccio, Stephane	227
Puhr, Barbara	636, 669
Pühringer, Dominic	101
Pulido, Angeles	529
Puphal, Pascal	378
Puschmann, Horst	754
Pyrih, Andrii	653

## Q

Qichun, Zhang	472
Queen, Wendy	498

## R

Raaijmakers, Hans	400
-------------------	-----

Rabeh, Wael.....	105
Rabending, Tina).....	288
Radacki, Krzysztof.....	281
Radanovic, Mirjana.....	209, 590
Radcliffe, Paul.....	250
Radoi, Antonio.....	641
Radoske, Thomas.....	731
Rae, Alan David.....	691
Raffy, Guillaume.....	504
Rahm, Martin.....	338
Ramakrishnan, Sitaram.....	322
Rambo, Robert.....	51
Rameshan, Christoph.....	298, 306
Rameshan, Raffael.....	298, 306
Ramsnes, Stian.....	701
Rao, Vincenzo.....	90
Raschhofer, Johannes.....	298
Rasmussen, Kim Krighaar.....	88
Rastall, Bob.....	119
Ravnsbæk, Dorthe.....	292
Ravy, Sylvain.....	749
Read, Randy.....	69, 148, 165, 180
Reddy, C. Malla.....	569
Redford, Sophie.....	4
Rega, Davide.....	427
Reichenbach, Tom.....	121
Reichert, Harald.....	713
Reid, David.....	493
Reikhard, Arsenii.....	186
Reime, Bernd.....	15
Reinsch, Helge.....	505
Reisenbichler, Anna Maria.....	61
Rejnhardt, Piotr.....	548
Rekis, Toms.....	370 532
Rembeza, Elzbieta.....	23
Remko, Milan.....	576
Remok, Firdaous.....	655
Rennhofer, Harald.....	177
Resel, Roland.....	510, 649, 703
Resnati, Giuseppe.....	475
Reuther, Christoph.....	262
Reykhart, Liudmila.....	186
Reyntjens, Steve.....	66
Ribeiro, Euripides.....	37
Richards, Logan.....	390
Richter, Carsten.....	273, 275
Richter, Dieter.....	117
Ridley, Christopher.....	256
Riegler-Berket, Lina.....	604
Riesinger, Christoph.....	421
Rigden, Daniel.....	141, 160, 166, 174
Righi, Lara.....	512
Rigin, Sergei.....	589
Rignanese, Gian-Marco.....	192
Ringkjøbing Jensen, Malene.....	88
Riobé, François.....	40
Rissanen, Kari.....	483, 494, 520
Ristau, Uwe.....	8
Ristic, Predrag.....	558
Riva, Michele.....	314
Roa PaixaoO, Luisa.....	538, 586, 591
Rodic, Marko.....	209, 590

Rodriguez Fernandez, Angel.....	729
Rodriguez, Alan.....	80
Rodríguez, José.....	390
Rodríguez-Carvajal, Juan.....	382
Rodriguez-Chamorro, Ariadna.....	126
Rodriguez-Mendoza, Ulises R.....	290
Rodríguez-Navarro, Alejandro.....	182
Roessle, Manfred.....	627
Rohlicek, Jan.....	667
Röhr, Caroline.....	363, 410
Rols, Stéphane.....	422
Romaguera, Arnau.....	377
Romanitan, Cosmin.....	641
Roodt, Andreas.....	474
Rooth, Victoria.....	465
Rosa, Bartłomiej.....	557
Rosa, Patrick.....	458
Rosales, Diego.....	375
Rosca, Robert.....	7
Rosenkranz, Stephan.....	412
Roseveare, Thomas.....	502
Roske, Yvette.....	127
Roslova, Maria.....	393
Rossi, Miriam.....	350
Rossi, Patrizia.....	528
Rossi, René M.....	575, 635
Rossin, Andrea.....	513
Rossjohn, Jamie.....	74
Rössli, Bertrand.....	381
Roth, Nikolaj.....	429, 430
Round, Ekaterina.....	732
Rouquette, Jerome.....	252
Roy, Siddhartha.....	55
Ruat, marie.....	607
Rubicic, Mirta.....	583
Rück, Denivy.....	7
Ruf, Michael.....	250, 344
Rüffer, Rudolf.....	237
Ruh, Thomas.....	298, 306
Ruiz-Fuertes, Javier.....	281
Rummel, Lena.....	342
Rupp, Bernhard.....	18
Rupprechter, Günther.....	642
Rutjes, Floris P.J.T.....	501
Ryde, Ulf.....	97, 150
Rydz, Agnieszka.....	358
Rywkin, Shanti.....	333
Rzepinski, Patryk.....	453, 593

## S

S. M. Abdelbaky, Mohammed.....	550
Saadoune, Ismael.....	266
Sachse, Carsten.....	136
Sadeghpour, Amin.....	575, 625, 635
Sadocha, Anna.....	593
Sagmeister, Theo.....	54, 179
Saifina, Alina.....	353, 447, 450
Sala, Fernanda Angelica.....	53
Saleem Batcha, Raspudin.....	110

Salim, OueniaA.....	183	Schroer, Martin A.....	627
Salzmann, Ingo.....	703	Schubert, Robin.....	732
Samanta, Dipak.....	469	Schuck, Götz.....	263, 301
Samigullina, Aida.....	447, 497, 541	Schulz, Eike.....	8, 16, 17, 96, 389
Sammito, Massimo.....	148, 161, 165, 167, 180	Schulz, Joachim.....	732
Samolová, Erika.....	552	Schumann, Florian.....	225
Samperisi, Laura.....	391	Schutte Smith, Marietjie.....	474
Sanchez Rodriguez, Filomeno.....	174	Schwalbe, Carl.....	758
Sander, Mathias.....	618	Schwarz, Marcus R.....	288
Sanloup, Chrystelee.....	236	Schwarz, Michael.....	363
Sans, Juan Angel.....	259	Schwarz, Thomas.....	128
Santiso-Quinones, Gustavo.....	402	Schwensow, Leif.....	295
Santoni, Gianluca.....	40, 155	Scilabra, Patrick.....	475
Santos, Hugo.....	7	Scurfield, Georgia.....	683
Sanyal, Suparna.....	647	Sears, Jennifer.....	382
Saouane, Sofiane.....	15	Sébastien, Pillet.....	467
Sapozhnikov, Philipp.....	186	Seidler, Tomasz.....	354
Saridakis, Emmanuel.....	30	Seidhofer, Beatrix-Kamelia.....	730
Sarma, Dipankar Das.....	242	Sekiguchi, Hiroshi.....	51
Sarrou, Iosifina.....	48	Sella, Andrea.....	247
Sartori, Andrea.....	676	Sellars, Jonathan.....	462
Sashuk, Volodymyr.....	547, 557	Senba, Yasunori.....	27
Sasniati, Popi.....	383	Senda, Toshiya.....	723, 728
Saunders, Lucy.....	255	Senior, Levi.....	516
Savko, Martin.....	160, 514	Senn, Mark.....	374
Sawai, Hitomi.....	130	Senyshyn, Anatoliy.....	673
Sbarcea, Beatrice Gabriela.....	696	Serre, Christian.....	514
Scavini, Marco.....	261	Seryotkin, Yuriy.....	287
Schaffer, Robert.....	7	Seshadri, Vasudevan.....	55
Schaniel, Dominik.....	467, 680	Shablinskii, Andrey.....	257
Scheer, Manfred.....	342, 421, 478, 518	Shaikh, Ra'eesah.....	78
Schefer, Jürg.....	379	Shang, Tian.....	322, 379
Scheidl, Katharina.....	239	Sharma, Suresh.....	533
Scheinost, Andreas.....	270, 731	Sheng, Xiang.....	102
Schewa, Siawosch.....	627	Shepard, William.....	160, 514
Schiavoni, Marco.....	231	Sheptyakov, Denis.....	379
Schifferle, Andreas.....	420	Sherman, Dov.....	334
Schikora, Hendrick.....	16	Shi, Wuxian.....	5
Schindelin, Hermann.....	65	Shilova, Anastasiia.....	14
Schirmer, Tilman.....	79	Shimon, Linda.....	446, 469
Schlesinger, Carina.....	329, 526	Shintake, Tsumoru.....	388, 401
Schlosser, Dieter.....	608	Shiro, Yoshitsugu.....	2, 130
Schlüter, Dieter.....	413	Shokr, Mohammad.....	608
Schmahl, Wolfgang.....	181, 182	Shteingolts, Sergey A.....	353, 486
Schmid, Michael.....	314	Shubin, Kirill.....	522
Schmidt, Ella Mara.....	426	Shvanskaya, Larisa.....	221
Schmidt, Martin U.....	232, 329	Sibille, Roman.....	381
Schmitt, Andreas.....	83	Sics, Igors.....	13
Schmitt, Bernd.....	4	Sidebottom, Philip.....	524
Schmitz, Carlo.....	118	Sidorov, Aleksei A.....	468
Schneider, Bohdan.....	85, 152	Siefker, Christof.....	26
Schneider, Hartmut.....	234	Sieh, Daniel.....	281
Schneider, Thomas.....	8, 16, 17, 95, 715	Šiffalovic, Peter.....	624
Schneiderová, Magdalena.....	39	Siidra, Oleg.....	230
Schnick, Wolfgang.....	191	Silenzi, Alessandro.....	7
Schoekel, Alexander.....	725	Simbrunner, Josef.....	703
Schoeller, Martin.....	580	Simenas, Mantas.....	503
Schönleber, Andreas.....	370	Simkovic, Felix.....	160, 166
Schorr, Susan.....	263, 301	Simonet Roda, Maria.....	181
Schrader, Tobias E.....	117	Simonov, Arkadiy.....	255, 413, 431, 418
Schreuer, Jürgen.....	262	Simons, Hugh.....	628
Schrode, Benedikt.....	703	Simpkin, Adam.....	154, 160, 166

Singh, Manrose .....	350
Singh, Rajendra .....	20
Skalova, Tereza .....	44, 104, 656
Skibsted, Jørgen .....	688
Skinner, John .....	5
Skorepa, Ondrej .....	44
Skorepova, Eliska .....	667
Skotnicki, Marcin .....	587
Skoulatos, Markos .....	322
Skovhede, Kenneth .....	722
Skubak, Pavol .....	154
Škultétyová, Lubica .....	39
Sliwiak, Joanna .....	372
Smeets, Stef .....	332, 393, 699
Smietanska, Joanna .....	372
Smith, Luke .....	125
Smith, Mark .....	581
Smith, Vernon .....	45, 205
Smith, Zachary J. ....	659
Smokrovic, Kristina .....	336
Smo'yakov, Alexander .....	677
Smrecki, Neven .....	544, 584
Sniechowska, Justyna .....	599
Soares, Alexei .....	5
Sobolev, Egor .....	142, 158
Sobolev, Oleg V. ....	69
Socha, Pawel .....	497
Soeken, Mathias .....	698
Soler, Nicolas .....	140
Sommer, Sanna .....	685, 688
Søndergaard-Pedersen, Frederik .....	631
Song, Jenn-Ming .....	694
Soo, Yun-Liang .....	697
Sorg, Isabel .....	79
Souhassou, Mohamed .....	337
Souici, Abdelhafid .....	634
Souto, Manuel .....	455
Sovago, Ioana .....	529
Spackman, Mark A .....	457
Spano, Fabrizio .....	635
Spek, Ton .....	744
Spingler, Bernhard .....	648
Spirzewski, Michal .....	7
Sponga, Antonio .....	125, 126
Stachowicz, Marcin .....	244
Stadnicka, Katarzyna .....	354, 358
Stalke, Dietmar .....	436, 439
Stallinger, Amrutha .....	129
Stangarone, Claudia .....	238
Staniec, Dominika .....	115
Stefania, Valeria .....	37
Stefanovich, Sergey .....	233
Stefanski, Tomasz .....	355
Steffien, Michael .....	724
Steinfeld, Gunther .....	402
Stelhorn, J.R. ....	407
Stepien, Dominik .....	309
Stevens, Joanna .....	529, 745
Stilinic, Vladimir .....	482
Stock, Norbert .....	505
Stöcker, Hartmut .....	262
Stöcker, Walter .....	118

Stockwell, Duncan H. ....	148, 165
Stoffel, Ralf .....	249
Storm, Selina .....	6
Stránský, Jan .....	39, 44, 104
Strüder, Lothar .....	608
Strzalka, Radoslaw .....	365, 372
Stuart, Dave .....	20
Stübe, Nicolas .....	15
Stüble, Pirmin .....	363
Stuerzer, Tobias .....	205, 250, 609
Sugden, Isaac .....	535, 536
Sugimoto, Hiroshi .....	2, 130
Sugimoto, Kunihsa .....	619
Suh, Jeong-Yong .....	99
Sulcek, Lara .....	598, 603
Sun, Junliang .....	331, 332
Sun, Yuh-Ju .....	89
Suskiewicz, Martin J. ....	60
Sutter, Jean-Pascal .....	755
Suttle, Martin D. ....	194
Sutula, Szymon .....	244, 438
Suwinska, Kinga .....	546
Svane, Bjarke .....	343
Švecová, Leona .....	104
Svergun, Dmitri I. ....	627
Symeou, Elli .....	305
Szalayová, Andrea .....	116
Szarejko, Dariusz .....	621, 622
Szegletes, Zita .....	734
Székely, Edit .....	445
Szumna, Agnieszka .....	557

## T

Taberman, Helena .....	22, 724
Tabti, Charef .....	530
Taciak, Przemyslaw .....	441
Taftø, Johan .....	305
Tailleur, Elodie .....	458
Takagi, Hidenori .....	321
Takakura, Hiroyuki .....	366
Takayama, Tomohiro .....	321
Takeda, Hanae .....	130
Takeda, Hiroaki .....	619
Takeuchi, Tomoyuki .....	27
Takouachet, Radhwane .....	459, 563
Talla, Dominik .....	199, 282
Tamraoui, Youssef .....	266
Tanaka, Masahiko .....	323
Tandrup, Tobias .....	107
Tarrés-Solé, Aleix .....	86
Tasci, Emre .....	746
Tchon, Daniel .....	564
Tedesco, Consiglia .....	456
Tellkamp, Friedjof .....	8, 16, 17, 96
TEOBALDI, Gilberto .....	422
Terasaki, Osamu .....	443
Terraneo, Giancarlo .....	573, 475
Terwilliger, Thomas C. ....	69
Teufel, Robin .....	110

Tews, Ivo .....	6, 94
Thalal, Abdelmalek .....	700
Thersleff, Thomas.....	393
Thiele, Dennis J.....	107
Thifault, Darretn.....	57
Thomä, Sabrina.....	613, 632
Thomä, Sabrina.....	613
Thomas, Jens.....	141, 154, 160, 166
Thomas, Pamela .....	267
Thomas, Sajesh.....	457
Thomaston, Jessica.....	123
Thominet, Vincent.....	4
Thompson, Amber L.....	683, 761
Thompson, Stephen .....	502
Thomsen, Maja K.....	356
Thorkildsen, Gunnar .....	701
Thorn, Andrea.....	65, 740
Thune, Elsa .....	672
Tickle, Ian .....	145
Tien, Nguyen-Dung.....	575
Timerghazin, Qadir.....	466
Timofeeva, Tatiana.....	589
Tinnemans, Paul.....	501
Tissot, Antoine.....	514
Többens, Daniel .....	263, 301
Tocher, Derek.....	524
Todorovic, Tamara.....	554, 558
Togashi, Hiromi .....	130
Tolborg, Kasper.....	339, 615
Tolkiehn, Martin .....	721
Tombesi, Alessia .....	513
Tonceli, Claudio.....	625
Topic, Edi .....	583
Topic, Filip.....	481
Topnikova, Anastasiia.....	219
Törnroos, Karl Wilhelm .....	666
Tosha, Takehiko.....	2
Tovborg, Morten .....	107
Trebbin, Martin .....	8
Trebosc, Julien .....	599
Trif, László.....	578
Tritschler, Felix .....	48
Triviño, Josep .....	167
Trojanowski, Sebastian.....	7
Trundová, Mária .....	104
Truong, Khai-Nghi .....	520
Trzybinski, Damian .....	564
Tsai, A. P.....	407
Tseng, Eric Nestor.....	383
Tseng, Jo-Chi .....	725
Tsirlin, Alexander.....	237, 285
Tsurkan, Vladimir.....	375
Tuci, Giulia .....	513
Turk, Dušan.....	108
Turner, Douglas.....	147
Turowska-Tyrk, Ilon .....	254
Tusar, Livija .....	113
Tzschaschel, Christian.....	759

## U

Ueno, Go .....	27
Ugale, Bharat.....	592
Ullah, Najeeb .....	41
Umayahara, Akihiro.....	190
Unge, Johan.....	162
Urbschat, Jakob .....	15
Ursby, Thomas.....	9
Urzhumtsev, Alexandre.....	69, 760
Urzhumtseva, Ludmila.....	760
Usenik, Aleksandra .....	108
Ushakov, Ivan .....	335, 452, 605
Uski, Ville.....	141, 154, 160
Usón, Isabel.....	52, 54, 140, 144, 161, 167, 180, 390
Ustrnul, Lukáš.....	520
Uzelac, Lidija.....	544

## V

Vaganova, Ekaterina .....	500
Vagin, Alexy.....	141
Vakhrushev, Sergey.....	415
Vaknin, Uriel.....	334
Valadares, Napoleao.....	52
Valcarcel, Ricardo.....	29, 736
Valenta, Rudolf .....	56
Valkonen, Arto .....	483
van Beek, Wouter.....	106, 665
van Cleuvenbergen, Stijn .....	659
Van de Velde, Jasper.....	543
van der Boom, Milko .....	446
van der Veen, Monique .....	427, 503, 659
van Driel, Tim.....	617
van Smaalen, Sander .....	285, 322, 370
van Well, Natalija .....	322
van de Velde, Christophe .....	509
Vandyukova, Irina .....	450
Vanek, Ondrej .....	44
Vanková, Pavla .....	39
Vapnik, Yevgeny .....	189
Varasteanu, Pericle.....	641
Varming, Anders .....	88
Vasylevskiy, Serhii .....	504
Vaughan, Gavin B. M. ....	670
Veber, Philippe.....	235
Vejevovic, Djenana .....	54, 179
Velankar, Sameer .....	172
Velázquez, Matias .....	235
Vera, Laura .....	4
Verbiest, Thierry.....	659
Vergasova, Lidiya.....	257
Véron, Muriel.....	17
Vicent-Morales, Maria .....	455
Viciosa, Maria Teresa .....	591
Villanueva, Jorge.....	29, 736
Vinci, Doriana.....	223
Vinter, Brian .....	722

Virovets, Alexander.....	478, 518
Virovets, Alexander.....	478
Vismara, Rebecca.....	513
Vlieg, Elias.....	501
Vogel, Antonia.....	59, 80
Vojinovic-Ješić, Ljiljana.....	209, 590
Volkov, Anatoly.....	219
Volkov, Sergey.....	233
Vollmar, Melanie.....	157, 174
Volodin, Alexander.....	359, 468, 605, 677
Vologzhanina, Anna.....	452, 468, 605
von Stetten, David.....	8, 16, 17, 715
von Wachenfeldt, Claes.....	97
Vonck, Janet.....	54, 102, 179
Voronina, Julia.....	488
Voronova, Evgenia.....	452, 605
Vrdoljak, Višnja.....	583
Vujin, Slobodan.....	128
Vukovic, Vedran.....	357
Vulic, Predrag.....	558
Vušak, Darko.....	517, 544, 584
Vymazalová, Anna.....	214

## W

Wachsmann Hogiu, Sebastian.....	659
Wagh, Ajay.....	35
Wagner, Armin.....	733
Wagner, Lucas.....	610
Wagner, Tristan.....	40
Wahiduzzaman, Mohammad.....	505
Wahl, Markus.....	82
Wahyudi, Olivia.....	662
Walker, David.....	267
Wallacher, Dirk.....	46
Wallden, Karin.....	64
Walsh, James P. S.....	356
Wanat, Monika.....	441
Wang, Biao.....	246
Wang, Bin.....	393, 699
Wang, Chih-Chieh.....	551
Wang, Haiyan.....	328
Wang, Jun.....	123
Wang, Meitian.....	4
Wang, Mengying.....	50
Wang, Zhendong.....	332
Wanker, Erich E.....	127
Ward, Jas.....	494, 556
Ward, Suzanna.....	15, 156
Warias, Jonas.....	676
Waroquiers, David.....	192
Warren, Mark.....	255, 502
Warscheid, Bettina.....	126, 128
Warshamanage, Rangana.....	68
Waterman, David.....	157
Watson, Gabrielle.....	74
Watson, Kim.....	119
Wattiaux, Alain.....	235
Weber, Thomas.....	413, 759
Webster, Nathan.....	220

Weidenbacher, Lukas.....	635
Weidenthaler, Claudia.....	260
Weigel, Tina.....	275, 273
Weinberger, Peter.....	308
Weiss, Manfred.....	22, 46, 724
Welberry, Richard.....	13, 428
Welzmler, Simon.....	296
Wen, Yuh-Sheng.....	416
Wendt, Mario.....	725
Wenger, Emmanuel.....	357
Wentzcovitch, Renata M. M.....	243
Wenz, Sergej.....	725
Werzer, Oliver.....	510, 649
Weselski, Marek.....	545
Wetzel, Marius H.....	288
Wharmby, Michael.....	505, 725
White, Fraser.....	748
White, Jonathan S.....	378
Wick, Peter.....	625
Widdra, Wolf.....	225
Wieduwilt, Erna.....	340
Wierenga, Rikkert.....	97
Wiggin, Seth.....	156
Wiker, Geir.....	665
Wildner, Manfred.....	196, 199, 282
Wilke, Manuel.....	660
Willart, Jean-Francois.....	586
Willhammar, Tom.....	465
Wilson, Keith.....	10
Winkelmann, Aimo.....	448
Winn, Martyn.....	67, 157
Woinska, Magdalena.....	441
Wojciechowski, Jakub.....	748
Wojdyr, Marcin.....	154, 160
Wojnarska, Joanna.....	354
Wolf, Wojciech.....	576
Wollenhaupt, Jan.....	22, 724
Wolny, Janusz.....	366, 367, 372
Wolpert, Emma.....	385, 431
Wolter, Bettina.....	735
Wood, Ian.....	207
Wood, Peter.....	529
Worthy, Anna.....	457
Wortmann, Judith.....	47, 56
Wozniak, Krzysztof.....	244, 438, 441, 491
Wrenger, Carsten.....	41
Wright, Jonathan P.....	217
Wright, Gareth.....	53
Wu, Lai-Chin.....	719
Wu, Tai-Sing.....	697
Wu, Yibing.....	123

## X

Xu, Hongyi.....	64, 399, 465
Xutang, Tao.....	472

## Y

Yaghi, Omar .....	427
Yago, Takehiko.....	239
Yakacki, Christopher M.....	671
Yakubovich, Olga .....	221, 222
Yakushevska, Alevtyna.....	66
Yamada, Yusuke .....	723, 728
Yamaguchi, Kotaro .....	300, 303
Yamamoto, Masaki.....	27
Yamasaki, Hiroshi.....	27
Yamashita, Keitaro .....	27
Yamaura, Kazunari.....	323
Yan, Zeyin .....	337
Yang, Chia-Wei .....	416
Yang, Weimin .....	332
Yano, Junko .....	122
Yarema, Maksym.....	645
Yatsenko, Dmitriy .....	637
Ye, Zuo-Guang .....	661
Yefanov, Oleksandr .....	48
Yeung, Hamish .....	255
Yildiz, Özkan .....	62
Yoon, Hyejin .....	537
Yorke, Briony.....	8
Yoshihiro, Tsujimoto .....	323
Youngman, Christopher.....	7
Yu, Jinlong.....	631, 640
Yu, Ming .....	77
Yue, Wyatt.....	23
Yukhno, .....	258
Yumoto, Hirokatsu .....	27

## Z

Zabrocki, Janusz .....	576
------------------------	-----

Zaharko, Oksana.....	375
Zair, Touriya.....	655
Zaitsev, Viatcheslav .....	120, 175
Zajonc, Dirk.....	75
Zakharov, Boris.....	287, 674
Zakharychev, Dmitry V.....	353
Zalden, Peter .....	729
Zamofing, Thierry.....	4
Zanghellini, Benjamin.....	177
Zanotti, Giuseppe.....	131
Zápražný, Zdenko .....	624
Zchornak, Matthias.....	269
Zep, Anna .....	198, 561
Zerraf, Soufiane .....	566
Zhang, Weiguo.....	265
Zhang, Xiaodong.....	377
Zhao, Jianbo .....	147
Zhao, Jingjing.....	39, 692
Zhao, Yue .....	330
Zhao, Zengying .....	218
Zhaodong, Liu .....	246
Zheng, Lirong.....	323
Zheng, Weili.....	128
Zhou, Jingjing.....	64
Zhu, Jun.....	7
Zickmantel, Till.....	627
Ziegler, Andreas.....	181
Zimmermann, Robert .....	604
Zizak, Ivo .....	263
Zobel, Mirijam .....	295, 613, 632
Zodge, Amit.....	445
Zollner, Eva Maria .....	225
Zolotarev, Andrey.....	197
Zorina-Tikhonova, Ekaterina N.....	468
Zou, Xiaodong .....	
Zschech, Ehrenfried .....	327
Zschornak, Matthias.....	273, 275
Zvoníček, Vít.....	667
Zweckstetter, Markus .....	83

